Studies on the immunosuppressive effects and detection of naturally-occurring toxins

A thesis submitted for the degree of Ph.D.

by

Edwina C. Stack B.Sc. (Hons.) M.Sc. (Hons.)

December 2011

Based on research carried out at

School of Biotechnology,

Dublin City University,

Dublin 9,

Ireland.

Under the supervision of Professor Richard O' Kennedy.

This thesis is dedicated to my parents, Edmond and Breda, for their love and support throughout the years

I hereby certify that this material, which I now submit for assessment on the programme of study leading to the award of Doctor of Philosophy is entirely my own work, that I have exercised reasonable care to ensure that the work is original, and does not to the best of my knowledge breach any law of copyright, and has not been taken from the work of others save and to the extent that such work has been cited and acknowledged within the text of my work.

Signed: _____

ID No.: 52431769

Date: _____

Acknowledgements

I would like to thank my supervisor, Richard O'Kennedy for the opportunity to undertake this research work in his laboratory. I also thank him for his constant encouragement and enthusiasm during my time in DCU.

I wish to thank Professor Chris Elliott, Institute of Agri-Food and Land Use, Queen's University, Belfast for the provision of genetic material and toxin reagents for the work on azaspiracid antibody generation.

A big thank you also to my friends and co-workers in the lab, Niamh, Valarie, Paul C, Carol, Caroline M, Jenny and Elaine – for the daily banter that brightened my day and the daily torment that convinced me to leave! Thanks also to the other members of the 'ROK' lab (both past and present) that made the past four years enjoyable: Jodie, Stephen, Paul L, Gregor, Carolyn, Catherine H, Gillian, Sue, Seán, Meg, Chandra, Jessie, Conor, Barry B., Barry Mc, Hannah and Sarah.

To the non-DCU people who kept me sane with nights out, great chats and trips away during the years. Thanks for helping me to keep things in perspective – Ciara, Siobhan and Mary, I owe you one!

A very special thanks goes to my family, without whose never-ending support, this work would not have been completed. To Angela and Maria, for the encouragement and pep talks that kept me going when times were tough and for the frequent treats! To my parents, Edmond and Breda, to whom I dedicate this work – thank you for the endless encouragement and love you have given me. Finally, to Ger, my best friend, for always listening, being a constant support and for proof-reading this thesis. Thanks for everything.

Table of Contents

List of Figures

List of Tables

Abbreviations

2D	Two-dimensional
3D	Three-dimensional
α	Alpha
AC	Alternating current
Adda	(2S,3S,8S,9S)-3-amino-9-methoxy-2,6,8-trimethyl-10-phenyldeca-4,6-dienoic
AFAR	Aflatoxin B_1-aldehyde reductase
AFB_1	Aflatoxin B_1
AFB_2	Aflatoxin B_2
AFG_1	Aflatoxin G_1
AID	Activation-induced (cytidine) deaminase
AIDA	Advanced image data analysis
Ala	Alanine
AP	Antarctic phosphatase
AP-1	Activator protein-1
APC	Antigen-presenting cell
APS	Ammonium persulfate
APTES	3-aminopropyltriethoxysilane
ASC	Apoptosis-associated speck-like protein
ASP	Amnesic shellfish poisoning
ATA	Alimentary toxic aleukia
AZA	Azaspiracid
AZP	Azaspiracid shellfish poisoning
β	Beta
BCR	B-cell receptor
BLyS	B lymphocyte stimulator
bp	Base pair
BSA	Bovine serum albumin
BTG	Bovine thyroglobulin
C	Constant
Ca^{2+}	Calcium ions
cAMP	Cyclic adenosine monophosphate
CARD	Caspase activation and recruitment domain
Caspase	Cysteinyl aspartate-specific proteases
CBE	Cyanobacterial bloom extract
cBSA	Cationised BSA
CD14	Cluster of Differentiation 14
cDNA	Complementary DNA
CDRs	Complementary determining regions
CFE	Colony-forming efficiency

CIPPIA	Colorimetric immuno-protein phosphatase inhibition assay
CLRs	C-type lectin receptors
CO_2	Carbon dioxide
COX-2	Cyclooxygenase-2
CRM	Certified reference material
CTAB	Cetyltrimethylammonium bromide
DAMPs	Danger-associated molecular patterns
dATP	Deoxyadenosine triphosphate
DCC	Dicyclohexylcarbodiimide
dCTP	Deoxycytidine triphosphate
DCU	Dublin City University
δ	Delta
dGTP	Deoxyguanosine triphosphate
dH_2O	Distilled water
DMEM	Dulbecco's modified Eagle's medium
DMSO	Dimethyl sulfoxide
DNA	Deoxyribonucleic acid
dNTPs	Deoxynucleotide triphosphates
DPBS	Dulbecoo's phosphate buffered saline
DSP	Diarrhetic shellfish poisoning
DTT	Dithiothreitol
dTTP	Deoxythymide triphosphate
DTX1	Dinophysis toxin-1
ε	Epsilon
E.coli	*Escherichia coli*
EC	Electron coupling
ECACC	European collection of cell cultures
ECIS	Electric cell-substrate impedance sensing
EDC	*N*-ethyl-*N*-(dimethyl-aminopropyl)-carbodiimide hydrochloride
EDPC	(1-(3 dimethylaminopropyl)-3-ethylcarbodiimide)
EDTA	Ethylenediaminetetra acetic acid
ELISA	Enzyme-linked immunosorbent assay
EP	Error prone
ESI	Electrospray ionisation
EPA	Environmental protection agency
EtOH	Ethanol
Fab	Fragment antigen-binding of antibody
FABMS	Fast atom bombardment mass spectrometry
FACS	Fluorescence activated cell sorting
FBS	Fetal bovine serum
Fc	Fragment-crystallisable region of antibody

FCA	Freund’s complete adjuvant
FIA	Freund’s incomplete adjuvant
FITC	Fluorescein isothiocyanate
FLICA	Fluorescent-labelled inhibitor of caspases
FMK	Fluoromethyl ketone
fMLP	formyl-Met-Leu-Phe
FPLC	Fast-performance liquid chromatography
FW	Framework region
GALT	Gut-associated lymphoid tissues
GC-MS	Gas chromatography-mass spectrometry
γ	Gamma
Glu	Glutamic acid
GPCR	G-protein-coupled receptor
GRAVY	Grand average of hydropathicity
GTX	Gonyatoxin
H	Heavy chain
HA	Haemagluttinin
HABA	4'-hydroxyazobenzene-2-carboxylic acid
HABs	Harmful algal blooms
HBS	Hepes buffered saline
HCC	Hepatocellular carcinoma
HCl	Hydrochloric acid
HEPES	4-(2-hydroxyethyl)-1-piperazineethanesulfonic acid
HF	High fidelity
His	Histidine
His_6	Hexahistidine
HPLC	High-performance liquid chromatography
HRP	Horseradish peroxidase
HSP	Heat-shock proteins
IARC	International agency for research on cancer
Ig	Immunoglobulin
IgA	Immunoglobulin A
IgD	Immunoglobulin D
IgE	Immunoglobulin E
IgG	Immunoglobulin G
IgY	Immunoglobulin Y
IKK	IκB kinase
IL	Interleukin
IMAC	Immobilised metal affinity chromatography
iNOS	Inductible nitric oxide synthase
IPTG	Isopropyl-beta-D-thiogalactopyranoside
IRAK	IL-1 receptor-associated kinase
K^+	Potassium ion
κ	Kappa

KLH	Keyhole limpet haemocyanin
L	Light chain
λ	Lamda
LB	Lauria-Bertani
LC	Long chain
LC-MS	Liquid chromatography-mass spectrometry
LDH	Lactate dehydrogenase
LDLR	Low-density lipoprotein receptor
LOB	Limit of blank
LOD	Limit of detection
LPB	LPS-binding protein
LPS	Lipopolysaccharide
LRR	Leucine-rich repeats
LTA	Lipoteichoic acid
mAb	Monoclonal antibody
MALDI-TOF	Matrix-assisted laser desorption time of flight mass spectrometry
MAPK	Mitogen-associated protein kinase
MC	Microcystin
MDha	*N*-methyl-dehydroalanine
MDP	Muramyl dipeptide
MeAsp	β-methylaspartic acid
mer	Oligomer
MFI	Mean fluorescence intensity
MG	Molecular grade
$MgCl_2$	Magnesium chloride
MHC	Major histocompatability complex
$MnCl_2$	Manganese chloride
mRNA	messenger RNA
MS	Mass spectrometry
MS/MS	Tandem mass spectrometry
MTT	(3-(4,5-dimethylthiazol-2-yl)-2,5-diphenyltetrazolium bromide)
μ	Mu
MW	Molecular weight
MWCO	Molecular weight ‘cut-off’
MyD88	Myeloid differentiation primary-response, gene 88
N_2	Nitrogen
NaCl	Sodium chloride
NAD^+	Nicotinamide adenine dinucleotide
$NADP^+$	Nicotinamide adenine dinucleotide phosphate
NaOH	Sodium hydroxide
NBD	Nucleotide-binding oligomerisation domain
Neg	Negative

NH_2	Amino group
NHS	N-hydroxysuccinimide
Ni^+-NTA	Nickel-nitrilotriacetic acid
NK	Natural killer
NLR	'Nod-like' receptor
NMR	Nuclear magnetic resonance
NO	Nitric oxide
NOD	Nucleotide-binding oligomerisation domain
NSP	Neurotoxic shellfish poisoning
oligo(dT)	Oligodeoxythymidylic acid
OVA	Ovalbumin
PA	Protective antigen
pAb	Polyclonal antibody
PAGE	Polyacrylamide gel electrophoresis
PAMPs	Pathogen-associated molecular patterns
PBS	Phosphate buffered saline
PBST	Phosphate buffered saline with Tween 20
PCR	Polymerase chain reaction
PDA	Photodiode array
PDB	Protein data bank
PE	Phycoerythrin
PEG	Polyethylene glycol
PP	Protein phosphatase
PMN	Polymorphonuclear cell
PPIA	Protein phosphatase inhibition assay
PRRs	Pattern recognition receptors
PSP	Paralytic shellfish poisoning
PTX	Pectenotoxins
Q-TOF	Quadrolope-time-of-flight
QUB	Queens University Belfast
RIG	Retinoic acid-inducible gene
RLR	RIG-I-like receptor
RNA	Ribonucleic acid
RNase	Ribonuclease
ROS	Reactive oxygen species
RP-HPLC	Reversed-phase high-performance liquid chromatography
RS	Mitochondrial succinate-tetrazolium-reductase system
RT	Reverse transcriptase
RTCA	'Real-time' cell analysis
SB	Super broth
scFv	Single chain antibody fragment

SDS	Sodium dodecyl sulfate
SEB	Staphylococcal enterotoxin B
SIM	Selected ion monitoring
SMC	Spleen mononuclear cell
SOC	Super optimal catabolite
SOE	Splice overlap extension
SPE	Solid-phase extraction
STX	Saxitoxin
Sulfo-NHS	*N*-hydroxysulfosuccinimide
TACI	Transmembrane activator calcium modulator and cyclophilin ligand interactor
TAE	Tris-acetate-EDTA
Taq	*Thermus aquaticus*
TB	Terrific broth
TCR	T-cell receptors
TEMED	N,N,N',N'-Tetramethylethylenediamine
TFA	Trifluoroacetic acid
TH	Helper T-cells
TIR	Toll/Interleukin-1 receptor domain
TLR	'Toll-like' receptor
TMB	3, 3', 5, 5' tetramethylbenzidine
TNF	Tumor necrosis factor
TRAF-6	Tumor necrosis factor-receptor-associated factor 6
Tris HCL	Tris(hydroxymethyl)aminomethane hydrochloride
TY	Tryptone yeast extract
UPLC	Ultra-performance liquid chromatography
V	Variable
UV	Ultraviolet
V_H	Variable heavy
V_L	Variable light
WHO	World Health Organisation
YTX	Yessotoxin
YVAD	Tyrosine-valine-alanine-aspartic acid
ZY	Auto-induction media

Units

%	Percent
A	Absorbance
ANOVA	Analysis of variance
AU	Arbitary units
C	Concentration
^{o}C	Degrees Celsius
cfu	Colony-forming unit
CI	Cell index
cm	Centimeter
CV	Coefficient of variation
Da	Dalton
EC_{50}	Half-maximal effective concentration
g	Acceleration
hrs	Hours
IC_{50}	Half-maximal inhibitory concentration
kb	Kilobase
kDa	Kilodalton
kg	Kilogram
kV	Kilovolt
L	Litre
LD_{50}	Half-maximal lethal does
M	Molar
m/z	Mass-to-charge ratio
mAu	Milli-absorbance unit
mg	Milligram
min	Minute
mL	Millilitre
mM	Millimolar
mm	Millimetre
mmol	Millimoles
mS	Microsiemen
mV	Millivolt
n	Number of observations
ng	Nanogram
nm	Nanometre
nM	Nanomolar
OD	Optical density
Ω	Ohm
P	Probability
pg	Picogram
pH	Negative logarithm of the hydrogen ion concentration
pI	Isoelectric point

pM	Picomolar
R^2	R-squared
RMSD	Root mean square deviation
rt	Retention time
RU	Response unit
SD	Standard deviation
SE	Standard error
sec	Second
SEM	Standard error of the mean
U	Units
µF	Microfarad
µg	Microgram
µL	Microlitre
µm	Micrometer
µM	Micromolar
V	Voltage
v/v	Volume per unit volume
w/v	Weight per unit volume
Z	Impedance

Publications

Bruneau, J.C., **Stack, E**., O'Kennedy, R., Loscher, C.E. (Submitted; 2011) Aflatoxins B_1, B_2 and G_1 Modulate Cytokine Secretion and Cell Surface Marker Expression in Murine Macrophages. *Toxicology Letters*.

Byrne, B., **Stack, E**., O'Kennedy R. (Chapter in Press; 2011) The application of biosensors for the sensitive detection of agricultural contaminants, pathogens and food-borne toxins, *Food Biochemistry and Food Processing*.

Byrne B., **Stack E.**, Gilmartin N., and O'Kennedy R. (2009) Antibody-Based Sensors: Principles, Problems and Potential for Detection of Pathogens and Associated Toxins. *Sensors* **9**, 4407-4445.

Presentations and posters

Stack, E., Murphy, C., and and O'Kennedy R. (4-5th May, 2011) Development of recombinant antibody fragments for detection of microcystins. Second Annual Research Consortium Meeting for BEACONS: Biosafety for Environmental Contaminants using Novel Sensors, Fermanagh, Ireland (Presentation).

Stack, E., Murphy, C., Devlin, S., Elliott, C., and O'Kennedy R. (21-24th March, 2011) Development of recombinant antibody fragments for microcystin detection. International Asset Conference on Food Integrity and Traceability, Belfast, Ireland (Poster; Awarded best poster presentation).

Stack E., and O' Kennedy R. (28th January, 2011) Development of recombinant antibody fragments for detection of microcystins. The 3rd Annual Biotechnology Research Day, Dublin, Ireland (Poster).

Stack, E., Murphy, C., and and O'Kennedy R. (21-22nd September, 2010) Development of recombinant antibody fragments for detection of microcystins. Research Consortium Meeting for BEACONS: Biosafety for Environmental Contaminants using Novel Sensors, DCU, Dublin, Ireland (Presentation).

Stack E., Steward, L., Elliott, C., and O'Kennedy R. (12th February, 2010) Development of recombinant antibody fragments for detection of marine biotoxins. First Annual Beaufort Sensors & Communications project workshop, Dublin, Ireland (Poster and Presentation; Awarded best poster presentation).

Stack E., and O' Kennedy R. (1st July, 2008) New Technologies for the Detection of Biotoxins in Foods 4th Safefood Biotoxin Research Network Meeting and Workshop, Belfast, Ireland (Presentation).

Education and outreach work

The Centre for Talented Youth in Ireland (CTYI) works with young people with exceptional academic ability. CTYI run summer courses, correspondence courses and discovery days for young people between the ages of six and sixteen.

Stack, E., (2010) Instructor for Biomedical Diagnostics course, Summer Program, Centre for Talented Youth, Ireland (CTYI), DCU, Dublin

Stack, E., (2009) Instructor for MAMBO (Me and My Body) Young Student Program, CTYI and BDI, DCU, Dublin

Stack, E., (2008) Instructor for Chemistry Weekend Program, CTYI, DCU, Dublin.

Stack, E., (2007) Teaching Assistant and Residential Assistant for CTYI, DCU, Dublin.

The Education and Outreach programme at the Biomedical Diagnostics Institute (BDI), DCU contributes to science education from primary to fourth level through school visits, workshops and classroom lessons.

Stack, E., (2007-2008) Teaching assistant, BDI Education and Outreach Primary School Science Programme Workshops, DCU, Dublin.

The Access Service at DCU runs courses aimed at increasing participation in higher education by students who do not view going to university as a viable option for social and financial reasons.

Stack, E., (2009) Instructor for Forensic Science, DCU Access Programme, DCU, Dublin.

The Discover Science and Engineering Science Bus is an interactive mobile science laboratory, specifically designed for primary school children. It travels to schools around Ireland, giving children the opportunity to participate in fun, hands-on science experiments.

Stack, E., (2008) Instructor on Discover Science and Engineering Science Bus, Dublin.

Abstract

Episodes of toxin-producing phytoplankton occur worldwide, causing both animal and human fatalities. Toxicity occurs through consumption of phycotoxins, including azaspiracid, which accumulate in filter-feeding shellfish. Microcystins are hepatotoxins, produced mainly by freshwater cyanobacteria. Aflatoxins are potent, fungal hepatocarcinogens, which occur mainly in food and feed products. The purpose of this research was to examine the cytotoxic and immunosuppressive effects of aflatoxins (B_1, B_2 and G_1), azaspiracid-1 and microcystin-LR *in vitro*, using the murine macrophage cell line, J774A.1. The results clearly demonstrated that azaspiracid and microcystin had a significant effect on host defence functions, through deregulation of IL-6, IL-10, IL-12p40 and TNF-α cytokine expression. Microcystin exposure significantly decreased IL-1β expression. 'Toll-like' receptor (TLR2 and CD14) expression was altered following aflatoxin exposure, while apoptotic marker (caspase-1) expression was affected following microcystin exposure. This knowledge should be taken into consideration in the implementation of detection limits, aimed at minimising risks to human health through toxin exposure.

Increased awareness of the hazards presented by toxins led to the requirement for recombinant antibodies for these targets, for incorporation into sensitive detection immunoassays. This thesis describes the production of leprine and avian immune libraries for azaspiracid and microcystin, respectively. Attempts were made to isolate azaspiracid-specific antibodies with little success. Phage display was utilised to successfully isolate two single chain antibody fragments (scFvs) to microcystin from the avian library. Error-prone PCR resulted in the isolation of a mutant clone which displayed a 2.3-fold improvement in sensitivity by ELISA, with an LOD of 1.4 ng/mL. The mutant scFv displayed an altered cross-reactivity profile to the microcystin variants tested using Biacore™ inhibition analysis. The recombinant antibodies were successfully applied to the development of fluorescence-based immunoassay formats. The biotinylated mutant scFv was incorporated into a slide-based assay format on a functionalised glass substrate (IC_{50} ~ 1 µg/L). This assay had the potential to accurately detect microcystin and its variants, below the regulatory limit of 1 µg/L. The application of these highly-sensitive recombinant antibodies into rapid and inexpensive fluorescence detection systems could aid in the development of an early warning system for toxin outbreaks.

CHAPTER 1

Introduction

1.1 Introduction

This chapter will introduce the concepts of innate and adaptive immunity with a focus on inflammatory cells, including macrophages and their related inflammatory mediators, including cytokines and chemokines. Pattern recognition, including 'toll-like' receptor (TLR) and 'nod-like' receptor (NLR) recognition mechanisms and microbial sensing, especially in relation to macrophages, will be described. These concepts will be discussed to provide a basis for the investigation of the effects of phycotoxins and mycotoxins on the immune response to infection. Adaptive immunity, including T-cell and B-cell recognition and development, leading to a specific immune response and antibody development will be introduced.

The area of recombinant antibody generation to small-molecular weight marine toxin targets, for the purpose of immunosensor development is also introduced. The key stages involved in successful immune response generation to hapten targets in host animals are outlined, including immunogen preparation, conjugate carriers, coupling chemistries and conjugate purification. Introductions to recombinant antibody technology and immune library preparation are given. The current literature on marine toxins and mycotoxins, including cases of toxin outbreaks, their chemical structures and properties, source organisms, occurrence and accumulation is reviewed.

1.2 The immune system

The body is protected from damage caused by infectious agents and from other harmful substances, including toxins, by the immune system. A successful immune response to an invading pathogen relies on recognition of the infection, recruitment and trafficking of relevant immune cells, and proper activation and execution of their effector functions. The immune system consists of several organs, lymphocytes and a large number of extracellular messengers. A vast array of receptor-ligand interactions control these events (Rudd *et al*., 2004; Long *et al*., 2006).

Innate immunity represents a non-specific first line of defence to the body, in which the host's cell surface receptors recognise components of foreign pathogens. The adaptive immune response is characterised by the production of antibodies and activation of T-cells and is developed during the lifetime of an individual in response to a specific infection. Considerable co-ordination occurs between the innate and adaptive immune systems (Akira *et al*., 2006). In the absence of vital innate effector functions, including antigen-presentation and cytokine production, adaptive responses would be ineffectual. However, innate responses do not lead to immunological memory, as it is solely the adaptive immune response that provides such specificity and complexity. Essentially, the innate immune system functions as a delaying mechanism, temporarily preventing infection while a more specific adaptive response is mounted.

1.3 Innate Immunity

1.3.1 The frontline of host defence

When an infectious agent is first encountered, the initial defences are physical and chemical barriers, which prevent microbes from entering the body. These have been reviews in detail by Janeway and Medzhitov (2002). The epithelial surfaces form a physical barrier that is highly impermeable to most infectious agents, acting as the first line of defence against invading organisms. In the gastrointestinal and respiratory tract, movement due to peristalsis or cilia aid in the removal of infectious agents. The trapping effect of mucus that lines these tracts aids in the protection of the lungs and digestive system from infection. The gut flora can prevent the colonisation of pathogenic bacteria by competing with pathogenic bacteria for nutrients or attachment to cell surfaces. The flushing action of tears and saliva helps prevent infection of the eyes and mouth. It is only when these barriers are overcome, that the immune system is activated.

1.3.2 Inflammation

The inflammatory response to an infection, as part of innate immunity, involves the triggering of physiological responses, including fever, pain, redness and swelling and a

build-up of white blood cells at the site of infection (White, 1999; Akira *et al*., 2006). This response will recruit effector cells (Section 1.3.3) and chemical factors (Section 1.3.4) of the innate immune system to the site of infection from local blood vessels. A local environment is formed, which promotes the migration of white blood cells to the site of infection, the destruction of the invasive agents and the repair of the damaged tissue. Acute inflammation is initiated by certain cells present in all tissues of the body, known as mononuclear phagocytes, or macrophages. These cells possess unique receptors on their surface, known as PRRs. PRRs recognise molecules that are broadly shared by pathogens, but distinguishable from other molecules and are referred to as pathogen-associated molecular patterns (PAMPs). Pattern recognition will be discussed in detail in Section 1.3.5. On the on-set of infection, macrophages undergo activation and release inflammatory mediators, including TNF-α and IL-1, leading to the clinical signs of inflammation. Chemical factors including histamine, bradykinin, serotonin, leukotrienes and prostaglandins are produced by basophils and mast cells in response to inflammation (White, 1999). These factors are involved in the sensitisation of pain receptors, cause vasodilation of blood vessels and attract phagocytes, especially neutrophils.

1.3.3 Macrophages

A key element of the inflammatory response is the recruitment of polymorphonuclear neutrophils (PNMs) and macrophages to sites of infection. Pathogens that overcome the epithelial barrier first encounter macrophages in residing tissues and subsequently interact with PMNs, including neutrophils and monocytes, recruited to the site of infection, where they phagocytose and kill invading organisms internally. They also contribute to tissue damage which occurs during inflammation. These cells possess PRRs which induce the engulfing of microbes into membrane-bound vesicles or 'phagosomes' (Underhill *et al*., 2002). Multiple receptors are simultaneously engaged to mediate internalisation, activate microbial killing, and induce the production of inflammatory cytokines and chemokines (Table 1.3.3.1). Binding to PRRs will ultimately trigger cell signaling, producing soluble mediators such as cytokines, chemokines, acute phase proteins and complement initiating an inflammatory response. The surface receptors of macrophages and other PMN*s* regulate

a number of key functions, including growth, differentiation, survival, phagocytosis and cytotoxicity (Janeway and Medzhitov, 2002; Russell and Ley, 2002). This ability to recognise and respond to a wide range of endogenous and exogenous ligands is essential for homeostasis, inflammation and host defence in innate and acquired cellular activation by the macrophage.

Macrophages are immune effector cells which have a well established role in pathogen recognition, host defence and immune regulation. They have been reviewed extensively in relation to pattern recognition and innate immunity (Tsan and Gao, 2004; Taylor *et al*., 2005; Mosser and Edwards, 2008; Kumar *et al*., 2011). Macrophages were first recognised in 1905 as important phagocytes (Metchnikoff, 1968) and have been under constant investigation by immunologists since then. Macrophages originate from myeloid progenitor cells in the bone marrow and, when committed to the monocyte lineage, they exit the bone marrow and enter the blood stream. Macrophages can leave the circulation to migrate into tissues throughout the body. They also function in phagocytosis and intracellular killing, usually involving the production of reactive oxygen species (ROS) which can be released into a phagocytosed microbe following phagolysosome formation or engulfment. Furthermore, macrophages contribute to tissue repair and act as antigen-presenting cells, which are required for the induction of specific immune responses. Studies have shown that tissue macrophages express remarkably heterogeneous surface receptors and have very different phenotypes, which reflect specialisation of function within different microenvironments (Gordon and Taylor, 2005; Taylor *et al*., 2005; Mosser and Edwards, 2008).

Macrophages have distinct sub-populations in lymphoid and non-lymphoid tissue, including liver (Kupffer cells), lung (alveolar), nervous system (microglia), epidermis (Langerhans cells), reproductive organs and serosal cavities. Macrophages can also be found in the lamina propria of gut and the interstitial fluid of the heart, pancreas and kidney. In response to inflammatory stimulation, additional monocytes are recruited to the site of infection, where they will display different phenotypes to the already resident macrophages (Taylor *et al*., 2005). Macrophages have the ability to initiate adaptive immunity by presenting antigen to CD4+ T-cells via MHC class II molecules of the

adaptive immune system (Janeway *et al*. 2001). Macrophages can be stimulated through two distinct routes; classical activation and alternative activation, and regulatory macrophages also form an important homeostatic subset (Mosser and Edwards, 2008).

Table 1.3.3.1: Overview of macrophage receptors involved in the innate response.

Receptor Family	Example	Cell Type	Function
Scavenger	SR-A CD36	Macrophage	• Phagocytosis of bacteria and apoptotic cells
GPI-anchored	CD14	Macrophage	• LPS-binding • Interaction with MD2/MyD88 • TLR signalling • Apoptotic cell recognition
'Toll-like' receptors	TLR2 TLR4	Macrophage	• Response to Peptidoglycan • Response to LPS
NOD (nucleotide-binding oligomerisation domain) receptor	NOD1 NOD2	Macrophage Epithelial cells Paneth cells of gut	• Recognise Peptidoglycan and muramyl dipeptide (MDP) or stress responses and form oligomers • Activate inflammatory caspases (e.g. caspase-1), cleavage and activation of IL-1, and/or activate the NF-κB signaling
IgG superfamily	FcR (ITAM/ ITIM), TREM-1	Macrophages, neutrophils, dendritic and mast cells	• Antibody-dependent binding • Up-take and killing • Regulation of inflammation
TNF-receptor superfamily	CD40	B-cells, macrophages and dendritic cells	• Macrophage signalling to CD4+ T-cells

1.3.4 Cytokines

Cells of the immune system are continuously sending and receiving messages. Cytokines are small protein molecules, usually less than 30 kDa in size, secreted by T-cells and macrophages (Stow *et al*., 2009). Cytokines are pleiotropic or multi-functional and the specific response elicited by a given cytokine is dependent upon the cellular context, the environment and the cell's state of maturation. Cytokines frequently function in a redundant manner, in that multiple cytokines can produce the same physiological response. Furthermore, individual cytokines can be produced simultaneously and act synergistically. The response elicited by a cytokine or group of cytokines can have an expansive effect, in that one signal can trigger a cascade of cytokine signaling events. Cytokines usually operate in a targeted fashion, operate over short distances and have short life-spans. The overall result of successful cytokine signaling is the rapid activation and recruitment of the appropriate cells of the immune system in response to a pathogenic agent.

There are five families of cytokines and cytokine receptors including: the Toll/IL-1 family, the tumor necrosis factor (TNF) family, the haematopoietic receptors, the interferon receptors and the chemokine receptors (Dinarello, 2000). Interleukins of the Toll/IL-1 subgroup are produced mainly by T-cells, but are also produced by monocytes and macrophages. Cytokine signaling to B-cells and T-cells promotes growth, proliferation and differentiation. In addition to Toll/IL-1 cytokines, tumor necrosis factor (TNF) receptors and their associated cytokines are involved in the coordination and regulation of growth, proliferation and survival of leukocytes. They coordinate the development of lymphoid organs and temporary inflammatory structures and they play a central part in the adaptive immune response. TNF-type cytokines have a key role in homeostasis and the maintenance of stability in the inflammatory process. Hematopoietin receptors or Class I cytokine receptors are a family of over 20 signalling molecules involved in lymphocyte signalling. The interferon/IL-10 receptors or Class II cytokine receptors mediate anti-viral responses through signalling to other leukocytes and up-regulating anti-viral genes. Moreover, interferons act as anti-tumour agents through down-regulation of genes involved in proliferation and they are involved in regulating genes essential for the adaptive immune response. TNF-α acts as an inducer of the local inflammatory response, aiding in the

containment of infection. It also has systemic effects, many of which are harmful. IL-8 is involved in the local inflammatory response, which helps to attract neutrophils to the site of infection. IL-1β, IL-6 and TNF-α have a crucial role in acute phase response in the liver and fever induction. IL-12 activates natural killer (NK) cells of the innate immune response and favors the differentiation of CD4 T–cells into T_H1 cells during adaptive immunity. Table 1.3.4.1 outlines the most prominent cytokines secreted by macrophages and dendritic cells as part of the inflammatory response.

Table 1.3.4.1: Inflammatory cytokines

Cytokine	Producer	Effect
IL-1	Macrophages Keratinocytes	• Proliferation and enhanced responses in lymphocytes • Induces acute-phase protein secretion
IL-6	Macrophages Dendritic cells	• Proliferation and differentiation and Ig production • Enhance innate immune response • Induces acute-phase protein secretion
IL-8	Phagocytes	• Chemoattractant for neutrophils
IL-10	Monocytes	• Inhibits cytokine production
IL-12	Naïve T-cells	• Diverts immune response to T_H1 • Pro-inflammatory cytokine secretion
TNF-α	Vascular endothelium	• Induces changes in vascular endothelium • Changes in cell-cell junctions with increased fluid loss • Local blood clotting

1.3.5 Pattern recognition receptors

Our innate immune system has evolved a number of pattern recognition receptors that cooperate to recognise microbial pathogens or endogenous danger signals. The two main receptor families include the 'toll-like' receptor system (TLRs) and the 'nod-like' receptors (NLRs), although a number of other receptor subtypes exist. The TLR and NLR family will be discussed in detail in this work. Pattern recognition is a concept first proposed by Janeway and Medzhitov (2002). It is based on the recognition of evolutionary conserved microbial structures, named pathogen-associated molecular patterns (PAMPs) (Takeda and Akira, 2005). These are recognised by a small number of non-clonal germline-encoded antigen-presenting cell (APC) pattern recognition receptors (PRRs). Individual PRRs with unique expression patterns react with specific PAMPs, resulting in the activation of a distinct signalling pathway and immune response. Some of the unique cell wall components of bacteria are recognised by immune cells and act as PAMPs, which are recognised by individual TLRs.

Bacteria can be classified into two major groups, gram-positive and gram-negative, named for their staining characteristics of their cell walls. Gram-positive are stained dark blue by gram staining as they retain the crystal violet stain due to their substantial peptidoglycan cell wall. In contrast, gram-negative bacteria cannot retain the crystal violet dye because of their thin cell wall and are instead identifiable using a counter-stain, such as safranin. The innate immune response can be stimulated by components of the gram-positive cell wall, including lipoteichoic acid (LTA), lipoproteins and peptidoglycan. LTA is an amphiphilic molecule (contains both hydrophilic and lipophilic properties), negatively-charged glycolipid and functions as an immune activator. Lipoproteins and peptidoglycan, as components of both gram-positive and gram-negative bacteria, are potent immuno-stimulators (Figure 1.3.5.1).

Lipopolysaccharide (LPS) is a complex amphiphilic molecule which varies widely in chemical composition in bacterial species. Bacterial LPS is a cell-wall component of gram-negative bacteria, which activates monocytes and macrophages to produce cytokines. LPS mediates inflammation through receptor interactions with various immune cells. LPS binds

the CD14/TLR4/MD2 receptor complex, which promotes the secretion of pro-inflammatory cytokines, including TNF-α, IL-1 and IL-6, in many cell types but especially in macrophages and B-cells. LPS is a large molecule, consisting of a lipid and a polysaccharide joined by a covalent bond (Figure 1.3.5.1). LPS also acts as an exogenous pyrogen or fever-inducing substance. The term "LPS challenge" refers to the process of exposing a subject to LPS that may act as a toxin. In humans, an over-exposure to LPS leads to a condition known as septic shock, which is caused by an overwhelming secretion of cytokines, as a result of systemic bacterial infection or sepsis.

A detailed structure of LPS is illustrated in Figure 1.3.5.1. Lipid A is the lipid component of LPS which contains the hydrophobic, membrane-anchoring region. Lipid A consists of a phosphorylated *N*-acetylglucosamine dimer with 6 to 7 saturated fatty acid chains attached. The core antigen or polysaccharide of LPS is attached to the sixth position of the *N*-acetylglucosamine and consists of a short chain of sugars. The O antigen is attached to the core antigen and consists of repeating oligosaccharide subunits made up of 3 to 5 sugars. The individual chains can be up to 40 repeat units in length. Moreover, the O antigen is much longer than the core antigen and is responsible for maintaining the hydrophilic domain of the LPS molecule. There is considerable variation in the composition of the sugars in the O antigen between species and strains of gram-negative bacteria and at least 20 different sugars are known to occur (Lerouge and Vanderleyden, 2002).

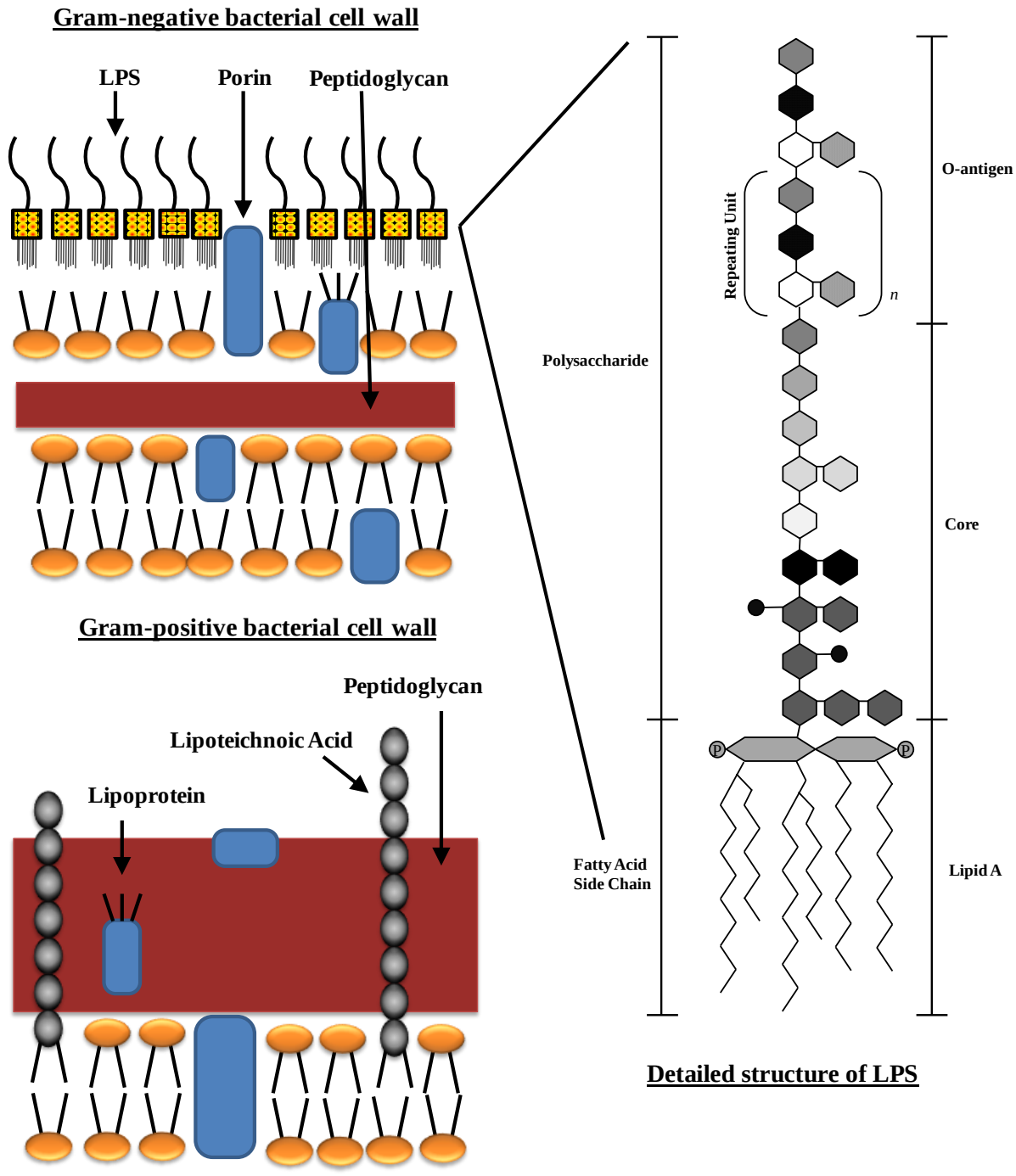

Figure 1.3.5.1: Schematic representation of bacterial cell walls of gram-positive and gram-negative bacteria. Gram negative cell walls are characterised by the presence of LPS, while gram-positive cell walls are characterised by a thick layer of peptidoglycan. A detailed structure of LPS is illustrated, containing the characteristic O-antigen, core and lipid A portions.

1.3.5.1 'Toll-like' receptor (TLR) family

It has been well established that 'toll-like' receptors (TLRs) represent a first line of defence against invading pathogens in mammals, plants and insects (Akira and Takeda, 2004; Kumar *et al*., 2011). TLRs are evolutionarily conserved from the worm *Caenorhabditis elegans*. Toll, one of the first members discovered of the TLR superfamily, was identified as a gene essential for the development of embryonic dorsoventral polarity in *Drosophilia*. TLRs are type I integral membrane glycoproteins. Recognition of microbial components by these receptors triggers the innate immune response and will eventually lead to the expression of inflammatory genes and clearance of the infection. Lipids, carbohydrates and nucleic acids are among the PAMPs recognised by TLRs (Table 1.3.5.1). TLR receptors are evolved to distinguish between different PAMP structures. However, this recognition is one of the most complex and undefined areas of TLR signalling (Hopkins and Sriskandan, 2005; Ostuni *et al*., 2010). Eleven TLRs have been identified in humans, while 13 have been discovered, to date, in the mouse genome. TLRs 1-9 are conserved between these species.

The TLR receptors all share a cytosolic TIR (Toll/ Interleukin-1 receptor) domain, which is also found in the Interleukin-1 receptor family, and an extracellular 'leucine-rich' repeat (LRR), which functions in microbial recognition. The LRR domains are composed of 19-25 tandem LRR motifs, each of which is 25-29 amino acids in length, containing the motif XLXXLXLXX, as well as other conserved amino acid residues. Each LRR contains a β-strand and an α-helix, connected by loops. It has been suggested that the LRR motif forms a horseshoe structure, with the ligand binding on the concave surface (Bell *et al*., 2005). TLR1, TLR2, TLR4, TLR5 and TLR6 are all localised on the plasma membrane, whereas, TLR3, TLR7, TLR8 and TLR9 are preferentially expressed in intracellular compartments, such as endosomes. Based on their structural characteristics, TLRs can be further subdivided into subfamilies which recognise different PAMPs; TLR1, TLR2 and TLR6 bind lipids, whereas TLR7, TLR8 and TLR9 bind nucleic acids (Table 1.3.5.1). However, some TLRs are capable of binding structurally diverse ligands. For example, TLR4 can recognise the lipopolysaccharide, LPS, the viral protein, RSV, fibronectin and heat shock proteins. TLRs are expressed on a number of different immune cell types, including

macrophages, dendritic cells, B-cells, some types of T-cells and non-immune cells, including fibroblasts and epithelial cells. Expression of TLR is constantly changing in response to different pathogenic stimuli, cytokines and environmental stimuli.

TLR2 recognises a wide variety of microbial components including lipoproteins from various pathogens, peptidoglycan from gram-positive bacteria, glycophosphatidylinositol (GPI) anchors from malaria-causing parasites, zymosan from fungi and forms of LPS that are structurally distinct from those recognised by TLR4 (Figure 1.3.5.2). TLR2 is able to recognise a wide range of compounds because of its inherent ability to form heterodimers with other TLRs, namely TLR1 and TLR6. TLR1:TLR2 association allows for the recognition of triacyl lipopeptides, whereas TLR2:TLR6 heterodimers recognise diacyl lipopeptides.

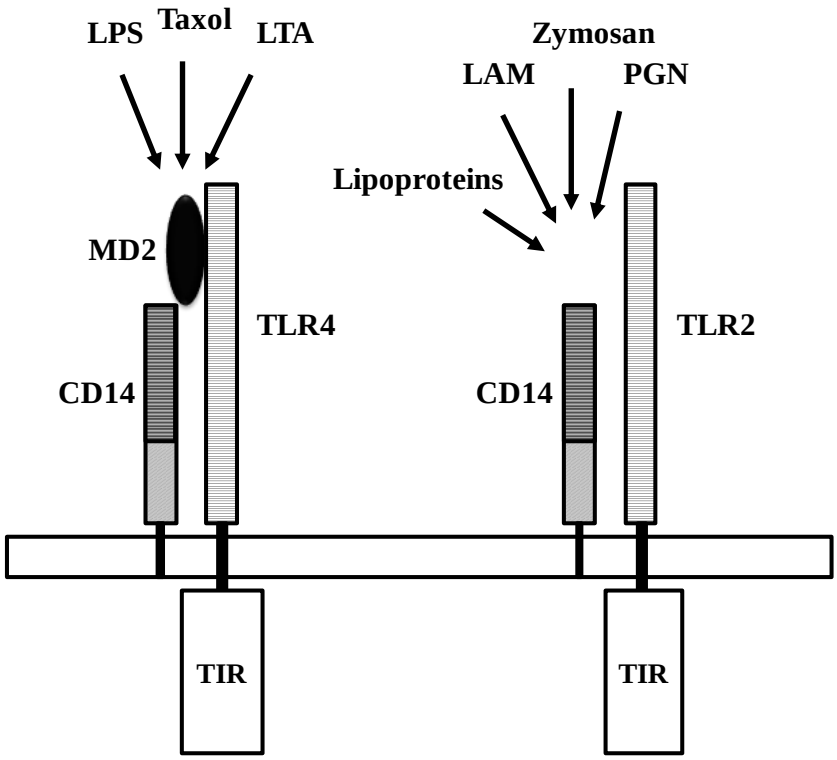

Figure 1.3.5.2: Putative ligands for TLR receptors. TLR4 is required for the signaling of LPS from Gram-negative bacteria, LTA from Gram-positive bacteria and taxol. In contrast, TLR2 recognises PGN, zymosan, LAM and lipoproteins from various bacteria (Adapted from Takeuchi *et al*., 2001).

Table 1.3.5.1: TLR receptors and ligands (Adapted from Hopkins and Sriskandan, 2005)

'Toll-like' Receptor	Ligand
TLR1	Soluble bacterial factors: Triacyl Lipopeptides (*Mycobacteria, Neisseria* and *Borrelia*)
TLR2	Bacterial: Diacyl Lipopeptides (*Mycoplasma*), PGN, LTA, porins, LPS (*Pseudomonas, Helicobacter*) Fungal: Zymosan Viral: HCV core, NS3 proteins, measles virus, human CMV, HSV-1 Endogenous: HSP60 and 70, Cys3Pam, defensins
TLR3	Viral: dsRNA Synthetic: Poly (I:C), siRNA, shRNA
TLR4 (with CD14 and MD-2)	Bacterial: LPS (Gram-negative bacteria), Lipotechnoic acid (Gram-positive bacteria), *Pseudomonas* exoS, *C. Pneumonia, H. pylori* HSP60 Viral: Virus envelope proteins (RSC, MMTV) Endogenous: Fibrinogen, HSP70, heparin, hyaluronic acid Synthetic: Taxol, MPL (LPS mimetic)
TLR5	Bacterial: Flagellin Synthetic: Discontinous 13 amino acid peptide
TLR6	Diacyl lipopeptides (Mycoplasma)
TLR7	Viral: ssRNA (e.g. influenza, HIV) Synthetic: Imidazoquinolines
TLR8	DNA: G-rich oligonucleotides Viral: ssRNA (e.g. influenza, HIV) Synthetic: Imidazoquinolines
TLR9	Bacterial and viral DNA (HSV, CMV), Unmethylated CpG DNA

Cell surface receptors, including TLR receptors, utilise membrane-spanning hydrophobic residues to interact with the plasma membrane. There are a number of key co-receptors that are essential for TLR signaling, including CD14 and CD40. It has also been demonstrated that surface receptors can utilise GPI-based glycolipids e.g. CD14 for anchoring to the cell membrane. CD14 is relevant to macrophage immune recognition and is mainly expressed on cells of a myeloid lineage, including monocytes, macrophages and granulocytes and is also expressed on other cell types, including B-cells, liver parenchymal cells and fibroblasts. Various ligands for CD14 have been identified, including LTA (lipotechnoic acid), PGN and apoptotic cells (Schütt, 1999). CD14 does not have a transmembrane domain, accessory molecules or co-receptors, including TLR2 and TLR4 are essential for signal transduction (Triantafilou and Triantafilou, 2002). CD14 can be present as a soluble form (sCD14) or a glycosylphosphatidylinositol (GPI)-linked form (mCD14). TNF-α and LPS induce the secretion of sCD14, whereas IL-4 and IFN-γ inhibit it. In cases of septic shock, increased levels of sCD14 in serum correlate with increased mortality.

The accessory molecule, CD40, is expressed on a number of different cell types, including antigen-presenting cells (APC), such as B-cells, macrophages and dendritic cells. The CD40 ligand, CD154, is primarily found on activated CD4+ T-cells. CD40 is a co-stimulatory molecule that has an important role in the regulation of antigen-presentation. Binding of CD154 to CD40 on dendritic cells and macrophages causes T-cell expansion and macrophage activation. LPS is known to up-regulate CD40 on dendritic cells and it has been suggested that CD40 signalling regulates TLR4 and MD-2 expression and function (Frleta *et al*., 2003). MD-2 is a protein involved in binding LPS with TLR4. Binding of the MD/ LPS complex to CD40 on monocytes and macrophages results in an increased expression of pro-inflammatory cytokines including IL-1α and IL-1β, TNF-α, IL-6, IL-12, as well as chemokines, including IL-8. CD40 stimulation has additional effector functions, including the expression of matrix metalloproteinases and production of nitric oxide (NO). Matrix metalloproteinases are involved in the degradation of extracellular matrix proteins, the cleavage of surface receptors, cytokine/ chemokine release, and the release of apoptotic ligands. Overall, stimulation of CD40 directs macrophages, monocytes and dendritic cells to a phenotype which promotes antigen presentation and pro-inflammatory activation.

1.3.5.2 'Nod-like' receptors and inflammasome activation

For mammalian hosts to survive infection, the immune system must recruit an arsenal of defence mechanisms to combat invading microorganism, which has been widely discussed thus far in Section 1.3. It has now been widely demonstrated that in addition to sensing microbial components, PRRs have a key role in sensing endogenous products or danger signals, referred to as danger-associated molecular patterns (DAMPs), which are released from damaged or dying cells (Kono and Rock, 2008). Damaged cells release endogenous signalling molecules, including nucleic acid, ATP and uric acid crystals, which trigger the same responses as those produced during microbial detection by the innate immune system. These responses can however be detrimental to the host and often cause an inflammatory response. This is evident in the case of 'nod-like' receptors (NLRs), particularly the NLRP3 inflammasome. Numerous microbial components, including LPS, single-stranded RNA, peptidoglycans and CPG DNA have been identified as activators of the NLRP3 inflammasome (Kanneganti *et al*., 2006; Kanneganti *et al*., 2007).

The NLRs are cytosolic receptors which regulate production of pro-inflammatory cytokines, including interleukins, IL-1β and IL-18. IL-1β is produced by many immune cell types and is a key mediator of systemic and local response to infection and immunological challenge by generating fever, activating lymphocytes and promoting translocation to sites of injury. IL-18 does not possess the pyrogenic activity of IL-1β, but it does induce interferon-γ (IFN-γ) production by activated T-cell and NK cells in the presence of IL-12, thereby contributing to T_H1 polarisation. The production, processing and release of IL-1β are tightly controlled and it requires two distinct levels of stimulation Firstly, pro-IL-1β is accumulated in intracellular stores via transcriptional regulation and released upon stimulation to the mature cytokine, IL-1β. The first is a microbial stimulus, signalled though PRRs, for example TLR4, which results in the accumulation of intracellular pro-IL-1β. The mechanisms controlling the transcription of pro-IL-1β are still not fully known, but NF-κB and mitogen-activated protein kinase (MAPK) signalling have been implicated (Gretten *et al*., 2007; Hedl and Abraham, 2011).

Macrophages are known to secrete IL-1β in response to stimulation with LPS and subsequent treatment with a high concentration of ATP (Ferrari *et al*., 2006). LPS is required both to induce expression of pro-IL-1β and to prime cells for caspase-1 activation in response to ATP. The effect of ATP is mediated by an ionotropic ATP receptor, $P2X_7$, which upon activation, causes a rapid K^+ efflux from the cytosol. Recently, it has been demonstrated that pannexin-1 is required for ATP release during apoptosis but not for inflammasome activation (Qu *et al*., 2011). The ATP-gated $P2X_7$ receptor is an ATP-gated ion channel, responsible for potassium conductance through the cell membrane (Figure 1.3.5.3). ATP-dependent activation of NLRP3 occurs through binding of ATP to the $P2X_7$ receptor, resulting in the opening of a pore via pannexin-1. Pannexin-1 is an ATP-releasing hemi-channel protein, associated with the $P2X_7$ receptor and was also found to be essential for NLRP3 activation by ATP, maitotoxin (a potent marine phycotoxin), nigericin and LPS (Kanneganti *et al*., 2007; Pelgrin and Surprenant, 2007). It was shown that pannexin-1 is essential for caspase-1 activation and IL-1β secretion in LPS-stimulated macrophages pulsed with ATP (Pelegrin and Surprenant, 2006). Potassium ionophores (lipid membrane transporter), $P2X_7$ and pore-forming toxins all induce IL-1β activation and secretion. Therefore, K^+ efflux may be essential for NLRP3 activation.

The second stimulus required for the cleavage of pro-IL-1β involves multi-protein complexes, known as inflammasomes. This dual stimulation may operate to control accidental or un-controlled NLRP3 activation, which could lead to host destruction. The fact that a priming stimulus is required for NLRP3 inflammasome activation suggest that immune cells, including macrophages, require either a signal which indicates the presence of infection via PRR activation or the presence of other pro-inflammatory cytokine-stimulated cells in order to sense danger signals in their environment. Excess IL-1β production has been associated with a number of hereditary disorders, including autoimmune and inflammatory diseases, such as gout and rheumatoid arthritis (McDermott and Tschopp, 2007). Inflammasome signaling was shown to play a key role in the progression of auto-inflammatory and autoimmune diseases, particularly in the pathogenesis of obesity, atherosclerosis, multiple sclerosis and insulin resistance (Lukens *et al*., 2011; Stienstra *et al*., 2011).

Inflammasomes are multi-protein complexes and have an approximate molecular mass of 700 kDa. The main role of the NALP3 inflammasome is to control the activation of the cysteine aspartic acid-specific protease -1 (caspase-1) and to control the cleavage of pro-IL-1β. Caspases are described as apoptotic initiators or effectors and can be divided into two sub-classes, based on substrate specificity; pro-apoptotic and pro-inflammatory. Caspase-1 can be described as pro-inflammatory. The NALP3 inflammasome functions to convert inactive pro-caspase-1 to active caspase-1, which then cleaves inactive cytokine precursors to a secreted and active form. The known substrates that are processed by caspase-1 are the precursors of IL-1β and IL-18. Studies have shown that NALP3 and the adapter protein, ASC are essential for caspase-1-mediated activation in response to bacterial ligands, nucleic acids and synthetic anti-viral components (Kanneganti *et al*., 2006; Sutterwala et al., 2006).

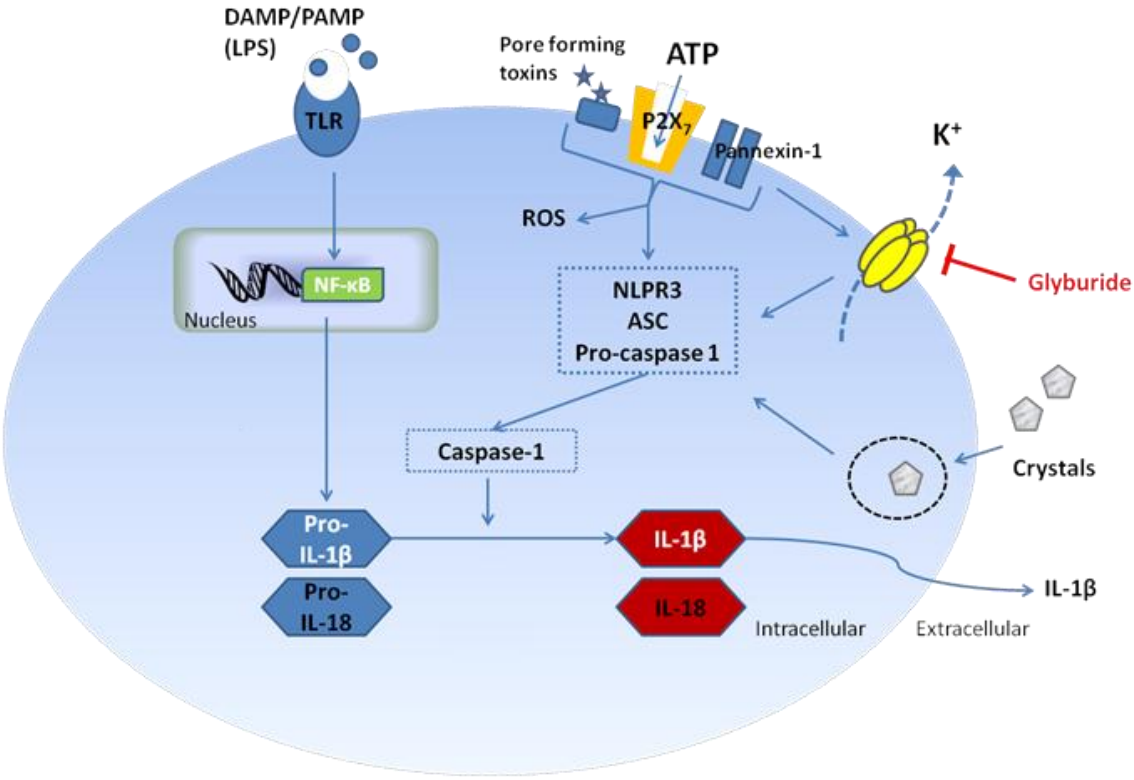

Figure 1.3.5.3: The NLRP3 inflammasome. A priming signal through TLRs activates NF-κB-dependent transcription of pro-IL-1β and pro-IL-18. Pro-IL-1β is cleaved to IL-1β by caspase-1. Caspase-1 is activated by the NLRP3. NLRP3 oligmerises upon activation by danger signals and recruits the adapter ASC, which subsequently recruits and activates caspase-1 (Adapted from Bauernfeind *et al*., 2011).

1.4 Adaptive Immunity

The adaptive immune response consists of two main components, a cellular response mediated by T lymphocytes and a humoral response, mediated by antibodies, produced by B lymphocytes. It takes several days or weeks for the adaptive immune response to take effect and during this period the innate immune response contains the infection. Vertebrates are constantly under threat from invasion against microorganisms and over time have evolved systems of host defence in order to eliminate infectious agents from the body. The acquired or adaptive immune system is involved in the elimination of pathogens in the late phase of infection, as well as in the generation of immunological memory. The role of the adaptive immune response is to produce a specific response to a foreign substance, in the form of immune cells and antibodies, which can specifically interact with them and protect the host from invasion. Acquired immunity is characterised by specificity, which is generated by a complicated clonal selection process from a vast repertoire of lymphocytes bearing antigen-specific receptors generated by gene rearrangement.

1.4.1 Antigen recognition by T-Cell and B-Cell receptors

Adaptive immunity utilises antigen-specific receptors, which are mainly found on lymphocytes, including B-cells and T-cells, to direct effector functions (Pancer and Cooper, 2006; Palm and Medzhitov, 2009). Lymphocytes, or white blood cells, are highly mobile cells which have the ability to migrate from blood into tissue and back into blood (Figure 1.4.1.1). They respond to infection by attacking and destroying the causative agents, or pathogens. They are involved in inflammatory immune responses, innate immune responses and adaptive immune responses. Both T-cells and B-cells originate from progenitor cells in the bone marrow. T-cells mature and migrate to the thymus, whereas B-cells undergo further development in the bone marrow. Antigen specificity is conferred by B-cell receptors (BCRs) or membrane-bound antibodies and T-cell receptors (TCRs) on B-cells and T-cells, respectively. Specificity is attributed to rearrangements of the genes encoding membrane-bound antibodies and TCRs, resulting in a vast repertoire of antigen-binders (Arstila *et al.*, 2000). Naïve lymphocytes enter peripheral lymphoid organs where the

majority of immune responses occur. Each lymphocyte cell bears surface receptors for a single antigen. However, high specificity combined with the huge repertoire of lymphocytes means only a small number of lymphocytes are able to recognise a given antigen.

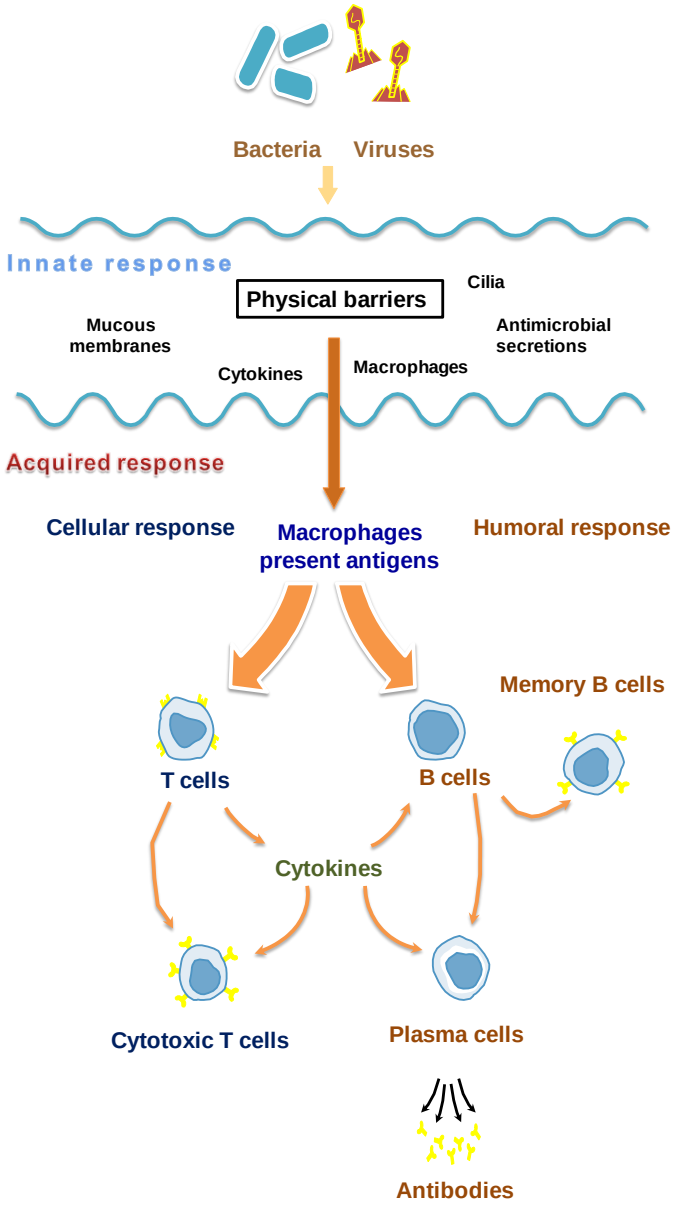

Figure 1.4.1.1: Diagrammatic representation of cellular response to infection. Foreign pathogens, including bacteria and viruses must first penetrate the physical barriers of innate immunity. Through a process of antigen recognition and presentation, innate immune cells, including macrophages, present potential pathogens to the acquired immune system, which mounts a specific cell-based immune response i.e. B- and T-cell development and antibody production.

Major histocompatability complexes (MHCs) play a key role in antigen recognition. To elicit a cellular response to infection, at least two distinct signals are required. The first step is antigen binding to the BCRs and TCRs, in association with CD4 and CD8 co-receptors. The B-cell ingests the antigen-antibody complex, processes the antigen, and in combination with an MHC Class II complex, the antigen is displayed on the B-cell surface. Activated helper T-cells (T_H), which have specific receptors for this antigen, convey the second signal and trigger the production of cytokines. The second set of signals is sent into the cell via co-stimulatory pathways. The most prominent of the co-stimulatory pathways are the CD28/B7 system and the CD40/CD40L signalling pathway. These cytokines bind their receptors on the B-cell, which triggers B-cell differentiation and proliferation.

TCRs recognise short peptide sequences, typically 8 to 15 residues long, which belong to antigens which have been processed and bound to MHC Class II molecules expressed on the surface of antigen-presenting cells. The TCR recognition process differs from BCR antigen recognition since the latter targets entire molecules, either denatured or native forms of proteins or cell-bound carbohydrates. MHC receptors are key in distinguishing self from non-self. Class I MHCs bind peptides derived from molecules encountered in the cytosol and are therefore able to display fragments of viral proteins on the cell surface. Class II members bind peptides from molecules broken down in endosomes and intracellular vesicles and display peptides derived from pathogens resident in macrophage vesicles or internalised by phagocytic cells and B cells.

1.4.2 Humoral immune response and B-cell development

Antibodies are produced by the host's immune system in response to a foreign antigen by B-cell lymphocytes, which play a major role in generating the humoral response of the host immune system (LeBien and Tedder, 2008). Each B-cell is programmed to make a single type of antibody for a particular immunogen. When a B-cell encounters an antigen, a plasma cell is generated, which produces antibodies with specificity and affinity for an epitope on the antigen. B-cells are stimulated to proliferate when they are exposed to the CD40 ligand (CD40L) and interleukin-4 (IL-4), which is produced by activated T_H2 cells

when they recognise their specific ligand on the B-cell surface. Therefore, IL-4 and CD40L cooperate in B-cell proliferation to drive the clonal expansion which precedes antibody production. The TNF receptor family members including CD30, the CD30 ligand and BLyS (B lymphocyte stimulator) and its receptor on B-cells, TACI, are also involved in B-cell stimulation (Kurosaki *et al*., 2010). After several rounds of proliferation, B-cells can further differentiate into antibody-secreting plasma cells. Two additional cytokines, IL-5 and IL-6, both secreted by T_H2 cells, contribute to the later stages of B-cell activation.

1.4.3 Antibody structure and function

Immunoglobulins (IgGs) are natural biological scaffolds with structurally variable antigen-binding domains, which are used by the immune system of higher organisms to mount a humoral immune response. More than 10^8 different antibodies can be in circulation at any one time. Gene rearrangement is used in the production of a primary repertoire of antibodies. Foreign antigens trigger the clonal expansion of naïve B-lymphocytes that express a cognate antibody of low affinity. Rapid and specific affinity maturation is achieved by subjecting the immunoglobulin genes in the B-cells to a period of intense mutation. Due to clonal expansion and affinity maturation, immunoglobulins with highly evolved molecular recognition properties are generated. Affinity maturation is achieved by somatic hypermutation, a mutational process in which single nucleotide substitutions are introduced into rearranged variable (V) gene segments.

Antibodies are large glycoprotein structures with a characteristic 'Y' shape (Figure 1.4.3.1). There are five main antibody classes, designated according to their heavy chain structure (IgG, IgA, IgM, IgD and IgE). All naïve B-cells express cell-surface IgM and IgD prior to isotype switching but little IgD is produced at any time, so the early stages of the antibody response are dominated by IgM. Later, IgG and IgA are the predominant isotypes, with IgE contributing a small but biologically important part of the response. The overall predominance of IgG_1 results from its longer lifetime in the plasma of approximately 21 days. An IgG antibody consists of two heavy chains and two light chains, which are covalently linked by disulfide bonds. In addition to an inter-chain disulfide bond, an IgG

has two intra-chain disulfide bonds. Each light chain has an N-terminal variable domain (V_L) and a constant domain (C_L). Each heavy chain is composed of an N-terminal variable domain (V_H), three constant domains (C_H1- C_H3) and a hinge region. There are 5 classes of heavy chains α, γ, μ, δ, ε, and two classes of light chains, κ and λ. The heavy chains confer different biological functions to a specific isotype and they differ in their size and carbohydrate context. Most species produce both types of light chains, but the ratio of κ to λ varies with the species (Scott and Potter, 1983).

Table 1.4.3.1: Structure and function of IgG components and recombinant fragments.

Structure	Function
scFv molecule	• Smallest recombinant fragment of ~26-27 kDa. • Consists of a complete binding site of the individual heavy and light chain V domains • Connected with a short linker peptide of 10-25 amino acids
Fab molecule	• Recombinant fragment of ~50 kDa with a shortened heavy chain. This heavy chain fragment is referred to as an Fd fragment. • Two domains, V_L-V_H and C_L-C_H1, interact to form the two-chain structure of the Fab molecule, which is further stabilised by a disulfide bridge between C_L and C_H1.
Fragment antigen-binding (Fab fragment)	• Region on an antibody that binds to antigens. • It is composed of one constant and one variable domain of each of the heavy and the light chain.
Fragment-crystallisable region (Fc region)	• Tail region of an antibody that interacts with cell surface receptors called Fc receptors and some proteins of the complement system. • This property allows antibodies to activate the immune system.
Disulphide bridges	• Important for structural determination and conformation • Stabilise the interaction between heavy and light chains
Carbohydrate	• Fc regions of IgG's have a highly conserved *N*-glycosylation site. Glycosylation of the Fc fragment is essential for Fc receptor-mediated activity. The *N*-glycans attached to this site are predominantly core-fucosylated diantennary structures.

Each antibody has only one light chain and heavy chain type, which determine the subclass. The V_H and V_L chain form the antigen-binding site of the molecule. The sequence and structural variation in the variable domains is generally restricted to three short hypervariable loops, known as complementary determining regions (CDRs). The variable domain also consists of a framework region, which is highly conserved. The combination of amino acid residues in the CDRs determines the antibodies ability to recognise a specific antigenic determinant. A number of specific amino acid residues account for the predominant interaction of the antibody with the antigen. These locations are referred to as "hot spots" (Copley *et al*., 1996; Murphy *et al*., 2006).

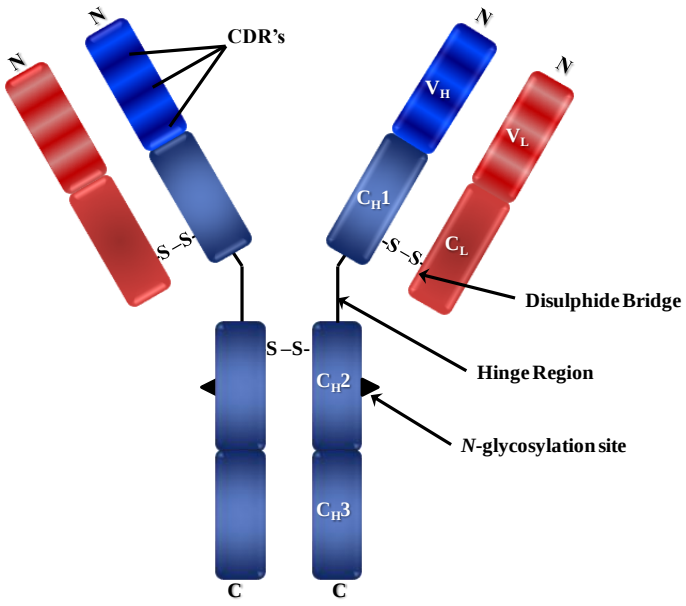

Full Length IgG

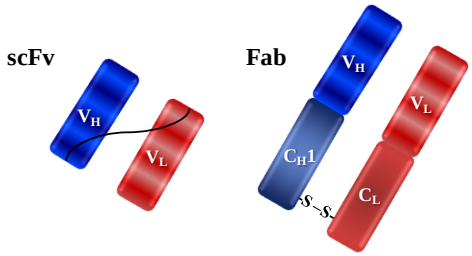

Figure 1.4.3.1: Immunoglobulin formats. Structure of intact immunoglobulin G (IgG) molecule, an scFv molecule and a Fab molecule. Heavy chain domains are represented by blue boxes and light chain domains by red boxes. Variable domains of heavy and light chains are represented by striped blue and red boxes, respectively. S-S represents a disulphide bridge. N and C represent the N and C terminus, respectively.

1.5 Immune response generation

1.5.1 Immunogen preparation for immunisation

The ability of the antigen to generate an immune response depends on its immunogenicity. An antigen capable of generating a humoral or a cell-mediated immune response by itself is known as an immunogen. The immunogenicity of an antigen is conferred by distinctive molecular structural features, recognised as foreign by the host's immune system. These features act as targets for the immune response to produce large numbers of antibodies with varying specificity, whose purpose is to bind the immunogen, rendering it ineffective. However, not all antigens are immunogens. Small molecules or "haptens" are unable to stimulate an immune response unless they are coupled to a larger reactive molecule, known as a carrier (Singh *et al*., 2004). When an immune response is generated against a hapten-carrier molecule, the B-cells will produce antibodies that are specific for both the hapten and the carrier and possibly also to chemical linkers or any combination of the three.

The first step in the successful production of an antibody to a hapten target, involves the careful consideration of a number of key issues including, conjugation strategy and point of attachment, functionalisation of the hapten, choice of carrier molecule, hapten to carrier ratio and purification and characterisation of the conjugate.

1.5.1.1 Conjugate Carriers

The most commonly used carriers are large molecules, which give haptens immunogenicity when they are coupled covalently to them. Examples of carriers include proteins, liposomes, polymers, such as dextran, agarose and poly-L-lysine, or synthetic organic molecules (dendrimers). A good carrier molecule will have suitable immunogenicity, functional groups for conjugation and reasonable solubility, even after derivitisation (Hermanson *et al*., 2008). The most common protein carriers are keyhole limpet haemocyanin (KLH), bovine from serum albumin (BSA), cBSA (cationised BSA), thyroglobulin, ovalbumin (OVA) and toxoid protein, such as tetanus toxoid. cBSA is

prepared by modification of BSAs carboxylate groups with ethylene diamine. This leads to the masking of BSAs native negatively-charged carboxylates and positively charged amines are created in their place. This highly positive charge dramatically increases BSAs immunogenicity by increasing the binding to antigen-presenting cells (APCs) *in vivo*. cBSA conjugates get incorporated by APCs faster and generate quicker immune response with a greater concentration of specific antibody (Muckerheide *et al*., 1987). Thyroglobulin and ovalbumin are widely used as conjugate carriers for antibody characterisation and screening. Table 1.5.1.1 outlines some of the most commonly used carrier proteins, along with details of their molecular weight, structural and stability properties and some requirements for conjugation.

1.5.1.2 Coupling Chemistry

The coupling chemistry used to prepare the immunogen is extremely important for the successful production of an antibody with the desired specificity. The conjugation process is dependent on the functional groups present primarily on the hapten and also on the carrier molecule. The most commonly used linkage involves the formation of an amide bond between a carboxylic acid moiety on the hapten and a primary amino group on the carrier. Usually, the correct functional group is not present on the hapten and needs to be introduced using a derivitisation step or alternatively, a structural analogue of the hapten can be used. As well as introducing a functional group for attachment, this step may also introduce a bridge or spacer arm between the hapten and the carrier. A spacer arm may have the advantage of reducing steric hindrance of the protein molecule on the hapten, allowing the hapten to be easily recognised by circulating lymphocytes. A disadvantage of a coupling molecule or spacer arm is the possibility of generating an antibody response to it.

Table 1.5.1.1: Properties of carrier proteins for conjugation

Carrier Protein	KLH	BSA and cBSA	Thyroglobulin	Ovalbumin
Molecular Weight (Da)	• 4.5×10^5 to 1.3×10^7	• 67,000	• 660,000	• 43,000
Structure	• Large, multi-subunit • At physiological pH, exists in multi-subunit aggregate states	• Presence of numerous carboxylate groups confers BSA with a negative charge	• Large multi-subunit protein composed of several polypeptide chains	• Phosphoprotein containing one *N*-glycosylation site and 386 amino acids
Stability	• Increased immunogenicity and solubility, when dissociated into subunits • Highly stable and soluble in 0.9 M NaCl • Should not be frozen or freeze-thawed	• Cationisation significantly increases pI of protein • DMSO may be added to solubilise hapten molecules • Highly soluble, even after extensive hapten modification	• Acidic pI (4.7) due to presence of multiple carboxylate groups	• Sensitive to temperature (above 56°C), electric fields and vigorous shaking • Extremely soluble in DMSO (70 percent)
Conjugation Requirements	• High salt concentrations required for multi-subunit KLH to preserve solubility	• DMSO may be added to solubilise hapten molecules	• Limited solubility • DMSO may be added to solubilise hapten molecules	• Care should be taken in handling to prevent denaturation and precipitation
Functional Group Availability (per mole)	• 2,000 amines (lysine residues) • 700 sulfhydryls (cysteine groups) • 1,900 tyrosines • 300-600 malemide groups (after SMCC* activation)	• 59 lysine ε-amine groups (35 available) • 1 free cysteine sulfhydryl (17 disulphides buried in structure) • 19 tyrosine phenolate residues • 17 histidine imidazole groups	• Large number of tyrosine residues • Glycosylated; contains 8-10 carbohydrates	• 20 lysine residues • 14 aspartic acids • 33 glutamic acid groups • 20 ε-amine groups, N-terminal amine, 47 side chain carboxylates, C–terminal carboxylate, 4 sulfhydryl groups, 10 tyrosine, 7 histidine groups

* Succinimidyl-4-(*N*-maleimidomethyl) cyclohexane-1-carboxylate
(Data modified from Hermanson, 2008)

A number of coupling strategies have been employed including, carbodiimide-mediated synthesis, NHS-ester mediated synthesis and glutaraldehyde-mediated synthesis. Carbodiimides are short cross-linking agents which react with carboxylate groups for coupling with amine-containing proteins. This results in the formation of an amide or a phosphoamidate linkage between a carboxylate and an amine or a phosphate and an amine, respectively. Hapten-carrier conjugation can also be carried out using homobifunctional reagents, containing NHS ester groups at both ends. The active esters are highly reactive to amines on proteins and form stable amide linkages. Crosslinking agents of various lengths can be used in this method, including sulfo-NHS ester analogs, which are more water soluble. Glutaraldehyde is a homobifunctional crosslinking agent that can be used in a one- or two-step conjugation reaction. It can react with primary amine groups to form Schiff bases or double bond (Michael-type) addition products. Schiff bases can form resonance-stabilised products with α,β-unsaturated aldehydes of the glutaraldehyde polymers, which predominate at basic pH. Reduction of the Schiff base can yield stable secondary amine linkages (Hermanson, 2008).

Another important consideration is designing the conjugation so that the hapten is orientated in the correct manner for proper presentation to the immune system. Landsteiner's principle determines the most suitable point of attachment to link the hapten and carrier molecules (Landsteiner, 1990). This law states that antibody specificity is directly related to the portion of the hapten molecule furthest away from the point of attachment or functional group that is used to link it to the carrier. The part of the hapten closest to the point of attachment is sterically hindered by the carrier protein. Landsteiner's principle also states that the carrier protein should be attached at a site remote from the point of chemical or metabolic activity. Therefore, in carrying out hapten-carrier conjugation, consideration must be given to the reaction group chosen as the point of attachment, in addition to the number of reaction groups that are present on the hapten. This should result in the exposure of the portion of the hapten most desirable for antibody development. Pedersen and colleagues investigated the influence of different conjugation ratios and orientations on antibody affinity and titre to haptens (Pedersen *et al*., 2006). This report showed that differing types of molecular orientation influenced the antibody titre to the immunised molecule. It also appeared that a lower conjugation ratio of peptide to carrier increased the antibody affinity.

1.5.1.3 Purification and characterisation of conjugates

Purification of the crude immunogen is essential for a number of reasons. Firstly, it is necessary to remove excess reagents and un-reacted starting material, which may cause toxicity when injected into an animal, and carrier which may result in a excessive carrier-only response. Purification ensures specificity of the immune response to the targeted epitope or antigenic determinant on the antigen. Secondly, it is essential for any subsequent conjugate characterisation, including determination of the carrier:hapten ratio. The most commonly used methods for purification involves initial dialysis and gel filtration chromatography, such as Sephadex G25, which is efficient at removing non-covalently linked material based on size. If the hapten has a characteristic UV or visible absorbance spectrum that distinguishes it from the carrier protein, this property can be easily used to determine the degree of incorporation to the conjugate. Indirect methods can also be used if the reaction involves lysine ε-amino residues, as the extent of incorporation can be calculated by the degree of free amino groups remaining on the conjugate (Hermanson *et al*., 2008). Two of the main and most widely used methods for conjugate characterisation include nuclear magnetic resonance (NMR) and matrix-assisted laser desorption time of flight mass spectrometry (MALDI-TOF- MS) (Singh *et al*., 2004). These advanced techniques are capable of unequivocally demonstrating effective conjugation. MALDI-TOF-MS has the advantage of also providing quantitative information on conjugation ratios. Nuclear magnetic resonance (NMR) has the advantage of discriminating between covalently and non-covalently bound hapten.

1.5.2 Hapten and conjugate processing by B-cells

As previously mentioned, most small molecular weight haptens do not provoke a significant immune response in animals. These haptens may be capable of binding cell surface receptors on B-cells and T-cells, but they are incapable of stimulating a B-cell response. Therefore it is necessary to functionalise haptens with large molecular weight carrier molecules to promote immunogenicity. The carrier molecule functions to stimulate T-helper cells, which cooperate with B-cells to provoke a response to the hapten. As shown in Figure 1.5.2.1, one determinant on a protein antigen can behave as a hapten in binding to the B-cell, while other determinants promote a carrier function in recruiting T-helper cells (Janeway *et al*., 2001).

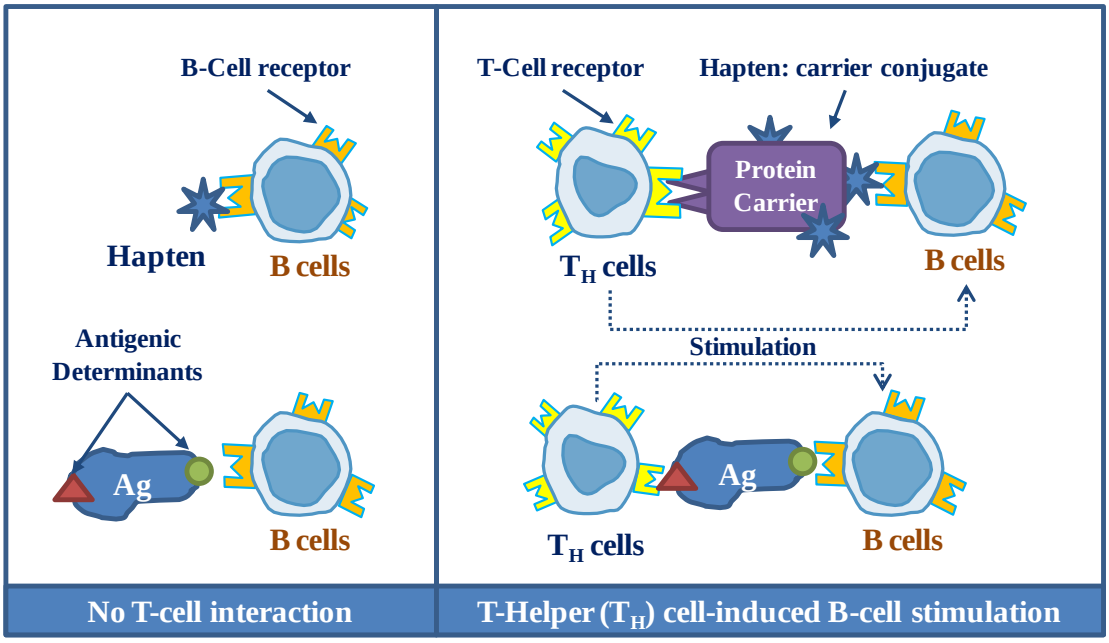

Figure 1.5.2.1: Processing of antigens by B-cells and T_H cells. T-helper cells interact with B-cells through antigenic determinants to aid in the response to a protein antigens and hapten:carrier conjugates by providing signals via accessory receptors and MHC molecules (Adapted from Roitt and Delves, 2001) .

The requirement for a physical linkage between the hapten and large molecular weight protein carrier suggests that T-Helper (T_H) cells must recognise the antigenic determinants of the carrier on the B-cell in order to provide the relevant accessory stimulus. However, T-cells only recognise processed membrane-bound antigen in complex with major histocompatibility complex (MHC) molecules. Therefore, T_H cells cannot recognise native protein antigens or conjugates bound to the B-cell receptors, as depicted in simplified scheme in Figure 1.5.5.1. Protein antigens bound to surface B-cell receptors are internalised to endosomes which fuse with vesicles containing MHC class II molecules. Processing of the protein antigen then occurs and the resulting antigenic peptide is recycled to the surface in association with the MHC class II molecules. These displayed peptides are now available for recognition by specific T_H cells. Significantly, the carrier portion of a hapten:carrier complex causes the hapten to be simultaneously processed for B-cell recognition, leading to the stimulation of T_H cells and the production of anti-hapten antibodies.

1.5.3 Immune response generation and diversification in a leporine host

Rabbit antibodies are widely used in research due to their evolutionary distance of the animal from humans and mice, making them ideal for immune response generation to conserved antigens, otherwise not recognised by rodents. Rabbits also make very suitable hosts for peptides and hapten targets and often exhibit a better immune response, compared to mice and other animals (Rader *et al*., 2000). Unlike rodents and other mammals, the generation of diversity in rabbits does not depend on the use of many variable gene segments. Most B-lymphocytes produce the same V_H gene in the V(D)J rearrangement. The advantage of this for recombinant antibody work is that a relatively small number of primer sets are required, compared to mice and other primates. Li *et al*. (2000) demonstrated that high-affinity scFv fragments could be successfully generated against four different hapten molecules simultaneously, namely the herbicides mecoprop, atrazine, simazine, and isoproturon, from a single immunised rabbit.

Overall, the organisation of rabbit sequences are similar to that of humans and mice. The heavy chain locus of rabbits contains a single gene for the constant region of IgG and multiple copies of genes for the constant region of IgA (Mage *et al.*, 1999). Combinational diversity is limited in rabbits, as only approximately 100 V_H genes are known to be rearranged. The main diversification of the primary antibody repertoire is a result of somatic hypermutation and gene conversion-like changes of re-arranged V_H in B-cells, which migrate to the appendix and other gut-associated lymphoid tissues (GALT) in young rabbits. The rabbit GALT is seen as the mammalian equivalent for the Bursa of Fabricus in chickens. Most rabbit B-cell development, including rearrangement and diversification of V genes, occurs early in life. However, some B-cells in adult rabbits have rearranged V_H sequences that are identical or near-identical to germ line sequences. Also, in rabbit C_H rearrangement, there is a preference for expansion of B-lymphocytes that utilise V_H1, the first gene in the locus, that is nearest to the D_H and J_H genes (Knight, 1992). This limited diversity means that less primers are used in the amplification of rabbit V_H genes. There are a three allelic allotypes of the V_H1 gene, namley a1, a2 and a3 (Figure 1.5.6.1).

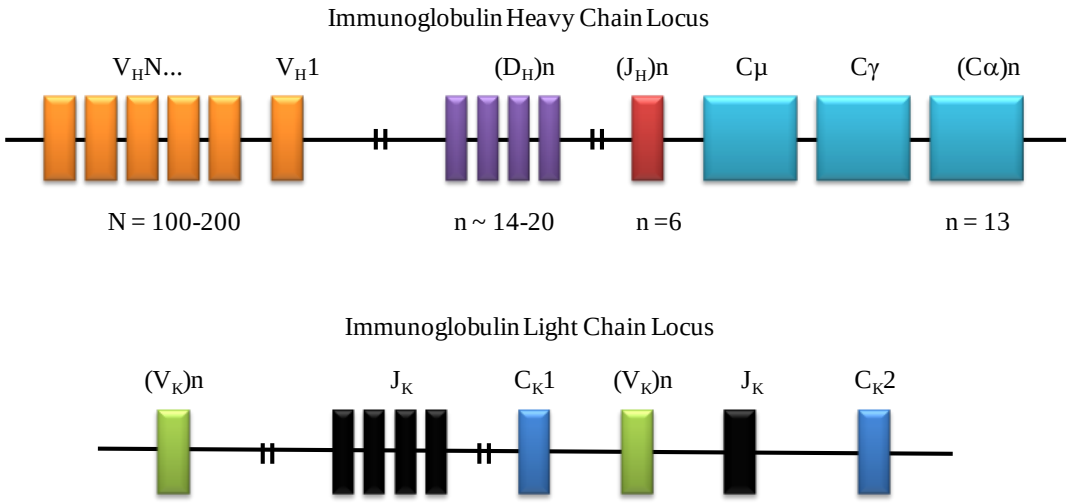

Figure 1.5.3.1: Development of rabbit B lymphocyte repertoire (Adapted from Mage *et al.*, 1999). There are multiple allelic forms of the V_H1 gene, known as the V_Ha allotypes (a1, a2 and a3). There are multiple allelic allotypic forms of the rabbit kappa light chain (b4, b5, b6, and b9) due to many amino acid differences in the constant regions.

The rabbit kappa light chain has four different variants (b4, b5, b6 and b9), due to amino acid substitutions in the constant regions. At some point in evolution of the rabbit ancestor, a duplication in the kappa locus occured, leading to two variants kappa 1, the major expressed type and kappa 2, the minor expressed type (Popkov *et al.*, 2003). More diversity in the immune repertoire is contributed from the kappa light chain regions compared to the heavy chain regions. This is due to the presence of the two variants of the kappa locus and also due to germline V_K-encoded variability in the length of complementarity determining region 3 (LCDR3) (Mage *et al.*, 2006). Although, antibody diversity generated by V_HDJ_H rearrangements in rabbits is much more restricted than in mice or humans, a significant amount of diversity is obtained from V_KJ_K rearrangements. The unique diversification and gene rearrangement features of the rabbit make it an excellent choice for recombinant antibody development as it combines high specificity with high avidity and affinity.

1.5.4 Immune response generation and diversification in an avian host

Chickens or *Gallus gallus domesticus* are phylogenetically more distant from other mammalian laboratory animals, such as mice and rabbits. Therefore, the use of chickens is especially beneficial when generating recombinant antibodies to protein targets. This

is especially true for mammalian targets, as they are recognised as foreign by the avian immune system, thus generating a greater immune response. Birds and mammals originated from a common reptilian ancestor and have evolved common immunological systems. The bursa of Fabricus, a sac-like structure attached to the proctodeal region of the bird's cloaca (posterior opening) has been shown to be essential for antibody-mediated immunity. In addition, the avian thymus has a role in cell-mediated immunity (Davison, 2008). The mammalian equivalent for the bursa of Fabricus is the bone marrow, were B– and T-cell development occurs simultaneously. The division of the adaptive immune response into B- and T- cell classes, originated from the early study of avian immunology, where the physical separation of antibody-mediated and cell-based immunity, allowed for a clear understanding of the functionality of the immune response. The term B-lymphocyte is derived from "bursa-derived lymphocyte" in honour of the originally investigated avian lymphoid structure.

In humans and mice, the antibody repertoire of B-cells is produced by a process known as Ig gene rearrangement. Unlike humans and mice, the V_L and J_L genes in the antibody light chain sequences of chickens only have a single functional copy. Therefore, diversity due to V_LJ_L linking is very limited and the effect of V_J rearrangement is minimal (Ratcliffe, 2008). Little diversity is generated by the antibody heavy chain locus as only single functional copies of the V_H and J_H genes are present to generate the V_HDJ_H rearrangement. Clusters of pseudogenes upstream of the heavy and light chain Ig loci have a critical role to play in the generation of chicken antibody diversity. Pseudogenes are sequences of nucleotides that probably once were functional but have lost the ability to produce a gene product, because they lack the necessary promoter and leader sequences. Upstream of the functional variable gene sequences, 80-100 V_H pseudogenes are present in the IgH locus and 26 V_L pseudogenes are present in the V_L locus (McCormack *et al*., 1991). There are approximately 16 D_H sequences present in the IgH locus. An illustration of the development of diversity in the avian immune system is shown in Figure 1.5.4.1.

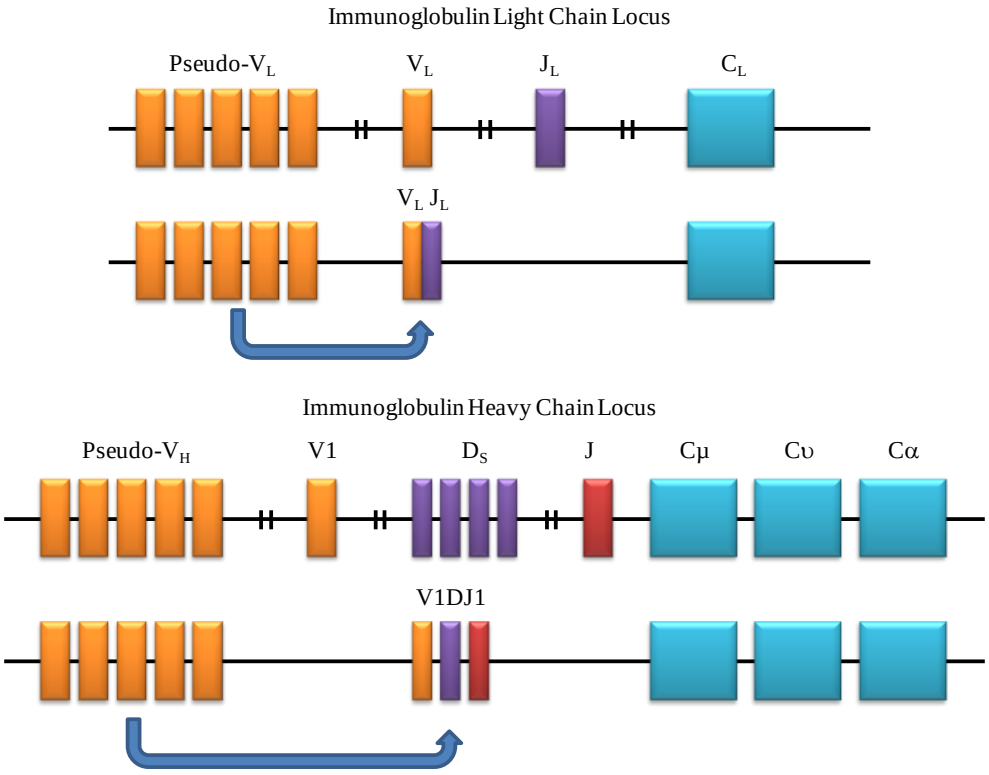

Figure 1.5.4.1: Development of avian B-lymphocyte repertoire (Adapted from Fellah *et al*., 2008). The chicken Ig light chain and heavy chain loci only carry a single functional variable gene (V_L and V1 for the heavy chain) downstream from a cluster of pseudo-genes. Between the two loci, there are unique J_L and J_H sequences. Approximately 15 functional D elements are present on the IgH locus. The 3' ends of the heavy and light chain loci contain the constant (C) regions.

In the process of somatic gene conversion in chickens, which solely occurs in the bursa of Fabricus, V_H and V_L gene sequences are replaced with pseudogene sequences. This process creates a high rate of diversity, as there is already substantial diversity in the hypervariable regions of the donor V pseudogenes. Therefore, somatic gene conversions can accumulate within single functional V_H and V_L genes. Chicken sequences have the unique ability to undergo somatic gene conversion to generate a large antibody repertoire, which is comparable to the repertoires of mammals that possess multiple functional copies of the V_H and V_L genes (Davison, 2008). In chicken, somatic gene conversion occurs continuously from the late embryonic stage and a mature antibody repertoire is formed at around 5-7 weeks, when the bursa is fully developed (Tizard, 2002).

1.6 Recombinant antibody library generation

Recombinant antibodies, generated through phage display and bio-panning against a target of interest (Bradbury and Marks, 2004, Hoogenboom *et al*., 2005) have been utilised for the detection of a range of structurally diverse antigens, including haptens (Byrne *et al*., 2009), cell surface markers (Marty *et al*., 2006) and proteins (Tully *et al*., 2008). Four types of libraries may be used as sources of antibody pools, synthetic, semi-synthetic, naïve and immune. Synthetic and naïve antibody libraries are non-immune sources, derived from natural, rearranged V genes. Naïve libraries, consisting of the variable region repertoires can be generated from collections of variable genes from the IgM/IgG messenger RNA (mRNA) of B-cells of non-immunised human donors, isolated from peripheral blood lymphocytes, tonsils, bone marrow and spleen cells. Polymerase chain reaction (PCR) using specific primer sets are used to amplify variable regions from IgM and IgG mRNA and these regions are cloned into selection and screening vectors (Barbas *et al*., 1992).

An ideal naïve library should contain a representative sample of the primary repertoire of immune systems, although it lacks antibodies with somatic hypermutations produced by natural immunisation. Therefore, naïve libraries often yield antibodies with low affinity, as they have not undergone somatic mutation or affinity maturation. Synthetic libraries are produced by PCR-based randomisation of complementarity-determining regions (CDR) from heavy and light chains. CDRs are modified by pre-determined levels of mutagenesis. These repertoires are cloned into an antibody domain framework and are sub-cloned into a phage display vector to generate a library of $10^7 – 10^{10}$ clones. Semi-synthetic libraries can also be created using combinations of natural and synthetic sources by selecting one or more antibody frameworks within the CDR loops. The CDR loops can be partially or completely randomised using oligonucleotide primers. A high level of diversity in composition and length can be achieved, particularly in the CDRH3 domain, which significantly contributes to antigen binding (Johnson and Wu, 1998).

Immune libraries are constructed from RNA isolated from splenocytes or the bone marrow of a host (avian, murine, leporine etc.) immunised with an antigen that generates a specific immune response. Immune libraries do not need to be as large as non-immune libraries; 10^{6-7} unique and functional scFv clones are sufficient. Antibody

fragments isolated from immune libraries will generally be highly specific and have a high affinity, due to affinity maturation in the host. The RNA is converted into complementary DNA (cDNA), which in turn serves as a template for the amplification of variable heavy (V_H) and variable light (V_L) gene sequences. These are fused through an overlapping-extension splicing PCR reaction and subsequently cloned into a suitable phage or phagemid vector. The introduction of this construct into suppressor strains of *Escherichia coli* (*E. coli*) by electroporation, in conjunction with the packaging of phage particles via the addition of helper phage (a process referred to as rescuing), allows the encoded antibody structure to be 'presented' on the exterior of a bacteriophage particle. In the phage display technique, the scFv fragments encoded by the antibody library are expressed as fusion partners of a coat protein, pIII, on the surface of the phage molecule (See Figure 1.6.1).

E. coli is the best choice as host because of its ease of use in transformation and manipulation. A number of alternative host options are also available, including mammalian, yeast and insect (Verma *et al.*, 1998). A tight control over transcription is essential for efficient expression of antibody fragments. The lac promoter system is the most commonly used, as it can be readily induced with isopropyl-beta-D-thiogalactopyranoside (IPTG) and repressed by glucose, if necessary. Bacterially-expressed protein can be isolated from a number of locations, including the cytoplasm, the periplasm and the culture supernatant. Proteins with no signal sequence are expressed in the cytoplasm and are known to form aggregates of insoluble protein or inclusion bodies, which produces a low expression yield. With the inclusion of an *N*-terminal signal sequence, the antibody fragment can be exported to the bacterial periplasm (Tudyka and Skerra, 1997). In the periplasmic space, the antibody fragment can fold correctly, remain soluble and form intra-domain disulphide bonds, which is only possible in the oxidation environment of the periplasm.

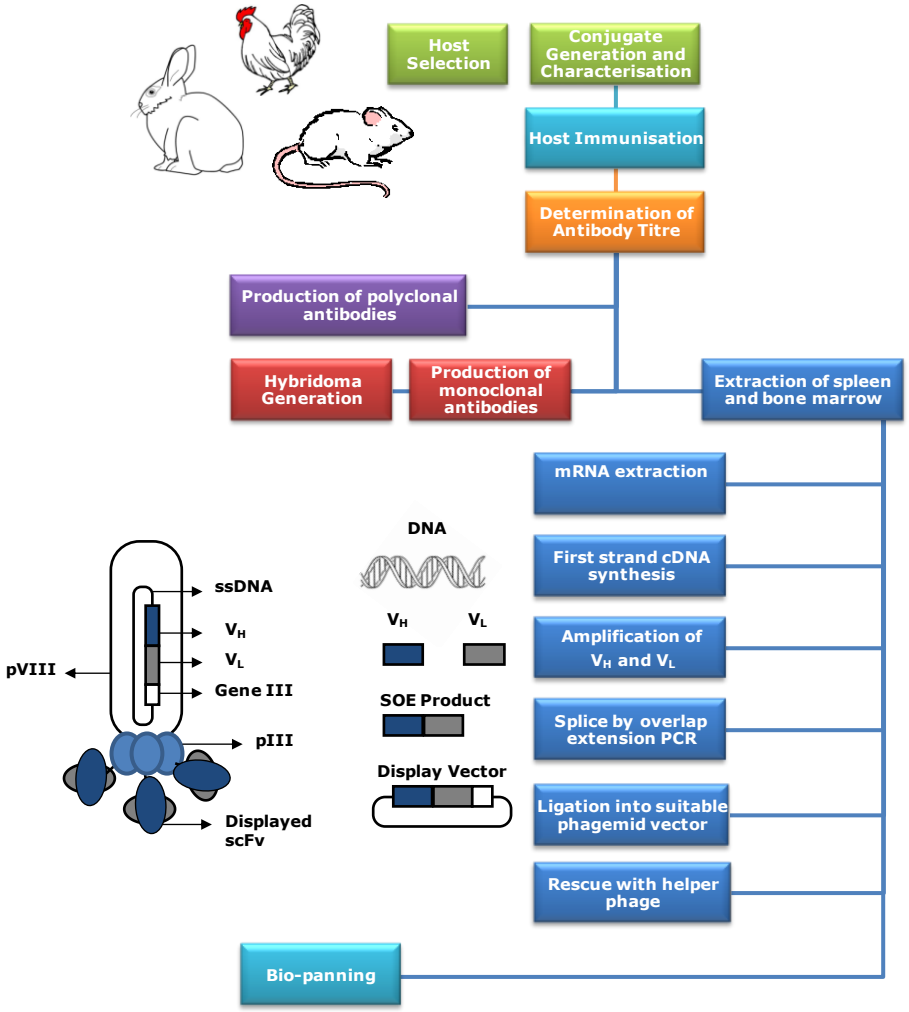

Figure 1.6.1: Overview of antibody generation strategies. Polyclonal antibodies can be isolated from immune serum and monoclonal antibodies can be generated using hybridoma technology. In recombinant antibody generation, the genetic material is harvested from the host's lymphoid organs (spleen and bone marrow). The immune library can be displayed on the surface of filamentous phage and screened using bio-panning.

The linker between the variable region domains has to be long enough to span the distance from the C-terminal of one domain to the N-terminal of the second domain. It has been reported that longer linkers can increase antibody affinity and decrease the formation of aggregrates. (Whitlow *et al.*, 2003). The linker can affect domain orientation, which influences the conformation and affinity of the binding site. The extent of scFv multimerisation is also determined by linker structure and length. The $((Gly)^4Ser)^3$ linker was designed so that the glycine residues conferred the inherent flexibility of peptide bonds, while the serine residues provided hydrophilicity. A

number of advances involving both rational and evolutionary approaches have made it possible to produce scFv fragments with improved affinity and stability (Jermutus *et al*., 2001; Wörn and Plückthun, 2001). Fragment antigen binding (Fab) antibodies are heterodimer structures containing an antibody light chain and the VH and the CH1 domains of the heavy chain. In general, Fabs are difficult to assemble, have lower yields as soluble fragments and are more likely to be unstable in phage, due to the fact that Fabs have two protein chains (Barbas *et al*., 2001). Fabs also have a number of advantages; they do not undergo dimerisation, they are more stable and can be converted into full length IgG (Guo *et al*., 1997).

1.6.1 Display Techniques

The development of advanced display techniques has allowed the screening of large antibody libraries, leading to selection of an antibody with a desirable trait, for example in affinity antibody selection. Display techniques include bacterial (Daugherty *et al*., 2007), yeast (Feldhaus and Siegel, 2004; Gai and Wittrup, 2007), mRNA (Gold, 2001; Fukuda *et al*., 2006), phage and ribosomal display. The choice of selection technology for a given antibody depends on a number of different parameters, including the diversity of the library, the properties of antigen and the intended use. It is desirable to have combinational libraries with the maximum functional diversity to increase the possibility of finding molecules with the desired function (Benhar *et al*., 2007).

1.6.1.1 Phage Display

Phage display, first described by Smith (1985), was the first molecular diversity selection platform and the forerunner of all subsequent molecular diversity techniques (Figure 1.6.1.1). Filamentous phage and phagemid (M13, f1 and fd) are the most commonly used for phage display, although T7 and lambda have also been used. McCafferty *et al*. (1990) was the first to use phage display to isolate antibodies from a large naïve library. Phage selection involves repeated rounds of growth, panning, and infection, which selects for binding of antibody fragments that are expressed on phage. Both phage and phagemid vectors can be used for the display of antibodies and other proteins on the surface of filamentous phage. Phage vectors are derived from the phage

genome and contain a phage origin of replication and genes for assembly of phage particles. Phagemid vectors contain a recombinant version of g3p on the plasmid (phagemid), which also contains the packaging signal for Ff phage. Phagemids contain both phage and phagemid origins of replication, but do not contain an antibiotic resistance gene. The phagemid will produce large amounts of the recombinant display protein, but it is unable to produce phage without the assistance of helper phage, such as M13K07 and VCSM13, which contain mutated or deleted pIII and a defective packaging signal for phage replication and assembly. The disabled packaging signal does not prevent the helper phage from making phage in bacteria. However, the presence of phagemid, which contains the optimal functional packaging signal, results in the preferential packaging of the phagemid over the helper phage. Overall, phagemid vectors are preferred over phage vectors because of their ease of use, selection of high affinity clones with large diversity and the presence of an amber stop codon for soluble expression (Bradbury and Marks, 2004).

In phage display, the phagemid vector contains the expression genes which encode the phage coat protein to be displayed. Additionally, the 5' end of the pIII protein is required for phage infectivity. It mediates the attachment of the phage to the tip of the F' pilus of *E.coli*. Therefore, to allow infection with helper phage, the amino terminal domain of pIII in the fusion protein expressed by the phagemid vector should be deleted. Otherwise, the phagemid pIII would make the cell immune to super-infection with helper phage. A truncated pIII, consisting of the carboxyl terminal alone serve as a fusion partner for the displayed scFv. This mutant pIII can mediate the incorporation of the fusion protein into the phage coat, without producing immunity to helper phage infection.

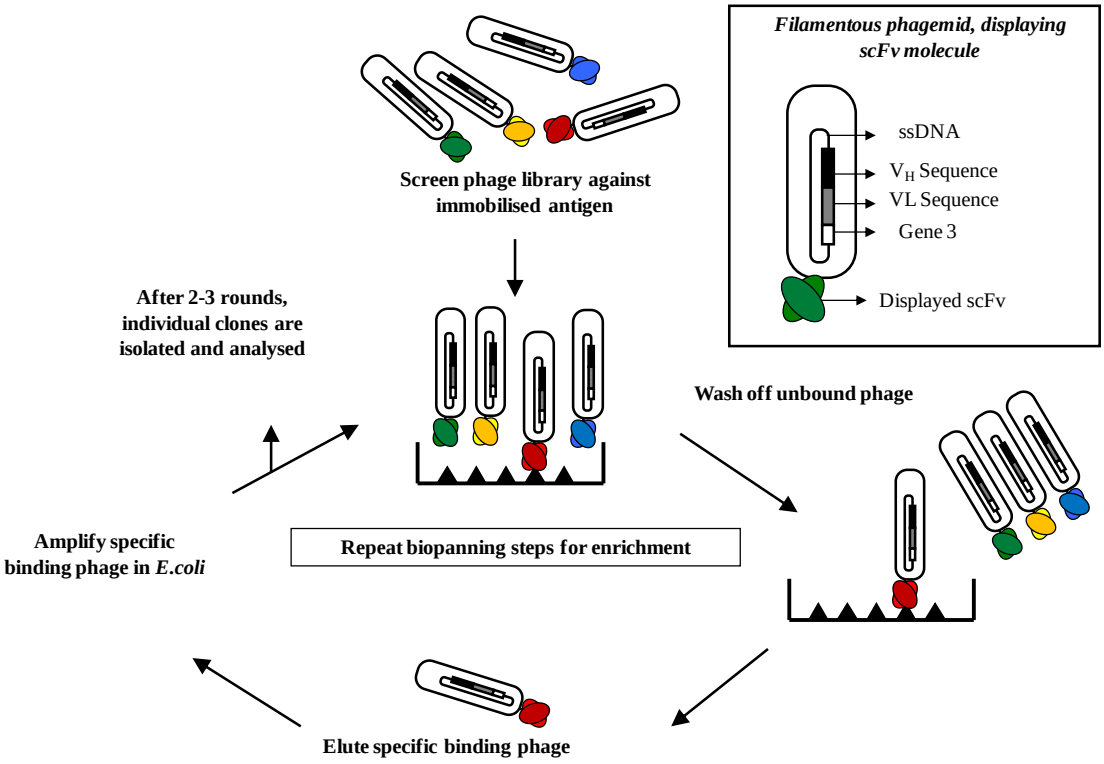

Figure 1.6.1.1: Recombinant antibody phage display. Bio-panning, utilising conjugated antigen, immobilised on solid phase and repeated cycles of enrichment.

Phage display is accomplished by fusing the antibody library to the N-terminus of either the minor coat protein (pIII) or the major coat protein (pVIII) of filamentous bacteriophages. Approximately 2,700 copies of pVIII are displayed per virion, while only 3-5 copies of pIII are displayed. The small number of copies per virion for pIII is used to great advantage for displaying large polypeptides and monovalent display allows for selection of high affinity clones, as avidity is not an issue (Kirsch *et al.*, 2005). pIII is the phage protein involved in bacterial infection and is responsible for binding to the F pilus. It has a tripartite structure consisting of three domains, separated by glycine-rich regions (Lubkowski *et al.*, 1998). Expression of these fusion proteins in bacteria results in the incorporation of the antibody fragment into the mature phage coat, which is then displayed on the phage surface. Importantly, the genetic material that relates to the antibody fragment is still contained within the phage genome. This link between antibody genotype and phenotype allows for isolation of antigen-specific phage antibodies using immobilised antigen in the bio-panning process. Bound phage are eluted, re-infected into bacteria and re-grown for the next round of selection, resulting in enrichment of the phage pool.

Bio-panning (Figure 1.6.1.1) is used for the selection of binders from an antibody library which may contain between 10^7 and 10^{10} different antibody-encoding gene sequences. In bio-panning, the antigen is immobilised onto a solid phase (e.g. on a column or immunotube) or bead-conjugated (in solution phase) and the antibody pool is subjected to recurrent rounds of selection against the antigen with increasing levels of stringency in terms of binding ability. Selected binders are retained and subjected to additional screening to increase their specificity for the target (affinity maturation), which can be monitored by ELISA-based analysis. Following selection, the phage particles can be infected into a non-suppressor strain of *E.coli*, such as Top10F' or HB2151 for soluble expression. These hosts recognise the amber (AUG) codon engineered between the scFv and gIII gene (Hoogenboom *et al*., 1991) producing scFv or Fab fragments independent of the phage coat proteins.

1.6.1.2 Isolation and affinity maturation of toxin-specific antibodies

A number of technological advances have made detection of hazardous toxins and organism faster and more reliable. Nucleic acid and immunosensor-based identification of hazardous microorganisms and their products, including antigens and toxins, have wide applications in testing of food, clinical and environmental samples. In order to develop an effective and applicable detection system for specific identification, the assay system must work on the requisite or 'real' sample. Immunological detection methodologies have been successful in the sensitive detection of bacterial cells, spores, viruses and toxins in the environment (Leonard *et al*., 2003; Byrne *et al*., 2009). Production of polyclonal or monoclonal antibodies requires continuous maintenance of animals or cultures of hybridomas, respectively. For both approaches, the life span of the animal and subsequent maintenance through a course of immunisations and bleedings is costly and time-consuming. Phage display has proven invaluable in selecting high affinity antibodies specific for toxins. Current detection methodologies for biological threats, including the use of phage display for toxin biosensors, have been widely reviewed (Iqbal *et al*., 2000; Petrenko and Vodyanoy, 2003; Petrenko and Sorokulova, 2004).

For example, mRNA from mice immunised with botulinum neurotoxin was employed in the successful generation of a recombinant antibody library with a repertoire of

binding specificities. The combinatorial library was biopanned to select and isolate phage displayed antibodies that specifically recognised botulinum neurotoxin (Emanuel *et al*., 1996). These recombinant antibodies demonstrated a high affinity to the neurotoxin (0.9 –7 nM) and were superior to the related monoclonal antibody when analysed by surface plasmon resonance, flow cytometry, enzyme-linked immunosorbent assay (ELISA) and immunochromatographic assay (Emanuel *et al*., 2000). Phage display was also used to isolate anti-botulinum toxin scFvs with affinities in the nanomolar range from very large non-immune human library (Sheets *et al*., 1998).

A commercially available phage peptide library (NEB) was employed to isolate phage specific for anthrax toxin and staphylococcal enterotoxin B (SEB), a toxin associated with food poisoning, (Goldman *et al*., 2000; Mourez *et al*., 2001, respectively). This combinational library consists of random peptides (12-mer) fused to the minor coat protein (pIII) of M13 phage. Mourez *et al*. (2001) panned the library on a cleaved heptamer of protective antigen (PA), which is responsible for binding and internalisation of the two different forms of anthrax toxin, lethal toxin and edema toxin. They subtractively panned on intact PA to avoid peptides that recognised the unprocessed protein. Goldman *et al*. (2000) labelled the phage particles, expressing the 12-mer of an anti-SEB clone, with fluorescent tags and incorporated it into an immunofluorescence assay using the RAPTOR fiber-optic biosensor. Moghaddam *et al*. (2001) screened two phage antibody libraries, including a human lymphocyte antibody library and the semi-synthetic antibody library, against aflatoxin B_1, conjugated to BSA and soluble aflatoxin B_1. The isolated scFvs were specific for the conjugate molecule and were unable to bind soluble aflatoxin B_1. A variation in the elution strategy, involving a switch from triethylamine elution to competitive elution with free aflatoxin B_1 for 16 hours, resulted in the isolation of scFv with specific binding to soluble aflatoxin B_1 with high affinity. Ma *et al*. (2006) constructed a number of cyclic peptide libraries, where the random amino acid sequences were surrounded by cysteine residues, which formed disulfide loops. These libraries were biopanned against *Clostridium botulinum* neurotoxin, resulting in the isolation of a single clone specific for neurotoxin A, while not binding other botulinum neurotoxins. Although recombinant antibody technology has allowed for the isolation of antibodies to almost any type of antigen, it remains difficult to obtain high affinity antibodies to certain rare

haptens. Either very large libraries have to be constructed or stringent selection strategies need to be employed, incorporating affinity maturation of isolated antibodies.

1.7 Toxins and their occurrence in nature

1.7.1 Azaspiracid Shellfish Poisoning

Single-celled microalgae or phytoplankton have an important role in the aquatic environment. They provide nourishment for a large quantity of heterotrophic marine animals, including filter-feeding bivalve molluscs such as mussels, clams and scallops. Among the reported 5,000 species of marine phytoplankton, 300 have been shown to occur in high numbers causing algal blooms or 'red-tide' events. Of these 300 species, there are approximately 40 which have been shown to produce potent toxins as secondary metabolites, known as phycotoxins (Sournia *et al*., 1991). Algal blooms occur due to mass proliferation of phytoplankton in localised regions that have become temporarily rich in inorganic nutrients, such as nitrogen, phosphorus and iron. Most algal blooms are harmless, but if a bloom of toxic microalgae occurs, toxins are released to the aquatic marine environment. Blooms of toxic algae are also known as harmful algal blooms or HABs. HABs pose a threat to human health because of their potential to cause respiratory, neurological and gastrointestinal problems, including mortalities, at very low toxin concentrations. They also pose a threat to coastal economies and the shellfish industry. Lengthy port closures due to bloom events, reduced tourist activity and costly monitoring programs all contribute to economic losses.

Phycotoxins include a variety of toxins from different phytoplankton groups. Phycotoxins are low molecular weight, non-proteinaceous compounds. They vary widely in their physical properties, chemical structure and toxic mechanisms. The type of poisoning and, therefore, the phycotoxin groups are classified according to the associated symptoms: paralytic shellfish poisoning (PSP), neurotoxic shellfish poisoning (NSP), amnesic shellfish poisoning (ASP), diarrhetic shellfish poisoning (DSP), and azaspiracid shellfish poisoning (AZP) associated with shellfish; and ciguatera poisoning associated with finfish. Health concerns have been raised around shellfish and fish poisoning which have been caused by different types of phycotoxins. A number of countries have established regulations and specific concentration limits to

monitor the levels of these phycotoxins in seafood (Van Egmond, 2004). AZP will be discussed in detail for the purpose of this research study.

1.7.1.1 Cases and outbreaks of azaspiracid poisoning (AZP)

Azaspiracids (AZAs) were first identified in 1995 in the Netherlands as a result of the consumption of mussels (*Myltilus edulis*) cultivated in Killary Harbour in Ireland (Satake *et al*., 1997). Similar mussel toxicity was recorded in Donegal in 1996, followed by a reoccurrence in 1998 (McMahon and Silke, 1996; 1998). Since these toxic events, AZA was isolated and characterised from shellfish as AZA-1 (Satake *et al*., 1998) and subsequently structurally revised (Nicolaou *et al*., 2006a, b, c). AZA toxin outbreaks have since been identified in several parts of the world. However, the problem poses a major threat to the Irish shellfish industry, due to the re-occurrence of toxin outbreaks. In the past, detection has proven inaccurate due to massive underestimation of AZA concentrations in shellfish with the analytical tests currently in use (EFSA, 2008). Regulatory laboratories, public health laboratories and the aquaculture industry are demanding the ability to monitor for the presence of AZA toxin at very low concentrations. This would mean contaminated beds could be closed long before the toxin concentrations would be high enough to pose significant health threats to the consumer. Extensive studies on AZA have been limited by the poor availability of purified material. Certified reference material (CRM) has now become available in small quantities (Perez *et al*., 2010). Reference materials are simple mixtures, solutions or complex natural materials that have been collected and homogenised to provide a stable, representative matrix for proper evaluation of analytical techniques. Presently, reference standards and reference materials are not available or are in short supply for most toxin groups.

1.7.1.2 Chemical structure and properties of AZP toxin

Symptoms of AZP are closely related to diarrhetic shellfish poisoning (DSP) symptoms and AZP was initially classified as DSP (Satake *et al*., 1997). AZA was subsequently discovered to be a nitrogen-containing polyether toxin with a unique spiral ring assembly, a cyclic amine and a carboxylic acid (Satake *et al*., 1998) with a unique mode

of action (Ito *et al.*, 2000). Therefore, AZP was re-classified into its own group. The structure which was reported in 1998 was found to contain an error, after attempts were made to synthesise the molecule in 2003 (Nicolaou *et al*, 2003 a,b). The product of this synthesis was found to have a different chromatographic pattern and differences in its nuclear magnetic resonance (NMR) spectrum, compared to naturally sourced compound. Further extensive research and analysis by NMR resulted in a revised structure (Nicolaou *et al*., 2006 a,b,c) (Figure 1.7.1.1).

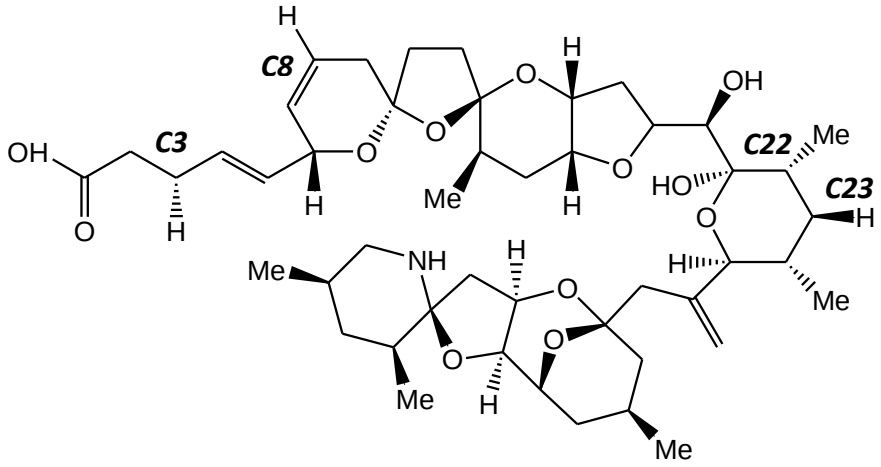

Figure 1.7.1.1: Molecular structure of azaspiracid-1

After the AZA-1 structure had been definitively characterised, four different analogs were identified, isolated and their structure determined using MS and NMR techniques (Ofuji *et al.*, 1999; Ofuji *et al*., 2001). Three of these analogs differ only in the number of methyl groups. In comparison to AZA-1, AZA-3 is lacking the methyl group at C22 and AZA-2 has an additional methyl group at C8 (Figure 1.7.1.1). The other two analogs of the toxin (AZA-4 and AZA-5) are hydroxyl analogs of AZA-3, having an additional OH group at either C3 (AZA-4) or at C23 (AZA-5). Only AZA 1-5 have been preparatively isolated, with their structure confirmed using NMR techniques. Structure elucidation of other analogs has relied on the analysis of fragmentation patterns of their respective MS/MS spectra. To date, 27 analogs to AZA have been identified, as reviewed by Rehmann *et al*. (2008).

1.7.1.3 Source organisms for AZP

One of the major controversies surrounding AZP is the origin of the associated toxin. Studies on the seasonal and episode accumulation of azaspiracid in filter-feeding bivalve molluscs, especially the mussels *Mytilus edulis*, have always suggested a plankton source. Much research has gone into establishing a clear and definitive link between AZA toxins in shellfish and their planktonic source. Structural homology studies between AZA and other lipophilic phycotoxins indicated a dinoflagellate source (Satake *et al*., 1998). The heterotrophic dinoflagellate, *Protoperidinium crassipes* was proposed as the causative organism on the basis of micropipette isolation and pooling of cells, followed by confirmatory analysis by liquid chromatography coupled to mass spectrometry (LC–MS) (James *et al*., 2003). However, surveys carried out by the Irish Marine Institute failed to show any correlation between occurrence of AZA in shellfish and blooms of *P. crassipes* or other Protoperidinium species during a four year monitoring period along the Irish coast (Moran *et al*., 2005). Work in other countries, including Norway and the UK also has failed to support any clear association with this organism. Gribble *et al*. (2007) reported that little correlation between the occurrence of Protoperidinium spp. in plankton and azaspiracids in shellfish existed. Tillmann *et al*. (2009) definitively identified *Azadinium spinosum* spp. as the primary producer of azaspiracid toxins.

1.7.1.4 Occurrence and accumulation of AZP in seafood

Polyether toxins are known to concentrate in the digestive glands or hepatopancreas of shellfish. However, azaspiracid and its methyl- and demethyl-analogues, AZA2 and AZA3, respectively, are not confined to the hepatopancreas but are also distributed throughout shellfish tissues. Toxin profiles for AZA in different mussel tissues have been shown to differ significantly, with AZA-1 as the predominant toxin in digestive glands (James *et al*., 2002a). Mussel digestive glands initially contain most of the azaspiracid content due to grazing on toxic dinoflagellates. However, the transport of AZA to other tissues in the shellfish may cause a prolonged period of shellfish intoxication due to the low rate of natural depuration of AZA. Azaspiracids have shown an unusual solvent distribution during the extraction procedure, leading to the

suggestion that the polar amino acid and the non-polar polyether regions of the molecule confer unique properties to AZA (James *et al*., 2004). This may explain how azaspiracid moved though different polarities and how it can penetrate different tissues of shellfish and mammals.

Detailed global surveys on the bio-geographical distribution of AZA toxins have not been conducted, but AZA contaminated mussels have been found on the east coast of England and along the Norwegian west coast (James *et al*., 2002b). Following its initial identification and confirmation of AZA-1 as the cause of human poisoning events, other cases of intoxication from consumption of mussels from Ireland, France and Italy were also attributed to AZP (Magdalena *et al*., 2003; James *et al*., 2004). The European Commission have set the maximum permitted level of AZP toxins in bivalve molluscs, echinoderms, tunicates and marine gastropods, to 160 µg/kg in 2002.

1.7.1.5 Toxicological studies for AZP

Human consumption of AZA-contaminated shellfish can result in severe acute symptoms that include nausea, vomiting, diarrhoea and stomach cramps. Due to a limited amount of data available for AZP events, most information on AZA toxicity has derived from *in vitro* and *in vivo* toxicological experiments. All symptoms appear within hours of ingestion and persist for 2-3 days. However, little is known about the effects of long term exposure to AZA, as all work has focused on acute effects. Also, given the EU regulatory limit of 160 µg/kg of shellfish meat, production sites have remained open where AZA contamination levels have remained below this level, resulting in marketing and consumption of contaminated produce throughout Europe.

Considerable work was carried out to understand the mode of action of AZA in mammalian models from studies using purified toxin (Twiner *et al*., 2008). *In vivo* studies in mice showed that AZA-1 caused acute necrosis of the lamina propria of the small intestine and chronic damage to lymphoid tissues (Ito *et al*., 2002). Furthermore, AZA-1 decreases F-actin concentrations on a cellular level (Román *et al*., 2002) and causes teratogenic effects in Japanese rice fish (medaka) embryos (Colman *et al*., 2005). It has also been shown to be cytotoxic to several cell types (reviewed by Twiner *et al*.,

2005) and it also modulates calcium concentrations in human lymphocytes (Alfonso *et al*., 2005). On the neuronal level, AZA-1 inhibits bioelectrical activity of spinal cord neuronal networks (Kulagina *et al*., 2006) and also decreases neuronal viability (Vale *et al*., 2007).

1.7.2 Cyanobacterial poisoning

Cyanobacteria (blue-green algae) are photo-autotrophic micro-organisms which are found in both terrestrial and aquatic environments. In many parts of the world, surface water is used as the drinking water supply and its quality can be variable. In developed countries, the water is treated by filtration in water treatment and purification plants. Conventional water treatment plants use flocculation, precipitation, sand filtration and chlorination, however, this is not enough to remove cyanobacterial toxins from water supplies with high levels of eutrophication. A key factor for cyanobacterial decontamination in water treatment plants is the removal of both cell-bound and dissolved toxins. Cyanotoxins can be released during water treatment processes as a result of mechanical and chemical stress factors (Schmidt *et al*., 2002). Removal or degradation of cyanotoxins can also occur naturally by the action of bacteria or sunlight (Shephard *et al*., 1998). However, in less developed areas, sophisticated water treatment plants are unavailable and people have to rely on untreated water. Cyanobacteria are a normal part of the phytoplankton of surface waters, but if they are present in sufficient quantities, they may pose a threat to consumers.

Cyanotoxins are resistant to boiling and have the ability to pass through conventional water treatment facilities. In clean, oligotrophic lakes and rivers, the concentration of cyanobacteria is low and a range of species may be present at any given time. The cyanobacterial cell population is limited due to the lack of nutrients, particularly phosphates. As nutrient activity increases through human activity, including intensive agriculture and waste disposal, the cyanobacterial population rises rapidly. The condition of the freshwater is now described as eutrophic, where there are sufficient nutrients to support a large population of phytoplankton. The key factor which allows a particular species of cyanobacterium to become dominant is the ability to produce toxins. Cyanobacteria are the primary food source for organisms in freshwater. Toxin producers are given a competitive advantage by suppressing consumption, allowing the

toxic species to outgrow non-toxic phytoplankton. Globally, the most frequently found cyanobacterial toxins, in blooms from fresh and brackish waters, are the cyclic peptide toxins of the microcystin and nodularin family. They pose a major challenge for the production of safe drinking water from surface waters containing cyanobacteria with these toxins.

1.7.2.1 Cases and outbreaks of cyanobacterial poisoning

Microcystin contamination in water has led to fatalities in both wild and domestic animals worldwide and has been associated with human illness. There are several reports of animal and human deaths due to the consumption of water contaminated with cyanobacterial heptatoxins (Azevedo *et al.*, 2002; Falconer and Humpage, 2005). Human poisoning associated with cyanobacterial poisoning in drinking water has been identified in Europe, Brazil, Africa, Australia and the US, although many cases remain unreported. This is due to the fact that cyanobacterial poisoning is primarily associated with vomiting, diarrhoea, a tender abdomen and headache, which are also the symptoms of common viral, bacterial and protozoal gastrointestinal illnesses. Therefore, poisoning events may often go unreported for medical diagnosis or treatment. Poisoning events are only reported when a substantial number of individuals are affected in a population and no infectious diseases have been found. Testing for cyanobacterial agents will only take place when other eventualities, such as heavy metal poisoning or industrial or agricultural chemicals, have been eliminated.

In 1989, a direct case of poisoning from exposure to *Microcystis aeruginosa* scum was reported in the UK. Twenty army recruits who carried out exercises in a reservoir in Staffordshire became ill with malaise, vomiting, sore throat, dry cough and pneumonia. In 1996 in Brazil, a major disaster occurred in a dialysis clinic, affecting 131 patients, who had received dialysis over the course of one week. Dialysis patients are particularly vulnerable to soluble, low molecular weight chemicals in the water supply, as 120-150 litres can be used in the treatment of one patient. Of the 131 patients, 76 died due to liver failure (Azevedo *et al.*, 2002). The water supply originated from the Tabocas reservoir, which had a history of cyanobacterial poisoning. Most reported cases of human injury have been reported for drinking water supplies, therefore it is clear that

safe drinking water guidelines are essential. Another exposure route for microcystins is through contaminated food supplies, such as shellfish. Cyanobacterial toxins can accumulate in some species of mussel (Vasconcelos, 1995) and there is some evidence for the concentration of microcystin in fish (Carbis *et al.*, 1997).

1.7.2.2 Chemical structure and properties of the cyanobacterial toxin, microcystin

Microcystins contain five constant amino acids, namely, D-alanine, D-methylaspartic acid, Adda, D-glutamic acid and *N*-methyldehydroalanine, as well as two variable L-amino acids (Figure 1.7.2.1). The unique Adda or (2S,3S,8S,9S)-3-amino-9-methoxy-2,6,8-trimethyl-10-phenyldeca-4,6-dienoic acid is a β-amino acid. Microcystins are named according to the variable amino acids at position X and Y. Microcystin-LR contains the amino acids leucine (L) and arginine (R) at these positions. Currently, over 90 variants of microcystin have been identified and characterised and differ according to their toxicities (Falconer and Humpage, 2005). The different toxicities of the variants of microcystin provide some insights into the mechanism of their toxic effect. The most toxic of the microcystins are those with more hydrophobic L-amino acids, for example microcystin-LR, -LA, -YM and –YR, with the hydrophilic microcystin-RR being less toxic (Gupta *et al.*, 2003). Loss of the methyl group from the D-methyl aspartic acid or from the methyldehydroalanine reduces toxicity roughly by half. The Adda group is also crucial for toxicity, as proven by removal or saturation of the group (Harada *et al.*, 1990).

Microcystin-LR is the most common variant in cyanobacteria, although it is common to find more than one in a strain of cyanobacterium. The similar cyclic pentapeptide, nodularin contains arginine, glutamic acid, β-methyl aspartic acid, *N*-methyldehydroalanine and Adda. Therefore, nodularins are structurally similar and exhibit similar toxicities to microcystin. The toxins act by inhibiting the serine and threonine protein phosphatases 1 and 2A, which are essential for many cell regulatory processes, such as growth, protein synthesis, glycogen metabolism and muscle contraction (Falconer and Humpage, 2005). The Adda group is essential for binding of the toxin to the phosphatase structure via highly specific, covalent bonding. Adda also provides microcystins and nodularins with a characteristic absorption wavelength at 238

nm due to the presence of a conjugated diene group in the long carbon chain. This special property provides a means of analysis for microcystin, especially for reverse phase chromatography.

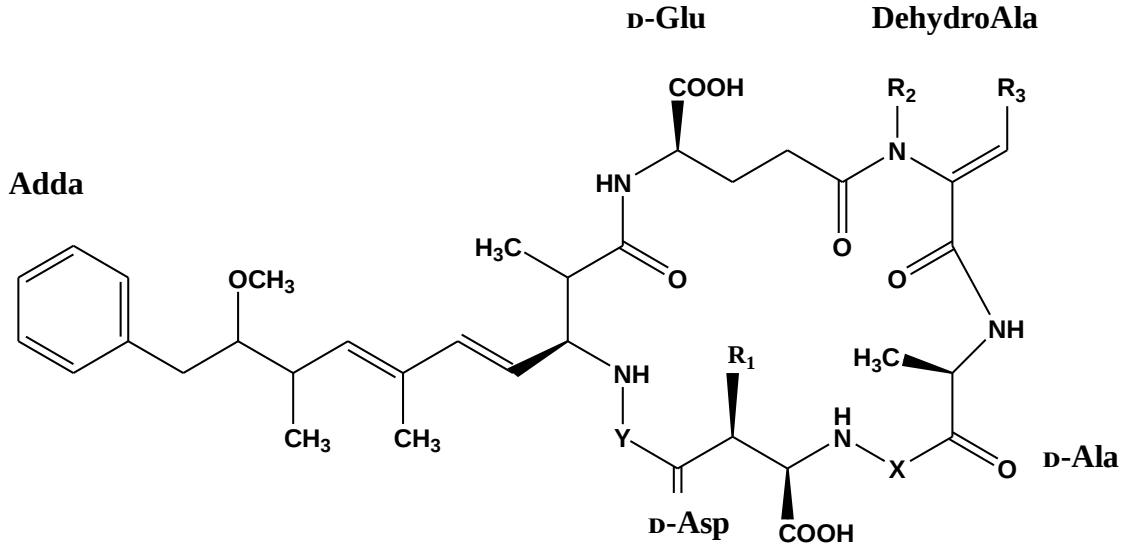

Microcystin Variant	X	Y	R1	R2	R3
MC-LR	Leu	Arg	CH_3	CH_3	H
MC-LW	Leu	Trp	CH_3	CH_3	H
MC-LF	Leu	Phe	CH_3	CH_3	H
MC-LA	Leu	Ala	CH_3	CH_3	H
MC-RR	Arg	Arg	CH_3	CH_3	H
MC-YR	Try	Arg	CH_3	CH_3	H

Figure 1.7.2.1: Microcystin structure and derivatives: Microcystin-XY: X and Y represent the one-letter abbreviations of the variable amino acids 2 (X) and 4 (Y). R1 to R3 represent variations in the methyl group position. At least 80 microcystin variants have been identified and MC-LR, MC-LW, MC-LF, MC-LA, MC-RR and MC-YR represent the most abundant. Microcystins also consist of a D-alanine (Ala); D-erythro β-methylaspartic acid (MeAsp); (2S,3S,8S,9S)-3-amino-9-methoxy-2,6,8-trimethyl-10-phenyldeca-4,6-dienoic acid (Adda); iso-linked D-glutamic acid (Glu) and *N*-methyl dehydroalanine (Mdha).

1.7.2.3 Source organisms for the production of microcystin

The cyanobacteria are ancient organisms, having been identified from rocks dating from the first thousand million years of the earth's history. As colonies of cyanobacteria occur in shallow water, they appear in the fossil record in sedimentary rocks deposited in shallow seas and lakes. Cyanobacteria are photosynthetic prokaryotes, which possess a single circular chromosome, which has been completely sequenced in several species (Kaneko *et al*., 1996). Their photosynthetic membranes contain chlorophyll-a and the pigment phycocyanin, which produces the characteristic blue-green colour of many species. Nitrogen fixation is an important feature of many species of cyanobacteria. Cyanobacterial poisoning is caused by the hepatotoxins microcystin and nodularin, during bloom events. They are produced by several genera of cyanobacteria including Microcystis, Anabaena, Nostoc, Anabaenopsis, Hapalosiphon and Planktothrix (Oscillatoria) (Carmichael, 1997) (Figure 1.7.2.2). Toxin-producing species are also seen in other groups besides phytoplankton and cyanobacteria, including raphidophytes, diatoms and prymnesiophytes.

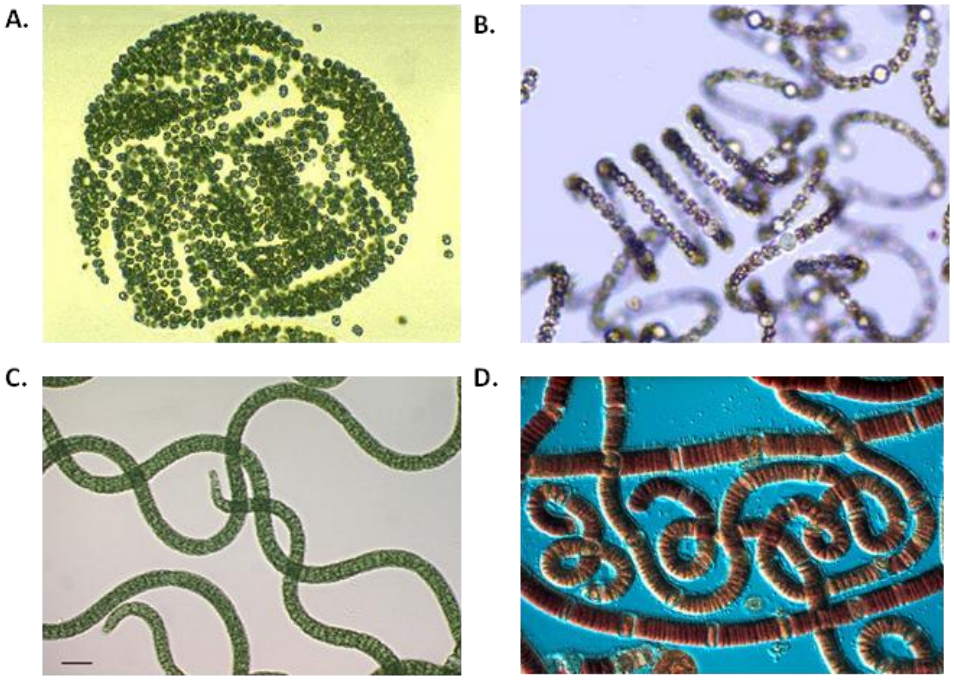

Figure 1.7.2.2: Photomicrographs of toxic species of cyanobacteria. A.*) Microcystis aeruginosa* B.) *Anabaena circinalis* C.) *Planktothrix species* D.) *Nodularia spumigena* (Images courtesy of Google Images).

Toxic water blooms of Microcystis have been reported widely across the world, associated with livestock, pet and wildlife deaths, as well as human injury through drinking water and food sources. Bishop *et al*. (1959) first isolated the "fast-death factor" from *M. aeruginosa* in culture. The first structural determination for microcystin was carried out on toxin samples from South Africa and Australia, using Fast Atom Bombardment Mass Spectrometry (FABMS) and NMR techniques at Cambridge University. The toxins were purified by ammonium bicarbonate extraction of cell homogenates, followed by multi-step column fractionation using Sephadex G-50 and DEAE cellulose (Botes *et al*., 1984). Once the structure of microcystin was elucidated, the structures of four further variants were published (Botes *et al*., 1985).

1.7.2.4 Occurrence and accumulation of microcystins in freshwater

Incidences of animal and human fatalities resulting from microcystins have led to the implementation of guideline values for drinking water by the World Health Organisation (WHO, 1998). The threat of microcystins was examined in detail by an expert group, who determined a provisional "guideline value" for microcystin-LR at 1 µg/L. This estimation was based on sub-chronic toxicity to rodents and pigs in the absence of sufficient data for carcinogenesis and teratogenesis. To minimise the danger to human health through exposure to microcystins, there is an urgent requirement for sensitive and reliable methods, capable of detecting these hepatopeptides in a wide variety of sample matrices. Increased awareness of the risks associated with microcystins has led to the development of a number of methods for their detection and quantification, ranging from biological-based screening methods to more sophisticated analytical techniques. Recently, routine sample screening using the mouse bioassay has been replaced with more sensitive and reliable assay methods such as enzyme-linked immunosorbent assay (ELISA; Nagata *et al*., 1995; Metcalf *et al*., 2000), and the protein phosphatase assay (Ward *et al*., 1997). Detection methodologies for microcystin are reviewed in detail in section 2.3.1

1.7.2.5 Toxicological studies for microcystins

The toxicity of microcystins is caused by the inhibition of serine/threonine protein phosphatases 1 and 2A (MacKintosh *et al*., 1990), which leads to hepatocyte necrosis and hemorrhage (Bhattacharya *et al*., 1997). Hepatotoxins, such as microcystin, induce massive haemorrhage and disruption in the mammalian liver (Falconer *et al*., 1983) and they have also been known to affect the kidneys (Milutinovic *et al*., 2002). Microcystins induce apoptotic effects in mammals (Fladmark *et al*., 1999; Mankiewicz *et al*., 2001) and morphological changes include membrane budding, cell shrinkage and organelle redistribution in human and rat cells (McDermott *et al*., 1998; Mankiewicz *et al*., 2001). Microcystins promote tumour precursor production, particularly in the liver, and research from southern China has demonstrated a link to human liver carcinoma (Yu *et al*., 1995). Microcystin was also implicated in the occurrence of liver and colorectal cancer (Hernández *et al*., 2009).

1.7.3 Mycotoxin poisoning

Mycotoxins are secondary metabolites of moulds that exert toxic effects on animals and humans. The toxic effect of mycotoxins on animal and human health is referred to as mycotoxicosis, the severity of which depends on the toxicity of the mycotoxin, the extent of exposure, age and nutritional status of the individual and possible synergistic effects of other chemicals to which the individual is exposed. The chemical structures of mycotoxins vary considerably, but they are all relatively low molecular mass organic compounds. Mycotoxins have significant economic impacts in a number of crops, especially wheat, maize, peanuts and other nut crops, cottonseed, and coffee. The Food and Agriculture Organization has estimated that 25% of the world's crops are affected by mycotoxins each year, with annual losses of around 1 billion metric tons of foods and food products. Aflatoxins are secondary fungal metabolites produced by strains of *Aspergillus flavus* and *A. parasiticus*. They are structurally related difuranocoumarin derivatives (Figure 1.7.6.1), incorporating the aflatoxin, trichothecenes, fumonisin and ochratoxin subgroups.

There are four major aflatoxin isoforms associated with food contamination: aflatoxin B_1, B_2, G_1 and G_2. Aflatoxin B_1 (AFB_1) and B_2 (AFB_2) are produced by *A. flavus*, while all four isoforms are produced by *A. parasiticus* (Creppy, 2002). Due to widespread incidence of Aspergillus contamination, aflatoxin can be found in a variety of foodstuffs, including cereals (maize, wheat, rice, sorghum, millet), nuts (pistachios, brazil, peanuts, walnuts, coconuts), spices (chili, turmeric, paprika, black pepper, ginger), dried fruit, and seeds (Pitt, 2000; Williams *et al.*, 2004). Trichothecenes are a group of mycotoxins which represent a number of different entities, all containing the trichothecene nucleus and are produced primarily by the Fusarium genus and also Myrothecium, Trichothecium, Stachybotrys, and Cephalosporium.

Toxicity generally occurs when a number of different trichothecene toxins are consumed simultaneously from mouldy cereal grains. Fumonisins are mycotoxins produced by *Fusarium verticillioides* (formerly known as *F. moniliforme*) and several other Fusarium species. Corn products contaminated with *F. verticilliodes* are responsible for agriculturally significant diseases in horses and swine (ICPS, 2000) and are currently being evaluated to determine the possible threat they pose to public health. Corn pests cause damage to the developing grain, which enables spores of the toxin-producing fungi, Fusarium, to germinate. The fungus then proliferates, which leads to ear and kernel rot and the production of potentially hazardous levels of fumonisins. Another mycotoxin produced by some Fusarium species is zearalenone. Zearalenone can occur in corn, barley, wheat, hay, and oats as well as other agricultural commodities. Zearalenone consumption can decrease the reproductive potential of farm animals, especially swine. Ochratoxin A is primarily produced by *Aspergillus ochraceous*, *A. carbonarius*, and *Penicillium verrucosum* and human exposure occurs as the result of contamination of small grains (barley, wheat and corn), coffee beans and grapes.

1.7.3.1 Cases and outbreaks of mycotoxin poisoning

Within the last decade, numerous outbreaks of mycotoxicoses have been reported worldwide. In 2004, 125 people died following a major outbreak of aflatoxicosis in the eastern and central provinces of Kenya. Three hundred and seventeen cases were reported, and most were linked to aflatoxin poisoning from contaminated maize. In 2005, more than 75 dogs died in the United States after consuming pet food contaminated with aflatoxins, and hundreds more experienced severe liver problems associated with the intoxication. There have been many reported cases of trichothecene toxicity in farm animals and a few in humans. One of the well-known cases of presumed trichothecene human toxicity occurred in Russia during 1944 in Orenburg, Siberia. Disruption of agriculture caused by World War II resulted in millet, wheat, and barley being overwintered in the field. Consumption of these commodities resulted in vomiting, skin inflammation, diarrhoea, and multiple haemorrhages, among other symptoms. About 10% of the population was affected and mortality rates were high at 60% in some countries. The causative agent was subsequently identified as alimentary toxic aleukia (ATA) (CAST, 2003).

1.7.3.2 Chemical structure and properties of aflatoxins

Four major aflatoxins: aflatoxin B_1, B_2, G_1, G_2 and two additional metabolic products, M_1 and M_2 are significant contaminants in foods and feed stocks. The aflatoxins M_1 and M_2 were first isolated from milk of lactating animals fed aflatoxin preparations; hence, the M designation. The B designation of aflatoxins B_1 and B_2 resulted from the exhibition of blue fluorescence under UV light and the G designation refers to the yellow-green fluorescence of the relevant structures under UV-light. These toxins have closely similar structures and form a unique group of highly oxygenated, naturally occurring heterocyclic compounds (Figure 1.7.6.1). Aflatoxins B_2 and G_2 were established as the dihydroxy derivatives of B_1 and G_1, respectively, whereas, aflatoxin M_1 is 4-hydroxy aflatoxin B_1 and aflatoxin M_2 is 4-dihydroxy aflatoxin B_2 (Fratamico *et al*., 2005).

Aflatoxin B_1

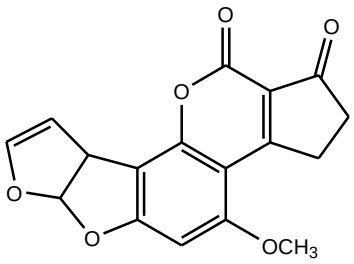

Aflatoxin B_2

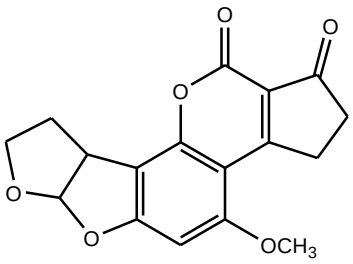

Aflatoxin G_1

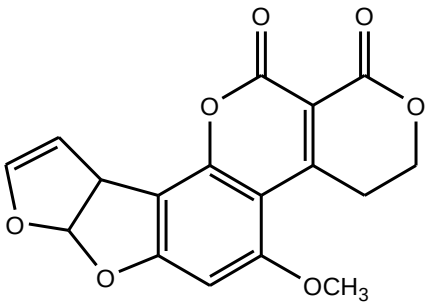

Aflatoxin G_2

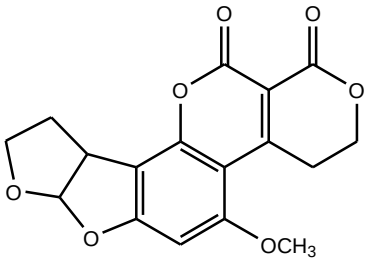

Fumonisin B_1

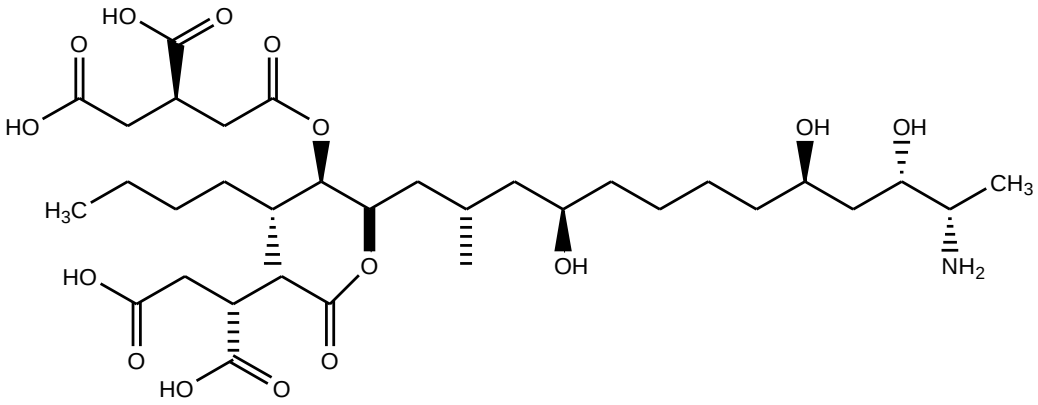

Figure 1.7.3.1: Structures of commonly-occurring aflatoxins: Aflatoxin B_1, Aflatoxin B_2, Aflatoxin G_1, Aflatoxin G_2 and Fumonisin B_1.

1.7.3.3 Occurrence and accumulation of aflatoxins

Mycotoxin contamination occurs during harvest time or during storage of food. Exposure to low levels of the mycotoxins through ingestion of the mouldy foods is common, depending on geographic location and type of food. Aflatoxins often occur in crops in the field prior to harvest. Postharvest contamination can occur if crop drying is

delayed and during storage of the crop if water is present. Insect or rodent infestations facilitate mould invasion in stored commodities. The most widely occurring contamination from aflatoxins is from Aspergillus species in stored grain, ochratoxin A, produced by Aspergillus and Penicillium in moulds, and zearalenone, a mycotoxin produced by Fusarium and Gibberella species (Al-Anati and Petzinger, 2006). Mycotoxins contamination can occur in a variety of plants used as food, including commodities such as cereal grains (barley, corn, rye and wheat), coffee, dairy products, fruits, nuts, peanuts, and spices. Contamination can also arise in animal products, in which animals consume contaminated feeds (e.g., milk). However, commodities such as cereal grains are eaten in the greatest quantities, therefore, the mycotoxins present in these foods represent the greatest risk (Cousins *et al*., 2005).

Moulds can be divided into two main groups: field fungi and storage fungi. The field fungi group contains species that proliferate under field conditions and do not multiply readily once grain is in storage. Field fungi may be superseded by storage fungi if there is sufficient moisture and oxygen conditions. However, the presence of a toxigenic mould does not guarantee the presence of a mycotoxin, which occurs only under certain conditions. Furthermore, more than one mould can produce the same mycotoxin (e.g., both *Aspergillus flavus* and several Penicillium species produce the mycotoxin cyclopiazonic acid). Also, more than one mycotoxin may be present in an intoxication event (Fratamico *et al*., 2005). Among the various mycotoxins, the aflatoxins have been the most intensively researched because of their extremely potent hepatocarcinogenicity, especially for aflatoxins B_1 and G_1. Generally, aflatoxins occur in susceptible crops as mixtures of aflatoxins B_1, B_2, G_1, and G_2.

A carcinogenic hydroxylated metabolite of aflatoxin B_1 (termed aflatoxin M_1) can occur in the milk from dairy cows that consume contaminated feed. Aflatoxins may occur in a number of susceptible commodities derived from them, including edible nuts (peanuts, pistachios, almonds, walnuts, pecans, brazil nuts), oil seeds (cottonseed, copra), and grains (corn, grain sorghum, millet). Since the discovery of the threat of aflatoxins to human health, progress has been made in decreasing the level of aflatoxins in specific commodities in developed countries. For example, in the United States and Western European countries, control measures include ensuring adequate storage conditions and careful monitoring of susceptible commodities for aflatoxin level and the

banning of lots that exceed the action level for aflatoxin B_1. Organic foods, produced without the use of insecticides and fungicides, may be more susceptible to mycotoxin contamination than foods produced using conventional agricultural practices. The UK Food Standards Agency found several organic maize meal products highly contaminated with fumonisin mycotoxins, whereas, conventional produced maize meal products analysed simultaneously had levels below recommended limits (UK Food Standards Agency, 2003).

1.7.3.4 Toxicological studies for aflatoxins

Aflatoxin exposure is detrimental to both human and animal health. AFB_1, the predominant isoform, is a potent hepatocarcinogen, and aflatoxin exposure has been linked to development of hepatocellular carcinoma (HCC) (Kew, 2003). Based on the toxicological data, the naturally occurring aflatoxins (B_1, B_2, G_1, and G_2, including mixtures of isoforms) and the metabolic product aflatoxin M_1 have been designated Group 1 carcinogens (carcinogenic to humans) by the International Agency for Research on Cancer (IARC) (IARC, 2002). Aflatoxins are also known to be teratogenic, mutagenic and immunosuppressive (Peraica *et al.*, 1999; Kihara *et al.*, 2000; Jiang *et al*., 2005). A number of mycotoxins produce nephrotoxicity such as aflatoxin B_1, citrinin, ochratoxins, fumonisins, and patulin (O'Brien and Dietrich, 2005). Fumonisins B_1 and B_2 are commonly found on corn and corn products and produce nephrotoxicity in rats and rabbits (Bucci *et al.*, 1998). There are few reports of acute intoxications caused by mycotoxins, however, prolonged exposure to small quantities of mycotoxin may lead to more dangerous effects including growth retardation, birth defects, impaired immunity, decreased disease resistance, and tumor formation in humans and decreased production in farm animals (CAST, 2003).

Aflatoxins are products of species of the genus Aspergillus, particularly *A. flavus*, a common fungus found as a contaminant of grain, maize and peanuts. First implicated in poultry diseases such as Turkey-X disease, they were subsequently shown to cause cancer in experimental animals and from epidemiological studies in humans. Aflatoxin B_1, the most toxic of the aflatoxins, must be activated enzymatically to exert its carcinogenic effect. Aflatoxin B_1 is acutely toxic in all species studied, with an LD_{50} of

60 mg/kg for mice with death usually resulting from hepatotoxicity. Aflatoxin B_1 is also highly mutagenic, hepatocarcinogenic, and possibly teratogenic. A problem in extrapolating animal data to humans is the extremely wide range of species susceptibility to aflatoxin B_1. Aflatoxin B_1 is an extremely reactive compound biologically, altering a number of biochemical systems. The hepatocarcinogenicity of aflatoxin B_1 is associated with its biotransformation to a highly reactive electrophilic epoxide, which forms guanine adducts and induces apoptotic cell death in human hepatocytes (Reddy *et al*., 2006). Damage to DNA is thought to be the initial biochemical lesion resulting in the expression of the pathological tumour growth (IARC, 2002). Species differences in the response to aflatoxin may be due in part to differences in biotransformation and susceptibility to the initial biochemical lesion.

Fumonisins are mycotoxins produced by the fungus Fusarium, primarily by *Fusarium moniliforme* and *Fusarium proliferatum* growing on corn. Ingestion by horses of corn contaminated with Fusarium mold causes "mouldy corn poisoning" or equine leukoencephalomalacia. In humans, an association with esophageal cancer has been suggested (Myburg *et al*., 2002). Trichothecenes are protein synthesis inhibitors which bind ribosomes. The extent of toxicity associated with the trichothecenes in humans and farm animals is poorly understood, owing in part to the number of entities in this group and the difficulty of assaying for these compounds. The acute LD_{50}'s of the trichothecenes range from 0.5 to 70 mg/kg, and there has been reports of possible chronic toxicity associated with certain members of this group (Li *et al*., 2011). However more research is required to study the adverse human health effects of this toxin group. Fumonisins have been associated with cancer, reproductive toxicity, and acute disease outbreaks where low-quality corn is consumed on a regular basis (Cousins *et al*., 2005). Fumonisins target different organs in different species, but the underlying mechanism is a disruption of lipid metabolism by inhibition of ceramide synthetase, an enzyme integral to the formation of complex lipids in membranes (ICPS, 2000). Ochratoxin A is nephrotoxic and carcinogenic in mice and rats. Ochratoxin A is absorbed from the gastrointestinal tract and enters the enterohepatic circulation and it is also absorbed by the kidney. It binds tightly to albumin in the blood and can therefore have a very long serum half-life. Epidemiologic evidence indicates nearly half the European population is exposed to ochratoxin A and there is an association of endemic nephropathy and renal tumors in humans in parts of Eastern Europe (CAST, 2003).

1.8 Thesis Aims

Intoxication events caused by consumption of seafood and water supplies with naturally-occurring marine toxins is becoming a worldwide problem. While phycotoxins and mycotoxins have been shown to modulate certain immune functions, their specific mechanisms of action remain unknown. Specifically, this work aims to elucidate mechanism involved in the effects of azaspiracid-1, microcystin-LR and the aflatoxins, B_1, B_2 and G_1 on the murine macrophage, J774A.1, responses to LPS. Herein, a tailored approach is taken to examine the possible mechanisms of toxin-mediated modulation of macrophage function by observing their effects on cellular function, cell surface marker expression and secreted cytokines. It is hoped to provide an insight into the mechanisms by which phycotoxins and mycotoxins modulate the host immune response to exert their immunosuppressive activity.

The second purpose of this research was to generate recombinant antibodies to azaspiracid for incorporation into a specific and sensitive immunoassays. Currently, no recombinant antibodies exist to this target, but polyclonal and monoclonal azaspiracid-specific antibodies have been generated (Forsyth *et al.*, 2006; Fredrick *et al.*, 2009) Immunoassays, incorporating novel recombinant antibodies, could potentially be incorporated into toxin detection systems in shellfish and water. Genetic material became available from an azaspiracid-immunised rabbit host. It was decided to harness this material to generate single chain antibody fragments (scFvs) to azaspiracid.

A third goal of this research was to generate recombinant antibodies for detection of microcystin through generation of avian immune libraries. No previous reports of avian immune recombinant antibodies to this compound exist. However, scAb fragments have been isolated from non-immune libraries, but they lack sensitivity and their cross-reactivity was shown to be variable (McElhiney *et al.*, 2000; Strachen *et al.*, 2002). Custom synthesised microcystin conjugate were generated for this purpose.

A final aim was to produce a sensitive immunosensor for toxin detection, using the recombinant antibodies generated over the course of the research. Ideally, the immunosensor would be in a format applicable to future in situ device development and that could accurately and sensitively detect toxin outbreaks in an algal matrix.

CHAPTER 2

Material and Methods

2.1 Media preparation

All the components are prepared in distilled water and autoclaved at 120^{o}C for 20 minutes to remove contaminants. All components were purchased from Sigma-Aldrich Ltd. and Cruinn Diagnostics Ltd.

Media	Components
2x Tryptone Yeast extract (2xTY)	Tryptone (16 g/L) Yeast extract (10 g/L) NaCl (5 g/L)
Super Broth (SB)	MOPS (10 g/L) Tryptone (30 g/L) Yeast extract (20 g/L)
Super Optimal Catabolite (SOC)	Tryptone (20 g/L) Yeast extract (5 g/L) NaCl (0.5 g/L) KCl (2.5 mM) $MgCl_2$ (20 mM) Glucose (20 mM)

2.2 Buffer preparation

2.2.1 General buffers

The constituents of each buffer are dissolved in 990 mL distilled and deionised water and adjusted to a final pH of 7.4. The solution is made up to a final volume of 1 Litre. All components were analytical grade.

Buffer Name	Components
Phosphate-buffered saline (PBS) 150 mM (pH 7.4)	NaCl (5.84 g/L) Na_2HPO_4 (4.72 g/L) NaH_2PO_4 (2.64 g/L)
PBS Tween 20 (PBST)	NaCl (5.84 g/L) Na_2HPO_4 (4.72 g/L) NaH_2PO_4 (2.64 g/L) Tween 20 (0.05 % (v/v))
HBS buffer	HEPES (2.38 g/L) NaCl (8.77 g/L) EDTA (1.27 g/L) Tween 20 (0.05 % (v/v)) HBS was filter sterilised through a 0.2 µm filter and degassed.
FACS Buffer	2 % (v/v) FCS 0.05 % (w/v) sodium azide The buffer was prepared in sterile PBS (150 mM, pH 7.4) and filter sterilised through a 0.2 µm filter

2.2.2 Buffers for sodium dodecyl sulfate-polyacrylamide gel electrophoresis (SDS-PAGE)

Preparation of 12.5 % Separation Gel	**1 gel/ 6 mL**
1 M TrisHCl (pH 8.8)	1.5 mL
30 % (w/v) acrylamide (Acrylagel)	2.5 mL
2 % (w/v) methylamine bisacrylamide (Bis-Acrylagel)	1.0 mL
Water	934 µL
10 % (w/v) sodium dodecyl sulfate (SDS)	30 µL
10 % (w/v) Ammonium persulfate (APS) (Fresh)	30 µL
N,N,N',N'-Tetramethylethylenediamine (TEMED)	6 µL

Preparation of 4.5 % Stacking Gel	**1 gel/ 2.6 mL**
1 M TrisHCl (pH 6.8)	300 µL
30 % (w/v) acrylamide (Acrylagel)	375 µL
2 % (w/v) methylamine bisacrylamide (Bis-Acrylagel)	150 µL
Water	1.74 mL
10 % (w/v) SDS	24 µL
10 % (w/v) APS	24 µL
TEMED	2.5 µL

10X Electrophoresis Buffer	**Volume (1 L)**
196 mM Glycine	144 g
50 mM Tris (pH 8.3)	30 g
0.1 % (w/v) SDS	10 g

4X Loading Dye	Volume (10 mL)
Tris 0.5M (pH 6.8)	2.5 mL
Glycerol	2 mL
2-mercaptoethanol	0.5 mL
20 % (w/v) SDS	2.5 mL
Bromophenol blue	20 ppm
Water	2.5 mL

Coomassie Stain	Volume (500 mL)
0.2 % (v/v) Coomassie blue R-250	1 g
45 % (v/v) Methanol	225 mL
45 % (v/v) Water	225 mL
10 % (v/v) Acetic acid	50 mL

Coomassie Destain	Volume (1 L)
10 % (v/v) Acetic acid	100 mL
25 % (v/v) Methanol	250 mL
65 % Water	650 mL

2.2.3 Buffers for western blotting

Transfer Buffer	Volume (1 L)
Tris	3.03 g
Glycine	14.4 g
Methanol	200 mL
	Adjust to 1L with dH_20

2.2.4 Buffers for immobilised-metal affinity chromatography (IMAC)

Lysis Buffer	**Volume (100 mL)**
300 mM NaCl	1.754 g
50 mM NaH_2PO_4	0.69 g
10 mM Imidazole	0.068 g
Adjust pH to 7.5, using 1 M NaOH	

Wash buffer A	**Volume (100 mL)**
50 mM NaH_2PO_4	0.69 g
1 M NaCl	5.844 g
10 % (v/v) glycerol	20 mL 50 % (v/v) solution
20 mM Imidazole	0.136 g
1 % (v/v) Triton X-100	1 mL
Adjust pH to 7.5, using 1 M NaOH	

Wash buffer B	**Volume (100 mL)**
50 mM NaH_2PO_4	0.69 g
300 mM NaCl	1.754 g
20 mM Imidazole	0.136 g
Adjust pH to 7.5, using 1 M NaOH	

Elution buffer	**Volume (100 mL)**
50 mM NaH_2PO_4	0.69 g
300 mM NaCl	1.754 g
250 mM Imidazole	1.7 g
Adjust pH to 7.5, using 1 M NaOH	

2.3 Reagents

All reagents were of analytical grade and purchased from Sigma-Aldrich Ireland Ltd (Dublin, Ireland), unless otherwise specified.

Reagent	Supplier
Biacore™ CM5 research grade sensor chips	GE Healthcare Bio-Sciences AB, SE-751 84 Uppsala, Sweden.
Bacteriological Agar **Yeast extract** **Tryptone**	Cruinn Diagnostics Ltd., Hume Centre, Parkwest Business Park, Nangor Road, Dublin 12, Ireland.
DNA Ligase **Helper phage** **Restriction enzymes** **Phusion High-Fidelity DNA polymerase** **Antarctic Phosphatase**	ISIS Ltd., Unit 1 & 2, Ballywaltrim Business Centre, Boghall Road, Bray, Co. Wicklow, Ireland.
dNTPs **GoTaq® DNA Polymerase** **RedTaq® DNA Polymerase**	Medical Supply Company Ltd, Damastown, Mulhuddart, Dublin 15, Ireland.
FPLC molecular protein standards	Phenomenex Ltd., Melville House, Cheshire SK10 2BN, UK.

PageRuler™ Plus Prestained Protein Ladder	AGB Scientific Limited - A VWR International Company, Orion Business Campus, Northwest Business Park, Ballycoolin, Dublin 15, Ireland.
PCR primers	Eurofins MWG Operon, 318 Worple Road, Raynes Park, London, SW20 8QU, UK.
Platinum® Taq DNA Polymerase High Fidelity **Trizol**	Bio-sciences, Crofton Road, Dun Laoghaire, Dublin, Ireland.
RNaseZap™ **RNAlater™** **Glycogen (5 mg/mL)** **3M Sodium acetate**	Applied Biosystems/Ambion, 2130 Woodward St., Austin, TX 78744-1832, USA.

2.4 Commercial antibodies and antigens

Reagent	Supplier
Goat anti-rabbit, peroxidase conjugated pAb **Rabbit anti-mouse, peroxidase conjugated pAb**	Sigma Aldrich, 3050 Spruce Street, St. Louis, MO 63103, USA.
Lipopolysaccharide (LPS) *E. coli*, serotype R515 **Microcystin-LR-BSA and OVA protein conjugates** **Microcystin-LR (MC-LR), MC-LW, MC-LF, MC-LA, MC-RR and MC-YR**	Enzo Life Sciences Inc. 10 Executive Boulevard Farmingdale, NY 11735, USA.
Mouse anti- haemagglutinin (HA) mAb	Cambridge Bioscience, 24-25 Signet Court, Newmarket Road, Cambridge CB5 8LA, UK.
Mouse anti-M13 antibody, horseradish peroxidase conjugated	GE Healthcare Bio-Sciences AB, SE-751 84 Uppsala, Sweden.
Rabbit anti-chicken IgY (H+L), horseradish peroxidase conjugated	Pierce, Thermo Fisher Scientific Inc., 3747 N Meridian Rd, Rockford, IL USA 61101.

2.5 Commercial kits

Reagent	Supplier
Cell proliferation reagent (WST-1) **Cytotoxicity detection Kit (LDH)**	Roche Diagnostics GmbH, Sandhoferstrasse 116, DE-68305 Mannheim, Germany.
DuoSet ELISA development kits	R&D Systems, Inc., 614 McKinley Place NE, Minneapolis, MN 55413, USA.
Perfectprep gel cleanup Kit	Eppendorf AG, Barkhausenweg 1, Hamburg 22339, Germany.
Superscript III reverse transcriptase kit	Invitrogen Corporation, 5791 Van Allen Way, Carlsbad, CA 92008, USA.
Wizard Plus SV Miniprep™ kit	Promega, 2800 Woods Hollow Road, Madison, WI 53711, USA.
NucleoSpin® Xtra Midi Plasmid Purification Kit	Macherey-Nagel, Fisher Scientific Ireland Ltd., Suite 3, Plaza 212, Blanchardstown Corporate Park 2, Ballycoolin, Dublin 15.

2.6 Cell culture reagents

Reagent	Supplier
RPMI-1640 liquid medium with L-Glutamine **DMEM/high glucose with sodium pyruvate** **Fetal bovine serum** **L-Glutamine** **Penicillin-Streptomycin solution (10,000 unit/mL Penicillin and 10,000 µg/mL Streptomycin in 0.85 % (w/v) NaCl)** **Trypsin solution (0.05 % w/v) (1X)** **DPBS (1X) without calcium and magnesium**	Thermo Scientific Hyclone™, Fisher Scientific Ireland Ltd., Suite 3, Plaza 212, Blanchardstown Corporate Park 2, Ballycoolin, Dublin 15.

2.7 Equipment

Equipment Name	Supplier
ÄKTA™ Explorer 100 system	GE Healthcare UK Ltd., Amersham Place, Little Chalfont, Buckinghamshire, England.
Biacore™ 3000	GE Healthcare Bio-Sciences AB, SE-751 84 Uppsala, Sweden.
Eppendorf™ Centrifuge 5810 R with swing-bucket rotor (A-4-62) and fixed-angle rotor (F-45-30-11)	AGB Scientific Ltd , VWR International, Co. Dublin, Ireland.
FACSCalibur™ Flow Cytometer	BD Biosciences, 1 Becton Drive, Franklin Lakes, New Jersey, 07417, USA.
Gene Pulser Xcell™ electroporator **Biorad Gel electrophoresis system** **HERA Cell 100 CO_2 incubator**	Bio-Rad Laboratories, Inc., 2000 Alfred Nobel Drive, Hercules, California 94547, USA.
GeneSnap™ 2D Imaging System	Syngene, 5108 Pegasus Court, Suite M, Frederick, MD 21704, USA.
MSC-Advantage Laminar Flow Cabinet **PX2 thermal cycler**	Thermo Electron Corporation, 81 Wyman Street, Waltham, Massachusetts (MA), 02454, USA.

Sceptor Handheld Automated Cell Counter	Millipore, 290 Concord Road, Billerica, MA 01821, USA.
Nanodrop™ ND-1000	NanoDrop Technologies, Inc., 3411 Silverside Rd 100BC, Wilmington, DE19810-4803, USA.
Perkin Elmer™ ScanArray Express Microarray Analysis System	75 Nicholson Ln, San Jose, California, 95134-1366, USA
Roller mixer SRT1	Sciencelab, Inc., 14025 Smith Rd, Houston, Texas 77396, USA
Safire™ 2 plate reader	Tecan™ Group Ltd. Seestrasse 103, CH-8708 Männedorf, Switzerland
Vibra Cell™ sonicator	Sonics and Materials Inc., 53 Church Hill Road, Newtown, CT 06470-1614, USA

2.8 Bacterial strains

All strains were purchased from Stratagene, La Jolla, Calfornia, USA.

- *E. coli* TOP10F′ strain: {lacI^{q}, Tn10(Tet^{R})} mcrA Δ(mrr-hsdRMS-mcrBC) ϕ 80lacZΔM15 ΔlacX74 recA1 araD139 Δ(ara-leu)7697 galU galK rpsL (Str^{R}) endA1 nupG
- *E. coli* XL1-Blue strain: recA1 endA1 gyrA96 thi-1 hsdR17 supE44 relA1 lac [F′ proAB lacI^{q}ZΔM15 Tn10 (Tet^{R})].

2.9 Safety precautions and protocols for handling toxin material and waste

Azaspiracid, microcystin and aflatoxin are all highly toxic and hazardous substances. Therefore, for all experiments involving these compounds, the correct protocols for their safe storage, handling and disposal were carried out, in accordance with approval from the DCU Safety Committee and the Environmental Protection Agency (EPA). All cell culture work was carried out in a designated toxin laminar flow hood. All biopanning and ELISA experiments were also carried out in a designated toxin fume hood. Toxin-containing liquid waste, including coating, blocking, washing, assay and cell culture media solutions were decanted into designated glassware containing Virkon®. This liquid waste was collected and disposed of by Ecosafe Ltd. Personal protective equipment was worn at all stages, including lab coat, goggles and two pairs of gloves.

2.10 Toxins and toxin conjugates

Toxins and toxin conjugates were stored in single-use aliquots at - 20^{o}C. Both aflatoxins (B_1, B_2 and G_1; Sigma-Aldrich Ireland Ltd.) and microcystin (MC-LR, M-RR, MC-LF, MC-LA, MC-YR and nodularin; Enzo Life Sciences Ltd.) were re-constituted, from lyophilised vials, according to manufacturer's instructions in molecular-grade methanol (prepared in 'endotoxin-free' water). Azaspiracid was provided in PBS (150 mM, pH 7.4).

The use of plastic tubes and of plastic pipette tips in the manipulation of MC-LR solutions has been shown to influence dissolved toxin concentrations (Hyenstrand *et al*., 2001). Therefore, microcystins were stored in glass vials and pipetting was minimised. In cases where multiple toxin dilutions in plastic microcentrifuge tubes were required, a stock solution of microcystin in 25 % (v/v) methanol was prepared, as the same study showed that MC-LR in a solution of above 25 % (v/v) methanol did not interact with plastics to any great extent (Hyenstrand *et al*., 2001).

2.11 Cell culture techniques

2.11.1 Culture of cell lines

The murine macrophage cell line J774A.1 was obtained from the European Collection of Cell Cultures (ECACC; Salisbury, UK). The cells were cultured in RPMI-1640 medium supplemented with 10 % (v/v) foetal bovine serum, 2 mM L-glutamine, 50 U penicillin and 50 µg streptomycin. The semi-adherent cell line, J774A.1 was sub-cultured by gently tapped to dislodge the cells from the surface of the flask. Cells were recovered by centrifugation at 400 g for 5 minutes, diluted in fresh medium and then transferred to a sterile 75 cm^2 tissue culture flasks for further growth.

The human hepatocellular cell line, HepG2, was obtained from the European Collection of Cell Cultures (ECACC; Salisbury, UK). The cells were cultured in DMEM supplemented with 10 % (v/v) foetal bovine serum, 2 mM L-glutamine, 50 U penicillin and 50 µg streptomycin. For sub-culturing, the media was carefully removed, the cells were washed twice with sterile PBS and 2 mL of 0.05 % (w/v) trypsin (Hyclone) was added and incubated for 2-6 minutes in a CO_2 incubator. Eight mL of fresh media was then added to deactivate trypsin, thus preventing cellular damage. The culture was centrifuged at 400 g for 5 minutes, resuspended in fresh media and transferred to a sterile 75 cm^2 tissue culture flasks for further growth.

All cultures were maintained in a 37°C, 5 % CO_2 humidified atmosphere. All work was carried out in a LaminAir flow cabinet to ensure sterility.

2.11.2 Long-term storage of cell lines

Cells were prepared by aliquoting into 1 mL cryovials at a concentration of 5-10X 10^6 cells/mL in freeze medium. Freeze medium consisted of 95 % of the appropriate medium and 5 % (v/v) dimethyl sulfoxide (DMSO). Once aliquoted, the vials were immediately transferred to a Nalgene® Mr. Frosty and placed in a -80ºC freezer for slow freezing. Once frozen, the vials were transferred to liquid nitrogen, for long-term storage.

2.11.3 Resuscitation of frozen cell line stocks

One aliquot of cells was thawed, when new cultures were required, or when the viability of the cells after cryopreservation needed to assessed. Ten mL of the appropriate medium was pre-warmed to 37°C in a 25 cm^2 sterile tissue culture flask. The cryovial was warmed briefly at room temperature before thawing in a 37ºC water bath. The contents of the vial were slowly transferred to the pre-warmed medium, which was then placed in the incubator. Cell growth was monitored by examining the cells, under a Nikon® inverted microscope. After 72-96 hours, the regular subculture routine was initiated to ensure that the optimal cell concentration and conditions were maintained.

2.11.4 Cell counting

Cells were counted and their viability assessed using trypan blue exclusion. Trypan blue is negatively charged, so it is excluded from viable cells. Therefore, only the cells with damaged cell membranes (e.g. dead cells) will stain blue. To count the cells, 10 µL of cell suspension was added to 90 µL of 0.04 % (v/v) trypan blue solution. The sample was loaded into the chamber of an improved Neubauer haemocytometer. Using a light microscope, cells were counted in 5 squares of either side of the chamber (10 in total). The concentration of the cells in the suspension (cells/mL) was calculated by multiplying the total number of cells in all 10 squares x dilution factor x 1000.

2.11.5 Mycoplasma testing

Regular testing for mycoplasma was carried out using a MycoAlert® Mycoplasma Detection Kit (Lonza), as per the manufacturer's instructions. This luminescence-technique was based on the measurement of ATP in a culture supernatant. Enzymes released from viable mycoplasma react with the kit substrate, catalysing the conversion of ADP to ATP.

2.11.6 Endotoxin testing

Regular testing for endotoxin contamination was carried out using an E-toxate™ kit (Sigma-Aldrich, Ireland), as per the manufacturer's instructions. This test is dependent

on the viscosity of the test sample in the presence of circulating amebocytes of the horseshoe crab, *Limulus polyphemus.*

2.12 Effects of marine toxin exposure on murine macrophage cell line

2.12.1 Toxin treatments

For cell culture analysis, all required toxin dilutions were prepared in cell culture media. For the toxins dissolved in methanol, including microcystin and aflatoxin, the final concentration of solvent exposed to cells was always less than 0.1 % (v/v) methanol. In all experiments, a control assay was prepared, in which cells were exposed to the equivalent vehicle concentration, to that used in the toxin treatment.

2.12.2 Lactate dehydrogenase assay

The lactate dehydrogenase (LDH) assay kit (Roche Applied Sciences) is a colorimetric assay for the quantification of cell death and cell lysis, based on the measurement of LDH activity released from the cytosol of damaged cells into the supernatant (Figure 2.12.1). To calculate the percent cytotoxicity, a number of controls were included in the experimental set-up. The background control or media control provided information on the background LDH activity of the assay medium. The absorbance value obtained in this control has to be subtracted from all other values. The low control provided information about the LDH activity released from the untreated normal cells. The high control provided information about the maximum releasable LDH activity in the cells. For this experiment the low control was molecular grade methanol, at the same concentration as toxin solvent in the final cell preparation. The high control was 1 % (v/v) Triton-X100, a non-ionic surfactant, which is used for the solubilisation of membranes under non-denaturing conditions. The permeabilisation of the membrane leads to a fast cell death by necrosis (Weyermann *et al*., 2005).

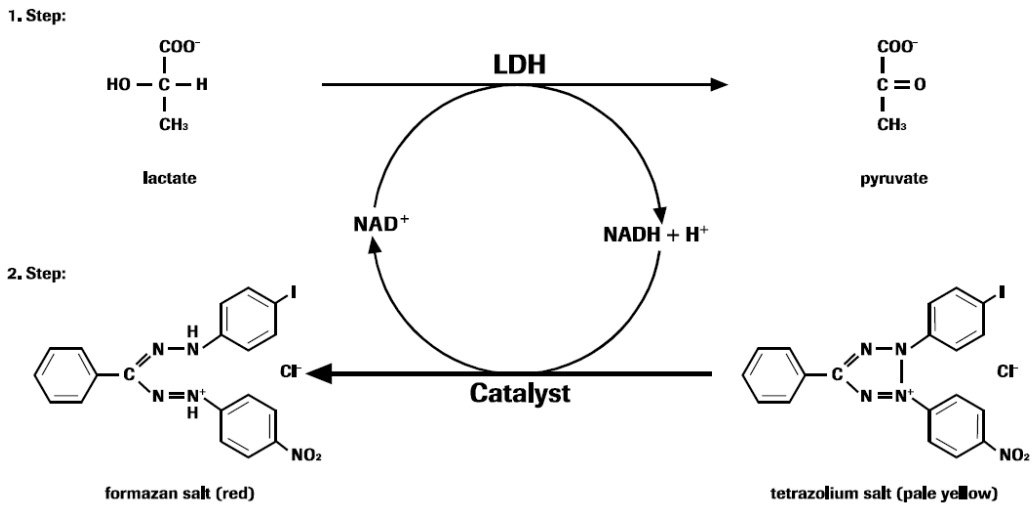

Figure 2.12.2.1: Lactate dehydogenase (LDH) assay principle (Image from Roche Applied Sciences). LDH activity is determined in a coupled enzymatic reaction; during which, the tetrazolium salt (INT) is reduced to formazan salt.

To determine the percentage cytotoxicity, the mean absorbance values of the triplicate experiments were calculated and the background measurement was subtracted from each. The resulting values are substituted in the following equation:

$$\% \text{ Cytotoxicity} = \frac{\text{Experimental Value - Low Control}}{\text{High Control - Low Control}} \times 100$$

For the experiment, 200 µL of murine macrophage cells, at a concentration of $1x10^6$ cells/mL in RPMI (with 10 % (v/v) FBS), was dispensed into each well of a 96 well cell culture plate (NUNC™). The plate was placed in a CO_2 incubator at 37°C, 5 % CO_2 and the cells were allowed to adhere overnight. The next day, 'serum-free' RPMI was pre-warmed to 37°C prior to experimental set-up. Dilutions of toxins and LPS were prepared in 'serum-free' media. The J774A.1 macrophage cells were checked under the inverted microscope to ensure that they adhered overnight and were viable. The toxins and controls were added to each well as appropriate. A positive and negative control was included each time the experiment was performed to both ensure that the cells are

behaving normally and to screen for contamination. In this situation, the negative control was medium alone and the positive control was 100 ng/mL LPS. The plate was incubated at 37°C, 5 % CO_2 for the predetermined time period.

After treatment, the 96 well plate was centrifuged at 400g for 5 minutes to minimise the presence of cellular material in the supernatant, which may affect subsequent results. One hundred µL of supernatant was transferred to new plate for the LDH assay. One hundred µL of LDH assay solution was added to the supernatant plate and incubated for 30 minutes at room temperature wrapped in tin foil to minimise exposure to light. The LDH assay solution was prepared immediately prior to use, according to manufacturer's instructions, by mixing 250 µL 'Bottle 1' (Diaphorase/NAD^+ mixture) with 11.25 mL 'Bottle 2' (Iodotetrazolium chloride and sodium lactate). After incubation, the absorbance of the LDH assay plate wells was measured at 490 nm using a Tecan™ Safire II instrument.

2.12.3 WST-1 cell death assay

The WST-1 assay is designed for spectrophotometric quantification of cell growth, viability and proliferation, through determination of mitochondrial dehydrogenase activity. The stable tetrazolium salt, WST-1, is cleaved to a soluble formazan by a complex cellular mechanism which occurs primarily at the cell surface. This bioreduction is largely dependent on the glycolytic production of NAD(P)H in viable cells. Therefore, the amount of formazan dye formed directly correlates to the number of metabolically active cells in the culture. (Figure 2.12.3.1).

Murine macrophages were prepared for analysis, as described in Section 2.12.1. After cells were treated for the pre-determined time period with controls and toxins, the 96 well plate was removed from the incubator. Supernatant was removed for LDH analysis, WST-1 assay solution added in a volume of 10 µL and incubated at 37^{o}C for time ranging from 0.5 to 4 hours. The WST-1 assay solution was thawed from a 1 mL frozen stock, immediately prior to use. Following incubation, the absorbance of the WST-1 assay plate was measured at 450 nm, using a Tecan™ Safire II instrument.

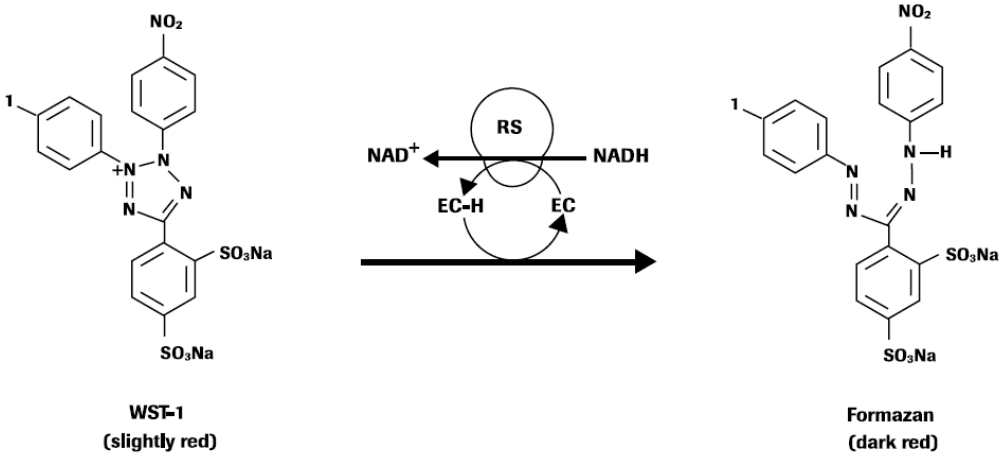

Figure 2.12.3.1: WST-1 (4-[3-(4-iodophenyl)-2-(4-nitrophenyl)-2H-5-tetrazolio]-1,3-benzene disulfonate) cell death assay principle, based on the cleavage of WST-1 to formazan (dark red). EC = Electron coupling reagent, RS = Mitochondrial succinate-tetrazolium-reductase system (Image from Roche Applied Sciences).

2.12.4 Analysis of effects of toxin on cytokine (IL-6, IL-10, IL-12p40, IL-1β and TNF-α) release in the J774A.1 murine macrophage cell line

TNF-α, IL-10, IL-6, IL-12p40, and IL-1β DuoSet ELISAs were performed according to the manufacturer's instructions (R&D Systems, Ltd). Each sample was assayed in duplicate for each of the cytokines indicated. Sterile 'serum-free' RPMI (Fisher Scientific, Ireland) was pre-warmed to 37^{o}C prior to the experimental set-up. Dilutions of toxin were prepared in a pre-determined assay range in 'serum-free' media. J774A.1 murine macrophage cells at 70 % confluency were detached from a T75 (NUNC™) flask by gently tapping. The cells were transfered to a 25 mL sterilin tube and centrifuged at 400 g for 5 minutes (Sigma Centrifuge 2K15). The pelleted cells were re-suspended in 10 mL fresh media, a sample was taken for trypan blue staining and a cell count was performed, as described in Section 2.22.4 The concentration was adjusted to 1x10^{6} cells/mL in a 25 mL volume. Five hundred µL of this cell suspension was aliquoted into a 48 well tissue culture plate (NUNC™). The toxins were added to a final concentration (100 pg/mL AZA-1; 1 and 5 µg/mL MC-LR; 0.01 and 0.1 ng/mL aflatoxins B_1, B_2 and G_1), with or without 100 ng/mL lipopolysaccharide (LPS) (Alexis Biochemicals), to induce an inflammatory response. Cells were incubated with an

equivalent methanol concentration, as a vehicle control for microcystin and aflatoxin toxicity analysis. The plates were placed in a 37^{o}C incubator (Thermo Scientific), 5 % CO_2, for the pre-determined time period. After the incubation period, the cell supernatant was harvested and aliquoted into sterile 1.5 mL tubes and used immediately or stored at -80^{o}C until required. All experiments were performed in triplicate.

2.12.5 Cell surface marker expression

Cell surface expression of TLR2, TLR4, CD14 and CD40 on J774A.1 cells was assessed by flow cytometry. Following 72 hour exposure to AFB_1, AFB_2 or AFG_1 alone or in combination (10 ng/mL), 1x10^6 cells were stimulated with and without 100 ng/mL LPS for 24 hours. At the end of the 24 hour incubation, cells were labelled to determine cell surface expression of CD14, TLR4, TLR2 and CD40 (eBio). For this, cells were scraped from the bottom of the well with a sterile transfer pipette and collected in a 15 mL falcon tube. Non-specific binding was blocked with an equal volume of foetal bovine serum (FBS) for 15 minutes at room temperature. After blocking, samples were centrifuged for 5 minutes at 400 g. Supernatant was discarded and the cells are washed once in 2 mL FACS buffer (See Section 2.13.2). The cell pellet was resuspended in 2 mL FACS buffer and 200 µL of cell suspension was dispersed into a 96 well round bottom plate. The plate was centrifuged at 805 g for 5 minutes, in an Eppendorf 5018R centrifuge. The supernatant was discarded and the pellets were resuspended in 100 µL of appropriate antibody. The plate was incubated at 4°C for 30 minutes. At the end of incubation time, the cells were pelleted, as previously described, and washed 3 times in 200 µL FACS buffer. The cells were fixed in 4 % (v/v) formaldehyde in a final volume of 500 µL per sample. The stained cells were transferred to a labelled FACS tube and stored at 4°C protected from light prior to analysis. Isotype controls for each cell surface marker included, respectively. A minimum of 10,000 events were acquired for each sample on a FACSCalibur flow cytometer (BD Biosciences).

2.12.6 Statistical analysis

Data was pooled and mean values ± 3SE was calculated. A one-way analysis of variance (ANOVA) was performed using JMP 7.0.1 (SAS Institute, Cary, NC). If the ANOVA table was significant (*P < 0.05; ** P < 0.01; *** P < 0.001), post-hoc

analysis was performed using Dunnett's two-tailed test to evaluate the differences between treatment and control groups.

2.13 Generation of immune library for azaspiracid (AZA)

2.13.1 Immunisation of New Zealand white rabbit with azaspiracid-br-cBSA

Immunisation of a New Zealand white rabbit was carried out by the Institute of Agri-Food and Land Use, Queens University, Belfast. The rabbit was immunised with an AZA-br-cBSA conjugate produced in their laboratory. The immunogen was mixed in a 1:1 ratio with montanide ISA 50V adjuvant (Seppic, France) by vortexing and then thickened by passing from one syringe to another connected by a narrow bore Pyrex cylinder. One mL of the resultant emulsion was administered to the rabbit sub-cutaneously over four sites (250 µL each). The rabbit was primarily immunised with 50 µg of immunogen and boosted at four weekly intervals with 50 and 100 µg concentrations. Bleeds were taken at intervals and analysed by direct ELISA. The rabbit was sacrificed and the spleen and two samples of bone marrow from two legs were removed with sterile surgical tools and stored in RNAlater® (Ambion, Applied Biosystems, UK) for transport.

2.13.2 Serum titre of AZA-cBSA –immunised Rabbit by ELISA

In order to determine an immune response against AZA, a bleed was taken, left to coagulate and centrifuged at 18,514 g for 20 minutes to harvest serum. A NUNC™ 96 well plate was coated with 10 µg/mL AZA-KLH conjugate, 10 µg/mL AZA-BTG conjugate, 10 µg/mL KLH and 10 µg/mL BTG, overnight at 4^{o}C. The antigen solution was flicked out from the overnight plate, wells were blocked with 3 % (w/v) Milk Marvel/PBS (150 mM, pH 7.4) solution, 200 µL per well at 37˚C for 1 hour. Following blocking, the plate was washed three times with PBST (150 mM, pH 7.4) and three times with PBS (150 mM, pH 7.4). The immune serum was serially diluted from 10^{-2} to 10^{-7} in 1 % (w/v) Milk Marvel/ 0.01 % (v/v) Tween 20/PBS (150 mM, pH 7.4) and added to the plate. This was incubated for 1 hour at 37^{o}C; following this it was washed as above. 100 µL of a secondary HRP-labelled anti-rabbit polyclonal antibody (Sigma Aldrich, Ireland) at a 1/2,000 dilution in a 1 % (w/v) Milk Marvel/PBS (150 mM, pH 7.4) solution was added to each well. The plate was incubated at 37˚C for 1 hour.

Following incubation, the plate was washed as above and 100 µL 3, 3', 5, 5' tetramethylbenzidine (TMB) substrate solution (Sigma Aldrich, Ireland) prepared in 0.05 M phosphate-citrate buffer, pH 5.0, was added to each well. The plate was then incubated for approximately 20 minutes under tinfoil to allow for colour development after which the reaction was stopped by addition of 50 µL of 10 % (v/v) HCl. The absorbance was then determined at 450 nm with a Tecan™ Safire II plate reader (Tecan™, UK).

2.13.3 Phenol-chloroform extraction of RNA

The spleen and bone marrow were centrifuged for 10 minutes at 2,500 g (Eppendorf 5810R, bucket rotor A-4-62) and all the RNAlater® was removed. All excess fat was trimmed from the spleen. Both bone marrow and spleen were transferred to fresh 'RNase-free' tubes. 10 mL of cold Trizol reagent (Invitrogen, Bio-Sciences) was immediately added and the samples was homogenised at 50 % output for 1 minute. A further 20 mL of Trizol was added after homogenisation. The samples were allowed to stand for 5 minutes at room temperature to allow for the total dissociation of nucleoprotein complexes, while maintaining the integrity of the RNA, before centrifuging at 2,500 g in an Eppendorf 5810R centrifuge (bucket rotor A-4-62) for 20 minutes at 4^{o}C. The supernatant was carefully removed and transferred to a polypropylene tube which had been pre-treated with RNaseZap and rinsed with 'RNase-free' MG-water prior to use. 6 mL of MG-chloroform was added and the samples were vortexed for 15 seconds. This resulted in the separation of the homogenised spleen preparation into an upper aqueous phase (containing RNA) and a lower organic phase (containing DNA and protein). The spleen and bone marrow samples were incubated at room temperature for 15 minutes before centrifugation (fixed angle, pre-cooled Sorval SS34 rotor) at 17,500 g for 20 minutes at 4°C.

The centrifugation produced 3 layers; a lower red phenol/chloroform phase, a protein interphase and a colourless liquid-upper phase with the RNA. The upper aqueous layer was very carefully removed and transferred to a polycarbonate tube. Molecular grade (MG)-isopropanol (15 mL) was added, vortexed for 15 seconds and incubated at room temperature for 10 minutes. The isopropanol precipitated the RNA from solution. The samples were centrifuged for 25 minutes at 4^{o}C and an RNA pellet was formed. The

supernatant was carefully removed and 30 mL of 75 % (v/v) MG-ethanol was added. The samples were centrifuged at 17,000 g for 20 minutes at 4^{o}C and the supernatant was again removed. The pellet was air dried and 500 µL of 'RNase-free' water was used to gently re-suspend the pellet. The samples were stored on ice before immediately proceeding with cDNA synthesis. The spleen and bone marrow RNA samples were quantified using a Nanodrop^{TM} spectrophotometer. Bone marrow RNA (1.47 µg/µL) and spleen RNA (5.1 µg/µL) was sufficient for cDNA synthesis were obtained

2.13.4 cDNA synthesis by reverse transcription

For cDNA synthesis, a Superscript III First Strand Synthesis System for RT-PCR (Invitrogen, Biosciences) kit was used. A total of 5 µg RNA is required for each reaction. Two mixtures are prepared; mixture 1 and mixture 2, which each contain a 20X reaction mixture.

The preparation of each mixture is outlined:

Mixture 1	**1X Reaction**	**20X Reaction**
RNA	Y µL (to give 5 µg)	20X µL
Oligo-$(dT)_{20}$ (50 µM)	1 µL	20 µL
dNTPs (10 mM)	1 µL	20 µL

Mixture 2	**1X Reaction**	**20X Reaction**
10X RT Buffer	2 µL	40 µL
$MgCl_2$ (25 mM)	4 µL	80 µL
DTT (0.1 M)	2 µL	40 µL
RNase OUT (40 U/µL)	1 µL	20 µL
Superscript III RT (200 U/µL)	1 µL	20 µL

Mixture 1 was divided into eight 25 µL aliquots and mixed by vortexing before Stage 1 on the Thermocycler was run, as described below. The tubes were placed on ice for 1 minute and 25 µL Mixture 2 was added and Stage 2 of the program was carried out. RNase H was added at a volume of 1 µL RNase H per 10 µL of reaction mixture. The purpose of RNase H was to digest template RNA from the RNA:cDNA hybrid mix

following cDNA synthesis. After, RNase H addition, Stage 3 of the program is followed. Following synthesis, the reaction mixture was aliquoted and stored at -80^{o}C. cDNA synthesis was carried out using a PX2 thermal cycler using the following PCR program:

Stage	Temperature	Time
Stage 1	65^{o}C	5 minutes
		Pause
Stage 2	50^{o}C	50 minutes
	85^{o}C	5 minutes
		Pause
Stage 3	37^{o}C	20 minutes
	4^{o}C	Hold

2.13.5 Amplification of antibody variable domain sequences using PCR

Bone marrow and spleen cDNA obtained from reverse transcription was used in the first round of polymerase chain reaction (PCR) to amplify the variable heavy and variable light chain genes. The primers were obtained from Eurofins-MWG-Operon. pComb3XSS series primer sequences were obtained from Barbas *et al*. (2001). The various primer combinations for the heavy and light variable chains were assigned abbreviations for convenience.

Variable kappa light chain combinations:

Abbreviation:	Forward:	Reverse:
VK1	RSCVK1	RKB9J10-BL
VK2	RSCVK1	RKB9J0-BL
VK3	RSCVK1	RKB42J0-BL
VK4	RSCVK2	RKB9J10-BL
VK5	RSCVK2	RKB9J0-BL
VK6	RSCVK2	RKB42J0-BL
VK7	RSCVK3	RKB9J10-BL
VK8	RSCVK3	RKB9J0-BL
VK9	RSCVK3	RKB42J0-BL

Variable lambda light chain combinations

Abbreviation:	Forward:	Reverse:
VLλ	RSCλ1	RJλo-BL

Variable Heavy chain combinations

Abbreviation:	Forward:	Reverse:
VH1	RSCVH1	RSCG-B
VH2	RSCVH2	RSCG-B
VH3	RSCVH3	RSCG-B
VH4	RSCVH4	RSCG-B

PCR reactions were carried out using a PX2 thermal cycler using the following PCR program:

Stage	Temperature	Time	No. of Cycles
Stage 1	94^{o}C	10 minutes	1 cycle
Stage 2	94^{o}C	15 seconds	30 cycles
	56^{o}C	30 seconds	
	72^{o}C	60 seconds	
Stage 3	72^{o}C	10 minutes	1 cycle
	4^{o}C	Hold	

The PCR reaction mixture was prepared:

Component	Concentration	50 µL Volume
GoTaq Buffer (5x)	1X	10.0 µL
V_L/V_H Forward Primer	60 pM	0.5 µL
V_H/V_L Back Primer	60 pM	0.5 µL
$MgCl_2$	1.5 mM	3.0 µL
cDNA	0.5 µg	1.0 µL
dNTP	0.2 mM	1.0 µL
H_2O	-	33.75 µL
GoTaq Polymerase	5 U/µL	0.25 µL

2.13.6 PCR optimisation using Phusion® Taq DNA polymerase

For PCR optimisation of variable light chain kappa regions, the high fidelity Phusion® Taq polymerase was required. The PCR program was set up:

Step	Temperature	Time	No. of Cycles
Stage 1	98°C	6 minutes	1 cycle
Stage 2	98°C	15 seconds	30 cycles
	56°C	30 seconds	
	72°C	90 seconds	
Stage 3	72°C	10 minutes	1 cycle
	4°C	Hold	

The PCR reaction mixture was prepared:

Component	Concentration	50 µL Volume
HF Buffer (5x)	1X	10.0 µL
V_L/V_H Forward Primer	60 pM	0.5 µL
V_H/V_L Back Primer	60 pM	0.5 µL
cDNA	0.5 µg	1.0 µL
dNTP	0.2 mM	1.0 µL
H_2O	-	36.8 µL
Phusion® Taq Polymerase	1 U/µL	0.2 µL

2.13.7 SOE-PCR using Platinum® Taq DNA polymerase (High Fidelity)

The variable heavy and variable light (both kappa and lambda) were combined in eqimolar concentrations and used for SOE-PCR. The following overlap PCR primers were used:

RSC-F (sense): 5´ GAG GAG GAG GAG GAG GAG GCG GGG CCC AGG CGG CCG AGC TC 3´
RSC-B (reverse): 5´ GAG GAG GAG GAG GAG GAG CCT GGC CGG CCT GGC CAC TAG TG 3´

The PCR program was set up:

Step	Temperature	Time	No. of Cycles
Stage 1	94°C	2 minutes	1 cycle
Stage 2	94°C	15 seconds	30 cycles
	56°C	30 seconds	
	72°C	2 minutes	
Stage 3	72°C	10 minutes	1 cycle
	4°C	Hold	

The PCR reaction mixture was prepared:

Component	Concentration	50 µL Volume
Buffer (10x)	1X	10.0 µL
$MgSO_4$	2mM	2.0 µL
V_H	100 µg	1.9 µL
V_L	100 µg	2.4 µL
Forward Primer RSC-F	60 pM	0.5 µL
Back Primer RSC-B	60 pM	0.5 µL
dNTP	0.2 mM	1.0 µL
H_2O	-	30.0 µL
Platinum® Taq Polymerase	1 U/µL	0.2 µL
DMSO	3 %	1.5 µL

2.13.8 Plasmid purification using Wizard® Plus SV Miniprep DNA purification system

The *Escherichia coli* strain, ER2925, containing the pComb3XSS plasmid was cultured on a 2xTY agar plate containing carbenicillin (100 µg/mL) and kanamycin (50 µg/mL). A single colony was then taken and inoculated into 10 mL of 2xTY also containing carbenicillin and propagated at 37^{o}C overnight in an orbital shaker. The Wizard® Plus Miniprep DNA purification system (Promega, US) was then used to isolate the pComb3XSS plasmid. A 5 mL of overnight culture was used in the miniprep. Once completed, the product was quantified using the Nanodrop™ and stored at -20^{o}C.

2.13.9 Agarose gel electrophoresis

A 1 % (w/v) agarose gel was prepared by adding 0.5 g of agarose to 50 mL of Tris-Acetate-EDTA (TAE) buffer and heating to 100^{o}C for 2-3 minutes. When the agarose was dissolved and partially cooled, 5 µL of SYBR®Safe DNA gel stain (Invitrogen) was added and poured into a prepared gel mold. DNA loading dye was added to the samples prior to loading along with a 1kb Plus DNA molecular weight ladder (Invitrogen) for size quantification. The gel was run at a voltage of 100V for approximately 40 minutes, viewed using a UV transilluminator Image Master VDS system (Amersham Pharmacia Biotech) and imaged using a Fujifilm Thermal Imaging System FT1-500.

2.13.10 DNA agarose Gel purification using QIAquick ™ gel extraction kit

All the DNA samples were gel-purified using the QIAquick Gel Extraction Kit (Qiagen). DNA was electrophoresed on a 1 % (w/v) agarose gel. The gel was visualised using a Darkreader transilluminator (Clare Chemical Research) and the required bands were excised from the gel with a sterile, sharp scalpel. The QIAquick protocol was followed and concentrations were obtained by measuring the absorbance at 260nm using the Nanodrop™. Samples were stored at -20^{o}C.

2.13.11 Digestion of scFv insert and pComb3XSS vector using the restriction enzyme *Sfi*I

The plasmid DNA and the scFv insert were digested using the *Sfi*I restriction enzyme. Absorbances were measured at 260 nm using the Nanodrop^{TM}. For the SOE insert, digestion was carried at 50^{o}C for 5 hours. The digested product was electrophoresed on a 1.5 % (w/v) agarose gel and subsequently gel-purified, using the QIAquick gel extraction kit. The pComb3XSS vector was digested with *Sfi*I for 5 hours at 50^{o}C. After digestion, the pComb3XSS vector was treated with Antarctic phosphatase (NEB, ISIS) to prevent re-annealing of the vector. The product was electrophoresed on a 0.8 % (w/v) agarose gel and gel-purified.

2.13.12 Ligation of SOE insert into pComb3XSS vector

For ligation of the scFv fragment, T4 DNA Ligase (NEB) was incubated with pComb3XSS and SOE insert in a 2:1 (insert:vector) ratio at room temperature overnight. In addition, ligation controls to check for stuffer contamination and empty vectors were also carried out.

2.13.13 Transformation of XL-1 Blue *E.coli* cells with library ligation

Library ligations were transformed using a Gene Pulser X-cell electroporation system (Bio-Rad, USA). Fifty µL of XL-1 Blue electrocompetent cells (Technopath), which had been previously thawed on ice, was mixed with 5 µL of ligation mix and stored on ice for 1 minute. The samples were then transferred to a pre-chilled electophorator cuvette and electophorated at a voltage of 2.5 kV, a capacitance of 2S µF, a resistance of 200 Ω and in a 2 mm cuvette. The cuvette was immediately rinsed with 1 mL of SOC medium and mixed well. The cells were transferred to a sterile tube containing 2 mL of SOC medium. This was incubated for 1 hour at 37^{o}C and 100 µL of each ligation was plated onto 2xTY agar plates containing carbenicillin (100 µg/mL). The library titre was approximately 1X 10^{7} cfu/mL. The plates were incubated overnight at 37^{o}C and colonies are then analysed using colony-pick PCR. For colony-pick PCR, a single colony was taken and inoculated into 5 µL of molecular grade water.

The PCR amplification was carried out as per protocol in Section 2.6.8, and electrophoresed on a 1 % (w/v) agarose gel.

2.13.14 Antibody selection from immune rabbit scFv library

2.13.14.1 Rescue of rabbit anti-AZA scFv-displaying phage

Five hundred µL of transformed library was inoculated into 400 mL of 2xTY medium (100 µg/mL carbenicillin). The culture was grown at 37^{o}C in and orbital incubator until an OD_{600} of 0.4 was reached. The scFv library was rescued by addition of 400 µL of commercial M13K07 helper phage (NEB), left static at 37°C for 20 minutes and then transferred to a 37^{o}C orbital shaker for 2 hours. Next, kanamycin was added, to a final concentration of 70 µg/mL, before propogating the culture overnight at 37°C.

2.13.14.2 Enrichment of rabbit phage library via bio-panning against immobilised-antigens

A NUNC^{TM} immunotube was coated overnight at 4°C with a 500 µL AZA-BTG in sterile-filtered PBS solution (150 mM, pH 7.4) see Table 2.6.19.1. The immunotube was blocked with 5 % (w/v) Milk Marvel-PBS (150 mM, pH 7.4) for 2 hours. The overnight phage induced scFv library was centrifuged at 3,220 g in a GSM rotor (brake-on) for 15 minutes at 4^{o}C. The phage were then precipitated with 4 % (w/v) PEG and 3 % (w/v) NaCl for 1 hour at 4^{o}C. The PEG-precipitated phage were harvested by centrifugation at 18,514 g in a GSM rotor (brake off) for 20 minutes at 4^{o}C. The pellet was resuspended in 1.5 mL of BTG solution [1 % (w/v) BSA/PBS (150 mM, pH 7.4)] and centrifuged. Subsequently 400 µL of this BTG-phage solution was added to a 100 µL 5 % (w/v) Milk Marvel to a final concentration of 1 % (w/v) milk. Four successive rounds of panning were performed (See Table 2.2.20.1).

Table 2.13.14.1: Panning Protocol for Azaspiracid Library Screening

Variable	PAN 1	PAN 2	PAN 3	PAN 4
Coating concentration of AZA-BTG	100 µg/mL	50 µg/mL	25 µg/mL	12.5 µg/mL
Number of Washes	5 x PBST 5 x PBS	5 x PBST 5 x PBS	5 x PBST 5 x PBS	5 x PBST 5 x PBS
Culture Volume	400 mL	100 mL	100 mL	100 mL
Phage Volume	400 µL	200 µL	200 µL	200 µL

The coated and blocked immunotube was washed once with PBST (150 mM, pH 7.4) and once with PBS (150 mM, pH 7.4). The input is added to the immunotube and left to incubate at 37°C for 2 hours. The immunotube was decanted and washed several times with PBST and PBS (See Table 2.2.20.1) to remove weak-binding phage. Eight hundred µL of 100 mM glycine was added to the immunotube and allowed to stand for 8 minutes. This eluted the phage-scFv antibodies from the surface antigen. After 8 minutes, the contents of the immunotube were added to 66 µL 1 M Tris, to neutralise the antibodies. This was the output of the first round of panning. For re-infection, 200 µL of output from the first round of panning was added into 4 mL of XL1-Blue cells (OD_{600} of approximately 0.5) and allowed to infect for 30 minutes at 37^{o}C. This was plated onto 2xTY plates with 100 µg/mL carbenicillin and incubated overnight at 37^{o}C. Input and output titres are determined by counting the number of colonies and calculating the number of transformants or colony forming units/mL (cfu/mL).

2.13.14.3 Polyclonal phage ELISA

A polyclonal phage ELISA was performed with the output phage from the un-panned library, Pan 1, Pan 2, Pan 3 and Pan 4. A NUNC^{TM} immunosorbent 96 well plate was coated with 10 µg/mL AZA-BTG conjugate in PBS (150 mM, pH 7.4) overnight at 4^{o}C. The antigen solution was flicked out from the plate, wells were blocked with 3 % (w/v) Milk Marvel/PBS (150 mM, pH 7.4) solution, 200 µL per well, at 37˚C for 1 hour. Following blocking, the plate was washed three times with PBST followed by three times with PBS. 100 µL of outputs from each round of panning was then added to the plate. The plate was incubated at 37˚C for 1 hour, following this it was washed as above. One hundred µL of a horse-radish peroxidase (HRP)-labelled anti-M13 antibody was added to each well, diluted 1/1,000 in a 1 % (w/v) Milk Marvel/PBS (150 mM, pH 7.4) solution. The plate was incubated at 37˚C for 1 hour. Following incubation, the plate was washed as above and 100 µL TMB substrate solution (Sigma-Aldrich, Ireland) prepared in 0.05M phosphate-citrate buffer, pH 5.0, was added to each well. The 0.05M phosphate-citrate buffer (Sigma-Aldrich, Ireland) solution was prepared by dissolving one tablet in 100 mL deionised water. The plate was then incubated for approximately 20 minutes under tinfoil to allow for colour development after which the reaction was stopped with 50 µL of 10 % (v/v) HCl. The absorbance was then determined at 450 nm with a Tecan™ Safire plate reader (Tecan™, UK).

2.13.14.4 Re-infection into Top10F' cells and scFv check via colony-pick PCR

For soluble expression, the output phage from Pan 4 was re-infected into *E. coli* Top10F′. For re-infection, 200 µL of Pan 4 output was added into 4 mL of Top10F′ cells (OD_{600} of approximately 0.5) and allowed to infect for 30 minutes at 37^{o}C. This was plated onto 2xTY plates with 100 µg/mL carbenicillin and incubated overnight at 37^{o}C. Individual colonies were selected from pan 4 agar plates, inoculated in 50 µL sterile water and incubated for 10 minutes at 95^{o}C to facilitate cell lysis. This mixture was then used as template DNA in the PCR protocol outlined in Section 2.6.8. The product was electrophoresed on a 1 % (w/v) agarose gel to check for the presence of scFv insert fragments.

2.13.14.5 Direct monoclonal ELISA of solubly-expressed scFv fragments

Single colonies, with one colony per well, from pan 4 Top10F′ re-infection plates, were inoculated into sterile non-absorbent 96 well plates, containing 200 µL of 2xTY and 100 µg/mL carbenicillin. These plates were grown at 37^{o}C in an orbital incubator overnight. Sixty µL of 50 % (v/v) glycerol was added to each well, to give a final concentration of 20 % (v/v) and this plate was stored at -80^{o}C as stock. A fresh 96 well plate was prepared by adding 170 µL of super broth (SB) with 100 µg/mL carbenicillin to each well. A 30 µL culture taken from the stock plate was aseptically transferred to inoculate the fresh plate. This was incubated at 37˚C in an orbital incubator and once growth was observed, 50 µL of a 5 mM IPTG solution was added, to give a final concentration of 1 mM IPTG, and incubated at 30˚C overnight in an orbital incubator. The next day, the plates were removed from the incubator and centrifuged at 3,220 g (Eppendorf centrifuge 5018R) for 10 minutes. The pellets were resuspended in 100 µL sterile MG water. The plate was freeze-thawed to facilitate cell lysis, by incubating at -80^{o}C for 15 minutes, then 37^{o}C for 15 minutes and this was repeated 3 times. The plate was centrifuged (Eppendorf centrifuge 5018R) at 3,220 g for 10 minutes and 100 µL of the supernatant was used for ELISA analysis.

Simultaneously, 96 well ELISA plates (Maxisorp™, NUNC™) were coated with AZA-BTG and AZA-KLH conjugates in PBS solution (150 mM, pH 7.4) (50 µL per well) and incubated overnight at 4°C. The following day, the antigen-coated plate was blocked with a 3 % (w/v) Milk Marvel-PBS (150 mM, pH 7.4) solution (200 µL per well) for 1 hour at 37°C. The culture supernatant was then added, at 100 µL per well, to the coated and blocked ELISA plate and incubated at 37°C for 1 hour. Following incubation, the plates were washed three times with PBST (150 mM, pH 7.4) and three times with PBS (150 mM, pH 7.4), to remove any unbound scFv. Binding was detected using a 1/2,000 dilution of an anti-rabbit, HRP-labelled, secondary antibody (Sigma Aldrich, Ireland). After 1 hour at 37°C, 100 µL of TMB was added and the reaction was left to develop for 20 minutes at 37°C. The reaction was stopped with 50 µL per well of 10 % (v/v) HCl, after which the plate was measured at 450 nm on a Safire II plate reader (Tecan™).

2.13.15 Conjugation of AZA-2 to protein carriers, BTG and KLH

For the conjugation of AZA-2 to Haemocyanin from *Megathura crenulata* (keyhole limpet) (KLH) (Sigma-Aldrich, Ireland), 0.05 mg toxin material was reacted with 8.5 mg of KLH protein via reactive amine group coupling. The N-hydroxysuccinimide (NHS) ester group reacts with the amine of lysine (κ) residues to produce a stable amide bond. Firstly, DCC (dicyclohexylcarbodiimide) was used to activate the amine groups on the KLH protein. Subsequently 50 µL DMSO and 50 µL pyridine were added to 50 µg AZA-2 on ice. After which 1.22 µL of 15 mg/mL DCC was prepared in pyridine, was added to the AZA-2 mixture and incubated further for 10 minutes, while stirring on ice. Next, a 0.7 µL solution of 15 mg/mL NHS (N-hydroxysuccinimide) that was prepared in pyridine, was added and stirred for 30 minutes. The process of DCC and NHS addition was then repeated and incubated for 30 minutes. The reaction was incubated overnight at 4^{o}C, while stirring. The next day, the reaction was stirred for 4 hours at room temperature, followed by removal of all solvents, except DMSO, using a Speedvac for 1 hour. A 28 mg/mL KLH solution was prepared with 0.05M potassium phosphatase di-basic (pH 8.2) in a final volume of 300 µL. The reaction was stirred slowly on ice, followed by the addition of 50 µg of the toxin ester. The reaction was stirred overnight at 4^{o}C. A Vivaspin molecular weight cut-off (MWCO) 5,000 column (Sartorius, Sarstedt) was used for buffer exchange and to concentrate the final product to a final volume of 2 mL in sterile-filtered PBS (150 mM, pH 7.4). The estimated concentration of this product was 4 mg/mL. This was stored at 4^{o}C.

For the conjugation of AZA-2 to bovine thyroglobulin (BTG) (Sigma Aldrich, Ireland), 0.15 mg toxin material was reacted with 2 mg of KLH protein via amine group coupling. Firstly, 15 mg/mL solutions of NHS and DCC were prepared in pyridine and sequentially added to the AZA-2 as before, this time with volumes of 2.1 µL NHS and 3.66 µL DCC. The reaction was incubated for 30 minutes and stirred overnight at 4^{o}C. The following day, the reaction was stirred at room temperature for 4 hours. A Speedvac was used for 1 hour to remove the solvents. A 10 mg/mL solution of BTG was prepared in 200 µL 0.05M potassium phosphate di-basic (pH 8.2). This was added to the toxin ester and stirred on ice for 2 hours. The reaction was again stirred overnight at 4^{o}C.

A Vivaspin MWCO 5,000 column (Sartorius, Sarstedt) was used for buffer exchange and to concentrate the final product to a final volume of 2 mL in sterile-filtered PBS (150 mM, pH 7.4). The estimated concentration of the conjugated product was 1 mg/mL.

2.13.16 Immunisations of Leghorn chicken with AZA-KLH conjugate

Prior to immunisation, a pre-bleed was taken from a female Leghorn chicken. The immunogen, AZA-KLH, was prepared in a final volume of 1 mL in a 1:1 ratio with Freund's complete adjuvant (Sigma Aldrich, Ireland) for the primary immunisation and Freund's incomplete adjuvant (Sigma Aldrich, Ireland) for subsequent immunisations. The immunogen was vortexed for 1 hour before immunisation to create a stable emulsion. 1 mL of the emulsion was administered to the chicken subcutaneously over four sites (250 µL each). For the primary immunisation, the animal was injected with 100 µg AZA-KLH and for subsequent boosts, 50 µg AZA-KLH was used. A period of three weeks was left between each immunisation. A bleed was taken only after the third boost to determine the level of immune response.

2.13.17 Pre-concentration and immobilisation of AZA-transferrin onto a CM5 chip

An AZA-transferrin conjugate (100 µL) was obtained from QUB at a 1 mg/ml concentration. Before immobilisation, a pre-concentration study was carried out to determine the optimal pH at which to immobilise the conjugate on the negatively charged dextran surface of a CM5 sensor chip surface. A pre-concentration study was performed using 10mM sodium acetate solution ranging from pH 3.8 to 5. The solutions were pH adjusted using 10 % (v/v) acetic acid solution. The AZA-transferrin conjugate was diluted at each respective pH to a final concentration of 20 µg/mL and sequentially passed over an un-activated carboxymethylated dextran sensor chip surface at a flow rate of 5 µL/minute. The pH showing the greatest degree of pre-concentration, shown by the highest response unit (RU) value and the sharpest slope was chosen as the buffer for immobilisation. The optimal condition was at a pH of approximately 4.0. An attempt was also made to immobilise the AZA-BTG conjugate (Prepared by QUB) on a CM5 chip but change in response was observed at the pre-concentration stage.

The carboxymethylated dextran matrix on the sensor chip was activated by mixing equal volumes of 100 mM NHS and 400 mM EDC (N-ethyl-N-(dimethyl-aminopropyl) carbodiimide hydrochloride) and injecting the mixture over the sensor chip surface at a flow rate of 5 µL/minute. The AZA-transferrin conjugate was diluted in 10 mM sodium acetate, pH 4.0, to a concentration of 20 µg/mL. This solution was then injected over the activated chip surface at a flow rate of 5 µl/minute. A 1M ethanolamine hydrochloride solution (pH 8.5) was injected, resulting in both capping of any un-reacted active groups and removal of loose non-covalently attached proteins. Finally, loosely bound material was further removed using two pulses of 5 mM NaOH.

2.13.18 Direct binding analysis on Biacore™ 3000 using an AZA-transferrin chip

Dilutions of serum from rabbit R922 (AZA-cBSA-immunised) were prepared in sterile HBS buffer, ranging from 1 in 2 to 1 in 1,000. There dilutions were passed over the AZA-transferrin-immobilised surface at a flow rate of 5 µL/minute for 20 minutes. A 20 % (v/v) acetonitrile solution was used for regeneration of the sensor chip surface.

2.14 Generation, screening and selection of chicken scFv library for microcystin

2.14.1 Derivatisation and protein conjugation of microcystin-LR

2.14.1.1 Preparation of aminoethanethiol-microcystin-LR

Derivatisation of microcystin-LR was carried out according to Moorhead *et al*. (1994). Microcystin-LR (2 mg) was dissolved in ethanol (500 µL) and added to a degassed solution of water (750 µL), DMSO (1 mL), 5 N NaOH (335 µL) and aminoethanethiol (500 µL, 1 mg/mL). The reaction mixture was incubated at 50ºC for 30 minutes under argon. The solution was cooled and glacial acetic acid (3 mL) was added. 0.1 % (v/v) TFA in water (24 mL) was added and the pH adjusted to 1.5 with TFA (approximately 250 µL). The resultant solution was applied to a solid-phase C_{18} cartridge (Supelco, 52606-U, DSC-18) previously equilibrated with 0.1 % TFA (v/v) /H_2O according to the supplier's instructions. The column was washed with 10 % (v/v) acetonitrile/0.1 % (v/v) TFA water and the aminoethanethiol-Microcystin-LR eluted with 100 % (v/v) acetonitrile/0.1 % (v/v) TFA. Volatile solvent was removed by rotary evaporation and the remaining aqueous solution lyophilised overnight to give a glassy solid.

2.14.1.2 HPLC analysis of aminoethanethiol-microcystin-LR

At the end of the above reaction period and prior to work up, the reaction mixture was analysed by reverse-phase high-performance liquid chromatography (HPLC) (Vydac 218TP54, 4.6 mm x 250 mm) employing a helium-degassed acetonitrile gradient of 5-95 % (v/v) acetonitrile (containing 0.1 % (v/v) TFA: water) run at 1.5 mL/minute and monitored spectrophotometrically at 230 nm (Figure 2.14.1.1 A). Consistent with Moorhead G., *et al* (1994), the reaction mixture showed conversion of starting material to >95 % of a single product peak, which did not co-elute with a spiked sample of MC-LR (Figure 2.14.1.1 B).

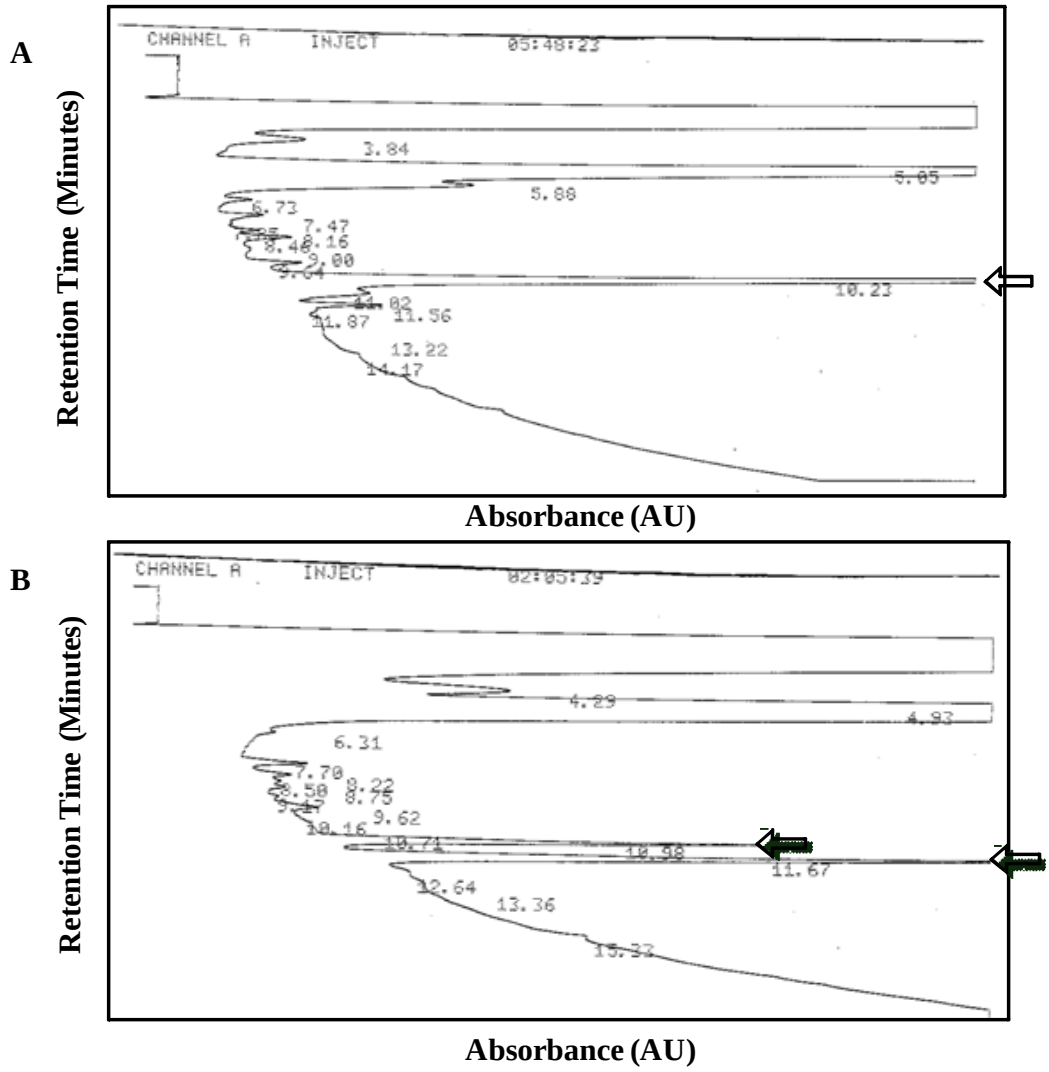

Figure 2.14.1.1: Reverse Phase HPLC analysis carried out by Enzo Life Sciences Ltd. A.) Analysis to verify presence of derivitised aminoethanethiol-MC-LR. The eluted peak at 10.23 minutes demonstrated the aminoethanethiol-derivatised MC-LR. The additional peaks are by-products of the derivitisation reaction B.) Analysis of aminoethanethiol-MC-LR with a spiked sample of un-derivatised microcystin-LR. The derivative at 10.23 minutes remained, with an additional peak at 11.67 minutes, corresponding to un-derivatised MC-LR. Conditions: Vydac 218TP54, (4.6 mm x 250 mm), helium-degassed acetonitrile gradient of 5-95 (v/v) % acetonitrile: water (with 0.1 (v/v) % TFA). The run was carried out at 1.5 mL/minute and monitored spectrophotometrically at 230 nm.

2.14.1.3 Preparation of microcystin-LR-aminoethanethiol-BSA conjugate

Aminoethanethiol-derivatised Microcystin-LR (~1 mg), as prepared in Section 3.2.1.1, was conjugated to bovine serum albumin (BSA) (~3 mg) using a one step glutaraldehyde coupling procedure
as outlined by Metcalf *et al*. (2000). The resultant conjugate was dialysed against 0.9 % (w/v) saline and supplied in a quantity of 1.2 mL at a concentration of ~2.5 mg BSA per mL.

2.14.1.4 Preparation of microcystin-LR-aminoethanethiol-OVA conjugate

Aminoethanethiol-derivatised Microcystin-LR (~1 mg) was conjugated to ovalbumin (OVA) (~3 mg) using a one step glutaraldehyde coupling procedure as outlined by Metcalf *et al*. (2000). The resultant conjugate was dialysed against 0.9 % (w/v) saline and supplied (Enzo Life Sciences, USA) in a quantity of 1.2 mL at a concentration of ~2.5 mg OVA per mL.

2.14.2 Immunisation of Leghorn chicken with microcystin-LR BSA conjugate

A female Leghorn chicken was immunised over a period of 12 weeks at 3 weekly intervals, with 500 µg microcystin–LR conjugated to bovine serum albumin (BSA). The injections were mixed and emulsified by vortexing in a 1:1 ratio with Freund's Complete Adjuvant (FCA) for the primary immunisation and with Freund's Incomplete Adjuvant (FIA) for each subsequent immunisation. The emulsions were administered to the chicken sub-cutaneously over four sites in a total volume of 1 mL. Bleeds were taken at three week intervals to determine the immune response of the animal. The chicken was sacrificed and the spleen and two samples of bone marrow from two legs were removed with sterile surgical tools in preparation for RNA extraction.

2.14.3 MC-LR-BSA chicken scFv library construction

2.14.3.1 RNA extraction and cDNA synthesis

Extraction from bone marrow and spleen samples was carried out, as described in Section 2.13.3, and cDNA was synthesised as described in Section 2.13.4.

2.14.3.2 Amplification of antibody variable domain sequences using PCR

To amplify the V gene rearrangements from the immunised chicken, one V_H amplification and one V_L (λ) amplification were performed. The following PCR primers were used:

V_H Primers

CSCVHo-F (sense) 5′ GGT CAG TCC TCT AGA TCT TCC GCC GTG ACG TTG GAC GAG 3′

CSCG-B (reverse) 5′ CTG GCC GGC CTG GCC ACT AGT GGA GGA GAC GAT GAC TTC GGT CC 3′

V_L Primers

CSCVK (sense) 5′ GTG GCC CAG GCG GCC CTG ACT CAG CCG TCC TCG GTG TC 3′

CKJo-B (reverse) 5′ GGA AGA TCT AGA GGA CTG ACC TAG GAC GGT CAG G 3′

For PCR optimisation of the V_H and V_L regions, a $MgCl_2$ concentration gradient was required. The PCR program was set up:

Step	Temperature	Time	No. of Cycles
Stage 1	94°C	10 minutes	1 cycle
Stage 2	94°C	15 seconds	30 cycles
	56°C	30 seconds	
	72°C	60 seconds	
Stage 3	72°C	10 minutes	1 cycle
	4°C	Hold	

The PCR reaction mixtures were prepared:

Component	Concentration	50 µL Volume
GoTaq® Flexi Reaction Buffer (5x)	1X	10.0 µL
V_L/V_H Forward Primer	60 pM	0.5 µL
V_L/V_H Back Primer	60 pM	0.5 µL
cDNA	0.5 µg	1.0 µL
dNTP (10 mM)	0.2 mM	1.0 µL
$MgCl_2$ and H_2O Mix	-	36.75 µL
GoTaq® Flexi DNA Polymerase	1 U/µL	0.25 µL

Final $MgCl_2$ conc./ per reaction	1.5 mM	2 mM	3 mM	4 mM
Volume of $MgCl_2$ (µL)	3	4	6	8
Volume H_2O (µL)	33.75	32.75	30.75	28.75

The reaction was repeated in large-scale, using an optimised $MgCl_2$ concentration of 3 mM for both V_H and V_L fragments. The products were ethanol-precipitated by adding a 0.1X volume of 3M sodium acetate, pH 5.2, a 10X volume of 100 % (v/v) ice-cold ethanol and 1 µL glycogen, and stored at -20°C overnight. The following day, the DNA was harvested by centrifuging at 18,514 g for 30 minutes. Subsequently, the ethanol supernatant was decanted and the pellet was washed with 70 % (v/v) ethanol and centrifuged for 10 minutes (18,514 g) at 4°C. The pellet was allowed to air-dry briefly and then gently dissolved in 5 µL of molecular grade H_2O. This product was gel-purified from a 1 % (w/v) agarose gel, using a QiaQuick Gel Extraction Kit (Qiagen) (See Section 2.13.10).

2.14.3.3 SOE-PCR using High Fidelity Platinum® Taq DNA polymerase

The purified V_H and V_λ fragments were used for SOE-PCR. The following overlap PCR primers were used:

CSC-F (sense) 5´ GAG GAG GAG GAG GAG GAG GTG GCC CAG GCG GCC CTG ACT CAG 3´
CSC-B (reverse) 5´ GAG GAG GAG GAG GAG GAG GAG CTG GCC GGC CTG GCC ACT AGT GGA GG 3´

The PCR program was set up:

Step	Temperature	Time	No. of Cycles
Stage 1	94°C	2 minutes	1 cycle
Stage 2	94°C	15 seconds	30 cycles
	56°C	30 seconds	
	72°C	2 minutes	
Stage 3	72°C	10 minutes	1 cycle
	4°C	Hold	

The PCR reaction mixture was prepared:

Component	Concentration	50 µL Volume
HF Buffer (10X)	1X	10 µL
$MgSO_4$	2 mM	2 µL
V_H	100 µg	0.34 µL
V_L	100 µg	0.23 µL
CSC-F	60 pM	0.5 µL
CSC-B	60 pM	0.5 µL
10 mM dNTP	0.2 mM	1.0 µL
H_2O	-	33.73 µL
High Fidelity Platinum® Taq	1 U/µL	0.2 µL
DMSO	3 %	1.5 µL

The approximately 750 bp fragment from this reaction was ethanol-precipitated and purified on a 1 % (w/v) agarose gel, using a QiaQuick gel extraction kit (Qiagen).

2.14.3.4 Digestion of scFv insert and pComb3XSS vector using *Sfi*I

The *Sfi*I restriction enzyme allows for unidirectional cloning of the scFv fragment library into the pComb3XSS vector. The enzyme recognises 8 bases which are interrupted by 5 random nucleotides (5′ ggccnnnnnggcc 3′), thus eliminating internal digestion in antibody sequences.

Digests of the scFv insert and pComb3XSS vector were prepared as follow:

Component	150 µL Volume
SOE product (50 µg)	74.63 µL
10X Buffer 2	15 µL
100 X BSA	1.5 µL
H_20	43.87 µL
***Sfi*I (6 U/ µg)**	15 µL

Component	50 µL Volume
pCom3xSS vector (20 µg)	3.7 µL
10X Buffer 2	5 µL
100 X BSA	0.2 µL
H_20	25.1 µL
***Sfi*I (16 U/ µg)**	16 µL

Digestions were incubated for 5 hours at 50^{o}C. Both digests were separated by electrophoresis on a 1 % (w/v) agarose gel and gel-purified, as described.

2.14.3.5 Treatment of pComb3XSS vector with antarctic phosphatase

In order to prevent pComb3XSS vector re-ligation without insert, the digested vector was treated with Antarctic phosphatase (NEB). Antarctic phosphatase (AP) causes the removal of 5´ phosphate groups from DNA. Since DNA fragments treated with AP lack the 5´ phosphate group needed by ligase, they cannot self-ligate. This would potentially decrease vector background in cloning. The reaction was prepared as follows:

Reagent	Volume
Antarctic phosphatase buffer	20 µL
Restricted pComb3XSS vector	200 µL
Antarctic phosphatase	16 µL

The reaction was incubated for 25 minutes at 15^{o}C and the enzyme was de-activated for 5 minutes at 65^{o}C.

2.14.3.6 Ligation of SOE insert into pComb3XSS vector

The restricted scFv fragment library was ligated into the pComb3XSS vector in a 2:1 (insert:vector) ratio under the conditions below and incubated overnight at room temperature.

Component	200 µL Volume
10X Ligase buffer	20
Digested pComb3XSS vector (1.4 µg)	3.4
Digested SOE insert (700 ng)	7.5
H_2O	159.1
T4 DNA Ligase (400 U/ µL)	10

The ligations were ethanol-precipitated, as described in Section 3.2.3.2.

2.14.4 Phage screening from a microcystin-specific immune library

2.14.4.1 Library transformation and rescue of chicken scFv-displaying phage

The ethanol-precipitated library ligations were centrifuged for 20 minutes at 4^{o}C at 18,514 g. The resulting pellets were washed twice with 1 mL 70 % (v/v) EtOH and dried briefly. The pellets were resuspended in 10 µL sterile MG H_2O and stored on ice. Commercial electro-competent *E.coli* XL1-Blue cells (Stratagene) were thawed on ice. 100 µL of cells were added to each library ligation and pipetted up and down. This was stored on ice for 1 minute. Electro-cuvettes (Bio-Rad®) were pre-chilled prior to transformations. The ligation:cell mixture was electroporated at 2.5 kV, 25 µF and 200 Ω using a Bio-Rad® electrophorator. The electro-cuvette was washed with 1 mL pre-warmed SOC media and transferred to 15 mL tubes, containing 3 mL SOC media. This was followed by incubated for 1 hour at 37^{o}C in an orbital shaker. Serial dilutions of the transformed library were prepared, from 10^{-1} to 10^{-8} and 100 µL was plated onto LB agar plates, containing carbenicillin (100 µg/mL), which were incubated at 37^{o}C overnight. The total transformants was the number of colonies, multiplied by the culture volume (25 mL) and divided by the plating volume (0.1 mL).

The library was transferred to a flask containing 600 mL 2xTY with 100 µg/mL carbenicillin and 20 µg/mL tetracycline and the cells were grown to an optical density (OD) of 0.6. 1 mL of $1X10^{11}$ pfu/mL M13KO7 helper phage (NEB) was added and the culture was incubated stationary at 37°C for 30 minutes. The culture was then propagated at 37°C for 2 hours in an orbital shaker. Subsequently, 50 µg/mL kanamycin was added and the culture was propagated overnight at 30°C. The overnight phage library was centrifuged at 10,414 g in a GSA rotor (brake off) for 20 minutes. The phage supernatant was transferred to 250 mL sorval tubes. Phage were precipitated by addition of PEG (4 % w/v) and NaCl (3 % w/v), dissolved in an orbital shaker for 20 minutes at 37°C and placed on ice for 30 minutes. The precipitated phage were centrifuged at 10,414 g in a GSA rotor (brake off) for 15 minutes at 4°C. The supernatant was discarded and the phage pellet dried by inversion for 10 minutes. The pellet was resuspended thoroughly in 2 mL 1 % (w/v) BSA/PBS (150 mM, pH 7.4) and transferred to a 2 mL microcentrifuge tube. The solution was centrifuged (Herlme Microlitre centrifuge Z 233 M-2) at 15,000 g for 5 minutes to remove debris and 0.02 % (w/v) sodium azide was added before storage at 4°C.

2.14.4.2 Enrichment of chicken phage library by bio-panning

The overnight phage library was centrifuged at 10,414 g (brake off) for 20 minutes. The phage supernatant was transferred to an 85 mL Nalgene® centrifuge tubes and PEG (4 % w/v) and NaCl (3 % w/v) added. The tubes were shaken for 20 minutes at 37°C to dissolve the PEG and NaCl, after which the tubes were placed on ice for 30 minutes. Subsequently, phage were precipitated by centrifuging at 10,414 g (brake off) for 15 minutes at 4°C. The supernatant was discarded and the resulting pellet dried on tissue. The pellet was re-suspended thoroughly in 2 mL of 1 % (w/v) BSA/PBS (150 mM, pH 7.4) and transferred to a 2 mL micro-centrifuge tube. The solution was centrifuged (Herlme Microlitre centrifuge Z 233 M-2) at 15,000 g for 5 minutes at 4°C, after which the supernatant was transferred to a fresh micro-centrifuge tube with 0.02 % (w/v) sodium azide and the solution stored at 4°C. An immunotube (Nalgene®) was coated overnight with MC-LR-OVA, according to coating concentrations specified in Table 3.2.3.1. The next day, the tube was blocked with 3 % (w/v) BSA/PBS (150 mM, pH 7.4) for 1 hour at 37°C. The immunotube was washed in PBS / 0.05 % (v/v) Tween 20. 1 mL of phage library, as prepared in Section 2.14.4.1, was placed in the immunotube

and incubated, rotating, for 2 hours at room temperature. The unbound phage were then carefully removed and the immunotube was washed, as specified in Table 2.14.4.1. One mL of 10 mg/mL trypsin, prepared in PBS (150 mM, pH 7.4) was added in the immunotube for 30 minutes at 37^{o}C, followed by vigorous pipetting. A total of 800 µL of output phage were re-infected into a 5 mL XL-1 Blue culture, with an OD_{600} of 0.6, and incubated static for 15 minutes at room temperature. The phage-infected culture was added to 6 mL of warm SB media containing 1.6 µL 100 mg/mL carbenicillin and 12 µL 5 mg/mL tetracycline, and incubated for 1 hour at 37^{o}C in and orbital shaker. A further 4 µL of 100 mg/ml carbenicillin was added and incubated for an additional 1 hour at 37^{o}C. M13K07 helper phage (800 µL, NEB) was added to the culture and this helper phage-infected culture was then added to 88 mL warm SB media, containing 46 µL carbenicillin and 184 µL tetracycline. The culture was propagated for 2 hours at 37^{o}C. Subsequently, 140 µL 50 mg/ml kanamycin was added and incubated overnight at 37^{o}C in an orbital shaker.

Output titres were prepared by preparing dilutions of the phage output in XL-1 Blue and plating on 2xTY agar plates, containing 100 µg/mL carbenicillin. Input titres were made by preparing dilutions of input phage in SB media and re-infecting into XL1-Blue cells (OD_{600} of 0.6) for 15 minutes at room temperature. These re-infected cultures were then plated and all plates were incubated at 37°C overnight.

Table 2.14.4.1: Panning Protocol for Microcystin Library Screening

Variable	PAN 1	PAN 2	PAN 3	PAN 4	PAN 5
Coating Concentration	100 µg/mL	50 µg/mL	25 µg/mL	10 µg/mL	5 µg/mL
Number of Washes	5 x PBST 5 x PBS	5 x PBST 5 x PBS	10 x PBST 10 x PBS	15 x PBST 15 x PBS	15 x PBST 15 x PBS
Culture Volume	600 mL	100 mL	100 mL	100 mL	100 mL

2.14.4.3 Analysis of anti-microcystin scFvs by soluble monoclonal ELISA

For re-infection and soluble expression, 200 µL of Pan 5 output was added into 4 mL of *E. coli* Top10F′ cells (OD_{600} of approximately 0.5) and allowed to infect for 30 minutes at 37°C. This was plated onto 2xTY plates with 100 µg/mL carbenicillin and incubated overnight at 37°C. Individual colonies were picked from these plates and analysed by colony-pick PCR, as described in Section 2.13.14.4. A large number of single colonies (384) were picked, solubly expressed and incorporated into a direct ELISA to identify scFv fragment binding. The picked clones were grown overnight in an orbital incubator at 37°C in 96 well plates, containing 100 µL 2xTY media with 100 µg/mL carbenicillin. These stock plates were then sub-cultured into 180 µL SB media, containing 100 µg/mL carbenicillin and glycerol was added to the stock plates to a final concentration of 15 % (v/v) and stored at -80°C

The sub-cultured plates were incubated at 37°C in an orbital incubator until an OD_{600} of ~0.6 was reached. Expression was then induced by addition of IPTG at a final concentration of 1 mM and incubating at 30°C in an orbital incubator. In addition, 96 well ELISA plates (Maxisorp™, NUNC™) were coated with 5 µg/mL microcystin-OVA in PBS solution (150 mM, pH 7.4) (50 µL per well) and incubated overnight at 4°C. The following day, the antigen-coated plate was blocked with a 3 % (w/v) Milk Marvel-PBS (150 mM, pH 7.4) solution (200 µL per well) for 1 hour at 37°C. Meanwhile, the overnight expression plates were freeze-thawed for the production of scFv-enriched lysate. The plates were placed at -80°C until frozen and then thawed at 37°C. This step was repeated a total of 3 times. The plates were then centrifuged at 3,220 g (Eppendorf™ Centrifuge 5810 R) for 15 minutes to isolate the scFv-enriched lysate supernatant. The resulting supernatant was then added, at 100 µL per well, to the coated and blocked ELISA plate, and incubated at 37°C for 1 hour. Following incubation, the plates were washed three times with PBST (150 mM, pH 7.4) and three times with PBS (150 mM, pH 7.4), to remove any unbound scFv. Binding was detected using a 1/2,000 dilution of an anti-chicken, HRP-labelled, secondary antibody (Sigma Aldrich, Ireland). After a one hour incubation at 37°C, 100 µL of TMB was added and the reaction was left to develop for 20 minutes at 37°C. The reaction was stopped with 50 µL per well of 10 % (v/v) HCl, after which the absorbance of the wells was measured at 450 nm on a Safire II plate reader (Tecan™).

2.14.4.4 Analysis of anti-microcystin scFvs by competition ELISA

Fresh 'scFv-rich' lysate was prepared from 10 mL cultures, as described in Section 3.2.5. A 96 well ELISA plate was coated overnight at 4^{o}C with 5 µg/mL microcystin conjugate or carrier alone (50 µL per well). The plate was blocked with 3 % (w/v) Milk Marvel-PBS (150 mM, pH 7.4) solution (200 µL per well) for 1 hour at 37°C. The scFv-enriched lysate from each clone was incubated on the coated plate with varying concentrations of free microcystin-LR (1,000 to 3.9 ng/mL) for 1 hour at 37^{o}C (100 µL per well). The scFvs ability to bind free microcystin was then determined by comparison of the absorbance response (A) to A_0. The A_0 represents the absorbance of the same lysate without free toxin. The captured avian scFv was detected using an anti-HA monoclonal antibody (HRP-labelled). After each stage, the ELISA plate was washed three times with PBST (150 mM, pH 7.4) and three times with PBS (150 mM, pH 7.4). Binding was detected using TMB substrate, stopped with 10 % (v/v) HCl and measured at 450 nm with a Safire II plate reader.

2.14.5 Restriction digestion profiling

Restriction digestion was carried out on the amplified SOE product with the enzyme, *Alu*I. The amplified SOE products were obtained by carrying out a colony-pick PCR, as described in Section 2.13.14.4, using the chicken overlap extension primers (CSC-F and CSC-B). The PCR amplified SOE product was digested with the frequent cutting enzyme, *Alu*I for 2 hours at 37^{o}C, using the following conditions:

Components	Total 20 µL volume
10x buffer 2	2 µL
SOE product	8 µL
*Alu*I enzyme	0.5 µL
100 X BSA	0.2 µL
Water	9.3 µL

The digestion products were electrophoresed on a 1 % (w/v) agarose gel and visualised using a UV light box.

2.14.6 Large-scale production of anti-microcystin scFvs and purification using immobilised metal affinity chromatography

Overnight cultures of the 2 selected clones, 2H1 and 2G1, were grown in 10 mL SB media, containing 100 μg/mL carbenicillin, by inoculating a single colony from a stock plate and growing overnight at 37°C in an orbital shaker. Five mL of this overnight culture was then inoculated into 500 mL fresh SB media containing 100 μg/mL carbenicillin. The sub-cultured clones were incubated at 37°C in and orbital incubator until an OD_{600} of approximately 0.6 to 0.8 was reached. The cultures were then induced by addition of IPTG to a final concentration of 1 mM and incubating at 30°C before propagating overnight. The overnight-expressed culture was transferred into sterile 50 mL tubes and centrifuged at 3,220 g for 30 minutes (Eppendorf 3810R), to pellet the bacterial cells. The supernatant was discarded and the excess media removed by inversion of the 50 mL tube onto a paper towel. The cell pellet was thoroughly resuspended in 5 mL of lysis buffer (Table 4.2.1.1) and put on ice. The sample was kept on ice and sonicated at an amplitude of 40 % for 6 second pulses for 3 minutes using a microtip Vibra Cell™ sonicator. The cell extract was centrifuged (Herlme Microlitre centrifuge Z 233 M-2) at 15,000 g for 20 minutes at 4°C, in order to remove cell debris. The lysate supernatant was then passed through a 0.2 μM filter to remove any residual cell debris.

Purification of scFv fragments using immobilised metal affinity chromatography (IMAC) was carried out using Ni^{+}-NTA agarose resin (Novagen). Two mL of Ni^{+}-NTA agarose resin was added to a 20 mL column and allowed to settle for 10 minutes. The column was equilibrated using 4 mL of lysis buffer (Section 2.2.4). The filtered lysate was passed through the column. The 'flow-through' was collected and passed through the column twice more. A 100 μL sample of this flow-through was kept for analysis on SDS-PAGE gel. The column was washed once with 8 mL wash buffer A (Section 2.2.4) and twice with 8 mL wash buffer B (Section 2.2.4) to remove any loosely bound non-specific proteins. The wash fractions were collected for SDS-PAGE analysis. The protein was eluted with 10 mL of elution buffer (Section 2.2.4) and twenty 0.5 mL fractions were collected in 1.5 mL tubes. The protein concentration of each fraction was measured at 280 nm using the Nanodrop™ ND-1000. The fractions containing a sufficient quantity of protein were pooled and thoroughly buffer exchanged against 20

mL filter-sterilised PBS (150 mM, pH 7.4) using a 5 kDa molecular weight 'cut-off' Vivaspin™ 6 column (AGB). The buffer exchanged scFv was again quantified using the Nanodrop™ ND-1000, aliquoted and stored at -20°C.

2.14.7 Size-exclusion chromatography of IMAC-purified scFvs

To separate affinity-purified scFv molecules from dimers and higher aggregates, and to control stability of separated monomers, size exclusion chromatography was performed. A HiLoad™ Superdex 200 16/60 column (GE Healthcare Ltd) was equilibrated with three column volumes of PBS (150 mM, pH 7.4) at a flow rate of 2 mL/minute. A 1 mL sample of concentrated antibody was passed through a 0.2 µm filter and manually injected onto the 2 mL loop. Size exclusion was carried out on a AKTA™ FPLC system (GE Healthcare Ltd) using an pre-programmed method running on UNICORN™ control software. A typical scFv size exclusion run was carried out at a flow rate of 0.5 mL/minute with sterile filtered (0.2 µM), degassed PBS (150 mM, pH 7.4). Fractions of 5 mL were automatically collected using a fraction collector (Frac-950). The system and column was cleaned between runs using distilled water and 20 % (v/v) ethanol.

2.14.8 Size determination of scFv by size-exclusion chromatography

A set of protein standards (Phenomenex Ltd.) was utilised to determine the exact molecular weight of the scFv molecule through comparison with the known molecular weights of the proteins used. The protein standard mixture contained; bovine thyroglobulin (670 kDa), human gamma globulin (150 kDa), ovalbumin (44 kDa), myoglobulin (17 kDa) and a separate vial containing uridine (244 Da). The protein standard kit consisted of 10 mg human gamma globulin, 5 mg bovine thyroglobulin, 5 mg ovalbumin and 2 mg myoglobin. The uridine sample contained 2 mg in total. The standard mixture was reconstituted with 1 mL of 100mM phosphate buffer, 100 µL of protein mixture and 6 µL of uridine sample. Of this, 10 µL was injected in a total volume of 500 µL, resulting in a protein mixture in the approximate following final concentrations: human gamma globulin (100 µg/mL), bovine thyroglobulin (50 µg/mL), ovalbumin (50 µg/mL), myoglobin (20 µg/mL) and uridine (12 µg/mL). The standard run was carried out at a flow rate of 0.5 mL/minute in PBS running buffer (150 mM, pH

7.4). The protein for size determination was subsequently loaded, after cleaning of the column and system, as described.

2.14.9 ScFv purification analysis by SDS-PAGE and western blotting

The purified scFv fragments were analysed for their purity and to verify correct molecular weight by separation on a 12.5 % (w/v) SDS-PAGE gel, using a Bio-rad® gel electrophoresis apparatus (Bio-Rad®). The preparation of all separation and stacking gels and buffers for SDS-PAGE was outlined in Section 2.2.3. The separation gel was prepared, cast between two clean glass plates and left to polymerise. After the gel polymerised, a stacking gel was prepared, poured and wells were formed using a 1mM plastic comb, for loading of protein samples. The samples were prepared by addition of appropriate volumes of 4X loading dye and deionised water and heated (to facilitate protein denaturation) for 5 minutes at 95^{o}C. Each protein sample was added into each well in a total volume of 20 µL. The gels were placed in an electrophoresis apparatus and submerged in 1X electrophoresis buffer. The gel was run at 100V until the tracker dye had reached the bottom of the gel, taking approximately 1 hour. The gels were taken out and stained using Coomassie Blue for 1 hour and the de-stained for 3-4 hours, using Coomassie de-stain solution, until the protein band is clearly visible and the background was removed.

Western blot analysis was also carried out to confirm the results obtained by SDS-PAGE and ELISA. SDS-PAGE gels were prepared, as outlined above, loading 20 µg protein per well. Six sheets of Whatman® Gel Blot paper (Sigma) and one sheet of 3 mm Protran BA 85 Nitrocellulose membrane (Carl Stuart Ltd.) were cut to the same dimensions as the SDS-PAGE gel and soaked in ice-cold transfer buffer (Section 2.2.4) for 30 minutes. The SDS-PAGE gel was also soaked in transfer buffer. Three layers of the soaked blotting paper were placed between the electrodes of Trans-Blot® Semi-Dry Transfer cell (Bio-Rad®) apparatus. The nitrocellulose membrane was placed over the blotting paper, followed by the SDS-PAGE gel containing the resolved proteins to be transferred. The gel was sandwiched by placing three more sheets of blotting paper on top. Any air bubbles were removed by carefully rolling each of the layers with a disposable 10 mL serological pipette. Proteins were transferred from the gel to the nitrocellulose by applying 15 V electric current for 15 minutes. The nitrocellulose

membrane was blocked with 20 mL of 5 % (w/v) Milk Marvel/PBS solution (150 mM, pH 7.4) overnight at 4°C. The blocked membrane was washed 3 times with PBST (150 mM, pH 7.4) and three times with PBS (150 mM, pH 7.4), followed by incubation with 20 mL of 1 % (w/v) milk/PBST solution containing a rat monoclonal anti-HA-HRP labelled antibody (1/2,000), for 1 hour at room temperature with gentle agitation. The membrane was then washed 3 times with PBST (150 mM, pH 7.4) and three times with PBS (150 mM, pH 7.4). The membrane was developed by the addition of TMB substrate for western blotting (Sigma). Once sufficient colour development had occurred, the reaction was stopped by repeatedly washing with distilled water.

2.14.10 Inhibition ELISA for detection of MC-LR in solution

A 96 well ELISA plate was coated overnight at 4^{o}C with 500 ng/mL of MC-LR-OVA conjugate (50 µL per well). The plate was blocked with 3 % (w/v) Milk Marvel-PBS (150 mM, pH 7.4) solution (200 µL per well) for 1 hour at 37°C. The purified scFv fragments, at an optimised dilution (1/20,000) was incubated on the coated plate with varying concentrations of free microcystin-LR (200 to 0.78 ng/mL) for 1 hour at 37^{o}C (100 µL per well). The scFvs ability to bind free microcystin was then determined by comparison of the absorbance response (A) to A_0. The A_0 represents the absorbance of the scFv fragment without free toxin. The captured avian scFv was detected using an anti-HA monoclonal antibody (HRP-labelled). After each stage, the ELISA plate was washed three times with PBST (150 mM, pH 7.4) and three times with PBS (150 mM, pH 7.4). Binding was detected using TMB substrate, stopped with 10 % (v/v) HCl and measured at 450 nm with a Safire II plate reader.

2.14.11 Inter- and Intra-day ELISA analysis of avian scFvs

Inter-day and intra-day assay studies were performed to verify the accuracy and precision of the ELISA inhibition format. The standard curve was generated (n=3) on a single day (intra-day) and on three consecutive days (inter-day) and the mean and standard error were calculated (n=3). The percentage coefficients of variation (% CV) were determined for each concentration and calibration curves were generated from the data with a four-parameter equation, using BIAevaluation™ software. The percentages accuracies were calculated for

each concentration of MC-LR from the curve, according to current assay validation techniques (DeSilva et al., 2003; Kelley and DeSilva, 2007)

2.15 Mutagenesis of scFv clone, 2H1, by error-prone PCR and chain shuffling

2.15.1 Amplification of variable heavy chain gene from 2H1 scFv clone

The 2H1 wild type clone was chosen for mutagenesis studies. A stored plasmid preparation of the clone in the pComb3x phagemid vector was used for amplification of the V_H region for chain shuffling with the light chain mutant library. For gene amplification of the V_H region, the following PCR program was set up:

Step	Temperature	Time	No. of Cycles
Stage 1	94°C	10 minutes	1 cycle
Stage 2	94°C	15 seconds	30 cycles
	56°C	30 seconds	
	72°C	60 seconds	
Stage 3	72°C	10 minutes	1 cycle
	4°C	Hold	

The PCR reaction mixtures were prepared:

Component	Concentration	50 µL Volume
GoTaq® Flexi Reaction Buffer (5X)	1X	10.0 µL
V_H Forward Primer	60 pM	0.5 µL
V_H Back Primer	60 pM	0.5 µL
pComb3x (2H1)	0.5 µg	1.0 µL
dNTP (10 mM)	0.2 mM	1.0 µL
$MgCl_2$ (25 mM)	1.5 mM	3.0 µL
H_2O	-	33.75 µL
GoTaq® Flexi DNA Polymerase (5 U/µL)	1 U/µL	0.25 µL

The product from this reaction was ethanol-precipitated and purified on a 1 % (w/v) agarose gel, using a QiaQuick gel extraction kit (Qiagen).

2.15.2 Amplification of the avian light chain library using error-prone PCR and light chain shuffling

Light chain shuffling of the 2H1 clone against the original, un-panned avian scFv library (microcystin-specific) was carried out. A total of 50 µL of the phage library (Pan 1 Input-See Section 2.14.4.1), previously stored at -80^{o}C, was infected into XL-1 Blue *E.coli* cells (OD 0.6 - 0.8) containing 20 µg/mL tetracycline. The culture was incubated at room temperature for 15 minutes and 5 µL of 100 mg/mL carbenicillin was subsequently added. The culture was shaken in an orbital shaker for 1 hour at 37^{o}C. The phage library was titred at this stage to ensure phage infectivity and library was found to have 5 x 10^{7} cfu/mL, which was sufficient for further work. A further 45 µL carbenicillin was added to the culture in 45 mL of pre-warmed media and the culture was shaken overnight at 37^{o}C. A large-scale plasmid purification was carried out the next day using a NucleoSpin® Xtra Midi Plasmid Purification Kit (Macherey-Nagel).

For error-prone PCR of the V_L gene library, the following PCR program was set up using RedTaq® DNA polymerase:

Step	Temperature	Time	No. of Cycles
Stage 1	94^{o}C	10 minutes	1 cycle
Stage 2	94^{o}C	1 minute	30 cycles
	55^{o}C	2 minute	
	72^{o}C	3 minute	
Stage 3	72^{o}C	10 minutes	1 cycle
	4^{o}C	Hold	

Error-prone PCR reactions were prepared with a higher concentration of $MgCl_2$ (7 mM) compared to a basic PCR reaction (1.5 mM). The purpose of this was to stabilise non-complementary nucleotide pairing. Manganese chloride ($MnCl_2$) can also be added to increase the error-rate of amplification and the mutation rate was also modified by varying the ratios of nucleotides in the reaction. The optimal $MnCl_2$ concentration for

the PCR reaction was empirically determined using an initial concentration gradient of 10 to 40 µM. This concentration range was chosen as DNA polymerases are often inhibited at high $MnCl_2$ concentrations. The PCR reaction mixtures were prepared as follows:

Component	Stock Concentration	Final Concentration	50 µL Volume
RedTaq® Reaction Buffer	10X	1X	5.0 µL
V_L Forward Primer	100 µM	0.4 µM	0.2 µL
V_L Back Primer	100 µM	0.4 µM	0.2 µL
Plasmid Prep	100 mg/mL	100 ng	0.1 µL
dGTP	100 mM	0.2 mM	0.1 µL
dATP	100 mM	0.2 mM	0.1 µL
dTTP	100 mM	1 mM	0.5 µL
dCTP	100 mM	1 mM	0.5 µL
dH_2O	-	-	24.8-18.8 µL
$MgCl_2$	25 mM	7 mM	14 µL
$MnCl_2$	250 µM	10-40 µM	2-8 µL
RedTaq® DNA Polymerase	1 U/µL	0.05 U/µL	2.5 µL

The products from this reaction were pooled, ethanol-precipitated and purified on a 1 % (w/v) agarose gel, using a QiaQuick gel extraction kit (Qiagen).

In order to introduce further errors into the sequence, PCR reactions were set up with varying concentration of template (light chain of avian library in pComb3x vector). A high error rate was introduced by using a low concentration of template (6 ng total) and a low error rate was introduced by using a high concentration of template (600 ng total). A higher concentration of Red Taq® polymerase was also incorporated:

Component	Stock Concentration	Final Concentration	50 µL Volume
RedTaq® Reaction Buffer	10X	1X	5.0 µL
V_L Forward Primer	100 µM	0.4 µM	0.2 µL
V_L Back Primer	100 µM	0.4 µM	0.2 µL
Plasmid Prep	100 mg/mL	6/ 600 ng	0.06/ 6 µL
dGTP	100 mM	0.2 mM	0.1 µL
dATP	100 mM	0.2 mM	0.1 µL
dTTP	100 mM	1 mM	0.5 µL
dCTP	100 mM	1 mM	0.5 µL
dH_2O	-	-	22.34/ 16.4 µL
$MgCl_2$	25 mM	7 mM	14 µL
$MnCl_2$	250 µM	10 µM	2 µL
RedTaq® DNA Polymerase	1 U/µL	0.1 U/µL	5 µL

The products from this reaction were pooled, ethanol-precipitated and purified on a 1 % (w/v) agarose gel, using a QiaQuick gel extraction kit (Qiagen).

2.15.3 SOE PCR for mutant library construction

The purified V_H (2H1) and V_L error-prone amplification products were used for SOE-PCR using Phusion® Taq DNA polymerase. The overlap PCR primers, CSC-F and CSF-B, as described, were used for amplification.

The PCR program was set up:

Step	Temperature	Time	No. of Cycles
Stage 1	98°C	6 minutes	1 cycle
Stage 2	98°C	15 seconds	30 cycles
	56°C	30 seconds	
	72°C	90 seconds	
Stage 3	72°C	10 minutes	1 cycle
	4°C	Hold	

The PCR reaction mixture was prepared:

Component	**Concentration**	**50 µL Volume**
HF Buffer (10X)	1X	10 µL
$MgSO_4$	2 mM	2 µL
V_H (2H1)	100 µg	0.34 µL
V_L (EP)	100 µg	0.23 µL
CSC-F	60 pM	0.5 µL
CSC-B	60 pM	0.5 µL
10 mM dNTP	0.2 mM	1.0 µL
H_2O	-	33.73 µL
High Fidelity Platinum® Taq	1 U/µL	0.2 µL
DMSO	3 %	1.5 µL

The approximately 750 bp fragment from this reaction was ethanol-precipitated and purified on a 1 % (w/v) agarose gel, using a QiaQuick gel extraction kit (Qiagen).

Re-cloning of the mutated scFv library into the pComb3XSS vector was carried out as described. The scFv insert and the pComb3X vector were first digested using *Sfi*I (Section 2.14.3.4). In order to prevent pComb3XSS vector re-ligation, the digested vector was treated with Antarctic phosphatase (NEB) (Section 2.14.3.5). Library ligation and transformation were carried out according to Section 2.14.3.6 and Section 2.14.4.1, respectively.

2.16 Selection and characterisation of mutant clones

2.16.1 Enrichment of the mutagenised avian phage library by biopanning, against immobilised MC-OVA.

Bio-panning was carried out, as described in Section 2.14.4.2, with a number of modifications. Phage rescue was carried out from overnight phage culture (600 mL) (Section 2.14.4.1). For the first three rounds of panning, trypsin elution was used to isolate phage from the immunotube. In subsequent rounds, the phage were split so that both trypsin elution and competitive elution were carried out simultaneously (Table 2.16.1.1). The washing steps were increased in stringency over the successive rounds of biopanning.

For bio-panning rounds 4 and 5, a competitive elution strategy was employed. After the phage had been incubated for two hours at room temperature on the immunotube, the unbound phage were removed and the tube was washed the required number of times (See Table 2.27.1) with PBST. The bound phage were eluted from the immunotube with 1 mL of free MC-LR toxin for 2.5 hours at room temperature. The competitively-eluted output phage were re-infected into 5 mL XL-1 Blue culture (O.D.600 of 0.6) and incubated static at room temperature for 15 minutes. After phage re-infection, bio-panning was carried out as described in Section 2.14.4.2. A library size of 2.14×10^7 cfu/mL was obtained for the light chain shuffle library.

Table 2.16.1.1: Bio-panning strategy for enrichment of mutagenised avian MC library

	PAN 1	PAN 2	PAN 3	PAN 4	PAN 5
Coating Concentration (Trypsin Elution)	50 µg/mL	2 µg/mL	100 ng/mL	5 ng/mL	0.25 ng/mL
Coating Concentration (Competitive Elution)	50 µg/mL	2 µg/mL	100 ng/mL	100 ng/mL	100 ng/mL
Competitive Elution Solution	-	-	-	500 ng/mL	5 ng/mL
Number of Washes	5 x PBST 5 x PBS	5 x PBST 5 x PBS	10 x PBST 10 x PBS	15 x PBST 15 x PBS	15 x PBST 15 x PBS
Culture Volume	400 mL	100 mL	100 mL	100 mL	100 mL

2.16.2 Selection and screening from light chain-shuffled library

2.16.2.1 Polyclonal phage ELISA of mutant library

The outputs from each round of bio-panning was analysed by direct ELISA using HRP-labelled anti-M13 antibody. This procedure is described in detail in Section 2.24.4.3.

2.16.2.2 Soluble monoclonal and inhibition ELISA of mutant avian scFvs

Soluble monoclonal ELISA was carried out on clones from round 4 and round 5 from the light-chain shuffled mutant scFv library. Both competitively and trypsin-eluted phage were re-infected into Top10F' *E. coli* cells and soluble-expressed scFvs were analysed by direct ELISA, as described in Section 2.14.4.3. Inhibition analysis of the resulting clones was performed by ELISA with free MC-LR (See Section 2.14.4.4).

2.17 Development of Biacore™ inhibition assay for microcystin and microcystin congeners

2.17.1 Immobilisation of MC–LR onto a CM5 sensor chip for Biacore™ inhibition analysis

For immobilisation of MC-LR onto the sensor chip surface, a direct conjugation strategy was undertaken on the laboratory bench. This procedure was carried out in Queen's University, Belfast, as part of a collaborative project, by a Ph.D student, Shauna Devlin. Firstly, equal volumes of EDC (N-ethyl-N'-(dimethylaminopropyl) carbodiimide) and NHS (N-hydroxysuccinimide) were pre-mixed and applied to a CM5 chip surface in a 50 µL volume. This was incubated at room temperature for 30 minutes, protected from light. MC-LR (0.5 mg, Enzo) was dissolved in 25 µL 100 % (v/v) EtOH and made up to 100 µL with 75 µL dH_2O, which was added dropwise. One hundred µL 0.6mM CTAB, 0.10 mM HEPES, pH 7.4, was mixed with 100 µL 5 mg/mL of prepared MC-LR in 25 % (v/v) EtOH. The EDC/NHS mixture was removed from the chip surface and 50 µL MC-LR/CTAB/HEPES mixture was applied. This was incubated at room temperature overnight, protected from light. The mixture was removed from the chip surface the next day and 50 µL 1M ethanolamine-HCl, pH 8.5, was applied. This was incubated at room temperature for 20 minutes, protected from light. The chip was

washed with 2-3 drops of dH_2O and dried under N_2. The chip was stored at 4^oC until required.

2.17.2 Optimisation of assay parameters

To determine the optimal flow rate and contact time for use on the immobilised MC-LR chip, a range of different flow rates and contact times were investigated. Contact times of 4 minutes, 2 minutes and 48 seconds, each at flow rates of 5, 10 and 25 µL/minute were evaluated. This was to determine what parameters gave the highest response change with respect to analyte concentration. To assess the stability of the immobilised surface, regeneration scouting was performed. A known concentration of antibody was passed over the chip surface, and the surface regenerated using a panel of different regeneration solutions. The solutions used included 10 mM glycine at pH of 1.5, 2.5 and 3.0, 1 M NaCl, 10 mM HCl, pH 1.3, 50 mM HCl, pH 1.3, 20 mM NaOH, pH 12, 20 mM NaOH/ 1 % (v/v) Acetonitrile, pH 12, and 200 mM NaOH, pH 12. The regeneration studies demonstrated that two pulses of 200 mM NaOH for 1 minute was the most effective regeneration buffer.

2.17.3 SPR inhibition analysis of scFv clones

Analysis was performed using a Biacore™ 3000 instrument and data analysis was performed using BIAevaluation™ 3.0 (BIAcore™, Uppsala, Sweden). The binding ability of the scFvs was assessed with the microcystin-LR-immobilised sensor chip surface. A dilution of the IMAC-purified scFv clones in HBS buffer was passed over the sensor chip at a flow rate of 5 µL/minute for 4 minutes. Bound scFvs were dissociated with a pulse of 200 mM NaOH and the baseline was restored with the injection of HBS running buffer over the chip surface. For the inhibition studies, an optimal scFv dilution was mixed with free microcystin toxin, MC-LR in an optimal 1:10 ratio, at concentrations ranging from 300 to 0.69 ng/mL. These were analysed using a flow rate of 25 µL/minute with 2 minute injections. The surface was regenerated with two pulses of 200 mM NaOH for 1 minute.

2.17.4 Cross-reactivity studies of 2H1 and 2G1 clones on Biacore™ 3000

For the cross-reactivity analysis using Biacore™ inhibition, an optimal scFv dilution was mixed with free microcystin toxins, MC-LR, MC-LW, MC-LF, MC-LA, MC-RR and MC-YR, at concentrations ranging from 300 to 0.69 ng/mL in HBS assay buffer. Toxin: antibody dilutions were pre-incubated for 30 minutes at room temperature prior to analysis. Samples were analysed using a flow rate of 25 µL/minute with 2 minute injections. The surface was regenerated with two pulses of 200 mM NaOH for 1 minute. The inhibition analysis for each toxin cogener was performed in triplicate. The IC_{50} values of the calibration curve, for each respective toxin cogener, was directly compared to that of MC-LR to determine the degree of cross reactivity.

2.17.5 Inter- and intra-day for Biacore™ assay development

Inter-day and intra-day assay studies were performed to verify the accuracy and precision of the Biacore™ inhibition format. The standard curve was generated (n=3) on a single day (intra-day) and on three consecutive days (inter-day) and the mean and standard error were calculated (n=3). The percentage coefficients of variation (% CV) were determined for each concentration and calibration curves were generated from the data with a four-parameter equation, using BIAevaluation™ software. The percentages accuracies were calculated for each concentration of MC-LR from the curve.

2.18 Fluorescence immunoassay development

2.18.1 Generation of an antibody response to microcystin in a leporine host

A New Zealand white rabbit was immunised over a period of 12 weeks at 3 weekly intervals, with 500 µg microcystin–LR conjugated to ovalbumin (OVA) in 1 mL. The injections were mixed and emulsified by vortexing in a 1:1 ratio with Freund's Complete Adjuvant (FCA) for the primary immunisation and with Freund's Incomplete Adjuvant (FIA) for each subsequent immunisation. The emulsion was administered to the rabbit sub-cutaneously over four sites (250 µL at each site). Bleeds were taken at three week intervals to determine the immune response of the animal. The rabbit was sacrificed and approximately 100 mL of blood was harvested. The blood was allowed to

clot at 4°C and was centrifuged at 18,514 g for 30 minutes to remove all cellular content. The serum was aliquoted into 2 mL volumes and stored at -20°C.

2.18.2 Protein-G purification of anti-microcystin immunoglobulin G (IgG) from leporine serum

A 2 mL suspension of immobilised protein G (immobilised on Sepharose 4B, stored in sterile-filtered PBS containing 20 % (v/v) ethanol) was equilibrated in a column with 30 mL of sterile-filtered PBS (150 mM, pH 7.4). Five mL of serum from the sacrificed rabbit was thawed on ice and pooled and made up to a final volume of 10 mL with sterile-filtered PBS (150 mM, pH 7.4). The diluted pAb-rich serum was then passed through the column and the eluant collected and passed through the column twice more. A total of 30 mL of wash buffer (sterile-filtered PBS, 150 mM, pH 7.4) was passed through the column and the bound IgG was eluted with 0.1 M glycine-HCl buffer (pH 2.5). Protein G binds the Fc portion of IgG. Fractions of eluate were collected in micro-centrifuge tubes containing 150 µL of neutralisation buffer (2 M Tris-HCl, pH 8.5). This step allowed for the neutralisation of the highly acidic environment of the elution buffer, thus preventing denaturation of the eluted IgG. The fractions were quantified using the NanoDrop™ ND-1000 spectrophotometer employing an extinction coefficient of 13.7 at 280 nm. The fractions containing high concentrations of IgG were pooled, buffer-exhanged on a Vivaspin™ 5,000 MWCO column into sterile-filtered PBS (150 mM, pH 7.4) and stored at -20°C. Verification of the purification was carried out by separating and visualising the purified IgG using SDS-PAGE (See Section 2.2.3).

2.18.3 Labelling of scFvs and IgG antibodies with Alexa Fluor® 647 dye

An Alexa Fluor® 647 protein labelling kit (Molecular Probes) was employed to directly label both IgG and scFv molecules with fluorescent dye. The reactive dye possesses a succinimidyl ester moiety which reacts with primary amines on the protein to form stable amide bond-linked dye:protein conjugates. Conjugates of Alexa Fluor® 647 have an absorption and emission fluorescence maxima of 650 nm and 668 nm, respectively. Each fluorescence labelling reaction contained 1 mg of scFv or 2 mg of IgG in a volume of 500 µL. Accurate protein quantification was carried out using a Modified Lowry protein assay kit (Pierce). A 1M solution of sodium bicarbonate was prepared, as per the

manufacturer's instructions, and the antibody of interest was diluted to a concentration of 2 mg/mL in 500 µL sterile-filtered PBS (150 mM, pH 7.4). Fifty µL of 1M sodium bicarbonate was added to the antibody solution. Sodium bicarbonate (pH ~ 8.3) functions to raise the pH of the reaction mixture, as succinimidyl ester groups react efficiently at pH 7.5 to 8.5. A vial of reactive dye was allowed to warm to room temperature, the antibody solution was directly added and the dye was allowed to fully dissolve. The reaction was stirred for 1 hour at room temperature.

Purification of the labelled antibody from un-reacted antibody and free dye was carried out using size exclusion chromatography on a Bio-Rad® BioGel P-30 purification resin. The resin was packed into a 10 mL chromatography column and allowed to settle. The sample was directly loaded and allowed to enter the resin bed. The reaction vial was rinsed with 100 µL of elution buffer (PBS, 150 mM, pH 7.4) and the solution was allowed to enter the column. Elution buffer was diluted from a 10X stock solution and contained 0.1M potassium phosphate, 1.5M NaCL pH 7.2, with 2 mM sodium azide. To separate and elute the antibody and dye components, elution buffer was added to the resin. The dye:antibody conjugate was distinguishable from the free dye, because two blue band fronts could be observed. The first band front representing labelled-protein and the latter front represented unincorporated dye. All eluted fractions were collected.

To determine the degree of labelling, the absorbance of the dye:antibody conjugate fractions were calculated at 280 nm and 650 nm (A_{280} and A_{650}), using a Nanodrop™ ND-1000 spectrophotometer. The molar concentration of antibody and the number of moles of dye/ mole of antibody were calculated as follows:

$$\text{Antibody Concentration (M)} = \frac{(A_{280} - [A_{650} \times 0.03]) \times \text{Dilution Factor}}{\text{Molar Extinction Coefficient of Antibody}}$$

$$\text{Moles Dye per mole antibody} = \frac{A_{650} \times \text{Dilution Factor}}{239{,}000 \times \text{Antibody Concentration (M)}}$$

A correction factor of 0.03 was incorporated to account for the absorption of dye at 280 nm. The molar extinction coefficient of the Alexa Fluor® 647 dye is 239,000 M^{-1} cm^{-1} at 650 nm. The molar extinction coefficient of a typical IgG is 203,000 000 M^{-1} cm^{-1}. The

molar extinction coefficient of the scFv molecule was calculated in three ways. Firstly, a value of 51,130 M^{-1} cm^{-1} was extracted from the literature (Pace et al., 1995; Grovender *et al.*, 2004). The ProtParam Expasy Tool (http://web.expasy.org/protparam/) was utilised to calculate the extinction coefficient of the 2G1 scFv as 38,390 M^{-1} cm^{-1}. The ProParam tool computes parameters including: molecular weight, theoretical pI, amino acid composition, atomic composition, extinction coefficient, estimated half-life, instability index, aliphatic index and grand average of hydropathicity (GRAVY), using the molecular sequence of the protein. Also, the molecular weight of the 2G1 scFv was extrapolated from a protein standard curve using size exclusion chromatography to give a value of 29,649 M^{-1} cm^{-1}. It was clear that an average of 1 mole of dye was incorporated per mole of the 2G1 scFv (mean of three extrapolated values) and approximately 6 moles of dye was incorporated per mole of protein G purified-rabbit IgG.

Antibody	**Molar extinction coefficient (M^{-1} cm^{-1})**	**Moles dye/ Mole Antibody**
2G1 scFv clone	51,130 (Typical scFv)	**1.30**
	38,390 (Calculated from ProtParam)	**0.96**
	29,649 (Extrapolated by Size Exclusion)	**0.74**
Rabbit IgG	203,000 (Typical IgG)	**5.70**

2.18.4 Biotinylation of scFv and IgG antibodies

The size exclusion chromatography-purified chicken anti-MC scFvs (2G1 and C12) and protein G-purified rabbit IgG were biotinylated using Sulfo-NHS-Long Chain (LC)-Biotin (Pierce). Sulfo-NHS-LC-Biotin can be used for the efficient labelling of antibodies through conjugation to primary amino groups ($-NH_2$) to form stable amide bonds. *N*-Hydroxysuccinimide (NHS)-activated biotins react with primary amines found in the side chain of lysine residues and the N-terminus of peptides that are available for labelling. Prior to conjugation the molar antibody concentration and amount of biotin to add to the reaction had to be calculated. A 100-fold molar excess of biotin reagent was incubated with the antibody to ensure a high ratio level of biotin per antibody molecule. Two milligram of antibody was used for each reaction.

The millimoles (mmol) of biotin reagent to add to the antibody to have a 100-fold molar excess were calculated using the equation:

$$\text{mmol Biotin} = \text{mL protein} \times \frac{\text{mg protein}}{\text{mL protein}} \times \frac{\text{1 mmol protein}}{\text{mg protein}} \times \frac{\text{100 mmol Biotin}}{\text{1 mmol protein}}$$

To calculate the microlitres of 10 mM biotin reagent solution required to add to the antibody conjugation reaction, the following equation was used:

$$\mu\text{L Biotin for reaction} = \text{mmol Biotin} \times \frac{\text{1,000,000 } \mu\text{L}}{\text{L}} \times \frac{\text{L}}{\text{10 mmol}}$$

Directly prior to use, the sulfo-NHS-LC biotin was equilibrated at room temperature and a 10 mM biotin solution was prepared by dissolving the required amount of biotin in ultra pure H_2O. The required volume of biotin was then incubated with the protein solution for 2 hours on ice. After the incubation period, the biotinylated antibody was buffer-exchanged to remove any un-reacted biotin. This was carried out using a Vivaspin™ 10,000 MWCO (molecular weight cut-off) spin column. The column was centrifuged at 3,220 g until all the solution was removed and the column was washed and centrifuged three times with 10 mL sterile-filtered PBS (150 mM, pH 7.4). The labelled antibody was then collected, adjusted to the required concentration and stored at -20^{o}C in aliquots.

2.18.5 Biotin quantification

Successful labeling with biotin will depend on the number and distribution of available amino groups on the antibody, the protein concentration and the ratio of reagents used. The degree of biotin incorporation onto the scFv and IgG molecules was determined using the biotin quantification kit (Pierce). In this procedure, the biotinylated antibody was incubated with a mixture of HABA and avidin. The inherent high affinity of avidin for biotin resulted in the displacement of the HABA from avidin and the absorbance at 500 nm decreased proportionately.

The HABA/avidin mixture was warmed to room temperature and re-constituted by adding 100 µL of ultrapure water. One hundred and sixty µL of sterile-filtered PBS

(150 mM, pH 7.4) was pipetted into a NUNC™ microtitre plate and 20 µL of the HABA/ avidin mixture was added. This was mixed well by vortexing and the absorbance measured at 500 nm (A_{500} HABA/avidin). Twenty µL of the biotinylated protein were added to the well and the solution was mixed well again. Biotinylated HRP of a known biotin:HRP ration of 1:1.4, was used as a positive control for all reactions. The HABA/avidin/biotin absorbance at 500 nm was determined (A_{500} HABA/avidin/biotin). The moles of biotin per mole of protein was calculated using the Beer Lambert Law:

$$A_\lambda = \varepsilon_\lambda bC$$

A is the absorbance at a particular wavelength (λ), ε is the absorptivity or extinction coefficient at the wavelength (λ). b is the cell path length expressed in centimetres (cm). For the microtitre plate format the path length is 0.5 cm. C is the concentration of the protein sample expressed in molarity (= mol/L = mmol/mL). To calculate the number of moles of biotin per mole of antibody, the concentration of biotinylated antibody in mmol/mL needed to be calculated as:

$$\text{mmol antibody per mL} = \frac{\text{Antibody Concentration (mg/mL)}}{\text{MW of Antibody (mg/mmol)}}$$

The calculated molecular weight (MW) of the scFv was 29,648 grams/mole, as determined by size exclusion chromatography (See Section 2.14.7) and the typical MW of an IgG was 150,000 grams/mole. The change is absorbance at 500 nm between the HABA/avidin (H/A) alone and the HABA/avidin/biotin (H/A/B) mixture was calculated as:

$$\Delta A_{500} = (A_{500}\ \text{H/A}) - (A_{500}\ \text{H/A/B})$$

This change in absorbance value was then incorporated into an equation to calculate the concentration of biotin in mmol/mL:

$$\text{mmol Biotin/mL Reaction} = \frac{\Delta A_{500}}{(34{,}000 \times b)}$$

b is the pathlength (cm) which is equal to 0.5 for a microtitre plate and the extinction coefficient of HABA/avidin at 500 nm is equal to 34,000 $M^{-1}cm^{-1}$. The number of moles of biotin per mole of antibody can then be calculated as:

$$\text{mmol Biotin/mmol Antibody} = \frac{(\text{mmol/mL Biotin})(10)(\text{Dilution Factor})}{\text{mmol/mL Antibody}}$$

The biotinylated protein was diluted by a factor of 10 in the original reaction mixture (10) and an addition dilution factor was also incorporated if the sample was further diluted prior to the assay.

Table 2.18.5.1: Quantification of biotin in reaction after antibody biotin-labelling with Sulfo-NHS-LC-Biotin

Antibody format	Biotin incorporation ratio (mmol biotin/mmol protein)
IgG	6.70
C12	2.00
2G1	2.27

2.18.6 Optimisation of fluorescence immunoassay conditions

2.18.6.1 Optimisation of fluorescence parameters for fluorescence immunoassay development

Fluorescence parameters were established using a direct immunoassay format where 100 µL of a 500 ng/mL MC-OVA solution was coated on a NUNC™ black Maxisorp® plate and a 1 in 100 dilution of Alexa Fluor®-labelled anti-MC IgG was incubated for 1 hour at 37°C. The plate was washed three times with PBS (150 mM, pH 7.4) and three times with PBST (150 mM, pH 7.4) and 100 µL PBS was pipetted into each well before a fluorescence measurement was taken. A wavelength absorption scan was performed with an excitation wavelength between 550 nm and 750 nm and a fixed emission wavelength of 668 nm. The gain and Z position were calculated automatically from the wells and were 79 arbitrary units and 6000 µM, respectively. A wavelength emission scan was performed with a fixed excitation wavelength of 650 nm and an emission wavelength of between 550 nm and 750 nm. The gain and Z position were calculated automatically from the wells and were 72 arbitrary units and 9900 µM, respectively. The step size was set at 5 nm and the excitation and emission bandwidths were both set at 5 nm for each scan. For each experiment, the gain was set at 255 arbitrary units (in order to maximise the fluorescence signal) and the Z position was calculated individually for each plate on a Safire II plate reader (Tecan™).

2.18.6.2 Checkerboard immunoassay for Alexa Fluor® 647-labelled anti-microcystin antibodies

A 96 well black microtitre plate (Maxisorp™, NUNC™) was coated with varying concentrations of microcystin conjugate (0.5 to 16 µg/mL), in sterile-filtered (150 mM, pH 7.4) and incubated overnight at 4°C. The following day, the conjugate-coated plate was blocked with a 5 % (w/v) Milk Marvel/ PBS solution (200 µL per well) for 1 hour at 37°C. Either Alexa Fluor®-labelled polyclonal antibody or Alexa Fluor® - labelled 2G1 scFv, were serially diluted in 1 % (w/v) Milk Marvel in PBST (1/100 to 1/12,500) and 100 µL was added in triplicate to the coated and blocked wells and incubated at 37°C for 1 hour. Following incubation, the plates were washed using three times with PBST (150 mM, pH 7.4) and three times with PBS (150 mM, pH 7.4) to remove any

unbound antibody. For detection, 100 µL PBS (150 mM, pH 7.4) was pipetted into each well before a fluorescence measurement was taken with an excitation and emission wavelength of 646 nm and 674 nm, respectively.

2.18.6.3 Competitive immunoassay with Alexa Fluor® 647-labelled anti-microcystin antibodies

A 96 well black microtitre plate (Maxisorp™, NUNC™) was coated with microcystin-OVA conjugate at an optimised concentration of 4 µg/mL and incubated overnight at 4°C. The following day, the coated plate was blocked with a 5 % (w/v) Milk Marvel/PBS solution (200 µL per well) for 1 hour at 37°C. Dilutions of MC-LR (10X concentrated) were prepared from a stock solution of 10 µg/mL in 50 % (v/v) methanol/dH_20, ranging in concentration from 0.8 - 2000 ng/mL. Optimised antibody concentrations (1/500 for 2G1- Alexa Fluor® 647 and 1/2000 for IgG - Alexa Fluor® 647) were prepared in 1 % (w/v) Milk Marvel/ PBST. Toxin preparations were diluted 1/10 in the antibody solution and incubated for 30 minutes at room temperature. One hundred µL was added in triplicate to each well of the coated and blocked plate and incubated at 37°C for 1 hour. The plate was then washed three times with PBST (150 mM, pH 7.4) and three times with PBS (150 mM, pH 7.4), to remove any unbound material. For detection, 100 µL PBS (150 mM, pH 7.4) was pipetted into each well before a fluorescence measurement was taken on a Tecan™ Safire II reader, using excitation and emission wavelengths of 646 nm and 674 nm, respectively.

2.18.6.4 Checkerboard immunoassay for biotinylated anti-microcystin antibodies

For the biotinylated antibodies, coating and blocking were carried out as described in Section 2.18.6.2, this time with an optimal coating concentration of 0.5 µg/mL. Either biotinylated polyclonal antibody or biotinylated 2G1 or C12 scFv, were serially diluted in 1 % (w/v) Milk Marvel in PBST and 100 µL was added in triplicate to the coated and blocked wells and incubated at 37°C for 1 hour. Following incubation, the plates were washed using three times with PBST (150 mM, pH 7.4) and three times with PBS (150 mM, pH 7.4) to remove any unbound antibody. Serial dilutions of streptavidin-Alexa Fluor® 647 conjugate or streptavidin – HRP conjugate were prepared in 1 % (w/v) Milk Marvel in PBST and added to the plate. After a one hour incubation at 37°C, the plates were washed as before. For fluorescence detection, 100 µL PBS (150 mM, pH 7.4) was

pipetted into each well before a fluorescence measurement was taken with an excitation and emission wavelength of 646 nm and 674 nm respectively. For colorimetric detection, TMB substrate was then added (100 µL per well) and left to react for 15 minutes at room temperature. The reaction was quenched by the addition of 100 µL per well of 10 % (v/v) HCl, after which the absorbance was determined at 450 nm on a Safire II plate reader (Tecan™).

2.18.6.5 Competitive immunoassay with biotinylated anti-microcystin antibodies and streptavidin conjugates

A 96 well black microtitre plate (Maxisorp™, NUNC™) was coated with microcystin-OVA conjugate at an optimised concentration of 0.5 µg/mL and incubated overnight at 4°C. The following day, the coated plate was blocked with a 5 % (w/v) Milk Marvel/PBS solution (200 µL per well) for 1 hour at 37°C. Dilutions of MC-LR (10X concentrated) were prepared from a stock solution of 10 µg/mL in 50 % (v/v) methanol/ dH_20, ranging in concentration from 2000 to 0.8 ng/mL. Optimised antibody concentrations (1/10,000 2G1-Biotin, 1/2,000 C12-Biotin and 1/2,000 IgG-Biotin) were prepared in 1 % (w/v) Milk Marvel/ PBST. Toxin preparations were diluted 1/10 in the antibody solution and incubated for 30 minutes at room temperature. One hundred µL was added in triplicate to each well of the coated and blocked plate and incubated at 37°C for 1 hour. The plate was then washed three times with PBST and three times with PBS (150 mM, pH 7.4) to remove any unbound material.

For fluorescence detection, a solution of streptavidin Alexa Fluor® 647 (1/1,000) was prepared in 1 % (w/v) Milk Marvel/ PBST and 100 µL was incubated in each well for 1 hour at 37°C. After the incubation period, the wells were washed, as described, and 100 µL PBS (150 mM, pH 7.4) was pipetted into each well before a fluorescence measurement was taken with an excitation and emission wavelength of 646 nm and 674 nm, respectively. For colorimetric detection, solutions of streptavidin-HRP (IgG-Biotin 1/2,000, C12-Biotin 1/2,600 and 2G1-Biotin 1/1,000) was prepared in 1 % (w/v) Milk Marvel/ PBST and 100 µL was incubated in each well for 1 hour at 37°C. After the incubation period, the wells were washed, as described, and TMB substrate was added (100 µL per well) and left to react for 15 minutes at room temperature. The reaction was

quenched by the addition of 100 µL per well of 10 % (v/v) HCl, after which the absorbance was determined at 450 nm on a Safire II plate reader (Tecan™).

2.18.7 Functionalisation of glass substrates for fluorescence-based slide assay

All glass slides (75 mm x 25 mm) are cleaned before silanisation, to remove any debris and to ensure a clean surface for functionalisation. The slides were cleaned by sonicating in a solution of 4 % (v/v) Hellmanex® in distilled water for 1 hour. Hellmanex® II is an alkaline liquid detergent which produces an effective cleaning solution for glass surfaces when mixed with water. The slides are rinsed with distilled water and subsequently silanised using a solution of 2 % (v/v) aminopropyltriethoxysilane (APTES) in 95 % (v/v) molecular grade ethanol. After 30 minutes, the slides were rinsed with 95 % (v/v) absolute ethanol and cured at 60^{o}C for at least 2 hours. After baking, functionalised slides were stored in a dessicator for up to two weeks until ready to use. Prolonged storage beyond one month could reduce the efficacy of the slides.

2.18.8 Fluorescence-based slide immunoassay for sensitive microcystin detection

Poly-L-Lysine-coated slides (VWR international) and APTES-treated glass slides (Section 2.29.7) were both used for slide-based immunoassay development. Adhesive micro-well cartridges were prepared by Dr. Robert Gorkin, School of Physical Chemistry, DCU, using laser cutting technology. Briefly, the well structures were created by laser machining (Zing 16 Laser, Epilog) using a laminate of double-sided pressure sensitive adhesive (PSA, Adhesives Research) and poly(methylmethacrylate) (PMMA) sheets (Radionics). In the design, the depth of the well was determined by the thickness of the PMMA (1.5mm), while the tacky nature of the PSA allowed for easy assembly. Following production, the carrier layer of the PSA was removed and the top polymer assembly could then be adhered to the poly-L-lysine and APTES-treated glass slides. For an immunoassay, the cartridges was attached to the slides and secured carefully with a hand-held roller to prevent leakage.

All incubations were carried out in a simple humidity container to prevent drying. The wells were coated with microcystin-LR-OVA or BSA conjugate at an optimised

concentration in 60 µL and incubated overnight at 4°C. The following day, the coated slide was blocked with a 5 % (w/v) Milk Marvel/PBS solution (100 µL per well) for 1 hour at 37°C. Dilutions of MC-LR (10X concentrated) were prepared from a stock solution (10 µg/mL) in 50 % (v/v) methanol/ dH_2O. Optimised antibody concentrations were prepared in 1 % (w/v) Milk Marvel/ PBST. Toxin preparations were diluted 1/10 in the antibody solution and incubated for 30 minutes at room temperature. Sixty µL of the antibody:toxin mixture was added in duplicate to each well of the coated and blocked slide and incubated at 37°C for 30 minutes. The slide was washed carefully twice with PBST (150 mM, pH 7.4) and twice with PBS (150 mM, pH 7.4) to remove any unbound material.

Binding could now be directly quantified if the detection antibody was directly labelled with Alexa Fluor® 647. If the detection antibody was biotinylated, a secondary streptavidin- Alexa Fluor® 647 (1/1,000) was prepared in 1 % (w/v) Milk Marvel/ PBST and 100 µL was incubated in each well for 1 hour at 37°C. After the incubation period, the wells were washed, as described, and the slide divider was carefully removed. Fluorescence was quantified using a Perkin Elmer Scanarray Express fluorescence scanner with a 633 nm excitation laser (Gain: 80 %, Resolution: 5 µM). The Alexa Fluor® 647 dye has maximum excitation and emission wavelength of 640 and 668 nm, respectively. Advanced Image Data Analysis (AIDA) software was employed to quantify fluorescence intensity. Square measurement areas of identical size were placed over each fluorescent spot, and the fluorescence intensities were quantified and compared.

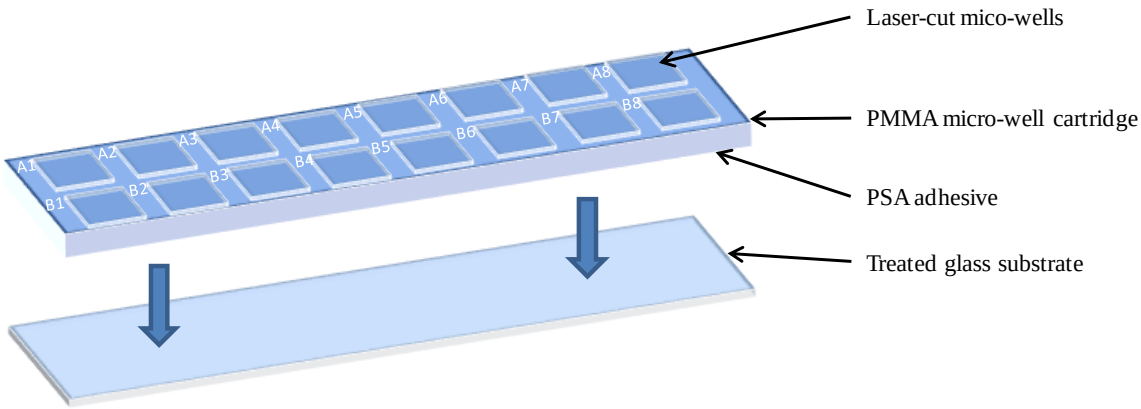

Figure 2.18.8.1: Adhesion of PMMA micro-well cartridge to functionalised-glass substrate, using attached PSA adhesive strip. Sixteen well were laser cut in total, with a maximum volume of 100 µL per well.

CHAPTER 3

Effect of phycotoxin and mycotoxin exposure on murine macrophage cells

3.1 Introduction

The work described in this chapter focused on how products of naturally-occurring microalgae and fungi may affect the signaling pathways and associated immune functions of macrophages. The immunomodulatory effect of the algal toxins, azaspiracid and microcystin, as well as the mycotoxins, aflatoxin B_1, B_2 and G_1, were analysed on the basis of their ability to repress immune function in response to LPS, a bacterial cell wall component. This work may aid in the understanding of how toxins exert their toxic effects to suppress the immune system in humans and animals.

The J774A.1 murine macrophage cell line was utilised in the course of this research. The J774A.1 cell line originating from cultured murine lymphoblastoid cells (Snyderman *et al*., 1977). The study of continuous cell line, such as murine cells with macrophage properties provides important information concerning biochemical parameters associates with certain macrophage functions. Macrophages isolated from murine peritoneal cavity are commonly used for studying the activation properties of this immunologically important cell type. However, the behaviour of the J775A.1 murine model closely mimics the physiological behaviour of a human macrophage *in vivo*, making it an ideal candidate to study the effects of immunotoxicity *in vitro*.

3.1.1 Effect of azaspiracid on immune cell function

Early toxicological studies to analyse the effect of azaspiracid (AZA) on cultured cells demonstrated that AZA was cytotoxic to a hepatocellular carcinoma cell line (HepG2) and a human bladder carcinoma cell line (ECV-304), following a 24 hour exposure to crude mussel extracts (Flanagan *et al*., 2001). This cytotoxic effect was also confirmed using purified toxin with a number of human, mouse and rat cell lines (Twiner *et al*., 2005). Twiner and colleagues showed that AZA-1 was cytotoxic to a number of different cell lines (kidney, lung, neuronal, pituitary and immune cell cultures), both in a concentration- and time-dependent manner. The Jurkat T-lymphocyte cell line was one found to be most sensitive to AZA-1, and significant contraction and elimination of actin-containing pseudopodia was observed. However, the cytotoxic effects of AZA appeared to be broad-spectrum in action overall, which correlated with previous pathological studies in mice (Ito *et al*., 2000; 2002). These studies in mice demonstrated

that AZA targeted the liver, lung, pancreas, thymus, spleen and especially the murine small intestine. In the later study, T- and B-cell necrosis occurred in the lymphoid tissues (thymus, spleen and Peyer's patches) and in lamina propria of the small intestine. Chronic exposure to AZA was associated with the development of lung tumours in mice (Ito *et al*., 2002).

Román *et al*. (2002) demonstrated that AZA had marked effects on cytosolic calcium (Ca^{2+}), cAMP and F-actin in human T-cells and neuroblastoma cells. The actin cytoskeleton has a key role in signal transduction and regulatory pathways. F-actin depolymerisation or disruption results in reduced cell proliferation. A change in intracellular calcium concentration is one of the main pathways by which information from the extracellular environment is transferred into the cell. Calcium is generally maintained at low levels in the cytosol, through sequestering by the mitochondria and the smooth endoplasmic reticulum. Calcium release from intracellular stores leads to signalling protein activation, resulting in cell injury and cell death. It has been suggested that AZA-4, unlike any other AZA analogue, is a novel inhibitor of plasma membrane Ca^{2+} channels (Alfonso *et al*., 2005). In this report, it was demonstrated that AZA-4 inhibited Ca^{2+} entry by membrane channels in human T-lymphocytes. Alteration in intracellular pH and cytosolic Ca^{2+} levels was also demonstrated in human lymphocytes in relation to AZA-1 to 5 (Alfonso *et al*., 2008). The variable effect of different AZA analogs on intracellular calcium modulation has been attributed to differences in chemical structure. This would indicate that the presence of a methyl or a hydroxyl group can significantly affect changes in calcium influx. To further investigate the significant effect of AZA-1 on T-lymphocytes, whole genome microarray analysis was employed to assess the differential expression of genes over a period of 24 hours (Twiner *et al*., 2008). This analysis revealed increased expression of the low-density lipoprotein receptor (LDLR), which is involved in cholesterol biosynthesis. Analysis revealed that a number of other gene expression pathways were also targeted, including the insulin/glucagon pathway, the WNT signaling pathway, and other pathways that are involved in inflammation, ion channel activities, the cytoskeleton, and cell growth/division. In a recent review, it was highlighted that azaspiracids are significantly different from other classes of toxins, as they possess unusual toxicity profiles, resulting in erratic and unpredictable intoxication patterns (Furey *et al*., 2010).

3.1.2 Effect of microcystin on immune cell function

It was widely reported that microcystin toxicity is associated with the inhibition of the serine/threonine protein phosphatases (PP) 1 and 2A at the cellular level (MacKintosh *et al*., 1990). The PP1 and PP2A regulatory enzymes are critical for maintaining homeostasis in eukaryotic cells. Inhibition by microcsytin can lead to hepatocyte necrosis, affecting cell proliferation and differentiation, leading to tumour promotion (Falconer and Humpage, 2005). In hepatocytes, microcystin utilises the bile duct transporter system to penetrate into cells and inhibit protein phosphatase activity in the cytoplasm (Fischer *et al*., 2005). This inhibition generates a sustained hyperphosphorylation cascade, eventually leading to hepatocyte and liver toxicity. Microcystin can also exert their toxic effects through immunomodulation of a number of immune cell types, and it is this particular area, which is of relevance for human and livestock toxicity events (Hernández *et al*., 2000; Yea *et al*., 2001).

In relation to the immunomodulatory activities, it was speculated that microcystin may rely on over-stimulation of the immune system for effectiveness. For many years, microcystin compounds have been known to regulate the production of IL-1, TNF-α and inducible nitric oxide synthase in macrophages (Nakano *et al*., 1989; Nakano *et al*., 1991; Pahan *et al*., 1998). Investigation into the immunosuppressive effects of microcystin on mice peritoneal macrophages showed that both short term (6 hour) and long term (24 hour) exposure had a significant inhibitory effect on iNOS (inductible nitric oxide synthase) and the macrophage-related cytokines, IL-1β, TNF-α, GM-CSF and IFN- γ (Chen *et al*., 2004, 2005). Another study employing mouse peritoneal macrophages demonstrated that supernatant from microcystin-treated macrophages induced electrogenic intestinal effects in rabbit ileum in a time-dependent manner (Rocha *et al*., 2000). In contrast to the studies by Chen and colleagues, the toxin-treated macrophages increased the secretion of TNF-α and IL-1β into the supernatant, but the authors speculate that these cytokines were not involved in the intestinal secretory effect.

Interestingly, a study on the effects of MC on a number of mammalian cell lines, including human colon adenocarcinoma (Caco-2), astrocytoma (IPDD-A2) and lymphoblastoid (NCNC), showed that microcystin exposure in the NCNC cells (which

originate from an established cell line of peripheral blood lymphocytes), had very little effect on ROS production or DNA damage at concentrations of up to 10 µg/mL. This insensitivity to MC-LR exposure in human lymphoblastoid cell line (TK6) was also observed at low concentrations (< 80 µg/mL) by Zhan and co-workers (2004). In contrast, an investigation into the effect of MC-LR on peripheral human and chicken blood lymphyocytes, showed that toxin exposure significantly affected cytokine secretion and down-regulated B- and T-cell function by inducing apoptosis and necrosis, at low concentrations (Lankoff *et al*., 2004). For example, human lymphocytes increased production of IL-6 and decreased production of IL-2 following MC-LR exposure at concentrations of less than 2 µg/mL.

In addition, microcystin can affect the spontaneous adherence properties of human peripheral polymorphonuclear leukocytes (PMN) (Hernández *et al*., 2000). It has also been reported that concentrations of microcystin below the recommended WHO limit affect human PMNs (Kujbida *et al*., 2006). Two microcystins (MC-LR and [Asp^3]-MC-LR) induced the production of reactive oxygen species (ROS), which enhanced neutrophil migration and increased phagocytosis and killing of *Candida albicans.* Interestingly, Yea and colleagues demonstrated that microcystin down-regulated the production of IL-2 mRNA in splenocytes and thymocytes (Yea *et al*., 2001). Their analysis revealed that microcystin decreased lymphocyte responsiveness to LPS, and produced a dose-dependent inhibition of the *in vitro* polyclonal antibody response. Moreover, MC-LR induced DNA damage in rat lymphocytes and inhibited natural killer (NK) cell activity (Zhang *et al*., 2001). Kujbida *et al*., (2009) investigated the ability of three structurally distinct microcystin toxins (MC-LA, MC-LR and MC-YR) to increase intracellular calcium and to affect neutrophil migration, especially in response to the chemoattractant, fMLP (formyl-Met-Leu-Phe). They demonstrated that toxins are chemoattractants for neutrophils, which may be linked to the interaction of microcystin with membrane components and their penetration into the cell.

In many of these studies it is speculated that the immunotoxicity of microcystin is caused by an over-stimulation of the immune system (Pahan *et al*., 1998; Yea *et al*., 2001). One of the unique approaches taken to assess the immunotoxic potential of microcystins was to analyse the apoptotic effects, induced by algal bloom extracts on rat hepatocytes and human lymphocytes (Mankiewicz *et al*., 2001). This was followed by a

study of DNA damage in human lymphocytes that demonstrated the genotoxic potential of these extracts (Mankiewicz *et al*., 2002). Shen *et al*. (2003) subsequently demonstrated the effect of cyanobacterial bloom extract (CBE) on immune functions, including phagocytosis of peritoneal phagocytes, inhibition of LPS-induced lymphocyte proliferation, and a dose-dependent decrease in the number of antibody-producing cells in mice.

3.1.3 Effect of aflatoxin on immune cell function

Mycotoxins, as secondary metabolites of fungi that grow on various food stuffs and feeds, have the potential to elicit a wide variety of toxicological effects, including immune-suppression and immune-stimulation. For the trichothecene family of mycotoxins, exposure to sublethal doses has the potential to either stimulate or suppress immune functions, such as lymphocyte proliferation, cell-mediated immunity and humoral immunity, depending on dose and exposure time (Pestka and Bondy, 1994). Production of cytokines by monocytes and macrophages in response to inflammatory stimuli and microbial products is well established (Bendtzen *et al*., 1988). Several studies have shown that aflatoxins can affect macrophages, both *in vitro* (Cusumano *et al*., 1990, Moon *et al*., 1998, Moon *et al*., 1999a and Moon *et al*., 2000) and *in vivo* (Moon *et al*., 1999b). Liu *et al*., (2002) showed that fumonisin B and aflatoxin B_1 were immunotoxic to swine alveolar macrophages, employing techniques such as DNA laddering, nuclear fragmentation and phagocytosis and by analysis of apoptosis-related heat shock protein 72 (hsp72) and cytokines IL-1β and TNF-α.

Numerous animal studies have demonstrated that aflatoxins have immunosuppressive activity. Poultry (chickens and turkeys), pigs and lambs in particular, are susceptible to aflatoxin-induced immunosuppression (Smith *et al*., 1995; Devegowda and Murthy, 2005). Furthermore, cell-mediated immunity is affected by aflatoxin exposure. Murine macrophages exposed to aflatoxins *in vivo* (Dugyala and Sharma, 1996) and *in vitro* (Moon *et al*., 1999a; Moon *et al*., 1999c) exhibited decreased cytokine secretion. Other macrophage functions, such as release of reactive intermediates (Moon *et al*., 1999a; Moon *et al*., 1999b) and phagocytosis (Moon *et al*., 1999b; Liu *et al*., 2002) are decreased in macrophages exposed to AFB_1. For example, human monocytes show decreased mRNA and protein secretion levels of pro-inflammatory cytokines (Rossano

et al., 1999), in addition to decreased phagocytosis and anti-microbial activity (Cusumano *et al.*, 1996).

The immunotoxicity of mycotoxins was extensively reviewed by Bondy and Pestka, 2000. Mycotoxins can produce cellular depletion in lymphoid organs, cause alterations in T-cell and B-cell function, suppress antibody responses, suppress NK cell activity, decrease delayed-type hypersensitivity responses, and increase susceptibility to infectious disease. In addition, the T-2 mycotoxin has also been implicated as a developmental immunotoxicant, which targets fetal lymphocyte progenitors (Holladay *et al.*, 2002). The dose, the route of administration, and the species type, are all critical factors in the immunotoxicity of the mycotoxin, ochratoxin (Al-Anati and Petzinger, 2006). The effects of aflatoxins on the human immune system has not yet been fully characterised, but concerns have arisen, in countries such as West Africa, where widespread aflatoxin contamination has resulted in 99% of children in some areas possessing aflatoxin–albumin adducts in their blood (Gong *et al*., 2003).

The effect of the tricothecene group of aflatoxins on immune function has shown that the mechanism of impairment is related to inhibition of protein synthesis. Interestingly, high doses of trichothecenes induce lymphocyte apoptosis along with immune suppression (Pestka and Bondy, 1994). In contrast, low dose trichothecene promotes expression of a diverse array of cytokines including IL-1, IL-2, IL-5, and IL-6. Tricothecenes also activate mitogen-activated protein kinases (MAPK's) *in vivo* and *in vitro*, via the ribotoxic stress response (Zhou *et al*., 2003; Pestka *et al*., 2004). It was shown that LPS exposure can markedly increase the toxicity of deoxynivalenol by amplifying the pro-inflammatory cytokines: TNF-α, IL-6 and IL-1β (Zhou *et al*., 1999). Luyendyk *et al*. (2002) demonstrated that exposure to LPS increased liver injury and hepatotoxicity caused by $AFB_{1.}$ Similarly, Pestka and Zhou *et al*., (2006) showed that pre-exposure with LPS sensitised murine RAW264.7 macrophages and peritoneal murine macrophages to the pro-inflammatory effects of deoxynivalenol. Prolonged consumption of deoxynivalenol by mice was shown to induce elevation of IgA and IgA immune complex formation, in addition to kidney mesangial IgA deposition (Pestka, 2003). Although the immunomodulatory effects of the aflatoxins have been demonstrated previously, the mechanism by which these compounds exert their immunosuppressive effects is still unknown. Previous investigations have shown that

AFB_1 pretreatment, followed by LPS stimulation, decreases CD14 expression in murine peritoneal macrophages. However, CD14 expression was unaffected in cells that were pre-treated with AFB_1, but not challenged with LPS (Moon and Pyo, 2000).

3.1.4 Chapter aims

The purpose of this chapter was to study the effects of certain naturally-occurring toxins on the immune response to infection, using the murine macrophage cell line, J774A.1 as a model for host defence. This data provides further insight into the mechanisms by which phycotoxins and mycotoxins modulate the host immune response to exert their immunosuppressive activity.

- This included analysis of the cytotoxic effect of the phycotoxin, azaspiracid, on murine macrophages, using end-point assays to examine cell viability and cytotoxicity. The expression of a number of pro- and anti- inflammatory cytokines, including TNF-α, IL-12p40, IL-6 and IL-10, after azaspiracid exposure, was studied. In addition, the effect of toxin exposure on cytokine expression after macrophage activation with the TLR4 ligand, lipopolysaccharide (LPS), was also examined. Importantly, this is the first report of the immunomodulatory effect of AZA on macrophages *in vitro*.
- The anti-proliferative activity of the cyanobacterial toxin, MC-LR on the murine macrophage model was also studied using end-point assays to analyse cytotoxicity and viability. MC-LR was used to analyse the effect of toxin exposure on NLR3 inflammasome activation, a multi-protein complex responsible for activation of key inflammatory processes. The parameters under investigation included: inflammatory IL-1β and active caspase-1, which are both markers of inflammasome activation. The effects of microcystin exposure was studied following the exposure of J774A.1 cells to danger signals from adenosine triphosphate (ATP) and LPS endotoxin, which are know activators of the NLR3 inflammasome.
- The effect of aflatoxin B_1 (AFB_1), aflatoxin B_2 (AFB_2) and aflatoxin G_1 (AFG_1) exposure, alone and in combination, on the secretion of TNF-α, IL-12p40, IL-6 and IL-10 from murine macrophages, was investigated. In addition, the effect of aflatoxin exposure on the expression levels of key cell surface markers, involved in the inflammatory response, was also examined. Expression levels of 'Toll-like' receptor 2 (TLR2), 'Toll-like' receptor 4 (TLR4) and Cluster of Differentiation 14 (CD14), along with the macrophage activation marker, CD40, were studied.

3.2 Results

3.2.1 Cytotoxicity analysis of azaspiracid on murine macrophage and hepatocellular carcinoma cell lines

3.2.1.1 WST-1 cell death assay

The WST-1 assay (Roche) measures cell proliferation and viability through determination of mitochondrial dehydrogenase activity. An increase in enzyme activity leads to a increase in formazan dye formed, which is proportional to the number of metabolically-active cells. The growth rate of the J774A.1 murine macrophage cell line, in the presence of AZA-1 at concentrations, ranging from 0.01 to 100 pg/mL, was assessed using the WST-1 proliferation assay (Figure 3.2.1.1). A graph was plotted, which compared the percentage viability of the control groups (methanol control), with that of the toxin-treated cells. The results indicate AZA-1 has a potent cytotoxic activity on J774A.1 macrophages. The percentage viability decreased significantly ($P < 0.01$) at a concentration of 100 pg/mL AZA-1, compared to 0 pg/mL AZA-1. Certain experimental samples exceed 100 % viability, as they may have a higher mitochondrial dehydrogenase activity, compared with the methanol control (100 % viable).

The inflammatory processes in the macrophage are activated by the endotoxin, LPS. Therefore, LPS was included in the WST-1 analysis, to analyse the effect of toxin exposure on macrophage activation and proliferation. LPS is a potent stimulator of the 'toll-like' receptor 4 (TLR4) pathway in the immune response to infection, especially in macrophages and B-cells. With the inclusion of LPS stimulation, AZA-1 did not have any clear effect on cell viability, over a range of concentrations, compared with the LPS control (0 pg/mL AZA-1 and 100 ng/mL LPS) (Figure 3.2.1.1).

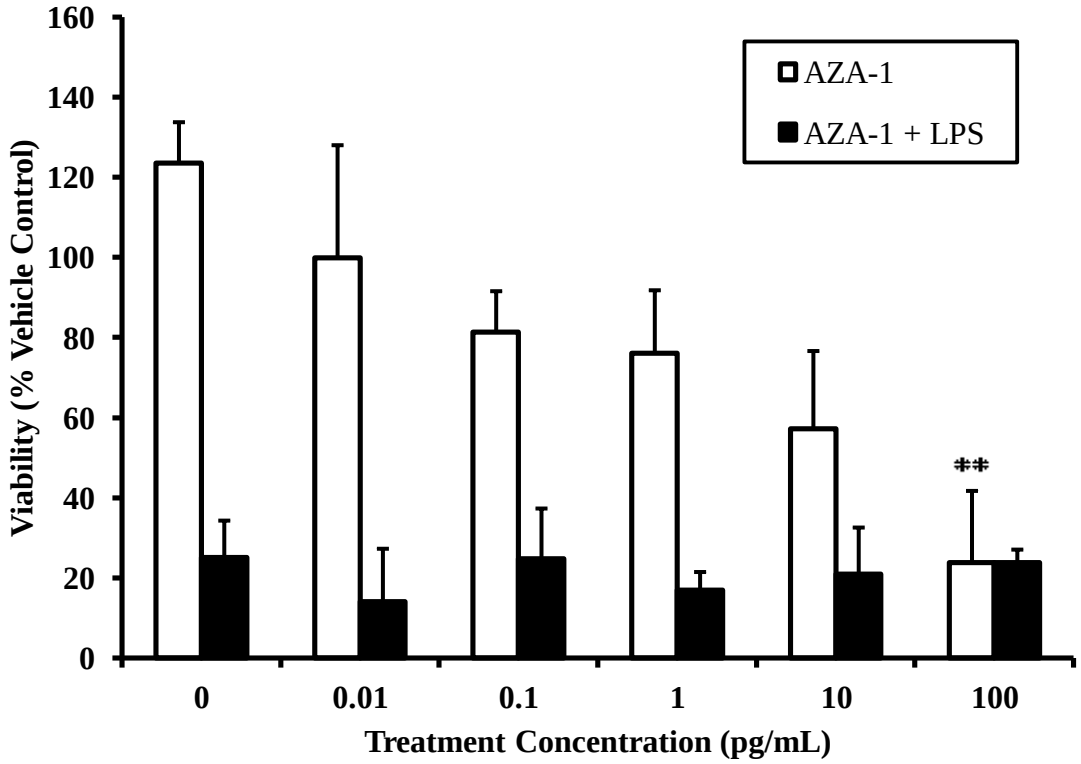

Figure 3.2.1.1: WST-1 proliferation assay to analyse the effect of AZA-1 on the J774A.1 macrophage cell line. J774A.1 cells were treated for 24 hours with AZA-1 toxin, ranging in concentration from 0.01 to 100 pg/mL, with and without LPS (100 pg/mL). The white bars (□) represent AZA-1 treatment alone and the black bars (■) represent AZA-1 treatment with LPS stimulation. Triton-X detergent (0.01% (v/v)) was included as a positive control of cytotoxicity (5.16 % viability, compared with vehicle (methanol) control). Results indicate a mean value from three independent experiments and error bars represent mean 3SE (standard error of mean) (n=3). AZA-1: $P < 0.01$** (100 pg/mL AZA-1, versus 0 pg/mL).

3.2.1.2 LDH proliferation assay

The LDH cytotoxicity assay (Roche) assesses cell death and cell lysis, based on the measurement of lactate dehydrogenase (LDH) activity, released from the cytosol of damaged cells into the supernatant. The amount of colour formed, measured at an absorbance of 490 nm, is proportional to the number of lysed cells. Data was plotted as percent cytotoxicity, as a percent of the high control (Triton-X) versus toxin treatment concentration (pg/mL). The LDH activity in the high control is measured following solubilisation of the cells with 1 % (v/v) Triton-X. A significant decrease ($P > 0.05$) in cytotoxicity, from 34 % (negative control) to 22 %, was observed, at an AZA-1 concentration of 0.01 ng/mL. A significant decrease ($P > 0.01$), from 34% to 19 %, also occurred after AZA-1 exposure, at a concentration of 0.1 ng/mL (Figure 3.2.1.2).

However, significant alterations in cellular cytotoxicity were only observed at concentration of 0.01 and 0.1 ng/mL, respectively. At lower (0.001 pg/mL) and higher (1 - 100 pg/mL) AZA-1 concentrations, no discernable change in cytotoxicity was observed, relative to the control value. A very similar U-shaped graph was obtained when macrophages were co-treated with LPS (100 ng/mL) and AZA-1 (0 to 100 pg/mL), with concentrations of 0.1 and 0.01 ng/mL displaying a significant decrease ($P > 0.05$) in % cytotoxicity, compared with the LPS control (no toxin).

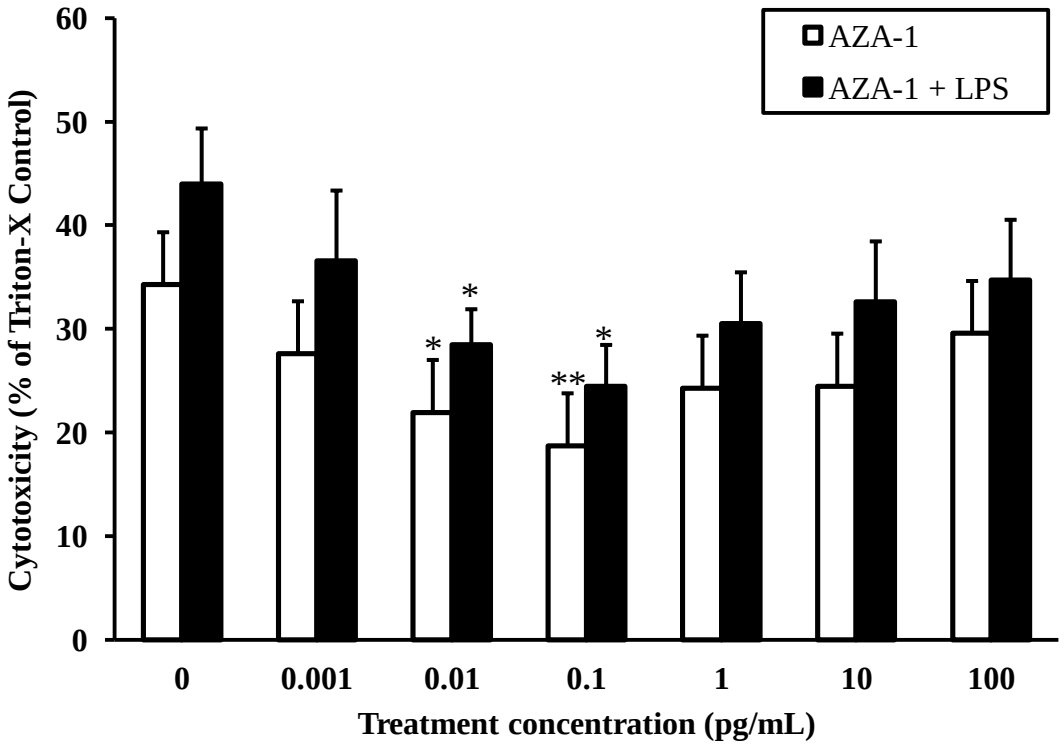

Figure 3.2.1.2: LDH cytotoxicity assay to analyse the effect of exposure to AZA-1 on the J774A.1 macrophage cell line. J774A.1 cells were treated for 24 hours with AZA-1 toxin, ranging in concentration from 0.001 to 100 pg/mL, with and without LPS (100 pg/mL). The white bars (□) represent AZA-1 treatment alone and the black bars (■) represent AZA-1 treatment with LPS stimulation. Results indicate a mean value from three independent experiments and error bars represent the mean 3SE (n=3). - LPS: $P < 0.05$* (0.01 pg/mL, versus 0 pg/mL), $P < 0.01$** (0.1 pg/mL, versus 0 pg/mL). + LPS: $P < 0.05$* (0.01 and 0.1 pg/mL, versus 0 pg/mL).

3.2.1.3 Effect of AZA-1 on cytokine secretion in J774A.1 murine macrophages

Following the confirmation of the cytotoxic effects of AZA-1 on immune macrophage cells by WST-1 and LDH cell assays, it was decided to further investigate the effect of AZA-1 on the immune macrophage cell line, J774A.1. An approach was taken to analyse the cytokine secretion from macrophages after a 24 hour exposure to AZA-1 (100 pg/mL). The concentration was selected from the cytotoxicity analysis as it significantly influenced cell viability, without causing a killing effect (See Section 3.2.1.1 and 3.2.1.2). Cells were simultaneously challenged with LPS to analyse the ability of the cell to respond to endotoxin exposure.

ELISA analysis was carried out on harvested supernatant in an antibody sandwich format. A capture antibody specific to the cytokine of interest (IL-6, IL-10, TNF-α and IL-12p40) was used for capture. Samples, standards (1,000 to 16 pg/mL) and controls were added to the capture surface, followed by a biotin-conjugated detection antibody. The biotinylated detection antibody bound to a different epitope of the cytokine being measured, thus completing the sandwich immunoassay. The detection reagent was streptavidin-labeled horse-radish peroxidase (HRP) and colour was developed using TMB substrate. A standard curve was prepared of concentration (pg/mL) versus absorbance (450 nm) and unknown values were extrapolated using linear regression analysis.

The cytokine response of J774A.1 macrophages to AZA-1 exposure varied, depending on the exposure time and the presence or absence of an LPS challenge. Incubation with AZA-1 (100 pg/mL) for 24 hours (no LPS) resulted in a statistically significant increase in IL-12p40 secretion ($P < 0.001$). In addition, a further increase was observed after 72 hours of AZA-1 exposure, compared with the vehicle (methanol) control. Interestingly, IL-12p40 secretion also increased in a time-dependent manner following LPS exposure, but the results were not significant (Figure 3.2.1.3). There appeared to be a decrease in IL-12p40 after 72 hours of AZA-1 exposure, compared with the vehicle control.

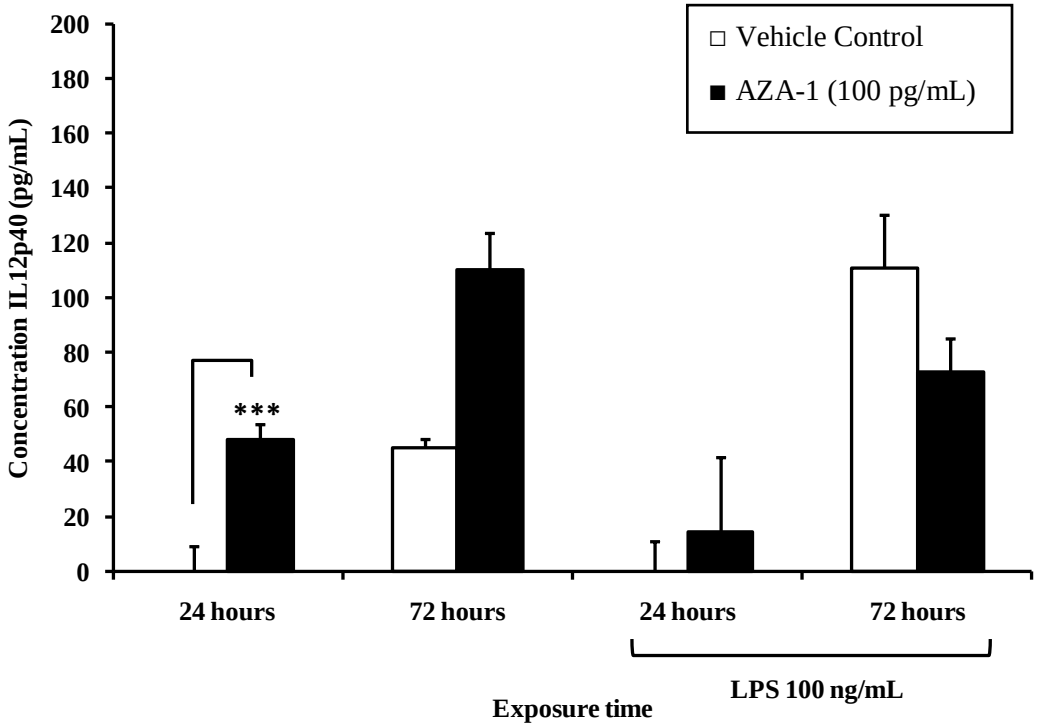

Figure 3.2.1.3: Analysis of IL-12p40 cytokine secretion from J774A.1 murine macrophages, treated for 24 and 72 hours with AZA-1 (100 pg/mL) and also stimulated with and without LPS (100 ng/mL). Results indicate a mean value from three independent experiments and error bars represent mean 3SE (n=3). Vehicle control (methanol) treatments are represented by the white bars (□) and toxin treatments are represented by the black bars (■). – LPS: $P < 0.001$*** for 24 hours AZA-1, versus vehicle control.

There was a very significant increase in TNF-α secretion ($P < 0.001$) with AZA-1 treatment for 24 hours (Figure 3.2.1.4). In contrast, a significant decrease in TNF-α expression was observed when cells were exposed to AZA-1 for 24 hours and simultaneously stimulated with LPS for 24 hours ($P < 0.001$). No significant changes in TNF-α expression were observed for the 72 hour time point. Surprisingly, no TNF-α expression was observed for the control LPS-stimulated cells after the 72 hour treatment. It is postulated that this extended time point may have been too long to observe TNF-α expression and cells were unable to respond to LPS challenge.

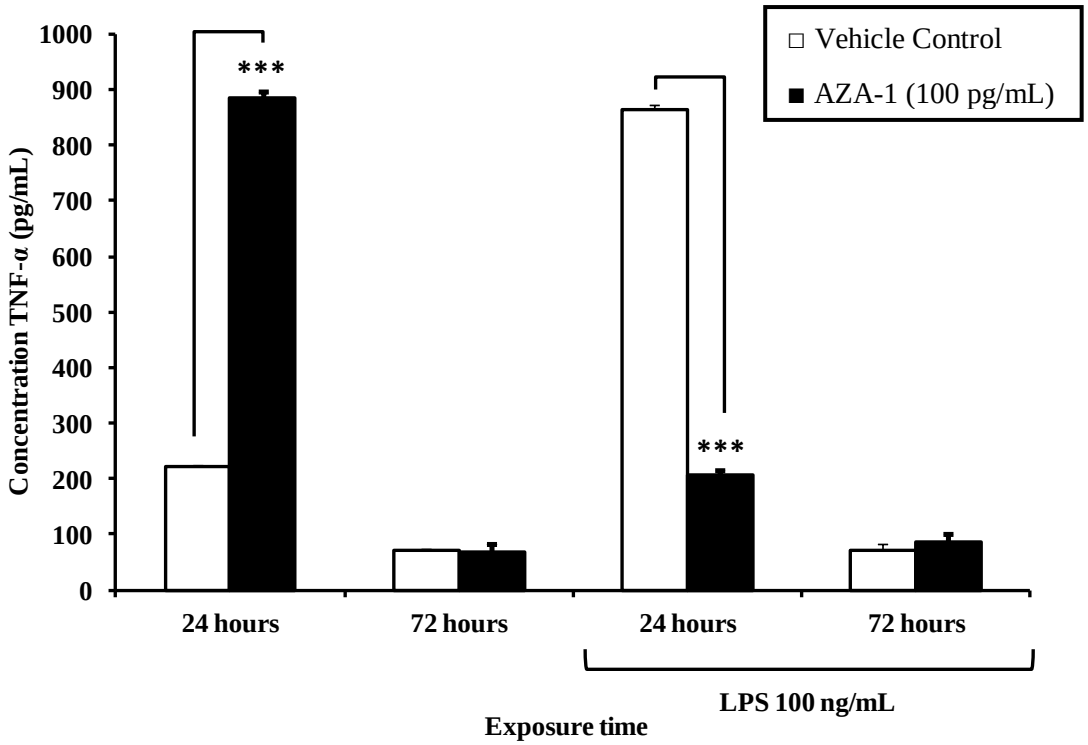

Figure 3.2.1.4: Analysis of TNF-α cytokine secretion from J774A.1 murine macrophages treated for 24 and 72 hours with AZA-1 (100 pg/mL) and also stimulated with and without LPS (100 ng/mL). Results indicate a mean value from three independent experiments and error bars represent mean 3SE (n=3). Vehicle control (methanol) treatments are represented by the white bars (□) and toxin treatments are represented by the black bars (■). - LPS: $P < 0.001$*** for 24 hours of AZA-1, versus vehicle control. + LPS: $P < 0.001$*** for 24 hours of AZA-1, versus vehicle control.

There was a significant decrease in the production of IL-10 by macrophages treated with AZA-1 for 24 hours, compared to the basal expression level (no LPS) ($P < 0.05$). However, there was no statistically significant change in IL-10 at 72 hours. No observable effects on IL-10 expression were observed for toxin-treated cells exposed to LPS challenge (Figure 3.2.1.5).

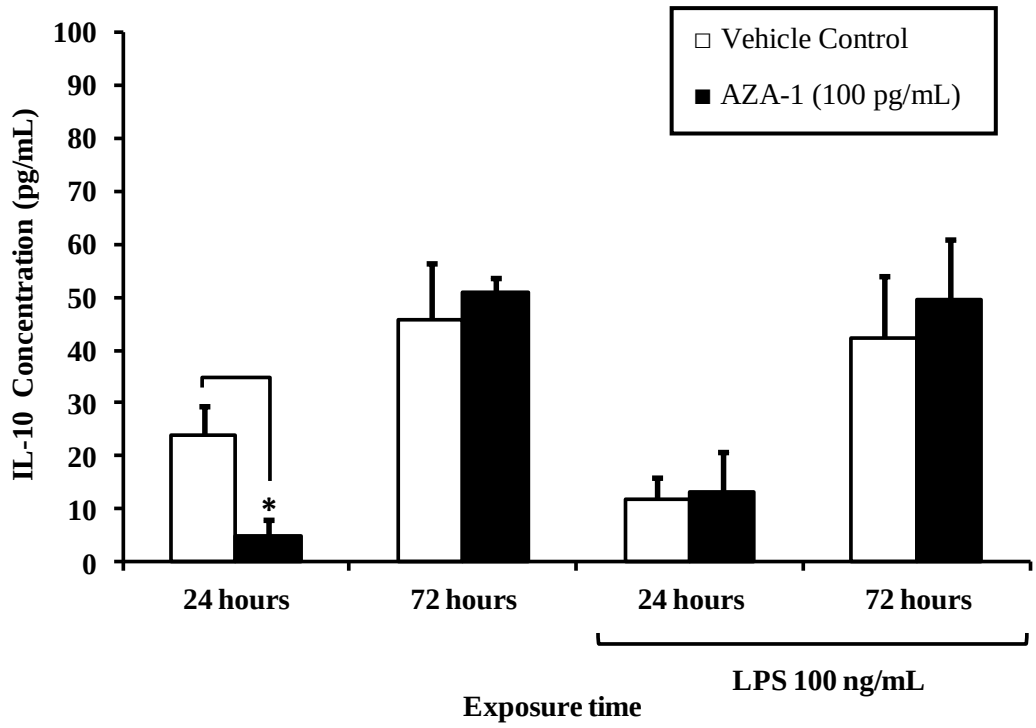

Figure 3.2.1.5: Analysis of IL-10 cytokine secretion from J774A.1 murine macrophages treated for 24 and 72 hours with AZA-1 (100 pg/mL) and also stimulated with and without LPS (100 ng/mL). Results indicate a mean value from three experiments and error bars represent mean 3SE (n=3). Vehicle control (methanol) treatments are represented by the white bars (□) and toxin treatments are represented by the black bars (■). – LPS: $P < 0.05$* for 24 hours of AZA-1, versus vehicle control.

Closely mimicking the effect of AZA-1 exposure on TNF-α, levels of IL-6 expression by J774A.1 macrophages were significantly increased ($P < 0.001$) following 24 hours of AZA-1 exposure (Figure 3.2.1.6). In contrast, after LPS challenge, there was a decrease in anti-inflammatory IL-6 macrophage expression at 24 hours ($P < 0.001$). However, following 72 hours of exposure, no significant changes were observed.

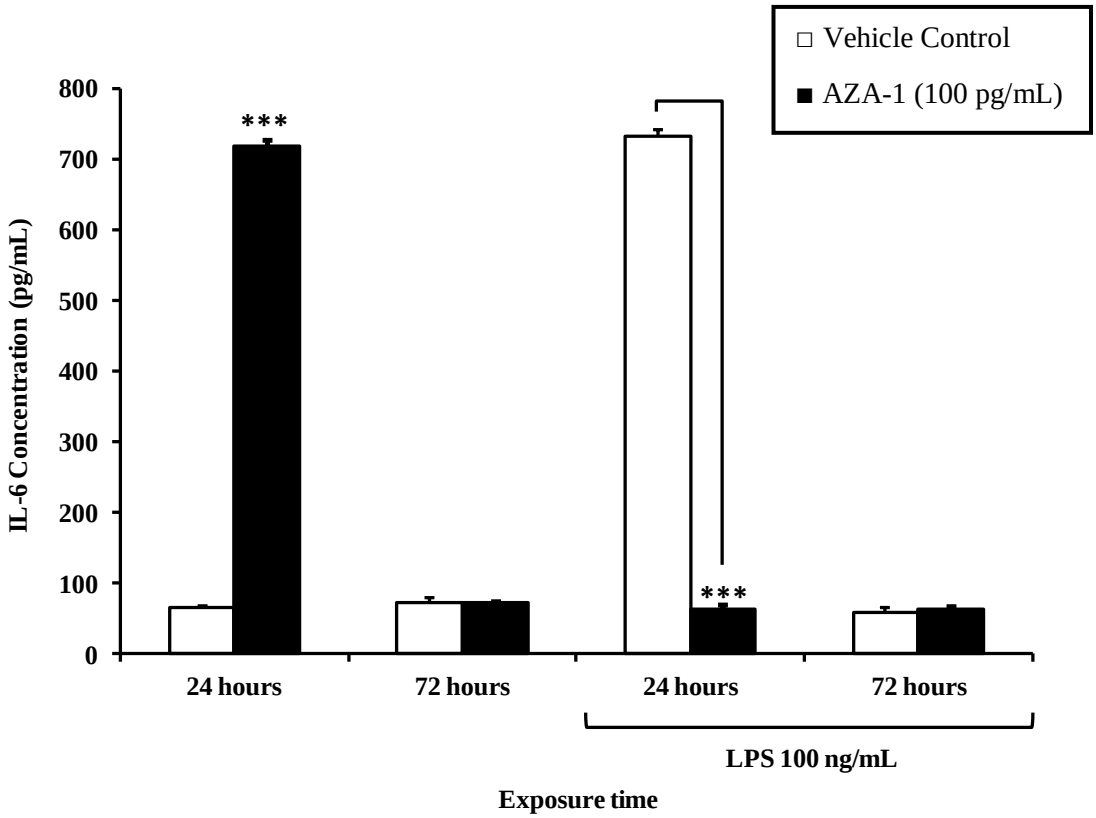

Figure 3.2.1.6: Analysis of IL-6 cytokine secretion from J774A.1 murine macrophages treated for 24 and 72 hours with AZA-1 (100 pg/mL) and also challenged with LPS (100 ng/mL). Results indicate a mean value from three experiments and error bars represent mean 3SE (n=3). Vehicle control (methanol) treatments are represented by the white bars (□) and toxin treatments are represented by the black bars (■). – LPS: $P < 0.001$*** for 24 hours of AZA-1, versus vehicle control. + LPS: $P < 0.001$*** for 24 hours of AZA-1, versus vehicle control.

3.2.2 Effect of cyanobacterial toxin, microcystin on J774A.1 macrophage function

3.2.2.1 Cytotoxicity analysis of microcystin on the murine macrophage cell line

The proliferation of the murine macrophage cells, J774A.1 exposed to microcystin-LR (MC-LR) for 12, 24 and 48 hours were compared on the basis of mitochondrial dehydrogenase activity, using the LDH assay. The toxins were incubated with the macrophages for the designated time points at two different MC-LR concentrations (10 and 0.1 µg/mL) in media, both with and without LPS stimulation (100 ng/mL). The calculated cytotoxicity, expressed as a percentage of a high control (highly cytotoxic Triton-X detergent), increased in a time-dependent manner from 12 to 48 hours. The response of cells to microcystin did not appear to be dose-dependent when analysed over a range of MC-LR toxin concentrations (data not shown). In contrast, there was a significant increase in percent cytotoxicity from 12 to 48 hours, both in the presence and absence of LPS co-stimulation ($P < 0.05$) for the high MC-LR dose (10 µg/mL) (Figure 3.2.2.1 A). A similar trend was observed for the lower MC-LR concentration (0.1 µg/mL), where a significant effect ($P < 0.05$ with toxin; $P < 0.01$ with toxin and LPS) was observed from 12 to 48 hours (Figure 3.2.2.1 B).

For the WST-1 cell death analysis for macrophages exposed to MC-LR (10 and 0.1 µg/mL), the trend was less clear. For example, there was no statistically significant change in percent viability, compared with a vehicle control (methanol) for cells exposed to 10 µg/mL of MC-LR for 12, 24 and 48 hours. However, there was a notable decrease in viability at the 24 hour time point for MC-LR alone, followed by an increase in percent viability at 48 hours (Figure 3.2.2.2 A). Conversely, at the lower toxin concentration (0.1 µg/mL) there was a significant reduction in cell viability following MC-LR exposure from 12 to 24 hours ($P < 0.01$). This was followed by a significant cell recovery at 48 hours, compared with the 24 hour time point ($P < 0.01$). No significant effect was observed for cells co-stimulated with LPS after MC-LR exposure (0.1 µg/mL) (Figure 3.2.2.2 B).

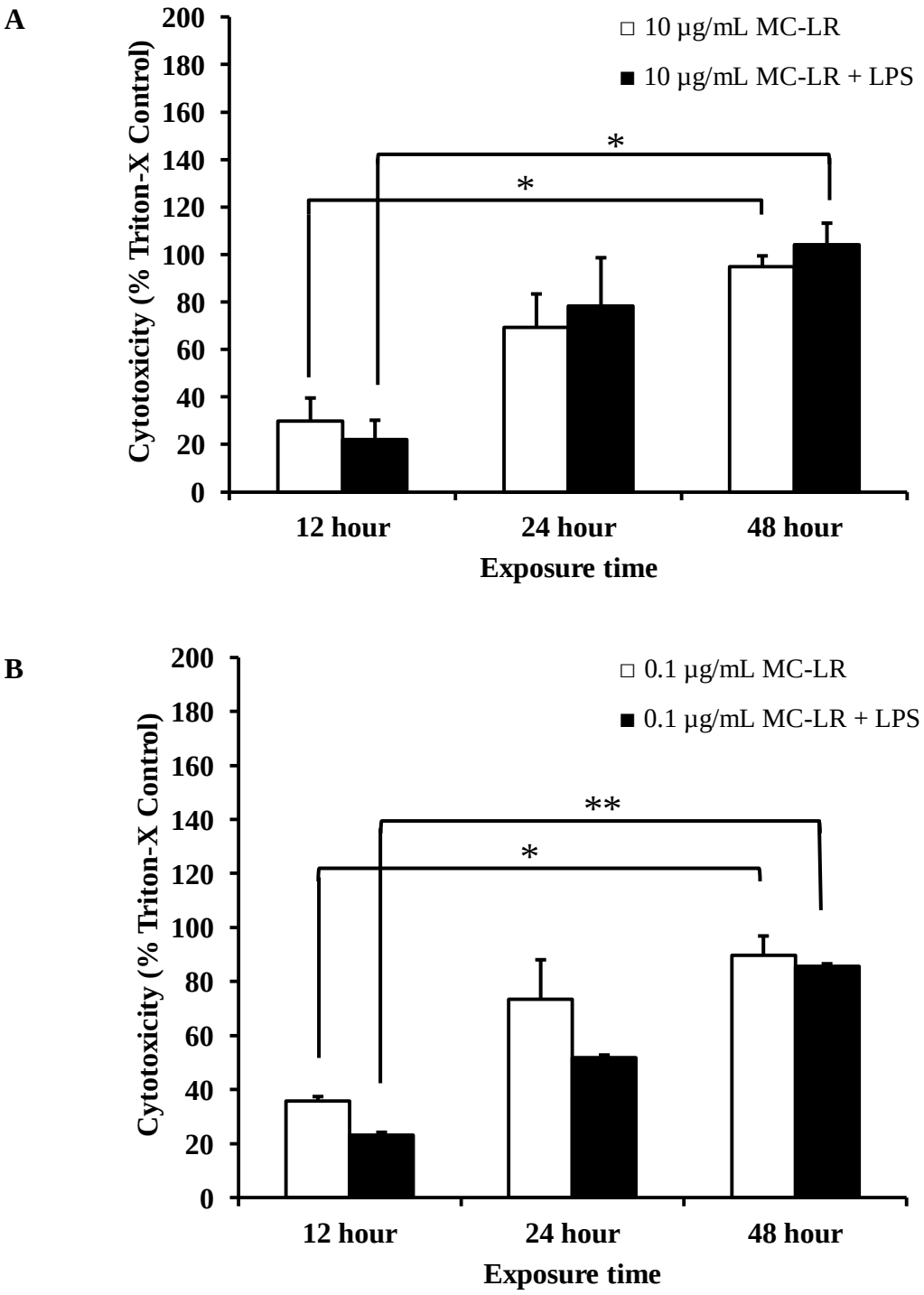

Figure 3.2.2.1: LDH cytotoxicity assay to analyse effect of exposure of MC-LR on J774A.1. Macrophages were cultured in the presence of MC–LR (A. 10 and B. 0.1 µg/mL MC-LR) for 12, 24 and 48 hours and stimulated simultaneously both with and without LPS. Toxin treatments alone are represented by the white bars (□) and toxin treatments with LPS challenge are represented by the black bars (■). A.) - LPS: $P < 0.05$*, + LPS: $P < 0.05$* (12 to 48 hours, 10 µg/mL). B.) - LPS: $P < 0.05$*, + LPS: $P < 0.01$** (12 to 48 hours, 0.1 µg/mL).

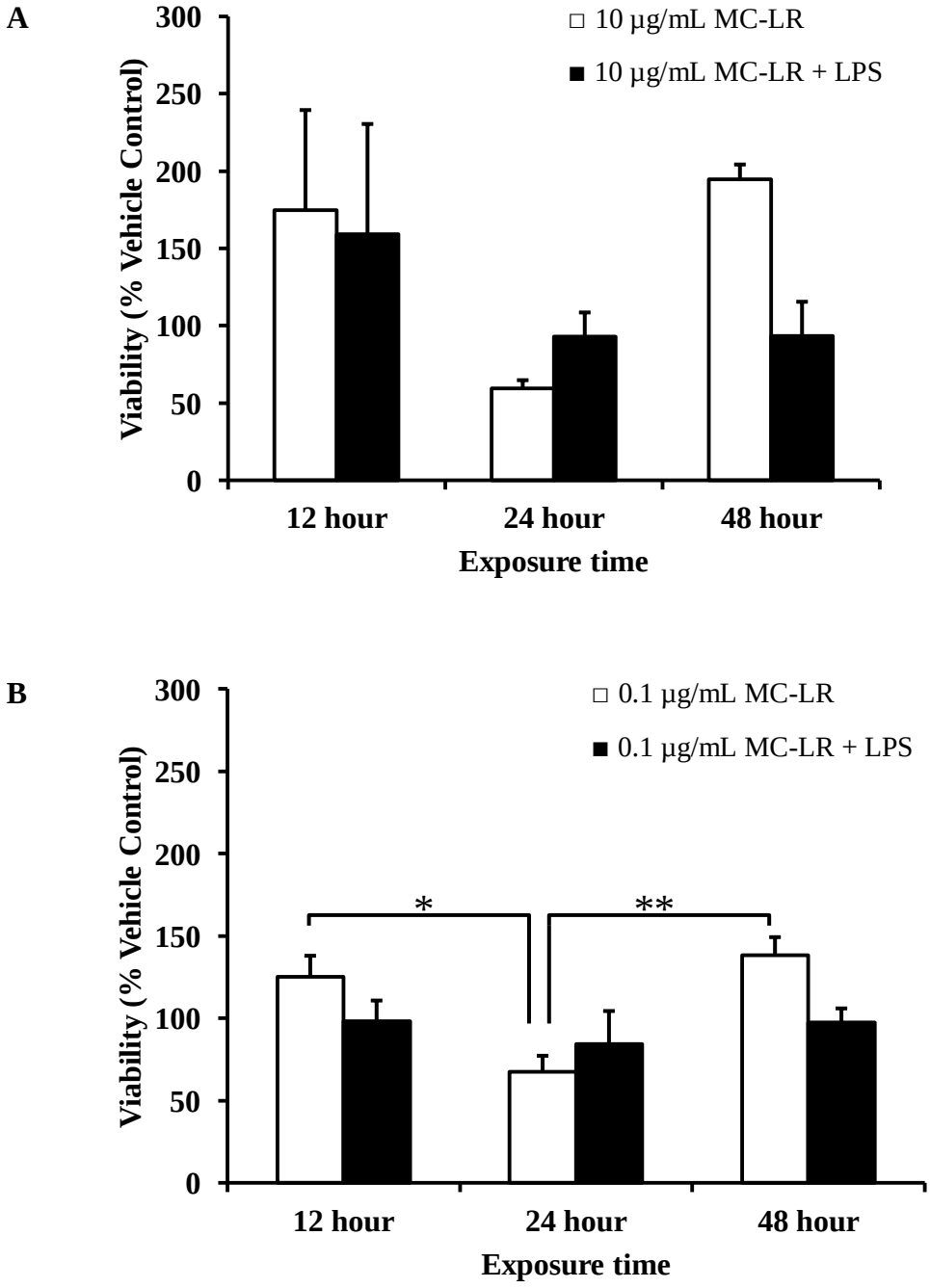

Figure 3.2.2.2: WST-1 proliferation assay to analyse the effect of MC-LR on J774A.1 macrophage cell line. Macrophages were cultured in the presence of MC–LR (A. 10 and B. 0.1 µg/mL) for 12, 24 and 48 hours and simultaneously stimulated with and without LPS. Toxin treatments alone are represented by the white bars (□) and toxin treatments with LPS challenge are represented by the black bars (■). B.) - LPS: $P < 0.05$* (12 to 24 hours, 10 µg/mL), $P < 0.01$** (24 to 48 hours, 10 µg/mL).

3.2.2.2 IL-1β cytokine release by J774A.1 murine macrophages following microcystin exposure and LPS challenge

Interleukin-1β (IL-1β) production by murine macrophages was measured in cell culture supernatants. IL-1β is a pro-inflammatory cytokine generated at sites of injury as part of the innate immune response, following danger signals from ATP and inflammasome activation. Initially, a control experiment was prepared to assess the ability of ATP to propagate a danger signal in the macrophages. It was also relevant to assess the ability of the TLR4 ligand, LPS, to activate the TLR4 signalling pathway. Such activation would result in the production of pro-IL-1β. Following APT stimulation, NLRP3 inflammasome activation would result in the cleavage of inactive pro-caspase-1 to active caspase-1, facilitating the conversion of pro-IL-1β to IL-1β, which would be released from the macrophage cell and subsequently detected in the supernatant, using ELISA.

Two different concentrations of ATP (10 and 20 nM) were assessed for their ability to stimulate IL-1β production in the presence and absence of an optimised concentration of LPS (100 ng/mL) (Figure 3.2.2.3). Supernatants were harvested and analysed for IL-1β secretion by ELISA. It is clear that both LPS and ATP are required for active IL-1β production. A concentration of 20 mM ATP was sufficient for IL-1β production ($P < 0.001$), whereas a concentration of 10 mM had no clear stimulatory effect. Glyburide (glybenclamide) is an inhibitor of ATP-sensitive K^+ channels and blocks inflammasome activation in response to ATP. A concentration of 25 µg/mL glyburide was also added, as part of the control experiment, to assess whether IL-1β production could be inhibited in macrophages stimulated with both LPS and ATP ($P < 0.001$). It was apparent that glyburide decreased the production of IL-1β secreted from the LPS-stimulated macrophage in the presence of the ATP stress signalling molecule (Figure 3.2.2.3). This effect was only apparent when ATP was present at a concentration of 20 mM.

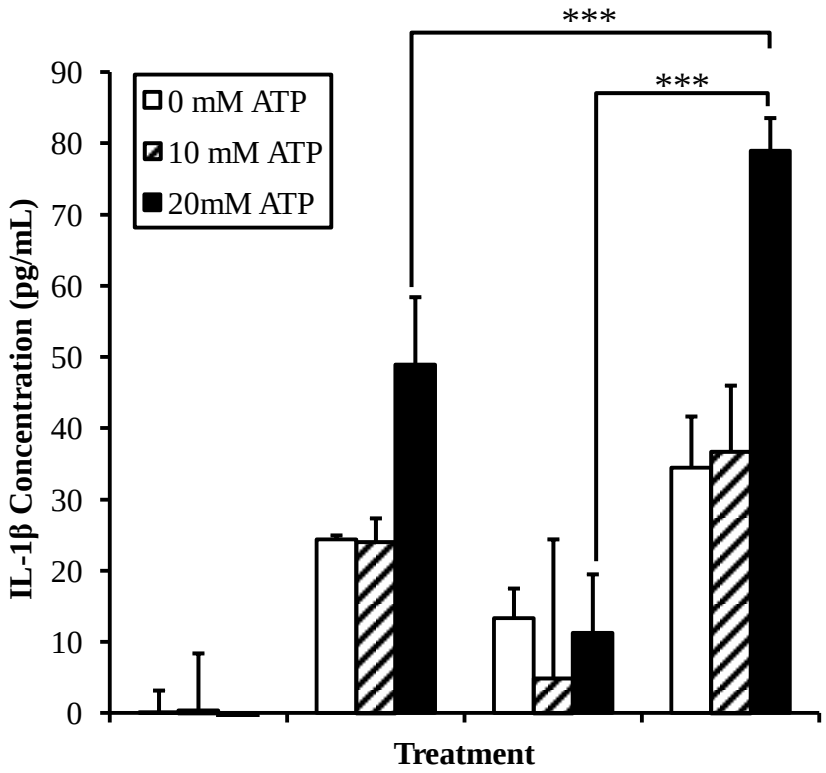

LPS (100 ng/mL)	-	+	-	+
Glyburide (25 µg/mL)	+	+	-	-

Figure 3.2.2.3: Optimisation of ATP, glyburide and LPS concentrations for analysis of ATP- and LPS-dependent inflammasome activation and glyburide inhibition in a macrophage model. J774A.1 cells were stimulated with and without 100 ng/mL LPS for 3 hours. Cells were subsequently exposed to varying concentrations of ATP (0, 10 and 20 mM), along with glyburide (25 µg/mL) for 24 hours. Supernatants were analysed by ELISA for the presence of active IL-1β (pg/mL). Results indicate a mean value from three independent experiments and error bars represent mean 3SE (n=3). $P < 0.001$*** (- / + glyburide, + LPS, + 20 mM ATP), $P < 0.001$*** (- / + LPS, + 20 mM ATP).

J774A.1 macrophages were exposed to MC-LR for 24 hours at two concentrations: 1 and 5 µg/mL. The high dose of MC-LR, 5 µg/mL significantly reduced IL-1β basal expression after 24 hours, compared with the media control ($P < 0.05$). The lower MC-LR concentration (1 µg/mL) also reduced IL-β basal expression but not in a statistically significant manner (Figure 3.2.2.4). The magnitude of IL-1β inhibition appeared to be significant and dose-dependent.

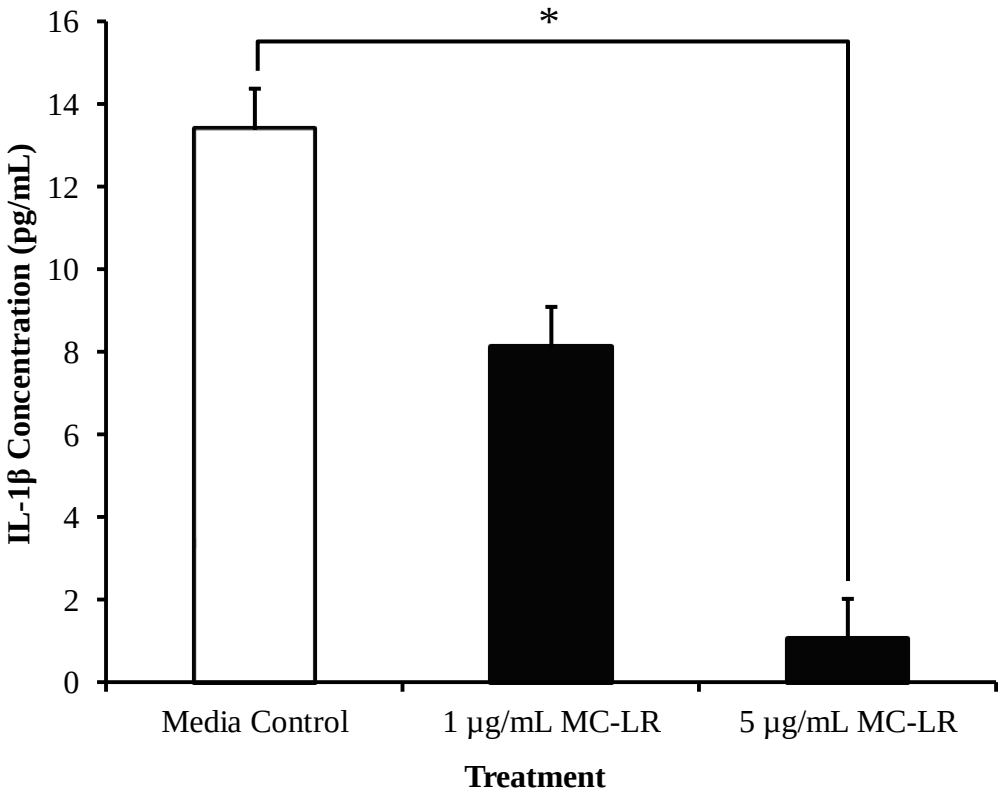

Figure 3.2.2.4: Effect of MC-LR on IL-1β cytokine secretion in J774A.1 murine macrophages. J774A.1 cells were exposed to two concentrations of MC-LR (1 µg/mL and 5 µg/mL), along with a media control, for 24 hours. Supernatants were harvested and analysed for IL-1β secretion by ELISA. Results indicate a mean value from three independent experiments and error bars represent mean 3SE (n=3). $P < 0.05$* (5 µg/mL MC-LR, versus media control).

To further investigate the immunosuppressive effects of MC-LR on murine macrophages *in vitro,* cells were pre-stimulated in the presence or absence of LPS (100 ng/mL) and exposed to extracellular ATP (20 mM) and MC-LR (5 µg/mL) for 3 hours. Supernatants were harvested and analysed for IL-1β secretion by ELISA. MC-LR exposure did not significantly alter LPS-stimulated or un-stimulated cells in the presence of ATP (Figure 3.2.2.5). However, MC-LR exposure did significantly reduce IL-1β expression in LPS-stimulated and un-stimulated cell in the absence of ATP ($P < 0.05$).

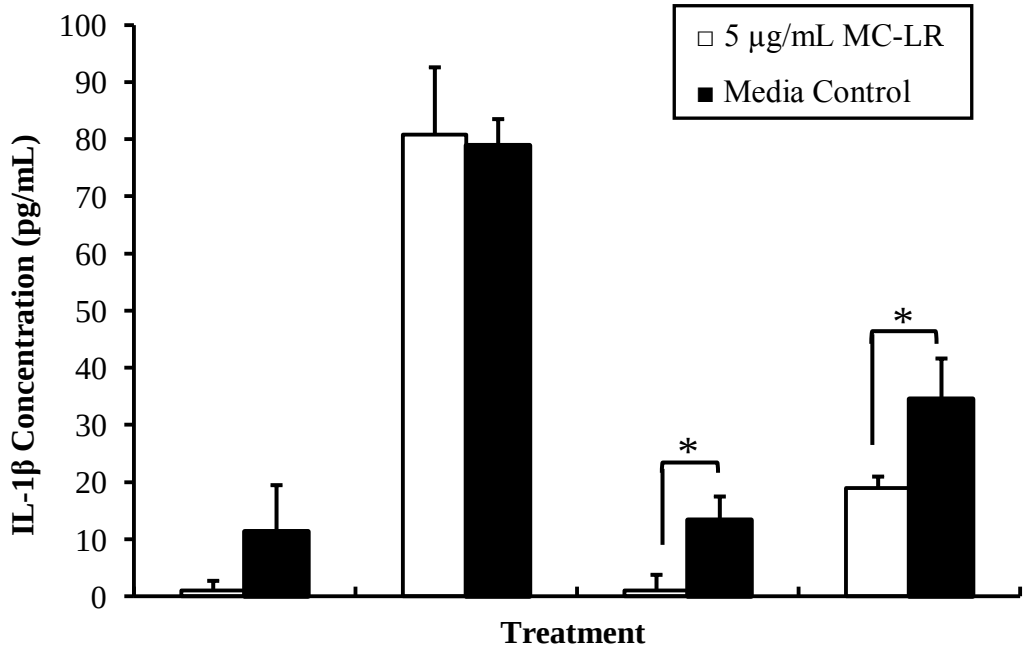

LPS (100 ng/mL)	-	+	-	+
ATP (20 mM)	+	+	-	-

Figure 3.2.2.5: Effect of MC-LR on IL-1β cytokine secretion in J774A.1 murine macrophages, following NLRP3 inflammasome activation. J774A.1 cells were stimulated with and without LPS (100 ng/mL) and then exposed to ATP, a NLRP3 and caspase-1 activator, and MC-LR (5 µg/mL) for 3 hours. Results indicate a mean value from three independent experiments and error bars represent mean 3SE (n=3). Toxin treatments are represented by the white bars (□) and control treatments (media only) are represented by the black bars (■). $P < 0.05$* (- LPS/- ATP: 5 µg/mL MC-LR, versus media control), $P < 0.05$* (+ LPS/- ATP: 5 µg/mL MC-LR, versus media control).

3.2.2.3 Analysis of caspase-1 activity after microcystin exposure using FLICA™ (Fluorochrome-labelled inhibitors of caspases) analysis

For sensitive detection of apoptotic cells *in vitro*, a fluorescence inhibitor probe, FAM-YVAD-FMK was utilised to label active caspase-1 in the murine macrophages. FLICA™ (Fluorescent-labelled inhibitor of caspases) probes are comprised of three main components; an inhibitor peptide sequence that binds to active caspase enzymes, a fluoromethyl ketone (FMK) moiety which irreversibly binds the enzyme and a fluorescent reporter tag (carboxyfluorescein) (FAM). For caspase-1 inhibiton, the multi-enzyme recognition sequence is tyrosine-valine-alanine-aspartic acid (YVAD). The FLICA™ FAM-YVAD-FMK probe interacts with the enzymatic reactive centre of activated caspase-1 via the YVAD recognition sequence, forming a covalent thioether adduct with the enzyme through the FMK moiety. The resulting fluorescence can be quantified using a fluorescence plate reader, giving an accurate indication of caspase-1 activity in a cell population.

In order to investigate the effect of MC-LR treatment on apoptosis in J774A.1 murine macrophages *in vitro*, cells were incubated with 5 µg/mL of MC-LR for 24 hours. Cells were incubated with FLICA solution and analysed for fluorescence activity on a Tecan® Safire II plate reader, using an excitation wavelength of 490 nm and an emission wavelength of 520 nm. The optimal gain and Z-Position were 255 AU and 3900 µM, respectively. The effects of non-specific binding were reduced by subtracting a background value of an un-stained cell population for each experiential parameter. Assessment of caspase-1 activation, via FLICA™ analysis, showed that MC-LR significantly increased the mean fluorescence intensity value and, thus, the amount of active caspase-1, in comparison with the media control ($P < 0.001$). This dramatic increase in active caspase-1 and, therefore, apoptotic cell number was only apparent when cells were exposed to MC-LR in the presence of two priming and stimulating signals from LPS and ATP, respectively. When the macrophages were subject to an LPS challenge alone, no significant increase in caspase-1 activity was observed (Figure 3.2.2.6).

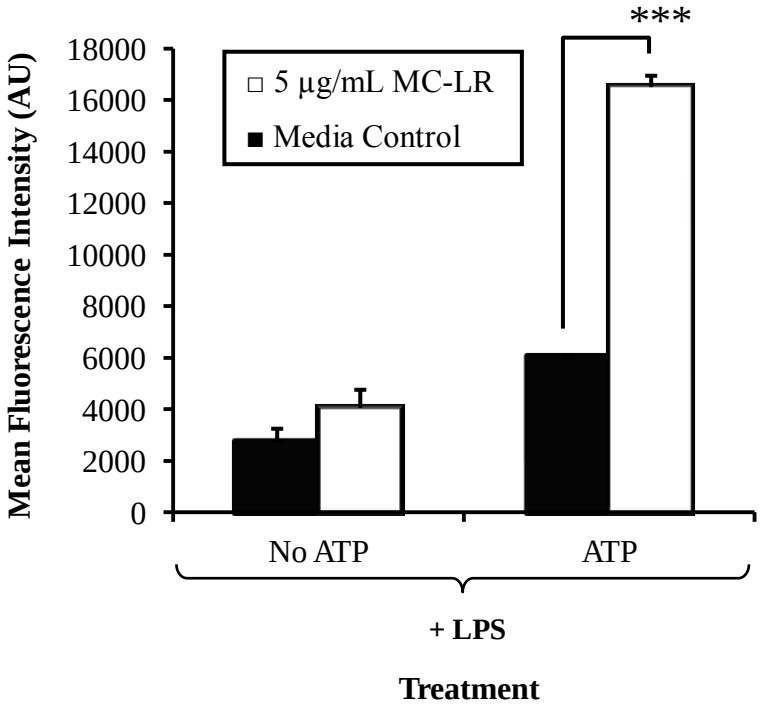

Figure 3.2.2.6: FAM-YVAD-FMK fluorescence detection of active caspase-1 in J774A.1 cells. Macrophages were stimulated with LPS (100 ng/mL), with and without ATP (20 mM) for 3 hours, followed by exposure to MC-LR (5 µg/mL) for 24 hours. Results indicate a mean value from three independent experiments and error bars represent mean 3SE (n=3). + LPS / + ATP: $P < 0.001$*** (5 µg/mL MC-LR, versus media control).

3.2.3 Analysis of aflatoxin exposure on the murine macrophages

3.2.3.1 Cytokine secretion by J774A.1 macrophages after exposure to aflatoxin G_1, B_1 and B_2 following LPS challenge

Initial cytokine analysis was carried out by Dr. Johanna Bruneau, as part of a collaborative publication. All subsequent data compilation and evaluation, for thesis work and publication, was carried out by Edwina Stack. The cytokine response of J774A.1 macrophages to LPS challenge varied depending on the aflatoxin isoform. Each graph shows concentration of cytokine released into supernatant compared to control, following high (0.1 ng/mL) and low (0.01 ng/mL) doses of AFB_1, AFB_2 or AFG_1 toxin alone and toxin with LPS challenge. Data was expressed as the mean for each experiment (n=3), with error bars indicating 3 SE. Significant differences in cytokine secretion were observed for the basal expression levels of cytokine, however, the major focus of these experiments was the effect of aflatoxin exposure, following

LPS challenge. Incubation with AFB_1 for 72 hours resulted in a statistically significant increase in IL-6 secretion with LPS stimulation at 0.1 ng/mL AFB_1 ($P < 0.01$) (Figure 3.2.3.1 A). Statistically, secretion of IL-12p40 and TNF-α were not significantly affected following LPS stimulation, but expression of IL-12p40 did decrease with an increasing AFB_1 concentration (Figure 3.2.3.1 B and D, respectively). With LPS stimulation, there was a significant decrease in anti-inflammatory IL-10 at 0.01 ng/mL AFB_1 and a significant increase at 0.1 ng/mL AFB_1 ($P < 0.001$), compared with the LPS stimulation alone (Figure 3.2.3.1 C).

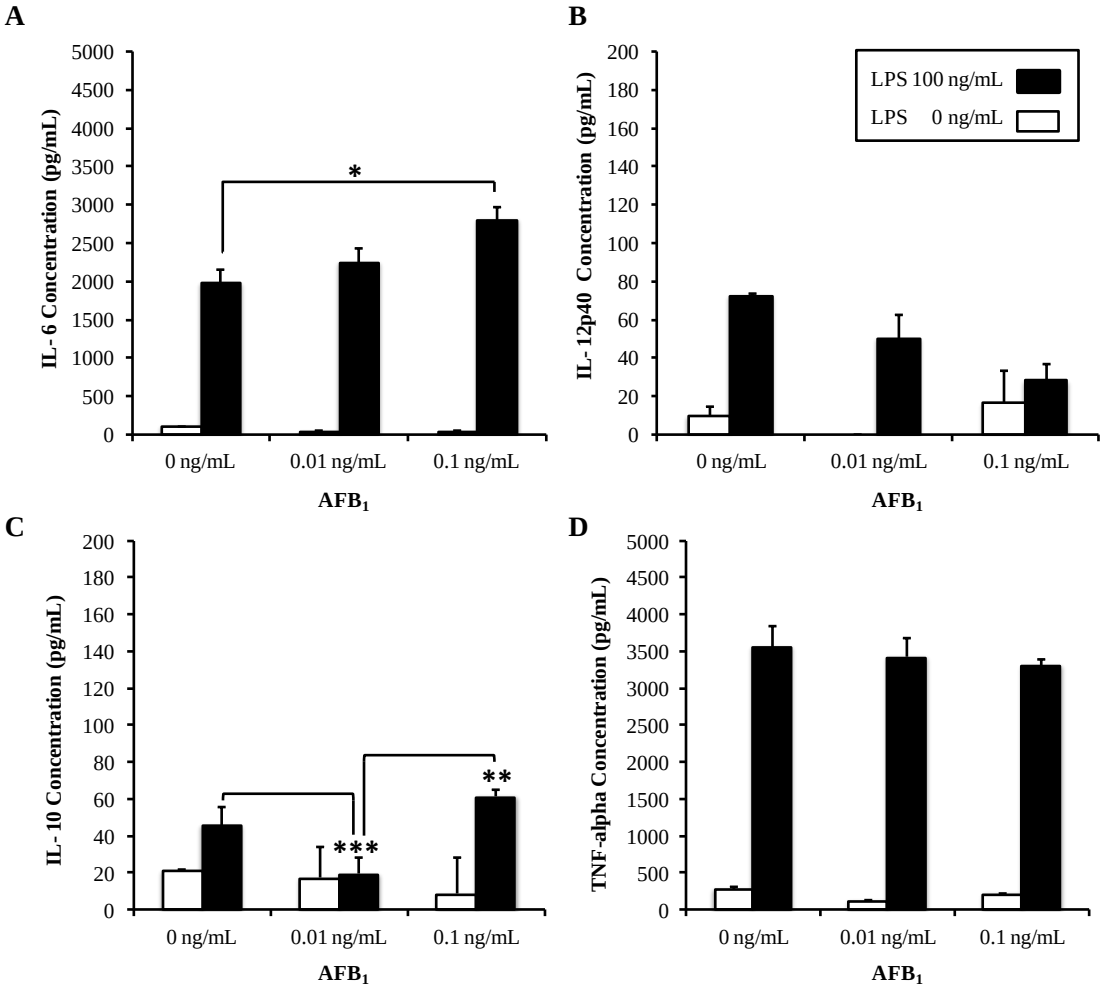

Figure 3.2.3.1: Exposure of J774A.1 macrophages to **AFB_1** modulates cytokine secretion. Expression of IL-6, IL-10, IL12p40 and TNF-α in supernatants of J774A.1 murine macrophage cells, cultured in the presence of AFB_1 for 72 hours were stimulated with LPS for 24 hours. The 72 hour toxin treatments are represented by the white bars (□) and toxin treatments with 24 hour LPS challenge are represented by the black bars (■). A.) LPS: $P < 0.05$* (0.1 ng/mL AFB_1, versus 0 ng/mL) C.) LPS: $P < 0.001$*** (0.01 ng/mL AFB_1, versus 0 ng/mL); $P < 0.01$** (0.1 ng/mL AFB_1, versus 0 ng/mL).

In comparison to AFB_1, treatment with AFB_2 (0.1 ng/mL), followed by stimulation with LPS, also resulted in a significant increase ($P < 0.001$) in IL-6 secretion (Figure 3.2.3.2 A). There was a significant decrease ($P < 0.05$) in IL-10 at the lower dose of 0.01 ng/mL AFB_2 (Figure 3.2.3.2 C). Levels of IL-12p40 were also decreased significantly ($P < 0.001$) after AFB_2 exposure, particularly at the lower dose (Figure 3.2.3.2 B). While TNF-α expression was inhibited by AFB_2 treatment, the effect was not significant (Figure 3.2.3.2 D).

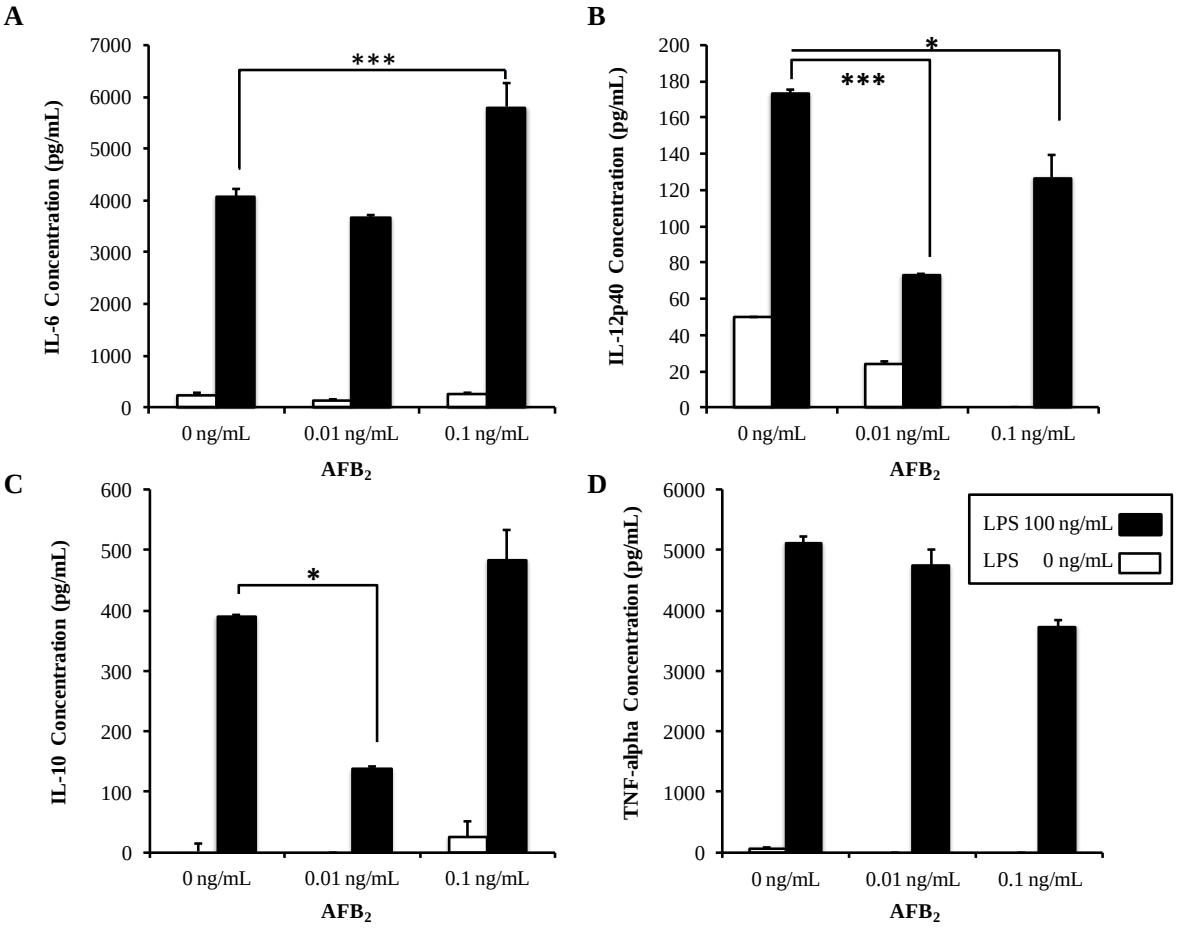

Figure 3.2.3.2: Exposure of J774A.1 macrophages to **AFB_2** modulates cytokine secretion. Expression of IL-6, IL-10, IL12p40 and TNF-α in supernatants of J774A.1 murine macrophage cells, cultured in the presence of AFB_2 for 72 hours and stimulated with LPS for 24 hours. The 72 hour toxin treatments are represented by the white bars (□) and toxin treatments with 24 hour LPS challenge are represented by the black bars (■). A.) LPS: $P < 0.001$*** (0.1 ng/mL AFB_2, versus 0 ng/mL) B.) LPS: $P < 0.001$*** (0.01 ng/mL AFB_2, versus 0 ng/mL), $P < 0.05$* (0.1 ng/mL AFB_2, versus 0 ng/mL) C.) LPS: $P < 0.05$* (0.01 ng/mL).

Of the three aflatoxin isoforms tested, AFG_1 had the least effect on cytokine secretion in the presence of LPS. When the murine macrophages were exposed to 0.01 ng/mL AFG_1 for 72 hours, and stimulated with LPS, a decrease in TNF-α expression was observed (Figure 3.2.3.3 D). Secretion of IL-6, IL-10 and IL-12p40 by the macrophages was not affected by AFG_1 at either dose tested (Figure 3.2.3.3 A-C).

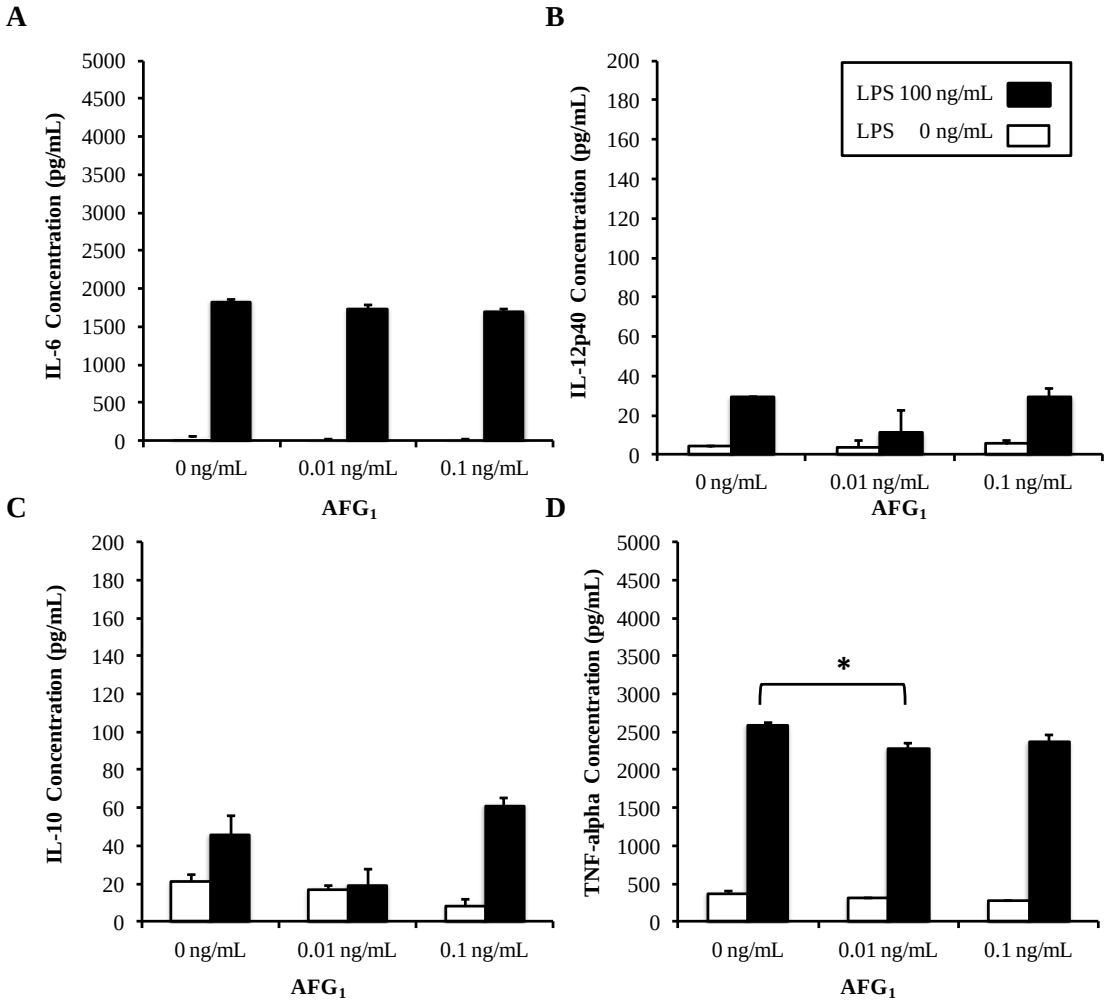

Figure 3.2.3.3: Effect of exposure of **AFG_1** on cytokine expression. Expression of IL-6, IL-10, IL12p40 and TNF-α in supernatant of J774A.1 murine macrophage cells, cultured in the presence of AFG_1 for 72 hours were stimulated with LPS for 24 hours. The 72 hour toxin treatments are represented by the white bars (□) and toxin treatments with 24 hour LPS challenge are represented by the black bars (■). D.) $P < 0.05$* (0.01 ng/mL).

The effect of combining different aflatoxin isoforms on cytokine secretion, by J774A.1 cells, varied depending on the isoform. Results for all isoform combinations are shown in Figures 3.2.3.4 and 3.2.4.5. Secretion of IL-6 was significantly increased ($P < 0.001$) following LPS exposure with a combination of AFB_1 and AFB_2, both at a concentration of 0.01 ng/mL (Figure 3.2.3.4 A). Significantly, there was no observable change in IL-6 expression at this lower dose when the macrophages were exposed to AFB_1 or AFB_2 alone. Although there was a significant decrease in LPS-induced IL-10 secretion from cells treated with 0.01 ng/mL AFB_1 or AFB_2 alone, IL-10 release was unaffected by any of the toxin combinations at either concentration (Figure 3.2.3.4 B). However, when AFB_1 and AFB_2 were combined at a concentration of 0.1 ng/mL, a significant increase in IL-10 basal expression levels was observed ($P < 0.001$).

Incubation with every toxin combination, including AFB_1 + AFB_2, AFB_1 + AFG_1, and AFB_2 + AFG_1, significantly decreased ($P < 0.001$) IL-12p40 secretion in LPS-stimulated macrophages (Figure 3.2.3.5 A). Previously, a significant decrease in IL-12p40 had only been observed for treatment with AFB_2 alone. Incubation with each toxin combination also inhibited the basal turnover of TNF-α expression across the board ($P < 0.01$ and $P < 0.001$). While there was little or no effect of single isoform treatment on TNF-α secretion observed, there was a significant ($P < 0.01$) decrease in LPS-induced TNF-α secretion for 0.01 ng/mL AFB_1 + AFG_1 and 0.1 ng/mL AFB_1 + AFB_2, compared with the vehicle controls (Figure 3.2.3.5 B).

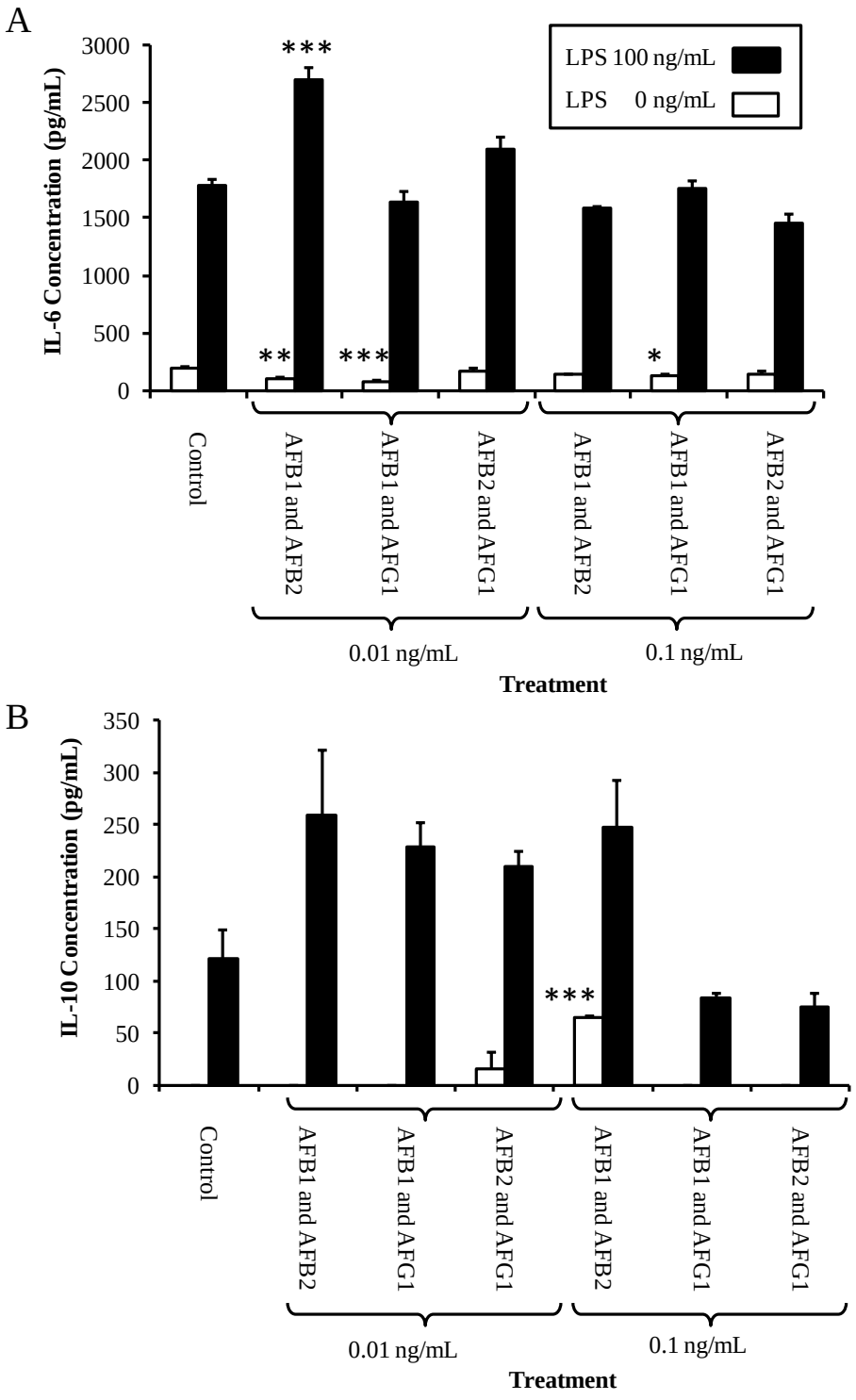

Figure 3.2.3.4: Expression of IL-6 and IL-10 in the supernatants of J774A.1 murine macrophage cells, cultured in the presence of different combinations of **AFB_1, AFB_2 and AFG_1** for 72 hours, and stimulated with LPS for 24 hours. The 72 hour toxin treatments are represented by the white bars (□) and toxin treatments with 24 hour LPS challenge are represented by the black bars (■). Data was expressed as the mean for each experiment (n=3), with error bars indicating 3SE. Significance: $P < 0.05$*; $P < 0.01$**; $P < 0.001$*** as illustrated, all relative to the LPS control (no toxins).

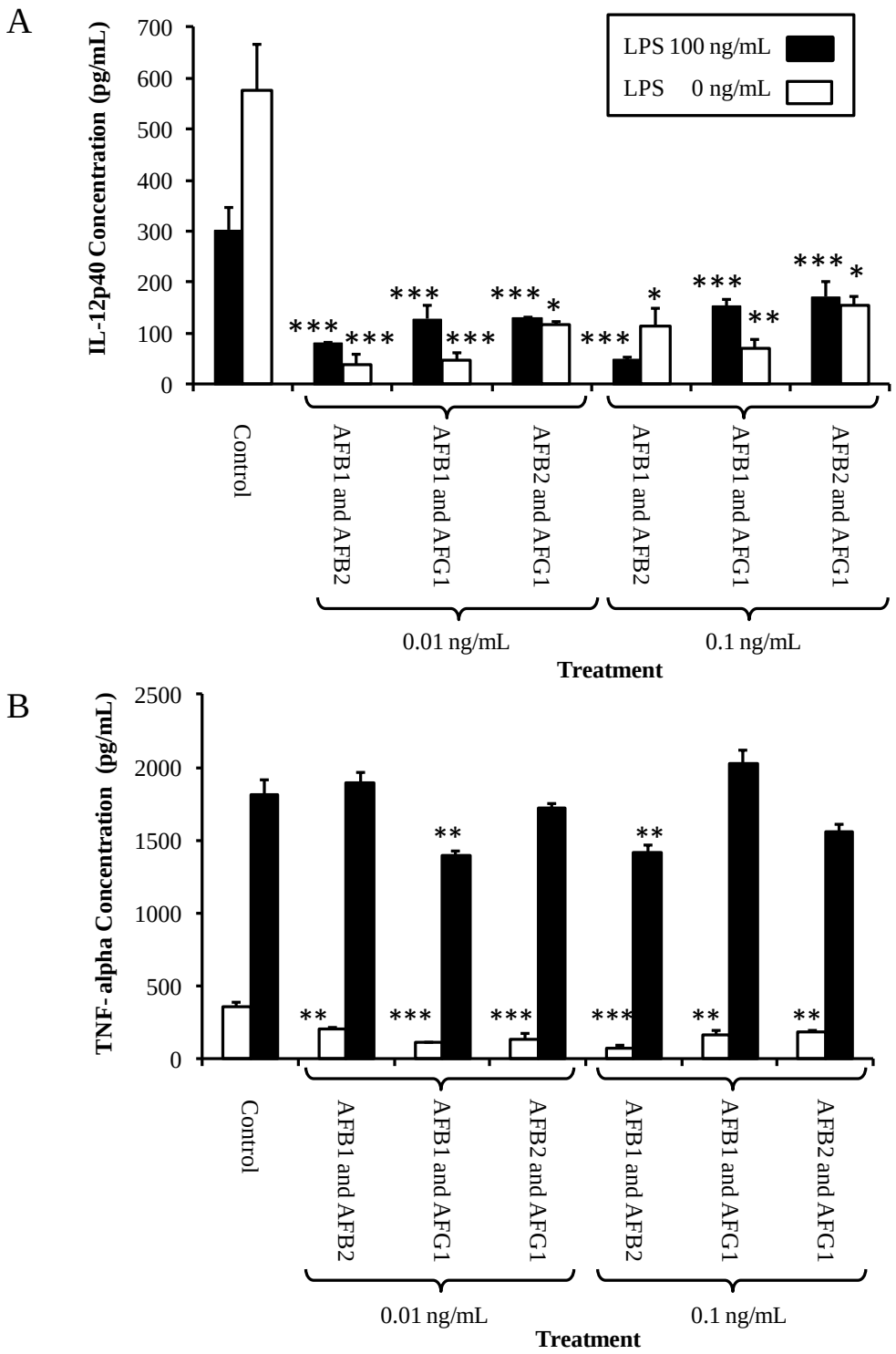

Figure 3.2.3.5: Expression of IL12p40 and TNF-α in supernatant of J774A.1 murine macrophage cells, cultured in the presence of different combinations of **AFB_1, AFB_2 and AFG_1** for 72 hours, and stimulated with LPS for 24 hours. The 72 hour toxin treatments are represented by the white bars (□) and toxin treatments with 24 hour LPS challenge are represented by the black bars (■). Data was expressed as the mean for each experiment (n=3), with error bars indicating 3SE. Significance: $P < 0.05$*; $P < 0.01$**; $P < 0.001$*** as illustrated, all relative to the LPS control (no toxins).

3.2.3.2 Cell surface marker expression on murine macrophage after exposure to Aflatoxin G_1, B_1 and B_2 with LPS challenge

Since cell surface markers play a critical role in the initiation of an inflammatory response, the effect of aflatoxin exposure on the expression of TLR2, TLR4, CD14 and CD40 in a murine macrophage cell line (J774A.1), was investigated. The results are summarised in Table 3.2.3.1. Treatments were performed at two concentrations, 0.1 ng/mL and 0.01 ng/mL, but significant changes were only observed at the lower concentration (data not shown for 0.1 ng/ml). Data was analysed using mean fluorescence intensity (MFI) values. MFI is defined as the arithmetic mean of the data, in which the linear scaled fluorescence was averaged and the result is weighted by outliers at the high end of the distribution.

A significant decrease was observed in expression of TLR2 on the murine macrophages, after treatment with AFB_2 or AFG_1 with endotoxin challenge ($P < 0.01$). With AFB_1 exposure alone, a slight increase in TLR2 expression was observed, compared with the solvent control ($P < 0.05$). Significantly, CD14 expression was significantly ($P < 0.01$) decreased following treatment with AFB_1 + AFB_2, both with and without LPS challenge. TLR4 and CD40 expression levels were not significantly affected by any of the toxin treatments, either in the presence or absence of LPS (data not included). For each experimental acquisition, the isotype-control antibody-stained cells indicated no non-specific binding of fluorophores. The isotype controls were rat anti-IgG2a (fluorescein (FITC)-labelled), rat anti-IgG2b (FITC-labelled) and rat anti-IgG2a (phycoerythrin (PE)-labelled).

Table 3.2.3.1: Cell surface marker analysis, following aflatoxin exposure. J774A.1 murine macrophage cells were incubated with 0.01 ng/mL singly or in combination with aflatoxins, **AFB_1, AFB_2 and AFG_1** for 72 hours and subsequently stimulated with or without 100 ng/mL of LPS for 24 hours. Cells were stained with anti-TLR2 antibody, labelled with FITC (eBio), anti-TLR4 antibody, labelled with PE (eBio), anti-CD40 antibody, labelled with PE (BD) and anti-CD14 antibody, labelled with FITC (eBio). Samples were analysed in three independent experiments using a FACSCalibur™ flow cytometer (BD). The data is represented as the mean value ± 3SE. TLR2 (- LPS): $P < 0.05$* (AFB_1 alone, versus control). TLR2 (+ LPS): $P < 0.01$** (AFB_2, AFG_1 alone, versus control), CD14 (- LPS): $P < 0.01$** (AFB_1 + AFB_2, versus control), CD14 (+ LPS): $P < 0.01$** (AFB_1 + AFB_2, versus control).

Treatment	LPS	TLR2	CD14
Solvent Control	-	35.55 ± 2.16	8.70 ± 0.03
AFB_1	-	44.43 ± 3.46 *	9.80 ± 0.04
AFB_2	-	33.68 ± 0.93	12.96 ± 3.86
AFG_1	-	33.55 ± 1.65	7.69 ± 0.03
Treatment	**LPS**	**TLR2**	**CD14**
Solvent Control	+	81.50 ± 1.44	16.20 ± 0.17
AFB_1	+	76.75 ± 2.88	16.17 ± 0.77
AFB_2	+	65.26 ± 2.42 **	12.07 ± 4.25
AFG_1	+	65.82 ± 4.36 **	17.20 ± 0.67
Treatment	**LPS**	**TLR2**	**CD14**
Solvent Control	-	45.75 ± 1.66	43.11 ± 0.78
AFB_1 + AFB_2	-	37.14 ± 2.51	34.37 ± 1.07 **
AFB_1 + AFG_1	-	37.59 ± 2.53	44.63 ± 1.23
AFB_2 + AFG_1	-	38.38 ± 0.47	46.51 ± 0.00
Treatment	**LPS**	**TLR2**	**CD14**
Solvent Control	+	70.87 ± 3.67	88.78 ± 3.89
AFB_1 + AFB_2	+	63.70 ± 3.54	35.42 ± 1.08 **
AFB_1 + AFG_1	+	57.69 ± 4.74	105.40 ± 5.86
AFB_2 + AFG_1	+	65.78 ± 0.18	97.91 ± 0.23

3.3 Discussion

Under normal healthy circumstances, the immune system defends the host against pathogenic infections. However, certain environmental factors, including toxins, can alter the development and function of the immune response, leading to autoimmunity, hypersensitivity or immunosuppression. However, understanding of the biological processes underlying immune system dysfunction is incomplete. A functioning immune system is essential for survival as it defends the body against infection to foreign agents. A key element of immune function is the ability to distinguish 'self' from potentially harmful foreign components ('non-self'). Failure to make this distinction results in autoimmune disease. Immunotoxicology is the study of undesired effects resulting from the interactions of xenobiotics, including toxins, with the immune system. There is evidence that certain xenobiotics cause immune suppression (Kaminski *et al*., 2008; Luster and Gerberick, 2010). It is clear that there are a vast number of cellular and molecular targets for xenobiotics that act as immunosuppressants, as reviewed by Grinyó *et al*. (2012).

Xenobiotics, such as toxins, may interfere with receptor-ligand binding at the cell surface or with the cascade of signalling events that leads to transcription of genes responsible for generating and regulating the appropriate immune responses. One of the major adverse consequences of immunosuppression is that host resistance against microbial pathogens is impaired, leading to infection. Moreover, immunostimulation and immunosuppression can occur with the same xenobiotic depending on the exposure conditions, including dosage and time. Chemicals such as cadmium, lead and selenium have the ability to enhance immune function at very low exposure levels, although high exposure levels led to immunosuppression (Zelikoff and Thomas, 1998). Such experimental observations have given rise to the term 'immunomodulation' which accounts for this dual effect. It is important to stress that any deregulation of immune cell homeostasis can result in serious consequences for immune functions, increasing the susceptibility to infections and cancer, as well as favouring the development of autoimmune diseases. Therefore, any significant change in the functionality of immune cells must be considered as a hazard.

3.3.1 Azaspiracid

Azaspiracid accumulation in shellfish and its ongoing risk to human health is a prevalent issue in the waters of Europe, Africa, and North and South America (James *et al*., 2002a; Taleb *et al*., 2006; Twiner *et al*., 2008; Álvarez *et al*., 2010). The lack of understanding of the molecular mechanisms of AZA toxicity has hindered researchers in identifying its acute and chronic effects on humans and other animals. To date, few studies have reported on the immunomodulatory effects of azaspiracid on macrophages *in vitro*. For example, Ito *et al*. (2000) is one of the few publications that demonstrated a decrease in the number of non-granulocyte cells, including monocytes, lymphocytes and macrophages in the spleen, following AZA exposure. According to Twiner and colleagues, AZA-1 was cytotoxic (EC_{50}s as low as 1 nM) to a number of mammalian cell lines, including Jurkat, Raji, THP-1, HEK-293, A549, GH_4C_1 and Neuro-2A, with the Jurkat cell line (human T-lymphocyte) being particularly sensitive (Twiner *et al*., 2005). Due to the lack of experimental evidence regarding molecular immunotoxicity of azaspiracid on cytotoxicity and cytokine production in macrophages, it was therefore important to investigate whether azaspiracid could regulate these pivotal parameters in a murine macrophage model. This investigation is the first to assess the *in vitro* effects of AZA on murine macrophages, although other phycotoxins including yessotoxin, have been shown to inhibit macrophage function (Orsi *et al*., 2010).

In this study, two commonly used colorimetric, end-point cytotoxicity assays, the WST-1 cell death assay and the LDH proliferation assay, were used to analysis azaspiracid toxicity in a J774A.1 murine model. The WST-1 assay provides a measurement of cell viability and proliferation, through determination of mitochondrial dehydrogenase, while the LDH assay is based on the measurement of lactate dehydrogenase activity in the cytosol of damaged cells. The J774A.1 murine macrophage cell line was exposed to various concentrations of AZA-1, and the WST-1 assay was used to analyse mitochondrial dehydrogenase activity. There was a significant change in the percentage viability of the macrophages, incubated with AZA-1 for 24 hours (0.001 to 100 pg/mL). Interestingly, no significant change in cell viability was observed when macrophages were co-stimulated with both LPS and AZA-1. It is clear that the presence of AZA-1 affected the ability of the cells to proliferate, and this may have lead to cell death. However, this effect was negated through stimulation of the cell with LPS. For the LDH

cytotoxicity assay, the percentage cytotoxicity, relative to the vehicle control, showed an unexpected decrease in cytotoxicity at the lower AZA-1 concentration, followed by a subsequent increase in cytotoxic effect at higher concentrations. It is possible that a protection mechanism is preventing cellular injury at low toxin concentrations, perhaps though internalisation or secretory products. In biological investigations, the occurrence of U-shaped dose-response relationships is well-documented and is commonly known as hormesis (Calabrese and Baldwin, 2001). This effect is identifiable as a favourable biological response to low exposures to toxins and other stressors. Historically, this effect was characterised by the Arndt–Schulz rule or Schulz' law, which states that 'for every substance, small doses stimulate, moderate doses inhibit, large doses kill'.

The molecular mechanisms involved in AZA toxicity are still not well understood. This is despite numerous cytotoxicity experiments in which a variety of different morphological effects were observed (Román *et al*., 2002; Twiner *et al*., 2005; Ronzitti *et al*., 2007; Twiner *et al*., 2008). For instance, T-lymphocytes responded to AZA-1 through reduction in membrane integrity, organelle protrusion and a retraction of pseudopodia, followed by protracted cell lysis (Twiner *et al*., 2005). In the study by Twiner *et al*., 2008, filamentous actin (F-actin) appeared to follow the retraction of the pseudopodia. AZA induced considerable morphological and cytoskeletal effects on human neuroblastoma cells, following 24 to 48 hour exposures (Vilariño *et al*., 2007).

Macrophages are a major source of cytokines, including IL-1β, TNF-α, IL-6, IL-10 and IL-12 and participate as major effector cells in resistance to pathogens, including bacteria and viruses. In the current study, exposure to AZA-1 significantly suppressed the ability of macrophages to respond to LPS activation. LPS is a component of the outer membrane of the cell wall of Gram-negative bacteria. A notable inhibition in the abundance of TNF-α and IL-6 was achieved through AZA-1 exposure in LPS-stimulated macrophages, which suggests that AZA-1 can antagonise the function and proliferation of macrophages through modulation of TNF-α and IL-6. TNF-α and IL-6 are pro-inflammatory cytokines, secreted by activated macrophages. TNF-α is a multi-functional cytokine, which serves to recruit and stimulate other cells to sites of microbial invasion and infection. These cytokines have important roles in host defence; however, their over-production or under-production can contribute to inflammatory diseases, including rheumatoid arthritis, cerebral malaria, and AIDS (McInnes and

Schett, 2007). IL-6 acts as both a pro-inflammatory and anti-inflammatory cytokine to stimulate the immune response to infection by promoting T- and B-cell proliferation. In addition, IL-6 functions as a mediator of the acute response to infection (Mosser and Edwards, 2008).

In contrast, levels of IL-12p40 and IL-10 were increased by AZA-1 exposure in a time-dependent manner; however, there was no significant effect on responsiveness to LPS stimulation. IL-12 is a regulator of cell-mediated immune responses. It is produced primarily by antigen-presenting cells, including activated B-cells, dendritic cells and macrophages. It is secreted as a 75 kD heterodimer glycoprotein, composed of a 40 kD and a 35 kD subunit, joined by a disulphide bond. Active IL-12 has multiple effects on T-cells and NK cells, including cytotoxicity stimulation, proliferation, cytokine production and T_H1 cell development. As an anti-inflammatory molecule, IL-10 blocks cytokine production and the expression of membrane co-stimulatory receptors, therefore decreasing the ability of macrophages and dendritic cells to present antigens (Pestka *et al*., 2004). The work presented in this chapter shows that murine macrophages generate a significant immune response to toxin exposure, particularly through production of the regulatory cytokine, IL-12p40. Moreover, it is possible that AZA-1 exposure can negate the ability to mount a host response to invasion by Gram-negative bacteria, by inhibiting the secretion of pro-inflammatory TNF-α and IL-6.

3.3.2 Microcystin

It is clear that macrophage function was down-regulated by the cyanobacterial hepatotoxins, microcystin (MC). The potent anti-proliferative activity of MC on J774A.1 macrophages was significant, as this effect had not been demonstrated previously. Most studies on the cytotoxicity of cyanobacterial toxins to immune cells utilised peritoneal macrophages, as previously discussed (Rocha *et al*., 2000; Nobre *et al*., 2003; Chen *et al*., 2004; Chen *et al*., 2005). Therefore, J774A.1 murine macrophages were chosen to examine the effects of MC-LR on cell growth and apoptosis. Exposure to MC-LR generated a time-dependent increase of LPS-induced and un-induced cytotoxicity, as measured by the LDH assay *in vitro*. This data is consistent with the LDH data obtained by Chong *et al*. (2000). These authors demonstrated the toxic effect of MC on numerous mammalian cell lines. Significantly,

this effect was only observed after 48 hours, indicating the cytotoxicity may be chronic in nature. The selected doses (10 µg/mL and 0.1 µg/mL) showed similar toxicity profiles. The inhibition of J774A.1 cell proliferation provoked by MC-LR was also examined by WST-1 analysis, but only the lower concentration of 0.1 µg/mL MC-LR showed a significant response after 24 hours of exposure. Therefore, based on WST-1 analysis, it appears that murine macrophage MC-LR-induced toxicity is both time-and dose-dependent.

Members of the 'nod-like' receptor (NLR) family assemble into multi-protein complexes, termed inflammasomes (Tschopp *et al*., 2003). Inflammasomes activate caspase-1, a proteolytic enzyme, which cleaves and activates the secreted pro-inflammatory cytokines, IL-1β and IL-18. Inflammasomes regulate pyroptosis, a caspase-1-dependent form of cell death that is highly inflammatory (Byrant and Fitzgerald, 2009). One of the most fully-characterised inflammasomes consists of NLRP3, ASC and caspase-1, and is termed the NLRP3 or NALP3 inflammasome. To test whether immunomodulation elicited by MC-LR was due to its influence on NLRP3 inflammasome activation or de-activation, a number of key inflammasome mediators were examined, including active IL-1β and caspase-1. IL-1β was significantly modulated by MC-LR exposure at a concentration of 5 µg/mL (Figure 3.2.2.4). These results corroborated with data published by Chen and co-workers, who showed that mRNA levels of iNOS, IL-1β and TNF-α were decreased, in a dose-dependent manner, in murine peritoneal macrophages, which were exposed to MC-LR (Chen *et al*., 2004). It is well documented that the pro-inflammatory cytokine, IL-1β play a critical role in the initiation of the immune response to toxins and in resulting peripheral tissue destruction (Black *et al*., 2005; Church *et al*., 2008). The results of this study showed that MC-LR significantly inhibited expression of IL-1β, relative to the vehicle control. IL-1β has a wide range of action in many cells, including B-cells, T-cells and monocytes. Previously, microcystin has been shown to cause significant immunomodulation effects in macrophage models. High levels of TNF-α were secreted after 24 hours of exposure to microcystin (Chen *et al*., 2005). It was possible that this may represent an adaptive response of macrophages to the inhibitory effect of microcystin, since it is known that TNF-α also stimulates phagocytosis in macrophages. Similarly, a number of investigations have demonstrated a decrease in IL-2 production in immune cells, following MC-LR exposure (Yea *et al*, 2001; Lankoff *et al*., 2004).

Given the inhibitory effect of MC-LR in the basal level of IL-1β secretion in murine macrophages, it was important to investigate whether this effect was related to NLRP3 inflammasome activation. The secretion of IL-1β is dependent on the levels of pro-IL-1β induced at the transcriptional level by pro-inflammatory stimuli from TLR ligands, including LPS. A large number of microbial components have been shown to activate the NLRP3 inflammasome including *Staphylococcus aureus, Listeria moncytogenes, Escherichia coli* and *Mycobacterium marinum* (Mariathasan *et al*., 2006; Mariathasan and Monack, 2007). In addition to microbial stimulation, endogenous danger signals, including ATP, generally released from damaged tissues, are essential for triggering inflammasome activation. The requirement for two distinct stimuli in the regulation of IL-1β production ensures that it is not inappropriately released, which may cause deleterious effects in the host. Excessive production of IL-1β has been associated with hereditary periodic fever syndromes, autoimmune and inflammatory diseases, such as gout and rheumatoid arthritis (Masters *et al*., 2009).

Through optimisation of the inflammasome activation in the J774A.1 macrophage model, it was clear that stimulation from both LPS and ATP was essential for the activation of IL-1β production, at a concentration of 100 ng/mL and 20 mM, respectively (Figure 3.2.2.3). The ATP-sensitive K^+ channel inhibitor, glyburide was also effective in reducing IL-1β production, in response to ATP and LPS, proving that the inflammasome could be inhibited in the murine macrophage. Following microcystin exposure (5 µg/mL) in an ATP- and LPS- activated macrophage, it was clear that microcystin inhibited IL-1β production, independent of LPS or ATP stimulation (Figure 3.2.2.5). Stimulation with ATP (both in the presence and absence of LPS) showed no significant effect on IL-1β production in response to microcystin. However, inhibition of IL-1β production was evident both in the presence and absence of LPS, with no ATP stimulation. It is clear that microcystin reduced the basal expression level of IL-1β, while also influencing the macrophages ability to respond to LPS stimulation. However, it is unknown whether this effect is influenced by inflammasome assembly or activation.

Freche *et al*. highlighted the ability of toxins to activate the inflammasome (Freche *et al*., 2007). Furthermore, it was demonstrated that aerolysin from *A. hydrophilia* triggers

the activation of caspase-1 (McCoy *et al*., 2010). Aerolysin is also known to cause pore-formation, which results in the permeabilisation of the plasma membrane to ions, particularly calcium and potassium. In response to pore formation, cells of the immune system, including lymphocytes, produce inflammatory molecules and undergo apoptosis. Potassium efflux can also be triggered by the purinergic receptor, $P2X_7$, by ATP, which has long been used as an activator of caspase-1 (Perregaux and Gabel, 1994). Opening of potassium-selective channels is followed by the opening of a larger pore, known as pannexin-1 (Pelegrin and Surprenant, 2006). Interestingly, pannexin-1 was recently shown to also be crucial for maitotoxin-induced caspase-1 activation (Pelegrin and Surprenant, 2007). Maitotoxin is a potent marine phycotoxin isolated from the dinoflagellate, *Gambierdiscus toxicus*. Currently, the mode of action of both microcystin and maitotoxin remains unknown.

In vivo and *in vitro* models demonstrated the stimulation of apoptosis, as a result of MC-LR exposure, via a mitochondrial pathway (Fladmark *et al*., 2002) and alternatively through expression of pro-apoptotic proteins (Fu *et al*., 2005). MC-LR induced reactive oxygen species formation, cytochrome-c and Ca^{2+} release, caspase activation and cytoskeletal damage, resulting in apoptosis (Ding *et al*., 2002; Ding and Ong, 2003; Weng *et al*., 2007). Analysis of caspase-1 activation in murine macrophages provides further insight into the mechanism by which microcystin induces apoptotic cell death. From the results, it is evident that MC-LR stimulated caspase-1 production in an ATP-dependent manner (Figure 3.2.2.6). In LPS-stimulated macrophages, no effect on caspase-1 activity was observed when cells were exposed to MC-LR, compared with the vehicle control. However, in the presence of ATP, there was a distinct production of active caspase-1 in LPS-stimulated macrophages. It is unclear how microcystin inhibits the production of IL-1β, while simultaneously stimulating caspase-1 production.

The immune system is highly susceptible to exposure and damage caused by toxic materials. It has previously been reported that MC can bind okadaic acid receptors in various cells, due to the similar tertiary structure between MC and okadaic acid (Bagu *et al*., 1997). Microcystin is transported into hepatocytes, as in intact molecule, via anion-transporting polypeptides, OATP1B1 and OATP1B3. In both acute and chronic exposure, MC-LR induces immune suppression via inhibition of protein phosphatases (PP- 1 and PP-2A) leading to the formation of ROS and heat shock protein-70, which

contribute to decreased immune responsiveness (Jayaraj *et al*., 2006). However, there is still no evidence of a specific transporter molecule or receptors for aiding microcystins in their interaction with immune cells. It has been suggested that a similar mechanism to the hepatocyte transport system is utilised in immune cells, given the number of reported incidences of microcystin immune cell toxicity (Mankiewicz *et al*., 2001; Chen *et al*., 2004; Chen *et al*., 2005; Kujbida *et al*., 2006; Kujbida *et al*., 2009). The mechanism of immunomodulation in murine macrophages requires further investigation, especially in relation to toxin transport into the cell, which is currently unknown.

3.3.3 Aflatoxins

The effect of the various aflatoxins on the immune system has been widely investigated (Dugyala and Sharma, 1996; Moon *et al*., 1999a, b; Moon *et al*., 2000; Hinton, 2003; Minervini *et al*., 2005 and Ubagai *et al*., 2008). However, little is known about the effect of administering toxin mixtures at low concentrations for prolonged periods. It is well known that feed commodities can be contaminated with more than one mycotoxin, commonly produced by the same mould species. Therefore, exposure to different aflatoxins is highly probable, especially if co-infection occurs with Aspergillus and other aflatoxin-producing organisms. Also, if a food supply is contaminated with aflatoxin, a low level of consistent and prolonged exposure is possible. However, there is a limit in the amount of information available on the interactions between commonly occurring mycotoxins and their combined toxic effect (Speijers and Speijers, 2004). A number of recent studies have demonstrated synergistic effects of mycotoxins *in vitro* (Thuvander *et al*., 1999, Luongo *et al*., 2006 and Kouadio *et al*., 2007) and *in vivo* (Theumer *et al*., 2003). Bernhoft *et al*., (2004) used the Isobole method developed by Berenbaum (Berenbaum, 1989) to definitively characterise the combined influence of pairing Penicillium mycotoxins, by examining their effect on mitogen-induced lymphocyte proliferation. Ouyang *et al*., (1995) demonstrated that trichothecenes could have markedly different effects on cytokine secretion and gene expression in primary CD4+ T-cells from murine mice. Theumer *et al*., (2003) examined the effect of inducing mycotoxicoses in rats using toxin mixtures of aflatoxin B_1 and fumonisin. In contrast to individual toxins, toxin mixtures had more pronounced affects on body

weight, mitogenic response, proliferation and cytokine production in spleen mononuclear cells (SMC's).

The aim of this study was to characterise the individual and combined effect of AFB_1, AFB_2 and AFG_1 in order to improve the understanding of the molecular mechanism of aflatoxin cytotoxicity. From the cytokine expression study, it was clear aflatoxins have varying effects on the expression of IL-6, IL-10, IL-12p40 and TNF-α, which was dependent on toxin isoform, dosage and exposure to LPS stimulation. From these results, it may be said that differing structural isoforms of aflatoxins, have different effects on the macrophage function and cytokine secretion. For example, AFB_1 and AFB_2 both significantly increased IL-6 at the higher dose tested and decreased IL-10 at the lower dose. However, AFB_2 also had a significant effect on the secretion of IL-12p40 which was not observed with AFB_1 treatment. These results demonstrate an isoform-specific effect on the modulation of cytokine secretion. Results obtained from experiments with AFG_1 provide further evidence for this isoform-specific effect. AFG_1 significantly decreased TNF-α secretion, which was unaffected by either AFB_1 or AFB_2. These results demonstrate that although these compounds are structurally similar, due to the differences in the ring structure between the three isoforms, they exert variable effects on cytokine production.

In addition to investigating the effect of single aflatoxin isoforms, the effect of exposure to multiple aflatoxins on the modulation of cytokine secretion was examined in murine macrophages. The results of these experiments show that the combination of toxin isoforms has a specific effect on cytokine secretion (Figures 3.2.3.4 and 3.2.3.5). Depending on the two isoforms used and the cytokine examined, the combinations had the ability to abrogate the effect observed in single treatments, or to act synergistically. For example, AFB_1 + AFB_2 acted synergistically at the lower dose to significantly increase IL-6 secretion (Figure 3.2.3.4 A), although neither isoform increased IL-6 at the 0.01 ng/ml dose independently (Figures 3.2.3.1 A and 3.2.3.2 A, respectively). However, IL-6 secretion did not change at the higher dose of AFB_1 + AFB_2 (Figure 3.2.3.4 A), although both AFB_1 and AFB_2 significantly increased IL-6 secretion individually at this dose (Figures 3.2.3.1 A and 3.2.3.2 A, respectively). IL-6 is an important mediator of the acute phase response, and also induces B- and T-cell proliferation (Mosser and Edwards, 2008).

Of particular interest are the results obtained on the effect of toxin mixtures on IL-12p40 and TNF-α secretion. All toxin combinations at both the low and high dose significantly decreased IL-12p40 expression (Figure 3.2.3.5 A) and exposure to AFB_1 + AFG_1 at a dose of 0.01 ng/mL and AFB_1 + AFB_2 at 0.1 ng/mL significantly reduced TNF-α expression (Figure 3.2.3.5 B), following LPS challenge. Such dramatic effects were not observed in IL-12p40 or TNF-α expression when macrophages were exposed to the aflatoxins individually. Individually, exposure to AFB_2 did reduce IL-12p40 expression and AFG_1 did slightly reduce TNF-α expression, but the effects were not as significant as the results observed following combined exposure. IL-10 levels were increased compared to controls, but not significantly (Figure 3.2.3.4 C). The results presented in the current study show that aflatoxin inhibited the LPS-mediated activation of macrophages, and it is possible that this could alter the host response to infection. This is the first report of the effect of aflatoxin isoform combinations on cytokine secretion from murine macrophages. When the macrophages were exposed to mixtures of aflatoxins, it may be possible that one aflatoxin is modulating the effect of the other aflatoxin by some unknown mechanism. A possible explanation for the additive or antagonistic effects of the toxins is that they may have common binding sites in the cell or on a receptor.

Macrophages express PRRs, which recognise conserved molecular patterns on the surface of the pathogen, known as PAMPs. PRRs expressed by macrophages include CD14 and TLRs. These cell surface markers play an important role in the ability of a host to respond to infection. Exposure of J774A.1 macrophages to low doses of AFB_1 + AFB_2 significantly decreased CD14 expression, both with and without LPS stimulation (Table 3.2.3.1). A decrease in the expression of CD14 on the cell surface impairs the ability of the cell to properly respond to LPS and mount a response to Gram-negative bacterial infection. Significantly, this effect was not observed when cells were exposed to AFB_1 or AFB_2 alone. Previous investigations of AFB_1 exposure on CD14 expression found a decrease in CD14 levels on macrophages after LPS challenge (Moon and Pyo, 2000). These indicate that aflatoxins inhibit the effectiveness of murine macrophages by decreasing their ability to respond to LPS stimulation, and to mount an inflammatory response. In addition to modulating CD14, TLR2 expression was also affected by aflatoxin exposure (Table 3.2.3.1). In the absence of LPS challenge, AFB_1 significantly

decreased TLR2 expression. Interestingly, following LPS stimulation, treatment with AFB_2 or AFG_1 significantly decreased TLR2 expression. TLR2 is a receptor for Gram-positive bacterial components, whereas, LPS is found in the outer membrane of the cell wall of Gram-negative bacteria. These results indicate that aflatoxins modulate the ability of macrophages to respond to both Gram-negative and Gram-positive bacteria.
Overall, the results demonstrate that aflatoxins, both singly and in combination, have the ability to modulate the typical inflammatory response of macrophages to LPS stimulus. In particular, aflatoxins affected the secretion of cytokines and cell surface marker expression that are critical for normal host response to infection. Clearly, mycotoxins that are known to co-occur, and have proven to be interactive in causing immunomodulation, are highly significant. When considering implementation of limits of detection and risk assessments, toxin interactions, and whether they are antagonistic, synergistic or additive, should be taken into account.

For this research, it is clear that certain toxins from natural sources, including the phycotoxin, azaspiracid, the cyanobacterial toxin, microcystin and the mycotoxins, aflatoxin B_1, B_2 and G_1, have the ability to cause macrophage dysfunction. Some of the molecular processes of toxicity are still not fully understood. However, this report has shed further light on the mechanisms by which toxins inhibit macrophage functions and, therefore, host defence functions, through deregulation of cytokine profiles, cell surface marker expression and activation of apoptotic markers, including caspases.

CHAPTER 4

Generation of recombinant antibody libraries to the phycotoxin, azaspiracid

4.1 Introduction

4.1.1 Azaspiracid as a Target

Outbreaks of phycotoxin contamination in shellfish are a major cause for concern in the Irish seafood industry. These toxins accumulate in the tissues of filter-feeding shellfish, which are consumed by humans. Although they are harmless to shellfish, they are toxic to humans. Azaspiracids (AZAs) are polyether phycotoxins associated with severe gastrointestinal intoxication in humans and other animals. Azaspiracid shellfish poisoning (AZP) was first reported in 1995 in the Netherlands, following the consumption of mussels cultivated in Killary Harbour, Ireland (Satake *et al*., 1998). Despite extensive research, little is known about azaspiracid, its toxicology or mode of action. Consumption of AZA-contaminated shellfish meat can cause severe acute symptoms, including nausea, vomiting, stomach cramps and diarrhoea. Toxin monitoring programmes have been implemented for AZA in Ireland and many other countries, to prevent the consumption of toxin-contaminated shellfish meat. Current detection methods include biological assays, such as the mouse bioassay, and chemical techniques, such as LC-MS and HPLC for regular AZA screening. Although they are the definitive methods for toxin detection, they require long extraction procedures and are not suitable for high throughput analysis. There is an ongoing requirement for the development of more sensitive, rapid and convenient testing for monitoring toxins such as AZA in shellfish.

4.1.2 Detection Methodologies

The European Commission have recognised the requirement for development of alternative methods to animal testing. One of the objectives of the EC's Sixth Framework Programme (EC, 2003) was to develop cost-effective tools for analysis and detection of hazards associated with seafood from coastal waters, including azaspiracid shellfish poisoning (AZP). Thus, there is an urgent need for rapid and effective detection technologies in this area. Several types of analytical techniques have already been developed including; bioassays, chromatographic techniques, immunoassays and enzyme inhibition-based assays.

4.1.2.1 Mouse Bioassay

Among the different bioassays, the *in vivo* mouse bioassay is the most commonly used, with the *in vivo* rat bioassay being an approved alternative. These bioassays involve the administration of potentially contaminated samples to mice or rats. The lethal dose and toxicity calculation are then determined, according to dose response curves established with reference material. Mussel extracts are intra-peritoneally injected into animal hosts and the azaspiracid response is characterised by hopping, scratching and progressive paralysis (Satake *et al*., 1998). This allows it to be distinguished from diarrheic shellfish poisoning (DSP), where these symptoms are atypical. Rodent death can range from 35 minutes to 30 hours, depending on the dose present in the sample. Generally, polyether toxins are concentrated in the digestive glands of shellfish, however, azaspiracids do not show this pattern. In contrast, AZA toxins are distributed throughout shellfish tissue. If conventional mouse bioassay protocols are used for AZA analysis, where only the hepatopancreas is tested, only 0 to 40% of total AZA content is quantified, causing false negative results (James *et al*., 2002). The mouse and rat bioassay is currently the approved regulatory method for detection for AZA. However, ethical concerns have been raised regarding the use of animals for experimentation. Furthermore, the method suffers from unreliability and insensitivity and this has led the EU to search for alternative AZA detection methodologies, which are more reliable, cost-effective and ethical.

4.1.2.2 Analytical Detection Methods

The lack of confidence in the use of bioassays for the regulatory control of shellfish toxins has led to the development of analytical methods to quantify individual toxins. A number of analytical methods, such as liquid chromatography (LC) with fluorometric detection and liquid chromatography with mass spectrometry (LC-MS), can be used as alternatives to the animal testing methods. Unfortunately, fluorescent labelling of the carboxyl or amino group in the azaspiracid molecule is very slow, due to the reduced reactivity of the two groups. One of the first LC-MS quantitative detection methods for AZA was based on selected ion monitoring (SIM) detection (Ofuji *et al*., 1999). This LC-MS method had a detection limit of 50 pg for azaspiracid. A micro-liquid

chromatography-tandem mass spectrometry method (micro-LC-MS-MS) was also developed with a detection limit of 20 pg, using a triple quadrupole instrument (Draisci *et al*., 2000). Subsequently, a number of robust and sensitive methods for the determination of AZA1-5, using ion-trap multiple tandem electrospray MS were developed (James *et al*., 2002b; Lehane *et al*., 2002). Lehane *et al*. (2002) reported the development of an LC-ESI-MS method for the determination of three of the most prevalent AZA toxins (AZA1-3), as well as the isometric hyroxylated analogues (AZA4-5). Subsequently, James *et al*. (2003) developed a multiple tandem MS (LC–MS^n) method for azaspiracid, leading to the identification of five analogs, AZA-7 to AZA-11. LC-MS^n methods, such as LC-MS^3, provide greater sensitivity than LC-MS/MS, as well as providing full spectral data.

However, when using techniques such as LC-MS for the analysis of a complex matrix, interferences can occur, especially with ion suppression (Suzuki and Yasumoto, 2000). One method to reduce interference and increase reliability is to introduce a clean-up step prior to analysis. Solid-phase extraction (SPE) was successfully employed for the analysis of AZA 1-3 using LC-MS (Ofuji *et al*., 1999). A comparison study using SPE methods for AZA determination in shellfish by LC-ESI-MS (Moroney *et al*., 2002) showed good recovery and reproducibility with a diol SPE cartridge and two octadecyl (C_{18}) SPE cartridge types. SPE is not required for multiple tandem MS techniques, but still needs to be employed in the development of routine analytical methods for the determination of AZA in seafood. Recent advances have shown that it is now possible to purify up to five AZA analogs from mussels contaminated with both DSP toxins and AZA (Alfonso *et al*., 2008). This procedure involved three consecutive steps, in which the toxins are first extracted from the mussels, followed by a solid phase extraction (SPE) procedure, which cleaned the samples and separated DSP and AZA toxins. Finally, a preparative HPLC technique was utilised to isolate each analog. Significantly, large amounts of AZA-1, AZA-2, AZA-3, AZA-4 and AZA-5 were obtained using this procedure. This technique may have utility in other areas, for example, in the preparation of reference material, toxicological analysis or antibody development.

However, for LC-MS^n detection purposes, complete chromatographic separation was not required for determination of AZA analogs. Lehane *et al*. (2004) demonstrated that LC-MS^3 can be utilised to resolve isomers using prescribed mass selection, making it

possible to identify unique ion fragments for each azaspiracid. More recently, an ultra-performance liquid chromatography (UPLC)–MS/MS method was capable of determining 21 individual marine toxins, including AZA-1, using predetermined precursor-product ion m/z combinations in 6.6 minutes (Fux *et al*., 2007). However, this analysis also resulted in signal suppression for AZA-1 analysis. A UPLC method coupled to quadrolope-time-of-flight (Q-TOF) MS/MS was employed to determine 20 previously unknown analogs of azaspiracid with additional hydroxyl and carboxyl substituents in blue mussels (Rehmann *et al*., 2008). Currently, there is strong scientific evidence that supports the incorporation of a validated LC-MS-MS method into EU legislation for AZA detection in naturally-contaminated mussels. This would serve as a replacement for the current mouse bioassay reference method (Hess *et al*., 2009; McCarron *et al*., 2011).

Despite the high sensitivity and reproducibility of these techniques, there is currently no means for performing rapid detection of azaspiracid toxin in algal blooms or in shellfish meat. Currently, LC-MS/MS-based methods have the greatest potential to replace bio-assays. They have the capacity to detect AZAs at concentrations well below the current regulatory limit of 160 μg AZA1 equivalents/kg shellfish meat. The method can also detect and quantify multiple toxin group analogs simultaneously. However, LC-MS/MS requires costly equipment and highly trained personnel, as well as reference material for identification and quantification. Certified reference materials (CRMs) are essential for shellfish toxin monitoring programs as they facilitate method validation, ensure accuracy of results and maintain consistency between laboratories. Nevertheless, shellfish toxin CRM, particularly for AZA, is limited in availability due to insufficient toxin quantities. This is mainly due to the complex structure of marine toxins including AZA, which do not allow for synthetic approaches, making naturally-occurring sources essential for CRM production. The isolation of shellfish toxins from natural sources is labour-intensive and yields relatively low quantities of purified toxin, making analytical techniques very challenging and costly, thus limiting the availability of reference material. Significant research time has been invested to produce certified reference material (CRM) for AZA and its analogs (Canas *et al*., 2010; Perez *et al*., 2010).

4.1.2.3 Immunological Detection Methods

Forsyth and co-workers developed polyclonal antibodies from sheep with broad specificity to the various forms of AZA. Their approach was to raise antibodies to synthetic haptens similar to the constant domain of the azaspiracid molecule, incorporating the common C28-C40 domain of AZA. The polyclonal antibodies detected natural AZA-1 in the range of 40 ng/mL (Forsyth *et al*, 2006). Moreover, Frederick *et al.* (2009) succeeded in generating a panel of monoclonal antibodies to synthetic AZA. This work was carried out with great difficulty, as the immunisation of mice with a synthetic azaspiracid-KLH conjugate resulted in the immediate death of the animals. It was postulated that the acute toxicity of the toxin-conjugate was attributed to the relative number of molecules immobilised on the surface of the KLH carrier. Immune response generation was achieved by reducing the conjugate dose by ten-fold, although an antibody response of only 1/ 3,200 to 6,400 was the highest achieved before sacrifice. The most sensitive clone had a limit of detection of 0.2 μM. No antibodies have yet been produced against naturally-occurring AZA. In addition, no recombinant antibodies have been developed.

4.1.3 Chapter aims

The purpose of this research was to generate a recombinant antibody to azaspiracid (AZA) for incorporation into a specific and sensitive immunoassay-based screening test. This immunoassay could potentially be incorporated into an AZA detection system in shellfish, for application in the seafood farming industry. In collaboration with Queen's University Belfast (QUB), the AZA toxin was sourced from the EU Reference Library in Vigo, Spain and this material was used for antibody production. A rabbit single chain fragment (scFv) antibody library was constructed from the spleen and bone marrow of an AZA-cBSA-immunised rabbit. The polyclonal immune serum was screened for binders using two available AZA protein conjugates; AZA-BTG and AZA-KLH. Bio-panning was carried out on the AZA scFv library using the AZA-BTG conjugate for the selection of high affinity clones. A chicken host was also immunised with AZA conjugates, generated 'in-house', and conjugate analysis was performed using surface plasmon resonance.

4.2 Results

4.2.1 Immunisation of rabbit host with AZA-1-cBSA

Immunisation of a New Zealand white rabbit took place in the Institute of Agri-Food and Land Use, Queen's University. Serum samples were obtained from the AZA-1-cBSA-immunised rabbit by Queen's University Belfast (QUB) and transferred to DCU for analysis. The serum was tested by direct ELISA using two AZA conjugates; AZA-BTG and AZA-KLH, synthesised at QUB (data not shown). Unfortunately, the immune serum displayed considerable non-specific background binding and it also appeared responsive to both the KLH and BTG protein carriers. It was apparent that the conjugates and resulting anti-sera were of poor quality. Moreover, the concentration of the conjugates appeared to be ambiguous, as a greater response was obtained to the carrier control, compared to the conjugates.

It was clear that there were major issues with conjugate quality and solubility, which made it difficult to establish a true titre value of the immune serum and, therefore, the responsiveness of the host animal to AZA. Unfortunately, due to the rarity of toxin material, no purified AZA toxin or AZA conjugates were available commercially and no definitive analytical methods were available for conjugate analysis. Despite these drawbacks, it was decided to generate an recombinant library with the immunised rabbit, which may potentially have generated an immune response for azaspiracid.

4.2.2 Construction and screening of the azaspiracid scFv rabbit library

4.2.2.1 Amplification of rabbit antibody heavy and light chains and PCR optimisation

Bone marrow and spleen were extracted from the immunised rabbit and phenol-chloroform extraction was carried out for isolation of RNA material, as described in Section 2.13.3. The cDNA from both the bone marrow and spleen were synthesised by reverse transcription and subsequently quantified and pooled in a 1:1 ratio. PCR amplifications for the four variable heavy (V_H) chain primer combinations were carried out, as outlined in Section 2.13.4.

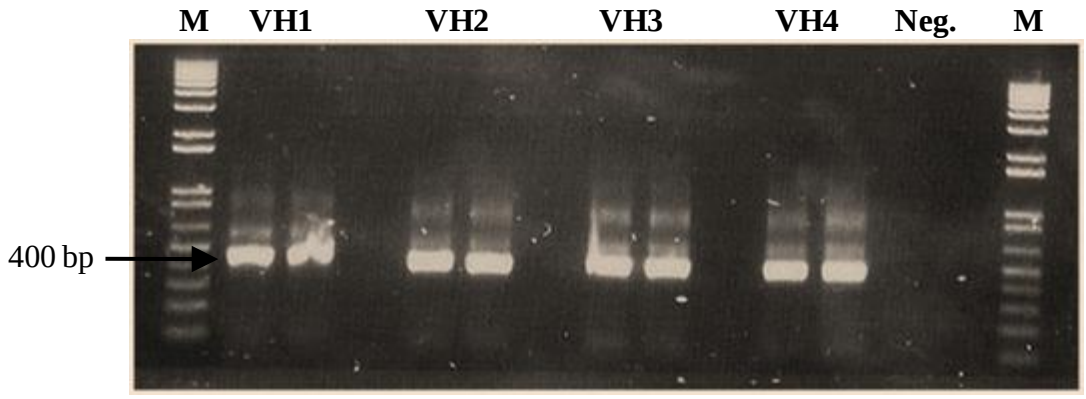

Figure 4.2.2.1: Amplification of rabbit heavy chain regions. The 4 combinations for the heavy chain regions were amplified successfully, utilising the primer combinations; RSCVH1 and RSCG-B (VH1), RCSVH2 and RSCG-B (VH2), RSCVH3 and RSCG-B (VH3), and RSCVH4 and RSCG-B (VH4). The amplifications are shown in duplicate along with a negative control (Neg.), which did not contain DNA template. The M lanes represent a 1 kb Plus DNA molecular weight ladder (Invitrogen).

The amplifications for the variable heavy chains were performed using GoTaq™ polymerase and all four reactions amplified successfully (Figure 4.2.2.1). A band of approximately 400 base pairs (bp) was obtained for the variable heavy chain, which represented the correct amplicon size for that chain fragment. No optimisation for amplification of the variable heavy chains was required.

PCR amplifications were carried out for the variable light (kappa) regions, using the primers sets RSCVK3 and RKB9J_{10}-BL (VK7), and RSCVK3 and RKB9J_o-BL (VK8) (Figure 4.2.2.2). All the variable kappa chains amplified successfully at 400 bp with GoTaq™ polymerase, except for the VK7 and VK8 primer sets, which required further optimisation. This optimisation of the VK7 and VK8 PCRs included; $MgCl_2$ concentration gradients, temperature gradients, DMSO addition, asymmetric PCR and use of alternative polymerases including *Phusion*® Taq DNA Polymerase (NEB) and *Platinum*® Taq (Hi-Fi) DNA Polymerase (Invitrogen).

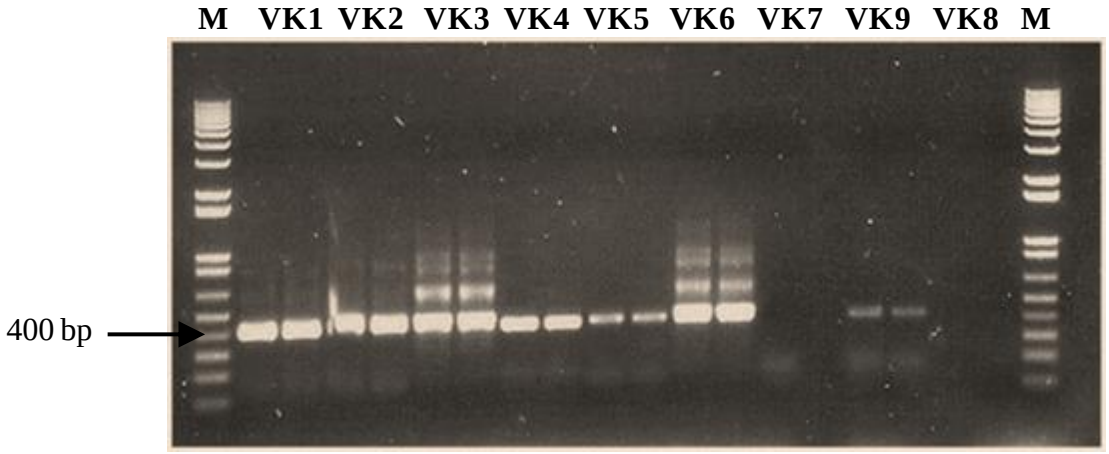

Figure 4.2.2.2: PCR amplifications for the variable light (kappa) regions. The single variable light (lambda) chain products amplified successfully at 400 base pairs and are represented as VK1 to VK9. M represents the 1 kb Plus DNA ladder.

A DMSO concentration gradient was performed to optimise the VK7 and VK8 primer combinations using the VK9 primer combination as a positive control. The concentrations used in the reaction mixtures were 2%, 4%, 6% and 8% (v/v) DMSO, respectively. The same reaction conditions and PCR program was used for GoTaq™ polymerase amplification, as outlined in Section 2.13.5. The addition of DMSO resulted in the successful amplification of the VK8 primer combination (Figure 4.2.2.3). For all further VK8 and VK9 PCR reactions, a concentration of 2% (v/v) DMSO was used.

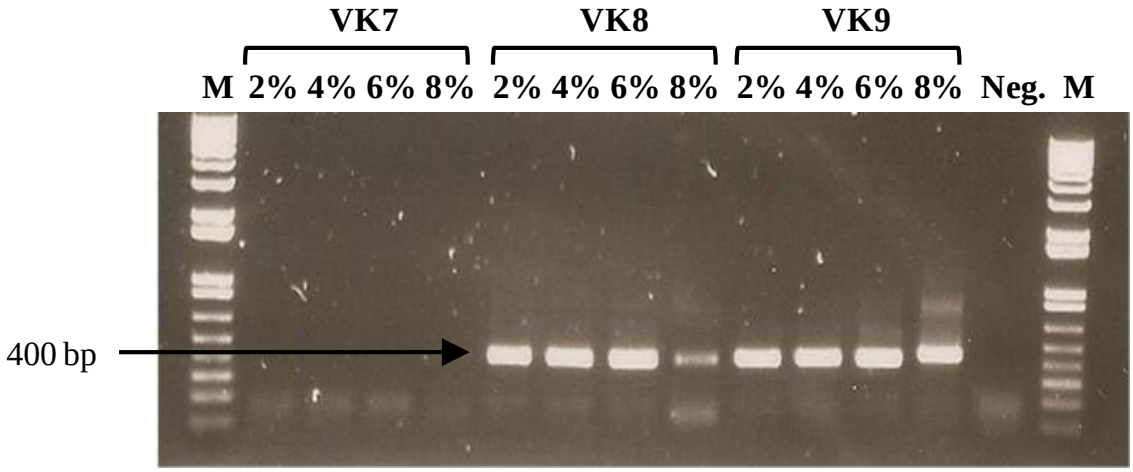

Figure 4.2.2.3: PCR amplifications of VK7, VK8 and VK9 variable light chain kappa with varying concentrations of DMSO, ranging from 2% to 8% (v/v). A band of 400 bp was observed for the variable light chain kappa gene fragment. A negative control was also included (Neg.), which did not contain DNA template. M represents the 1 kb Plus DNA ladder.

To optimise the VK7 variable light kappa primer combination, high-fidelity *Phusion*® Taq DNA polymerase (NEB) was employed. The reaction conditions for this PCR are outlined in Section 2.13.6. There are two possible reaction buffers for PCR reactions using *Phusion*® Taq polymerase, 5X *Phusion*® GC buffer and 5X *Phusion*® HF buffer. The error rate of HF buffer (4.4×10^{-7}) is lower than that in GC buffer (9.5×10^{-7}). The GC buffer can improve performance on difficult or longer templates. A hot start reaction was carried out for this PCR to aid in amplification efficiency. When a minute was left in Stage 1 of the PCR program, the machine was paused and the *Phusion*® Taq was added before proceeding with the program. As illustrated in Figure 4.2.2.4, the correct band was obtained for amplification of VK7 and VK8 with the inclusion of HF buffer. A smaller band was obtained for VK7 with the inclusion of GC buffer.

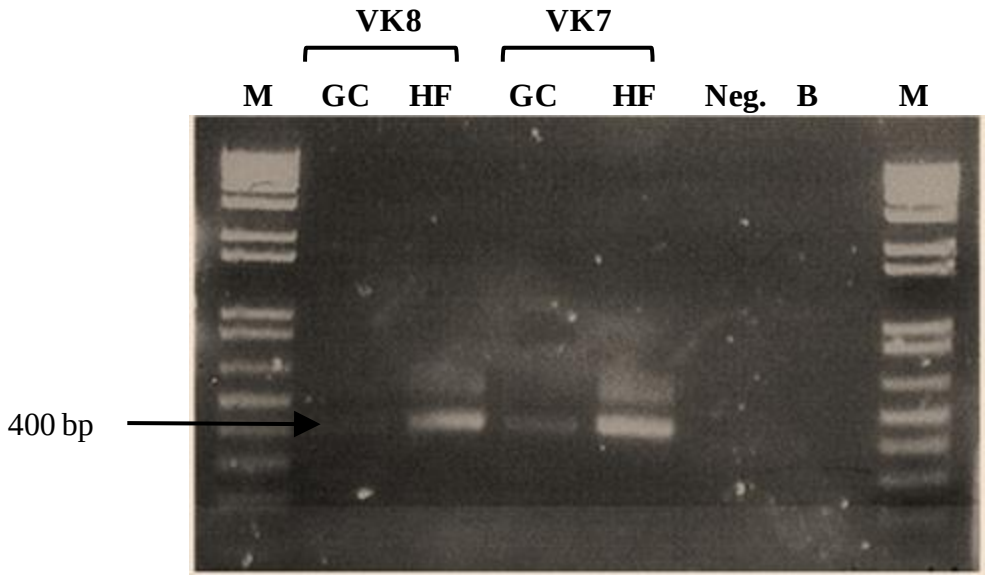

Figure 4.2.2.4: PCR optimisation of VK7 variable light chain primer combination using *Phusion*® Taq polymerase and a hot start reaction. The VK8 primer combination was used as a positive control. The GC and HF reaction buffers were both used for comparison and optimisation. M represents the 1 kb Plus DNA ladder, in addition, a negative control was included (Neg.), which did not contain DNA template. 'B' denotes a blank well.

Further optimisation was carried out on the VK7 variable light kappa primer combination, for the purpose of obtaining a sufficient quantity of DNA material for library construction. A $MgCl_2$ concentration gradient from 2 to 5 mM was prepared. The reaction buffer for this optimisation was 5X GC buffer. *Phusion*® Taq DNA polymerase was utilised in the PCR reaction, as described in Section 2.13.6. The clearest band with the least amount of smearing was obtained with a $MgCl_2$ concentration of 2 mM (Figure 4.2.2.5). An additional band at 250 bp was also obtained due to non-specific amplification. The correct band of 400 bp was isolated using gel electrophoresis (Section 2.13.9) and purified using QIAquick gel extraction (Section 2.13.10).

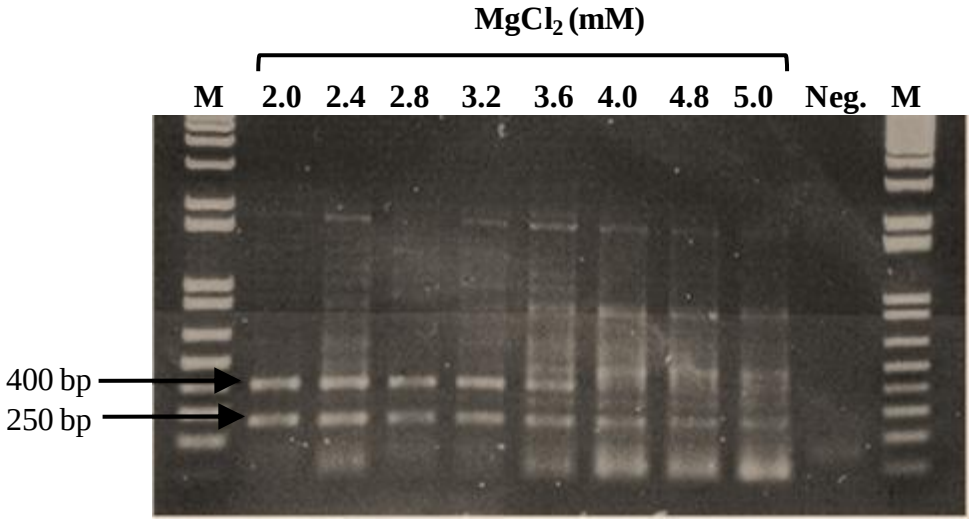

Figure 4.2.2.5: PCR optimisation of VK7 variable kappa light chain primer combination, with a gradient of $MgCl_2$ concentration and *Phusion*® Taq DNA polymerase. The $MgCl_2$ concentration, ranged from 2 to 5 mM. M represents the 1 kb Plus DNA ladder. A negative control was also included (Neg.), which did not contain DNA template.

The variable light chain lambda ($V_L\lambda$) primer combination was amplified using GoTaq™ polymerase. A number of reactions were carried out and subsequently pooled to have sufficient quantities for library construction. No optimisation for amplification of the variable light chain lambda region was required. The PCR was performed using the method described in Section 2.13.6. The amplifications are shown in Figure 4.2.2.6. The bands amplified at a molecular weight of 400 bp, which is the correct size for the variable λ light chain fragments.

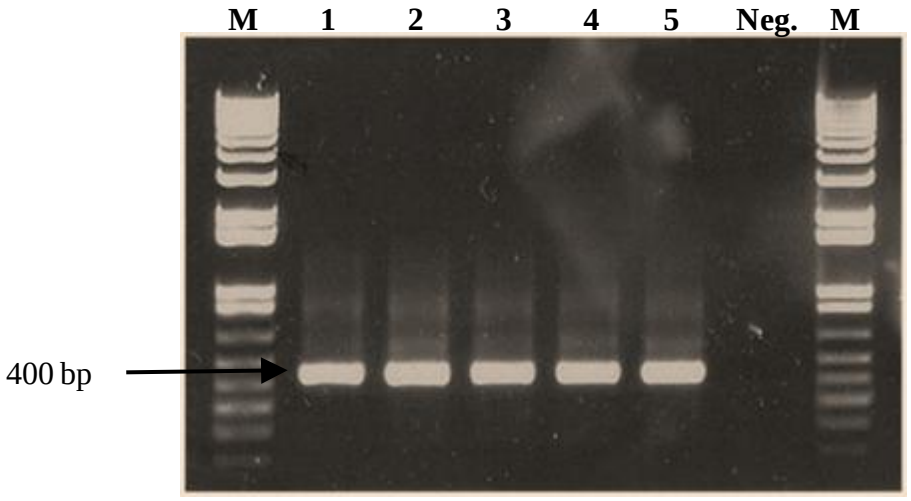

Figure 4.2.2.6: Amplification of light chain lambda ($V_L\lambda$) primer combination including a negative control. Five of the same reactions (lanes 1-5) were carried out and the PCR products pooled. M represents the 1 kb Plus DNA ladder. A negative control (N) was also included, which did not contain DNA template.

Following successful small-scale amplification of the variable heavy and light chain domains and PCR optimisation using methods described, large-scale PCR reactions (10X) were performed for all combinations. The large-scale PCR products were individually ethanol-precipitated, analysed via agarose gel electrophoresis (Section 2.13.9) and purified by gel extraction (Section 2.13.10). The purified products were combined in equimolar amounts for each of the 3 variable chains (heavy, kappa and lambda). This master mix was subsequently used for splice-by-extension overlap PCR (SOE-PCR).

4.2.2.2 SOE-PCR of the variable heavy and light chains of the rabbit library

Construction of the rabbit scFv library proceeded by fusing of equimolar concentrations of the variable heavy and variable light chain mixtures using the overlap primers, RSC-F and RSC-B (See Section 2.13.7). These primers were utilised to amplify a fusion product with a long serine-glycine linker (SSGGGGSGGGGGGSSRSS). The reaction was carried out both in the presence and absence of 2% (v/v) DMSO. No optimisation of the PCR was required; a sufficient band was obtained at approximately 750 bp (Figure 4.2.2.7).

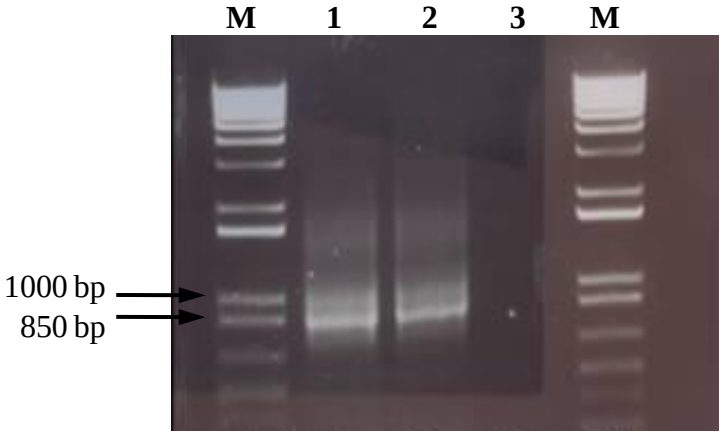

Figure 4.2.2.7: Splice by extension overlap PCR (SOE-PCR) of variable heavy and variable light chain fragment to form complete scFv fragment. The expected molecular weight of this fragment was 750 base pairs. A negative control was included (lane 3) which excluded DNA template and M represented the 1 kb Plus DNA ladder.

The Platinum® *Taq* High Fidelity DNA polymerase, which has proof-reading capacity, was chosen for the SOE-PCR. This enzyme was used to ensure that minimal mutations were incorporated into the scFv gene product. A 12X SOE-PCR was performed using the conditions outlined in Section 2.13.7. The scFv gene product was purified by gel extraction, as described in Section 2.13.10.

4.2.2.3 Library transformation and bio-panning of the AZA immune rabbit library

The scFv SOE product was cloned into the pComb3XSS vector using an *Sfi*I restriction enzyme. The *Sfi*I digests were prepared as outlined in Section 2.13.11. Before the ligation reaction was carried out, the *Sfi*I-digested pComb3XSS vector was treated with the enzyme, antarctic phosphatase (NEB). This enzyme was added to prevent self-ligation of the vector. Following SOE vector ligation (Section 2.13.12), the rabbit scFv library was electroporated into commercial *E. coli*. XL-1 Blue cells (Section 2.13.13). The size of the transformed rabbit scFv library was determined to be 1.02×10^7 cfu/mL.

The library was 'rescued' with M13K07 helper phage (NEB) and enriched via phage display bio-panning using the immobilised-AZA-BTG conjugate (Sections 2.13.14.1 and 2.13.14.2). Four rounds of bio-panning were carried out using decreasing concentrations of conjugate, which was coated onto an immunotube. Conjugate concentrations ranged from 100 to 12.5 µg/mL. During bio-panning the number of wash steps was kept constant at 5 washes of PBS-T and 5 washes of PBS. The objective was to use a low stringency bio-panning approach in order to enhance the selection of binding clones. The inputs and outputs from each bio-panning round are presented (Table 4.2.2.1). The AZA-BTG conjugate was chosen for bio-panning, as it showed a greater response to the immune serum compared with an alternative AZA-KLH conjugate (Data not shown). However, this analysis also indicated a high level of BTG carrier-binders. For this reason, a negative selection strategy was employed during the bio-panning process, whereby the phage were re-suspended in a solution of BTG and BSA, prior to incubation on the AZA-BTG conjugate-immobilised immunotube. The goal was to eliminate any phage specific for BTG alone by capturing them in solution and then discarding these binders, as this would aid the selection of AZA-specific clones. However, no enrichment was observed by polyclonal phage ELISA or by monoclonal soluble ELISA.

Table 4.2.2.1: Bio-panning inputs and outputs of the rabbit AZA phage library

Pan Number	Input (cfu/mL)	Output (cfu/mL)
Pan 1	1.28×10^{11}	4.46×10^{5}
Pan 2	1.88×10^{11}	2.38×10^{4}
Pan 3	3.13×10^{11}	2.28×10^{4}
Pan 4	2.51×10^{11}	2.30×10^{5}

4.2.2.4 Polyclonal phage ELISA and scFv check via 'colony-pick' PCR

A polyclonal phage ELISA was carried out on the pre-pan, pan 1, pan 2, pan 3 and pan 4 output phage, as outlined in Section 2.13.14.3. Commercial M13K07 helper phage was also incorporated as a negative control. However, no discernable response or change in response was observed after each round of bio-panning. To ensure that the antibody library contained scFv inserts, a colony-pick PCR was carried out. Ten colonies were picked from the pan 4 transformation plate. The colonies were used to amplify the SOE insert from the transformed library using PCR (See Section 2.13.14.4). The extension primers, RSC-F and RSC-B, were used for SOE PCR amplification and the PCR products analysed on a 1% (w/v) agarose gel. In total 8 out of 10 colonies were positive for the PCR insert check (Figure 4.2.2.8 A). All colonies were grown in small-scale (10 mL) cultures and the plasmid was purified using the Wizard® plasmid purification kit. The PCR was repeated and all 10 colonies amplified a PCR product of 750 bp, as illustrated in Figure 4.2.2.8 B.

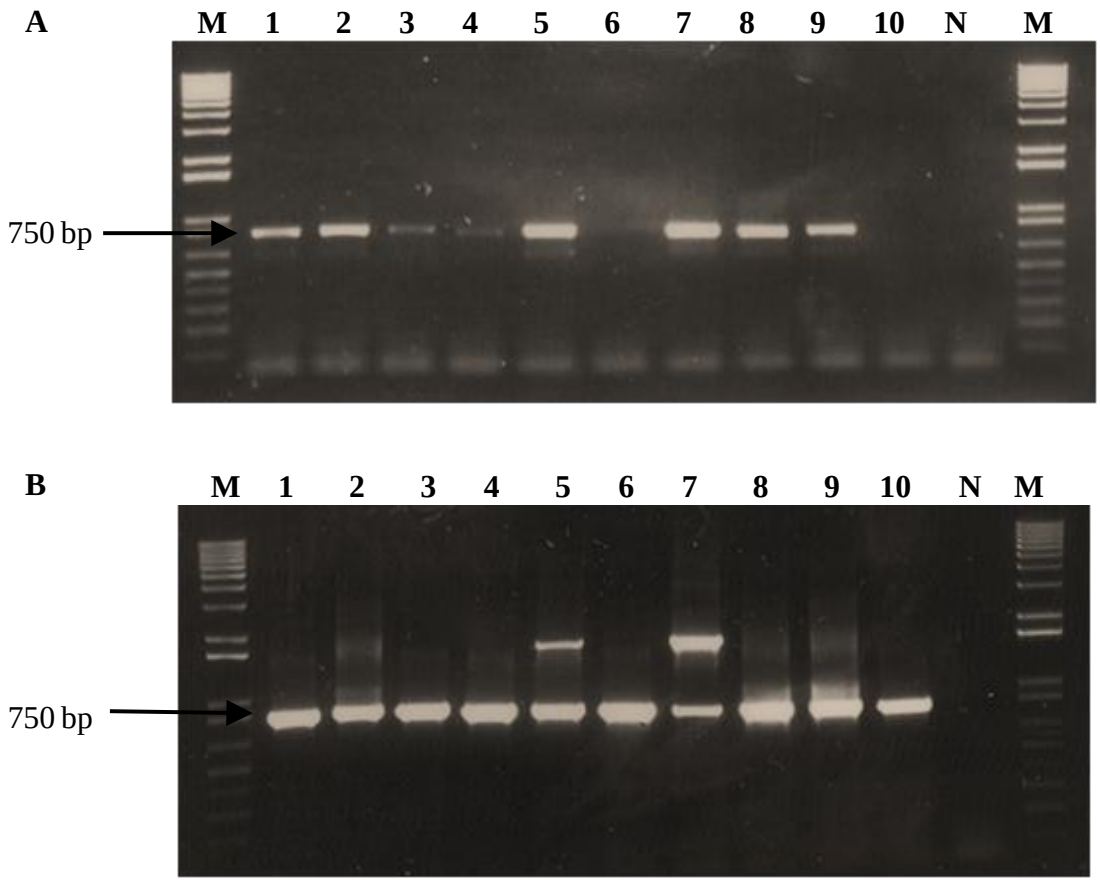

Figure 4.2.2.8: PCR insert check for successful cloning of SOE products into the pComb3XSS vector system. A.) Ten random colonies were studied (colony 1-10) by colony-pick PCR using the cloned phagemid as the template for PCR amplification. B.) The plasmids were purified from the isolated colonies and the same PCR was performed. A negative control was incorporated into each PCR (N). A 1 kb Plus DNA ladder was used for size confirmation of the SOE insert at 750 base pairs (M).

4.2.2.5 Direct monoclonal ELISA of solubly-expressed scFv fragments

The phage output from the final round of bio-panning round 4 (pan 4), were infected into Top10F′ cells for soluble expression (Section 2.13.14.4). The Top10F′ bacterial strain is a non-suppressor strain and is used for production of soluble protein. Single colonies (96) were selected from the transformed library and scFvs were solubly expressed using IPTG induction. The cells were freeze-thawed to facilitate cell lysis, and the supernatant was used for direct monoclonal ELISA, as described in Section 2.13.14.5.

A

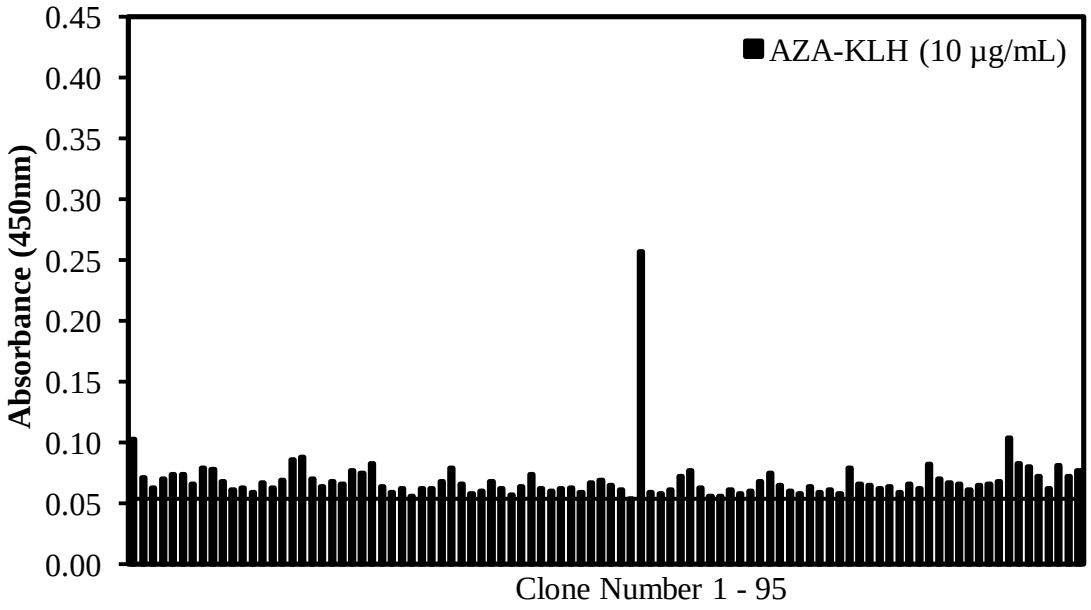

B

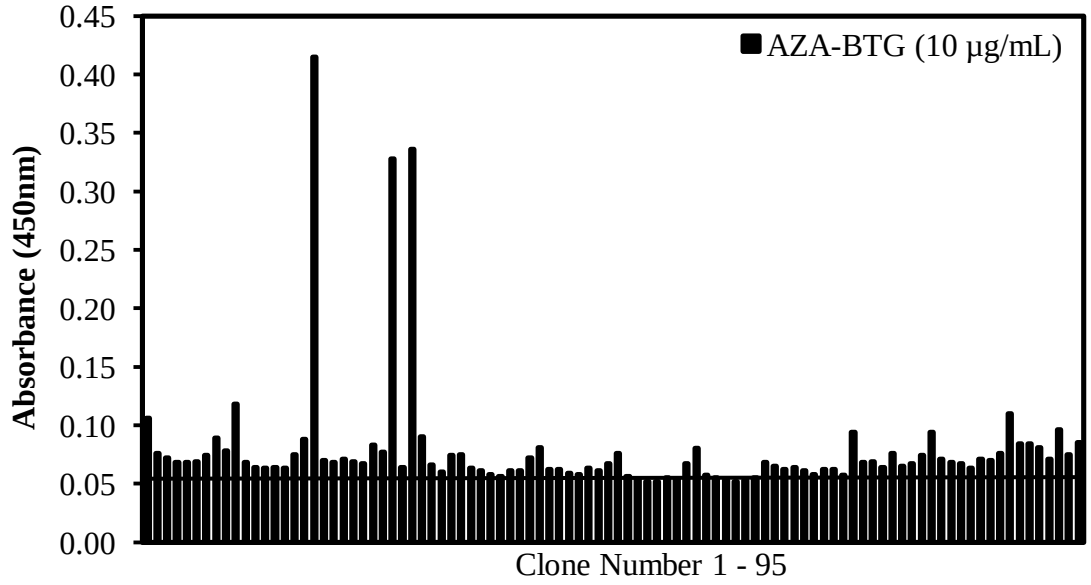

Figure 4.2.2.9: Direct monoclonal ELISA of solubly-expressed scFv fragments in lysate from transformed scFv clones from pan 4. A.) Binding response to the AZA-KLH conjugate. B.) Binding response to the AZA-BTG conjugate. The black horizontal line indicates background signal. Binding was detected using an anti-HA monoclonal antibody, labelled with HRP.

A number of positive clones were identified, however, the signal was very low (Figure 4.2.2.9). After repeating this monoclonal ELISA analysis using the same 96 clones, it was observed that the results were not reproducible and no AZA binding clones were isolated.

4.2.3 Analysis of AZA toxin conjugate using Biacore™ 3000

An alternative approach was employed to further analyse the serum from the AZA-immunised rabbit and to determine whether an alternative bio-panning conjugate could be successfully utilised for clonal isolation. An AZA-transferrin conjugate (QUB) was pre-concentrated and immobilised onto the surface of a CM5 sensor chip (GE Healthcare, Life Sciences) using EDC-NHS coupling chemistry, as outlined in Section 2.13.17. The pre-concentration of AZA-transferrin on to the surface is shown in Figure 4.2.3.1. A pH of 4.0 was chosen for immobilisation, as it showed the highest and steepest peak in the pre-concentration analysis. AZA-transferrin was successfully immobilised onto the surface of a CM5 dextran chip surface (Figure 4.2.3.2). Several dilutions of immune serum from the AZA-cBSA immunised-rabbit (R922) diluted in HBS buffer, were injected over the chip surface (Section 2.13.18). No change in response units was observed (data not shown).

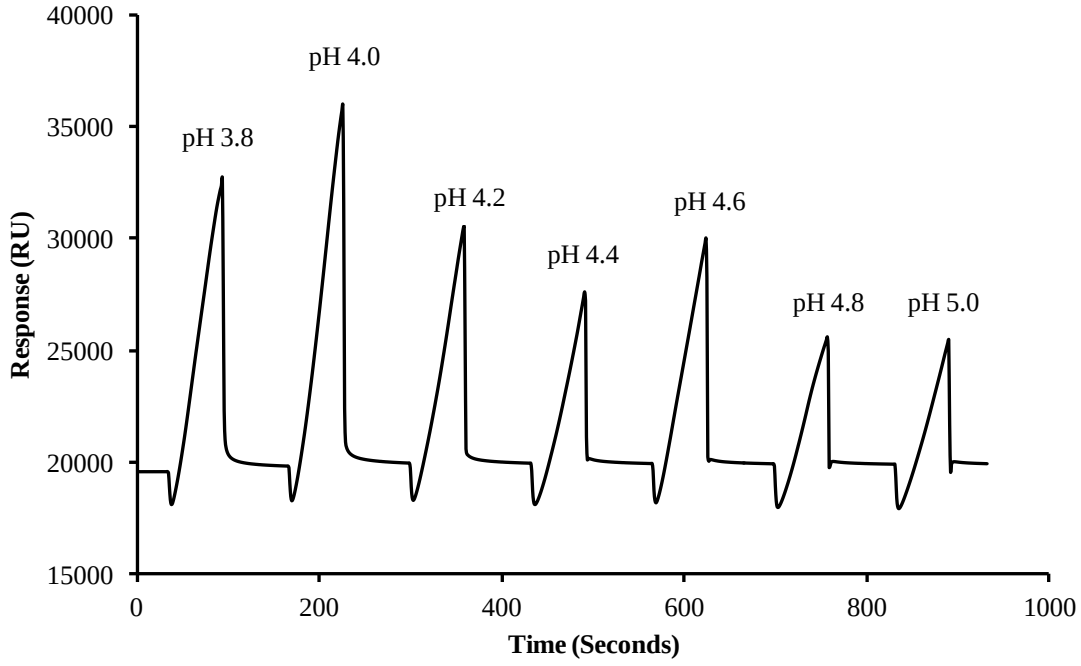

Figure 4.2.3.1: Pre-concentration study of AZA-transferrin conjugate on a CM5 sensor chip surface. AZA-transferrin (25 µg/mL) was diluted in sodium acetate buffers, with a pH range of 3.8 to 5.0. Each buffer solution was injected over the sensor surface at a flow rate of 5 µL/min for 1 minute. A pH of 4.0 was chosen for subsequent immobilisation.

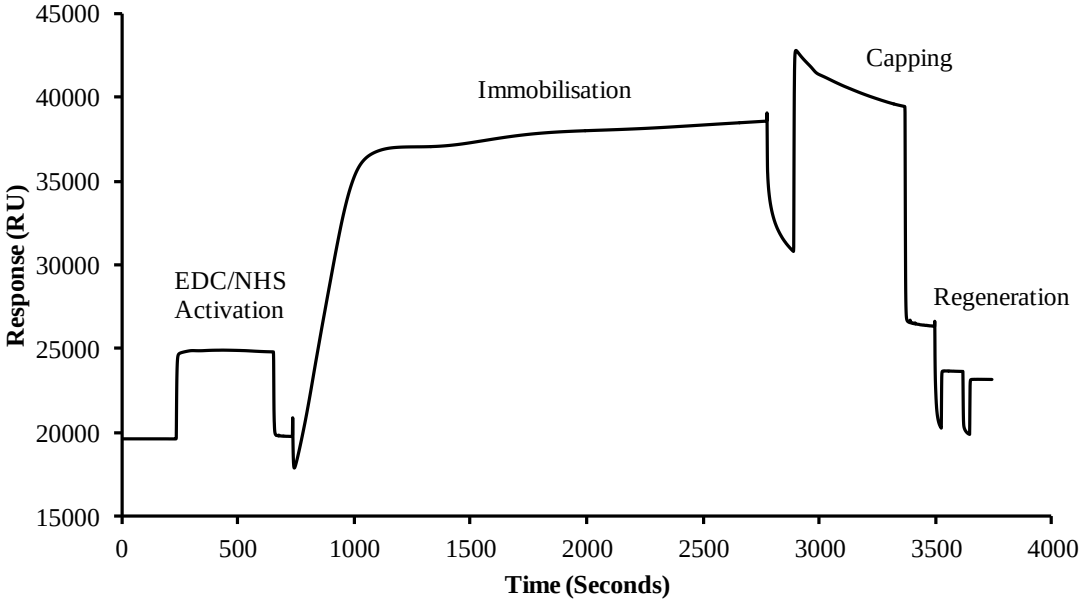

Figure 4.2.3.2: Immobilisation of AZA-transferrin onto a sensor surface. The CM5 chip was activated using EDC/NHS chemistry and immobilised with 25 µg/mL AZA-transferrin. The flow rate was 5 µL/min and the antigen contact time of 20 minutes. The non-reacted groups were capped using ethanolamine-HCl and the surface was regenerated using two pulses of 5 mM NaOH.

These results indicated that the AZA-transferrin conjugate was un-suitable for bio-panning of the R922 rabbit library, as no binding occurred between the rabbit immune serum and the immobilised AZA-transferrin. No clones were isolated from the R922 rabbit library using the AZA-KLH or AZA-BTG screening conjugates. Therefore, it was decided to generate new conjugates and repeat the immunisation process.

4.2.4 Production of a recombinant antibody library from an AZA-immunised chicken

4.2.4.1 Conjugation of AZA-2 to BTG and KLH

Conjugation reactions were carried out, in which a molar excess of AZA-2 was chemically linked to a protein carrier through an amide linkage (Section 2.13.15). This amide linkage was created using the NHS-ester method. The protein carriers were bovine thyroglobulin (BTG), with a molecular weight of 660,000 Da and keyhole limpet haemocyanin (KLH), with a molecular weight of 4.5 x 10^5 to 1.3 x 10^7 Da. A scheme of the conjugation is illustrated in Figure 4.2.3.1. No methods of analysis were available for these conjugates, as the size of the KLH and BTG molecules are too large for HPLC or MS determination and no AZA-specific antibodies were obtainable for immunological determination.

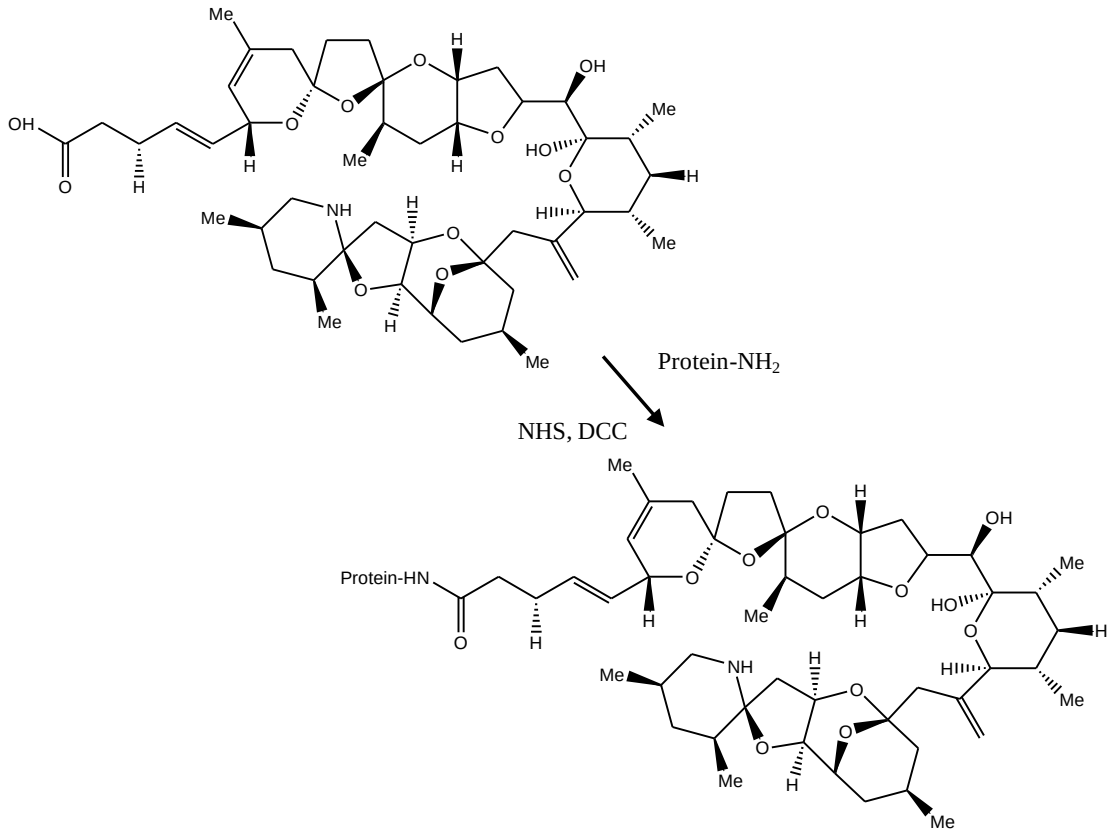

Figure 4.2.4.1: Illustration of the conjugation reaction of AZA-2 ester to either KLH or BTG carrier proteins using the NHS-ester method for conjugation. The image was created using ChemDraw Ultra software (Version 9.0).

4.2.4.2 Immunisation of AZA-KLH-immunised chicken and serum titre

A female leghorn chicken was immunised with the synthesized AZA-KLH conjugate (See Section 4.2.3.1). A pre-bleed was taken from the chicken prior to immunisation. For the primary immunisation, the chicken was injected with 100 µg of conjugate mixed with complete Freund's adjuvant. All subsequent boosts (50 µg of conjugate mixed with Freund's incomplete adjuvant) were administered subcutaneously at four sites and at three weekly intervals. After the third boost a serum bleed was taken and analysed by direct ELISA using a HRP-labeled anti-chicken (IgY) antibody.

The immune serum was screened using the AZA-BTG 'in-house' conjugate, using a direct titre ELISA format. A control included the un-conjugated carrier, BTG. The results show that no significant immune response was generated to AZA. A very low response to AZA-BTG was generated (approximately 1/1,000). However, the chicken immune serum also bound significantly to the BTG carrier alone. It was unknown how the serum was responsive to BTG. It is possible that the animal may have consumed a number of bovine products in feed. This may have caused a response to the bovine protein (BTG).

Screening with AZA-KLH and KLH carrier showed that there was a significant response to both proteins was generated (approximately 1/10,000) (data not shown). It cannot be determined whether this response was specific for AZA, as the AZA-KLH conjugate was used as the immunogen and the response may be solely KLH-specific. A negligible response was obtained when the conjugates and carriers were tested for binding to pre-immune serum from the chicken host (data not shown).

4.3 Discussion

Azaspiracid has previously been identified as a key target for establishment of alternative detection methodologies to animal toxicity assays and analytical techniques. Development of rapid testing methodologies, such as those incorporating immune recognition elements, would serve to support existing techniques, such as HPLC and mass spectral analysis, by providing a rapid warning mechanism for toxin outbreaks. Both monoclonal (Frederick *et al*., 2009) and polyclonal (Forsyth *et al*., 2006) antibodies have been generated to date, but no reported recombinant antibodies exists to azaspiracid. Recombinant antibodies have potential for incorporation of tags for functionalisation, immobilisation, purification and detection. They can be expressed in large quantities in bacterial systems. Additionally, they can be further improved using *in vitro* affinity maturation. In this work, an immune AZA single chain antibody fragment (scFv) library was constructed from an immunised rabbit host. A rabbit was chosen as the host animal because of its suitability for antibody generation to small-molecular weight targets and because of its unique diversification and gene rearrangement capabilities (See Section 4.1.3).

A rabbit host was immunised through successive injections with AZA, conjugated to BSA, to boost the immune system. Both genetic starting material and toxin conjugates were supplied from a different laboratory and no effective means was available to characterise or quantify these conjugates. As discussed, it was difficult to establish a true titre value, as there were significant and unexpected responses to the BTG and KLH carrier molecules, as well as significant background binding. The genetic material was extracted from the rabbit and the library was constructed using the polymerase chain reaction (PCR). The V_H and V_L (κ and λ) sequences were amplified, although some optimisation, using alternative high fidelity *Phusion*® Taq polymerase, DMSO and $MgCl_2$, was required. Genetic combinations of V_H and V_L sequences were spliced together via a short amino acid linker sequence (SOE-PCR), thereby creating a full length scFv gene fragment. An scFv fragment phage library was generated by cloning the gene fragment library into the pComb3XSS phagemid vector and transforming into *E. coli* cells. The phage library was rescued by infection with helper phage and screened against immobilised AZA-BTG conjugate.

Failure to isolate a recombinant antibody to AZA can be attributed to a number of factors, including ineffective immune response generation, the toxic nature of the immunogen, the size of the hapten and the quality of conjugation. Barbas *et al*. (2001) has specified that ideally recombinant antibody libraries should be built from animals that display a high serum titre to the antigen of interest. A high serum titre reflects a high level of antibody production and, therefore, a high level of specific mRNA for library construction. However, recombinant antibodies have been isolated from immune libraries with titres as low as 1/100 (Burton and Barbas, 1994; Barbas *et al*, 2001). In this work, considerable difficulty was encountered in generating a response in the AZA-conjugate–immunised rabbit. During the course of immunisation, the animal displayed poor health and this may have negatively impacted on the quality of the AZA-antibody response. The poor health of the animal may also have been attributed to the immunotoxic nature of azaspiracid (See Section 3.2.1). Despite the poor response to the AZA-conjugate, it was decided to construct a recombinant library from the genetic material of the rabbit.

A further challenge in this work was the inefficiency of toxin-protein conjugates. In an ideal situation, conjugates would be fully characterised with comprehensive analytical techniques, such as matrix-assisted laser desorption/ionization, with time of flight (MALDI-TOF), before immunisation or screening. This analysis would provide invaluable information regarding molecular mass of the conjugate and hapten incorporation ratios. However, in this project these systems were not available and the large size of the protein carriers would have made any analysis extremely complex and difficult to analyse. Furthermore, not enough conjugate material was available for this type of analysis.

In an attempt to further characterise the rabbit immune serum, an alternative AZA-transferrin conjugate was immobilised on a CM5 chip surface and binding to the immune serum was analysed by SPR. However, no serum antibody-conjugate binding was observed. In order to continue this work, new conjugates were required. Therefore, two new conjugates were generated for immunisation and screening using purified AZA-2 toxin; AZA-bovine thyroglobulin (BTG) and AZA-keyhole limpet haemocyanin (KLH) molecule. The AZA-KLH produced ‘in-house’ was employed for avian immunisations. In addition, attempts were made to characterise the ‘in-house’

conjugates through HPLC analysis, scanning absorbance spectrum analysis and surface plasmon resonance (data not shown). However, none of these techniques provided any definitive information about the quality of the conjugation, the number of toxin molecules bound or the concentration of the conjugate. Such information can only be elucidated by extensive and complex analytical analysis. It was not possible at this time to produce a recombinant avian AZA library, as the immunised chicken generated a greater response to the carrier molecules compared to the 'in-house' AZA-conjugates.

Frederick *et al*. (2009) encountered similar issues with immune response generation to AZA-conjugates in mice for monoclonal antibody development. Major problems were observed with mice immunisations, most resulting in death within 24 hours. The author's postulated that an unknown toxicity to the conjugate material, or the presence of un-conjugated material in the immunogen preparation was the cause of the deaths. Interestingly, it was discovered that a 10-fold reduction in the immunisation conjugate concentration had less harmful side effects in the mice. This positive effect was due to a decrease in the relative amount of toxin in the context of the carrier. Overall, this led to the successful production of polyclonal antibodies.

AZA is a problematic molecule. For instance, there are a number of ongoing issues surrounding its structural analysis, epidemiological analysis, toxicity analysis and isolation. Problems were encountered by the Yasumoto and Satake group who worked with minute quantities of purified toxin material in the structural elucidation of the molecule (Satake *et al.*, 1998). Interestingly, total synthesis of the azaspiracid structure by Nicolaou *et al*. (2003a, b) found that the previous proposed structure was incorrect. Nicolaou *et al*. (2006a, b and c) employed a combination of degradation studies and synthetic approaches to revise the structure of AZA. Also, little epidemiological data is available for AZA, as only a small number of AZA-poisoning events have been rigorously documented. This limitation has made the determination of a safety level very difficult.

The currently employed detection methodologies for AZA include HLPC, mass spectral analysis and the mouse toxicity assay. However, these methods are impractical due to their requirement for purified reference material, which is a rarity. Moreover, the in-humane use of animals in toxicology testing should be avoided (Twiner *et al*., 2008).

Certified reference material is vital for shellfish toxin monitoring programs to facilitate method validation and to ensure accuracy of results. AZA CRM is notoriously limited due to insufficient quantities of toxin, as previously discussed. The complex structure of marine toxins, such as AZA, do not allow for efficient synthetic approaches, so naturally-occurring sources are generally required. Isolation from natural sources is labour-intensive and the yields of purified material are very low.

The main limitation of this project work was the scarcity and high price of purified toxin material, as well as the immunotoxic nature of the immunogen, as reported previously in this thesis. Antibody generation does not require an excessively large amount of AZA material, however, a combination of factors, including inability to generate effective immune responses in two species of animal and the lack of characterisation capabilities, have made recombinant antibody production unattainable at this time. However, this is the first reported attempt to generate an immune recombinant library for AZA using naturally-sourced material. If a reliable, purified source of toxin material becomes available in the future, or if a more efficient purification process is established, it may be possible to isolate the first novel recombinant antibody to AZA from the existing immune libraries.

CHAPTER 5

Generation and characterisation of avian anti-microcystin antibodies

5.1 Introduction

This chapter outlines the process of generating a recombinant phage antibody library to the cyanobacterial toxin, microcystin-LR (MC-LR), and the isolation of specific clones via bio-panning. The development of a recombinant antibody to MC-LR would allow unlimited expression of the antibody in a bacterial host, greatly reducing cost and increasing availability of the antibody. Although, a number of recombinant antibodies were generated to microcystin (McElhiney *et al*., 2000; Strachen *et al*., 2002; McElhiney *et al*., 2002), these antibodies were from non-immune sources that included; a naïve human semi-synthetic phage display library, Griffin I, and the synthetic naïve library, Tomlinson I.

However, a major advantage of using immune libraries, over conventional naïve antibody libraries, is that the host animal immune system can refine and enhance antigen affinity and specificity. This increases the possibility of selecting higher affinity antibodies from a recombinant antibody fragment library, due to *in vivo* affinity maturation (Schmitz *et al*., 2000; Hoogenboom, 2005). Although naïve libraries are becoming increasingly popular for recombinant antibody selection, they may not have the same diversity as that of the immune system, which uses somatic hypermutation and gene rearrangement to generate large panels of diverse antibodies. Moreover, the affinity of antibodies generated from non-immune sources is frequently low, often requiring the use of antibody engineering for improved affinity (Gram *et al*., 1992).

This chapter describes the characterisation of the selected antibodies to microcystin by sequence analysis, molecular modelling and three-dimensional *in silico* docking analysis. Chromatographic techniques, including immobilised-metal affinity chromatography (IMAC) and size-exclusion chromatography (SEC), were employed for scFv purification and molecular weight characterisation. An inhibition ELISA was developed for sensitive detection of MC-LR, with a limit of detection of 0.5 ng/mL, utilising both the 2H1 and 2G1 anti-MC-LR scFv fragments. The MC assays were proven to be both accurate and precise following inter- and intra-day assay validation.

5.2 Microcystin as a target

5.2.1 Microcystin as a public health risk

The hepatotoxic cyclic peptides, including microcystin and nodularin, are part of the group of cyanobacterial toxins. Microcystins have been identified from species belonging to the genera Microcystis, Anabaena, Oscillatoria (Planktothrix), Nostoc, and Anabaenopsis. Nodularin is related to microcystin structurally and has a similar mode of toxicity. It was isolated from only a single species of cyanobacteria, *Nodularia spumigena* (Rinehart *et al*., 1988). Concern involving the presence of microcystins in drinking water and their possible contamination of food, such as salad, fish and shellfish; have resulted in an urgent need for reliable and accurate means for the detection and quantification of this class of toxin.

Although there is a lot of basic information available on the acute toxicity of microcystin, there are significant gaps in the understanding of chronic effects, caused by long term, low level exposure. The immunotoxicity of microcystins also remains an unresolved issue (see Chapter 3). Interestingly, there is strong evidence for tumour promotion in experimental animals (Nishiwaki-Matsushima *et al*., 1992), but the relevance of this in relation to human cancer has not yet been clearly demonstrated. As microcystin is taken up and excreted through the gut, there is the possibility of an increased rate of gastrointestinal tumours. In the mouse colon, tumour precursors were shown to grow faster with microcystin in the drinking water (Humpage *et al*., 2000). Until an exposure marker for cyanobacterial toxin intake in humans is clearly demonstrated, it is difficult to carry out effective human epidemiology. The implementation of appropriate regulatory limits for microcystin content requires the availability of suitable detection methods, which are sufficiently sensitive and reliable to detect the presence of microcystin at the stated levels.

Microcystin toxic episodes also impact society at both ecological and economic levels. For example, at an ecological level, marine wild animals that have fed on microcystin-contaminated material, such as marine mammals and birds may suffer intoxication and even death. Furthermore, the presence of microcystin blooms also generates economic losses to the aquaculture sector and fish industries. This is due to governmental regulations,

which determine the maximum acceptable limit of microcystins in freshwater. Breaches of such regulations and human poisoning events, often results in the closure of recreational and shellfish-handling areas. The growth of the world population and the subsequent increased demand on agricultural products has placed an increased demand on water supplies in recent years. Intensification of agricultural activity has also resulted in more water usage for irrigation, along with higher nutrient loads in water catchment areas. In circumstances where irrigation has depleted water flow in rivers, especially in the summer months, eutrophication often occurs. The use of eutrophic water for drinking supplies, which is prone to MC contamination, elevates the requirement for fast and effective MC detection and identification strategies.

5.2.2 Detection methodologies for the cyanobacerial toxin, microcystin

To protect the public from exposure to microcystin toxins, which may cause poisoning events, it is important to accurately quantify the identity and absolute quantity of the microcystin present in a sample. Potential sources of poisoning include; drinking water, dietary supplement and recreational swimming areas. The toxicity to humans is generally reported as acute poisoning and limits for the content of microcystin destined for human consumption have been set to protect human health. In 1998, the WHO published a guideline threshold for microcystin-LR in drinking water of 1 µg/L (WHO, 1998), leading to the requirement for a range of methodologies to detect, identify and quantify microcystins in natural and treated water (McElhiney and Lawton, 2005; Lawton and Edwards, 2008). Current routine analysis for microcystin involves high-performance liquid chromatography, with photodiode array detection (HPLC-PDA). A number of biological assays, such as the mouse toxicity assay and enzyme inhibition assays, exist for microcystin detection (Metcalf and Codd, 2003; McElhiney and Lawton, 2005; Msagatu *et al*., 2006). ELISA-based detection is, however, the most widely utilised because of its sensitivity and selectivity.

5.2.2.1 Mouse Bioassay

Until recently, the approved regulatory methods for most countries were based on laboratory animal bio-assays. The mouse bioassay plays an important role as a screening tool, as it gives the total toxic potential of the sample within a few hours and it can distinguish hepatotoxins from neurotoxins. The assay determines the minimum amount of microcystin required to kill a mouse and compares this value with lethal doses of a known amount of microcystin. The male swiss albino mouse is the most commonly used animal for toxicity testing for cyanotoxins. Toxicity is tested by intraperitoneal injection of cyanobacterial lysate prepared either by sonication or freeze-thawing of a cell suspension which has been sterilised by membrane ultra-filtration. The mice are observed for 24 hours and then sacrificed by an approved method. The observation time must be extended to seven days where cylindrospermopsin contamination is suspected. This toxin demonstrates protracted symptoms which result from progressive liver and kidney failure. Following animal sacrifice, the tissue injury is examined to determine which cyanotoxins are present. A disadvantage of this method is where more than one type of cyanotoxin is present, the more rapid-acting toxin may mask other symptoms. The final toxicity is expressed as LD_{50} mg cell dry weight per kg mouse body weight.

These assays raised a number of ethical issues, arising from the prolonged suffering and sacrifice of animals (Langley *et al*., 2007). Technical issues were also a key factor, including lack of specificity, duration of the assays and a high rate of false positives and negatives (Sauer *et al*., 2005). The assay does not detect toxins at low levels, especially in finished drinking-water, and it does not identify the specific toxic agent (Lambert *et al*., 1994). In most countries, there is a desire to move away from the approved animal testing methods, as demonstrated by European Directive 86/609/EEC. A large number of alternative methods have been proposed. However, regulatory authorities have set strict criteria around the possible substitution of these methods. Such rigid criteria have been set in order to ensure consumer protection. Consequently, solid evidence must exist to prove that any new method is comparable to internationally validated methods, before the authorities will accept its use in toxin testing.

5.2.2.2 Analytical Detection Methods

Analytical detection methods for microcystins are characterised based on their sensitivity and ability to detect the various toxin variants. Chemical analysis of microcystin is most commonly conducted on reversed-phase high-performance liquid chromatography (RP-HPLC), with UV detection at 238 nm. Microcystins have characteristic spectra at this wavelength, due to the presence of a chromophore and a diene in the Adda residue (Meriluoto *et al.*, 1997). The HPLC detection limit for microcystins, especially incorporating photo-diode array (PDA), is in the nanogram range (Meriluoto, 1997; Sangolkar *et al.*, 2006). Using this technique, Lawton *et al*. (1994) detected microcystin in a spiked water sample at 250 ng/L. Separation of microcystin variants is dependent on the composition of the mobile and stationary phases used for analysis. Microcystins can be separated using gradient elution or isocratic mobile phases, although gradient elution has the potential to separate a wider range of toxin variants.

C18 silica columns are the most widely used HLPC columns for separating toxins. They use a gradient of water and acetonitrile, both containing 0.05% (v/v) trifluoroacetic acid (TFA), which acts as an ion-pairing agent. This technique can separate up to 10 microcystin variants, but it is also necessary to analyse toxin standards in parallel, in order to accurately identify which variants are present (Lawton *et al.*, 1995). The use of more than one mobile phase is often necessary to ensure separation and identification of the full range of microcystin variants. HPLC with PDA detection is one method that is often used to determine the microcystin content of a sample. However, it is limited in its ability to distinguish between different microcystin variants, as most variants have a similar absorption peak between 200 and 300 nm. A major limitation for analytical detection methods for microcystins is the lack of reference material. There are approximately 90 different MC variants. However, commercial standards are available for only a few these variants (McElhiney and Lawton, 2005). In the absence of suitable standards, quantified microcystin variants are generally expressed as equivalents of MC-LR (McElhiney and Lawton, 2005).

More accurate identification of microcystins can be carried out using HPLC, followed by detection with mass spectrometry (LC/MS). In mass spectrometry, the molecules in a biological sample are converted to desolvated ions, which are resolved by mass analysers on the basis of mass and charge (Graves and Haystead, 2002). Different variations of this method have been developed for microcystin analysis, including fast atom bombardment (FAB) (Kondo *et al*.,1995), electrospray ionisation (ESI-MS) (Barco *et al*., 2002) and matrix-assisted laser desorption ionisation-time of flight (MALDI-TOF) (Welker *et al*., 2002). The structural information provided by these methods allows for definitive differentiation between the toxin variants. Techniques, such as HPLC-ESI-MS, have become more popular and are extensively used in the monitoring and identification of a range of cyanobacterial toxins, which include microcystins (Dahlmann *et al*., 2003). ESI-MS techniques provide molecular weight information, which can confirm the identity of toxin variants, previously detected by HPLC-PDA. When no mass data is available, in the case of unknown microcystin variants, the patterns obtained using tandem mass spectrometry (MS/MS) fragmentation are very useful for identification, especially for complex matrices (Lawton *et al*., 1995). Meriluoto *et al*. (1998) developed an electrochemical sensor for microcystin-LR, -RR and -YR, following HLPC analysis. In the study by Meriluoto and colleagues, measurement of the electrochemical response obtained by oxidation of arginine and tyrosine residues in the microcystin structure was carried out.

5.2.2.3 Immunological Detection Methods

Currently, the most promising techniques for the detection of microcystins involve the use of antibodies. Polyclonal, monoclonal and recombinant antibodies have been employed in a wide range of formats for toxin detection and quantification. These approaches have been reviewed according to conjugation strategies and carriers, used for immunogen preparation, as well as inhibitory concentration (IC_{50}), assay format and cross-reactivity, in Tables 5.2.3.1, 5.2.3.2 and 5.2.3.3, inclusively. The IC_{50} is defined as the inhibitory concentration of toxin required to cause half maximal binding.

Table 5.2.2.1: Strategies for polyclonal antibody development to microcystin. Antibodies were compared, according to their immunogen preparation (conjugation strategy and carrier molecule), IC_{50}, immunoassay format and cross-reactivity to microcystin variants. (*RIA: radioimmunoassay; *CIPPIA: Colorimetric immuno-protein phosphatase inhibition assay.

Toxin	Conjugation strategy	Carrier	IC_{50} (µg/L)	Format	Cross-reactivity	Reference
MC-LR and Nodularin	Aminoethylation of the *N*-methyldehydroalanine residue and one-step glutaraldehyde coupling	KLH	2.50	Indirect competitive	MC-LA, -LR, -LF, -LW, -D-Asp3-RR, -LY, NOD, MC-Asp (Z)-Dhb7-HtyR	Metcalf *et al*., 2000
MC-LR	Carbodiimide EDPC (1-(3 dimethylaminopropyl)-3-ethylcarbodiimide)	BSA Polyl-lysine	1.75	RIA*, direct and indirect competitive	MC-RR, -LR and –YR, NOD	Chu *et al.* 1989
MC-LR	Aminoethylation of the *N*-methyldehydroalanine residue and glutaraldehyde coupling	BSA	0.63	Direct competitive	MC-LR, -RR, -YR, -LF, -LW, NOD	Sheng *et al*., 2006
MC-LR/RR Nodularin	Carbodiimide	Polyl-lysine	10-50	Competitive inhibition	MC- LR,-RR Nodularin	Baier *et al*., 2000
Adda	Synthetic *N*-acetyl D-alanyl Adda	cBSA OVA	0.61	Indirect competitive	MC-LR, -RR, -YR,-LW, -LF, 3-dm-MC-LR, 3-dm-MC-RR, NOD	Fischer *et al*., 2001
MC-LR	Carbodimide method using activated EDC, via carboxylic acid group (Mixed anhydride)	BSA OVA HRP	0.50	Indirect and direct competitive	Abs with similar cross-reactivity pooled	Mhadhbi *et al*., 2006
MC-RR	Aminoethylation of the *N*-methyldehydroalanine residue and glutaraldehyde coupling	KLH	3.03	CIPPIA*	MC-LR, -RR, nodularin	Young *et al*., 2006

Table 5.2.2.2: Strategies for monoclonal antibody development to microcystin. Antibodies were compared, according to their immunogen preparation (conjugation strategy and carrier molecule), IC_{50}, immunoassay format and cross-reactivity to microcystin variants (EIA*: Enzyme immunoassay).

Toxin	Conjugation Strategy	Carrier	IC_{50} (µg/L)	Format	Cross-reactivity	Reference
MC-LR	Carbodiimide EDPC	BSA OVA KLH	0.13	Indirect competitive	_	Nagata *et al*., 1995
MC-LR	Aminoethylation of the *N*-methyldehydroalanine residue and glutaraldehyde coupling	BSA	1.8	Indirect competitive	Very low level	Sheng *et al*., 2007
MC-LR	Aminoethylation of *N*-methyldehydroalanine residue and glutaraldehyde coupling	BSA	1.00	Direct competitive	MC -RR, dmMC-LR, dmMC-RR, H_2N-etMC-LR, MC-YR, NOD	Mikhailov *et al*., 2001
Adda	Amide (activated ester) between carboxylic acid of Adda and primary amino groups	KLH BSA HRP	0.33	Direct competitive	All cogeners	Zeck *et al*., 2001
MC-LA	_	Polylysine Muramyl dipeptide	-	-	6 variants	Kfir *et al*., 1986
MC-LR	Carboxylic acid group via carbodimide	HRP	0.22	Direct competitive	All cogeners	Weller *et al*., 2001
MC-LR Nodularin	Aminoethylation on *N*-methyldehydroalanine	BSA	0.01	EIA*	MC-LR, -YR, -LA, NOD	Khreich *et al*., 2009
MC-LR	EDC/ NHS linkage via carboxylic acid groups	Biotin	0.05	Indirect inhibition	_	Lindner *et al*., 2004

Table 5.2.2.3: Strategies for recombinant antibody development to microcystin. Antibodies were compared, according to their immunogen preparation (conjugation strategy and carrier molecule), IC_{50}, antibody format, immunoassay format and cross-reactivity to microcystin variants.

Toxin	Conjugation Strategy	Carrier	Antibody Format	IC_{50} (µg/L)	Format	Cross-reactivity	Reference
MC-LR	Aminoethylation of the *N*-methyldehydroalanine residue and one-step glutaraldehyde coupling	KLH BSA	scAb from Tomlinson I library	4-9	Direct Competitive	MC-RR, -LW, -LF	McElhiney *et al*., 2000
MC-LR	Aminoethylation of the *N*-methyldehydroalanine residue and one-step glutaraldehyde coupling	KLH BSA	scAb from Griffin I library	0.0045	Direct Competitive	MC-RR, -LW, -LF	McElhiney *et al*., 2002
MC-LR	Aminoethylation of the *N*-methyldehydroalanine residue and one-step glutaraldehyde coupling	KLH BSA	scAb from Tomlinson I scab from Griffin I	0.013 4	Direct Competitive	-	Strachen *et al*., 2002

Microcystin antibodies have also been incorporated into an immuno-protein phosphatase inhibition assay (Metcalf *et al*., 2001), immunoaffinity chromatography (McElhiney *et al*., 2002; Aranda-Rodriguez *et al*., 2003) and, most recently, a lateral flow 'dipstick' style assay (Kim *et al*., 2003). Such kits have proven useful for screening water and cyanobacterial samples, but they have shown poor cross-reactivity to toxin variants (Rapala *et al*., 2002). In general, the analytical capacity of any ELISA in routine sample screening is dependent on the antibody's ability to recognise all microcystin variants. Polyclonal antibodies to microcystin have the advantage of being composed of a mixed pool of antibodies, which bind different sites on the microcystin molecule, including those that are common to all toxin variants. However, polyclonal antibody responses are highly variable and non-reproducible, especially when different batches of sera are used. A sheep polyclonal antibody was raised to the Adda moiety, which is found in 80 % of all microcystin and nodularin variants (Fischer *et al*., 2001).

Immunisation with a common structural feature, such as Adda, restricts the number of sites available for binding, giving greater reproducibility. The sheep pAb cross-reacted with MC-LR, -RR, -YR, -LW, -LF, 3-desmethyl-MC-LR, 3-desmethyl-MC-RR and nodularin. ELISA formats have also been developed for microcystin using monoclonal and recombinant antibodies. Monoclonal antibodies from hybridoma cell lines are more reliable and reproducible than polyclonal antibodies, as they can be generated in uniform batches, with comparable specificities. Isolation of single-chain antibody fragments to MC-LR, from a synthetic Tomlinson human phage library, was reported by McElhiney *et al*. (2000). The most sensitive antibody clone selected from the library detected MC-LR with an IC_{50} of 4 μg/L. The suitability of two naïve antibody libraries; the synthetic Tomlinson and the semi-synthetic Griffin phage libraries for recombinant antibody generation to MC-LR, were compared by Strachan *et al*. (2002). The Griffin library consists of human V_H and V_L chain gene fragments, with CDR3 diversity generated using synthetic oligonucleotides. The Tomlinson library is based on a single human framework with side chain diversity incorporated at 18 amino acid positions in the antigen-binding site. Selected antibodies (single chain antibody fragment, scAb) from the Griffin library were found to be 300 times more sensitive than those isolated from the Tomlinson library. McElhiney and colleague also employed the Griffin library to isolate recombinant antibody fragments (scAb) to MC-LR. It was reported that the most sensitive scAb isolated, was capable of detecting microcystin-LR at levels below the World Health Organisation limit in drinking water (1 μg/L). In addition, the antibody fragment cross-reacted with three purified microcystin variants (MC-RR, -LW, and -LF) and a related cyanotoxin, nodularin. The quantification of microcystins in toxic samples assayed by ELISA showed good correlation with analysis by high-performance liquid chromatography (McElhiney *et al*., 2002).

5.2.2.4 Phosphatase inhibition assays

Methods for detection of microcystin have been developed which exploit the biochemical properties of this hepatotoxin molecule. These assays are based on microcystins inherent ability to inhibit the catalytic subunit of protein phosphatases. There are a number of advantages to this approach; they provide a useful indication of the biochemical activity of the toxin sample, as a whole, and the assays are sensitive, rapid and inexpensive, due to the commercial availability of the enzymes. Protein

phosphatase inhibition assays (PPIAs) involve the ability of the catalytic subunit of protein phosphatase 1 (PP1) to dephosphorylate the chromogenic substrate *p*-nitrophenylphosphate. However, a limitation of this method is that the reactivity of different microcystins to protein phosphatases may not be the same, and the assay may be sensitive to other protein phosphatase inhibitors (Metcalf *et al*., 2001). Therefore, Metcalf *et al*. (2001) developed a modification of the PPIA to make it specific for microcystins and to decrease its sensitivity to other protein phosphatase inhibitors, such as okadaic acid, calyculin and tautomycin. They successfully combined immunoassay detection with protein phosphatase inhibition in a colorimetric, immuno-protein phosphatase inhibition assay system. Assays have been developed using both protein phosphatase 1 (PP1) and protein phosphatase 2A (PP2A), although the reaction of microcystin with PP1 is approximately 50 times less sensitive than with PP2A (Honkanen *et al*., 1994).

5.2.3 Detection Issues for Microcystin

Overall, there are a number of key issues causing concern in the area of microcystin detection. There is some concern that analytical techniques used for the detection of microcystins may fail to recognise toxin variants and this may result in a significant number of false negatives. This applies to instrumental techniques, as well as immunochemical assays. Also, certain methods have been hindered due to the presence of over 90 different purified variants, most of which are not commercially available. This may lead to the under-estimation of total microcystin in a sample. For example, some methods only report microcystin-LR equivalence, regardless of what other variants are present (McElhiney and Lawton, 2005). The availability of HPLC, coupled to mass spectral analysis, can aid in more accurate estimation of toxin variants. However, many microcystins share the same molecular mass, making definitive identification difficult. Another difficulty in analysing microcystins is the requirements for sample processing, including solid-phase extraction (SPE), in order to enrich environmental concentrations of microcystin and to eliminate contaminating animal and plant tissue from complex samples. New techniques involving recombinant antibodies have been exploited to develop assays and biosensors for microcystins, with higher sensitivities and a greater potential for cross-reactivity to toxin variants than other methods (McElhiney *et al*., 2002; Strachen *et al*., 2002).

5.2.4 Chapter aims

The purpose of this chapter is to give an overview of the successful generation of an avian scFv fragment to the cyanobacterial toxin, microcystin. An antibody is required that can detect microcystin and its variants with high sensitivity and specificity below the limit of detection of 1 µg/L. A chicken host was immunised, RNA extracted and cDNA synthesised. The antibody variable genes were amplified by PCR, gel-purified and cloned into a phagemid vector. Specific clones were isolated by bio-panning, which involved a selection process on MC-OVA-coated immunotubes, enrichment and affinity maturation. Five rounds of selection were performed on the avian anti-MC-LR single chain variable fragment (scFv) recombinant antibody library.

In addition, this chapter provides an insight into the molecular structure and binding characteristics of the recombinant antibody fragments to microcystin, isolated from an immune scFv avian library. Two antibodies were selected, 2H1 and 2G1, based on their binding characteristics by direct and competitive ELISA. DNA sequence information from the microcystin-binding scFvs allowed for a comprehensive comparison between the genetic sequences of each antibody and the three-dimensional (3-D) *in silico* modelling, which employed the Deepview–Swiss PDB Viewer. Docking analysis was performed with the scFv fragments and the microcystin-LR molecule, using the PDB NMR sequence data for microcystin (1LCM). This provided information about the interactions between the scFvs and the MC-LR molecule and also predicted possible docking positions for MC-LR with the scFv structures.

The availability of a hexa-histidine (His_6) tag on the scFvs fragments allowed for purification using an immobilised-nickel resin. These antibodies were further purified and characterised by size exclusion chromatography on an Akta™ Explorer FPLC instrument. An inhibition ELISA was optimised and preliminary assay validation was carried out, using the IMAC- and size exclusion-purified scFvs. The purpose of this chapter was to demonstrate the accuracy, precision and sensitivity of the isolated antibody fragments. The overall aim was to provide microcystin-binders for incorporation into a new immunosensor for microcystin that would be comparable or more effective than the detection technologies outlined in Section 5.2.2.

5.3 Results

5.3.1 Production of an avian recombinant scFv library for microcystin

5.3.1.1 Avian immune response generation to a microcystin conjugate

Two bespoke conjugates were generated through modification of the *N*-methyldehydroalanine residue to create an aminoethanethiol-microcystin-LR derivative (Section2.14.1). The derivatised microcystin-LR was subsequently conjugated to OVA and BSA using one-step glutaraldehyde coupling. An immune response was generated in an avian host using the MC-LR-BSA conjugate, as described in Section 2.14.2. Prior to the sacrifice of the immunised chicken, a serum titre was performed to determine whether a sufficient immune response was generated. Similar dilutions of serum, taken from the chicken prior to immunisation (pre-bleed), were also prepared. In order to characterise the true response to the toxin, an alternative coating conjugate, MC-LR-OVA was utilised.

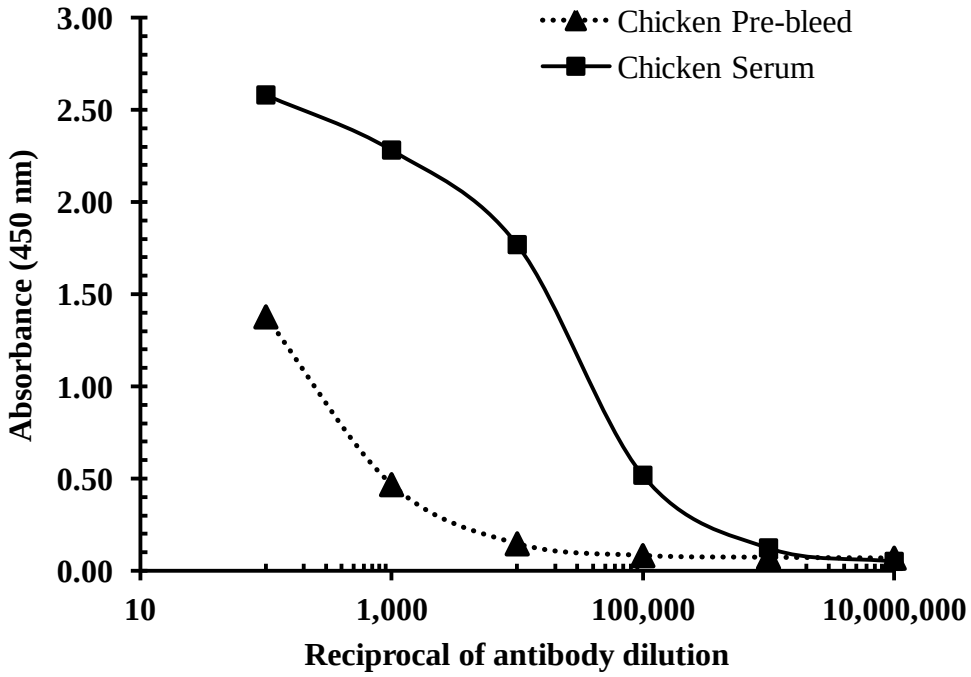

Figure 5.3.1.1: ELISA analysis of pre-bleed and immune serum from MC-LR-BSA-immunised avian host. The ELISA plate was coated with MC-LR-OVA conjugate, at a concentration of 10 µg/mL. Binding was detected with an anti-chicken (IgY) antibody, conjugated to horseradish peroxidase (HRP). The ELISA was developed with TMB substrate and the absorbance was measured at 450 nm, using a Tecan™ Safire II plate reader.

A clear immune response was generated in the chicken by administering four boosts with 500 µg of microcystin-BSA conjugate, at four weekly intervals. The titre was approximately 1/20,000 (Figure 5.3.1.1), which was sufficient for recombinant antibody generation. The pre-bleed showed some response with the conjugate, but this was largely due to non-specific binding of serum to the ELISA plate, despite the use of extensive blocking steps.

5.3.1.2 Extraction of RNA and reverse transcription to cDNA

RNA was extracted from the bone marrow and spleen of the immunised-animal and complementary DNA (cDNA) was synthesised using the First Strand® cDNA Synthesis Kit (Invitrogen). The cDNA from the bone marrow and spleen was electrophoresed on a 1 % (w/v) agarose gel to confirm the presence of good quality templates for further gene amplification (Figure 5.3.1.2).

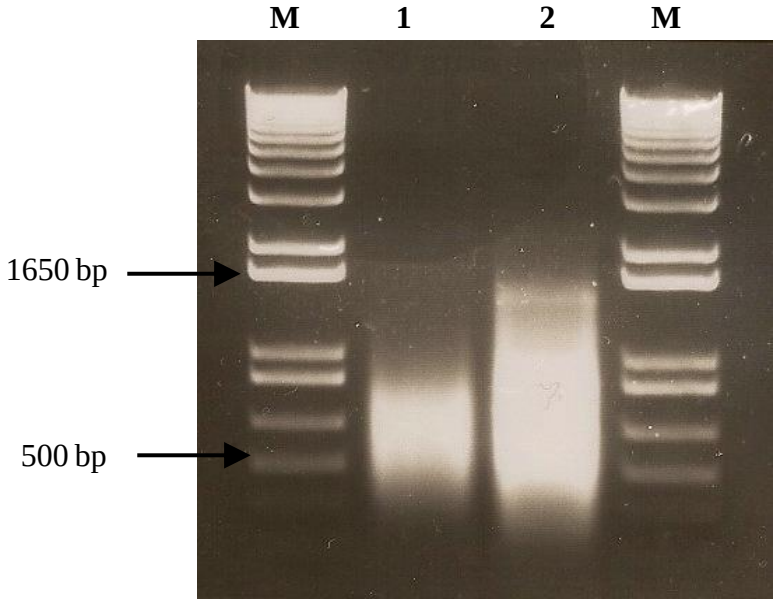

Figure 5.3.1.2: Agarose gel demonstrating successful cDNA synthesis from microcystin-immunised avian host. 1.) Spleen cDNA (5.6 µg) and 2.) Bone marrow cDNA (4.8 µg) were loaded on the 1 % (v/v) agarose gel. The presence of cDNA is characterised as a continuous smear from approximately 400-1650 bp. Lanes 'M' represent a 1 kb Plus DNA ladder (Invitrogen).

5.3.1.3 Amplification of avian heavy and light chains and PCR optimisation

The long linker primers, CSCVHo-F and CSCG-B (Barbas *et al*., 2001) were used to amplify V_H segments from the avian cDNA, as long linker scFv fragments have less tendency to dimerise and cause avidity effects. The sense primer has a sequence tail, which corresponds to the linker sequence that is used in the overlap extension PCR. The reverse primer has a sequence tail, containing an *Sfi*I restriction site. This tail is recognised by the reverse extension primer used in the second-round PCR. The CSCVK sense primer is combined with the CKJo-B reverse primer to amplify V_L gene segments from the avian cDNA. CSCVK has a 5´ sequence tail that contains an *Sfi*I site and is recognised by the sense extension primer in the second-round PCR. The reverse primer has a linker sequence tail that is used in the overlap extension. It was neccessary to optimise the $MgCl_2$ concentrations for both products. The PCR products were evaluated on 1 % (w/v) agarose gel (Figure 5.3.1.3).

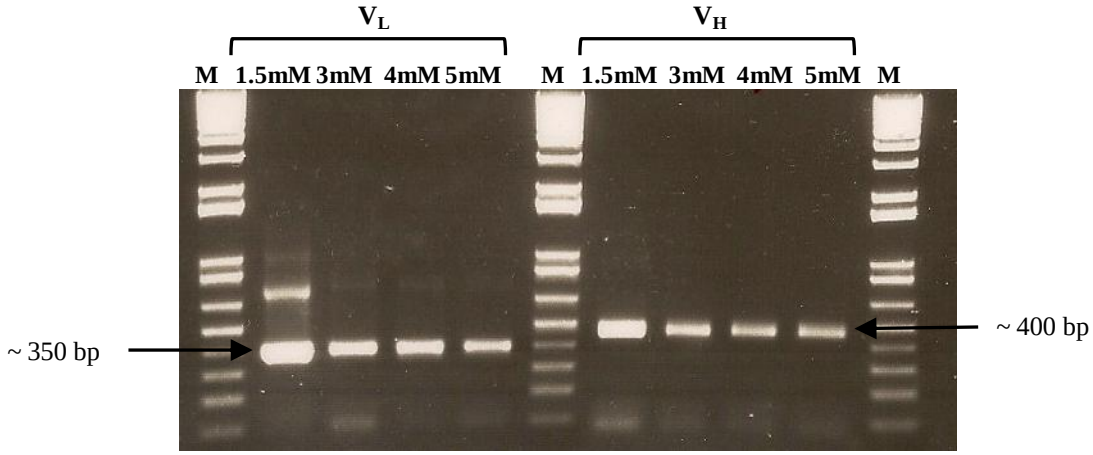

Figure 5.3.1.3: Optimisation of V_H and V_L PCR amplifications. $MgCl_2$ concentrations for each reaction were prepared from 1.5 mM to 5 mM, for both the V_H and V_L chains. 'M' represents a 1 kb Plus DNA ladder.

A 400 bp product amplified for the V_H reactions and a 350 bp amplicon was generated for the V_L reactions. These results indicated that the optimal $MgCl_2$ concentration for the V_L and V_H chain amplifications, were 3 mM and 1.5 mM, respectively. At 1.5 mM $MgCl_2$, a non-specific band was observed in the V_L reaction. Therefore, this concentration was not employed for further amplification. A large-scale PCR

amplification (10X reaction) was performed, using the optimised conditions, and the products were purified by gel extraction, using a QiaQuick gel extraction kit (Qiagen).

5.3.1.4 SOE-PCR of variable heavy and light chains from the avian library

Following purification of the V_H and V_L chains by gel extraction, SOE-PCR was carried out. SOE-PCR was performed, using the extension primers, CSC-F and CSC-R. This process joined the V_L and V_H regions, using the sequence tails introduced in the first round of PCR, to create a serine-glycine linker sequence. This second round of PCR produced a 750 bp product (Figure 5.3.1.4). An annealing temperature of 56^{o}C and a magnesium sulphate ($MgSO_4$) concentration of 2 mM were found to be optimal for the PCR, using the high fidelity Platinum® Taq DNA polymerase (Invitrogen).

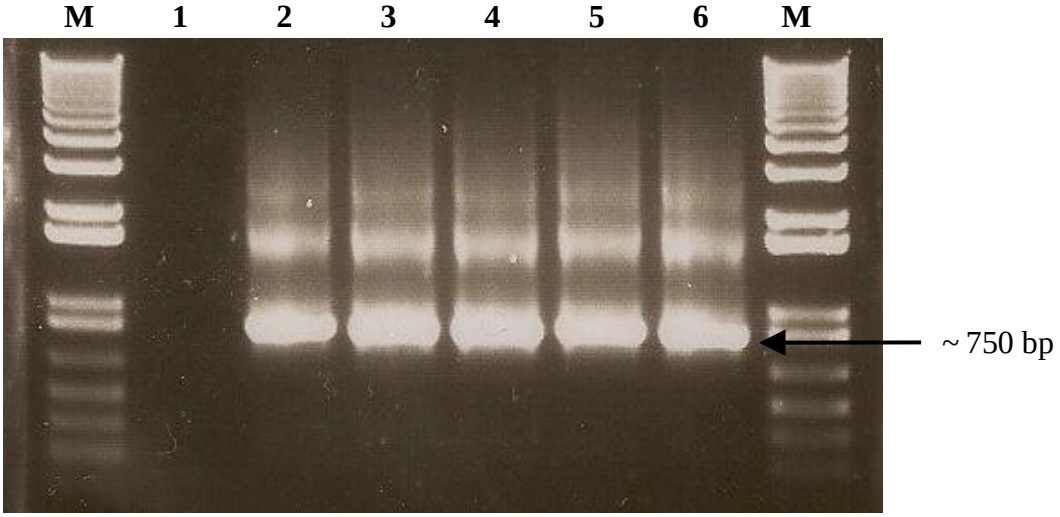

Figure 5.3.1.4: Large-scale amplification of SOE-PCR product. The approximate molecular weight of this fragment was 750 base pairs (bp). A negative control (no template) was included (1), and 'M' represents a 1 kb Plus DNA ladder. Lanes 2-6 contains repeat amplifications of the SOE product, employing the same PCR conditions.

Some non-specific bands were observed for the large-scale amplification (Figure 5.3.1.4), which were subsequently removed through gel purification. The purified SOE product, with a molecular weight of approximately 750 bp, was isolated, ethanol-precipitated and stored at -20^{o}C.

5.3.1.5 Antibody library construction and bio-panning

The SOE product was harvested, quantified (using a Nanodrop ND-1000™), and cloned into a pComb3xSS vector, using the restriction enzyme, *Sfi*I (see Section 2.14.3.4). *Sfi*I was used for cloning, as the sites at which it cuts are rare in antibody sequences and, therefore, the use of this enzyme eliminates the possibility of internal digestion and incorrect sequence lengths. Antartic phosphatase treatment (see Section 2.14.3.5) ensured that self-ligation of the vector did not occur. The ligated product was transformed into electro-competent *E. coli* XL1-Blue cells (Strategene), by electroporation. The transformed avian anti-microcystin scFv library had a size of 3.47 x 10^7 cfu/mL, which was sufficient for immune phage-displayed libraries.

5.3.1.6 Screening of microcystin chicken library using phage display

The library was 'rescued' using M13K07 helper phage, as outlined in Section 2.14.4.1. The immune library was subsequently enriched, via phage display bio-panning, against immobilised MC-LR-OVA conjugate (100 to 10 µg/mL). Five rounds of bio-panning were carried out, with decreasing concentrations of conjugate coated onto the immunotube for each round. The number of washes was increased to facilitate high stringency panning to select for all available binding clones (Table 2.14.4.1). The inputs and outputs from each round of bio-panning give an indication of panning efficiency and were optimal for each round (Table 5.3.1.1).

Table 5.3.1.1: Bio-panning inputs and outputs for the avian immune library

Pan Number	Input (cfu/mL)	Output (cfu/mL)
Pan 1	4.3 x 10^{11}	9.0 x 10^7
Pan 2	4.1 x 10^{10}	4.7 x 10^7
Pan 3	6.4 x 10^{10}	1.1 x 10^5
Pan 4	2.9 x 10^8	1.1 x 10^6
Pan 5	1.2 x 10^{11}	2.9 x 10^6

5.3.1.7 Polyclonal phage ELISA

The precipitated input phage from each round of bio-panning was analysed by polyclonal phage ELISA, as described in Section 2.13.14.3, to test for enrichment to the immobilised-MC-LR-OVA conjugate. The phage input contains a mixture of microcystin binders, with varying specificities and affinities, which are selectively enriched against the toxin-conjugate with each round of bio-panning. The polyclonal phage response is, therefore, an indication of bio-panning efficiency. An increase in the absorbance signal to MC-LR-OVA, in bio-panning rounds 4 and 5, is illustrated in Figure 5.3.1.5. A high signal of MC-OVA-specific scFv-phage can be observed in bio-panning round 1, which subsequently decreased, due to increased panning stringency. There is also an increase in selection to M13K07 helper phage in rounds 2 and 3, which subsequently decreased in rounds 4 and 5.

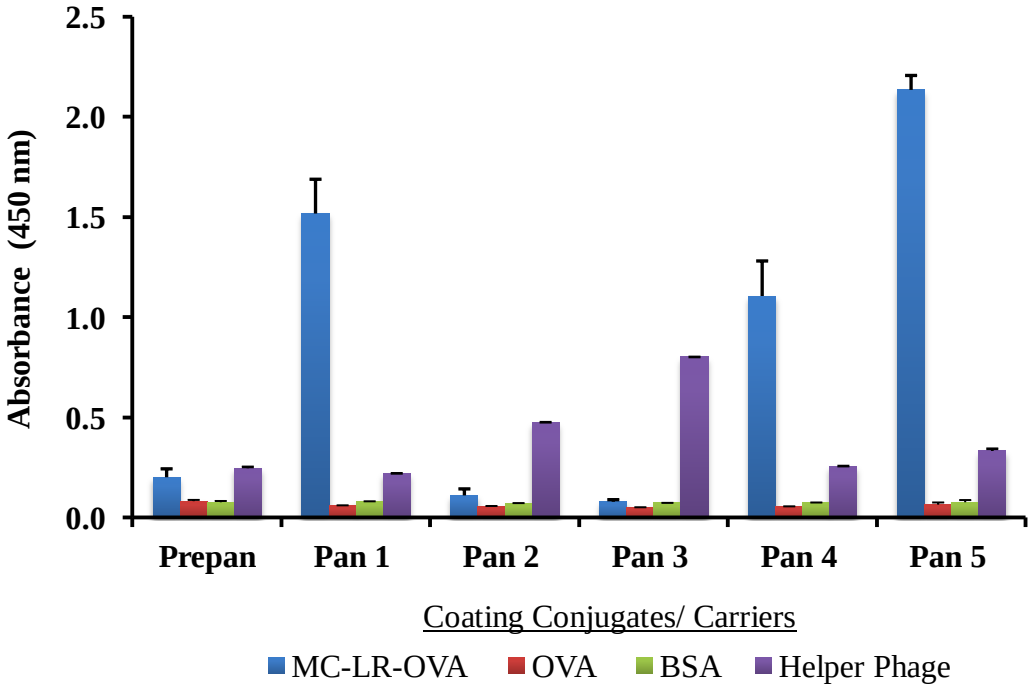

Figure 5.3.1.5: Polyclonal phage ELISA for the avian library. Input phage from each round of bio-panning was incubated with immobilised-MC-LR-OVA conjugate (10 µg/mL) and binding was detected using a HRP-labelled anti-M13 commercial antibody (GE Healthcare). Non-specific binding controls were included for the carrier immunogen, BSA (10 µg/mL) the screening carrier, OVA (10 µg/mL) and M13KO7 helper phage (1/100). Errors bars represent the standard error of the mean.

5.3.1.8 Direct soluble monoclonal ELISA and colony-pick PCR

It is possible to perform monoclonal phage ELISA from bio-panning outputs. However, it has been shown that the multivalent nature of display on the phage particle may cause avidity effects, resulting in selection of antibodies with lower affinities (Kwasnikowski *et al*., 2005). Therefore, phage outputs from panning rounds 4 and 5 were re-infected into *E.coli* Top10F' bacterial cells. Single colonies (150) were picked and sub-cultured overnight in 200 µL SB media, containing 100 µg/mL carbenicillin. The cultures were induced with 1 mM IPTG, for soluble expression, and subjected to three 'freeze-thaw' cycles. The scFv-enriched lysate was clarified by centrifugation and tested in a direct ELISA format for binding to immobilised MC-LR-OVA conjugate (5 µg/mL) (Figure 5.3.1.6). Ten of the best clones, selected on the basis of their absorbance values, were taken forward for cross-reactivity and inhibition analysis to assess their ability to bind MC-LR in solution.

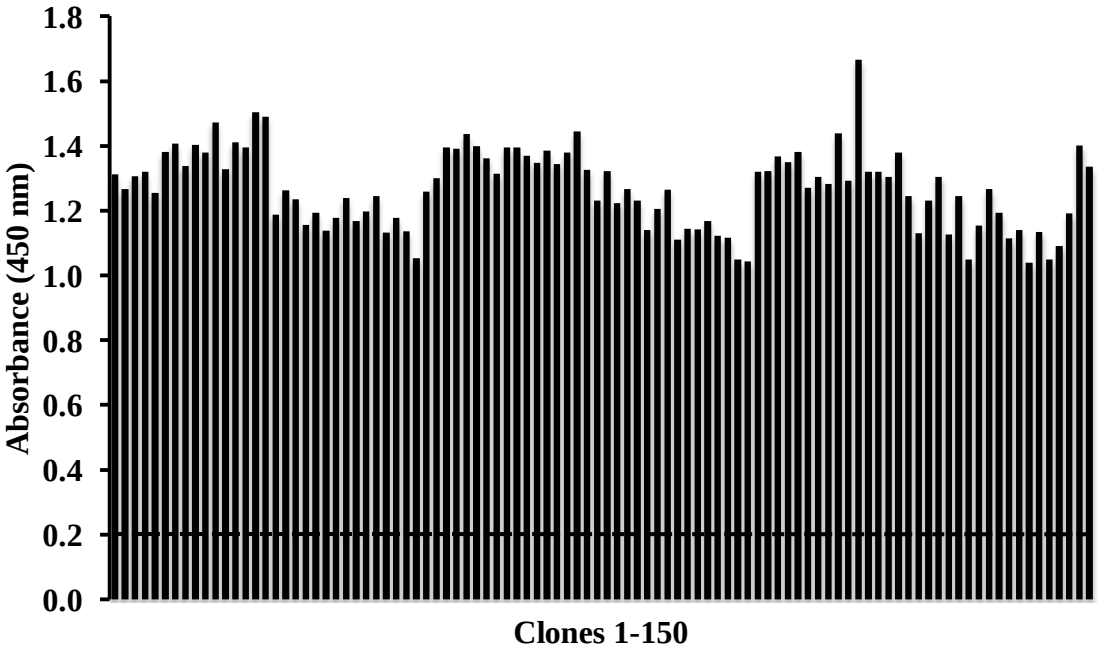

Figure 5.3.1.6: Soluble monoclonal ELISA of the anti-microcystin scFvs. One hundred and fifty clones were selected from panning rounds 4 and 5, for soluble expression analysis. Supernatant, containing solubly-expressed scFv, was incubated on MC-LR-OVA–coated plates (5 µg/mL) and binding was detected using HRP-labelled anti-HA commercial monoclonal antibody. All clones tested had an absorbance signal significantly above background. The ELISA background (three times the blank value) is marked with a horizontal line.

A ‘colony-pick’ PCR was performed on ten randomly selected individual colonies from the bio-panning rounds 4 and 5 of the avian scFv library. The bacterial colonies were inoculated into 50 µL of sterile, molecular-grade water and lysed at 94°C for 10 minutes. The amplified scFv products were analysed via gel electrophoresis on a 1% (w/v) agarose gel. An insert of approximately 750 bp was observed for every colony (data not shown).

5.3.1.9 Restriction digestion of the anti-microcystin scFvs

Ten of the scFv clones, identified by monoclonal soluble ELISA, were digested with *Alu*I restriction enzyme. The aim of this analysis was to characterise the antibodies, based on their characteristic restriction profiles, which may give an indication of library diversity (Figure 5.3.1.7). Four different digestion profiles were observed, based on the nucleotides identified by the *Alu*I enzyme (AG/CT), indicating that there was at least four distinct clones. Profile 1 is shown in lanes 1 and 7, resulting in four distinct bands. Profile 2 is shown in lanes 2 and 9, resulting in three distinct bands. Profile 3 is shown in lane 5, resulting in 2 distinct bands. Profile 4 is shown in lane 3, also resulting in two distinct bands. Some banding patterns may have resulted from partial enzymatic digestion. A number of clones remained un-digested, including lanes 4, 6, 8, 10, 11 and 12 (Figure 5.3.1.7).

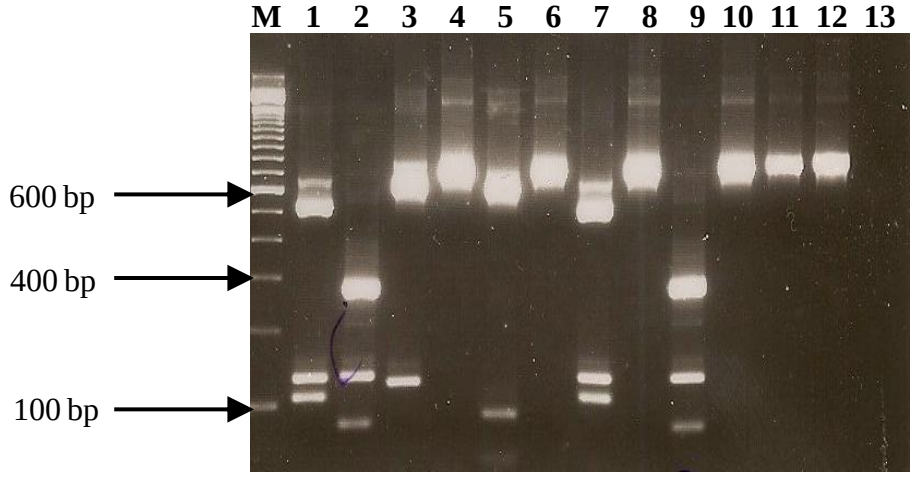

Figure 5.3.1.7: Restriction digestion analysis, utilising *Alu*I restriction enzyme. Lane 1: 2C3, Lane 2:2H1; Lane 3:1F11; Lane 4:5C9; Lane 5:2C5; Lane 6:2G1; Lane 7: 5A9; Lane 8: 2C1; Lane 9: 2C4; Lane 10: 1E11; Lane 11: 2G1; Lane 12: Un-digested control vector; Lane 13: Negative control (no colony). Lane ‘M’ represents a 100 bp DNA ladder (Invitrogen).

5.3.2 Characterisation of the microcystin-specific scFv fragments

5.3.2.1 Carrier cross-reactivity analysis of the anti-MC-LR clones

It was established that the ten clones, selected by soluble, monoclonal ELISA, were capable of binding microcystin in the context of a protein conjugate and that they possessed some genetic diversity, as illustrated by restriction analysis. It was, therefore, important to establish that the clones were not specific for the screening conjugate alone, and that they bound MC-LR in the context of other protein conjugates. The MC-LR-KLH (obtained from Queen's University) and the MC-LR-OVA (Enzo Life Sciences Ltd.) conjugates were utilised for screening. The screening protein carrier, ovalbumin (OVA), the immunogen carrier, bovine serum albumin (BSA) and the alternative conjugate protein, keyhole limpet haemocyanin (KLH) were included in the analysis (Figure 5.3.2.1).

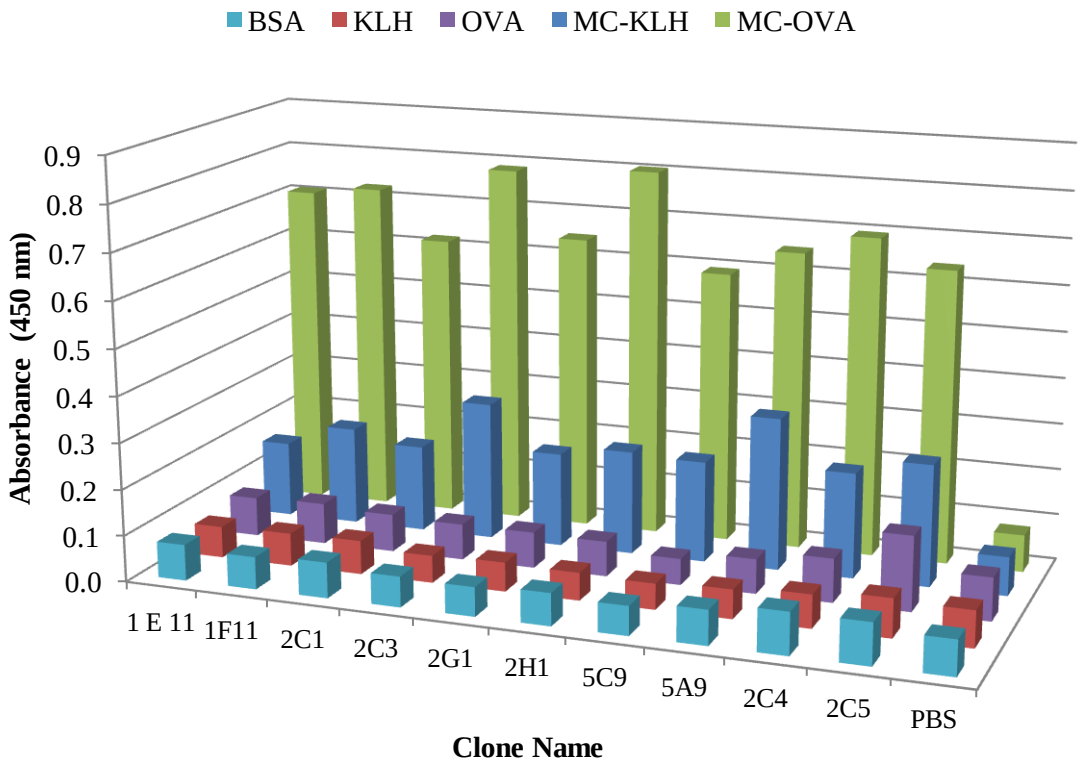

Figure 5.3.2.1: Direct ELISA analysis of crude lysate from cultures of ten selected clones. The clones were tested for reactivity to two microcystin conjugate, including MC-LR-KLH and MC-LR-OVA (5 µg/mL) and the carrier proteins, BSA, OVA and KLH (5 µg/mL). Ten mL cultures were grown, induced with IPTG and lysed using successive freeze-thaw cycles. Lysates were clarified by centrifugation and diluted (1/5) in 1 % (w/v) Milk Marvel/ PBS, containing 0.05 % (v/v) Tween 20.

The clones displayed some cross-reactivity to the MC-LR-KLH conjugate, which was not comparable to the binding of the MC-LR-OVA conjugate. The conjugates may have been synthesised using different techniques. Derivitisation and two-stage glutaraldehyde coupling were employed for the generation of the MC-LR-OVA conjugate. The conjugation technique employed for the functionalisation of MC-LR with KLH, remains unknown (undisclosed information). The conjugates may have different sites for conjugation and have different toxin:carrier ratios. Little or no binding was observed for the protein carriers, BSA, KLH and OVA.

5.3.2.2 Indirect inhibition ELISA of microcystin-binding clones in lysate

The MC-LR-specific scFvs were analysed for their capacity to bind free MC-LR in solution. Inhibition analysis was carried out by pre-incubating with free MC-LR for 30 minutes and adding the mixture to the pre-coated microplate. In total, ten scFvs were analysed for inhibition with MC-LR, ranging in concentration from 10 to 0.03 µg/mL of free microcystin in solution. The ability of the scFvs to bind the toxin in solution, relative to the immobilised conjugate on plate (A) was determined by analysing the same clone without any inhibition by the free antigen (A_0). The results were normalised by subtracting the absorbance at an excess of analyte (A_{excess}) from both A and A_0. The resulting normalised absorbance ($A-A_{excess}/A_0-A_{excess}$) was plotted as A/A_0, versus MC-LR concentration (ng/mL). This analysis showed that all of the scFvs selected were inhibited from binding the immobilised conjugate, for a given concentration of the free toxin in solution (Figure 5.3.2.2). It was observed that depletion of the free toxin was evident down to the low ng/mL range. This was important in relation to antibody characterisation and assay development, as the antibodies need to be able to recognise free toxin in solution.

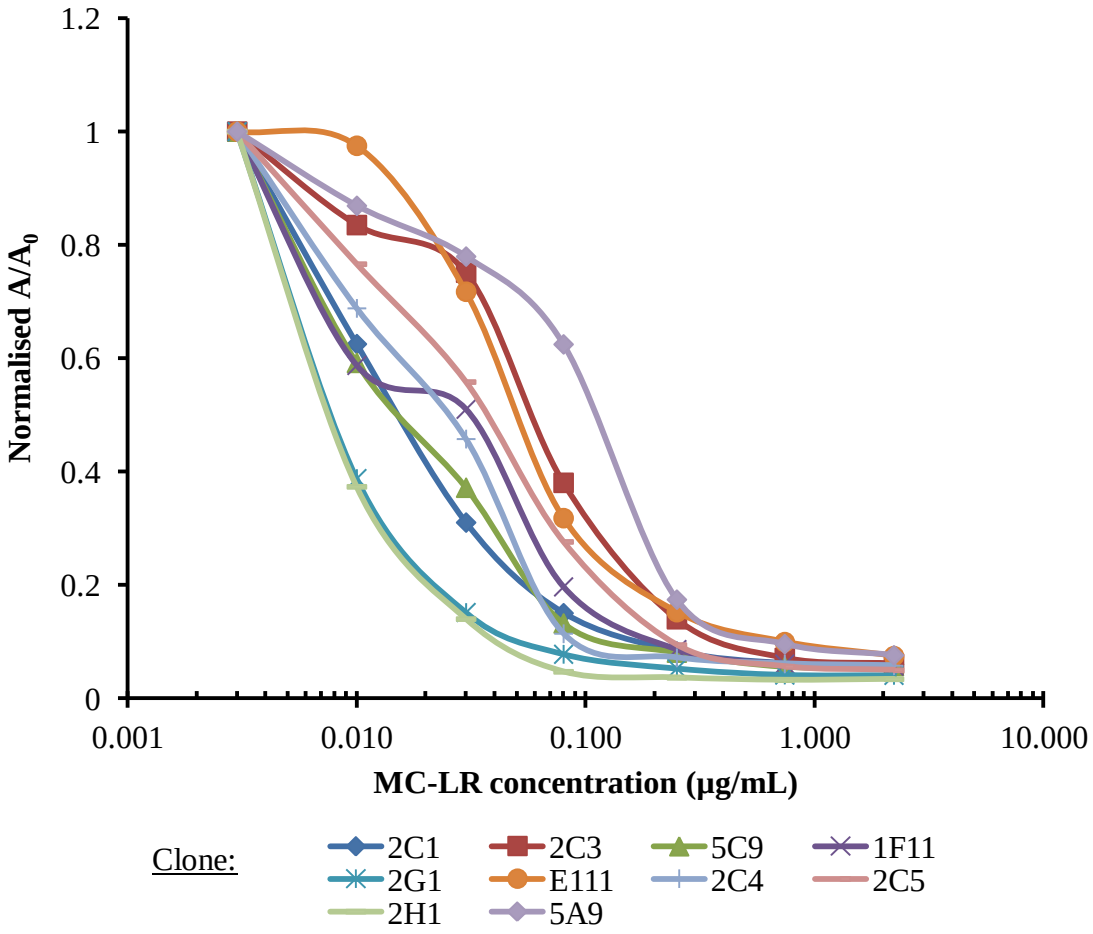

Figure 5.3.2.2: Crude inhibition ELISA of ten solubly-expressed MC-LR scFv clones. The ELISA plate was coated with 500 ng/mL MC-LR-OVA conjugate and inhibition occurred between free MC-LR, ranging in concentration from 10 to 0.03 µg/mL, and crude, induced lysate, diluted to a final concentration of 1/2,000 in 1 % (w/v) Milk Marvel/ PBS contain 0.05 % (v/v) Tween 20. The normalised absorbance (A/A_0) versus the free toxin concentration (µg/mL) was plotted.

5.3.2.3 Sequence analysis of four selected soluble microcystin-binding clones

Purified plasmids from four of the inhibitive clones, 2H1, 2G1, 2C1 and 5C9, were prepared using the Wizard® Plus SV Miniprep DNA purification system, as described in Section 2.13.8. The plasmids were sequenced by MWG-Operon, using the splice by extension overlap (SOE) primers. The light and heavy chain variable regions were identified using the Kabat numbering system and subsequently aligned (Figure 5.3.2.3). ClustalW is widely used for multiple alignments and for preparing phylogenetic trees (Thompson *et al.*, 1994). It is the third generation of the Clustal series of programs, where 'W' stands for weighting, which refers to the programs use of sequence weighting and position-specific gap penalties.

Considerable sequence diversity was evident between the 2H1 and 2G1 clones. The 2G1, 2C1 and 5C9 sequences were found to be genetically identical (Figure 5.3.2.3). CDRL1 and CRDL2 each have three amino acid differences and CDRH1 only has one difference, where alanine (Ala) in the 2H1 sequence was substituted to asparagine (Asp) in the 2G1 sequence. CDRL3, CDRH2 and CDRH3 are markedly different in 2H1 and 2G1, with 9, 6 and 9 amino acid differences between them, respectively. CDRL3 is shorter by two amino acids and CDRH3 is shorter by three amino in the 2G1 clone, compared to the related sequences in the 2H1 clone. The linker region is highlighted in blue, while the hexahistidine (His) tag is highlighted in yellow and the haemagglutinin (HA) tag is highlighted in green. The framework regions of the scFvs show high sequence similarity, with only 19 differences between the two molecules. There are a number of hydrophobic proline residues in the framework regions and in the CDRL2 region. Despite being hydrophobic, proline residues are frequently found on protein surfaces and play an important role in molecular recognition (Kay *et al.*, 2000). Tyrosine residues are present in CDRH1, CDRH2 and CDRL1 of both scFv fragments. Tyrosines are important in the formation of protein-protein interactions and, therefore, have an important role in molecular recognition (Koide and Sidhu, 2009).The most specific antibodies were those with the highest tyrosine content. In contrast, arginine content is associated with increased non-specific binding (Birtalan *et al.*, 2008).

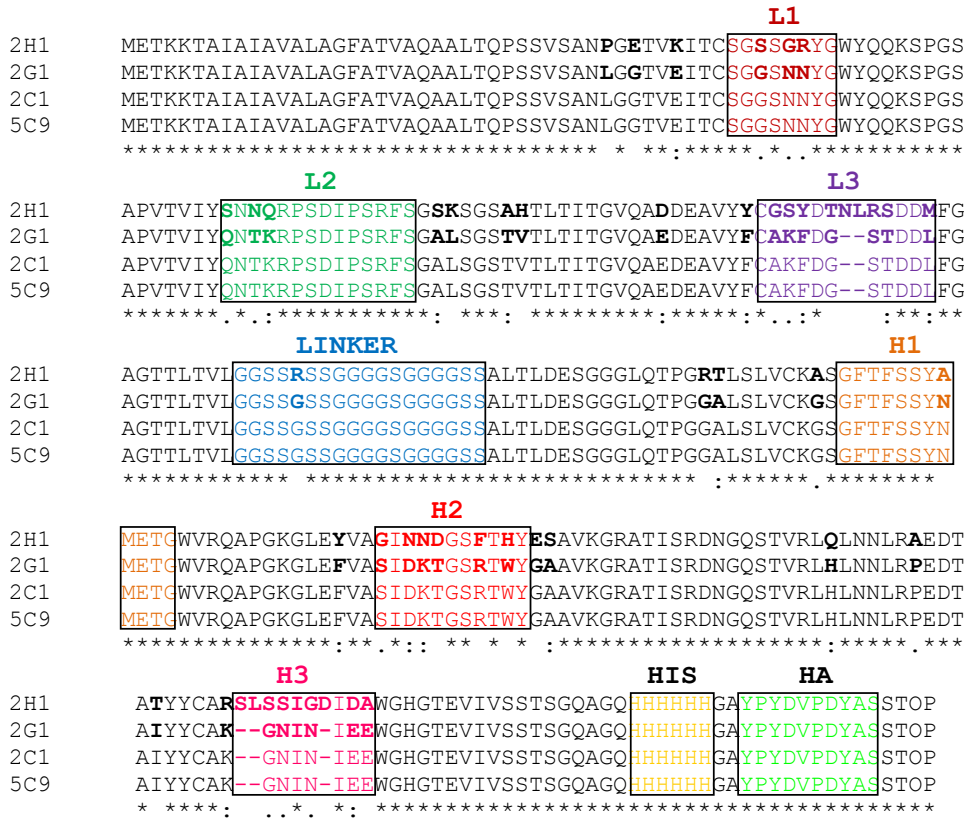

Figure 5.3.2.3: ClustalW sequence alignment for four MC-LR clones. CDR regions and tags, including His and HA, are highlighted in colour. Sequences 2G1, 2C1, 5C9 are identical. Key: CDRL1 = Red, CDRL2 = Green, CDRL3 = Purple, Linker = Blue, CDRH1 = Orange, CDRH2 = Red, CDRH3 = Pink, His Tag = yellow and HA Tag = Light Green.

5.3.2.4 Structural analysis of scFv clones using 3-D computer modelling

A murine scFv against IL-1β (2KH2, 2B chain) was found in the protein databank (PDB) that had a good homology to the 2H1 and 2G1 gene sequences using EMBL's T-Coffee alignment program. There is no current crystallographic structure for avian scFvs available. This ClustalW alignment was submitted to the Swiss Expasy protein structure homology-modelling server. The results from structural modelling studies for the two clones are illustrated in Figure 5.3.2.4. The hypervariable CDR domains were subsequently identified, from the Kabat numbering scheme for identification of residues belonging to CDR regions in the antibody structure. The 2H1 and 2G1 sequences have a high degree of homology. However, 2H1 has a longer CDRH3 and CDRL3 compared with 2G1 and residue differences can also be observed in all CDR regions.

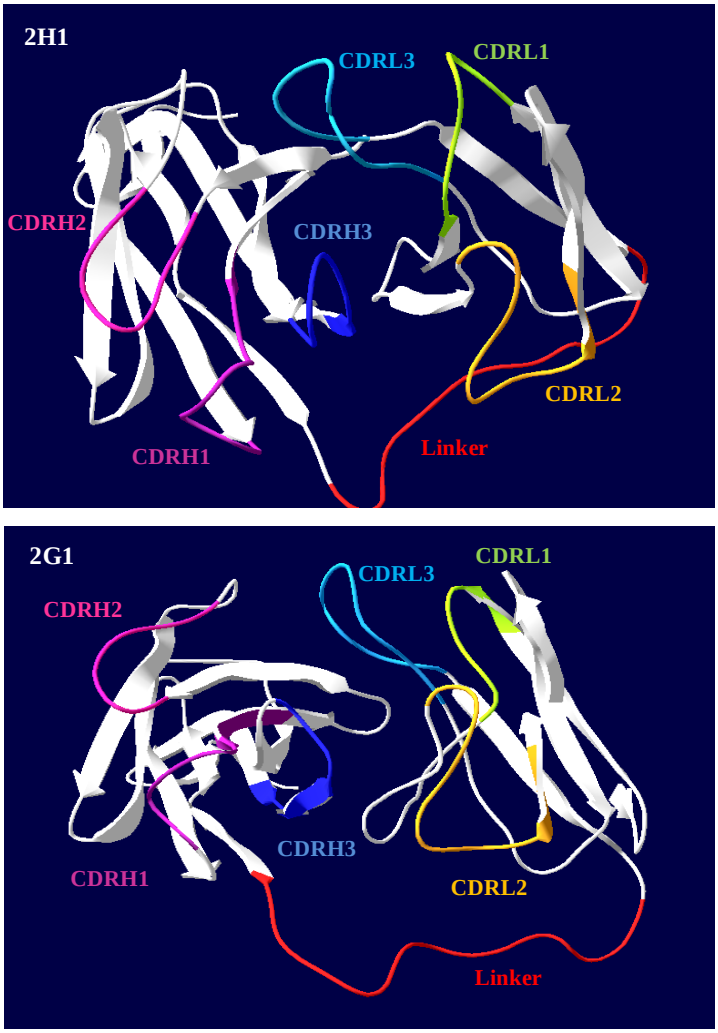

Figure 5.3.2.4: Three-dimensional (3D) structural models of the 2H1 and 2G1 scFv fragments, modelled to the known crystallographic structure of the scFv for the IL-1β complex (2KH2, 2B chain). CDRL1 = Green, CDRL2 = Orange, CDRL3 = Light Blue, Linker = Red, CDRH1 = Purple, CDRH2 = Pink and CDRH3 = Dark blue.

5.3.2.5 *In silico* docking of scFv clones to microcystin–LR

Once the protein structures of the scFv clones were known and the MC-LR peptide toxin were accessible through the Protein Data Bank (PBD), it was possible to carry out molecular docking, using Gramm-X software analysis. The aim of this analysis was to determine how the antigen-antibody interaction was occurring, thereby obtaining highly useful structural information. The MC-LR sequence was obtained from the PDB (Designation: 1LCM) and modelled using the Swiss-Model software programme (Kiefer *et al*., 2009) (Figure 5.3.2.5).

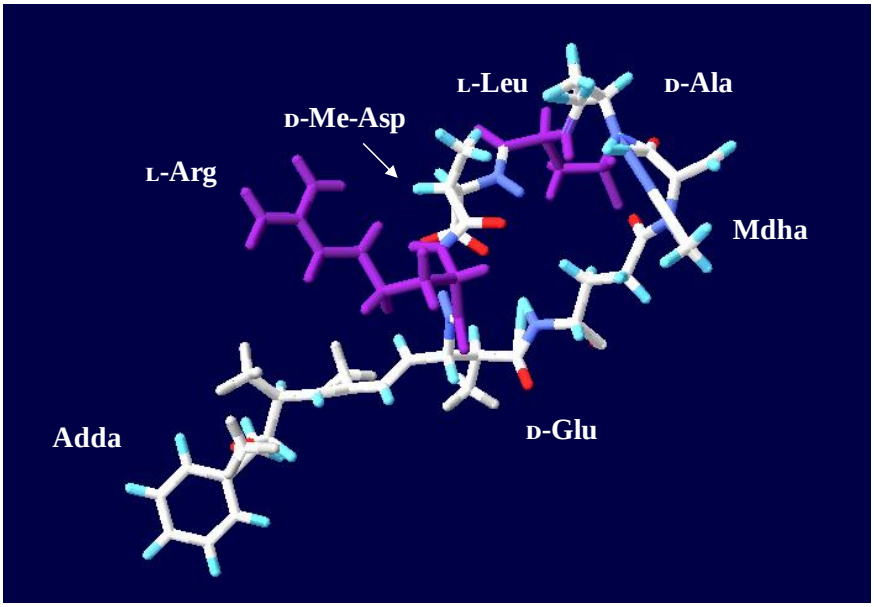

Figure 5.3.2.5: Structure of microcystin-LR (ILCM) created using the ExPASy homology-modelling server, SwissModel. Microcystin is characterised by the D-amino acids; D-Glutamic acid (D-Glu), D-Alanine (D-Ala) and D-erythro-methylaspartic acid (D-MeAsp) and the L-amino acids; L-Arginine (L-Arg) and L-Leucine (L-Leu). *N*-methyldehydroalanine (Mdha) and ß-amino acid side-group, 3-amino-9-methoxy-2-6, 8-trymethyl-10-phenyldeca-4, 6-dienoic acid (Adda) are also unique.

The Adda and arginine (Arg) side chains protrude from the ring structure distal from one another caused by the repulsion between the guanido function of Arg and the hydrophobic Adda (Rudolph-Böhner *et al*., 1994). Underlying the heterogeneity in MC variants is their common cyclic structure and possession of several rare, highly conserved amino acid moieties. The microcystin isoforms differ primarily at the two L-amino acids, and secondarily, by the presence or absence of the methyl groups on D-MeAsp and *N*-Mdha.

The purpose of the Gramm-X program is to add layers of possible docking protein sites, starting with the most probable prediction candidates (Tovchigrechko and Vakser, 2006).The input for modelling programs, such as Gramm-X, can be two molecules of any type: proteins, DNA, peptides or drugs. The output can be a list of potential complexes, sorted by shape complementarity criteria. Given two molecules, their surfaces are divided into patches according to the surface shape. Once the patches are

identified, they can be superimposed using shape matching algorithms. The best results can be re-scored using more advanced criteria, including energetic considerations, which should be more accurate in identifying the correct structural positions. Docking involves finding the most favourable binding modes of the ligand to the target. All docking methods require a scoring function to rank the various binding modes available and search methods to explore the variables.

Virtual screening on the basis of molecular distribution and physiochemical properties of ligands is very useful in proving leads for library mutagenesis and screening (Collis *et al*., 2003; Fellouse *et al*., 2004). Overall, it provides a three-dimensional structural hypothesis of how a ligand interacts with its target. Success of docking can be measured as the root mean square deviation (RMSD) of the Cartesian coordinates of the atoms of the ligand of the docked molecule in comparison to the actual crystallographic coordinates. A docking is seen as successful if the RMSD is less than the arbitrary threshold of 2 Å. Using the Gramm-X docking server, sequences for the 2H1 and 2G1 clones were submitted, along with the sequence for MC-LR (1LCM). The server provides the option of viewing multiple possible binding sites between the MC-LR molecule and the scFv. One possible binding combination of MC-LR with 2H1 and 2G1 is illustrated in Figures 5.3.2.6 A and D, respectively. Fifty possible MC-LR binding combinations are illustrated as layers of super-imposed molecules on the images for 2H1 and 2G1 (Figures 5.3.2.6 B and E, respectively). Figures 5.3.2.6 C and F illustrate the scFv structures, as red and green ribbon diagrams, with 50 possible microcystin positions super-imposed.

The green ribbon is representative of β-pleated sheet structures. For the 2H1 clone, the probable points of contact for MC-LR are characterised by the clustering of possible MC-LR binding sites (white circle) in Figure 5.3.2.6 B. These binding sites are in close proximity to the CDRL3, CDRH1, CDRH2 and CDRH3 regions of the 2H1 sequence and may be involved in recognition of the MC-LR peptide structure. For the 2G1 clone, the binding site is more ambiguous, with three possible points of contact identified (Figure 5.3.2.6 E). In this case, it is more difficult to determine which CDR regions may be involved in antibody:antigen recognition. All the RMSD values were below the arbitrary threshold of 2 Å.

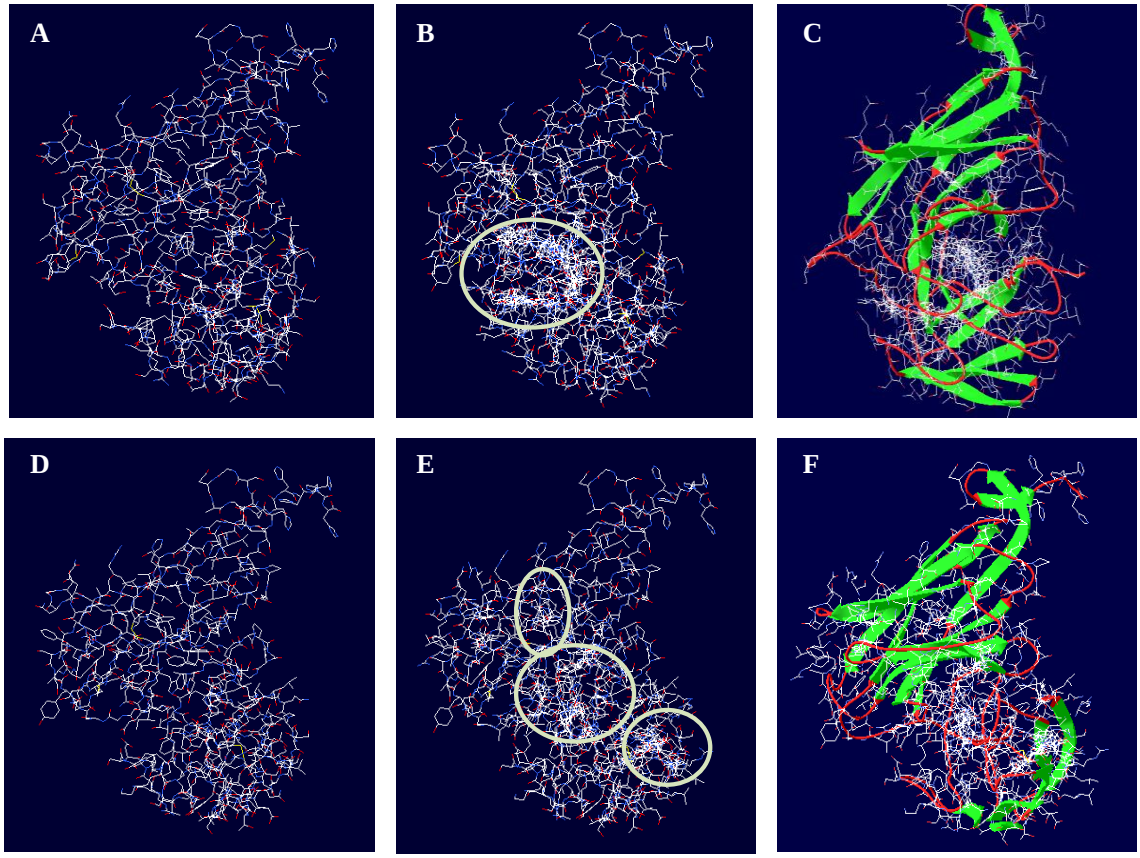

Figure 5.3.2.6: *In silico* docking prediction analysis, using Gramm-X software. A.) 2H1 clone docked with MC-LR (1LCM), with one visible layer B.) 2H1 clone docked with MC-LR (1LCM), 50 visible layers of possible docking sites C.) 2H1 clone ribbon structure (green indicating β-sheets and red strand), with 50 layers of possible MC-LR structures overlaid D.) 2G1 clone docked with MC-LR (1LCM), one visible layer E.) 2G1 clone docked with MC-LR (1LCM), 50 visible layers of possible docking sites F.) 2G1 clone ribbon structure, with 50 layers of possible MC-LR structures overlaid.

5.3.2.6 Recombinant antibody expression and purification using IMAC

Large-scale expression of the avian anti-MC scFvs, 2H1 and 2G1, was carried out in 500 mL culture volumes, as outlined in Section 2.14.6. Three culture media were compared for expression, including super broth (SB), terrific broth (TB) and auto-induction media (ZY). SB and TB are highly enriched media and contain high concentrations of tryptone and yeast. TB is a rich nutrient media for propagation of *E.coli* for the purpose of strain maintenance, plasmid propagation and protein expression. TB is also a phosphate-buffered rich medium and contains an additional 0.4 % (v/v) glycerol as an extra carbon source. SB is richer in peptone and yeast extract, compared with TB, and is used in high yield plasmid and protein production. This method of growth and induction relies on media components that are metabolised differentially to promote high-density growth and automatic induction of protein expression from *lac*-based promoters. The ZY auto-induction media contains carbon sources, which are optimised for tightly regulated un-induced growth to high cell density, followed by induction with lactose for continued growth and protein expression.

The antibody was extracted from both the IPTG-induced and auto-induced cultures by sonication and the bacterial pellets were isolated by centrifugation. The protein lysate was passed through a 0.2 µm filter, to reduce clogging of the nickel resin. Through application of the scFv-containing lysate, any expressed proteins containing a histidine-tag, were captured by the Ni^{+}-NTA agarose resin. Non-specific protein binding on the column was minimised by washing with 20 mL of wash buffer (containing 20 mM imidazole) and the protein was successfully eluted in fractions, using 250 mM imidazole. The IMAC-purified scFv fractions were quantified using a NanoDrop ND-1000™ and the fractions containing pure protein were pooled. The antibody was buffer-exchanged, to remove any residual elution buffer, and concentrated using Vivaspin™ 6 columns. Column ultra-filtration is a common technique used to separate proteins in size-graded fractions. The fractions for the 2H1 avian scFv clone (crude lysate and concentrated pure scFv) were analysed by SDS-PAGE to determine the degree of purity. The SDS-PAGE gel (Figure 5.3.2.7 A) verified that the scFvs were all of the correct molecular weight, at approximately 27 kDa. However, a number of impurities were present in the 'pure' SB and TB expression fractions. It was initially thought that

these products were as a result of protein degradation, so a suitable protease inhibitor cocktail (Sigma-Aldrich) was added and protein samples were handled and stored with the utmost care. However, this did not eliminate the impurities from the scFv preparation. Interestingly, a markedly pure band was observed for the ZY auto-induction media, which was verified by western blotting (Figure 5.3.2.7 B).The proteins were transferred to a nitrocellulose membrane and the blot was probed with anti-HA monoclonal antibody, labelled with HRP, which bound the HA tag of the scFv.

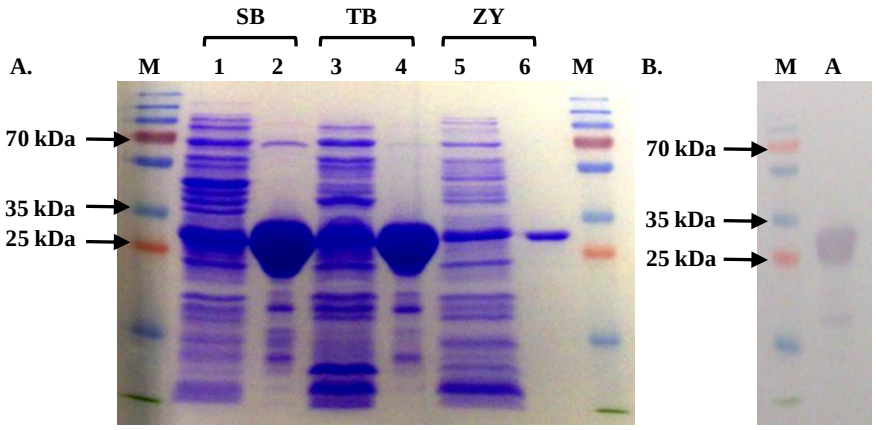

Figure 5.3.2.7: Analysis of avian scFv expression profiles A.) SDS-PAGE analysis for 2H1 growth media optimisation. Lanes 'M' contain the molecular weight marker, Page-Ruler™ Plus Ladder (Fermentas). Lanes 1, 3 and 5 contain crude lysate from 20 mL sonicated cultures. Lanes 2, 4, and 6 contain concentrated IMAC-purified 2H1 scFv. B.) Western Blot of purified 2H1 scFv (A) using ZY auto-induction as the growth medium. Fifty µg of protein were loaded for all samples.

5.3.2.7 Size exclusion chromatography of scFv fragments

The 2H1 scFv clone was expressed using ZY auto-induction media and purified by IMAC (Section 5.3.2.6). However, the protein yield from this expression was not sufficient for immunoassay development. In contrast, a high yield was obtained when the scFv was expressed in either SB or TB media and induced with IPTG, but SDS-PAGE analysis revealed a number of contaminating protein bands (Figure 5.3.2.7 A). Therefore, further purification of the scFv from the IMAC-pure material was performed, using size exclusion chromatography (SEC) on an ÄKTA™ Explorer 100 system (GE Healthcare, USA).

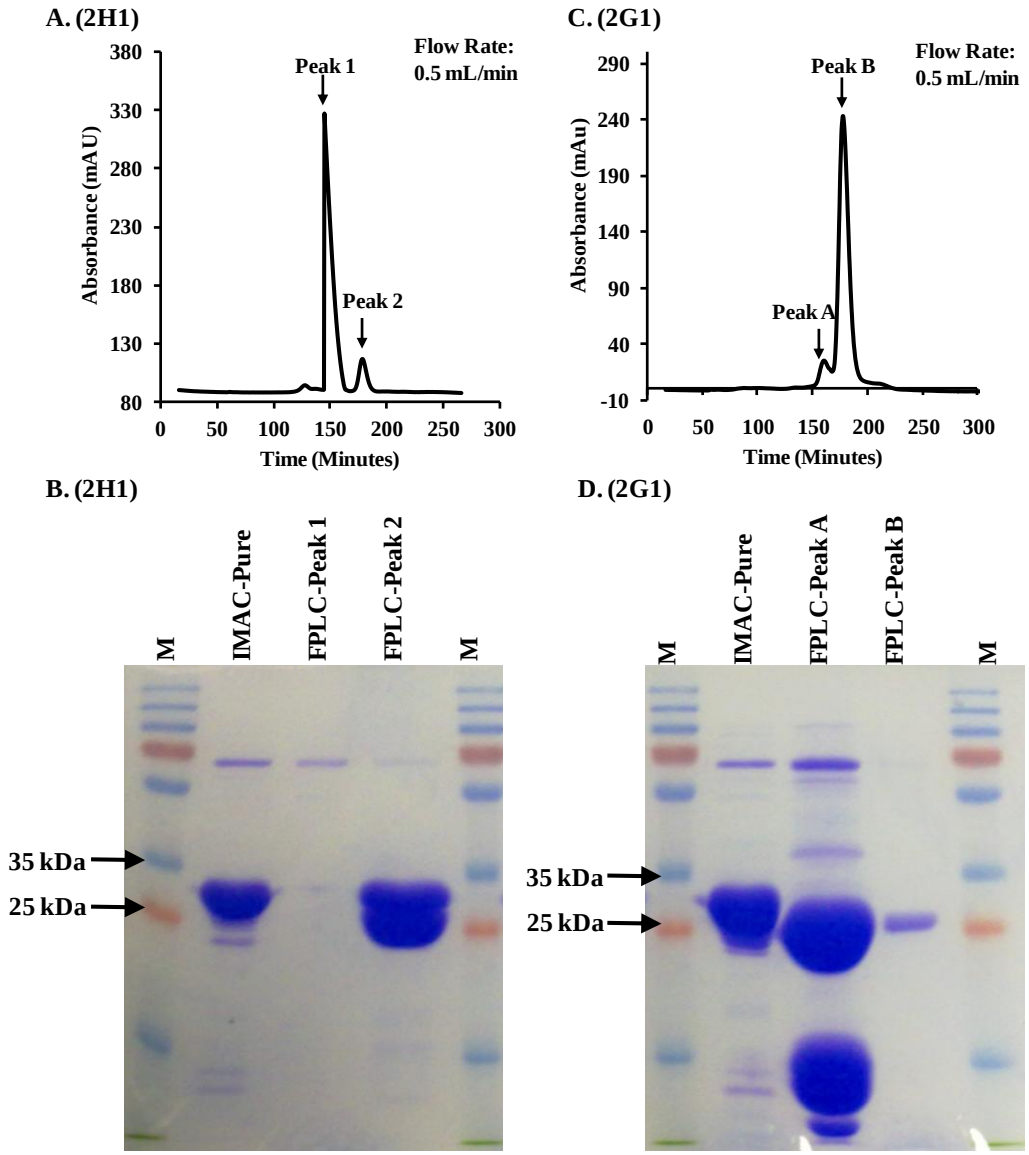

Figure 5.3.2.8: Size exclusion chromatography of avian scFv fragments. A.) Purification of 2H1 scFv clone on a HiLoad™ 16/60 Superdex™ 200 16/60 size-exclusion column. A graph of absorbance, measured as mAu, versus time (minutes) was plotted. B.) Selected fractions from the 2H1 analysis were compared to the IMAC-purified 2H1 fraction, by SDS-PAGE analysis. Fifty µg of protein was loaded for each fraction. 'M' represents a molecular weight marker, Page-Ruler™ Plus Ladder (Fermentas). ' FPLC-Peak 1' and ' FPLC-Peak 2' correspond to the peaks observed in the FPLC chromatogram in A. C.) Purification of 2G1 scFv clone on a Sephradex™ 200 16/60 size-exclusion column. D.) The protein content of the two 2G1 peaks was also compared to the IMAC-purified 2G1 fraction, by SDS-PAGE analysis. ' FPLC-Peak 1' and ' FPLC-Peak 2' correspond to the peaks observed in the FPLC chromatogram in C.

A HiLoad™ 16/60 Superdex™ 200 Prep-grade FPLC column was used with PBS (pH 7.2) mobile phase at a flow rate of 0.5 mL/min and monitored by UV absorbance spectroscopy, at 280 nm. Superdex™ is a composite matrix of dextran and agarose. The PBS buffer showed an expected conductivity of approximately 17.2 mS/cm. In this study, gel filtration was used as a final 'polishing' step to remove minor contaminants from the partially purified 2H1 and 2G1 scFv fragments. For each size exclusion run, the proteins were eluted and collected. Two major peaks were observed for the FPLC-purified 2H1 scFv size exclusion chromatogram (Figure 5.3.2.8 A). Peak locations for the separated fractions are indicated by arrows (Peak 1 and Peak 2). It was unknown, at this stage, whether each peak was representative of pure scFv, contaminants or aggregates.

Fractions (5 mL), corresponding to Peak 1 and Peak 2 were collected at approximately 154 and 174 minutes, respectively. The fractions were analysed by denaturing protein gel electrophoresis. The fractions from the 2H1 scFv gel filtration (FPLC-Peak 1 and FPLC-Peak 2) were compared to the pre-column, IMAC-pure 2H1 antibody fragment (Figure 5.3.2.8 B). It was clear that the 'FPLC-Peak 2' fraction contained the majority of the pure 2H1 scFv and the purity was significantly improved following gel filtration, compared to the IMAC-pure 2H1 scFv. The purified 2H1 scFv had an apparent molecular weight of approximately 29 kDa, which is the approximate size for a monomeric scFv fragment. There was a slight double band present on the SDS-PAGE gel (FPLC-Peak 2, Figure 5.3.2.8 B), which may be a result of the large amount of protein loaded on the gel. The fraction was re-analysed, with less protein, and demonstrated a clear single band (data not shown).

The size exclusion purification process was repeated for the 2G1 scFv fragment. Two peaks were also obtained (Peak A and B), but it is clear that these peaks are overlapping, indicating that the separation was not complete. Fractions, corresponding to the peak positions at 154 and 174 seconds were isolated for Peak A and Peak B, respectively. For the SDS-PAGE analysis of the 2G1 scFv FPLC fractions (FPLC-Peak A and FPLC-Peak B), it was clear that the majority of the 2G1 scFv was present in the FPLC-Peak A fraction, along with a number of concentrated impurities (Figure 5.3.2.8 D). The FPLC-Peak B fraction contained less 2G1 scFv, but no impurities were present. The purified 2H1 and 2G1 scFv fractions (Peak 2 and Peak B, respectively) were

analysed for the presence of functional antibodies by direct ELISA, using a HRP-labelled antibody, specific for the HA tag on the carboxyl terminus of the scFv fragment (data not shown). Functional scFv, denoted by high ELISA signals, were obtained for both fractions. The IMAC-SEC-purified 2H1 and 2G1 fractions were stored at -80^{o}C, with a protease inhibitor cocktail (Sigma-Aldrich) and subsequently used for immunoassay development.

Size exclusion chromatography was also applied to the determination of the native molecular weight of the monomer fraction of the scFv fragment, 2H1. Fifty µL of the monomer fraction of the 2H1 scFv was applied to a HiLoad™ 16/60 Superdex™ 200 FPLC column, using filtered and degassed PBS (pH 7.4), at a flow rate of 0.5 mL/min. A molecular weight standard preparation (Phenomenex), containing bovine thyroglobulin (670 kDa), human gamma globulin (150 kDa), ovalbumin (44 kDa), and myoglobin (17 kDa), was then directly analysed, under identical conditions. The FPLC chromatogram illustrated four main peaks with retention times of 60.67 minutes, 127.47 minutes, 163.60 minutes and 209.65 minutes, respectively, which represent the four protein constituents of the molecular weight standards (Figure 5.3.2.9 A). Some small, unknown peaks were also observed, which may be representative of degradation products, aggregates or small, UV active substances from the sample buffer.

The molecular weight of the scFv could be estimated from the peak position of the elution fraction, by comparing the retention time with that from the protein standards. The retention time of the 2H1 scFv fraction was 88.79 minutes (data not shown). The estimated molecular mass for the monomeric scFv fraction was extrapolated from the best fit line of the molecular weight standards ($y = - 0.0109x + 6.5042$, $R^2 = 0.99$), as 29,649 kDa. The data points should lie on a straight best fit line, as illustrated. If not, the column either has a separation range not suited or the gel-bed is not correctly packed and the column should be repacked or discarded.

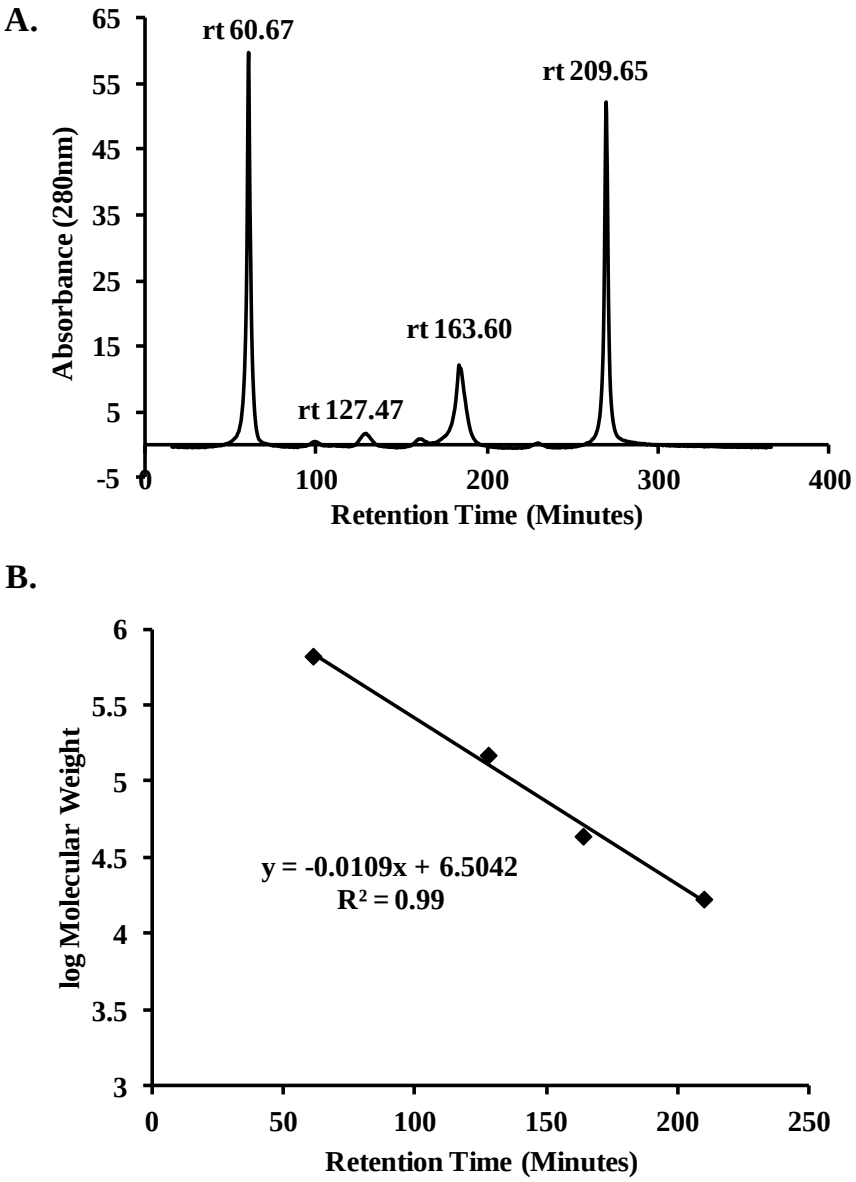

Figure 5.3.2.9: FPLC analysis of molecular weight standards A.) FPLC chromatogram of molecular weight standards, plotted as absorbance versus retention time. The retention time (rt) of the molecular weight standards are indicated: Bovine thyroglobulin (670 kDa), 60.67 minutes; human gamma globulin (150 kDa), 127.47 minutes; ovalbumin (44 kDa), 163.60 minutes and myoglobin (17 kDa), 209.65 minutes. B.) The retention time was plotted on the x axis, versus the log of the corresponding molecular weight on the y axis and the best-fit equation of the line was calculated as y = - 0.0109x + 6.5042) with an R^2 value of 0.99.

5.3.3 Validation of an inhibition ELISA for microcystin detection

5.3.3.1 Optimisation of the coating concentration and antibody dilution for inhibition ELISA development

Checkerboard ELISAs were carried out to determine the optimal coating concentration and optimal antibody dilution for use in an inhibition ELISA format. The sensitivity is significantly influenced by the coating concentration. High conjugate concentrations can result in binding bias towards the immobilised conjugate, thereby reducing sensitivity to free toxin in solution. Similarly, higher concentrations of free antibody will require a higher concentration of free toxin to inhibit binding to the immobilised conjugate, resulting in decreased sensitivity. Therefore, an important parameter in inhibition assay development is the optimisation of the conjugate and antibody concentrations. The accuracy and precision of any immunoassay are critical parameters and require the utmost attention for determining the sensitivity of the assay.

The optimal conjugate coating concentration and antibody dilution were determined by preparing serial dilutions of the MC-LR-OVA conjugate (1.25 to 4,000 ng/mL) and the scFvs, 2H1 and 2G1 (1/5,000 to 1/640,000). Analysis was carried out in a direct ELISA format (Figure 5.3.3.1). For the 2H1 and 2G1 scFv fragments tested, a coating concentration of 500 ng/mL was sufficient for signal generation, using the most economical amount of conjugate. The optimal 2H1 and 2G1 scFv concentration for immunoassay development, which gave the greatest change in absorbance per change in antibody dilution, was 1/20,000.

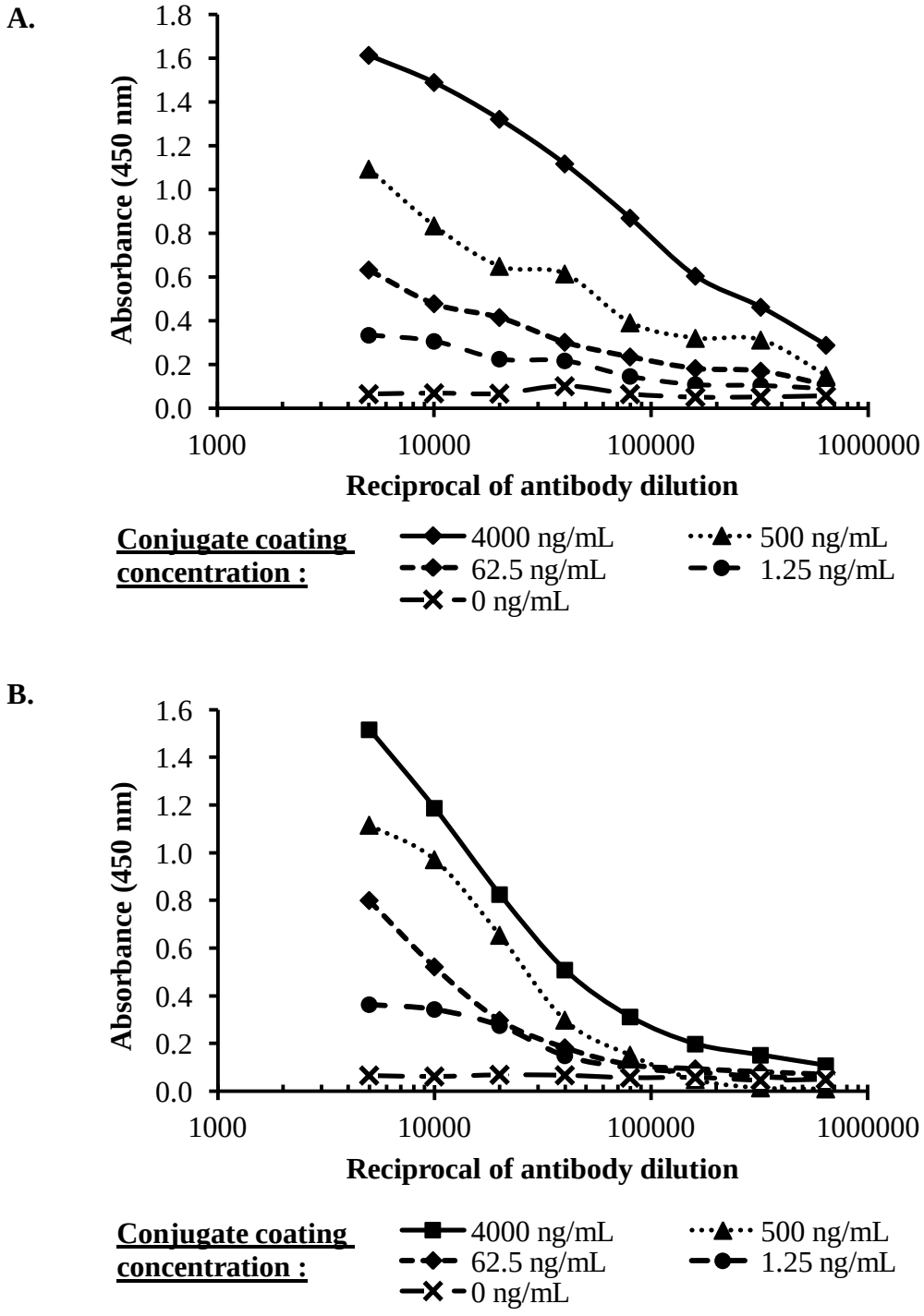

Figure 5.3.3.1: Checkerboard ELISA for inhibition assay development. A.) 2H1 scFv fragment. B.) 2G1 scFv fragment. To optimise the coating concentration, ELISA plates were coated with MC-LR-OVA conjugate, ranging in concentration from 4,000 to 1.25 ng/mL, in PBS (pH 7.4, 150 mM). Dilutions of scFv, ranging from 5,000 to 640,000 were prepared, using 1 % (w/v) Milk Marvel/ PBS (150 mM, pH 7.4), with 0.05 % (v/v) Tween 20. The serially-diluted scFvs was added to the ELISA plates. Binding was detected using a HRP-labelled anti-HA monoclonal antibody (Pierce).

5.3.3.2 Intra- and inter-day inhibition assay variability studies

Intra-day assay (variation within a day) and inter-day assay (variation between days) variability studies were performed to demonstrate the reproducibility of the inhibition ELISA for MC-LR detection. The % coefficient of variation (CV) was calculated, by expressing the standard deviation as a percentage of the mean values. To determine whether the measured concentrations agreed with the theoretical values, the % relative error (RE) was calculated, by expressing the measured concentration as a percentage of the back-calculated concentration. The limit of detection (LOD) was determined by selecting the mean normalised response for the negative standard (no MC-LR) and subtracting three standard deviations. This value was used to calculate an unknown value from the four-parameter fit equation, using BIAevaluation™.

Figure 5.3.3.3 illustrates the inter-day calibration curve using the 2G1 scFv fragment. As described previously, the A/A_0 value was plotted against the logarithm of the MC-LR concentration. The IC_{50} was calculated as 8.1 ng/mL.

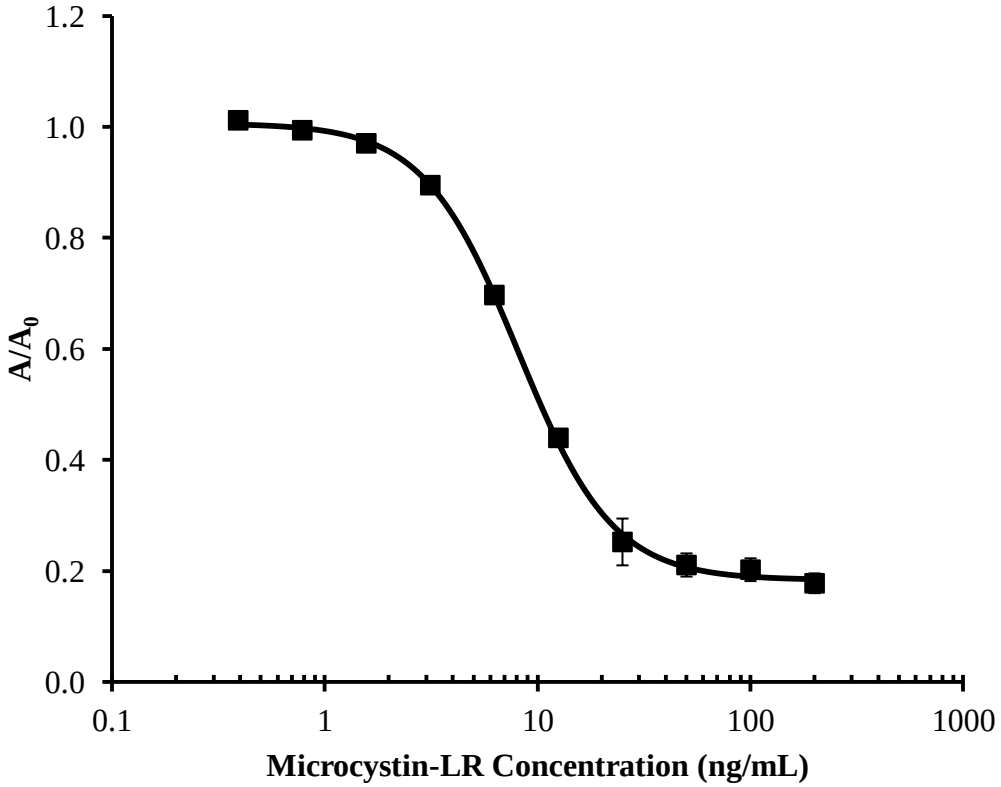

Figure 5.3.3.2: Inter-day assay calibration curve for the determination of MC-LR in PBS, for the 2G1 scFv. MC-LR concentrations, ranging from 200 to 0.39 ng/mL, were pre-incubated with an optimised dilution of the chicken 2G1 anti-MC-LR scFv (1/20,000) and added to the plate. Using BIAevaluation™ software (Version 3.1), the data was fitted using a 4-parameter equation. The error bars represent the standard deviation for each concentration.

Table 5.3.3.1: Inter-day and intra-day inhibition assay validation to determine the % coefficient of variation (CV) and % relative error (RE) for 2G1 scFv fragment.

MC-LR (ng/mL)	Inter-day Assay Validation			Intra-day Assay Validation		
	% CV	Back Calculated Concentration (ng/mL)	% RE	% CV	Back Calculated Concentration (ng/mL)	% RE
50.0	3.4	46.2	108.3	10.2	36.3	137.7
25.0	5.9	27.9	89.7	12.6	23.7	105.3
12.5	3.9	12.2	102.3	7.3	12.8	97.6
6.3	3.5	6.3	99.7	8.9	6.2	101.3
3.1	13.3	3.1	99.6	5.4	3.2	98.9
1.6	6.1	1.7	93.8	2.5	0.9	173.0
0.8	5.8	0.9	82.5	4.7	1.3	60.9

Both the inter-day and intra-day assays for the 2G1 scFv fragment displayed acceptable reproducibility (Table 5.3.3.1), as they were below the recommended precision level of 20 % (Findlay *et al*., 2000). The % RE values for the 2G1 scFv fragment were in the acceptable limits (80 to 120 %) (Findlay *et al*., 2000) from 3.1 to 25 ng/mL of MC-LR. Therefore, the 2G1 scFv assay had a useable assay range of 3.1 to 25 ng/mL for MC-LR. The overall LOD was calculated as 4.4 ng/mL.

Figure 5.3.3.5 illustrates the inter-day calibration curve using the 2H1 scFv fragment. As previously described, the A/A_0 value was plotted against the logarithm of the MC-LR concentration. The IC_{50} was calculated as 11.5 ng/mL.

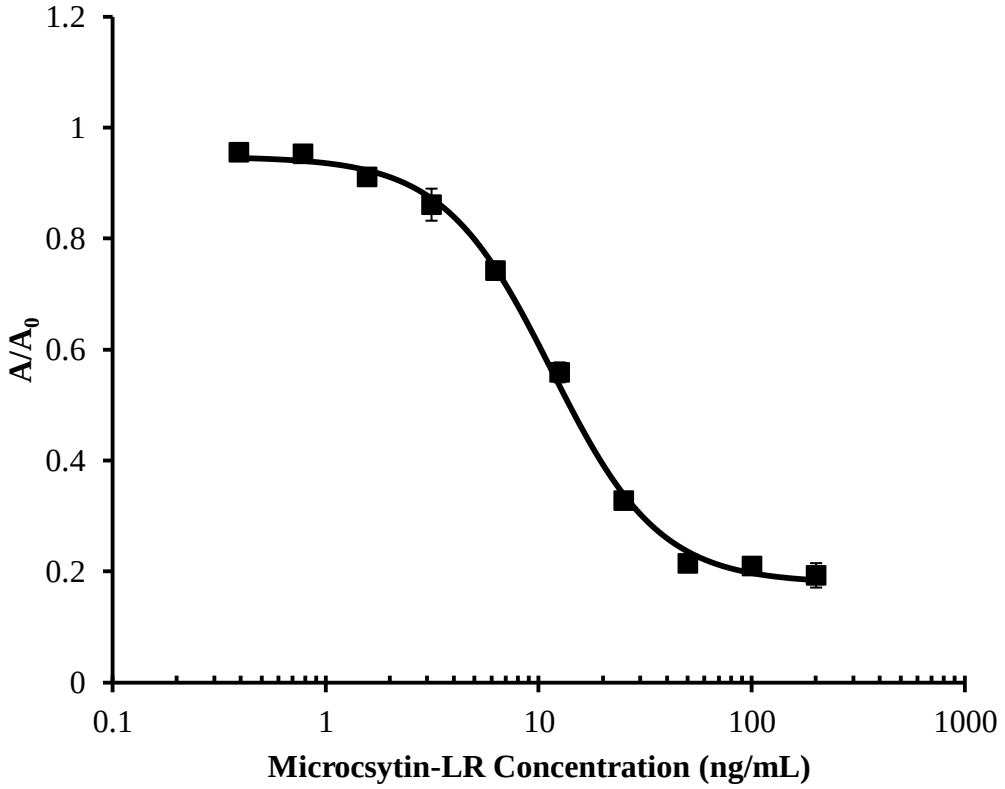

Figure 5.3.3.3: Inter-day assay calibration curve for the determination of MC-LR in PBS, for the 2H1 scFv. MC-LR concentrations, ranging from 200 to 0.39 ng/mL, were pre-incubated with an optimised dilution of the chicken 2H1 anti-MC-LR scFv (1/20,000) and added to the plate. Using BIAevaluation™ software (Version 3.1), the data was fitted using a 4-parameter equation. The error bars represent the standard deviation for each concentration.

Table 5.3.3.2: Inter-day and intra-day inhibition assay validation to determine the % CV and % RE for the 2H1 scFv fragment.

MC-LR (ng/mL)	Inter-day Assay Validation			Intra-day Assay Validation		
	% CV	Back Calculated Concentration (ng/mL)	% RE	% CV	Back Calculated Concentration (ng/mL)	% RE
100.0	2.0	73.2	136.6	32.3	89.5	111.7
50.0	1.5	67.2	74.4	24.7	57.6	86.9
25.0	14.8	26.5	94.4	14.6	25.6	97.8
12.5	8.2	11.7	107.1	9.5	11.6	108.0
6.3	6.8	6.4	97.7	13.4	6.7	93.9
3.1	1.5	3.5	90.3	9.4	3.1	99.6
1.6	2.4	2.0	77.4	9.9	1.4	109.0

The 2H1 assay had acceptable %CV values between 1.6 and 25 ng/mL.The intra-day CV values for high concentrations (50 and 100 ng/mL) were outside the acceptable range of 20 % (Table 5.3.3.2). The % RE values for the 2H1 scFv fragment were in the acceptable limits from 3.1 to 25 ng/mL. Therefore, for the 2H1 scFv fragment, the range of assay sensitivity was between 3.1 to 25 ng/mL MC-LR. The overall LOD was calculated as 3.2 ng/mL.

5.4 Discussion

The aim of this research was to generate a high affinity recombinant antibody to microcystin. An approach was taken to conjugate microcystin through its *N*-methyldehydroalanine residue for maximal exposure to the common Adda moiety. This seventh amino acid residue is located on the opposite side of the molecule from the two variable amino acid residues and the Adda moiety. This strategy increased the possibility of generating an antibody that was microcystin-specific and cross-reactive with other microcystin variants. Two MC-LR conjugates were generated commercially and the MC-LR-BSA conjugate was chosen for immunisation. The spleen, a rich source of antibody-producing B-lymphyocytes, was isolated from an avian host, after confirming anti-MC-LR-specific antibodies were present in the serum by ELISA. The RNA was extracted, using a phenol-chloroform method, and reversed transcribed to cDNA. The variable antibody genes (V_H and V_L) were successfully amplified, using PCR, and the desired single chain Fv fragments were assembled, with a glycine-serine linker in a V_L-$(G_4S)_4$-V_H orientation. The flexible linker region (20 amino acids) allowed for correct folding of the generated scFvs. While being considerably smaller in size compared with a full IgG antibody, scFv fragments consisting of linked antibody heavy and light chains, still retain their specificity and affinity to their cognate antigen. This recombinant phage display library was cloned into the pComb3XSS vector. The pComb3XSS phagemid vector contains an amber stop codon (TAG) between the scFv and g3p, which is suppressed in *E. coli* XL-1 Blue cells. A library size of 3.47×10^7 transformants per mL was obtained.

Phage display technology has facilitated the selection and enrichment of recombinant antibodies against a range of different haptens, including microcystin, from large antibody libraries (McCafferty, 1990). In order to select from the avian scFv library, five rounds of bio-panning were carried out, and stringency was introduced by increasing the number of washes for each round of bio-panning and decreasing the conjugate coating concentration on the immunotube. After five rounds of selection, on MC-LR-OVA-coated immunotubes, a polyclonal ELISA revealed the presence of positively binding anti-MC-LR-OVA phage-scFv clones. The selected soluble binders from phage selection were transformed into the non-suppressor TOP10F' *E. coli* cells and the soluble scFv fragments were transcribed, without any g3p fusion tag.

A panel of scFvs were selected, based on their diverse and inhibitive nature, as proven by restriction analysis and ELISA, respectively. These antibodies have the potential to be incorporated into an immunoassay for microcystin analysis. The most widely used format for microcystin immunoassays is the direct competitive format (Zeck *et al*., 2001; Weller *et al*., 2001; Sheng *et al*., 2006), although a number of other formats were also employed (Nagata *et al*., 1999; Metcalf *et al*., 2000; Mhadhbi *et al*., 2006). However, none of these immunoassays are in widespread use, most likely due to their poor sensitivity, unfavourable cross-reactivity and lack of commercial availability. In contrast, an immunoassay that has broad specificity to all microcystin variants would be extremely useful, especially for regulatory purposes. Interestingly, an scFv fragment from an immune source has not previously been generated to microcystin, although recombinant single chain antibody fragments (scAbs) have been developed from non-immune sources (McElhiney *et al.*, 2002; Strachen *et al*., 2002).

Protein modelling technology was used to predict possible three-dimensional structures of the anti-MC-LR scFvs, which aided in the prediction of possible microcystin-binding sites. The sequencing data generated for the 2H1 and 2G1 scFvs were used to create a computer-generated model of the structure of the scFv. As no crystallographic structure was available for a chicken scFv molecule, the scFvs were modelled against an IL-1β murine scFv (Wilkinson et al., 2009). This murine scFv had a high sequence homology to the microcystin clones. A structure that is sequentially most homologous to the antibody of interest is the preferred template for framework modelling. The modelling procedure was started at the variable domain framework region (FW), which is well conserved in structure among different antibodies. In the case of antibody sequences, structural variability is restricted to the hypervariable regions. CDRs are described as CDR-L1, L2 and L3 in the light chain and CDR-H1, H2 and H3 for the heavy chain. All CDRs, except for CDRH3, are classified to the structural canonical classes, which facilitates modelling of their structures (Decanniere *et al*., 2000). From the Gramm-X MC-LR docking site analysis, it can be hypothesised that the 2H1 and 2G1 scFv molecules bind microcystin through different interaction sites. For the 2H1 scFv fragment, a large concentration of possible binding-sites were localised at one location. However, the 2G1 scFv had three different locations where binding was highly probable. Docking programs, such as Gramm-X, provide a good indication of binding site position and hapten orientation. This information may be useful in the design of

site-directed mutagenesis approaches for antibody improvement and in future modelling studies. However, docking analysis using a best-fit approach only provides an estimation of antibody-antigen binding, based on a mathematical prediction model. Therefore, crystallographic analysis is essential to definitively verify binding sites and interaction residues.

The 2H1 and 2G1 clones were grown in large-scale cultures and antibody fragment expression was induced, using IPTG. An auto-induction media was also utilised. Auto-induction is more convenient than IPTG induction because the bacterial stock is simply inoculated into the auto-inducing medium and grown to saturation, eliminating the need to follow culture growth and to add inducer (IPTG) at the correct time. Furthermore, the culture density and concentration of the expressed protein, per volume of culture, are generally higher than IPTG induction. In this report, a larger protein yield was obtained when the bacterial clones were cultured in enriched growth media, including SB and TB, compared with auto-induction media. Interestingly, a highly pure fraction was obtained after IMAC purification of the auto-induced culture. It is possible that expression in the auto-induced culture is tightly-controlled by the inducible T7 system, preventing transcription of contaminating protein products. However, the protein yield for the auto-induced cultures was insufficient for immunoassay development. Therefore, further purification or 'polishing' of the IPTG-induced cultures was carried out, using size-exclusion chromatography.

The 2H1 and 2G1 scFv fragments were successfully purified by fast protein liquid chromatography (FPLC), and subsequently analysed by ELISA and gel electrophoresis. FPLC protein purification produced a high yield of pure scFv fragments. These scFv fragments were used to further develop the microcystin immunoassay. FPLC size exclusion also allowed for the successful determination of the native molecular weight of the 2H1 scFv (29 kDa). A large number of chromatographic separation techniques are applicable to FPLC, including; ion exchange (Easton *et al*., 2010), chromatofocusing (Rausell *et al*., 1997), gel filtration (Madadlou *et al*., 2011), hydrophobic interaction (Zera *et al*., 2002), and reverse phase (Gerber *et al*., 2004). Gel filtration has proven to be a useful technique for the analysis of antibody fragments, including scFv fragments, which have a tendency to form large multimeric aggregates (Kortt *et al*., 1997; Laroche-Traineau *et al*., 2000). A single peak, in the purification of

the 2H1 scFv fragment, was identified as a large molecular weight aggregate. The formation of aggregates often depends on the specific antibody fragment, the linker design (Schmiedl *et al*., 2006), and the concentration of the antibody fragments (Arndt *et al*., 1998). The tendency of scFv antibody fragments to form aggregates is also an indicator for their stability, because high aggregation levels lead to lower long-term stability of the scFvs. By using SEC, antibody fragments can be isolated from aggregates, including dimers. For this reason, it has become a standard technique to purify and characterise antibody fragments (Voedisch and Thie, 2004).

Following the successful expression and purification of the anti-MC antibody fragments, 2H1 and 2G1, ELISA inter- and intra-day analysis was carried out to determine the assay ranges and limits of detection of the scFvs. ELISA conditions, including coating concentration and antibody dilution, were optimised. Assay performance, including detection range, % precision and % relative error, were investigated. The 2H1 scFv fragment was found to have a range of detection of 3.1 to 25 ng/mL and a limit of detection of 3.2 ng/mL. When compared to the 2H1 scFv, the 2G1 scFv fragment displayed the same MC-LR range of 3.1 to 25 ng/mL and an LOD of 4.4 ng/mL. The MC-LR ELISA-based assays proved to be reasonably sensitive and precise, with the majority of analysis within 20 % of the acceptable range.

In summary, two novel avian scFv fragments were generated to the cyanobacterial toxin MC-LR. This is the first known report of recombinant microcystin antibodies in an scFv format, generated from an immune source. These antibodies are not sensitive enough for the required detection limit of 1 µg/L (WHO, 1998). The most sensitive antibody fragment (scAb) generated to microcystin cross-reacts with MC-RR, MC-LW, MC-LF, and nodularin and had a limit of detection of 0.8 nM (0.8 ng/L) (McElhiney *et al*., 2002). A major advantage of recombinant antibody technology for microcystin detection is that it provides a means to manipulate sensitivity, specificity and affinity at a molecular level at the molecular level (McElhiney *et al*., 2000), making them ideal for incorporation into immunosensor formats. Ideally, assay sensitivity well below the limit of detection is required for the immunoassay to be accepted as a validated technique for toxin detection. Therefore, it was necessary to employ affinity maturation strategies for the improvement of the selected MC-LR clones. A number of assay formats, including an SPR-based immunosensor and fluorescence-based immunoassay techniques will also be employed to reach the required detection limit.

CHAPTER 6

Random mutagenesis of the anti-microcystin scFv and subsequent immunoassay development

6.1 Introduction

In the work described in this chapter, maturation techniques were exploited to improve the binding potential of a previously isolated anti-microcystin scFv fragment. The light chain sequence of the 2H1 scFv was diversified by error-prone PCR. Subsequently, this error-prone light chain library was shuffled with the original heavy chain of the 2H1 clone. The mutant gene repertoire was displayed on the surface of filamentous phage and alternative binders were selected using both trypsin and competitive elution strategies. The major focus of this work was the development of sensitive immunoassays for the detection of MC-LR and its variants, MC-LW, MC-RR, MC-YR, MC-LA and MC-LF. Biacore™ inhibition assays were developed and validated for the scFv fragments, with an MC-LR-immobilised sensor chip surface. The immunosensor-based assays displayed good accuracy and precision in the low ng/mL range.

The wild-type scFv fragment (2H1) were compared to the mutant antibody using ELISA and Biacore™ analysis. The C12 mutant clone displayed a 2.3-fold improvement in the limit of detection, when compared by ELISA. Surprisingly, the 2G1 scFv fragment displayed excellent sensitive and reproducibility using SPR bio-sensing, compared to the 2H1 and C12 scFvs, with a limit of detection of 1.7 ng/mL. The limits of detection for the 2H1 and C12 scFvs were 13.8 and 14.8 ng/mL, respectively. Significantly, the C12 scFv displayed a better cross-reactivity profile, compared with the 2H1 parental scFv.

High assay sensitivity was achieved through development of fluorescence-linked immunosorbent assays (FLISAs), particularly using a poly-L-lysine functionalised slide-based format. The avian anti-microcystin scFvs, 2G1 and C12, were successfully biotinylated and incorporated into an indirect FLISA, using a streptavidin-Alexa Fluor® 647 conjugate (LODs of 1.4 and 0.6 ng/mL, respectively). The 2G1 scFv-Alexa Fluor® 647 and C12-biotin conjugates were incorporated into slide-based inhibition formats for rapid microcystin detection (IC_{50} of 6 and 1 ng/mL, respectively). A rabbit polyclonal microcystin-specific antibody was purified using immobilised-protein G chromatography. This antibody was incorporated into an alternative, highly-sensitive FLISA for MC-LR detection, on a functionalised glass substrate (IC_{50} = 0.4 ng/mL).

6.1.1 Antibody mutagenesis strategies for affinity improvement

In the human immune system, high affinity antibodies are generated in two stages. Firstly, a diverse primary repertoire of antibodies is produced through the combinatorial rearrangement of germline V-gene segments, followed by clonal selection of B-cells that produce higher affinity antibodies. Subsequently, antibody affinities are further improved by somatic hypermutation and further rounds of selection. Advances in phage-displayed antibody technology have enabled the affinity maturation process to be mimicked *in vitro*. It is now possible to improve the antigen-binding affinity and alter the binding specificity of recombinant antibodies (Barbas *et al*., 1992; Jackson *et al*., 1995). In the process of *in vitro* affinity maturation, the V-gene sequences are generally targeted, thus mimicking the *in vivo* process of somatic hypermutation.

During *in vivo* somatic hypermutation, mutations are preferentially targeted to the CDR regions, over the framework regions. The location of these CDR mutations generally mimics the locations where diversity is generated in the primary antibody repertoire (Tomlinson *et al*. 1996). Many CDR residues, particularly CDRH3 and CDRL3, are responsible for high energy interactions with the antigen. The mutation of residues within these regions may eliminate or reduce antigen-binding. Alternatively, the mutation of residues within the CDR regions may also increase affinity by introducing new contact residues, or by replacing low affinity or "repulsive" contact residues with more favourable energetics. It has been observed that many mutations, introduced both *in vivo* and *in vitro* by directed evolution, exert their effect on affinity indirectly. This may occur when insertions or deletions cause a shift in the position of the CDR regions, relative to one another, or by altering the side chains of contact residues for optimal interaction with the antigen (Foote and Winter, 1992).

Mutations have been introduced by chain-shuffling (Marks *et al*., 2004; Lou *et al*., 2010), error-prone PCR (Pritchard *et al*., 2005; Cirino *et al*., 2003), DNA-shuffling (Crameri *et al*., 1996), or by propagation of phage in mutator strains of *E. coli.* (Low *et al*., 1996). These approaches have yielded large increases in affinity for hapten targets (up to 300-fold) (Irving *et al*., 1996; Low *et al*., 1996). In site-directed mutagenesis approaches, sequence analysis of binding clones can result in the identification of both conserved structural and functional residues which may modulate affinity (Schier *et al*.

1996). These sequences can guide subsequent mutagenic efforts to further improve affinity.

Random introduction of mutations is the simplest approach, as it makes no assumptions as to which sites are the best to mutate in order to increase affinity, and more closely mimics the *in vivo* process of somatic hypermutation (Lou and Marks, 2010). This can be achieved by error-prone PCR, in which a low-fidelity DNA polymerase is utilised to introduce random point mutations into a selected V-region. Mutational error may be further increased, using suboptimal PCR conditions during DNA amplification. In another approach, synthetic oligonucleotides can be used to focus mutations on residues involved in antigen-binding, whilst avoiding key structural residues. The repertoire of mutant antibody sequences is then displayed on phage, and mutant antibodies with improved affinities are selected under stringent selection conditions (Rajpal *et al*., 2005).

Chain-shuffling and site-directed mutagenesis have been employed to increase the affinity of an anti-ErbB2 single chain antibody by 1,200-fold (Marks *et al*., 1992). These workers reported that mutagenesis of the CDR3 regions of the antibody were the most effective in improving affinity, using phage display. Similarly, Yang and co-workers increased the affinity of an anti-gp120 Fab by 420-fold. This was achieved by generating mutations in the CDR regions of five separate mutagenised libraries, which were subsequently combined (Yang *et al*., 1995). Interestingly, they observed that the largest affinity gain occurred when the CDR3 regions were mutated. In addition, light-chain shuffling of an anti-halofuginone-specific scFv fragment resulted in a 185-fold improvement in antibody affinity (Fitzgerald *et al*., 2011).

Selection of high affinity antibodies from mutant libraries is often achieved in phage display bio-panning by using increasingly harsh conditions in each successive round. For example, decreasing the antigen concentration, increasing the number of washing steps and reducing incubation times (Hust *et al*., 2008). A drawback of this approach is that bio-panning on immobilised surfaces can increase the tendency to isolate binders that are prone to dimerisation, particularly when using the scFv format. Dimerisation issues can be reduced by bio-panning with the antigen in solution (Schier *et al*., 1996). This can be achieved by utilising a biotinylated antigen, in combination with

streptavidin-coated beads. Moreover, it is possible to use un-biotinylated antigen after antibody phage binding has occurred, to introduce competition and to improve selection for better 'off-rates'. Monoclonal soluble binders can be assessed and affinity ranked through analysis of crude cell supernatants by competitive ELISA. In recent years, alternative techniques for affinity and specificity ranking have been employed, including SPR and flow cytometry (Geuijen *et al*., 2005; Leonard *et al*. 2007).

6.1.2 Immunosensors for toxins from marine microalgae

Chromatographic techniques have been widely employed for the sensitive detection of toxins produced by marine microalgae. Chromatography allows for separation, highly selective identification and sensitive quantification of the various toxin mixtures present in a sample. Moreover, limits of detection are generally one order of magnitude lower than those obtained with the mouse bioassay. However, toxin chromatographic techniques require expensive equipment and trained personnel. Furthermore these methods are laborious and time-consuming. The lack of standards is also a key concern, since non-certified or unknown toxins cannot be evaluated. Other reported issues include peak spreading, poor resolution and the need for continuous calibration (Botana, 2008) The versatility of biosensor-based analytical platforms for pharmacological, environmental and food safety detection has been extensively reviewed (Ivnitski *et al*., 1999; Baeumner, 2003; Amine *et al*., 2006; Rodriguez-Mozaz *et al*., 2006; Byrne *et al*., 2009; Van Dorst *et al*., 2010). Biosensors provide a cost-effective alternative for marine toxin detection, as well as, group specificity, sensitivity, portability, repeatability and robustness. However, a key issue in the analysis of marine toxins is the lack of uniformity between analytical techniques in different laboratories.

Biosensors have the potential to fulfil increasing demand for certification and traceability of seafood products. A biosensor is an analytical device incorporating a bio-recognition element which is associated with or integrated within a transducer that converts a biological response into an electrical signal. A large number of detection techniques can be incorporated into a biosensor format. The biological response can include enzymatic activity, antibody binding, receptor binding or cell responses. Biosensor technologies include transduction platforms based on electrochemical (potentiometric, amperometric, impedance), piezoelectric, thermal or optical methods

(reflectrometric interference spectroscopy, interferometry, optical waveguide lightmode spectroscopy, total internal reflection fluorescence, surface plasmon resonance). The sensitivity and the portability of a biosensor will depend on the signal transducer used. Recently, micro-fabrication tools have made it possible to manufacture micro-biosensors and nano-biosensors (Pumera *et al*., 2007; Jaffrezic-Renault *et al*., 2008). An immunosensor is a biosensor, incorporating an antibody as its biological detection element. Immunosensors can also be applied to the detection of small molecular weight toxins produced by toxic marine microalgae. A summary of electrochemical immunosensors for phycotoxin detection is presented in Table 6.1.2.1.

An electrochemical biosensor was developed for the detection of a number of marine toxins with disposable screen printed electrodes (SPEs), using a monoclonal antibody to okadaic acid and polyclonal antibodies to domoic acid and saxitoxin, as the recognition elements (Kreuzer *et al*., 2002). The assay was based on the detection of *p*-aminophenol and alkaline phosphatase-labelled antibodies. *P*-nitrophenol can be detected electrochemically at a low working potential of +300mV, versus Ag/AgCl. The sensors all achieved detection limits in the µg/L range, well within the limits of detection for each target. Micheli *et al*. (2004) also developed a disposable immunosensor for domoic acid, with a 5 µg/L detection limit. The assay was bases on an electrochemical immunosensor, using screen-printed electrodes coated with a domoic acid-BSA conjugate, as a transducer for differential pulse voltammetry (DPV). The assay format had a good percentage recovery making it suitable for accurate determination of domoic acid in real shellfish samples.

A novel electrochemical immunosensor was developed for detection of microcystin, employing functionalised single-walled carbon nanohorns (SWNHs) and HRP-labelled polyclonal antibodies (Zhang *et al*., 2010). The numerous carboxylic acid groups on the cone-shaped tips of the SWNHs enhanced the immobilisation capacity of MC-LR, resulting in an accurate, precise and reproducible assay. The same antibodies were employed to develop a technique for determination of microcystin residues in water, based on the magnetic relaxation of super paramagnetic nanoparticles, using nuclear magnetic resonance technology (Ma *et al*., 2009). Hayat *et al*. (2011) developed a competitive immunosensor, based on superparamagnetic nanobeads, for the detection of

okadaic acid. The electrochemical sensing was carried out using DPV and a limit of detection of 0.38 µg/L was achieved.

Table 6.1.2.1: Electrochemical immunosensors for the detection of marine toxins

Toxin	Antibodies	LOD	Reference
Okadaic acid **Brevetoxin** **Domoic acid** **Tetrodotoxin**	Anti-OA monoclonal-AP; Anti-BTX-AP; anti-DA sheep polyclonal; anti-sheep IgG-AP labelled	1.5 µg/L 1 µg/L 2 µg/L 0.016 µg/L	Kreuzer *et al*., 2002
Brevetoxin **Saxitoxin**	Goat polyclonal anti-PTX-glucose oxidase; Donkey polyclonal anti-STX-glucose oxidase; Rabbit anti-STX	15 µg/L	Carter *et al*., 1993
Okadaic acid	Monoclonal (on quartz crystal microbalance)	3.6 µg/L	Tang *et al*., 2002
Okadaic acid	Monoclonal (on super paramagnetic nanobeads)	0.38 µg/L	Hayat *et al*., 2011
Domoic acid	Polyclonal anti-DA; Anti-goat IgG-AP labelled	5 µg/L	Micheli *et al*. 2004
Domoic acid	Rabbit polyclonal; goat anti-rabbit IgG- biotin; Strep-HRP conjugate	0.6 µg/L	Kania *et al*.,2003
Microcystin	Monoclonal (on silver nanoparticles)	7.0×10^{-6} µg/L	Loyprasert *et al*., 2008
Microcystin	Rabbit polyclonal (on magnetic nanoparticles)	0.6 ng/g	Ma *et al.*, 2009
Microcystin	Rabbit polyclonal (SWNHs)	0.03 µg/L	Zhang *et al*., 2010
Microcystin	Monoclonal (MC10E7) and polyclonal (undisclosed source)	0.10 µg/L (mAb)/ 1.73 µg/L (pAb)	Campàs and Marty, 2007
Okadaic acid	Monoclonal: AP-labelled OA	2 µg/L	Tang *et al*., 2003
Okadaic acid	Monoclonal; goat anti-mouse-HRP or AP	0.03 µg/L	Campàs *et al*., 2008

Carter *et al*. (1993) described one of the first amperometric immunosensors for the detection of saxitoxin and brevetoxin. The biosensor utilised solid support membranes for immobilisation of toxin conjugates. Detection was based on a glucose oxidase-labelled antibody in a competitive format with immobilised and free toxin. The glucose oxidase label caused the conversion of a β-D-glucose substrate to its product with the release of H_2O_2, which was detected using a platinum electrode. The limit of detection for this assay format was 15 µg/L. Campàs and Marty (2007) utilised both anti-microcystin monoclonal and polyclonal antibodies to develop a competitive ELISA on screen-printed graphite electrodes. Tang *et al*. (2003) also produced a disposable immunosensor based on screen-printed electrodes for okadaic acid with a commercial monoclonal antibody, with a 2 ng/ml detection limit.

Optical-based immunosensors for toxin detection, particularly those that incorporate SPR, are widely used (Table 6.1.2.2). Kreuzer *et al*. (1999) developed a highly sensitive, optical immunosensor for okadaic acid using commercial murine monoclonal antibodies. They discovered that changing from a competitive to a displacement ELISA format affected the selectivity of the assay for okadaic acid and dinophysis-1. This work highlights the importance of assay format on overall specificity. A semi-automated membrane-based chemiluminescent biosensor was also developed for the detection of okadaic acid in mussels by Marquette *et al*. (1999). An okadaic acid-BSA conjugate was immobilised onto a pre-activated membrane connected to a fibre optic-based chemiluminescent flow injection configuration. The membranes minimised non-specific protein adsorption and showed good regeneration potential. Anti-okadaic acid monoclonal antibodies were mixed with spiked samples and antibody binding onto the membrane was monitored. The combination of the membranes and sensitive chemiluminescent detection resulted in a high sensitivity of 0.1 ng/ml in spiked mussel extracts.

A number of surface plasmon resonance (SPR)-based methods for paralytic shellfish poisoning (PST) toxins were developed. The aim was to develop methods that could detect saxitoxin below the regulatory limit. In addition, another goal was to assess if these SPR-based methods were comparable to the mouse bioassay and current HPLC techniques. Significantly, cross-reactivity to PST congeners was also evaluated (Campbell *et al*., 2007; Fonfria *et al*., 2007). Both these SPR methods utilised an anti-GTX2/3 monoclonal antibody and were capable of detection saxitoxin (STX) and its

congeners below the required regulatory limit. In addition, Campbell *et al*., (2007) also employed a rabbit polyclonal antibody raised to saxitoxin, along with a saxitoxin-binding sodium channel receptor. Haughey *et al*., (2011) also compared the same polyclonal and monoclonal antibodies using two SPR instruments; a Biacore™ Q biosensor and a Biacore™ T100. A novel approach was used for the detection of saxitoxin by Chen and co-workers (Chen *et al*., 2007). This group employed self-assembled monolayers (SAMs) of a calix[4]arene derivative to sensitively detect saxitoxin, using SPR. STX, a bis-guanidinium structure, binds calix[4]arene, based on its guanidinium ion selectivity. In addition, Yakes and co-workers developed an improved SPR immunoassay for saxitoxin detection, by optimisation of the sensor chip surface chemistry and determination of optimal antibody:analyte mixing ratios and incubation times (Yakes *et al*., 2011).

Table 6.1.2.2: Optical immunosensors for the detection of marine toxins

Toxin	Competition Format	Antibodies	LOD	Reference
Okadaic acid	Direct	Monoclonal-AP; OA-AP	5×10^{-4} to 4 μg/L	Kreuzer *et al*., 1999
Okadaic acid	Direct	Monoclonal-HRP	0.1 μg/L	Marquette *et al*., 1999
Domoic acid	Indirect	Monoclonal	1.8 μg/L	Lotierzo *et al*., 2004
Domoic acid	Indirect	Monoclonal	0.1 μg/L	Yu *et al*., 2005
Domoic acid	Indirect	Rabbit polyclonal	3.0 μg/L	Stevens *et al*., 2007
Microcystin	Direct	Monoclonal; Cy5 – labelled	0.03 μg/L	Long *et al*., 2009
Saxitoxin	Direct	Donkey polyclonal	0.5 μg/L	Yakes *et al*., 2011

Surface plasmon resonance has also been applied to the detection of domoic acid by Yu *et al*. (2005). In this biosensor format, the toxin was linked covalently to a mixed SAM-modified chip. The assay used a competition format between free domoic acid in

solution, and anti-domoic acid monoclonal antibodies. The detection limit achieved was 0.1 ng/mL, which was superior to that of a conventional colorimetric ELISA. This improvement was due to the lack of non-specific antibody adsorption on the SAM and the high sensitivity of the SPR instrument. Le Berre and Kane, (2006) developed Biacore™-based assays for detection of domoic acid, using polyclonal, monoclonal and recombinant antibodies. Interestingly, they demonstrated that the polyclonal antibody was the most sensitive for domoic acid analysis. A sensitive toxin inhibition SPR assay was also developed, using a monoclonal antibody, which detected MC-LR below the regulatory limit of 1 µg/L (Hu *et al*., 2009). In addition, monoclonal antibodies were also employed to detect MC-LR in Spirulina and *Aphanizomenon flos-aquae* blue-green algae food supplements**,** using SPR (Vinogradova *et al*., 2011).

Increased awareness has lead to the development of a diverse range of sensor techniques for phycotoxin and hepatotoxin monitoring, as reviewed by Byrne *et al*. (2009). Unfortunately, very few antibody-based sensors for phycotoxins have been approved as regulatory methods. This is due to the scarcity of sufficient quantities of pure toxin for the development of anti-toxin antibodies and assay validation (Hirama, 2005). Also, a poor supply of reference materials and cross-reactivities with non-target molecules pose significant problems. To reduce the risk to human health of exposure to marine bio-toxins, there is a requirement for more sensitive and reliable detection methods. An important aspect for immuno-detection of marine algal toxins is the structural similarity between toxin cogeners, therefore, care must be taken to characterise the toxin antibody for cross-reactivity to structurally similar molecules of the same phycotoxin grouping. If a mixture of toxin cogeners is analysed in an immuno-sensor format, underestimation or overestimation of toxicity may occur, due to the inability of the antibody to recognise one or multiple isomers of the toxin molecule. Ideally, biosensors for marine toxins should also be capable of detecting mixtures of toxins in complex matrices, such as shellfish meat. The described biosensor formats for marine toxins were all created in an attempt to replace the current regulated methods of detection, including the mouse bioassay and physiochemical analysis, including HPLC-MS. However, it remains to be seen whether they will be incorporated into legislation or routine monitoring programmes in the future.

6.1.3 Chapter aims

This chapter describes the application of random mutagenesis strategies for the generation of improved anti-microcystin binding recombinant antibody fragments. The light chain of the 2H1 scFv fragment was shuffled and a library of mutagenised clones with alternative V_H-V_L chain combinations were screened for improved microcystin binding and specificity. Random errors were introduced into the light chain sequences by error-prone PCR. Subsequently, phage display was used to isolate novel microcystin binders. An alternative, competitive elution strategy was also employed in the bio-panning process to select for scFv-phage particles that had an increased affinity for free toxin in solution. The amplified antibody variable genes were assembled by SOE-PCR and ligated into the Barbas pComb3XSS vector (Barbas *et al*., 2001).

An alternative mutant scFv (C12) was isolated using random mutagenesis techniques. The major aim of this research was to assess whether the mutations introduced into the amino acid sequence of the new clone, caused an improvement in assay sensitivity. The parent and mutant clones were compared by ELISA and Biacore™ inhibition analysis. This chapter also investigated the potential of different immunoassay formats to produce a robust and sensitive assay for microcystin. The parental, 2H1, and 2G1 and mutant C12 scFvs were biotinylated and functionalised with the fluorophore, Alexa Fluor® 647. The potential of a functionalised glass slide-base detection format was also investigated with some 'proof-of-concept' studies.

6.2 Results

6.2.1 Random mutagenesis of the 2H1 scFv fragment

To improve the binding characteristics of the 2H1 scFv, a random mutagenesis approach was employed, in which the un-panned variable light chain library, from the MC-LR-BSA immunised avian host, was mutagensied using error-prone PCR. Mutations were introduced using sub-optimal PCR reaction conditions, including unbalanced concentrations of template, dNTPs, $MnCl_2$ ions and $MgCl_2$ and a low-fidelity DNA polymerase (RedTaq®). This was then re-shuffled with the variable heavy chain of the parental, 2H1, scFv. The overall aim was to increase the sequence diversity of the light chain pool.

6.2.1.1 PCR amplification of the variable heavy chain (V_H) from the 2H1 scFv clone

Initially, the variable heavy (V_H) gene sequence was amplified from a plasmid preparation of the anti-microcystin scFv clone, using GoTaq® polymerase. The CSCHo-FL and CSCG-B primers were utilised for amplification. Successful amplification of the heavy chain fragment was achieved, at approximately 400 base pairs (bps) (Figure 6.2.1.1).

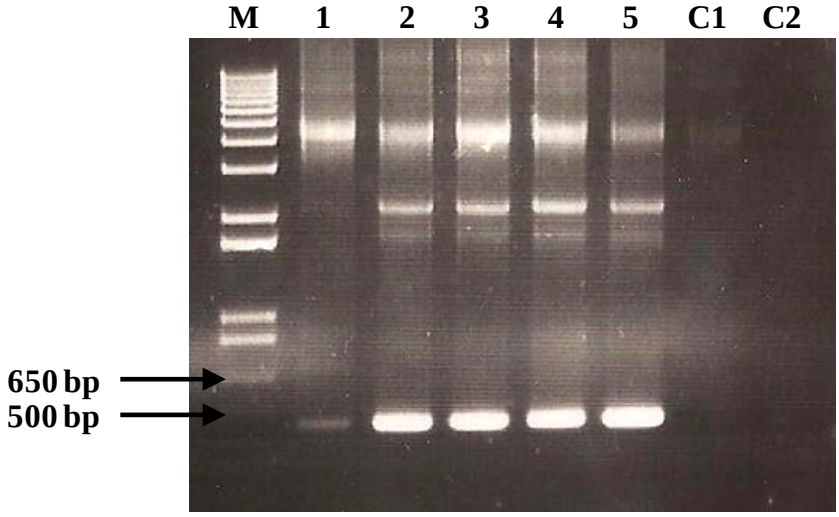

Figure 6.2.1.1: PCR amplification of variable heavy (V_H) sequence from the 2H1 plasmid DNA preparation. Lanes 1-5 contain amplifications of the same heavy chain product. A control amplification, with no primer (C1) and a control with no template (C2), were also included. 'M' represents the 1 kb Plus DNA ladder.

The pComb3XSS vector was also visible on the 1 % agarose gel (Figure 6.2.1.1). A non-specific band at approximately 2,500 bp was also observed (Lane 2-5). This band was eliminated in the process of gel extraction, using a QiaQuick gel extraction kit (Qiagen). The band in Lane 1 appeared to be faint, which may have resulted from a gel loading error.

6.2.1.2 Amplification of the light chain regions using error-prone PCR

Error-prone PCR is based on the lack of fidelity of the Taq polymerase in the presence of an unbalanced mixture of deoxyribonucelotides. The low-fidelity DNA polymerase RedTaq® lacks a 3' to 5' exonuclease activity. The error rate of RedTaq® is approximated at $1x10^{-4}$ bps/kb under normal amplification conditions. However, under certain error-prone amplification conditions, a higher error rate, of between 1-20 nucleotides in 1000, can be achieved (Vanhercke *et al*., 2005).

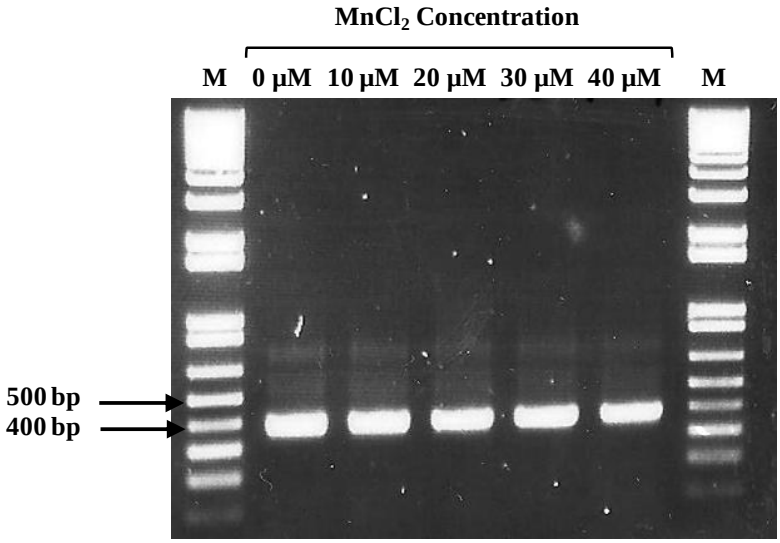

Figure 6.2.1.2: Optimisation of variable light (V_L) error-prone PCR amplification conditions. Manganese chloride ($MnCl_2$) concentrations were prepared from 1 to 40 µM for each reaction, along with 7 mM $MgCl_2$. Deoxyribonucleotide concentrations included 0.2 mM dATP and dGTP, and 1 mM dCTP and dTTP. The PCR reaction contained 0.5 U/µL of RedTaq® DNA polymerase. 'M' represents 1 kb Plus DNA ladder.

The addition of $MnCl_2$ stabilised non-complementary base-pairing and promotes the introduction of random mutations throughout the amplified product (Cadwell and Joyce, 1992). It was necessary to optimise the concentration of $MnCl_2$, as too high a concentration can result in a substantial reduction in PCR amplification. Concentrations of $MnCl_2$, ranging from 10 to 40 µM, were investigated. In order to increase the potential mutation rate, a higher concentration of $MgCl_2$ was also included in the PCR reaction buffer (Cirino *et al*., 2003).

Additionally, in error-prone PCR, A and T residues are more likely to be mutated, compared with G and C residues. This type of bias could potentially alter the type of mutations observed in the mutant library. Therefore, to eliminate this possibility, an unbalanced mixture of dNTPs was used in the PCR mix (Cirino *et al*., 2003; Pritchard *et al*., 2005). The PCR reaction contained an increased concentration of dTTP and dCTP (1 mM) and a decreased concentration of dGTP and dATP (0.2 mM). A 350 bp product was amplified, for the V_L chain library mutagenesis reaction (Figure 6.2.1.2). All the $MnCl_2$ concentrations tested resulted in successful PCR amplification. Each of the error-prone PCR products were pooled and subsequently purified by gel extraction.

To ensure a sufficient level of mutation, a low (6 ng) and high (600 ng) concentration of the light chain library was used as the input DNA template for error-prone PCR. The template concentration can influence the potential error rate, with lower template concentrations resulting in higher mutation frequencies. Therefore, the low and high template concentrations were included to amplify genes with both high and low mutation frequencies. The successful amplification of the V_L library under these conditions using RedTaq® DNA polymerase, 10 µM $MnCl_2$ and 7 mM $MgCl_2$ is shown in Figure 6.2.1.3. All the products from the $MnCl_2$ amplification and the template concentration reactions were pooled, to achieve maximum V_L mutant library diversity. PCR products were subsequently purified by gel extraction.

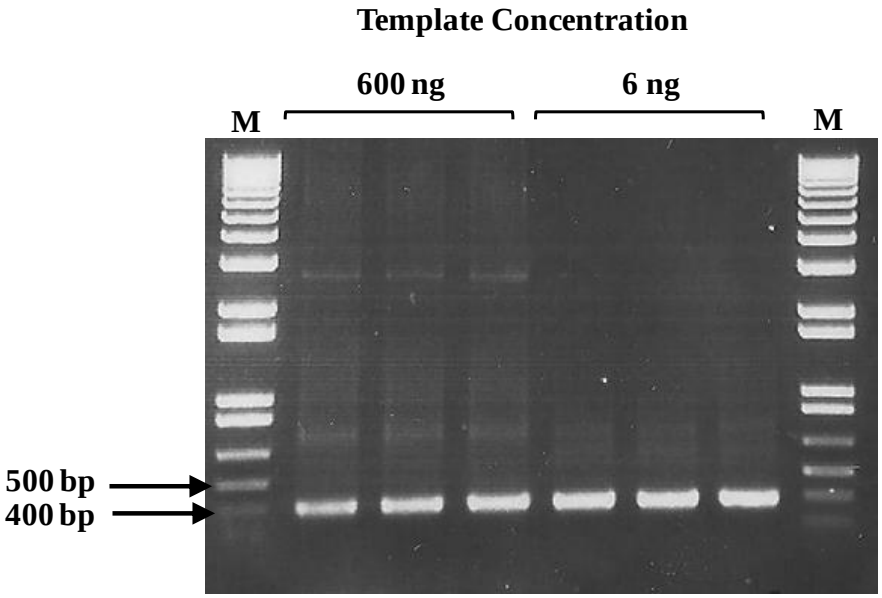

Figure 6.2.1.3: Optimisation of light chain library template concentrations. Concentrations of 600 and 6 ng of DNA template (three lanes each) were used in the amplification of the light chain library. A high RedTaq® polymerase concentration (0.1 unit/µL) was also used in the amplification reaction. Deoxyribonucleotide concentrations included 0.2 mM dATP and dGTP, and 1 mM dCTP and dTTP. 'M' represents 1 kb Plus DNA ladder.

6.2.2 Construction of mutant light chain-shuffled library

6.2.2.1 SOE-PCR of variable heavy and mutant light chain regions

Following purification of the V_H and V_L chains by gel extraction, SOE-PCR was carried out, using the extension primers, CSC-F and CSC-R. This process joined the V_L and V_H regions, using the sequence tails introduced in the first round of PCR to create a serine-glycine linker sequence. This second round of PCR produced a 750 bp product (Figure 6.2.2.1). The high fidelity Phusion® Taq DNA polymerase (Fermentas) was employed for further PCR amplification, in order to minimise the possibility of introducing mis-sense or non-sense mutations in the linker or cloning regions.

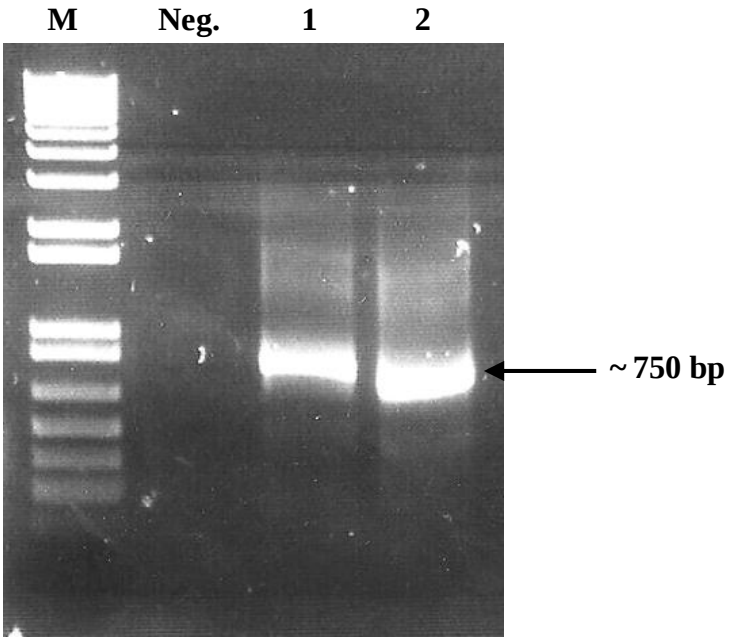

Figure 6.2.2.1: Large-scale amplification of the SOE-PCR product from the light chain-shuffled library. The approximate molecular weight of this fragment was 750 base pairs (bp). A negative control (no template) was included (Neg.), and 'M' represents the 1 kb Plus DNA ladder. Lanes 1 and 2 contain the same PCR amplicon.

The purified SOE product was amplified by large-scale PCR, purified by gel extraction, ethanol-precipitated and stored at -20^{o}C.

6.2.2.2 Mutant library construction and bio-panning

The SOE product was harvested, quantified using a Nanodrop ND-1000™ and cloned into the pComb3XSS vector, using the restriction enzyme, *Sfi*I. Antartic phosphatase treatment ensured that self-ligation of the vector did not occur. The ligated product was transformed into electro-competent *E. coli* XL1-Blue cells (Strategene), by electroporation. The transformed mutant avian anti-microcystin scFv library had a size of 2.14 x 10^{7} cfu/mL. The library was 'rescued' using M13K07 helper phage.

In order to isolate the most sensitive clones from the mutant library, two different selection strategies were employed. Using the standard bio-panning strategy, the library was initially enriched against an immobilised MC-LR-OVA conjugate (50 to 0.25 µg/mL) and eluted using trypsin (Rounds 1-3). Bio-panning were carried out with

decreasing concentrations of conjugate coated onto the immunotube for each round. The number of washes were increased, in order to facilitate high stringency bio-panning (Table 2.16.1.1). For rounds 4 and 5, the library was split and trypsin and competitive elution was carried out simultaneously. The inputs and outputs from each round of bio-panning give an indication of bio-panning efficiency. Table 6.2.2.1 shows that the inputs and outputs were optimal for rounds 1-4. However, bio-panning round 5 did not result in any input or outputs as the panning stringency was too severe.

Table 6.2.2.1: Bio-panning inputs and outputs for the mutant avian immune library

Round	Input (cfu/mL)	Output (cfu/mL)
1	1.4×10^{10}	5.7×10^{5} (Trypsin Elution)
2	1.3×10^{12}	1.5×10^{6} (Trypsin Elution)
3	5.0×10^{10}	7.4×10^{4} (Trypsin Elution)
4	8.4×10^{11}	1.2×10^{6} (Competitive Elution)
		6.9×10^{4} (Trypsin Elution)

For the competitive elution strategy in the final rounds of bio-panning (round 4 and 5), the phage library was incubated on the immunotube with immobilised MC-LR-OVA conjugate, and subsequently eluted with a decreasing concentration of MC-LR toxin in solution (500 ng/mL and 5 ng/mL). The aim of this strategy was to elute phage-scFv binders from the immunotube, which showed a high sensitivity for free toxin in solution. This should result in the isolation of mutant clones that bound MC-LR in its free form, and not in the context of a protein conjugate. A high affinity for the toxin attached to the conjugate is generally undesirable, because such antibodies do not dissociate readily, resulting in a reduction in assay sensitivity. Care must also be taken to avoid selection of 'interface binders' (Tuomola *et al.*, 2000). These antibodies recognise haptens in the context of the conjugate and bind to some extent to the linker or carrier protein close to the point of conjugation. Hence, they often show higher affinity for conjugate than for free hapten (Charlton and Porter, 2002). Selection and characterisation of mutant clones

6.2.2.3 Polyclonal phage ELISA of a light chain-shuffled and error-prone mutant library

The precipitated input phage, from each bio-panning round of the mutant library, was analysed by polyclonal phage ELISA. A high signal from the MC-OVA-specific scFv-phage can be observed in bio-panning round 2, which subsequently decreased, due to increased panning stringency. Enrichment was observed for panning round 4, from the trypsin-eluted (TE) phage only (Figure 6.2.2.2). No enrichment was observed for the competitively-eluted (CE) outputs.

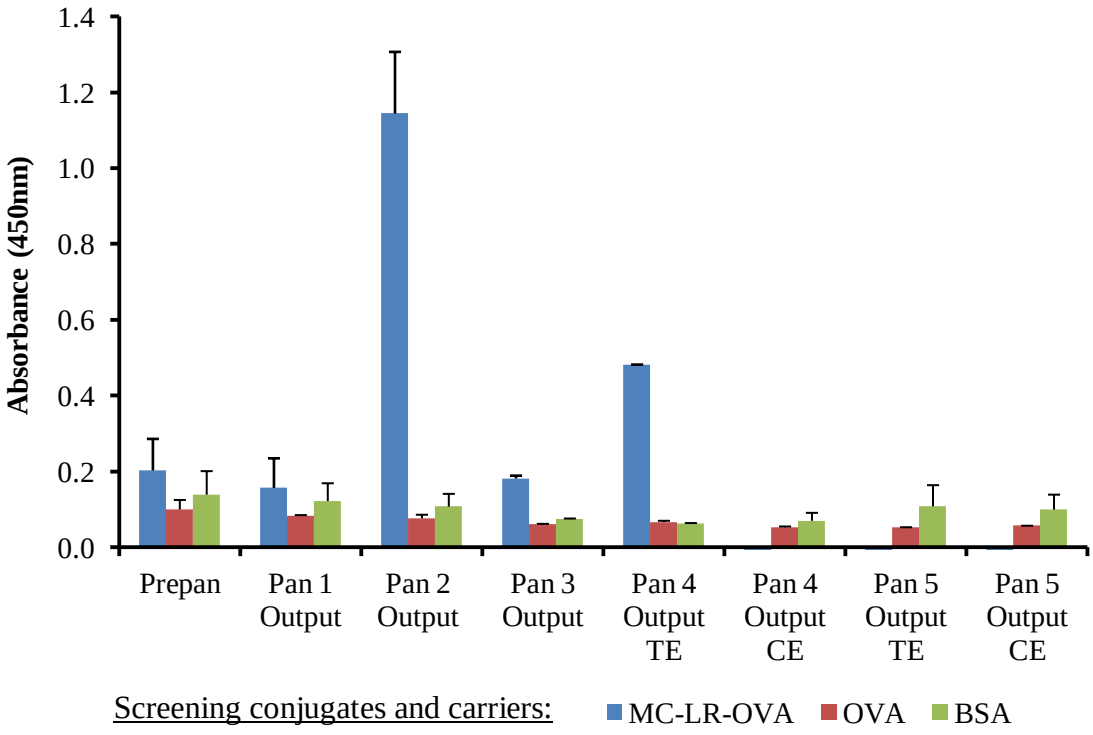

Figure 6.2.2.2: Polyclonal phage ELISA for the avian mutant library. Output phage from each round of bio-panning were incubated with immobilised MC-LR-OVA conjugate (10 µg/mL) and binding was detected using a HRP-labelled, anti-M13 commercial antibody (GE Healthcare). Non-specific binding controls were included; BSA (10 µg/mL) and OVA (10 µg/mL). Errors bars represent the standard deviation above the mean value.

6.2.2.4 Direct soluble ELISA of the light chain-shuffled avian library

Soluble monoclonal ELISA was performed on clones selected from rounds 4 and 5 of the trypsin-eluted and competitively-eluted bio-panning methods. No enrichment was detected for round 5, but it was decided to check for any positive binders. The quantity of phage may have been too small to generate a positive signal by polyclonal phage ELISA. Initially, phage outputs from bio-panning rounds 4 and 5 were re-infected into *E.coli* Top10F' bacterial cells for soluble expression. The scFv-enriched lysates were tested by monoclonal soluble ELISA for binding to immobilised MC-LR-OVA conjugate (5 µg/mL).

All clones were tested in parallel for cross-reactivity to the OVA and BSA carrier protein. No cross-reactivity pattterns were observed (data not shown). The majority of clones, from both the trypsin and competitively-eluted methods, had ELISA signals which were more than three-fold higher than that of the control proteins, BSA and OVA. The monoclonal ELISA screening results, from bio-panning round 4, are illustrated in Figure 6.2.2.3. The trypsin and competitively-elute clones displayed a percentage binding, above background, of 94 % and 72 %, respectively. It was clear that highest-binding clones were obtained from the trypsin-eluted library in this round.

The mean background value for all clones analysed was 0.359 AU. Similarly, the trypsin and competitively-eluted clones from bio-panning round 5 displayed a percentage binding, above background, of 95.8 % and 99 %, respectively (Figure 6.2.2.4). Thirty randomly-selected clones from rounds 4 and 5 (both trypsin and competitive elution) were taken forward for cross-reactivity and inhibition analysis to assess their ability to bind MC-LR in solution.

A.

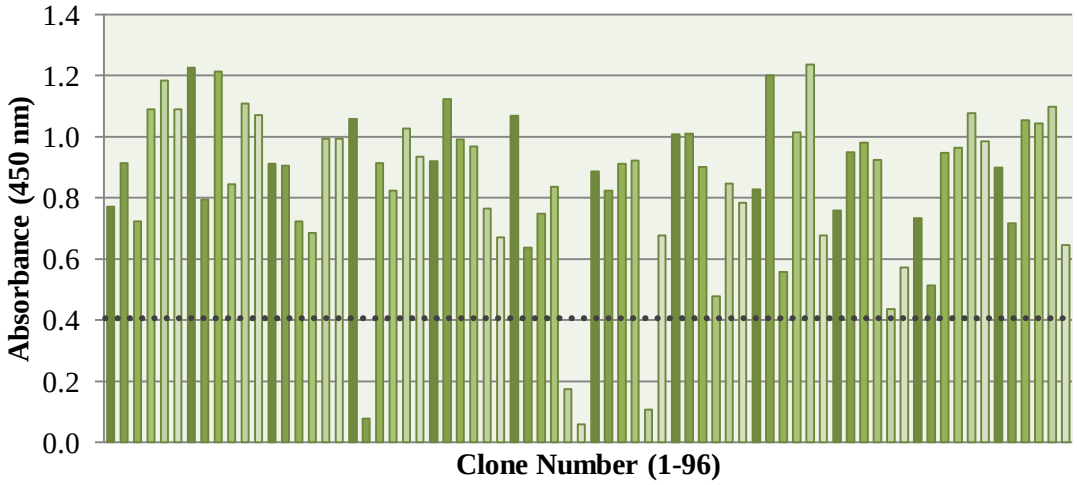

B.

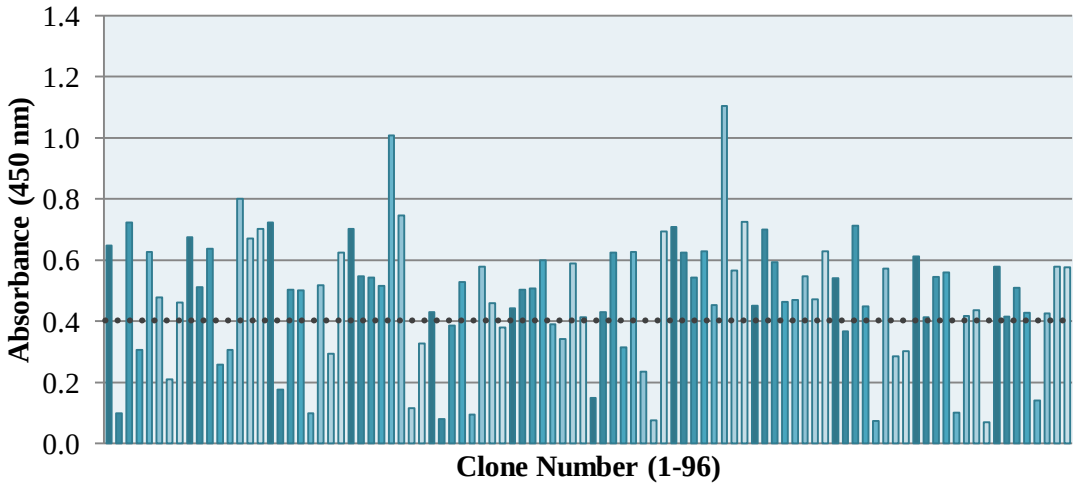

Figure 6.2.2.3: Soluble monoclonal ELISA of mutant, solubly-expressed scFvs from bio-panning round 4. Ninety six clones each were selected from the trypsin-eluted (A) and competitively-eluted (B) round 4 of bio-panning. Supernatant, containing solubly-expressed scFv was incubated on MC-LR-OVA–coated plates (5 µg/mL) and binding was detected using a HRP-labelled anti-HA monoclonal antibody.

A.

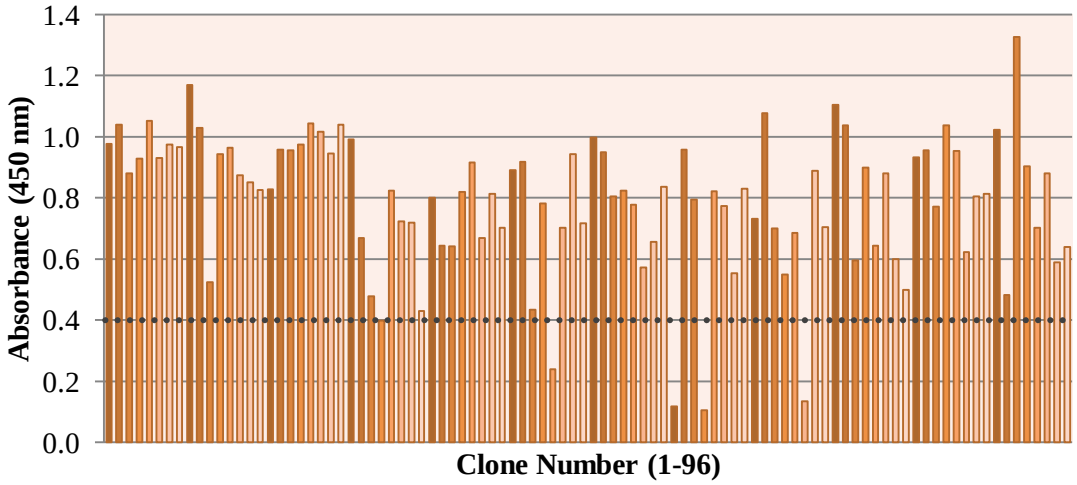

B.

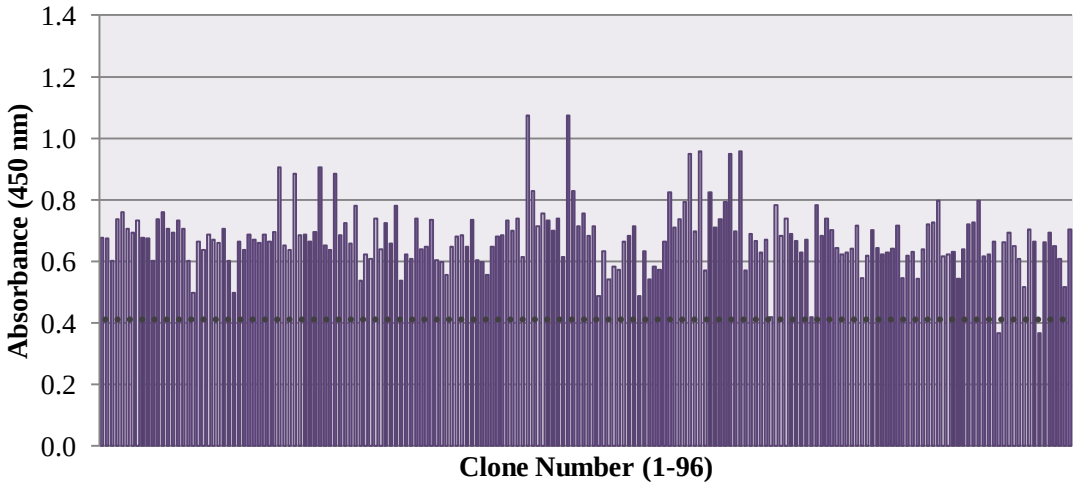

Figure 6.2.2.4: Soluble monoclonal ELISA of mutant, solubly-expressed scFvs from bio-panning round 5. Ninety six clones each were selected from the trypsin-eluted (A) and competitively-eluted (B) round 5 of bio-panning. Supernatant, containing solubly-expressed scFv, was incubated on MC-LR-OVA–coated plates (5 µg/mL) and binding was detected using a HRP-labelled anti-HA monoclonal antibody.

6.2.3 Sequence analysis of wild-type and mutant clones

The clones, 2H1, 3BA1, 4CF8, 4TC2 and 5TC12, which demonstrated the best inhibition ELISA profiles (data not shown) were sequenced by MWG-Operon, using the splice by extension overlap (SOE) primers. The light and heavy chain variable regions were identified using the Kabat numbering system (Johnson and Wu, 2000) and subsequently aligned using ClustalW (Figure 6.2.3.1).

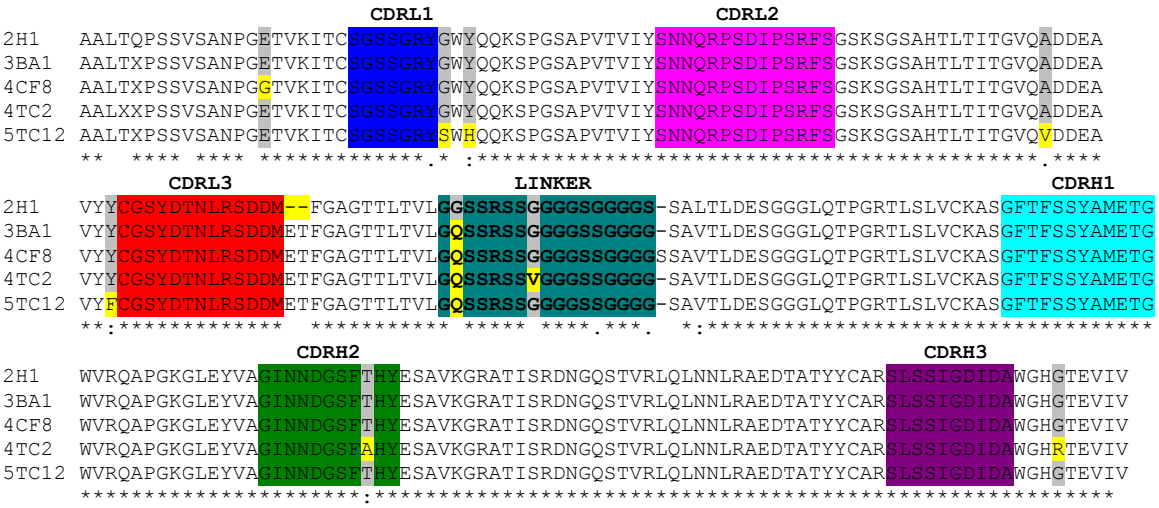

Figure 6.2.3.1: ClustalW sequence alignment for four MC-LR clones, compared to the 2H1 parent scFv clone (Top). CDR regions are highlighted with colour. Regions of sequence diversity are highlighted in yellow. Key: CDRL1 = Blue, CDRL2 = Pink, CDRL3 = Red, Linker = Turquoise, CDRH1 = Light Blue, CDRH2 = Green, CDRH3 = Purple.

The sequence comparison between the wild-type scFv (2H1) and the error-prone PCR, light chain-shuffled clones (2BA1, 4CF8, 4TC2 and 5TC12) clearly illustrates that the majority of sequence substitutions were located in the framework regions. Significantly, no alternative light chains were incorporated into the mutant clones. However, one substitution from threonine (T) to alanine (A) in the CDRH2 region was evident in the 4TC2 clone. The clone displaying the best inhibition profile by ELISA, 5TC12 (shortened to C12) was also the clone with the most amino acid substitutions (5), most likely caused by point mutations in the error-prone PCR replication process. In this process, the point mutations introduced a mis-sense error in the reading frame, caused by a malfunction in DNA replication. These changes are classified as either transitions

or transversions. Most common mis-sense mutations include the exchange of a purine for a purine (A ↔ G) or a pyrimidine for a pyrimidine, (C ↔ T). The threonine to alanine substitution in the CDRH2 region was most likely an A → G substitution. Notably, all the mutant clones had an insertion mutation (ET) close to the CDRL3 region (glutamic acid, E and threonine, T). Insertions and substitutions of nucleotides in the antibody-encoding genes are natural components of the hypermutation process, which may expand the possible interaction sites and conformations for antibody:antigen binding. Although mutations of amino acids have also been widely utilised in antibody engineering, little is known about the functional consequences of such modifications.

6.2.4 ELISA comparison of wild-type and mutant clones

The MC-LR-specific wild-type (2H1) and mutant (C12) scFvs were analysed for their capacity to bind free MC-LR in solution. The C12 clone was chosen for comparison, as it displayed the best inhibition profile in preliminary ELISA analysis, performed in crude lysate (data not shown). In addition, the C12 scFv displayed the most amino acid substitution, compared with the 2H1 clone. Inhibition analysis was carried out by pre-incubating the scFv fragments with MC-LR for 30 minutes before adding the mixture to the microplate, coated with MC-LR-OVA conjugate. Inter- and intra-day variability analysis was also performed, using the light chain-shuffled scFv fragment, C12. Satisfactory % CV and RE values were obtained in the validation studies, and the assay had a range of 0.8 to 50 ng/mL (Table 6.2.4.1).

The current ELISA analysis showed that the C12 scFv fragment was marginally more sensitive, in comparison to the 2H1 parent clone. The limit of detection (LOD) of the C12 mutant scFv was 1.4 ng/mL, while the LOD of the parental 2H1 was calculated as 3.2 ng/mL. Therefore, the mutagenesis strategy resulted in a 2.3-fold improvement in the limit of detection value of the 2H1 scFv fragment. The ELISA inhibition curves are compared in Figure 6.2.4.1.

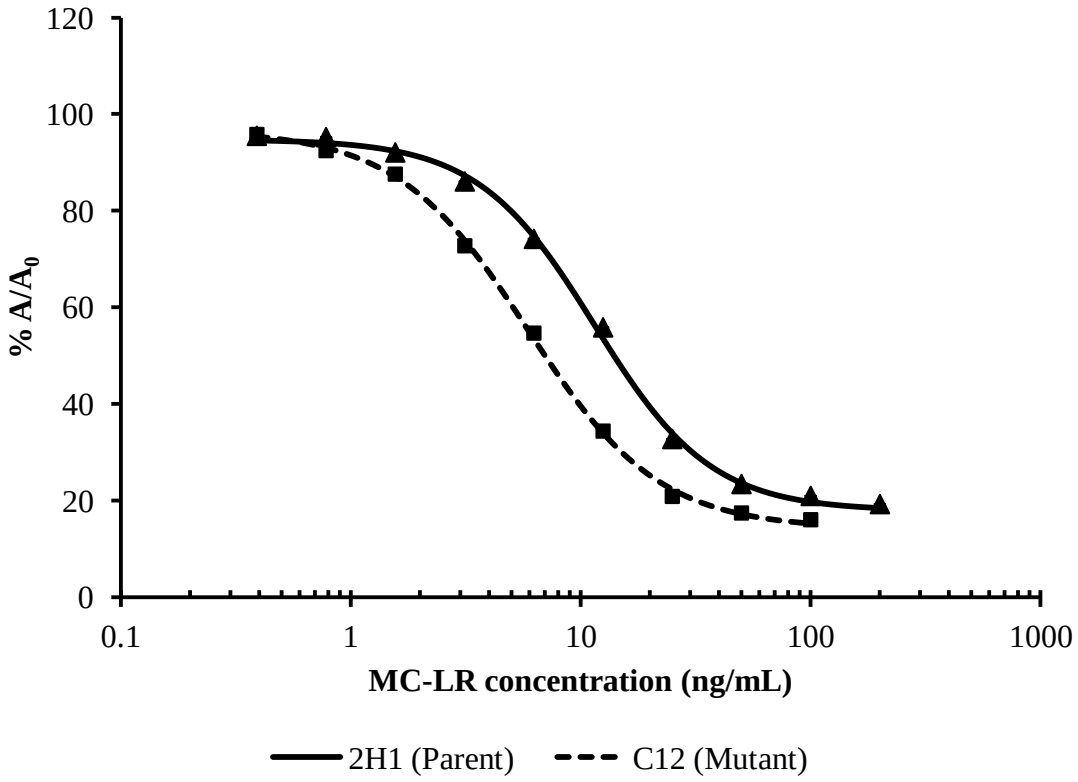

Figure 6.2.4.1: Comparison of 2H1 wild-type and C12 mutant scFv fragments by inhibition ELISA. The ELISA plate was coated with 500 ng/mL MC-LR-OVA conjugate. Inhibition between MC-LR (200 to 0.78 ng/mL) and purified scFv, diluted to a final concentration of 1/20,000, was observed. The normalised absorbance for a given MC-LR concentration ($A-A_{excess}$), divided by the normalised absorbance for negative sample (A_0-A_{excess}), was expressed as a percentage (% A/A_0) and plotted versus the MC-LR concentration (ng/mL).

Table 6.2.4.1: Inter- and intra-day variability studies for the C12 mutant scFv fragment

MC-LR (ng/mL)	Inter-day Assay Validation			Intra-day Assay Validation		
	% CV	Back Calculated Concentration (ng/mL)	% RE	% CV	Back Calculated Concentration (ng/mL)	% RE
100.0	6.0	57.3	174.6	1.7	70.1	142.7
50.0	2.1	60.4	82.8	10.8	48.2	103.8
25.0	2.5	25.9	96.5	2.9	29.1	85.9
12.5	3.7	12.4	100.7	18.4	12.3	101.3
6.3	12.1	6.2	101.2	19.9	6.0	103.5
3.1	5.7	3.5	88.8	12.2	3.3	95.4
1.6	5.8	1.4	115.4	5.7	1.5	104.5
0.8	6.5	0.7	118.2	6.9	0.9	90.6

6.2.5 Development of a Biacore™ inhibition assay for microcystin and microcystin congeners

Inhibition assays for the detection of MC-LR were developed by employing a CM5 dextran chip surface, immobilised with the heptapeptide toxin, MC-LR. For successful assay development, optimisation of a number of parameters was required. Inter-day and intra-day analysis was carried out for the 2H1 and 2G1 wild-type scFv fragments, as well as the C12 mutant clone, which was a product of mutagenesis and light chain shuffling of the 2H1 scFv clone. The three scFv fragments were compared in terms of their sensitivity and cross-reactivity to the microcystin variants; MC-LW, MC-RR, MC-YR, MC-LA and MC-LF.

6.2.5.1 Immobilisation of MC-LR onto a CM5 chip surface for Biacore™ analysis

MC-LR was directly conjugated to a CM5 dextran chip surface using EDC-NHS coupling chemistry (Queen's University, Belfast). The chip was firstly activated by (*N*-ethyl-*N*'-(dimethylaminopropyl) carbodiimide) (EDC) and (*N*-hydroxysuccinimide) (NHS), the toxin was subsequently incubated on the chip surface. The EDC solution in the presence of NHS, activates the CM dextran carboxyl groups, converting them into functional ester groups. The surface NHS esters react with primary amino groups, such as lysine residues on MC-LR, causing covalent binding of the toxin to the surface (Murphy *et al*., 2006; Vinogradova *et al*., 2011). Any remaining available unbound functional ester groups are deactivated by injecting a 1 M ethanolamine hydrochloride solution (pH 8.5) over the chip surface. Surface regeneration was optimised, as described in Section 2.17.2. The surface was regenerated using two pulses of 200 mM NaOH, to remove non-covalently attached proteins from the surface.

6.2.5.2 Inhibition assay optimisation for wild-type and mutant scFv fragments

In order to optimise the sensitivity of the standard curves for detection of MC-LR, various parameters, including the antibody dilution and contact time, were examined. The effect of antibody concentration on the standard curve was examined using dilutions of each scFv (1/900, 1/2,000, 1/3,000, 1/5,000 and 1/7,000) and the effect of

the flow rate was examined using three different rates (5, 10 and 25 µL/min) (data not shown). A flow rate of 5 µL/min was chosen for the generation of an inhibition assay for all three scFv fragments, as it produced the most stable and reproducible curve under the defined conditions. Overall, the flow rate did not affect the sensitivity of the assay over the range examined. However, in the current study, a longer contact time was chosen to generate a robust standard curve. Antibody dilution of 1/7,000, 1/2,000 and 1/3,000 and a flow rate of 5 µL/min were found to be optimal for the generation of a sensitive and reproducible inhibition assay using the 2G1, 2H1 and C12 scFv fragments, respectively.

6.2.5.3 Inter- and intra-day Biacore™ studies of wild-type and mutant clones

Optimal antibody dilutions (2H1, 2G1 and C12) were prepared in HBS-EP buffer, and mixed with MC-LR, to give final concentrations of between 0.7 and 200 ng/mL MC-LR. Samples were incubated for 30 minutes at room temperature, to allow equilibration, and subsequently injected over the MC-LR-immobilised chip surface, at a flow rate of 5 µL/min for 4 minutes. This was followed by two 5 second pulses of 200 mM NaOH, which allowed complete regeneration of the chip surface. The antibody response values (R) for each concentration were normalised by the transformation to % R/R_0, according to the equation:

$$\% R/R_0 = \frac{R - R_{excess}}{R_0 - R_{excess}}$$

where R is the relative response, R_0 is the response at a zero concentration of analyte, and R_{excess} is the response at an excess of analyte. The % R/R_0 value was plotted against the logarithm of the MC-LR concentration (ng/mL). To demonstrate the reproducibility of the assays, both inter- and intra-day variability studies were performed. The results of the inter-day assay for the 2H1, 2G1 and C12 scFv fragments are presented in Figures 6.2.5.1, 6.2.5.2 and 6.2.5.3, respectively.

The inter-day calibration curve for the 2H1 scFv fragment is illustrated in Figure 6.2.6.1. The IC_{50} was calculated as 33.5 ng/mL. The limit of detection was calculated from the mean of the zero analyte concentration, minus three standard deviations, as 13.8 ng/mL.

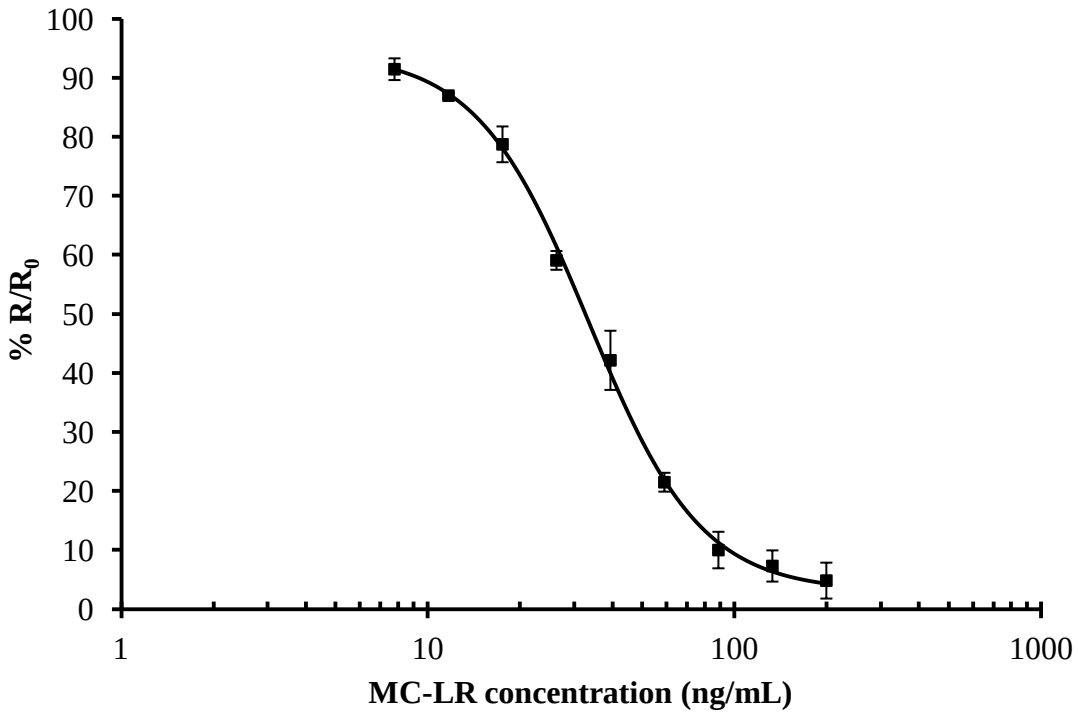

Figure 6.2.5.1: Inter-day Biacore™ assay calibration curve for the determination of MC-LR in PBS, for the 2H1 (wild-type) scFv fragment. MC-LR concentrations, ranging from 200 to 7.8 ng/mL were pre-incubated with an optimised dilution of the avian 2H1 anti-MC-LR scFv (1/2,000) and injected over the MC-LR-immobilised surface. Using BIAevaluation™ software (Version 3.1), the data was fitted using a 4-parameter equation. The error bars represent the standard deviation for each concentration.

Table 6.2.5.1: Inter-day and intra-day Biacore™ inhibition assay validation to determine the precision (% CV) and relative error (% RE) for the 2H1 (wild-type) scFv fragment.

scFv: 2H1	Inter-day Assay Validation			Intra-day Assay Validation		
MC-LR (ng/mL)	% CV	Back Calculated Concentration (ng/mL)	% RE	% CV	Back Calculated Concentration (ng/mL)	% RE
200	1.9	156.1	128.1	65.75	172.34	116.05
133.3	0.2	123.1	108.3	29.3	118.9	112.1
88.9	2.2	69.2	128.5	17.9	102.9	86.4
59.3	4.8	51.7	114.7	13.5	59.7	99.3
39.5	1.8	46.6	84.7	17.2	37.8	104.6
26.3	0.4	27.2	96.9	11.6	27.5	95.9
17.6	4.0	15.1	116.7	8.8	17.1	102.7
11.7	3.1	13.1	89.7	7.2	11.8	98.8
7.8	2.5	7.1	110.0	9.6	7.7	102.0

The precision and relative error of the inhibition analyses was evaluated by extrapolating the % CV and % RE. Inter- and intra-day assay CVs for the 2H1 scFv were all well below the acceptable limit of 20 %, indicating excellent reproducibility. The 2H1 inhibition assay was reproducible in the range of 7.8 to 59.3 ng/mL (Table 6.2.5.1).

The inter-day calibration curve for the 2G1 scFv fragment is presented in Figure 6.2.6.2. The IC_{50} was calculated as 6.2 ng/mL. The limit of detection was calculated from the mean of the zero analyte concentration, minus three standard deviations, as 1.7 ng/mL.

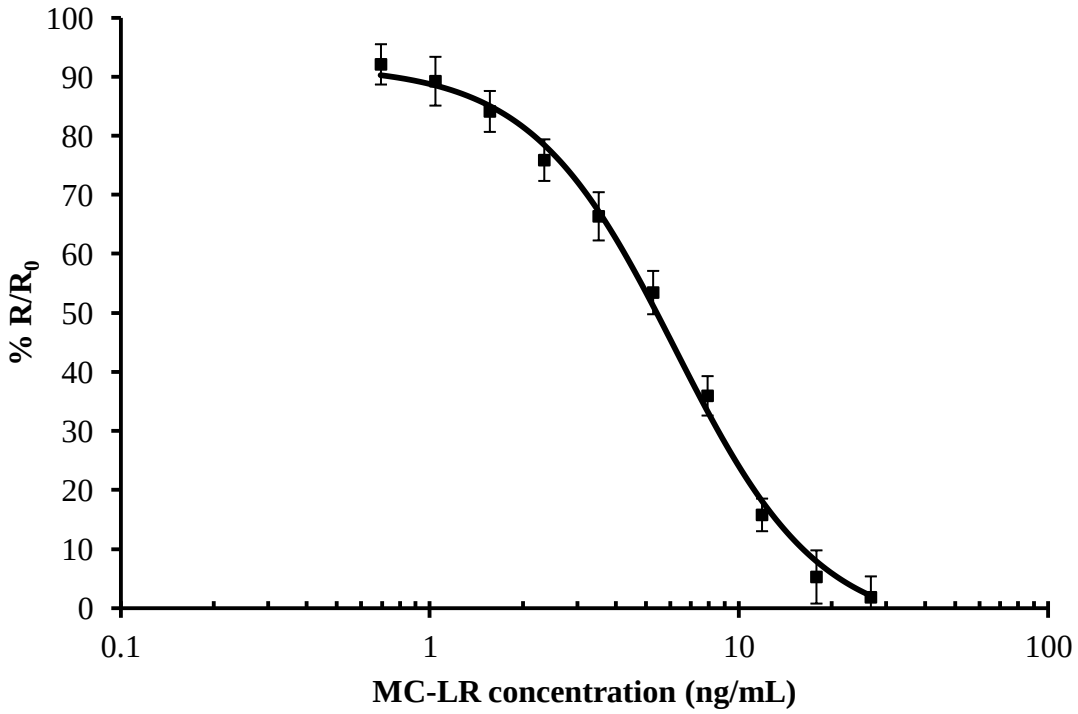

Figure 6.2.5.2: Inter-day Biacore™ assay calibration curve for the determination of MC-LR in PBS, for the 2G1 (wild-type) scFv fragment. MC-LR concentrations, ranging from 200 to 7.8 ng/mL were pre-incubated with an optimised dilution of the avian 2G1 anti-MC-LR scFv (1/7,000) and injected over the MC-LR-immobilised surface. Using BIAevaluation™ software (Version 3.1), the data was fitted using a 4-parameter equation. The error bars represent the standard deviation for each concentration.

Table 6.2.5.2: Inter-day and intra-day Biacore™ inhibition assay validation to determine the precision (% CV) and relative error (% RE) for the 2G1 (wild-type) scFv fragment.

scFv: 2G1	Inter-day Assay Validation			Intra-day Assay Validation		
MC-LR (ng/mL)	% CV	Back Calculated Concentration (ng/mL)	% RE	% CV	Back Calculated Concentration (ng/mL)	% RE
40.00	13.3	27.6	144.9	60.9	30.7	130.1
26.67	15.9	27.2	98.0	79.9	25.9	102.9
17.78	12.2	21.4	83.1	82.8	20.3	87.76
11.85	9.8	13.3	89.0	28.9	13.3	89.0
7.90	8.0	7.5	106.1	7.8	6.9	113.4
5.27	5.8	4.9	108.3	12.6	5.5	96.3
3.51	4.6	3.5	101.8	3.5	3.5	101.9
2.34	3.44	2.5	92.8	6.8	2.4	96.9
1.56	5.2	1.7	90.3	5.3	1.8	88.9
1.04	3.9	1.2	87.0	1.9	0.9	107.9
0.69	4.7	0.9	80.9	0.8	0.5	155.9

For the 2G1 scFv intra-day analysis, the % CV values for the high MC-LR concentrations were outside the acceptable limit. Therefore, the assay was not reproducible within this range. The 2G1 scFv was reproducible in the range of 1 to 7.9 ng/mL, for both inter-day and intra-day analysis (Table 6.2.5.2).

The inter-day calibration curve for the C12 scFv fragment is illustrated in Figure 6.2.6.3. The IC_{50} was calculated as 28.2 ng/mL. The LOD was calculated from the mean of the zero analyte concentration, minus three standard deviations, as 14.8 ng/mL.

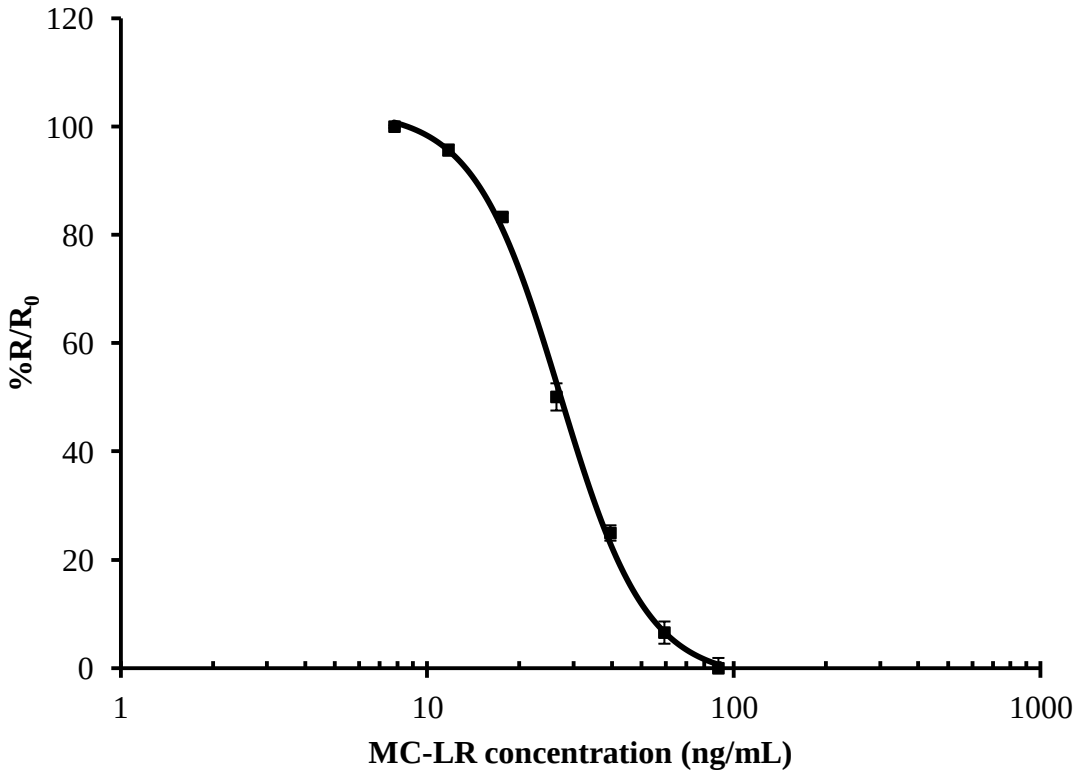

Figure 6.2.5.3: Inter-day Biacore™ assay calibration curve for the determination of MC-LR in PBS for the C12 (mutant) scFv fragment. MC-LR concentrations ranging from 100 to 7.8 ng/mL were pre-incubated with an optimised dilution of the avian C12 anti-MC-LR scFv (1/3,000) and injected over the MC-LR-immobilised surface. Using BIAevaluation™ software (Version 3.1), the data was fitted using a 4-parameter equation. The error bars represent the standard deviation for each concentration.

Table 6.2.5.3: Inter-day and intra-day Biacore™ inhibition assay validation to determine the precision (% CV) and relative error (% RE) for the C12 (mutant) scFv fragment.

scFv: C12	Inter-day Assay Validation			Intra-day Assay Validation		
MC-LR (ng/mL)	% CV	Back Calculated Concentration (ng/mL)	% RE	% CV	Back Calculated Concentration (ng/mL)	% RE
88.9	0.9	97.1	91.5	15.4	72.0	123.4
59.3	3.6	59.3	99.9	12.0	57.5	103.0
39.5	2.2	38.2	103.3	9.3	40.9	96.7
26.3	6.4	27.2	96.7	7.3	26.1	100.8
17.6	3.0	16.8	104.3	6.7	16.1	108.9
11.7	4.4	11.7	100.1	10.7	15.2	76.9
7.8	3.7	8.6	90.6	4.4	6.8	114.4

For the C12 inhibition analysis, the % RE indicated reasonable error, with the majority of values with 80 to 120 %. The % CV and % RE values for the mutant clone are outlined in Table 6.2.5.3. The C12 scFv fragment had an acceptable assay range, with good reproducibility between 7.8 and 59.3 ng/mL.

6.2.5.4 Comparison of wild type and mutant clones on Biacore™

The results of the Biacore™ inhibition assays, employing the wild-type scFv fragments, 2H1 and 2G1, were compared to the light chain-shuffled C12 scFv fragment, in terms of assay sensitivity. The Biacore™ inhibition curves for the three antibody fragments are shown in Figure 6.2.5.4.

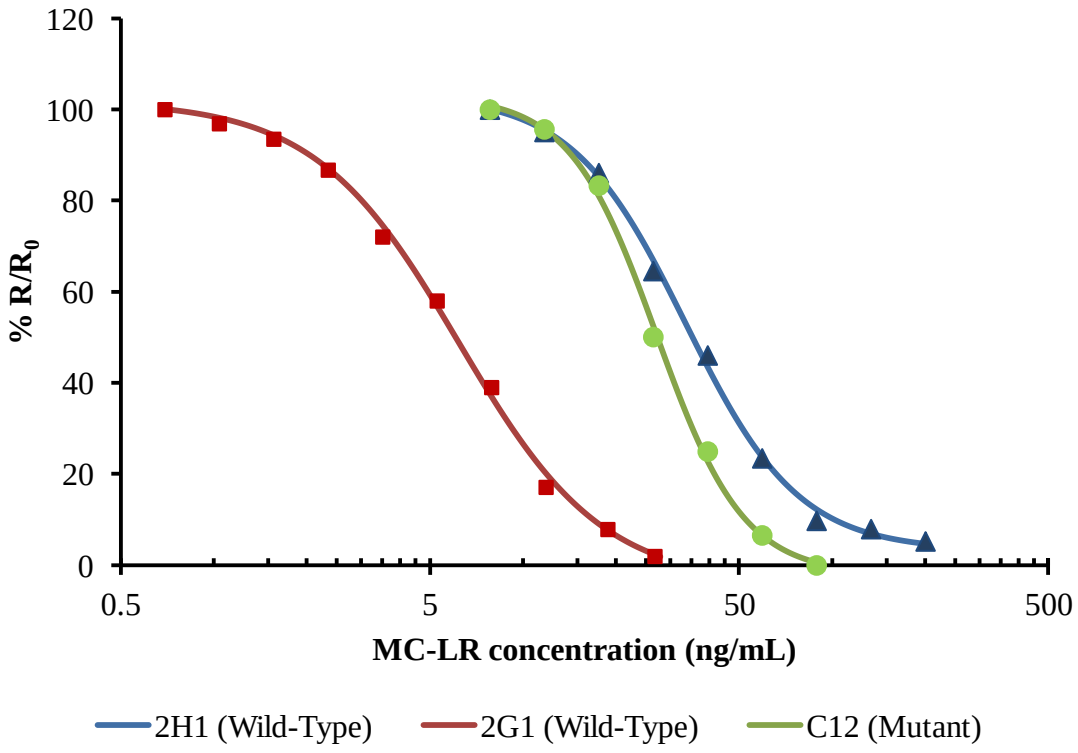

Figure 6.2.5.4: Comparison of Biacore™ inhibition analysis for the detection of MC-LR in HBS-EP buffer, using the 2H1, 2G1 and C12 scFv fragments. The mutant C12 fragment was derived from the 2H1 clone by error-prone PCR and light-chain shuffling. The normalised responses (R), expressed as % R/Ro, were plotted against the logarithm of the MC-LR concentration (ng/mL).

The range of detection, IC_{50} and limit of detection values are summarised in Table 6.2.5.4. The 2H1 scFv fragment (LOD = 13.8 ng/mL) displayed a similar sensitivity to the C12 mutant clone (LOD = 14.8 ng/mL), from which it was derived by mutagenesis and light–chain shuffling. The 2G1 scFv fragment was approximately 2.6-fold more sensitive in an SPR format, compared with the original ELISA format (Section 6.2.5) (ELISA LOD = 4.4 ng/mL; Biacore LOD: 1.7 ng/mL). Moreover, the 2G1 scFv showed

an estimated 9-fold greater assay sensitivity, compared with the C12 and 2H1 scFv fragments, in the SPR assay. It was clear that the 2G1 scFv fragment displayed excellent sensitivity for MC-LR in an immunosensor format, which was extremely close to the WHO detection limit of 1 µg/L (1 ng/mL).

Table 6.2.5.4: Comparison of assay range, IC_{50} and limit of detection (LOD) of the 2H1, 2G1 (wild-type) and C12 (mutant) scFv fragments.

scFv Fragment	Range (ng/mL)	IC_{50} (ng/mL)	LOD (ng/mL)
2H1 (Wild-Type)	7.8 – 59.3	33.5	13.8
C12 (Mutant 2H1)	1 – 7.9	28.2	14.8
2G1 (Wild-Type)	7.8 – 59.3	6.2	1.7

6.2.5.5 Cross-reactivity studies of wild-type and mutant clones

To determine the degree of cross-reactivity of the scFv fragments, 2H1, 2G1 and C12, with the five, structurally-related variants or 'cogeners' of microcystin, MC-LW, MC-RR, MC-YR, MC-LA and MC-LF, a Biacore™ inhibition analysis was performed. All the assay conditions were consistent. Percentage cross-reactivities (% CR_{50}) were extrapolated by comparing the relevant IC_{50} of the microcystin variants to the IC_{50} of the MC-LR toxin. The % CR_{50} was calculated using the equation:

$$\% \text{ Cross-reactivity 50 } (CR_{50}) = \frac{IC_{50} \text{ MC Variant}}{IC_{50} \text{ MC-LR}} \text{ X } 100$$

The cross-reactivity profiles for the 2G1 scFv clone for MC-YR, MC-LW and nodularin are illustrated in Figure 6.2.6.5 A, while the profiles for the MC-RR, MC-LF and MC-LA variants are illustrated in Figure 6.2.6.5 B. Each microcystin variant IC_{50} is compared to the IC_{50} of the MC-LR variant in each four-parameter fit profile. Figure 6.2.6.6 illustrates the cross-reactivities of the most commonly-occurring MC variants to the 2H1 scFv fragment. The IC_{50} and % CR_{50} for the 2G1, 2H1 and C12 scFv fragments

are shown in Table 6.2.6.5. It was not possible to generate four-parameter fit equations for the C12 mutant scFv cross-reactivity analysis, as the data was poor. This may have occurred due to the degradation of the chip surface with extended use over time. Therefore, the IC_{50} and CR_{50} values were estimated from a graph of normalised response ($\%R/R_0$) versus the logarithm of the MC variant concentration (ng/mL) (data not shown).

The results, listed in Table 6.2.5.5, indicate that the 2G1 scFv fragment had lower percentage cross-reactivities, compared with the 2H1 and C12 scFvs. However, the overall reactivity of the 2G1 scFv for MC-LR toxin and its variants is still considerably more sensitive, in comparison with the 2H1 and C12 scFv fragments. The degree of cross-reactivity of the 2G1 scFv to the MC variants was variable, with MC-YR and MC-LA showing a high cross-reactivity relative to MC-LR (Table 6.2.5.5).

The 2H1 scFv showed considerable cross-reactivity to the MC-LF variant, which contains leucine and phenylalanine, at the variable amino acid positions. However, the binding of the 2H1 scFv to the MC-LW and MC-RR were low, at 43.2 and 39.3 %, respectively. MC-LW is characterised by the presence of leucine and the bulky, aromatic-ring containing tryptophan, while MC-RR contains two long-chain arginine residues, at the variable positions. This may suggest that binding of the 2H1 scFv to the structurally-diverse MC variants is inhibited by the presence of bulky side chains.

Preliminary cross-reactivity studies were also carried out on the mutant C12 scFv, revealing that that the antibody offered greater specificity towards certain MC variants, in comparison with the parent scFv, 2H1. Binding to the MC-LA, nodularin and MC-RR variants were improved by approximately 190 %, 67 % and 47 %, respectively. However, binding to the C12 scFv mutant to the MC-LF variant was reduced by almost 50 % and reactivity to MC-YR and MC-LW was also reduced, in comparison with the wild-type 2H1 scFv.

A.

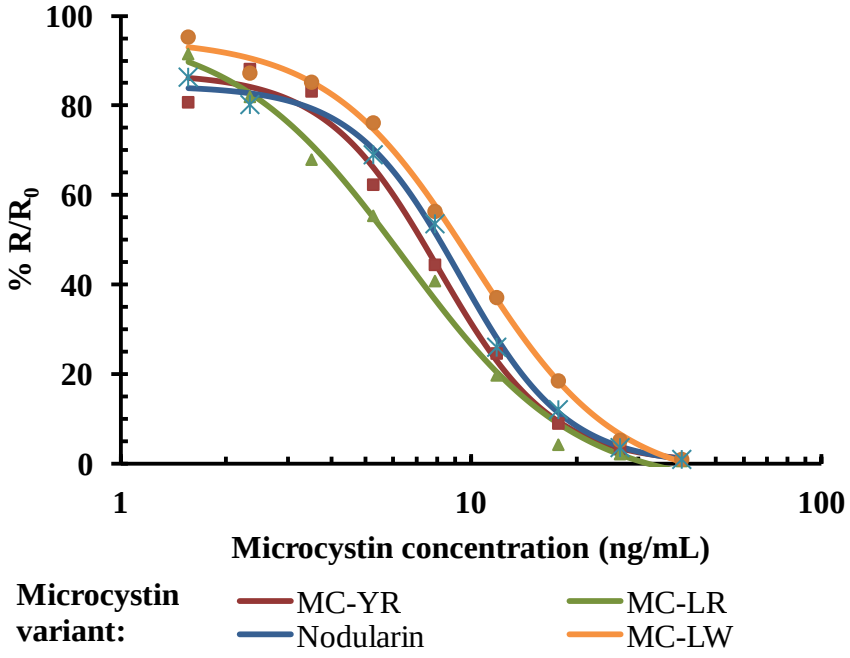

B.

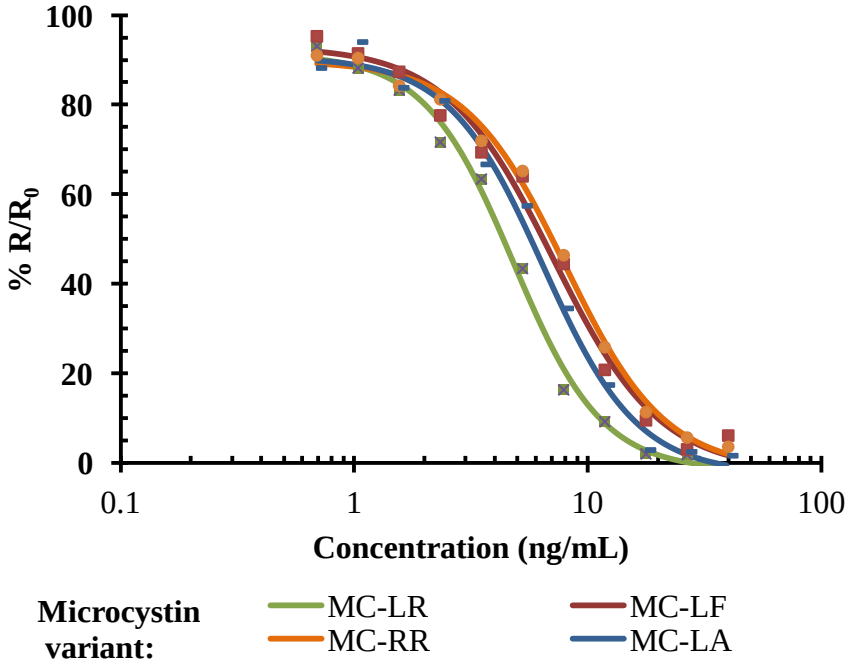

Figure 6.2.5.5: Cross-reactivity characterisation of the 2G1 scFv fragment, in HBS-EP buffer. A.) Comparison of MC-LR with the MC-YR, MC-LW variants and the related toxin, nodularin. B.) Comparison of MC-LR with the MC-LF, MC-RR and MC-LA variants. The normalised responses (R), expressed as % R/R_0, were plotted against the logarithm of the MC variant concentration (ng/mL).

A.

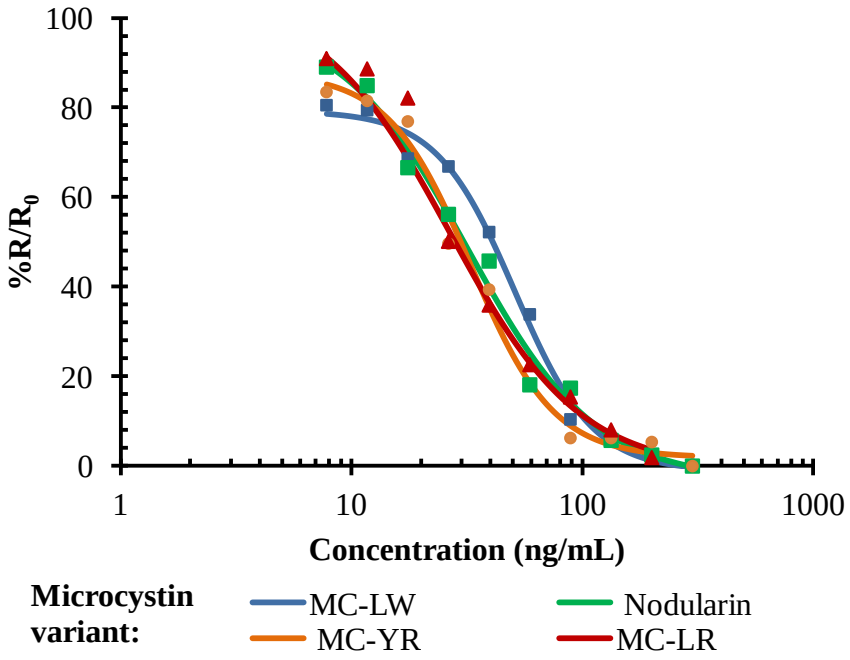

B.

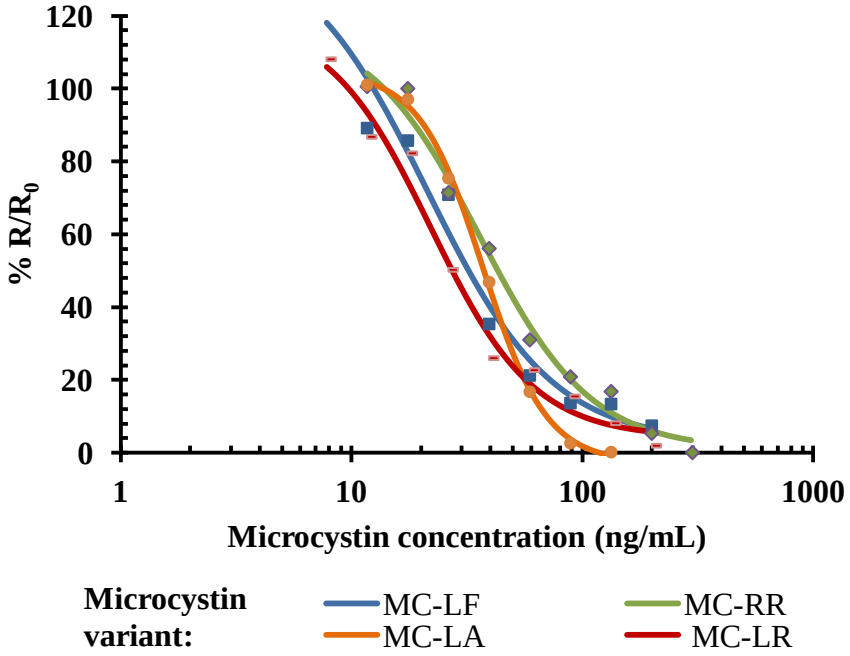

Figure 6.2.5.6: Cross-reactivity characterisation of the 2H1 scFv fragment, in HBS-EP buffer. A.) Comparison of MC-LR with the MC-YR, MC-LW variants and the related toxin, nodularin. B.) Comparison of MC-LR with the MC-LF, MC-RR and MC-LA variants. The normalised responses (R), expressed as % R/R_0, were plotted against the logarithm of the MC variant concentration (ng/mL).

Table 6.2.5.5: Summary of cross-reactivity analysis of 2G1, 2H1 and C12 antibody fragments. The cross-reactivity values were extrapolated from the IC_{50} value, which was estimated as 50 % B/B_0. The % CR_{50} values were determined as a percentage of the IC_{50} values for the MC-LR variant.

Cross-reactivity of MC toxins to 2G1 scFv fragment in HBS-EP buffer		
Analyte	**IC_{50} (ng/mL)**	**% CR_{50}**
MC-LR	4.8	100.0
MC-YR	8.1	79.7
MC-LA	6.4	74.8
MC-LF	7.1	67.5
MC-LW	10.1	63.7
MC-RR	7.9	60.1
Nodularin	9.3	69.3
Cross-reactivity of MC toxins to 2H1 scFv fragment in HBS-EP buffer		
Analyte	**IC_{50} (ng/mL)**	**% CR_{50}**
MC-LR	21.9	100.0
MC-YR	32.9	66.9
MC-LA	37.0	59.4
MC-LF	21.2	103.8
MC-LW	50.9	43.2
MC-RR	55.9	39.3
Nodularin	31.9	68.7
Preliminary cross-reactivity of MC toxins to C12 scFv fragment in HBS-EP buffer		
Analyte	**IC_{50} (ng/mL)**	**% CR_{50}**
MC-LR	25	100.0
MC-YR	48	52.1
MC-LA	22	113.6
MC-LF	43	58.1
MC-LW	80	31.3
MC-RR	30	83.3
Nodularin	25	100.0

6.2.6 Fluorescence immunoassay development for microcystin

Fluorescence immunoassays were developed, in parallel, using two antibody formats, a purified ‘in house’ rabbit polyclonal anti-microcystin antibody, and the novel scFv fragments, 2G1 and C12. The 2G1 and C12 scFvs were selected based on their high sensitivity and cross-reactivity to microcystin variants. The performance of a number of fluorescence immunoassay formats were compared, including the use of biotinylated antibodies, which were detected with fluorescent-streptavidin conjugates, and fluorescently-labelled antibodies. The assays were also incorporated onto a convenient slide-based immunoassay system for sensitive detection of microcystin.

6.2.6.1 Serum titration of MC-LR-OVA-immunised rabbit host

Following successive rounds of immunisation of a rabbit host, with MC-LR-OVA conjugate, a serum titre was performed, using MC-LR-BSA as the screening conjugate. Serum from the immunised rabbit was diluted (1/10 to 1/2,000,000) in 1 % (w/v) Milk Marvel in PBS, containing 0.05 % (v/v) Tween 20. These dilutions were tested against immobilised MC-LR-BSA (10 µg/mL), in a direct ELISA format. The immune rabbit serum was compared to a pre-bleed serum, taken prior to immunisation. A graph of absorbance versus the logarithm of the rabbit serum dilution is shown in Figure 6.2.6.1. The rabbit serum displayed a high titre in excess of 1/300,000 to the microcystin conjugate, making it ideal for the production of polyclonal antibodies.

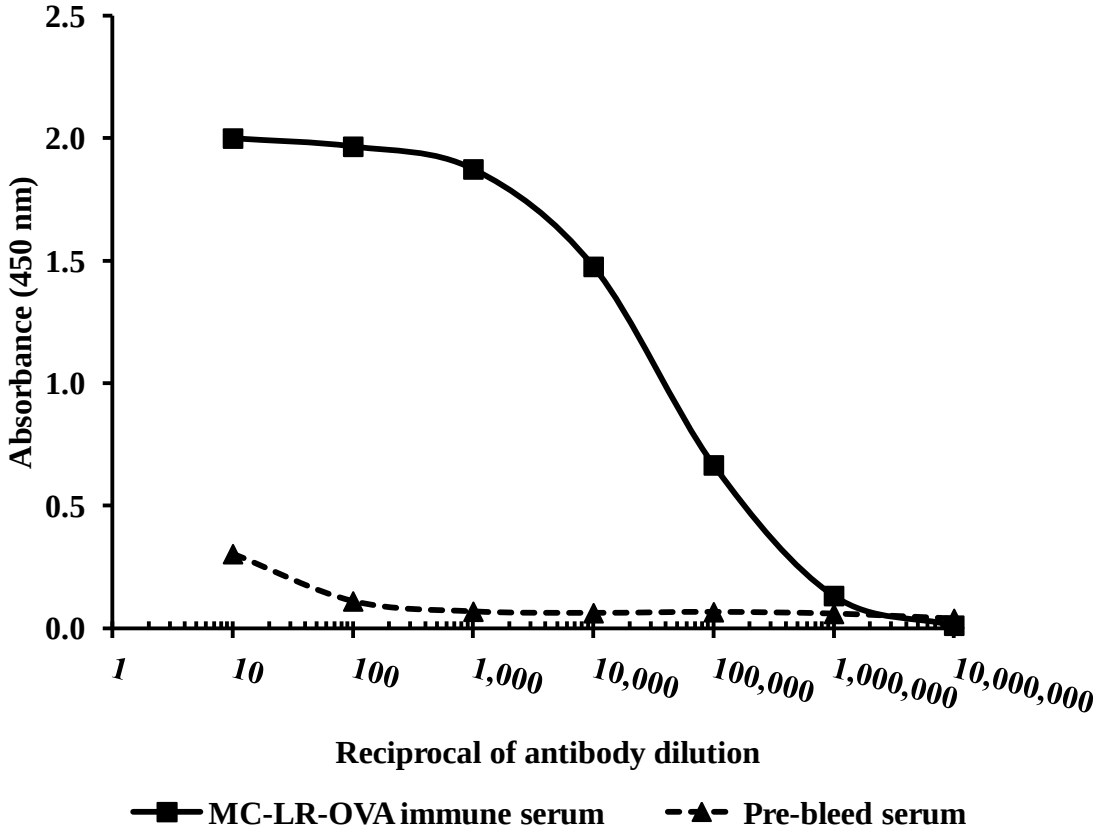

Figure 6.2.6.1: Titration of pre-bleed and immune serum from an MC-LR-OVA-immunised rabbit host. The ELISA plate was coated with an MC-LR-BSA conjugate, at a concentration of 10 µg/mL. Binding was detected with an anti-rabbit (IgG) antibody, conjugated to horseradish peroxidase (HRP). The ELISA was developed with TMB substrate and the absorbance was measured at 450 nm, using a Tecan™ Safire II plate reader.

6.2.6.2 Protein-G purification of rabbit IgG polyclonal antibody

The polyclonal antibody from the microcystin-immunised rabbit was purified from the immunoglobulin-rich immune serum, using protein G chromatography. Protein G affinity chromatography is a well established and reliable method for purifying whole antibodies from serum. The protein G-purified polyclonal antibody was compared to the crude immune serum, using SDS-PAGE analysis (Figure 6.2.6.2). The SDS-PAGE gel clearly illustrates that the antibody was efficiently purified from the impure serum sample. The two bands in lane B represent the heavy chain (~55 kDa) and the light chain (~25 kDa) of the polyclonal antibody, which had a high level of purity.

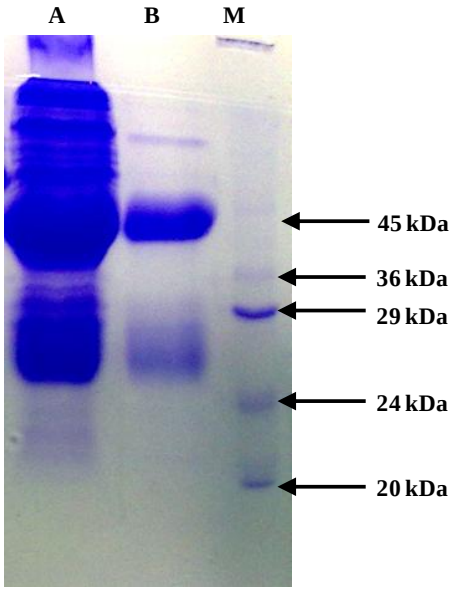

Figure 6.2.6.2: SDS-PAGE gel of fractions of protein G purification of rabbit anti-microcystin polyclonal antibody. The crude, unpurified serum (A), and the eluted purified polyclonal antibody (B), were analysed. A protein marker ladder (Sigma-Aldrich) was also loaded (M), for estimation of the apparent molecular weights of each of the protein samples.

6.2.6.3 Labelling of anti-microcystin scFv and polyclonal rabbit IgG with Alexa Fluor® 647 dye

A protein labelling kit was employed to directly label the recombinant (2G1) and polyclonal antibodies with Alexa Fluor® 647 reactive dye, via a succinimidyl ester moiety on the dye molecules. This moiety reacted with the primary amino groups on the antibody molecules to form stable amide linkages. The labelled antibodies were purified from the reaction mixtures, using size exclusion chromatography, on a P-30 purification resin. Differences in the molecular weight of the dye:antibody conjugate and the free dye, were used to separate the two components. The larger protein-dye conjugate eluted from the column first and was captured. The degree of labelling was calculated, based on the relative absorbances of the dye:antibody conjugates at 280 and 650 nm, respectively. It was estimated that the 2G1 scFv fragment contained approximately 1 mole of dye per mole of scFv and the rabbit IgG ratio was estimated at 6 moles dye per mole of IgG. The larger conjugation ratio for the IgG molecule was expected, as the full length antibody contains more primary amino groups for conjugation, in contrast to the single chain antibody fragment.

6.2.6.4 Biotinylation of anti-microcystin scFvs and polyclonal rabbit IgG

For the development of an indirect inhibition ELISA for MC-LR, the scFv fragments, 2G1 and C12 and the polyclonal antibody (IgG) were biotinylated, using a 100-fold excess of antibody (scFv or IgG) for efficient conjugation. A sulfo *N*-hydroxysuccinimde-LC activated biotin was used for labelling of the primary amino groups on the antibody molecules. After completion of the conjugation reaction, the conjugate was purified from non-conjugated biotin and microcystin, using molecular weight cut-off Vivaspin™ columns (10,000 Da MWCO). Identification of biotin in the conjugation reaction was assessed using a HABA (4'-hydroxyazobenzene-2-carboxylic acid)/ avidin assay. The scFv molecules (2G1 and C12) possessed approximately 2 millimoles of biotin per millimole scFv, and the IgG molecules contained approximately 7 millimoles of biotin per millimole of IgG. As expected, the IgG had a greater biotin incorporation ratio, compared to the smaller scFv fragments.

6.2.6.5 Optimisation of fluorescence immunoassay conditions

Before carrying out extensive assay development, the Z position and the bandwidth for the Tecan Safire II instrument were optimised. The Z position is defined as the optimal position of the well, corresponding to the focus of the optics of the instrument. The bandwidth of a monochromator is defined as the span of monochromator settings needed to move the image of the entrance slit across the exit slit. The bandwidth of the spectrofluorometer is changed by adjusting the width of the excitation and emission slits. Empirical optimisation revealed that a bandwidth of 12 nm was optimal for robust signal generation and a low signal to noise ratio.

The optimal plate coating concentration and antibody dilution was determined for the fluorescently-labelled 2G1 scFv fragment. Several concentrations of MC-LR-OVA (0.5 to 16 µg/mL) conjugate were compared with dilutions of 2G1-Alexa Fluor® 647, ranging from 1,00 to 1/12,000, in 1 % (w/v) Milk Marvel in PBS, containing 0.05 % (v/v) Tween 20. A graph of fluorescence intensity, arbitrary units (AU), versus the reciprocal of the labelled 2G1 scFv dilution was plotted (Figure 6.2.6.4). The optimal scFv concentration and corresponding conjugate coating concentration, which gave an adequate fluorescence signal, were determined. A signal of 20,000 AU was considered optimal for all fluorescence optimisation experiments. Dilutions were chosen to minimise the use of both protein and antibody conjugates. The optimal coating concentration was 8 µg/mL of MC-LR-OVA conjugate and the optimal scFv-fluorphore dilution was 1/500.

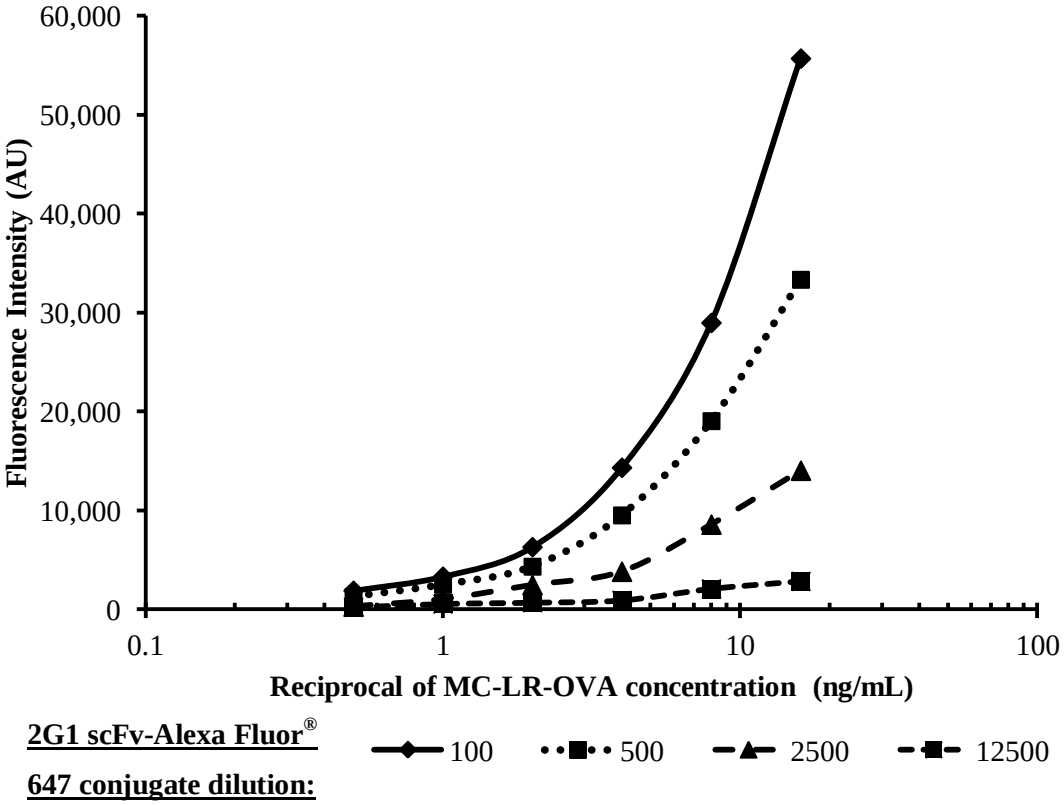

Figure 6.2.6.3: Checkerboard FLISA to determine optimal conjugate coating concentration (MC-LR-OVA) and optimal dilution of 2G1 scFv fragment. The scFv was directly-labelled with Alexa Fluor® fluorescent dye, using EDC-NHS conjugation. A graph of fluorescence intensity (AU) was plotted against the reciprocal of the conjugate concentration (ng/mL).

A checkerboard ELISA was also performed to calculate the optimal conditions for detection of IgG-Alexa Fluor® 647 binding (Figure 6.2.6.5). Similiar to the 2G1 scFv:fluorophore optimisation, different concentrations of MC-LR-OVA (0.5 to 16 µg/mL) were compared with dilutions of IgG-Alexa Fluor® 647, ranging from 1,00 to 1/12,000, in 1 % (w/v) Milk Marvel in PBS, containing 0.05 % (v/v) Tween 20. A graph of fluorescence intensity (AU), versus the reciprocal of the labelled IgG dilution was plotted (Figure 6.2.6.5). The optimal IgG concentration and corresponding conjugate coating concentration, which gave an adequate fluorescence signal, were calculated. The optimal coating concentration was 2 µg/mL of MC-LR-BSA conjugate and the optimal IgG-fluorphore dilution was 1/100.

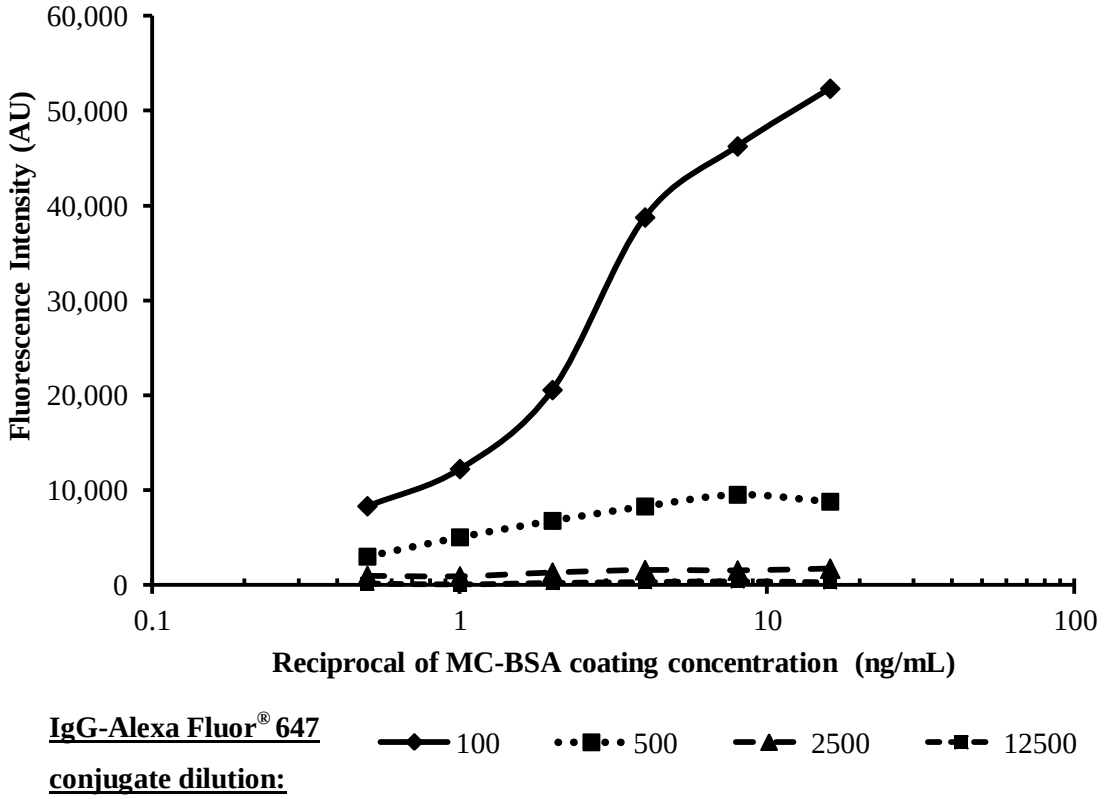

Figure 6.2.6.4: Checkerboard FLISA to determine optimal conjugate coating concentration (MC-LR-BSA) and optimal dilution of the Protein-G purified, rabbit polyclonal antibody. The IgG was directly-labelled with Alexa Fluor® fluorescent dye, using EDC-NHS conjugation. A graph of fluorescence intensity (AU) was plotted against the reciprocal of the conjugate concentration (ng/mL).

Optimisation experiments for fluorescence immunoassay development were also carried out for the biotinylated IgG, C12 and 2G1 antibodies. A number of parameters required optimisation, including the coating concentration, the dilution of biotinylated antibody and the dilution of streptavidin Alexa Fluor® 647 conjugate. The results of these optimisation experiments are summarised in Table 6.2.6.1.

Table 6.2.6.1: Optimisation of the conjugate coating concentration, the biotinylated antibody (rabbit IgG, 2G1 and C12 avian scFvs) dilution and the streptavidin-Alexa Fluor® 647 conjugate.

Biotinylated antibody	Conjugate	Conjugate coating concentration (ng/mL)	Biotinylated antibody dilution	Streptavidin Alexa Fluor® 647 conjugate dilution
Rabbit IgG-biotin	MC-LR-BSA	500 ng/mL	1/2,000	1/1,000
scFv 2G1-biotin	MC-LR-OVA	500 ng/mL	1/2,500	1/1,000
scFv C12-biotin	MC-LR-OVA	500 ng/mL	1/2,000	1/1,000

6.2.6.6 Fluorescence immunoassay development using the biotinylated mutant C12 scFv fragment

The fluorescence assay calibration curve for the C12 scFv fragment is shown in Figure 6.2.6.6. The normalised percentage fluorescence intensity (% F/F_0) was plotted against the logarithm of the MC-LR concentration (ng/mL), using BIAevaluation™ software. F represents the fluorescence intensity, while F_0 represents the fluorescence at a zero concentration of analyte. The data was normalised by expressing F as a percentage of F_0 (% F/F_0). The IC_{50} was calculated as 6.04 ng/mL. The preliminary limit of detection was calculated, as the mean of the normalised response for the zero value (no MC-LR), minus three standard deviations, at 0.6 ng/mL.

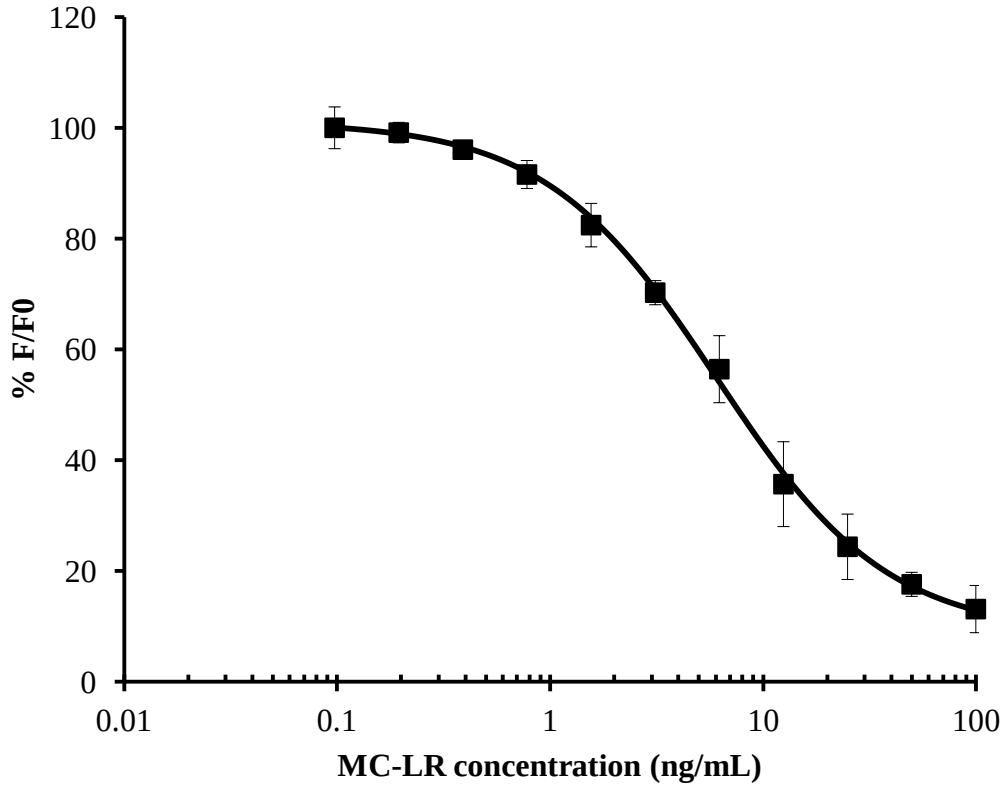

Figure 6.2.6.5: Calibration curve of FLISA with biotinylated mutant C12 scFv fragment, at an optimised concentration (1/2,000 dilution). Binding was detected using a streptavidin- Alexa Fluor® conjugate (1/1,000 dilution). Dilutions were prepared in 1 % (w/v) Milk Marvel, in PBS (150 mM, pH 7.4), containing 0.05 % (v/v) Tween. The error bars represent the standard deviation for each concentration.

6.2.6.7 Comparison of fluorescence immunoassay formats, using the labelled anti-microcystin antibodies

The fluorescence assay calibration curves for the labelled 2G1 scFv fragments are shown in Figure 6.2.6.7. The curves compare the sensitivity of the directly-labelled 2H1 scFv to the biotinylated scFv, as the percentage normalised fluorescence intensity (% F/F_0), versus the logarithm of the MC-LR concentration (ng/mL), using BIAevaluation™ software. The biotinylated scFv required a secondary detection fluorophore, in the form of a streptavidin Alexa Fluor® 647 conjugate. The use of biotin-streptavidin in the immunoassay resulted in a clear shift in assay sensitivity. This may be due to the presence of two millimoles of biotin, per millimole of scFv on the

2G1 scFv fragment. In contrast, the directly-labelled 2G1 scFv only contained approximately 1 mole of dye, per mole of scFv. Therefore, signal amplification may have occurred as a result of two-fold more biotin conjugated to the scFv, compared with the fluorophore-labelled scFv fragment (1:1 fluorophore:dye ratio). The antibodies may be analysed at different dilutions, but the F_0 values have been normalised (20,000 Au) to standardise the data.

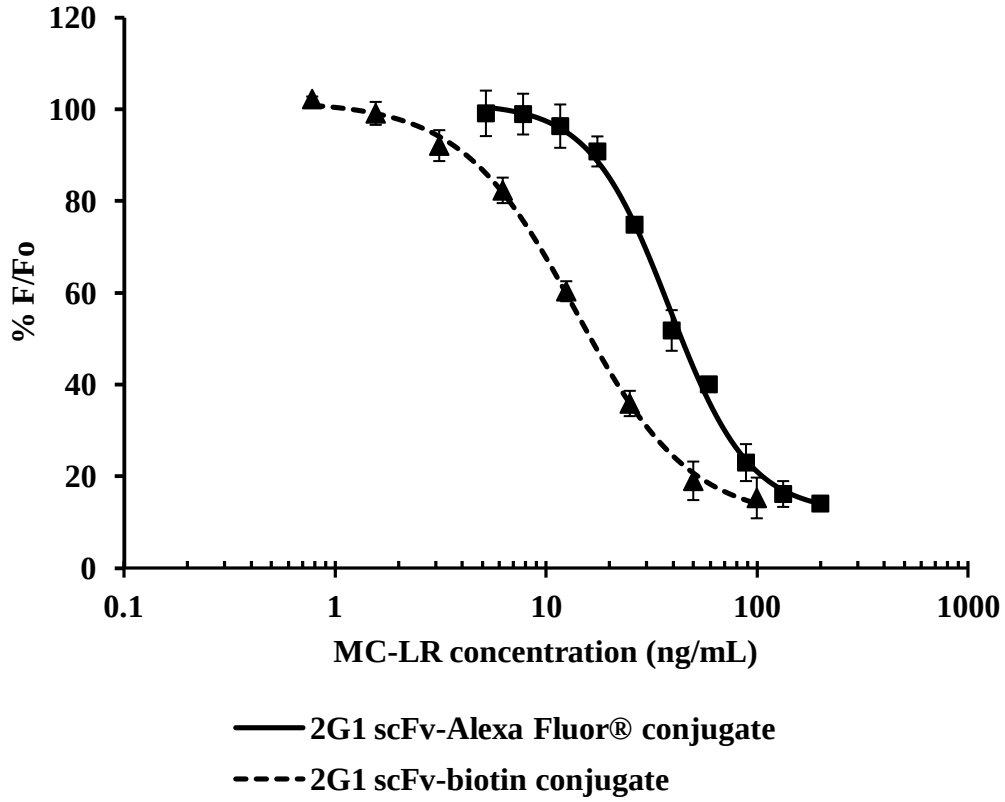

Figure 6.2.6.6: Comparison of calibration curves for FLISA with the 2G1 scFv-Alexa Flour® conjugate and the biotinylated 2G1 scFv fragment. Binding of the biotinylated 2G1 scFv fragment was detected with a streptavidin Alexa Fluor® 647 conjugate (1/1,000 dilution). Dilutions were prepared in 1% (w/v) Milk Marvel, in PBS (150 mM, pH 7.4), containing 0.05 % (v/v) Tween. The data was fitted into four-parameter fit equations, using BIAevaluation™ software.

The fluorescence assay calibration curves for the labelled IgG polyclonal antibody are illustrated in Figure 6.2.6.8. The curves compare the sensitivity of the directly-labelled IgG to the biotinylated IgG, as the percentage normalised fluorescence intensity (% F/F_0) versus the logarithm of the MC-LR concentration (ng/mL), using BIAevaluation™ software. The biotinylated IgG required a secondary detection fluorophore, in the form of a streptavidin Alexa Fluor® 647 conjugate. As the assay was already highly sensitive, little improvement in sensitivity was seen when the two assay formats were compared (Figure 6.2.6.8). As before, the antibodies may be analysed at different dilutions, but the F_0 values have been normalised (20,000 Au) to standardise the data.

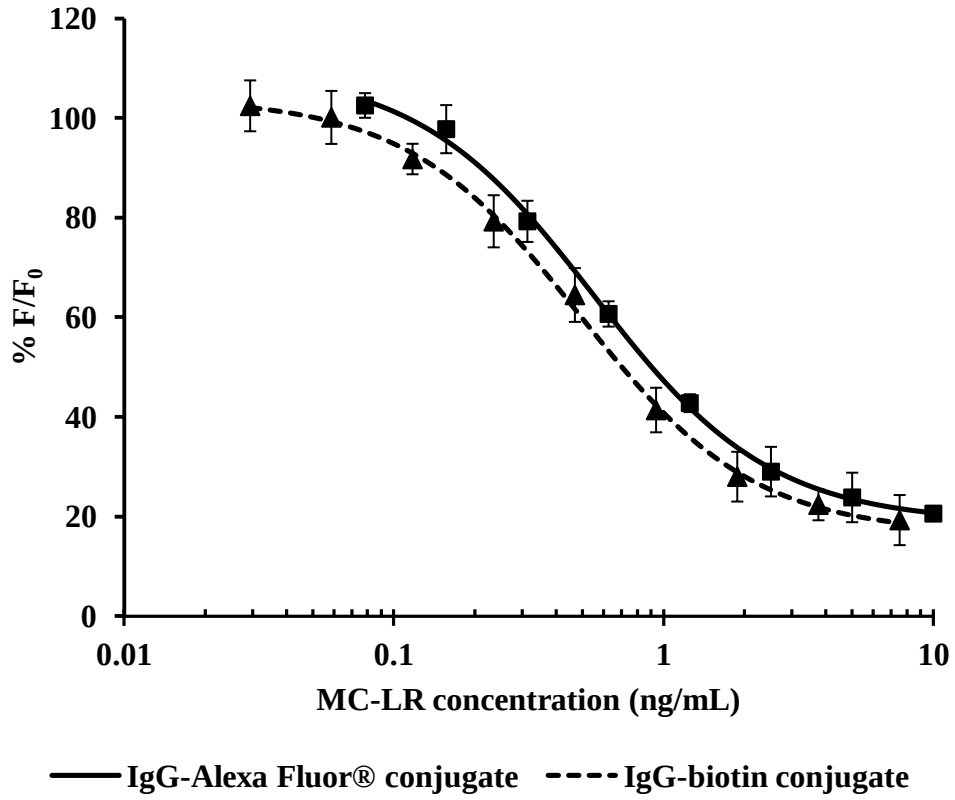

Figure 6.2.6.7: Comparison of calibration curves for FLISA with the IgG-Alexa Flour® conjugate and the biotinylated IgG polyclonal antibody. Binding of the biotinylated IgG was detected with a streptavidin Alexa Fluor® 647 conjugate (1/1,000 dilution). Dilutions were prepared in 1 % (w/v) Milk Marvel, in PBS (150 mM, pH 7.4), containing 0.05 % (v/v) Tween. The data was fitted into four-parameter fit equations, using BIAevaluation™ software.

A comparison of the assay sensitivities achieved using the fluorescence-immunoassay formats is summarised in Table 6.2.6.2. It is clear that the most sensitive antibody and assay formats were achieved using the fluorophore and biotin-labelled rabbit IgG antibodies, which resulted in limits of detection significantly lower than the regulatory limit of 1 ng/mL (0.3 and 0.2 ng/mL, respectively). Moreover, although the fluorescently-labelled 2G1 scFv did not reach the limit of detection (17.7 ng/mL), the biotin-labelled 2G1 scFv format achieved a limit of detection of 1.4 ng/mL. This change in fluorescence assay format resulted in an approximately 13-fold improvement in sensitivity. The biotinylated C12 mutant showed an excellent cross-reactivity below the limit of detection (0.6 ng/mL). Therefore, this fragment was used for further proof-of-concept immunoassay studies.

Table 6.2.6.2: Comparison of the IC_{50} and LOD values from the rabbit polyclonal and the 2G1 and C12 antibodies, using different immunoassay formats. Calibration curves were fitted, using a four parameter equation and the IC_{50} was calculated, as the MC-LR concentration, required to inhibit 50 % of antibody binding. The corresponding LOD was calculated from the equation, as the mean zero value, minus three standard deviations.

Antibody	Directly-labelled Alexa Fluor® 647 antibodies	Biotinylated antibodies, detected, using streptavidin Alexa Fluor® 647
Rabbit polyclonal (IgG)	IC_{50} = 0.6 ng/mL LOD = 0.3 ng/mL	IC_{50} = 0.5 ng/mL LOD = 0.2 ng/mL
2G1 scFv fragment	IC_{50} = 38.5 ng/mL LOD = 17.7 ng/mL	IC_{50} = 13.7 ng/mL LOD = 1.4 ng/mL
C12 scFv fragment	-	IC_{50} = 6.0 ng/mL LOD = 0.6 ng/mL

6.2.6.8 'Proof-of-concept' slide-based fluorescence immunoassay development

For 'proof-of-concept' a number of immunoassays were carried out on a poly-L-lysine functionalised glass slide, separated using a slide divider, to create wells for immunoassay spots. Optimised concentrations of antibody were incubated with a range of MC-LR concentrations (0.032 to 20 ng/mL) at room temperature for 20 minutes. The inhibition assay was carried out on the functionalised-glass substrate, which was previously coated with 4 µg/mL MC-LR-OVA and blocked with 5 % (w/v) Milk Marvel, in PBS.

Adhesive slide dividers were prepared, by the School of Physical Sciences, DCU, and all assay steps were carried out in the slide divider wells. After protein incubation and washing steps, the slide divider was removed and the fluorescence was quantified using a Perkin Elmer™ Scannarray Express scanner, under optimal conditions (see Section 2.18.9). Image analysis software (AIDA) was employed to quantify the pixel intensity in each spot in a defined area (Figure 6.2.6.9). The pixel intensity values were normalised to the negative spot intensity value (no MC-LR) and expressed as F/F_0. The F/F_0 value was plotted against the logarithm of the MC-LR concentration. Preliminary results for the inhibition assay curves generated for IgG-Alexa Fluor® 647, 2G1-Alexa Fluor® 647 and C12-biotin, detected with streptavidin-Alexa Fluor® 647, are shown in Figure 6.2.6.9 B, C and D, respectively. A representation and comparison of the assay sensitivities achieved using the microplate and slide-based assay is summarised in Table 6.2.6.3.

A.

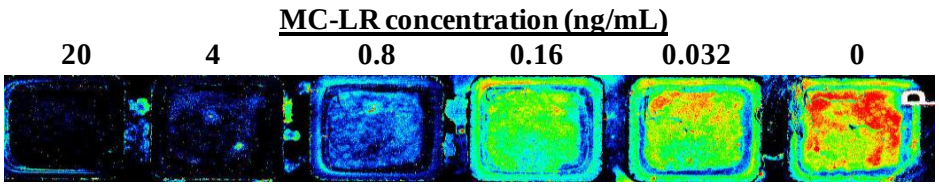
MC-LR concentration (ng/mL)
20
4
0.8
0.16
0.032
0

B.

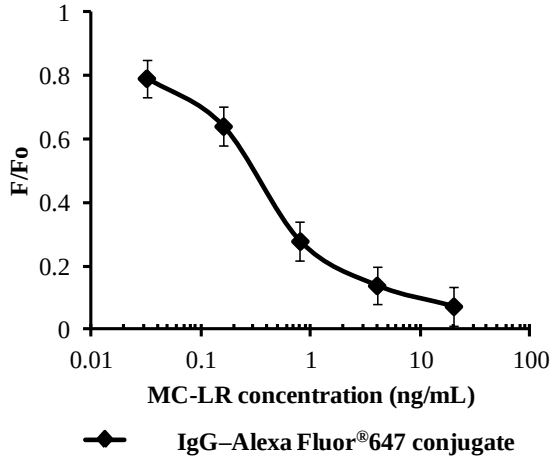
F/Fo
1
0.8
0.6
0.4
0.2
0
0.01
0.1
1
10
100
MC-LR concentration (ng/mL)
IgG–Alexa Fluor®647 conjugate

C.

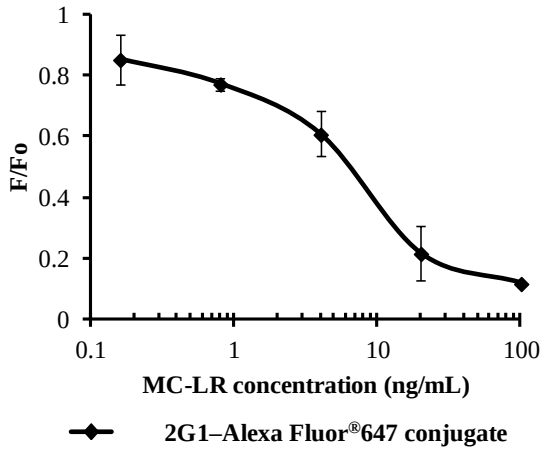
F/Fo
1
0.8
0.6
0.4
0.2
0
0.1
1
10
100
MC-LR concentration (ng/mL)
2G1–Alexa Fluor®647 conjugate

D.

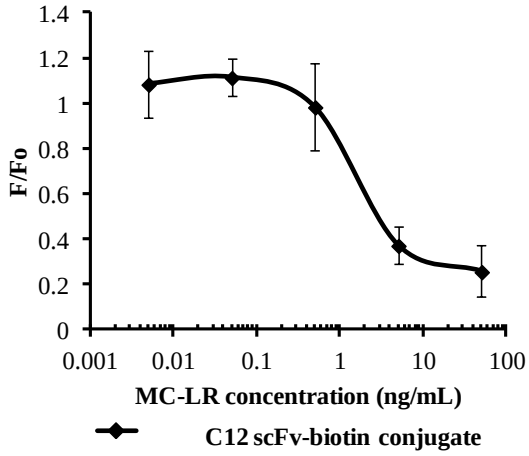
F/Fo
1.4
1.2
1
0.8
0.6
0.4
0.2
0
0.001
0.01
0.1
1
10
100
MC-LR concentration (ng/mL)
C12 scFv-biotin conjugate

Figure 6.2.6.8 (previous page): Proof of concept analysis of fluorescence immunoassay for detection of MC-LR, on poly-L-lysine functionalised glass slides. The inhibition immunoassay was carried out on individual conjugate-coated spots on the glass substrate, created using adhesive slide dividers. Fluorescence was quantified on a Perkin Elmer™ Scanarray Express instrument. Inhibition curves were generated as the normalised fluorescence (F/F_0), versus the MC-LR concentration (ng/mL). A.) Image of spots from an inhibition assay, using the Alexa Fluor® 647- labelled rabbit polyclonal antibody. As the MC-LR concentration decreased, the signal or pixel intensity increased, as measured by an increase in the colour intensity. B.) Inhibition assay curve of IgG-Alexa Fluor® 647 C.) Inhibition assay curve of 2G1-Alexa Fluor® 647. D.) Inhibition assay curve of C12-biotin, detected with streptavidin-Alexa Fluor® 647. The error bars represent the standard deviation for each data point and the mean was calculated from three separate experiments.

Table 6.2.6.3: Comparison of the IC_{50} values from the rabbit polyclonal and the 2G1 and C12 antibodies, using the microplate and slide-based fluorescence immunoassays. The IC_{50} values for the slide assays were calculated, as the MC-LR concentration, required to inhibit 50 % of antibody binding. The corresponding LOD was calculated from the equation, as the mean zero value, minus 3 standard deviations.

Antibody (Rabbit IgG)	**Directly-labelled Alexa Fluor® 647**
Plate Assay	IC_{50} = 0.55 ng/mL
Slide Assay	IC_{50} = 0.40 ng/mL (approximate)
Antibody (2G1 scFv)	**Directly-labelled Alexa Fluor® 647**
Plate Assay	IC_{50} = 38.52 ng/mL
Slide Assay	IC_{50} = 6.00 ng/mL (approximate)
Antibody (C12 scFv)	**Biotinylated antibody with streptavidin Alexa Fluor® 647 detection**
Plate Assay	IC_{50} = 6.04 ng/mL
Slide Assay	IC_{50} = 1.00 ng/mL (approximate)

6.3 Discussion

Recombinant antibodies can be covalently attached to drugs (Schrama *et al*., 2006) or toxins (Schmidt *et al*., 1999) for targeted cancer therapies or engineered for different specificities and affinities (Korpimäki *et al*., 2004; Holliger *et al*., 2005; Maynard and Georgiou, 2000). Both random and site-directed mutagenesis strategies can be employed for recombinant antibody improvement. In this work, novel recombinant scFv molecules were isolated from an immune library by phage display, and subsequently these scFvs were improved though affinity mutagenesis. The ability to mutate antibodies at the genetic level is a powerful tool in the antibody engineering repertoire. Specific properties of these molecules, such as stability, specificity, and in some cases catalysis, can be enhanced using mutagenesis techniques (Marks, 2004). Error-prone PCR has become one of the most common techniques for random mutagenesis. Using error-prone PCR, mutations can be precisely targeted to specific sequences, including CDR regions. Furthermore, the error rate of this technique can be tightly controlled and unlike other methods it avoids the use of hazardous chemicals. Furthermore, mutagenesis results using error-prone PCR can be obtained in a relatively short period of time (Cirino *et al*., 2003; Pritchard *et al*., 2005). Moreover, the employment of both chain shuffling and error-prone PCR in combination has the advantage of more closely mimicking the in vivo antibody maturation process.

The 2H1 avian scFv clone was chosen for affinity maturation. Following error-prone PCR amplification of the mutant light chain library, and non-error-prone PCR amplification of the parent heavy chain from the 2H1 scFv clone, the V_L and V_H gene fragments were joined by overlap extension PCR. The assembled single chain Fv fragments were cloned into the pComb3XSS phagemid vector. The library was subsequently transformed into electrocompetent *E.coli* XL-1 Blue cells. During the bio-panning process, a competitive elution strategy was performed in parallel with a trypsin elution strategy in the last rounds of bio-panning, with the aim of selecting improved binders in solution. Polyclonal phage ELISA showed that a large increase in the output phage was observed in round 2. These binders were eliminated during subsequent stringent bio-panning rounds. Encouragingly, a second enrichment of phage binders was observed in the fourth round of phage bio-panning, from the trypsin-eluted phage population.

No enrichment was observed for the competitively-eluted rounds, or for the fifth round of bio-panning. This may be because the bio-panning strategy was too stringent or the number of positive binders was too small to create a discernable signal. Clones were selected and screened from both bio-panning rounds, for both bio-panning strategies, by monoclonal phage ELISA. Phage pools were infected into a non-suppressor strain of *E. coli* (TOP10F′) and 96 clones from rounds 4 and 5 (trypsin and competitive elution) were solubly expressed and screened, by indirect ELISA. The majority of randomly-picked clones demonstrated significant binding reactivity to the MC-LR-OVA conjugate. A higher percentage of positive binders were evident in the trypsin-eluted clones, compared with the competitively-eluted clones. In addition, no significant binding was observed to the negative control proteins, BSA and OVA.

It has been reported that certain single amino acid insertions and deletions are generally well-tolerated and permit the production of correctly-folded recombinant antibody molecules, which retain their antigen recognition properties (Lantto and Ohlin, 2002). Sequence analysis of the anti-microcystin scFvs from the mutant avian library showed that no alternative light chain combinations were selected. This data strongly suggests that the existing light chain is the best partner for the parent heavy gene sequence, as re-selection from the light chain pool did not find a superior binding combination. A future avenue of research would be to reverse the chain shuffling process and perform heavy chain shuffling. It is possible that an alternative heavy chain combination could have yielded an improved anti-microcystin scFv with a higher sensitivity. In this research, the increased sensitivity of the C12 scFv most likely relates to its altered amino acid sequence. From the sequencing analysis, it is clear that the 2H1 and C12 clones are different, with five amino acid substitutions evident in the framework regions. Even though extensive PCR mutagenesis was carried out, only a small number of missense mutations occurred between the two sequences. It is possible that the mutant scFv library was highly diverse during the initial rounds of bio-panning. However, with subsequent rounds of harsh selection, the diversity of the scFv library was most likely reduced.

Even with this small number of amino acid changes in the framework region of the antibody, the binding properties of the antibody were significantly affected. In the ELISA comparison of the 2H1 and C12 clones, a two-fold increase was seen in the

LOD values, compared to the wild-type clone. Biacore™ inhibition analysis showed that the cross-reactivity profiles of C12 for the microcystin variants, MC-LA, nodularin and MC-RR, were significantly increased. In comparison to the parental 2H1 scFv, the C12 mutant scFv had a 190 % (MC-LA), 67 % (nodularin) and 47 % (MC-RR) improvement in binding to these MC variants. However, C12 reactivity to MC-LF, MC-YR and MC-LW were decreased. This is highly significant since a prerequisite for microcystin quantification is that the cognate antibody displays a good cross-reactivity profile for commonly-occurring microcystin variants. Therefore, the random mutagenesis approach resulted in an improved antibody specificity for some microcystin variants, which may aid in the accurate quantification of total toxin content in a sample. Importantly, this is the first report of an improved recombinant avian anti-MC scFv fragment.

The development of an easy-to-use, rapid, robust and non-expensive method for the measurement of low concentrations of microcystin has been recognised as a high priority (WHO, 1998). Biochemical methods for microcystin detection including immunoassay (Zeck *et al.*, 2001; Sheng *et al.*, 2007; Khreich *et al.*, 2009) and enzyme assays (protein phosphatase inhibition assay) (Metcalf *et al.*, 2001; Campàs *et al.*, 2005), are currently replacing un-ethical and inaccurate *in vivo* assays and expensive analytical detection systems. Although some of these methods are less qualitative, compared with the physiochemical methods, they are still equally sensitive. Moreover, some of these methods are more rapid, making them particularly useful for the screening of environmental samples (Carmichael and An, 1999).

Strachen *et al*. (2002) demonstrated that a highly-sensitive recombinant scAb antibody to microcystin could be selected from the non-immune Griffin I library, with sensitivities that ranged from 13 to 2,000 nM. Recombinant fragments (scAbs) were subsequently isolated from the Griffin I library with LODs as low as 0.8 nM (McElhiney *et al.*, 2002). Antibodies were previously isolated by the same group using the Tomlinson I library, however, these antibodies did not prove sensitive enough for detection below regulatory limits (4 µM) (McElhiney *et al.*, 2000). The CDRH3 of the Tomlinson I library is conserved at seven amino acids, while the Griffin I library incorporates variable heavy-chain CDR3 lengths. This may explain how a more sensitive antibody to microcystin was isolated from the Griffin I source, which had

CDRH3 of 10 amino acids long. This group postulated that improved antibody:hapten recognition may be associated with the length of the complementary determining region (CDRH3) in the heavy chain variable domain. The CDRH3 is known to play a major role in antigen binding (Johnson and Wu, 1998). Studies have shown that long CDRH3 regions are capable of forming anti-hapten binding pockets (Strachen *et al*., 2002).

A Biacore™ surface plasmon resonance biosensor was used as an assay platform to analyse the interaction of novel recombinant antibodies with covalently immobilised-microcystin-LR. The SPR detector monitors changes in resonance angle due to molecular interaction at the interface which is directly proportional to the change of mass at the surface. SPR biosensor techniques have proven to be versatile, robust and capable of producing rapid and reliable results, with minimum sample preparation (Baxter *et al*., 2001). Two of the clones from the original avian phage display library (2H1 and 2G1) were brought forward for SPR analysis, and their ability to bind microcystin was compared with the C12 mutant. The inhibition assays for the 2H1 and C12 scFv fragments had an IC_{50} value of 33.5 and 28.2 ng/mL, and LOD values of 13.8 and 14.8 ng/mL, respectively. The range of detection for these clones, at which the assays were both accurate and precise, was 7.8 to 59.3 ng/mL. However, the 2G1 scFv displayed a dramatically increased sensitivity to MC-LR and its variants, using Biacore™ inhibition analysis, compared to the ELISA analysis. The 2G1 scFv displayed an IC_{50} and limit of detection of 6.2 and 1.7 ng/mL, respectively. This was unexpected as the 2G1 had previously displayed comparable sensitivity to 2H1 by ELISA. The 2H1 scFv clone was chosen for mutagenesis based on ELISA analysis. It was not known at the time of mutant library construction that the 2G1 clone was more sensitive in an SPR format. It was demonstrated previously in this laboratory (unpublished results) that the same recombinant antibody may display remarkable different sensitivities depending on the format of analysis (ELISA or Biacore™).

Cross-reactivity analysis showed that the three antibodies were cross-reactive to varying extents with the microcystin variants MC-LW, MC-LF, MC-LA, MC-RR and MC-YR. The side-chains of MC-LR consist of a hydrophobic leucine (L) residue and a basic arginine (R) residue. The variant MC-LW and MC-LF both contain bulky tryptophan (W) and phenylalanine (F) residues respectively. These residues may have negatively impacted the interaction of the MC antigen with the binding sites on the scFv molecules

(Egloff *et al*., 1997). In this report, it was shown by *in silico* docking analysis that microcystin has the potential to bind to different sites of the 2G1 scFv structure (Section 5.3.2.5). Therefore, the 2G1 scFvs may bind microcystin and its variants in different ways and at different sites. Overall, the 2G1 scFv displayed the best specificity, with IC_{50} values in the range of 4.8 to 10.08 ng/mL, for all the variants tested, using Biacore™ inhibition analysis.

SPR has become a widely used technique, because 'real-time' and 'label-free' assays can be performed in complex matrices without the need for sample clean-up. A number of SPR immunosensors have recently been described for microcystin in drinking water (Herranz *et al*., 2010). In one such method, a competitive inhibition format is used, in which MC-LR was immobilised onto an SPR chip functionalised with a self-assembled monolayer. In this format, the assay gave an IC_{50} of 0.67 µg/L and cross-reacted with MC-RR and MC-YR. An SPR inhibition immunoassay was also developed using a monoclonal antibody to microcystin with a Biacore™ 3000 biosensor (Hu *et al*., 2009). In this assay, a MC-BSA conjugate was immobilised onto a CM5 chip surface and inhibition occurred with MC-LR in solution. The assay was sensitive in the 1 -100 µg/L range. Additionally, a rapid SPR immunobiosensor assay was developed for detection of microcystin in blue-green algae food supplements (Vinogradova *et al*., 2011). The biosensor results were in good agreement with an established LC–MS/MS assay. The assay is advantageous because it employs a simple clean-up procedure, compared to chemical assays. The SPR assays developed in this research compared favourably with these assays in terms of sensitivity and specificity. SPR has been successfully employed to detect small molecules and haptens in a multitude of food and environmental samples (Dostálek *et al*., 2006; Shankaran *et al*., 2007). Alternative biosensor techniques developed for microcystin detection include molecular-imprinted polymer (MIP)-sensors (Chianella *et al*., 2002), electrochemical immunosensors (Campàs *et al*., 2005; Campàs and Marty, 2007; Loyprasert *et al*., 2008) and evanescent wave immunosensors (Long *et al*., 2008; Long *et al*., 2009).

This chapter also described the production and characterisation of rabbit polyclonal antibodies and their subsequent use in the development of fluorescence-based immunoassays for the detection of microcystin. The applicability of a glass slide-based biosensor for the detection of MC-LR was investigated. Two recombinant scFv

antibodies, 2G1 and C12, were biotinylated, using EDC-NHS coupling chemistry. In addition, the 2G1 scFv was also directly labeled with an Alexa Fluor® 647 dye molecule via a succinimidyl ester moiety. In parallel the rabbit IgG was also functionalised with biotin and Alexa Fluor® 647. Initially, all reagents were tested in a FLISA plate format. For indirect FLISA analysis, the MC-LR toxin competed for antibody binding with the immobilised microcystin conjugate. In addition, the biotinylated antibody was detected using a commercially available streptavidin-Alexa Fluor® 647 conjugate.

A calibration curve was generated for the detection of MC-LR using the mutant C12 scFv-biotin conjugate. This assay displayed an IC_{50} and a limit of detection of 6 and 0.6 ng/mL, respectively. In contrast, the same clone displayed a limit of detection in a standard, ELISA format of 1.4 ng/mL. The introduction of fluorescence in combination with the biotin-streptavidin system resulted in an approximate 2-fold increase in assay sensitivity, bringing the detection limit below the WHO guideline value of 1 µg/L (1 ng/mL). The assay performance of the 2G1-Alexa Fluor® 647 conjugate was compared with the biotinylated-2G1 conjugate by FLISA. Significantly, the biotinylated-2G1, in combination with the streptavidin conjugate, displayed a 13-fold increase in assay sensitivity, compared with the fluorescently-labelled 2G1 scFv (LODs of 17.7 and 1.4, respectively). The same comparison was carried out, between biotinylated-IgG and fluorescently-labelled IgG polyclonal antibody, but no significant shift in assay sensitivity was observed. Previously, Pyo *et al*. (2007) compared fluorescence and colloidal gold-based immunochromatographic strip assays for detection of MC-LR using a fluorophore-conjugated MC-LR and gold-conjugated MC-LR monoclonal antibody, respectively. This assay was capable of sensitively detecting MC-LR at the test site without having to transfer to the laboratory. Additionally, Yu et al. (2011) incorporated antibody-conjugated quantum dots and antigen-coated magnetic beads into a bead-based fluorescence assay for microcystin detection. The assay displayed a limit of detection of 0.03 µg/L and an assay time of 30 minutes. It is clear that fluorescence assay development can provide unique advantages in terms of low detection limits, accuracy and short assay times.

Three highly sensitive FLISA assays, developed on black NUNC™ plates were transferred to an immunoassay on a functionalised glass slide for a ‘proof-of-concept’

experiment. These assays incorporated the IgG-Alexa Fluor® 647 conjugate and the 2G1-Alexa Fluor® 647, as well as the biotinylated C12 mutant scFv. The directly-fluorescently-labeled antibodies were included, as only one inhibition step is required prior to detection, which dramatically shortens the immunoassay time. The poly-L-lysine functionalised glass slides can be efficiently coated with microcystin conjugate and blocked, prior to addition of the test sample. This resulted in a rapid and sensitive FLISA format for MC detection. The preliminary inhibition curves obtained on the slide immunoassays clearly demonstrate improved IC_{50} values, compared with the plate immunoassays. The 2G1-Alexa Fluor® 647 conjugate displayed a 6-fold increase in sensitivity (IC_{50} values of 38.52 and 6 ng/mL, for plate- and slide-based assays, respectively). Due to time constraints, it was not possible to determine an accurate LOD value. The biotinylated C12 scFv fragment also displayed a 6-fold increase in sensitivity, with IC_{50} values of 6.04 and 1 ng/mL for the plate- and slide-based assays, respectively.

Recently, an ultra-rapid one-step fluorescence immunochromatographic assay was described for the detection of microcystin (Kim *et al*., 2003) which could detect contamination 'on-site' in 15 minutes. This assay utilised fabricated assay strips and a portable laser fluorescence scanner. Linder and co-workers reported the establishment of a highly sensitive immunoassay for the detection of MC-LR, based on the immobilisation of a biotin-MC-LR conjugate to the surface of a microplate and detection using a commercially-available monoclonal antibody, MC10E7 (Lindner *et al*., 2004). The immunoassay was used to detect microcystin in spiked water samples. It is apparent that the surface-based immunosensor format developed in this research displays great potential for the development of an 'easy-to-use', rapid and sensitive FLISA for microcystin detection. APTES-treated glass slides were also used in FLISA development, but the surfaces were not uniform and reproducible results could not be obtained. The novel slide dividers provided an effective method for the utilisation of plain, glass substrates for assay development. The rapid fabrication techniques used, allowed for the specific tailoring of the size, shape, well volume and substrate material, to meet the requirements for the various steps of assay development. In addition, the slide dividers can be made in large quantities and they are disposable, which is very convenient for toxin handling.

In conclusion, this chapter describes in detail the application of a random mutagenesis approach for the generation of improved anti-microcystin recombinant antibodies. The heavy chain of the 2H1 clone and the variable light chain genes of the pre-existing anti-microcystin avian library, in combination with error-prone PCR, were used in the construction of a mutant avian library. A mutant clone, C12, was isolated which displayed improved sensitivity. The recombinant antibodies were incorporated into Biacore™-based immunoassay formats, in which the 2G1 scFv displayed the best microcystin sensitivity (1.7 ng/mL). Interestingly, in comparison to the parent 2H1 antibody the C12 mutant scFv displayed better cross-reactivity to a panel of microcystin variants. It is probable that the small number of amino acid substitutions, in the framework region of the mutant sequence, has an effect on microcystin detection sensitivity and specificity. Mutations associated with affinity improvement are generally located in the CDR regions (Johnson and Wu, 1998; Lamminmaki *et al*., 1999). However, in this situation, a small number of framework mutations, resulted in improved binding capacity. These missense mutations may have caused slight shifts in the positioning of the CDR regions, thus improving antibody:antigen interaction. Fluorescence-based immunoassays were developed on glass substrates, with the mutant clone, C12, displaying high sensitivity, with an IC_{50} of approximately 1 ng/mL. With a limit of detection below 1 ng/mL, this assay format has the potential to be incorporated into a commercial, immunoassay microcystin detection system.

Chapter 7

Overall Conclusions

7.1 Overall conclusions

The research in this thesis describes an investigation of the immunomodulatory effects of phycotoxins and mycotoxins on murine macrophage function *in vitro*, using both 'real-time' and end-point analysis. In addition, the production of immune recombinant libraries to the shellfish and water contaminants, microcystin and azaspiracid are also described. Furthermore, the generation, purification and characterisation of highly, sensitive single chain antibody fragments to microcystin, is discussed in detail. Following affinity maturation of an scFv fragment, sensitive ELISA, Biacore™ and fluorescence-based assays were developed for detection of microcystin and its variants, below the WHO regulatory limit.

Chapter 3 contributed to the understanding of some of the biological processes underlying macrophage dysfunction in the presence of the toxins, azaspiracid-1, microcystin-LR and aflatoxins B_1, B_2 and G_1. One of the key parameters under investigation was the effect of immunosuppression on the macrophage response to microbial pathogens (LPS) and, therefore, host resistance. Under the threat of infection, activated macrophages produce pro-inflammatory cytokines (TNF-α, IL-1, IL-6 and IL-12p40) and anti-inflammatory cytokines (IL-10) to regulate the inflammatory response. In this report, the cytokine profile, following toxin exposure, provided vital information regarding the nature of the immunotoxic response. This is the first report of an investigation into the *in vitro* effects of AZA-1 on the murine macrophage cell line, J774A.1. AZA-1 significantly reduced the viability of the macrophages at a concentration of 100 pg/mL, in comparison to the control, but the effect was eliminated with the addition of stimulatory LPS (WST-1 assay). In the LDH cytotoxicity assay, the macrophages displayed a significant decrease in percentage cytotoxicity (i.e. increased cell survival), compared to the control, at concentrations of 0.1 and 0.01 pg/mL. This effect was replicated when the cells were exposed to toxin and LPS simultaneously. It is possible that a protection mechanism is activated in the macrophage cells when specific toxin concentrations (0.1 and 0.01 pg/mL) are reached, which aids in cell survival. However, at higher toxin concentrations (1-100 pg/mL), this unknown mechanisms may be overwhelmed, which results in cytotoxicity effects.

The significant effects of AZA-1 on macrophage viability and cytotoxicity, lead to the further investigation of AZA-1 *in vitro*. It was discovered that the AZA-1 significantly suppressed the ability of macrophages to respond to LPS activation, through analysis of

the pattern of cytokine expression. AZA-1 significantly reduced the expression of pro-inflammatory TNF-α and IL-6, in LPS-stimulated macrophages, thereby decreasing the macrophages ability to signal to other immune cells and to stimulate the inflammatory response to infection. In contrast, levels of pro-inflammatory IL-12p40 and anti-inflammatory IL-10 were significantly increased, through AZA-1 exposure, but there was no significant effect on responsiveness to LPS stimulation. Overall, it is possible that AZA-1 can modulate the ability of murine macrophages to mount an inflammatory response to invasion by Gram-negative bacteria, as shown by cytotoxicity and cytokine analysis. The murine and human genomes are 85 % homologous (Makalowski *et al*., 1996). Therefore, this murine model provides an insight into the possible threat that AZA-1 poses to the human immune system.

In this chapter, it was also shown that macrophage function was down-regulated through exposure to the cyanobacterial toxin, microcystin. The anti-proliferative effect of microcystin on the murine macrophages, J774A.1 was significant, as this effect has not been demonstrated previously. Exposure to MC-LR resulted in a time-dependent increase in cytotoxicity, both in the presence and absence of LPS, as quantified by the LDH cytotoxicity assay. The inhibition of macrophage proliferation by a low MC-LR concentration (0.1 µg/mL) was also demonstrated, by WST-1 cell proliferation analysis. An approach was taken to investigate whether microcystin was involved in the inflammasome activation process. Significantly, the marine toxin, maitotoxin has been previously shown to modulate NLRP3 inflammasome activation, by inducing caspase-1 production, which was dependent on activation of the pore-forming receptor, pannexin-1 (Mariathasan *et al*., 2006; Pelegrin and Surprenant, 2007).

The presence of two active markers of inflammasome activation, IL-1β and caspase-1 were investigated. Significantly, IL-1β was dramatically decreased by MC-LR exposure. Additionally, it was demonstrated that inflammasome activation was possible in the murine macrophages, through co-stimulation with the LPS and ATP danger signals. It was also shown that inflammasome inhibition was possible, using the ATP-sensitive K^+ channel inhibitor, glyburide. Following MC-LR exposure, in ATP and LPS-stimulated macrophages, it appeared that the MC-LR toxin inhibited IL-1β production, but that this effect was independent of either LPS or ATP stimulation. In contrast, ATP exposure, both in the presence and absence of LPS stimulation, had no discernable effect on IL-1β production, in response to microcystin. Analysis of caspase-1 activation, in relation to MC-LR provided a further insight into the mechanism of

apoptotic cell death following toxin exposure. It was shown that MC-LR induced caspase-1 activation, in an ATP-dependent manner. In LPS-stimulated macrophages, microcystin had no effect on caspase-1, compared with controls. However, in the presence of ATP and LPS, there was a dramatic increase in active caspase-1, following toxin exposure. It was therefore concluded that ATP is necessary for active caspase-1 production following microcystin exposure, but it remains unknown if microcystin is involved in the inflammasome assembly or activation process. Further investigations into the effect of microcystin exposure on the inflammatory mediators, IL-1β and caspase-1 are warranted.

The immunomodulatory effect of aflatoxin exposure on murine macrophages was also examined in detail. The major aim was to characterise the individual and combined effects of AFB_1, AFB_2 and AFG_1 exposure based on cytokine expression profiles and cell surface receptor expression. Addition of the aflatoxins, AFB_1 and AFB_2, resulted in significantly increased IL-6 (0.1 ng/mL) and significantly deceased IL-10 (0.01 ng/mL) expression levels. However, AFB_2 significantly decreased the expression of IL-12p40. In contrast, such an effect was not observed for AFB_1. These results demonstrated that the toxic effects, induced by these aflatoxins, are dependent on variations in the ring structure of the three toxin isoforms.

In studying the effect of multiple toxin isoforms on cytokine secretion, following LPS challenge, it was observed that AFB_1 + AFB_2 combined (0.01 ng/mL each), have an additive effect, by inducing IL-6 secretion. This is significant, as neither isoform modulated IL-6 secretion at this concentration independently. In analysing the effect of aflatoxin on IL-12p40 secretion, it was evident that all toxin combinations, at both low and high concentrations significantly reduced TNF-α expression. Moreover, exposure to AFB_1 + AFG_1 (0.01 ng/mL) and AFB_1 + AFB_2 (0.1 ng/mL) significantly reduced TNF-α expression. Importantly, the majority of these effects, particularly for IL-12p40 expression, were not observed when the macrophages were exposed to these toxins individually. In summary, these results suggest that aflatoxins inhibit the LPS-mediated activation of macrophages, thus inhibiting the host response to infection from Gram-negative bacteria. This is the first report of the effect of aflatoxin mixtures on TNF-α, IL-6, IL-10 and IL12p40 expression in a murine macrophage model. Exposure of AFB_1 + AFB_2 significantly reduced CD14 cell surface receptor expression, both in the presence and absence of LPS. Significantly, this effect was not evident when cells were exposed to AFB_1 or AFB_2 alone. Additionally, AFB_1 significantly reduced the

expression of the TLR ligand, TLR2. Interestingly, following LPS challenge, exposure to AFB_2 and AFG_1 significantly decreased TLR2 expression, thus inhibiting the ability of macrophages to respond to Gram-positive components. A further avenue of research would involve the study of the effects of aflatoxins on surface marker expression, in the presence of a TLR2 ligand, such as Pam_3CSK_4.

The initial part of this research project focused on the deregulation of immune system function by naturally-occuring toxins. Due to the obvious threat posed to both human and animal by toxin exposure, sensitive methods for their detection have become a priority. A number of aflatoxin-specific antibodies have already been produced in the laboratory (Daly *et al*., 2000; Dunne *et al*., 2005). However, no immune recombinant antibodies exist to either microcystin or azaspiracid. Therefore, the primary objective of this thesis was the generation and characterisation of recombinant antibodies that recognise azaspiracid and microcystin.

The beginning of chapter 4 described the generation and screening of a recombinant immune library to the phycotoxin, azaspiracid. A low titre rabbit immune scFv library was constructed and bio-panned. However, this library yielded no soluble AZA-1 binders. Novel AZA-BTG and AZA-KLH conjugates were generated and attempts were made to characterise these toxin conjugates, by Biacore™ analysis. The latter part of the chapter described the generation and characterisation of novel azaspiracid protein conjugates, AZA-KLH and AZA-transferrin. However, no binding to the AZA-transferrin-immobilised chip surface was observed. The AZA-KLH conjugate was used to immunise an avian host. However, no significant immune response to the AZA conjugate was observed. Azaspiracid proved to be a very difficult toxin target. In the future, if new well-characterised AZA conjugates become available, the existing recombinant library could be screened for novel binders. An isolated clone from this library would represent the only existing recombinant antibody to azaspiracid.

Chapter 5 focused on the isolation and characterisation of novel avian anti-microcystin scFv fragments. As previously outlined, chickens provided a number of advantages for recombinant antibody generation. Careful consideration and deliberation was given to the custom synthesis of the MC-LR conjugates. Derivitisation and one-stage glutaraldehyde coupling was used for conjugate generation, through the *N*-methyldehydroalanine residue of MC-LR. This residue is structurally separate from the Adda moiety, which is common to all microcystin variants. Antibody binding to the

Adda structure of the microcystin would, therefore, be advantageous for cross-reactivity purposes. The avian scFv library was constructed from the antibody variable regions genes of B-cells, derived from the spleen and bone marrow of an avian host, which was immunised with an MC-LR-BSA conjugate. The scFv library was screened using a MC-LR-OVA conjugate. Two scFv fragments (2H1 and 2G1) were selected for further characterisation, based on their potential to compete with MC-LR in solution-phase inhibition assays. The 2H1 and 2G1 scFvs were cultured in large-scale and purified by immobilised metal affinity chromatography, via an incorporated hexahistidine tag. FPLC was used for removal of minor contaminants or 'polishing' of the scFvs, prior to immunoassay development and labelling.

The 2H1 and 2G1 scFv fragments were successfully used in the development of an ELISA inhibition assay for MC-LR and the assays were validated using approved techniques. Under optimised conditions, the 2H1 and 2G1 scFv displayed limits of detection of 2.7 and 4.4 ng/mL, as quantified by extrapolating the zero value, minus three standard deviations, from a four-parameter fit equation. The range of these ELISA assays was found to be 3.1 to 25 ng/mL and both assays were accurate and reproducible within this range. This work is significant, as it demonstrates, for the first time, the generation of an anti-microcystin avian scFv, with sensitivity in the ng/mL range.

The work described in chapter 6 focused on a mutagenesis approach for the generation of an improved anti-microcystin antibody fragment. A random mutagenesis strategy was chosen for scFv diversification. The 2H1 scFv fragment was chosen for mutagenesis experiments, based on previous ELISA data. A light chain shuffling strategy was employed, in which the parental heavy chain from the 2H1 scFv clone was shuffled with a library of light chains from the original un-panned scFv immune library. Error-prone PCR was also incorporated into the amplification of the light chain regions to add to the pre-existing diversity of the library. The mutant scFv library was bio-panned with the MC-LR-OVA conjugate. Two bio-panning elution strategies were employed i.e. standard trypsin elution and competitive elution with free toxin. These strategies were used in order to maximise the chances of isolating an improved binder for microcystin. Analysis of the polyclonal phage pool from each round of bio-panning revealed that both methods produced large amounts of soluble, anti-microcystin scFv clones. This data showed that it was possible to co elute phage from the immunotube with toxin in solution. Such a strategy may aid in the isolation of binders with superior functionality in solution-phase and inhibition assay formats.

ELISA inhibition and sequencing analysis revealed one mutant clone, C12, which appeared to have a greater affinity for microcystin, in comparison to the 2H1 clone. An amino acid sequence alignment of the wild-type and mutant clones showed that they were genetically different. The clones had a number of amino acid substitutions in the framework region, but the majority of the sequences were identical. The only apparently significant amino acid substitution was the insertion of glutamic acid and threoine, in close proximity to the CDRL3 region. The lack of sequence variation between the 2H1 and C12 clones, in combination with the modest improvement in microcystin binding, indicates that the parent scFv format was already substantially optimised for microcystin binding *in vivo*. No alternative light chain combinations were selected, despite the presence of a highly diverse avian light chain for selection of alternative binding partners. However, presence of a number of amino acid substitutions in the framework region, introduced through error-prone PCR, decreased the MC-LR concentration required to inhibit antibody binding by 50 % (IC_{50}) by approximately 2-fold. The C12 mutant is a novel affinity-improved recombinant avian anti-microcystin scFv.

The Biacore™ proved to be an invaluable tool in the analysis of microcystin binders, especially in assay validation and the cross-reactivity analysis of microcystin variants. When the three antibodies were applied to the development of a Biacore™ inhibition assay, the 2H1 and C12 scFv displayed similar sensitivities (LODs: 13.8 and 14.8 ng/mL). On this platform, the 2G1 scFv demonstrated a better sensitivity than previously shown on ELISA. In this situation, there was a clear advantage of using an SPR-based biosensor format over a conventional ELISA assay. The limit of detection of 1.7 ng/mL compares favourably with other SPR-based methods in the published literature (Hu *et al*., 2009; Herranz *et al*., 2011).

Cross-reactivity studies carried out using Biacore™ inhibition analysis, on all three scFv fragments (2H1,C12 and 2G1), revealed that the C12 mutant scFv displayed an improved specificity to the microcystin variants (MC-LA, MC-RR and nodularin), in comparison with the 2H1 parent clone. While the sensitivities of the 2H1 parent and C12 mutant scFvs were comparable in the Biacore™ inhibition analysis, the specificity profile of the C12 was altered for a number of variants, with an improved binding to some of the most commonly-occurring microcystins. Therefore, the incorporation of the C12 clone into a sensitive immunoassay format would give a better estimation of the total toxin content in a sample, compared to the 2H1 scFv fragment.

The purified scFv fragments, 2G1 and C12 were biotinylated, using EDC-NHS coupling chemistry . The FLISA-based immunoassay showed a 2-fold improvement in the limit of detection, compared with the un-biotinylated C12 antibody fragment in ELISA (LODs: 0.6 and 1.4 ng/mL, respectively). The FLISA-based immunoassay with the biotinylated 2G1 clone displayed an 3-fold improvement in assay sensitivity, compared with the 2G1 clone in ELISA (LODs: 1.4 and 4.4 ng/mL). The incorporation of a biotin label with a secondary detection element increased the assay sensitivity significantly. In this research, rabbit polyclonal antibodies to microcystin were also generated, purified and evaluated for incorporation into a sensitive immunoassay format for microcystin. The antibodies (IgG) were directly labelled with Alexa Fluor® 647 and biotinylated for detection with a streptavidin Alexa Fluor® 647 conjugate and the formats were found to have limits of detection of 0.3 and 0.2 ng/mL, respectively.

The potential application of a disposable recombinant antibody-based bio-chip sensor, for the detection of microcystin, was also investigated. Initially, the fluorescent-based assays were developed on a microplate format, which proved to be highly sensitive. The microcystin conjugates were coated onto APTES-functionalised glass slides and inhibition was carried out on small spot areas, created using a custom built slide divider. This system enabled rapid, sensitive detection of microcystin, especially when directly labelled antibodies were utilised, as this system only requires one incubation step for detection. The use of fluorescence bio-chip platforms could potentially facilitate the generation of a highly sensitive, cheap, mass-produced disposable assay, for use in the laboratory or *in situ* testing environments. The 2G1-Alexa Fluor® 647 conjugate displayed a 6-fold increase in the IC_{50} value in the slide format, compared to the microplate format. The FLISA-based slide assay, employing the C12-Alexa Fluor® 647 scFv fragment, was estimated to have a IC_{50} of 1 µg/L. Importantly, this LOD is at the required WHO detection limit. Although further work on developing the bio-chip assay is required, the applicability of this format for microcystin detection is a possibility.

This thesis work has shown that certain toxins from natural sources, for example, azaspiracid-1, microcystin-LR and aflatoxin B_1, B_2 and G_1, have the ability to cause macrophage and, therefore, immune dysfunction. Many of the molecular processes involved in the immunotoxicity of phycotoxins and mycotoxins are still not fully understood. However, this research work has shed some light on the mechanisms in which toxins inhibit macrophage and host defence functionality, through deregulation of cytokine expression, TLR receptor expression and activation of apoptotic markers. In

addition, this work has also illustrated the utility of recombinant antibody technology for the production of anti-toxin antibodies. Furthermore, it has demonstrated that a random mutagenesis approach can improve the toxin binding capacity of a recombinant antibody fragment. Future work could include the development of a novel fluorescence-based bio-chip, capable of detecting microcystin and its variants below the regulatory limit. It is necessary to test the cross-reactivity of the antibodies in a fluorescence format to the microcystin variants. Finally, it is imperative to validate the assay in a matrix, to analyse whether sensitive microcystin detection is possible in real samples, including river water and processed cyanobacterial extracts of the Microcystis species. These assays would then have to be correlated with currently-accepted detection methods, including HPLC and mass spectrometry.

CHAPTER 8

Bibliography

Akira, S., Uematsu, S., and Takeuchi, O. (2006). Pathogen recognition and innate immunity. *Cell* **4**, 783-801.

Akira, S., and Takeda, K. (2004). Toll-like receptor signalling. *Nat. Rev. Immunol*. **7**, 499-511.

Al-Anati, L., and Petzinger, E. (2006). Immunotoxic activity of ochratoxin A. J. Vet. *Pharmacol. Ther*. **2**, 79-90.

Alfonso, C., Alfonso, A., Otero, P., Rodriguez, P., Vieytes, M.R., Elliot, C., Higgins, C., and Botana, L.M. (2008). Purification of five azaspiracids from mussel samples contaminated with DSP toxins and azaspiracids. *J. Chromatogr. B. Analyt Technol. Biomed. Life. Sci*. **1-2**, 133-140.

Alfonso, A., Román, Y., Vieytes, M.R., Ofuji, K., Satake, M., Yasumoto, T., and Botana, L.M. (2005). Azaspiracid-4 inhibits Ca^{2+} entry by stored operated channels in human T lymphocytes. *Biochem. Pharmacol.* **11**, 1627-1636.

Álvarez, G., Uribe, E., Ávalos, P., Mariño, C., and Blanco, J. (2010). First identification of azaspiracid and spirolides in *Mesodesma donacium* and *Mulinia edulis* from northern Chile. *Toxicon* **2-3**, 638-641.

Amine, A., Mohammadi, H., Bourais, I., and Palleschi, G. (2006). Enzyme inhibition-based biosensors for food safety and environmental monitoring. *Biosens. Bioelectron*. **8**, 1405-1423.

Aranda-Rodriguez, R., Kubwabo, C., and Benoit, F.M. (2003). Extraction of 15 microcystins and nodularin using immunoaffinity columns. *Toxicon* **6**, 587-599.

Armbruster, D.A., and Pry, T. (2008). Limit of blank, limit of detection and limit of quantitation. *Clin. Biochem. Rev*. **29** (suppl 1) S49-52.

Arndt, K.M., Muller, K.M., and Plückthun, A. (1998). Factors influencing the dimer to monomer transition of an antibody single-chain Fv fragment. *Biochemistry* **37**, 12918-12926.

Arstila, T.P., Casrouge, A., Baron, V., Even, J., Kanellopoulos, J., Kourilsky, P. (2000) Diversity of human alpha beta T-cell receptors. *Science* **288**, 1135.

Azevedo, S.M., Carmichael, W.W., Jochimsen, E.M., Rinehart, K.L., Lau, S., Shaw, G.R., and Eaglesham, G.K. (2002). Human intoxication by microcystins during renal dialysis treatment in Caruaru-Brazil. *Toxicology* **181-182**, 441-446.

Baeumner, A.J. (2003). Biosensors for environmental pollutants and food contaminants. *Anal. Bioanal Chem*. **3**, 434-445.

Bagu, J.R., Sykes, B.D., Craig, M.M., and Holmes, C.F. (1997). A molecular basis for different interactions of marine toxins with protein phosphatase-1. Molecular models for bound motuporin, microcystins, okadaic acid, and calyculin *A. J. Biol. Chem*. **8**, 5087-5097.

Baier, W., Loleit, M., Fischer, B., Jung, G., Neumann, U., Weiß, M., Weckesser, J., Hoffmann, P., Bessler, W.G., and Mittenbühler, K. (2000). Generation of antibodies directed against the low-immunogenic peptide-toxins microcystin-LR/RR and nodularin. *Int. J. Immunopharmacol*. **5**, 339-353.

Baneyx, F. (1999). Recombinant protein expression in *Escherichia coli*. *Curr. Opin. Biotechnol*. **5**, 411-421.

Barbas, C.F.,3rd, Burton, D.R., Scott, J.K., and Silverman, G.J. (2001). Phage Display: A Laboratory Manual, 1st Edition. Cold Spring Harbor Laboratory Press, New York, USA.

Barbas, C.F.,3rd, Bain, J.D., Hoekstra, D.M., and Lerner, R.A. (1992). Semisynthetic combinatorial antibody libraries: a chemical solution to the diversity problem. *Proc. Natl. Acad. Sci. U.S.A*. **10**, 4457-4461.

Barco, M., Rivera, J., and Caixach, J. (2002). Analysis of cyanobacterial hepatotoxins in water samples by microbore reversed-phase liquid chromatography-electrospray ionisation mass spectrometry. *J. Chromatogr. A* **1-2**, 103-111.

Bauernfeind, F., Ablasser, A., Bartok, E., Kim, S., Schmid-Burgk, J., Cavlar, T., and Hornung, V. (2011). Inflammasomes: current understanding and open questions. *Cell Mol. Life Sci*. **5**, 765-783.

Bell, J.K., Botos, I., Hall, P.R., Askins, J., Shiloach, J., Segal, D.M., and Davies, D.R. (2005). The molecular structure of the Toll-like receptor 3 ligand-binding domain. *Proc. Natl. Acad. Sci. U.S.A*. **31**, 10976-10980.

Bendtzen, K. (1988). Interleukin 1, interleukin 6 and tumor necrosis factor in infection, inflammation and immunity. *Immunol. Lett*. **3**, 183-191.

Benhar, I. (2007). Design of synthetic antibody libraries. *Expert Opin. Biol. Ther*. **5**, 763-779.

Berenbaum, M.C. (1989). What is synergy? *Pharmacol. Rev*. **2**, 93-141.

Bernhoft, A., Keblys, M., Morrison, E., Larsen, H.J., and Flaoyen, A. (2004). Combined effects of selected Penicillium mycotoxins on *in vitro* proliferation of porcine lymphocytes. *Mycopathologia* **4**, 441-450.

Bhattacharya, R., Sugendran, K., Dangi, R.S., and Rao, P.V. (1997). Toxicity evaluation of freshwater cyanobacterium *Microcystis aeruginosa* PCC 7806: II. Nephrotoxicity in rats. *Biomed. Environ. Sci.* **1**, 93-101.

Birtalan, S., Zhang, Y., Fellouse, F.A., Shao, L., Schaefer, G., and Sidhu, S.S. (2008). The intrinsic contributions of tyrosine, serine, glycine and arginine to the affinity and specificity of antibodies. *J. Mol. Biol.* **5**, 1518-1528.

Bishop, C.T., Anet, E.F., and Gorham, P.R. (1959). Isolation and identification of the fast-death factor in *Microcystis aeruginosa* NRC-1. *Can. J. Biochem. Physiol*. **3**, 453-471.

Black, S., Wilson, A., and Samols, D. (2005). An intact phosphocholine binding site is necessary for transgenic rabbit C-reactive protein to protect mice against challenge with platelet-activating factor. *J. Immunol.* **2**, 1192-1196.

Bondy, G.S., and Pestka, J.J. (2000). Immunomodulation by fungal toxins. *J. Toxicol. Environ. Health B Crit. Rev*. **2**, 109-143.

Botes, D.P., Wessels, P.L., Kruger, H., Runnegar, M.T.C., Santikarn, S., Smith, R.J., Barna, J.C.J., and Williams, D.H. (1985). Structural studies on cyanoginosins-LR, -YR, -YA, and -YM, peptide toxins from *Microcystis aeruginosa*. *J. Chem. Soc., Perkin Trans.* **1** 2747-2748.

Botes, D.P., Tuinman, A.A., Wessels, P.L., Viljoen, C.C., Kruger, H., Williams, D.H., Santikarn, S., Smith, R.J., and Hammond, S.J. (1984). The structure of cyanoginosin-LA, a cyclic heptapeptide toxin from the cyanobacterium *Microcystis aeruginosa* . *J. Chem. Soc., Perkin Trans.* **1,** 2311-2318.

Bradbury, A.R., and Marks, J.D. (2004). Antibodies from phage antibody libraries. *J. Immunol. Methods* **1-2**, 29-49.

Bucci, T.J., Howard, P.C., Tolleson, W.H., Laborde, J.B., and Hansen, D.K. (1998). Renal effects of fumonisin mycotoxins in animals. *Toxicol. Pathol*. **1**, 160-164.

Butler, J.E. (1998). Immunoglobulin diversity, B-cell and antibody repertoire development in large farm animals. *Rev. Sci. Tech.* **17**, 43-70.

Byrne, B., Stack, E., Gilmartin, N., and O'Kennedy, R. (2009). Antibody-based sensors: principles, problems and potential for detection of pathogens and associated toxins. *Sensors* **6**, 4407-4445.

Cadwell, R.C., and Joyce, G.F. (1992). Randomization of genes by PCR mutagenesis. PCR *Methods Appl*. **1**, 28-33.

Calabrese, E.J., and Baldwin, L.A. (2001). The frequency of U-shaped dose responses in the toxicological literature. *Toxicol. Sci.* **2**, 330-338.

Campàs, M., de la Iglesia, P., Le Berre, M., Kane, M., Diogène, J., and Marty, J. (2008). Enzymatic recycling-based amperometric immunosensor for the ultrasensitive detection of okadaic acid in shellfish. *Biosens. Bioelectron.* **4**, 716-722.

Campàs, M., and Marty, J. (2007). Highly sensitive amperometric immunosensors for microcystin detection in algae. *Biosens. Bioelectron.* **6**, 1034-1040.

Campàs, M., Szydlowska, D., Trojanowicz, M., and Marty, J. (2005). Towards the protein phosphatase-based biosensor for microcystin detection. *Biosens. Bioelectron.* **8**, 1520-1530.

Campbell, K., Stewart, L.D., Doucette, G.J., Fodey, T.L., Haughey, S.A., Vilariño, N., Kawatsu, K., and Elliott, C.T. (2007). Assessment of specific binding proteins suitable for the detection of paralytic shellfish poisons using optical biosensor technology. *Anal. Chem.* **15**, 5906-5914.

Canas, I.R., O'Callaghan, K., Moroney, C., Hamilton, B., James, K.J., and Furey, A. (2010). The development of a rapid method for the isolation of four azaspiracids for use as reference materials for quantitative LC-MS-MS methods. *Anal. Bioanal Chem*. **3**, 1477-1491.

Carbis, C.R., Rawlin, G.T., Grant, P., Mitchell, G.F., Anderson, J.W., and McCauley, I. (1997). A study of feral carp, *Cyprinus carpio* L., exposed to *Microcystis aeruginosa* at lake Mokoan, Australia, and possible implications for fish health. *J. Fish Dis*. **2**, 81-91.

Carmichael, W.W., and An, J. (1999). Using an enzyme-linked immunosorbent assay (ELISA) and a protein phosphatase inhibition assay (PPIA) for the detection of microcystins and nodularins. *Nat. Toxins* **6**, 377-385.

Carmichael, W.W. (1997). Advances in botanical research, In The Cyanotoxins, 1st Edition. Editor, Callow, J.A. Academic Press, London, UK, **27**, 211-256.

Carter, R.M., Poli, M.A., Pesavento, M., Sibley, D.E.T., Lubrano, G.J., and Guilbault, G.G. (1993). Immunoelectrochemical biosensors for detection of saxitoxin and brevetoxin. *Immunomethods* **2**, 128-133.

CAST (Council for Agricultural Science and Technology). (2003). Mycotoxins: risks in plant, animal, and human systems. *Task force Report,* Ames, Iowa, USA. **139,** 1-199.

Charlton, K.A., and Porter, A.J. (2002). Isolation of anti-hapten specific antibody fragments from combinatorial libraries. *Methods Mol. Biol.* **178**, 159-171.

Chen, H., Kim, Y.S., Keum, S., Kim, S., Choi, H., Lee, J., An, W.G., and Koh, K. (2007). Surface plasmon spectroscopic detection of saxitoxin. *Sensors* **7**, 1216-1223.

Chen, T., Shen, P., Zhang, J., and Hua, Z. (2005). Effects of microcystin-LR on patterns of iNOS and cytokine mRNA expression in macrophages *in vitro*. *Environ. Toxicol*. **1**, 85-91.

Chen, T., Zhao, X., Liu, Y., Shi, Q., Hua, Z., and Shen, P. (2004). Analysis of immunomodulating nitric oxide, iNOS and cytokines mRNA in mouse macrophages induced by microcystin-LR. *Toxicology* **1**, 67-77.

Chianella, I., Lotierzo, M., Piletsky, S.A., Tothill, I.E., Chen, B., Karim, K., and Turner, A.P.F. (2002). Rational design of a polymer specific for microcystin-LR using a computational approach. *Anal. Chem*. **6**, 1288-1293.

Chong, M.W., Gu, K.D., Lam, P.K., Yang, M., and Fong, W.F. (2000). Study on the cytotoxicity of microcystin-LR on cultured cells. *Chemosphere* **1-2**, 143-147.

Chu, F.S., Huang, X., Wei, R.D., and Carmichael, W.W. (1989). Production and characterization of antibodies against microcystins. *Appl. Environ. Microbiol*. **8**, 1928-1933.

Church, L.D., Cook, G.P., and McDermott, M.F. (2008). Primer: inflammasomes and interleukin 1[beta] in inflammatory disorders. *Na.t Clin. Pract. Rheum.* **1**, 34-42.

Cirino, P.C., Mayer, K.M., and Umeno, D. (2003). Generating mutant libraries using error-prone PCR. *Methods Mol. Biol*. **231**, 3-9.

Collis, A.V., Brouwer, A.P., and Martin, A.C. (2003). Analysis of the antigen combining site: correlations between length and sequence composition of the hypervariable loops and the nature of the antigen. *J. Mol. Biol*. **2**, 337-354.

Colman, J.R., Twiner, M.J., Hess, P., McMahon, T., Satake, M., Yasumoto, T., Doucette, G.J., and Ramsdell, J.S. (2005). Teratogenic effects of azaspiracid-1 identified by microinjection of Japanese medaka (*Oryzias latipes*) embryos. *Toxicon* **7**, 881-890.

Cousins, M.A., Riley, R.T., and Pestka, J.J. (2005). Foodborne mycotoxins: chemistry, biology, ecology, and toxicology. In Foodborne pathogens: microbiology and molecular biology. 1st Edition. Editors, Fratamico P.M, Bhunia A.K, Horizon Scientific Press, Norfolk, UK, 164.

Crameri, A., Whitehorn, E.A., Tate, E., and Stemmer, W.P. (1996). Improved green fluorescent protein by molecular evolution using DNA shuffling. *Nat. Biotechnol*. **3**, 315-319.

Creppy, E.E. (2002). Update of survey, regulation and toxic effects of mycotoxins in Europe. *Toxicol. Lett*. **1-3**, 19-28.

Cusumano, V., Rossano, F., Merendino, R.A., Arena, A., Costa, G.B., Mancuso, G., Baroni, A., and Losi, E. (1996). Immunobiological activities of mould products: functional impairment of human monocytes exposed to aflatoxin B_1. *Res. Microbiol*. **5**, 385-391.

Cusumano, V., Costa, G.B., and Seminara, S. (1990). Effect of aflatoxins on rat peritoneal macrophages. *Appl. Environ. Microbiol*. **11**, 3482-3484.

Dahlmann, J., Budakowski, W.R., and Luckas, B. (2003). Liquid chromatography-electrospray ionisation-mass spectrometry-based method for the simultaneous determination of algal and cyanobacterial toxins in phytoplankton from marine waters and lakes followed by tentative structural elucidation of microcystins. *J. Chromatogr. A* **1-2**, 45-57.

Daly, S.J., Keating, G.J., Dillon, P.P., Manning, B.M., O'Kennedy, R., Lee, H.A., and Morgan, M.R. (2000). Development of surface plasmon resonance-based immunoassay for aflatoxin B(1). *J. Agric. Food Chem.* **11**, 5097-5104.

Daugherty, P.S. (2007). Protein engineering with bacterial display. *Curr. Opin. Struct. Biol*. **4**, 474-480.

Davision, F. (2008). The importance of the avian immune system and its unique features. In Avian Immunology, 1st Edition. Editors, Davison, F., Kaspers, B. and Karel, S. A. Academic Press, London, UK, 1-11.

Decanniere, K., Muyldermans, S., and Wyns, L. (2000). Canonical antigen-binding loop structures in immunoglobulins: more structures, more canonical classes? *J. Mol. Biol.* **1**, 83-91.

DeSilva, B., Smith, W., Weiner, R., Kelley, M., Smolec, J., Lee, B., Khan, M., Tacey, R., Hill, H., and Celniker, A. (2003). Recommendations for the bioanalytical method validation of ligand-binding assays to support pharmacokinetic assessments of macromolecules. *Pharm. Res.* **11**, 1885-1900.

Devegowda, G., and Murthy, T.K.N. (2005). Mycotoxins: their adverse effects in poultry and some practical solutions. In The Mycotoxin blue book, 1st Edition. Editors, Diaz, D. E. Nottingham University Press, Nottingham, UK, 25-26.

Dinarello, C.A. (2000). Proinflammatory cytokines. *Chest* **2**, 503-508.

Ding, W., and Nam Ong, C. (2003). Role of oxidative stress and mitochondrial changes in cyanobacteria-induced apoptosis and hepatotoxicity. *FEMS Microbiol. Lett.* **1**, 1-7.

Ding, W.X., Shen, H.M., and Ong, C.N. (2002). Calpain activation after mitochondrial permeability transition in microcystin-induced cell death in rat hepatocytes. *Biochem. Biophys. Res. Commun*. **2**, 321-331.

Dostálek, J., and Homola, J. (2006). SPR biosensors for environmental monitoring. In Surface plasmon resonance based sensors. 1st Edition. Editor, Homola, J., Springer-Verlag, Berlin, Germany. 251.

Draisci, R., Palleschi, L., Ferretti, E., Furey, A., James, K.J., Satake, M., and Yasumoto, T. (2000). Development of a method for the identification of azaspiracid in shellfish by liquid chromatography-tandem mass spectrometry. *J. Chromatogr. A* **1-2**, 13-21.

Dugyala, R.R., and Sharma, R.P. (1996). The effect of aflatoxin B_1 on cytokine mRNA and corresponding protein levels in peritoneal macrophages and splenic lymphocytes. *Int. J. Immunopharmacol.* **10**, 599-608.

Dunne, L., Daly, S., Baxter, A., Haughey, S., and O'Kennedy, R. (2005). Surface Plasmon Resonance-Based Immunoassay for the Detection of Aflatoxin B1 Using Single-Chain Antibody Fragments. *Spectrosc. Lett.* **3**, 229-245.

Easton, L.E., Shibata, Y., and Lukavsky, P.J. (2010). Rapid, nondenaturing RNA purification using weak anion-exchange fast performance liquid chromatography. *RNA* **3**, 647-653.

EEC (1986). Council Directive 86/609/EEC of 24 November 1986 on the approximation of laws, regulations and administrative provisions of the Member States regarding the protection of animals used for experimental and other scientific purposes. *Offical Journal of the European Communities* **L358**, 1-29.

Egloff, M., Johnson, D.F., Moorhead, G., Cohen, P.T.W., Cohen, P., and Barford, D. (1997). Structural basis for the recognition of regulatory subunits by the catalytic subunit of protein phosphatase 1. *EMBO J*. **8**, 1876-1887.

Emanuel, P., O'Brien, T., Burans, J., DasGupta, B.R., Valdes, J.J., and Eldefrawi, M. (1996). Directing antigen specificity towards botulinum neurotoxin with combinatorial phage display libraries. *J. Immunol. Methods* **2**, 189-197.

European Food Safety Authority (2008) Marine biotoxins in shellfish – Azaspiracid group 1, Scientific Opinion of the Panel on Contaminants in the Food Chain. *The EFSA Journal* **723**, 1-52.

Falconer, I.R., and Humpage, A.R. (2005). Health risk assessment of cyanobacterial (blue-green algal) toxins in drinking water. *Int. J. Environ. Res. Public. Health*. **1**, 43-50.

Falconer, I.R., Beresford, A.M., and Runnegar, M.T. (1983). Evidence of liver damage by toxin from a bloom of the blue-green alga, *Microcystis aeruginosa*. *Med. J. Aust*. **11**, 511-514.

Feldhaus, M.J., and Siegel, R.W. (2004). Yeast display of antibody fragments: a discovery and characterization platform. *J. Immunol. Methods* **1-2**, 69-80.

Fellah, J.S., Jaffredo, T., and Dunon, D. (2008). Development of the avian immune system. In Avian Immunology, 1st Edition. Editors, Davison, F., Bernd, K. and Karel, S. A. Academic Press, London, UK, 51-66.

Fellouse, F.A., Wiesmann, C., and Sidhu, S.S. (2004). Synthetic antibodies from a four-amino-acid code: a dominant role for tyrosine in antigen recognition. *Proc. Natl. Acad. Sci. U.S.A.* **34**, 12467-12472.

Ferrari, D., Pizzirani, C., Adinolfi, E., Lemoli, R.M., Curti, A., Idzko, M., Panther, E., and Di Virgilio, F. (2006). The P2X7 receptor: a key player in IL-1 processing and release. *J. Immunol.* **7**, 3877-3883.

Findlay, J.W., Smith, W.C., Lee, J.W., Nordblom, G.D., Das, I., DeSilva, B.S., Khan, M.N., and Bowsher, R.R. (2000). Validation of immunoassays for bioanalysis: a pharmaceutical industry perspective. *J. Pharm. Biomed. Anal*. **6**, 1249-1273.

Fischer, W.J., Altheimer, S., Cattori, V., Meier, P.J., Dietrich, D.R., and Hagenbuch, B. (2005). Organic anion transporting polypeptides expressed in liver and brain mediate uptake of microcystin. *Toxicol. Appl. Pharmacol*. **3**, 257-263.

Fischer, W.J., Garthwaite, I., Miles, C.O., Ross, K.M., Aggen, J.B., Chamberlin, A.R., Towers, N.R., and Dietrich, D.R. (2001). Congener-independent immunoassay for microcystins and nodularins. *Environ. Sci. Technol*. **24**, 4849-4856.

Fitzgerald, J., Leonard, P., Darcy, E., Danaher, M., and O'Kennedy, R. (2011). Light-chain shuffling from an antigen-biased phage pool allows 185-fold improvement of an anti-halofuginone single-chain variable fragment. *Anal. Biochem*. **1**, 27-33.

Fladmark, K.E., Brustugun, O.T., Mellgren, G., Krakstad, C., Boe, R., Vintermyr, O.K., Schulman, H., and Doskeland, S.O. (2002). Ca^{2+}/calmodulin-dependent protein kinase II is required for microcystin-induced apoptosis. *J. Biol. Chem*. **4**, 2804-2811.

Fladmark, K.E., Brustugun, O.T., Hovland, R., Boe, R., Gjertsen, B.T., Zhivotovsky, B., and Doskeland, S.O. (1999). Ultrarapid caspase-3 dependent apoptosis induction by serine/threonine phosphatase inhibitors. *Cell Death Differ*. **11**, 1099-1108.

Flanagan, A.F., Callanan, K.R., Donlon, J., Palmer, R., Forde, A., and Kane, M. (2001). A cytotoxicity assay for the detection and differentiation of two families of shellfish toxins. *Toxicon* **7**, 1021-1027.

Fonfria, E.S., Vilariño, N., Campbell, K., Elliott, C., Haughey, S.A., Ben-Gigirey, B., Vieites, J.M., Kawatsu, K., and Botana, L.M. (2007). Paralytic shellfish poisoning detection by surface plasmon resonance-based biosensors in shellfish matrixes. *Anal. Chem*. **16**, 6303-6311.

Foote, J., and Winter, G. (1992). Antibody framework residues affecting the conformation of the hypervariable loops. *J. Mol. Biol*. **2**, 487-499.

Forsyth, C.J., Xu, J., Nguyen, S.T., Samdal, I.A., Briggs, L.R., Rundberget, T., Sandvik, M., and Miles, C.O. (2006). Antibodies with broad specificity to azaspiracids by use of synthetic haptens. *J. Am. Chem. Soc*. **47**, 15114-15116.

Freche, B., Reig, N., and van der Goot, F. (2007). The role of the inflammasome in cellular responses to toxins and bacterial effectors. *Seminars in Immunopathology* **3**, 249-260.

Frederick, M.O., De Lamo Marin, S., Janda, K.D., Nicolaou, K.C., and Dickerson, T.J. (2009). Monoclonal antibodies with orthogonal azaspiracid epitopes. *Chembiochem* **10**, 1625-1629.

Frleta, D., Noelle, R.J., and Wade, W.F. (2003). CD40-mediated up-regulation of Toll-like receptor 4-MD2 complex on the surface of murine dendritic cells. *J. Leukoc. Biol*. **6**, 1064-1073.

Fu, W.Y., Chen, J.P., Wang, X.M., and Xu, L.H. (2005). Altered expression of p53, Bcl-2 and Bax induced by microcystin-LR *in vivo* and *in vitro*. *Toxicon* **2**, 171-177.

Fukuda, I., Kojoh, K., Tabata, N., Doi, N., Takashima, H., Miyamoto-Sato, E., and Yanagawa, H. (2006). *In vitro* evolution of single-chain antibodies using mRNA display. *Nucleic Acids Res*. **19**, e127.

Furey, A., O'Doherty, S., O'Callaghan, K., Lehane, M., and James, K.J. (2010). Azaspiracid poisoning (AZP) toxins in shellfish: toxicological and health considerations. *Toxicon* **2**, 173-190.

Fux, E., McMillan, D., Bire, R., and Hess, P. (2007). Development of an ultra-performance liquid chromatography-mass spectrometry method for the detection of lipophilic marine toxins. *J. Chromatogr. A* **1-2**, 273-280.

Gai, S.A., and Wittrup, K.D. (2007). Yeast surface display for protein engineering and characterization. *Curr. Opin. Struct. Biol*. **4**, 467-473.

Gerber, F., Krummen, M., Potgeter, H., Roth, A., Siffrin, C., and Spoendlin, C. (2004). Practical aspects of fast reversed-phase high-performance liquid chromatography using 3 μm particle packed columns and monolithic columns in pharmaceutical development and production working under current good manufacturing practice. *J. Chromatogr. A* **2**, 127-133.

Geuijen, C.A., Clijsters-van der Horst, M., Cox, F., Rood, P.M., Throsby, M., Jongeneelen, M.A., Backus, H.H., van Deventer, E., Kruisbeek, A.M., Goudsmit, J., and de Kruif, J. (2005). Affinity ranking of antibodies using flow cytometry: application in antibody phage display-based target discovery. *J. Immunol. Methods* **1-2**, 68-77.

Gold, L. (2001). mRNA display: diversity matters during *in vitro* selection. *Proc. Natl. Acad. Sci. U.S.A.* **9**, 4825-4826.

Goldman, E.R., Pazirandeh, M.P., Mauro, J.M., King, K.D., Frey, J.C., and Anderson, G.P. (2000). Phage-displayed peptides as biosensor reagents. *J. Mol. Recognit.* **6**, 382-387.

Gong, Y.Y., Egal, S., Hounsa, A., Turner, P.C., Hall, A.J., Cardwell, K.F., and Wild, C.P. (2003). Determinants of aflatoxin exposure in young children from Benin and Togo, West Africa: the critical role of weaning. *Int. J. Epidemiol*. **4**, 556-562.

Gordon, S., and Taylor, P.R. (2005). Monocyte and macrophage heterogeneity. *Nat Rev Immunol* **12**, 953-964.

Gram, H., Marconi, L.A., Barbas, C.F. 3rd, Collet, T.A., Lerner, R.A., Kang, A.S. (1992) *In vitro* selection and affinity maturation of antibodies from a naive combinatorial immunoglobulin library. *Proc. Natl. Acad. Sci. U.S.A.* **89**, 3576-3580.

Graves, P.R., and Haystead, T.A. (2002). Molecular biologist's guide to proteomics. *Microbiol. Mol. Biol. Rev*. **1**, 39-63.

Greten, F.R., Arkan, M.C., Bollrath, J., Hsu, L.C., Goode, J., Miething, C., Goktuna, S.I., Neuenhahn, M., Fierer, J., Paxian, S., Van Rooijen, N., Xu, Y., O'Cain, T., Jaffee, B.B., Busch, D.H., Duyster, J., Schmid, R.M., Eckmann, L., and Karin, M. (2007). NF-kappaB is a negative regulator of IL-1beta secretion as revealed by genetic and pharmacological inhibition of IKKbeta. *Cell* **5**, 918-931.

Gribble, K.E., Nolan, G., and Anderson, D.M. (2007). Biodiversity, biogeography and potential trophic impact of *Protoperidinium* spp. (Dinophyceae) off the southwestern coast of Ireland. *Journal of Plankton Research* **11**, 931-947.

Grinyó, J.M., Cruzado, J.M., Bestard, O., Vidal Castiñeira, J.R., Torras, J. (2012) Immunosuppression in the ERA of Biological Agents. *Adv. Exp. Med. Biol*. **741**, 60-72.

Grovender, E.A., Kellogg, B., Singh, J., Blom, D., Ploegh, H., Wittrup, K.D., Langer, R.S., and Ameer, G.A. (2004). Single-chain antibody fragment-based adsorbent for the extracorporeal removal of beta2-microglobulin. *Kidney Int.* **1**, 310-322.

Guo, J., Jaume, J.C., Rapoport, B., and McLachlan, S.M. (1997). Recombinant thyroid peroxidase-specific Fab converted to immunoglobulin G (IgG) molecules: evidence for thyroid cell damage by IgG1, but not IgG4, autoantibodies. *J. Clin. Endocrinol. Metab*. **3**, 925-931.

Gupta, N., Pant, S.C., Vijayaraghavan, R., and Rao, P.V.L. (2003). Comparative toxicity evaluation of cyanobacterial cyclic peptide toxin microcystin variants (LR, RR, YR) in mice. *Toxicology* **2-3**, 285-296.

Hanes, J., Schaffitzel, C., Knappik, A., and Plückthun, A. (2000). Picomolar affinity antibodies from a fully synthetic naive library selected and evolved by ribosome display. *Nat Biotech* **12**, 1287-1292.

Harada, K., Ogawa, K., Matsuura, K., Murata, H., Suzuki, M., Watanabe, M.F., Itezono, Y., and Nakayama, N. (1990). Structural determination of geometrical isomers of microcystins LR and RR from cyanobacteria by two-dimensional NMR spectroscopic techniques. *Chem. Res. Toxicol.* **5**, 473-481.

Haughey, S.A., Campbell, K., Yakes, B.J., Prezioso, S.M., Degrasse, S.L., Kawatsu, K., Elliott, C.T. (2011). Comparison of biosensor platforms for surface plasmon resonance based detection of paralytic shellfish toxins. *Talanta* **85**, 519-526.

Hayat, A., Barthelmebs, L., and Marty, J.L. (2011). Enzyme-linked immunosensor based on super paramagnetic nanobeads for easy and rapid detection of okadaic acid. *Anal. Chim. Acta* **2**, 248-252.

Hedl, M., and Abraham, C. (2011). Distinct roles for Nod2 protein and autocrine interleukin-1beta in muramyl dipeptide-induced mitogen-activated protein kinase activation and cytokine secretion in human macrophages. *J. Biol. Chem*. **30**, 26440-26449.

Hermanson, G.T. (2008). Preparation of hapten–carrier immunogen conjugates. In Bioconjugate Techniques, 2nd Edition. Editor, Hermanson, G.T. Academic Press, New York, USA. 743-782.

Hernández, J.M., López-Rodas, V., and Costas, E. (2009). Microcystins from tap water could be a risk factor for liver and colorectal cancer: a risk intensified by global change. *Med. Hypotheses* **5**, 539-540.

Hernández, M., Macia, M., Padilla, C., and Del Campo, F.F. (2000). Modulation of human polymorphonuclear leukocyte adherence by cyanopeptide toxins. *Environ. Res*. **1**, 64-68.

Herranz, S., Bocková, M., Marazuela, M., Homola, J., and Moreno-Bondi, M. (2010). An SPR biosensor for the detection of microcystins in drinking water. *Analytical and Bioanalytical Chemistry* **398**, 2652-2634.

Hess, P., Nguyen, L., Aasen, J., Keogh, M., Kilcoyne, J., McCarron, P., and Aune, T. (2005). Tissue distribution, effects of cooking and parameters affecting the extraction of azaspiracids from mussels, *Mytilus edulis*, prior to analysis by liquid chromatography coupled to mass spectrometry. *Toxicon* **1**, 62-71.

Hinton, D.M., Myers, M.J., Raybourne, R.A., Francke-Carroll, S., Sotomayor, R.E., Shaddock, J., Warbritton, A., and Chou, M.W. (2003). Immunotoxicity of aflatoxin B_1 in rats: effects on lymphocytes and the inflammatory response in a chronic intermittent dosing study. *Toxicol. Sci.* **2**, 362-377.

Hirama, M. (2005). Total synthesis of ciguatoxin CTX3C: a venture into the problems of ciguatera seafood poisoning. *Chem. Rec.* **4**, 240-250.

Holladay, S.D., and Blaylock, B.L. (2002). The mouse as a model for developmental immunotoxicology. *Hum. Exp. Toxicol*. **9-10**, 525-531.

Holliger, P., and Hudson, P.J. (2005). Engineered antibody fragments and the rise of single domains. *Nat Biotech* **9**, 1126-1136.

Honkanen, R.E., Codispoti, B.A., Tse, K., Boynton, A.L., and Honkanan, R.E. (1994). Characterization of natural toxins with inhibitory activity against serine/threonine protein phosphatases. *Toxicon* **3**, 339-350.

Hoogenboom, H.,R. (2005). Selecting and screening recombinant antibody libraries. *Nat Biotechnology* **9**, 1105-1116.

Hoogenboom, H.R., Griffiths, A.D., Johnson, K.S., Chiswell, D.J., Hudson, P., and Winter, G. (1991). Multi-subunit proteins on the surface of filamentous phage: methodologies for displaying antibody (Fab) heavy and light chains. *Nucleic Acids Res.* **15**, 4133-4137.

Hopkins, P.A., and Sriskandan, S. (2005). Mammalian Toll-like receptors: to immunity and beyond. *Clin. Exp. Immunol*. **3**, 395-407.

Hu, C., Gan, N., Chen, Y., Bi, L., Zhang, X., and Song, L. (2009). Detection of microcystins in environmental samples using surface plasmon resonance biosensor. *Talanta* **1**, 407-410.

Humpage, A.R., Hardy, S.J., Moore, E.J., Froscio, S.M., and Falconer, I.R. (2000). Microcystins (cyanobacterial toxins) in drinking water enhance the growth of aberrant crypt foci in the mouse colon. *J. Toxicol. Environ. Health A.* **3**, 155-165.

Hust, M., Toleikis, L. and Dübel, S. (2008) Selection Strategies II: Antibody Phage Display, in Handbook of Therapeutic Antibodies. 1st Edition. Editors, Dübel, S. Wiley-VCH Verlag GmbH, Weinheim, Germany. 530.

Hyenstrand, P., Metcalf, J.S., Beattie, K.A., and Codd, G.A. (2001). Effects of adsorption to plastics and solvent conditions in the analysis of the cyanobacterial toxin microcystin-LR by high performance liquid chromatography. *Water Res.* **14**, 3508-3511.

IARC (International Agency for Research on Cancer) (2002). IARC monographs on the evaluation of carcinogenic risks to humans. WHO Press, Lyon, France. **82**, 1-590.

ICPS (International Chemical Safety Programme) (2000) Environmental Health Criteria - Fumonisin B1. In: Marasas, World Health Organisation. Editors, Miller, J.D., Riley, R.T., Visconti, A.WHO, Geneva, Switzerland. **219**, 1-174.

Iqbal, S.S., Mayo, M.W., Bruno, J.G., Bronk, B.V., Batt, C.A., and Chambers, J.P. (2000). A review of molecular recognition technologies for detection of biological threat agents. *Biosens. Bioelectron.* **11-12**, 549-578.

Irving, R.A., Kortt, A.A., and Hudson, P.J. (1996). Affinity maturation of recombinant antibodies using *E. coli* mutator cells. *Immunotechnology* **2**, 127-143.

Ito, E., Satake, M., Ofuji, K., Higashi, M., Harigaya, K., McMahon, T., and Yasumoto, T. (2002). Chronic effects in mice caused by oral administration of sublethal doses of azaspiracid, a new marine toxin isolated from mussels. *Toxicon* **2**, 193-203.

Ito, E., Satake, M., Ofuji, K., Kurita, N., McMahon, T., James, K., and Yasumoto, T. (2000). Multiple organ damage caused by a new toxin azaspiracid, isolated from mussels produced in Ireland. *Toxicon* **7**, 917-930.

Ivnitski, D., Abdel-Hamid, I., Atanasov, P., and Wilkins, E. (1999). Biosensors for detection of pathogenic bacteria. *Biosens. Bioelectron.* **7**, 599-624.

Jackson, J.R., Sathe, G., Rosenberg, M., and Sweet, R. (1995). *In vitro* antibody maturation. Improvement of a high affinity, neutralizing antibody against IL-1 beta. *J. Immunol*. **7**, 3310-3319.

Jaffrezic-Renault, N., and Dzyadevych, S.V. (2008). Conductometric microbiosensors for environmental monitoring. *Sensors* **4**, 2569-2588.

James, K.J., Fidalgo Saez, M.J., Furey, A., and Lehane, M. (2004). Azaspiracid poisoning, the food-borne illness associated with shellfish consumption. *Food Addit. Contam*. **9**, 879-892.

James, K.J., Sierra, M.D., Lehane, M., Brana Magdalena, A., and Furey, A. (2003). Detection of five new hydroxyl analogues of azaspiracids in shellfish using multiple tandem mass spectrometry. *Toxicon* **3**, 277-283.

James, K.J., Furey, A., Lehane, M., Ramstad, H., Aune, T., Hovgaard, P., Morris, S., Higman, W., Satake, M., and Yasumoto, T. (2002a). First evidence of an extensive northern European distribution of azaspiracid poisoning (AZP) toxins in shellfish. *Toxicon* **7**, 909-915.

James, K.J., Lehane, M., Moroney, C., Fernandez-Puente, P., Satake, M., Yasumoto, T., and Furey, A. (2002b). Azaspiracid shellfish poisoning: unusual toxin dynamics in shellfish and the increased risk of acute human intoxications. *Food Addit. Contam*. **6**, 555.

Janeway, C.A., and Medzhitov, R. (2002). Innate immune recognition. *Annu. Rev. Immunol***. 1**, 197-216.

Janeway, C.A., Travers, M., Walport, M., and Shlomchik, M.J. (2001). Immunobiology: the immune system in health and disease, 5th Edition. Garland Science, New York, USA.

Jayaraj, R., Anand, T., and Rao, P.V.L. (2006). Activity and gene expression profile of certain antioxidant enzymes to microcystin-LR induced oxidative stress in mice. *Toxicology* **2-3**, 136-146.

Jermutus, L., Honegger, A., Schwesinger, F., Hanes, J., and Plückthun, A. (2001). Tailoring *in vitro* evolution for protein affinity or stability. *Proc. Natl. Acad. Sci. U.S.A.* **1**, 75-80.

Jiang, Y., Jolly, P.E., Ellis, W.O., Wang, J.S., Phillips, T.D., and Williams, J.H. (2005). Aflatoxin B_1 albumin adduct levels and cellular immune status in Ghanaians. *Int. Immunol.* **6**, 807-814.

Johnson, G., and Wu, T.T. (2000). Kabat database and its applications: 30 years after the first variability plot. *Nucleic Acids Res.* **1**, 214-218.

Johnson, G., and Wu, T.T. (1998). Preferred CDRH3 lengths for antibodies with defined specificities. *International Immunology* **12**, 1801-1805.

Juan, T.S., Hailman, E., Kelley, M.J., Busse, L.A., Davy, E., Empig, C.J., Narhi, L.O., Wright, S.D., and Lichenstein, H.S. (1995). Identification of a lipopolysaccharide binding domain in CD14 between amino acids 57 and 64. *J. Biol. Chem*. **10**, 5219-5224.

Kaminski, N.E., Barbara, L., Faubert, K., and Holsapple, M.P. (2008). Toxic response of the immune system. In Casarett and Doull's toxicology: the basic science of poisons, 7th Edition. Editor, Klaassen, C. D. McGraw-Hill, Canada. 485-555.

Kaneko, T., Sato, S., Kotani, H., Tanaka, A., Asamizu, E., Nakamura, Y., Miyajima, N., Hirosawa, M., Sugiura, M., Sasamoto, S., Kimura, T., Hosouchi, T., Matsuno, A., Muraki, A., Nakazaki, N., Naruo, K., Okumura, S., Shimpo, S., Takeuchi, C., Wada, T., Watanabe, A., Yamada, M., Yasuda, M., and Tabata, S. (1996). Sequence analysis of the genome of the unicellular cyanobacterium *Synechocystis* sp. strain PCC6803. II. Sequence determination of the entire genome and assignment of potential protein-coding regions. *DNA Res*. **3**, 109-136.

Kania, M., Kreuzer, M., Moore, E., Pravda, M., Hock, B., and Guilbault, G. (2003). Development of polyclonal antibodies against domoic acid for their use in electrochemical biosensors. *Analytical Letters* **9**, 1851-1863.

Kanneganti, T.D., Lamkanfi, M., Kim, Y.G., Chen, G., Park, J.H., Franchi, L., Vandenabeele, P., and Nunez, G. (2007). Pannexin-1-mediated recognition of bacterial molecules activates the cryopyrin inflammasome independent of Toll-like receptor signaling. *Immunity* **4**, 433-443.

Kanneganti, T.D., Body-Malapel, M., Amer, A., Park, J.H., Whitfield, J., Franchi, L., Taraporewala, Z.F., Miller, D., Patton, J.T., Inohara, N., and Nunez, G. (2006). Critical role for Cryopyrin/Nalp3 in activation of caspase-1 in response to viral infection and double-stranded RNA. *J. Biol. Chem*. **48**, 36560-36568.

Kawai, T., and Akira, S. (2006). TLR signaling. *Cell Death Differ*. **5**, 816-825.

Kay, B.K., Williamson, M.P., and Sudol, M. (2000). The importance of being proline: the interaction of proline-rich motifs in signaling proteins with their cognate domains. *FASEB J*. **2,** 231-241.

Kelley, M., and DeSilva, B. (2007). Key elements of bioanalytical method validation for macromolecules. *AAPS J.* **2**, 156-63.

Kfir, R., Johannsen, E., and Botes, D.P. (1986). Monoclonal antibody specific for cyanoginosin-LA: Preparation and characterization. *Toxicon* **6**, 543-552.

Khreich, N., Lamourette, P., Renard, P., Clavé, G., Fenaille, F., Créminon, C., and Volland, H. (2009). A highly sensitive competitive enzyme immunoassay of broad specificity quantifying microcystins and nodularins in water samples. *Toxicon* **5**, 551-559.

Kiefer, F., Arnold, K., Kunzli, M., Bordoli, L., and Schwede, T. (2009). The SWISS-MODEL repository and associated resources. *Nucleic Acids Res*. **37**, D387-D392.

Kihara, T., Matsuo, T., Sakamoto, M., Yasuda, Y., Yamamoto, Y., and Tanimura, T. (2000). Effects of prenatal aflatoxin B_1 exposure on behaviors of rat offspring. *Toxicol. Sci.* **2**, 392-399.

Kim, Y.M., Oh, S.W., Jeong, S.Y., Pyo, D.J., and Choi, E.Y. (2003). Development of an ultrarapid one-step fluorescence immunochromatographic assay system for the quantification of microcystins. *Environ. Sci. Technol*. **9**, 1899-1904.

Kirsch, M., Zaman, M., Meier, D., Dubel, S., and Hust, M. (2005). Parameters affecting the display of antibodies on phage. *J. Immunol. Methods* **1-2**, 173-185.

Kleivdal, H., Kristiansen, S.I., Nilsen, M.V., Goksoyr, A., Briggs, L., Holland, P., and McNabb, P. (2007). Determination of domoic acid toxins in shellfish by biosense ASP ELISA-a direct competitive enzyme-linked immunosorbent assay: collaborative study. *J. AOAC Int.* **4**, 1011-1027.

Knight, K.L. (1992). Restricted VH gene usage and generation of antibody diversity in rabbits. *Annu. Rev. Immunol.* **1**, 593-616.

Koide, S., and Sidhu, S.S. (2009). The importance of being tyrosine: lessons in molecular recognition from minimalist synthetic binding proteins. *ACS Chem. Biol.* **5**, 325-334.

Kondo, F., Matsumoto, H., Yamada, S., Tsuji, K., Ueno, Y., and Harada, K. (2000). Immunoaffinity purification method for detection and quantification of microcystins in lake water. *Toxicon* **6**, 813-823.

Kondo, F., Ikai, Y., Oka, H., Matsumoto, H., Yamada, S., Ishikawa, N., Tsuji, K., Harada, K.-I., Shimada, T., Oshikata, M. and Suzuki, M. (1995). Reliable and sensitive method for determination of microcystins in complicated matrices by frit-fast atom bombardment liquid chromatography/mass spectrometry. *Nat. Toxins* **3**, 41–49.

Kono, H., and Rock, K.L. (2008). How dying cells alert the immune system to danger. *Nat. Rev. Immunol.* **4**, 279-289.

Korpimäki, T., Brockmann, E.C., Kuronen, O., Saraste, M., Lamminmäki, U., and Tuomola, M. (2004). Engineering of a broad specificity antibody for simultaneous detection of 13 sulfonamides at the maximum residue level. *J. Agric. Food Chem*. **1**, 40-47.

Kortt, A.A., Lah, M., Oddie, G.W., Gruen, C.L., Burns, J.E., Pearce, L.A., Atwell, J.L., McCoy, A.J., Howlett, G.J., Metzger, D.W., Webster, R.G., and Hudson, P.J. (1997). Single-chain Fv fragments of anti-neuraminidase antibody NC10 containing five- and ten-residue linkers form dimers and with zero-residue linker a trimer. *Protein Eng*. **4**, 423-433.

Kouadio, J.H., Dano, S.D., Moukha, S., Mobio, T.A., and Creppy, E.E. (2007). Effects of combinations of fusarium mycotoxins on the inhibition of macromolecular synthesis, malondialdehyde levels, DNA methylation and fragmentation, and viability in Caco-2 cells. *Toxicon* **3**, 306-317.

Kreuzer, M.P., Pravda, M., O'Sullivan, C.K., and Guilbault, G.G. (2002). Novel electrochemical immunosensors for seafood toxin analysis. *Toxicon* **9**, 1267-1274.

Kreuzer, M.P., O'Sullivan, C.K., and Guilbault, G.G. (1999). Development of an ultrasensitive immunoassay for rapid measurement of okadaic acid and its isomers. *Anal. Chem.* **19**, 4198-4202.

Kujbida, P., Hatanaka, E., Vinolo, M.A.R., Waismam, K., Cavalcanti, D.M.d.H., Curi, R., Farsky, S.H.P., and Pinto, E. (2009). Microcystins -LA, -YR, and -LR action on neutrophil migration. *Biochem. Biophys. Res. Commun*. **1**, 9-14.

Kujbida, P., Hatanaka, E., Campa, A., Colepicolo, P., and Pinto, E. (2006). Effects of microcystins on human polymorphonuclear leukocytes. Biochem. *Biophys. Res. Commun*. **1**, 273-277.

Kulagina, N.V., Twiner, M.J., Hess, P., McMahon, T., Satake, M., Yasumoto, T., Ramsdell, J.S., Doucette, G.J., Ma, W., and O'Shaughnessy, T.J. (2006). Azaspiracid-1 inhibits bioelectrical activity of spinal cord neuronal networks. *Toxicon* **7**, 766-773.

Kumar, H., Kawai, T., and Akira, S. (2011). Pathogen recognition by the innate immune system. *Int. Rev. Immunol*. **1**, 16-34.

Kurosaki, T., Shinohara, H., and Baba, Y. (2010). B cell signaling and fate decision. *Annu. Rev. Immunol.* **28**, 21-55.

Kwasnikowski, P., Kristensen, P., and Markiewicz, W.T. (2005). Multivalent display system on filamentous bacteriophage pVII minor coat protein. *J. Immunol. Methods* **1-2**, 135-143.

Lahti, K., Ahtiainen, J., Rapala, J., Sivonen, K., and Niemelä, S. (1995). Assessment of rapid bioassays for detecting cyanobacterial toxicity. *Lett. Appl. Microbiol*. **2**, 109-114.

Lambert, T.W., Boland, M.P., Holmes, C.F.B., Hrudey, S.E. (1994) Quantitation of the microcystin hepatotoxins in water at environmentally relevant concentrations with the protein phosphatase bioassay. *Envir. Sci. Tech.* **28**, 753-755.

Landsteiner, K. (1945). The Specificity of Serological Reactions, 1st Edition. Harvard University Press, Cambridge, Massachusetts, USA. 156.

Langley, G., Evans, T., Holgate, S.T., and Jones, A. (2007). Replacing animal experiments: choices, chances and challenges. *Bioessays* **9**, 918-926.

Lankoff, A., Carmichael, W.W., Grasman, K.A., Yuan, M. (2004). The uptake kinetics and immunotoxic effects of microcystin-LR in human and chicken peripheral blood lymphocytes *in vitro*. *Toxicology* **204**, 23-40.

Lantto, J., and Ohlin, M. (2002). Functional consequences of insertions and deletions in the complementarity-determining regions of human antibodies. *J. Biol. Chem*. **47**, 45108-45114.

Laroche-Traineau, J., Clofent-Sanchez, G., and Santarelli, X. (2000). Three-step purification of bacterially expressed human single-chain Fv antibodies for clinical applications. *J. Chromatogr. B. Biomed. Sci. Appl.* **1-2**, 107-117.

Lawton, L.A., and Edwards, C. (2008). Conventional laboratory methods for cyanotoxins. *Adv. Exp. Med. Biol*. **619**, 513-537.

Lawton, L.A., Edwards, C., Beattie, K.A., Pleasance, S., Dear, G.J., and Codd, G.A. (1995). Isolation and characterization of microcystins from laboratory cultures and environmental samples of *Microcystis aeruginosa* and from an associated animal toxicosis. *Nat. Toxins* **1**, 50-57.

Lawton, L.A., Edwards, C., and Codd, G.A. (1994). Extraction and high-performance liquid chromatographic method for the determination of microcystins in raw and treated waters. *Analyst* **7**, 1525-1530.

Le Berre, M., and Kane, M. (2006). Biosensor-based assay for domoic acid: comparison of performance using polyclonal, monoclonal, and recombinant antibodies. *Anal. Lett*. **8**, 1587-1598.

Le Bien, T.W. and Tedder, T.F. (2008). B lymphocytes: how they develop and function. *Blood*. **112**, 1570-80.

Lehane, M., Fidalgo Saez, M.J., Magdalena, A.B., Ruppen Canas, I., Diaz Sierra, M., Hamilton, B., Furey, A., and James, K.J. (2004). Liquid chromatography-multiple tandem mass spectrometry for the determination of ten azaspiracids, including hydroxyl analogues in shellfish. *J. Chromatogr. A*. **1-2**, 63-70.

Lehane, M., Braña-Magdalena, A., Moroney, C., Furey, A., and James, K.J. (2002). Liquid chromatography with electrospray ion trap mass spectrometry for the determination of five azaspiracids in shellfish. *J. Chromatogr. A*. **1-2**, 139-147.

Leonard, P., Safsten, P., Hearty, S., McDonnell, B., Finlay, W., and O'Kennedy, R. (2007). High throughput ranking of recombinant avian scFv antibody fragments from crude lysates using the Biacore A100. *J. Immunol. Methods* **2**, 172-179.

Leonard, P., Hearty, S., Brennan, J., Dunne, L., Quinn, J., Chakraborty, T., and O'Kennedy, R. (2003). Advances in biosensors for detection of pathogens in food and water. *Enzyme Microb. Technol.* **1**, 3-13.

Lerouge, I., Vanderleyden, J. (2002) *O*-antigen structural variation: mechanisms and possible roles in animal/plant-microbe interactions. *FEMS Microbiol. Rev*. **26**, 17-47.

Li, Y., Wang, Z., Beier, R.C., Shen, J., Smet, D.D., De Saeger, S., and Zhang, S. (2011). T-2 toxin, a trichothecene mycotoxin: review of toxicity, metabolism, and analytical methods. *J. Agric. Food Chem.* **8**, 3441-3453.

Li, Y., Cockburn, W., Kilpatrick, J.B., and Whitelam, G.C. (2000). High affinity scFvs from a single rabbit immunized with multiple haptens. *Biochem. Biophys. Res. Commun*. **2**, 398-404.

Lindner, P., Molz, R., Yacoub-George, E., Dürkop, A., and Wolf, H. (2004). Development of a highly sensitive inhibition immunoassay for microcystin-LR. *Anal. Chim. Acta* **1**, 37-44.

Liu, B., Yu, F., Chan, M., and Yang, Y. (2002). The effects of mycotoxins, fumonisin B1 and aflatoxin B_1, on primary swine alveolar macrophages. *Toxicol. Appl. Pharmacol*. **3**, 197-204.

Long, F., He, M., Zhu, A.N., and Shi, H.C. (2009). Portable optical immunosensor for highly sensitive detection of microcystin-LR in water samples. *Biosens. Bioelectron.* **8**, 2346-2351.

Long, F., He, M., Shi, H.C., and Zhu, A.N. (2008). Development of evanescent wave all-fiber immunosensor for environmental water analysis. *Biosens. Bioelectron.* **7**, 952-958.

Long, M., Lu, S., and Sun, G. (2006). Kinetics of receptor-ligand interactions in immune responses. *Cell. Mol. Immunol*. **2**, 79-86.

Lotierzo, M., Henry, O.Y., Piletsky, S., Tothill, I., Cullen, D., Kania, M., Hock, B., and Turner, A.P. (2004). Surface plasmon resonance sensor for domoic acid based on grafted imprinted polymer. *Biosens. Bioelectron*. **2**, 145-152.

Lou, J., Geren, I., Garcia-Rodriguez, C., Forsyth, C.M., Wen, W., Knopp, K., Brown, J., Smith, T., Smith, L.A., and Marks, J.D. (2010). Affinity maturation of human botulinum neurotoxin antibodies by light chain shuffling via yeast mating. *Protein Eng. Des. Sel*. **4**, 311-319.

Lou, J., and Marks, J.D. (2010). Affinity maturation by chain shuffling and site directed mutagenesis. In Antibody Engineering. 1st Edition. Editors, Kontermann, R. and Dübel, S. Springer-Verlag, Berlin, Germany. 377-396.

Low, N.M., Holliger, P., and Winter, G. (1996). Mimicking somatic hypermutation: affinity maturation of antibodies displayed on bacteriophage using a bacterial mutator strain. *J. Mol. Biol.* **3**, 359-368.

Loyprasert, S., Thavarungkul, P., Asawatreratanakul, P., Wongkittisuksa, B., Limsakul, C., and Kanatharana, P. (2008). Label-free capacitive immunosensor for microcystin-LR using self-assembled thiourea monolayer incorporated with Ag nanoparticles on gold electrode. *Biosens. Bioelectron*. **1**, 78-86.

Lubkowski, J., Hennecke, F., Plückthun, A., and Wlodawer, A. (1998). The structural basis of phage display elucidated by the crystal structure of the N-terminal domains of g3p. *Nat. Struct. Biol.* **2**, 140-147.

Lukens, J.R., Dixit, V.D., and Kanneganti, T.D. (2011). Inflammasome activation in obesity-related inflammatory diseases and autoimmunity. *Discov. Med*. **62**, 65-74.

Luongo, D., Severino, L., Bergamo, P., De Luna, R., Lucisano, A., and Rossi, M. (2006). Interactive effects of fumonisin B1 and alpha-zearalenol on proliferation and cytokine expression in Jurkat T cells. *Toxicol. In. Vitro*. **8**, 1403-1410.

Luster, M.I., and Gerberick, G.F. (2010). Immunotoxicology testing: past and future. *Methods Mol. Biol.* 598, 3-13.

Luyendyk, J.P., Shores, K.C., Ganey, P.E., and Roth, R.A. (2002). Bacterial lipopolysaccharide exposure alters aflatoxin B_1 hepatotoxicity: benchmark dose analysis for markers of liver injury. *Toxicol. Sci.* **1**, 220-225.

Ma, W., Chen, W., Qiao, R., Liu, C., Yang, C., Li, Z., Xu, D., Peng, C., Jin, Z., Xu, C., Zhu, S., and Wang, L. (2009). Rapid and sensitive detection of microcystin by immunosensor based on nuclear magnetic resonance. *Biosens. Bioelectron*. **1**, 240-243.

Ma, H., Zhou, B., Kim, Y., and Janda, K.D. (2006). A cyclic peptide-polymer probe for the detection of *Clostridium botulinum* neurotoxin serotype A. *Toxicon* **8**, 901-908.

MacKintosh, C., Beattie, K.A., Klumpp, S., Cohen, P., and Codd, G.A. (1990). Cyanobacterial microcystin-LR is a potent and specific inhibitor of protein phosphatases 1 and 2A from both mammals and higher plants. *FEBS Lett.* **2**, 187-192.

Madadlou, A., O'Sullivan, S., and Sheehan, D. (2011). Fast Protein Liquid Chromatography. *Methods Mol Biol*. **681**, 439-447.

Magdalena, A.B., Lehane, M., Krys, S., Fernández, M.L., Furey, A., and James, K.J. (2003). The first identification of azaspiracids in shellfish from France and Spain. *Toxicon* **1**, 105-108.

Mage, R.G., Lanning, D., and Knight, K.L. (2006). B cell and antibody repertoire development in rabbits: the requirement of gut-associated lymphoid tissues. *Dev. Comp. Immunol.* **1-2**, 137-153.

Mage, R.G., Sehgal, D., Schiaffella, E., and Anderson, A.O. (1999). Gene-conversion in rabbit B-cell ontogeny and during immune responses in splenic germinal centers. *Vet. Immunol. Immunopathol.* **1-2**, 7-15.

Makalowski, W., Zhang, J., and Boguski, M.S. (1996). Comparative analysis of 1196 orthologous mouse and human full-length mRNA and protein sequences. *Genome Res.* **9**, 846-857.

Mankiewicz, J., Walter, Z., Tarczynska, M., Palyvoda, O., Wojtysiak-Staniaszczyk, M., and Zalewski, M. (2002). Genotoxicity of cyanobacterial extracts containing microcystins from Polish water reservoirs as determined by SOS chromotest and comet assay. *Environ. Toxicol.* **4**, 341-350.

Mankiewicz, J., Tarczynska, M., Fladmark, K.E., Doskeland, S.O., Walter, Z., and Zalewski, M. (2001). Apoptotic effect of cyanobacterial extract on rat hepatocytes and human lymphocytes. *Environ. Toxicol*. **3**, 225-233.

Mariathasan, S., and Monack, D.M. (2007). Inflammasome adaptors and sensors: intracellular regulators of infection and inflammation. *Nat. Rev. Immunol*. **1**, 31-40.

Mariathasan, S., Weiss, D.S., Newton, K., McBride, J., O'Rourke, K., Roose-Girma, M., Lee, W.P., Weinrauch, Y., Monack, D.M., and Dixit, V.M. (2006). Cryopyrin activates the inflammasome in response to toxins and ATP. *Nature (London)* **7081**, 228-232.

Marks, J.D. (2004). Antibody affinity maturation by chain shuffling. *Methods Mol. Biol*. **248**, 327-343.

Marks, J.D., Griffiths, A.D., Malmqvist, M., Clackson, T.P., Bye, J.M., and Winter, G. (1992). By-passing immunization: building high affinity human antibodies by chain shuffling. *Biotechnology* **7**, 779-783.

Marquette, C.A., Coulet, P.R., and Blum, L.J. (1999). Semi-automated membrane based chemiluminescent immunosensor for flow injection analysis of okadaic acid in mussels. *Anal. Chim. Acta* **2-3**, 173-182.

Marty, C., Langer-Machova, Z., Sigrist, S., Schott, H., Schwendener, R.A., and Ballmer-Hofer, K. (2006). Isolation and characterization of a scFv antibody specific for tumor endothelial marker 1 (TEM1), a new reagent for targeted tumor therapy. *Cancer Lett.* **2**, 298-308.

Masters, S.L., Simon, A., Aksentijevich, I., and Kastner, D.L. (2009). Horror autoinflammaticus: the molecular pathophysiology of autoinflammatory disease. *Annu. Rev. Immunol.* **27**, 621-668.

Maynard, J., and Georgiou, G. (2000). Antibody engineering. *Annu. Rev. Biomed. Eng*. **2**, 339-376.

McCafferty, J., Griffiths, A.D., Winter, G., and Chiswell, D.J. (1990). Phage antibodies: filamentous phage displaying antibody variable domains. *Nature (London)* **6301**, 552-554.

McCarron, P., Emteborg, H., Nulty, C., Rundberget, T., Loader, J.I., Teipel, K., Miles, C.O., Quilliam, M.A., and Hess, P. (2011). A mussel tissue certified reference material for multiple phycotoxins. Part 1: design and preparation. *Anal. Bioanal Chem*. **3**, 821-833.

McCormack, W.T., Tjoelker, L.W., and Thompson, C.B. (1991). Avian B-cell development: generation of an immunoglobulin repertoire by gene conversion. *Annu. Rev. Immunol.* **1**, 219-241.

McCoy, A.J., Koizumi, Y., Toma, C., Higa, N., Dixit, V., Taniguchi, S., Tschopp, J., and Suzuki, T. (2010). Cytotoxins of the human pathogen *Aeromonas hydrophila* trigger, via the NLRP3 inflammasome, caspase-1 activation in macrophages. *Eur. J. Immunol*. **10**, 2797-2803.

McDermott, M.F., and Tschopp, J. (2007). From inflammasomes to fevers, crystals and hypertension: how basic research explains inflammatory diseases. *Trends Mol. Med*. **9**, 381-388.

McDermott, C.M., Nho, C.W., Howard, W., and Holton, B. (1998). The cyanobacterial toxin, microcystin-LR, can induce apoptosis in a variety of cell types. *Toxicon* **12**, 1981-1996.

McElhiney, J., and Lawton, L.A. (2005). Detection of the cyanobacterial hepatotoxins microcystins. *Toxicol. Appl. Pharmacol*. **3**, 219-230.

McElhiney, J., Drever, M., Lawton, L.A., and Porter, A.J. (2002). Rapid isolation of a single-chain antibody against the cyanobacterial toxin microcystin-LR by phage display and its use in the immunoaffinity concentration of microcystins from water. *Appl. Environ. Microbiol*. **11**, 5288-5295.

McElhiney, J., Lawton, L.A., and Porter, A.J. (2000). Detection and quantification of microcystins (cyanobacterial hepatotoxins) with recombinant antibody fragments isolated from a naïve human phage display library. *FEMS Microbiol. Lett*. **1**, 83-88.

McInnes, I.B., and Schett, G. (2007). Cytokines in the pathogenesis of rheumatoid arthritis. *Nat. Rev. Immunol.* **6**, 429-442.

McMahon, T. and Silke, J. (1998). Re-occurrence of winter toxicity. *Harmful Algae News* **17**, 12–16

McMahon, T. and Silke, J. (1996). Winter toxicity of unknown aetiology in mussels. *Harmful Algae News* **14**, 2.

Meriluoto, J., Kincaid, B., Smyth, M.R., and Wasberg, M. (1998). Electrochemical detection of microcystins, cyanobacterial peptide hepatotoxins, following high-performance liquid chromatography. *J. Chromatog. A.* **1-2**, 226-230.

Meriluoto, J. (1997). Chromatography of microcystins. *Anal. Chim. Acta* **1-3**, 277-298.

Metcalf, J.S., and Codd, G.A. (2003). Analysis of cyanobacterial toxins by immunological methods. *Chem. Res. Toxicol*. **2**, 103-112.

Metcalf, J.S., Bell, S.G., and Codd, G.A. (2001). Colorimetric immuno-protein phosphatase inhibition assay for specific detection of microcystins and nodularins of cyanobacteria. Appl. Environ. *Microbiol.* **2**, 904-909.

Metcalf, J.S., Bell, S.G., and Codd, G.A. (2000). Production of novel polyclonal antibodies against the cyanobacterial toxin microcystin-LR and their application for the detection and quantification of microcystins and nodularin. *Water Res*. **10**, 2761-2769.

Metchnikoff, E. (1959). Immunity in infective diseases. Review of some concepts of Metchnikoff. *Bacteriol Rev.* **2**, 48-60.

Mhadhbi, H., Ben-Rejeb, S., Cléroux, C., Martel, A., and Delahaut, P. (2006). Generation and characterization of polyclonal antibodies against microcystins-application to immunoassays and immunoaffinity sample preparation prior to analysis by liquid chromatography and UV detection. *Talanta* **2**, 225-235.

Micheli, L., Radoi, A., Guarrina, R., Massaud, R., Bala, C., Moscone, D., and Palleschi, G. (2004). Disposable immunosensor for the determination of domoic acid in shellfish. *Biosens. Bioelectron*. **2**, 190-196.

Mikhailov, A., Härmälä-Braskén, A., Meriluoto, J., Sorokina, Y., Dietrich, D., and Eriksson, J.E. (2001). Production and specificity of mono and polyclonal antibodies against microcystins conjugated through *N*-methyldehydroalanine. *Toxicon* **4**, 477-483.

Milutinovic, A., Sedmak, B., Horvat-Znidarsic, I., and Suput, D. (2002). Renal injuries induced by chronic intoxication with microcystins. *Cell. Mol. Biol. Lett*. **1**, 139-141.

Minervini, F., Fornelli, F., Lucivero, G., Romano, C., and Visconti, A. (2005). T-2 toxin immunotoxicity on human B and T lymphoid cell lines. *Toxicology* **1**, 81-91.

Moghaddam, A., Lobersli, I., Gebhardt, K., Braunagel, M., and Marvik, O.J. (2001). Selection and characterisation of recombinant single-chain antibodies to the hapten aflatoxin-B_1 from naive recombinant antibody libraries. *J. Immunol. Meth.* **1-2**, 169-181.

Moon, E.Y., and Pyo, S. (2000). Aflatoxin B_1 inhibits CD14-mediated nitric oxide production in murine peritoneal macrophages. *Int. J. Immunopharmacol*. **3**, 237-246.

Moon, E.Y., Rhee, D.K., and Pyo, S. (1999a). *In vitro* suppressive effect of aflatoxin B_1 on murine peritoneal macrophage functions. *Toxicology* **2-3**, 171-179.

Moon, E.Y., Rhee, D.K., and Pyo, S. (1999b). Inhibition of various functions in murine peritoneal macrophages by aflatoxin B_1 exposure *in vivo*. *Int. J. Immunopharmacol*. **1**, 47-58.

Moon, E.Y., Rhee, D.K., and Pyo, S. (1999c). Involvement of NO, H_2O_2 and TNF-alpha in the reduced antitumor activity of murine peritoneal macrophages by aflatoxin B_1. *Cancer Lett.* **2**, 167-176.

Moon, E.Y., Han, J.J., Rhee, D.K., and Pyo, S. (1998). Aflatoxin B_1-induced suppression of nitric oxide production in murine peritoneal macrophages. *J. Toxicol. Environ. Health A.* **7**, 517-530.

Moorhead, G., MacKintosh, R.W., Morrice, N., Gallagher, T., and MacKintosh, C. (1994). Purification of type 1 protein (serine/threonine) phosphatases by microcystin-Sepharose affinity chromatography. *FEBS Lett*. **1**, 46-50.

Moroney, C., Lehane, M., Braña-Magdalena, A., Furey, A., and James, K.J. (2002). Comparison of solid-phase extraction methods for the determination of azaspiracids in shellfish by liquid chromatography–electrospray mass spectrometry. *J. Chromatogr. A* **1-2**, 353-361.

Mosser, D.M., and Edwards, J.P. (2008). Exploring the full spectrum of macrophage activation. *Nat. Rev. Immunol*. **12**, 958-969.

Mourez, M., Kane, R.S., Mogridge, J., Metallo, S., Deschatelets, P., Sellman, B.R., Whitesides, G.M., and Collier, R.J. (2001). Designing a polyvalent inhibitor of anthrax toxin. *Nat. Biotechnol*. **10**, 958-961.

Muckerheide, A., Apple, R.J., Pesce, A.J., and Michael, J.G. (1987). Cationization of protein antigens. I. Alteration of immunogenic properties. *J. Immunol*. **3**, 833-837.

Murphy, M., Jason-Moller, L., and Bruno, J. (2006). Using Biacore to measure the binding kinetics of an antibody-antigen interaction. *Curr. Protoc. Protein Sci*. **19**, 14.

Myburg, R.B., Dutton, M.F., and Chuturgoon, A.A. (2002). Cytotoxicity of fumonisin B1, diethylnitrosamine, and catechol on the SNO esophageal cancer cell line. Environ. *Health Perspect*. **8**, 813-815.

Nagata, S., Tsutsumi, T., Yoshida, F., and Ueno, Y. (1999). A new type sandwich immunoassay for microcystin: production of monoclonal antibodies specific to the immune complex formed by microcystin and an anti-microcystin monoclonal antibody. *Nat. Toxins* **2**, 49-55.

Nagata, S., Soutome, H., Tsutsumi, T., Hasegawa, A., Sekijima, M., Sugamata, M., Harada, K., Suganuma, M., and Ueno, Y. (1995). Novel monoclonal antibodies against microcystin and their protective activity for hepatotoxicity. *Nat. Toxins* **2**, 78-86.

Nakano, M., Nakano, Y., Saito-Taki, T., Mori, N., Kojima, M., Ohtake, A., and Shirai, M. (1989). Toxicity of *Microcystis aeruginosa* K-139 strain. *Microbiol. Immunol*. **9**, 787-792.

Nakano, Y., Shirai, M., Mori, N., and Nakano, M. (1991). Neutralization of microcystin shock in mice by tumor necrosis factor alpha antiserum. *Appl. Environ. Microbiol*. **1**, 327-330.

Nicolaou, K.C., Chen, D.Y.-., Li, Y., Uesaka, N., Petrovic, G., Koftis, T.V., Bernal, F., Frederick, M.O., Govindasamy, M., Ling, T., Pihko, P.M., Tang, W., and Vyskocil, S. (2006a). Total synthesis and structural elucidation of azaspiracid-1. Synthesis-based analysis of originally proposed structures and indication of their non-identity to the natural product. *J. Am. Chem. Soc*. **7**, 2258-2267.

Nicolaou, K.C., Koftis, T.V., Vyskocil, S., Petrovic, G., Tang, W., Frederick, M.O., Chen, D.Y.-., Li, Y., Ling, T., and Yamada, Y.M.A. (2006b). Total synthesis and structural elucidation of azaspiracid-1. Final assignment and total synthesis of the correct structure of Azaspiracid-1. *J. Am. Chem. Soc*. **9**, 2859-2872.

Nicolaou, K.C., Pihko, P.M., Bernal, F., Frederick, M.O., Qian, W., Uesaka, N., Diedrichs, N., Hinrichs, J., Koftis, T.V., Loizidou, E., Petrovic, G., Rodriquez, M., Sarlah, D., and Zou, N. (2006c). Total synthesis and structural Elucidation of azaspiracid-1. Construction of key building blocks for originally proposed structure. *J. Am. Chem. Soc*. **7**, 2244-2257.

Nishiwaki-Matsushima, R., Ohta, T., Nishiwaki, S., Suganuma, M., Kohyama, K., Ishikawa, T., Carmichael, W.W., Fujiki, H. (1992) Liver tumor promotion by the cyanobacterial cyclic peptide toxin microcystin LR. *J. Cancer Res. Clin. Oncol.* **118**, 420-423.

Nobre, A.C., Martins, A.M., Havt, A., Benevides, C., Lima, A.A., Fonteles, M.C., and Monteiro, H.S. (2003). Renal effects of supernatant from rat peritoneal macrophages activated by microcystin-LR: role protein mediators. *Toxicon* **3**, 377-381.

O'Brien, E. (2005). Microtoxins affecting the kidney. In Toxicology of the Kidney, 3rd Edition. Editors, Tarloff, J.B. and Lash, L.H. Taylor & Francis, London, UK, 895–936.

Ofuji, K., Satake, M., Mcmahon, T., James, K.J., Naoki, H., Oshima, Y., and Yasumoto, T. (2001). Structures of azaspiracid analogs, azaspiracid-4 and azaspiracid-5, causative toxins of azaspiracid poisoning in Europe. *Biosci. Biotechnol. Biochem*. **3**, 740-742.

Ofuji, K., Satake, M., Oshima, Y., McMahon, T., James, K.J., and Yasumoto, T. (1999). A sensitive and specific determination method for azaspiracids by liquid chromatography mass spectrometry. *Nat. Toxins* **6**, 247-250.

Oh, M.Y., Joo, H.Y., Hur, B.U., Jeong, Y.H., Cha, S.H. (2007). Enhancing phage display of antibody fragments using gIII-amber suppression. Gene **1-2**, 81-89.

Orsi, C.F., Colombari, B., Callegari, F., Todaro, A.M., Ardizzoni, A., Rossini, G.P., Blasi, E., and Peppoloni, S. (2010). Yessotoxin inhibits phagocytic activity of macrophages. *Toxicon* **2-3**, 265-273.

Ostuni, R., Zanoni, I., and Granucci, F. (2010). Deciphering the complexity of Toll-like receptor signaling. Cell. Mol. Life Sci. **24**, 4109-4134.

Ouyang, Y.L., Azcona-Olivera, J.I., and Pestka, J.J. (1995). Effects of trichothecene structure on cytokine secretion and gene expression in murine $CD4^+$ T-cells. *Toxicology* **1-3**, 187-202.

Pace, C.N., Vajdos, F., Fee, L., Grimsley, G., and Gray, T. (1995). How to measure and predict the molar absorption coefficient of a protein. *Protein Sci.* **11**, 2411-2423.

Pahan, K., Sheikh, F.G., Namboodiri, A.M., and Singh, I. (1998). Inhibitors of protein phosphatase 1 and 2A differentially regulate the expression of inducible nitric-oxide synthase in rat astrocytes and macrophages. *J. Biol. Chem*. **20**, 12219-12226.

Palm, N.W. and Medzhitov, R. (2009). Pattern recognition receptors and control of adaptive immunity. *Immunol Rev.* **227**, 221-33.

Pancer, Z. and Cooper, M.D. (2006). The evolution of adaptive immunity. *Annu Rev Immunol*. **24**, 497-518.

Pedersen, M.K., Sorensen, N.S., Heegaard, P.M.H., Beyer, N.H., and Bruun, L. (2006). Effect of different hapten-carrier conjugation ratios and molecular orientations on antibody affinity against a peptide antigen. *J. Immunol. Methods* **1-2**, 198-206.

Pelegrin, P., and Surprenant, A. (2007). Pannexin-1 couples to maitotoxin- and nigericin-induced interleukin-1β release through a dye uptake-independent pathway. *J. Biol. Chem*. **4**, 2386-2394.

Pelegrin, P., and Surprenant, A. (2006). Pannexin-1 mediates large pore formation and interleukin-1β release by the ATP-gated P2X7 receptor. *EMBO J*. **21**, 5071-5082.

Peraica, M., Radic, B., Lucic, A., and Pavlovic, M. (1999). Toxic effects of mycotoxins in humans. *Bull. World Health Organ*. **9**, 754-766.

Perez, R., Rehmann, N., Crain, S., LeBlanc, P., Craft, C., MacKinnon, S., Reeves, K., Burton, I., Walter, J., Hess, P., Quilliam, M., and Melanson, J. (2010). The preparation of certified calibration solutions for azaspiracid-1, -2, and -3, potent marine biotoxins found in shellfish. *Anal. Bioanal. Chem*. **5**, 2243-2252.

Perregaux, D., and Gabel, C.A. (1994). Interleukin-1 beta maturation and release in response to ATP and nigericin. Evidence that potassium depletion mediated by these agents is a necessary and common feature of their activity. *J. Biol. Chem*. **21**, 15195-15203.

Pestka, J.J., and Zhou, H.R. (2006). Toll-like receptor priming sensitizes macrophages to proinflammatory cytokine gene induction by deoxynivalenol and other toxicants. *Toxicol. Sci*. **2**, 445-455.

Pestka, J.J., Zhou, H.R., Moon, Y., and Chung, Y.J. (2004). Cellular and molecular mechanisms for immune modulation by deoxynivalenol and other trichothecenes: unraveling a paradox. *Toxicol. Lett*. **1**, 61-73.

Pestka, J.J. (2003). Deoxynivalenol-induced IgA production and IgA nephropathy-aberrant mucosal immune response with systemic repercussions. *Toxicol. Lett*. **140-141**, 287-295.

Pestka, J.J., and Bondy, G.S. (1994). Immunotoxic effects of mycotoxins. In Mycotoxins in grain, compounds other than aflatoxin, 1st Edition. Editors, Miller, J. D., Trenholm, H. L. and Trenholm, L. Eagan Press, Minnesota, USA. 339-358.

Petrenko, V.A., and Sorokulova, I.B. (2004). Detection of biological threats. A challenge for directed molecular evolution. *J. Microbiol. Meth.* **2**, 147-168.

Petrenko, V.A., and Vodyanoy, V.J. (2003). Phage display for detection of biological threat agents. *J. Microbiol. Meth.* **2**, 253-262.

Pitt, J.I. (2000). Toxigenic fungi and mycotoxins. *Br. Med. Bull*. **1**, 184-192.

Popkov, M., Mage, R.G., Alexander, C.B., Thundivalappil, S., Barbas, C.F.,3rd, and Rader, C. (2003). Rabbit immune repertoires as sources for therapeutic monoclonal antibodies: the impact of kappa allotype-correlated variation in cysteine content on antibody libraries selected by phage display. *J. Mol. Biol.* **2**, 325-335.

Pritchard, L., Corne, D., Kell, D., Rowland, J., and Winson, M. (2005). A general model of error-prone PCR. *J. Theor. Biol*. **4**, 497-509.

Pumera, M., Sánchez, S., Ichinose, I., and Tang, J. (2007). Electrochemical nanobiosensors. *Sensors Actuators B: Chem.* **2**, 1195-1205.

Pyo, D. (2007). Comparison of Fluorescence Immunochromatographic Assay Strip and Gold Colloidal Immunochromatographic Assay Strip for Detection of Microcystin. *Anal. Lett*. **40**, 5.

Qavi, A.J., Washburn, A.L., Byeon, J.Y., and Bailey, R.C. (2009). Label-free technologies for quantitative multiparameter biological analysis. *Anal. Bioanal Chem*. **1**, 121-135.

Qu, Y., Misaghi, S., Newton, K., Gilmour, L.L., Louie, S., Cupp, J.E., Dubyak, G.R., Hackos, D., and Dixit, V.M. (2011). Pannexin-1 is required for ATP release during apoptosis but not for inflammasome activation. *J. Immunol*. **11**, 6553-6561.

Rader, C., Ritter, G., Nathan, S., Elia, M., Gout, I., Jungbluth, A.A., Cohen, L.S., Welt, S., Old, L.J., and Barbas, C.F. (2000). The rabbit antibody repertoire as a novel source for the generation of therapeutic human antibodies. *J. Biol. Chem*. **18**, 13668-13676.

Rajpal, A., Beyaz, N., Haber, L., Cappuccilli, G., Yee, H., Bhatt, R.R., Takeuchi, T., Lerner, R.A., and Crea, R. (2005). A general method for greatly improving the affinity of antibodies by using combinatorial libraries. *Proc. Natl. Acad. Sci. U.S.A.* **24**, 8466-8471.

Rapala, J., Erkomaa, K., Kukkonen, J., Sivonen, K., and Lahti, K. (2002). Detection of microcystins with protein phosphatase inhibition assay, high-performance liquid chromatography–UV detection and enzyme-linked immunosorbent assay: comparison of methods. *Anal. Chim. Acta* **2**, 213-231.

Ratcliffe, M.J.H. (2008). B cells, the Bursa of Fabricius and the generation of antibody repertoires. In Avian Immunology, 1st Edition. Editors, Davison, F., Kaspers, B. and Schat, K. A. Academic Press, London, UK, 67-89.

Rausell, C., Llorca, J., and Real, M.D. (1997). Separation by FPLC chromatofocusing of UDP-glucosyltransferases from three developmental stages of *Drosophila melanogaster*. *Arch. Insect Biochem. Physiol*. **3**, 347-358.

Reddy, L., Odhav, B., and Bhoola, K. (2006). Aflatoxin B_1-induced toxicity in HepG2 cells inhibited by carotenoids: morphology, apoptosis and DNA damage. *Biol. Chem*. **1**, 87-93.

Rehmann, N., Hess, P., and Quilliam, M.A. (2008). Discovery of new analogs of the marine biotoxin azaspiracid in blue mussels (*Mytilus edulis*) by ultra-performance liquid chromatography/tandem mass spectrometry. *Rapid Commun. Mass Spectrom*. **4**, 549-558.

Rinehart, K.L., Harada, K., Namikoshi, M., Chen, C., Harvis, C.A., Munro, M.H.G., Blunt, J.W., Mulligan, P.E., Beasley, V.R., Dahlem, A.M., and Carmichael, W.W., (1988). Nodularin, microcystin, and the configuration of Adda. *J. Am. Chem. Soc*. **25**, 8557-8558.

Rocha, M.F., Sidrim, J.J., Soares, A.M., Jimenez, G.C., Guerrant, R.L., Ribeiro, R.A., and Lima, A.A. (2000). Supernatants from macrophages stimulated with microcystin-LR induce electrogenic intestinal response in rabbit ileum. *Pharmacol. Toxicol.* **1**, 46-51.

Rodriguez-Mozaz, S., Lopez de Alda, M.J., and Barceló, D. (2006). Biosensors as useful tools for environmental analysis and monitoring. *Anal. Bioanal. Chem*. **4**, 1025-1041.

Roitt, IM and Delves, PJ. (2001). Essential Immunology, 10th Edition. Blackwell Science, Oxford, UK,

Román, Y., Alfonso, A., Louzao, M.C., de la Rosa, L.A., Leira, F., Vieites, J.M., Vieytes, M.R., Ofuji, K., Satake, M., Yasumoto, T., and Botana, L.M. (2002). Azaspiracid-1, a potent, nonapoptotic new phycotoxin with several cell targets. *Cell. Signal*. **8**, 703-716.

Ronzitti, G., Hess, P., Rehmann, N., and Rossini, G.P. (2007). Azaspiracid-1 alters the E-cadherin pool in epithelial cells. *Toxicol. Sci*. **2**, 427-435.

Rossano, F., Ortega De Luna, L., Buommino, E., Cusumano, V., Losi, E., and Catania, M.R. (1999). Secondary metabolites of *Aspergillus* exert immunobiological effects on human monocytes. *Res. Microbiol*. **1**, 13-19.

Rossi, D., and Zlotnik, A. (2000). The biology of chemokines and their receptors. *Annu. Rev. Immunol*. **18**, 217-242.

Rudd, P.M., Wormald, M.R., and Dwek, R.A. (2004). Sugar-mediated ligand-receptor interactions in the immune system. *Trends Biotechnol*. **10**, 524-530.

Rudolph-Böhner, S., Mierke, D.F., and Moroder, L. (1994). Molecular structure of the cyanobacterial tumor-promoting microcystins. *FEBS Lett*. **3**, 319-323.

Russell, J.H., and Ley, T.J. (2002). Lymphocyte-mediated cytotoxicity. *Annu. Rev. Immunol*. **20,** 323-370.

Sangolkar, L.N., Maske, S.S., and Chakrabarti, T. (2006). Methods for determining microcystins (peptide hepatotoxins) and microcystin-producing cyanobacteria. *Water Res*. **19**, 3485-3496.

Satake, M., Ofuji, K., Naoki, H., James, K.J., Furey, A., McMahon, T., Silke, J., and Yasumoto, T. (1998). Azaspiracid, a new marine toxin having unique spiro ring assemblies, isolated from Irish mussels, *Mytilus edulis* . *J. Am. Chem. Soc*. **38**, 9967-9968.

Satake, M., MacKenzie, L., and Yasumoto, T. (1997). Identification of *Protoceratium reticulatum* as the biogenetic origin of yessotoxin. *Nat. Toxins* **4**, 164-167.

Sauer, U.G. (2005). Animal vs. non-animal tests for the monitoring of marine biotoxins in the EU. *ALTEX*. **1**, 19-24.

Schier, R., Bye, J., Apell, G., McCall, A., Adams, G.P., Malmqvist, M., Weiner, L.M., and Marks, J.D. (1996). Isolation of high-affinity monomeric human anti-c-erbB-2 single chain Fv using affinity-driven selection. *J. Mol. Biol.* **1**, 28-43.

Schmidt, W., Willmitzer, H., Bornmann, K., and Pietsch, J. (2002). Production of drinking water from raw water containing cyanobacteria-pilot plant studies for assessing the risk of microcystin breakthrough. *Environ. Toxicol.* **4,** 375-385.

Schmidt, M., Maurer-Gebhard, M., Groner, B., Kohler, G., Brochmann-Santos, G., and Wels, W. (1999). Suppression of metastasis formation by a recombinant single chain antibody-toxin targeted to full-length and oncogenic variant EGF receptors. *Oncogene* **9**, 1711-1721.

Schmiedl, A., Zimmermann, J., Scherberich, J.E., Fischer, P., and Dubel, S. (2006). Recombinant variants of antibody 138H11 against human gamma-glutamyltransferase for targeting renal cell carcinoma. *Hum. Antibodies* **3**, 81-94.

Schmitz, U., Versmold, A., Kaufmann, P., and Frank, H.-. (2000). Phage Display: a molecular tool for the generation of antibodies - a review. *Placenta* **1**, S106-S112.

Schrama, D., Reisfeld, R.A., and Becker, J.C. (2006). Antibody targeted drugs as cancer therapeutics. *Nat Rev Drug Discov* **2**, 147-159.

Schütt, C. (1999). CD14. *Int. J. Biochem. Cell Biol*. **5**, 545-549.

Scott, C., Potter, M (1983) Diversity of immunoglobulin structural gene loci. *Immunol. Res.* **2**, 43-51.

Shankaran, D.R., Gobi, K.V., and Miura, N. (2007). Recent advancements in surface plasmon resonance immunosensors for detection of small molecules of biomedical, food and environmental interest. *Sensors Actuators B: Chem*. **1**, 158-177.

Sheets, M.D., Amersdorfer, P., Finnern, R., Sargent, P., Lindquist, E., Schier, R., Hemingsen, G., Wong, C., Gerhart, J.C., and Marks, J.D. (1998). Efficient construction of a large nonimmune phage antibody library: the production of high-affinity human single-chain antibodies to protein antigens. *Proc. Natl. Acad. Sci. U.S.A.* **11**, 6157-6162.

Shen, P.P., Zhao, S.W., Zheng, W.J., Hua, Z.C., Shi, Q., and Liu, Z.T. (2003). Effects of cyanobacteria bloom extract on some parameters of immune function in mice. *Toxicol. Lett*. **1**, 27-36.

Sheng, J., He, M., and Shi, H. (2007). A highly specific immunoassay for microcystin-LR detection based on a monoclonal antibody. *Anal. Chim. Acta* **1**, 111-118.

Sheng, J.W., He, M., Shi, H.C., and Qian, Y. (2006). A comprehensive immunoassay for the detection of microcystins in waters based on polyclonal antibodies. *Anal. Chim. Acta* **2**, 309-315.

Shephard, G.S., Stockenström, S., De Villiers, D., Engelbrecht, W.J., Sydenham, E.W., and Wessels, G.F.S. (1998). Photocatalytic degradation of cyanobacterial microcystin toxins in water. *Toxicon* **12**, 1895-1901.

Singh, K.V., Kaur, J., Varshney, G.C., Raje, M., and Suri, C.R. (2004). Synthesis and characterization of hapten-protein conjugates for antibody production against small molecules. *Bioconjug. Chem*. **1**, 168-173.

Smith, J.E., Solomons, G., Lewis, C., and Anderson, J.G. (1995). Role of mycotoxins in human and animal nutrition and health. *Nat. Toxins* **4**, 187-192.

Snyderman, R., Pike, M.C., Fischer, D.G., Koren, H.S. (1977) Biologic and biochemical activities of continuous macrophage cell lines P388D1 and J774.1. *J Immunol.* **119**, 2060-2066.

Sournia, A., Chrdtiennot-Dinet, M., and Ricard, M. (1991). Marine phytoplankton: how many species in the world ocean? *J. Plankton Res*. **5**, 1093-1099.

Speijers, G.J.A., and Speijers, M.H.M. (2004). Combined toxic effects of mycotoxins. *Toxicol. Lett.* **1**, 91-98.

Stevens, R.C., Soelberg, S.D., Eberhart, B.L., Spencer, S., Wekell, J.C., Chinowsky, T.M., Trainer, V.L., and Furlong, C.E. (2007). Detection of the toxin domoic acid from clam extracts using a portable surface plasmon resonance biosensor. *Harmful Algae* **2**, 166-174.

Stienstra, R., van Diepen, J.A., Tack, C.J., Zaki, M.H., van de Veerdonk, F.L., Perera, D., Neale, G.A., Hooiveld, G.J., Hijmans, A., Vroegrijk, I., van den Berg, S., Romijn, J., Rensen, P.C., Joosten, L.A., Netea, M.G., and Kanneganti, T.D. (2011). Inflammasome is a central player in the induction of obesity and insulin resistance. *Proc. Natl. Acad. Sci. U.S.A.* **37**, 15324-15329.

Stow, J.L., Low, P.C., Offenhauser, C., and Sangermani, D. (2009). Cytokine secretion in macrophages and other cells: pathways and mediators. *Immunobiology* **7**, 601-612.

Strachan, G., McElhiney, J., Drever, M.R., McIntosh, F., Lawton, L.A., and Porter, A.J. (2002). Rapid selection of anti-hapten antibodies isolated from synthetic and semi-synthetic antibody phage display libraries expressed in *Escherichia coli*. *FEMS Microbiol. Lett.* **2**, 257-261.

Studier, F.W. (2005). Protein production by auto-induction in high density shaking cultures. *Protein Expr. Purif.* **1**, 207-234.

Sutterwala, F.S., Ogura, Y., Szczepanik, M., Lara-Tejero, M., Lichtenberger, G.S., Grant, E.P., Bertin, J., Coyle, A.J., Galan, J.E., Askenase, P.W., and Flavell, R.A. (2006). Critical role for NALP3/CIAS1/Cryopyrin in innate and adaptive immunity through its regulation of caspase-1. *Immunity* **3**, 317-327.

Suzuki, T., and Yasumoto, T. (2000). Liquid chromatography-electrospray ionization mass spectrometry of the diarrhetic shellfish-poisoning toxins okadaic acid, dinophysistoxin-1 and pectenotoxin-6 in bivalves. *J. Chromatogr. A.* **2**, 199-206

Takeda, K., and Akira, S. (2005). Toll-like receptors in innate immunity. *Int. Immunol.* **1**, 1-14.

Takeuchi, O., Akira, S. (2001) Toll-like receptors; their physiological role and signal transduction system. *Int. Immunopharmacol*. **1**, 625-635.

Taleb, H., Vale, P., Amanhir, R., Benhadouch, A., Sagou, R., and Chafik, A. (2006). First detection of azaspiracids in mussels in North West Africa. *J. Shellfish Res*. **3**, 1067-1070.

Tang, A., Kreuzer, M., Lehane, M., Pravda, M., and Guilbault, G.G. (2003). Immunosensor for the determination of okadaic acid based on screen-printed electrode. *International Journal of Environmental Analytical Chemistry* **7-8**, 663-670.

Tang, A.X.J., Pravda, M., Guilbault, G.G., Piletsky, S., and Turner, A.P.F. (2002). Immunosensor for okadaic acid using quartz crystal microbalance. *Anal. Chim. Acta* **1**, 33-40.

Taylor, P.R., Martinez-Pomares, L., Stacey, M., Lin, H.H., Brown, G.D., and Gordon, S. (2005). Macrophage receptors and immune recognition. *Annu. Rev. Immunol*. **23**, 901-944.

Thedinga, E., Kob, A., Holst, H., Keuer, A., Drechsler, S., Niendorf, R., Baumann, W., Freund, I., Lehmann, M., and Ehret, R. (2007). Online monitoring of cell metabolism for studying pharmacodynamic effects. *Toxicol. Appl. Pharmacol*. **1**, 33-44.

Theumer, M.G., Lopez, A.G., Masih, D.T., Chulze, S.N., and Rubinstein, H.R. (2003). Immunobiological effects of AFB_1 and AFB_1-FB_1 mixture in experimental subchronic mycotoxicoses in rats. *Toxicology* **1-2**, 159-170.

Thompson, J.D., Higgins, D.G., and Gibson, T.J. (1994). CLUSTAL W: improving the sensitivity of progressive multiple sequence alignment through sequence weighting, position-specific gap penalties and weight matrix choice. *Nucleic Acids Res*. **22**, 4673-4680.

Thuvander, A., Wikman, C., and Gadhasson, I. (1999). *In vitro* exposure of human lymphocytes to trichothecenes: individual variation in sensitivity and effects of combined exposure on lymphocyte function. *Food Chem. Toxicol*. **6**, 639-648.

Tillmann, U., Elbrächter, M., Krock, B., John, U., and Cembella, A. (2009). *Azadinium spinosum* gen. et sp. nov. (Dinophyceae) identified as a primary producer of azaspiracid toxins. *Eur. J. Phycol*. **1**, 63.

Tizard, I. (2002). The avian antibody response. *Seminars in Avian and Exotic Pet Medicine* **1**, 2-14.

Tomlinson, I.M., Walter, G., Jones, P.T., Dear, P.H., Sonnhammer, E.L.L., and Winter, G. (1996). The imprint of somatic hypermutation on the repertoire of human germline V genes. *J. Mol. Biol.* **5**, 813-817.

Tovchigrechko, A., and Vakser, I.A. (2006). GRAMM-X public web server for protein–protein docking. *Nucleic Acids Research* **34**, W310-W314.

Triantafilou, M., and Triantafilou, K. (2002). Lipopolysaccharide recognition: CD14, TLRs and the LPS-activation cluster. *Trends Immunol*. **6**, 301-304.

Tsan, M.F., and Gao, B. (2004). Endogenous ligands of Toll-like receptors. *J. Leukoc. Biol*. **3**, 514-519.

Tschopp, J., Martinon, F., and Burns, K. (2003). NALPs: a novel protein family involved in inflammation. *Nat. Rev. Mol. Cell Biol*. **2**, 95-104.

Tudyka, T., and Skerra, A. (1997). Glutathione S-transferase can be used as a C-terminal, enzymatically active dimerization module for a recombinant protease inhibitor, and functionally secreted into the periplasm of *Escherichia coli*. *Protein Sci*. **10**, 2180-2187.

Tully, E., Higson, S.P., and O'Kennedy, R. (2008). The development of a 'labeless' immunosensor for the detection of *Listeria monocytogenes* cell surface protein, Internalin B. *Biosens. Bioelectron*. **6**, 906-912.

Tuomola, M., Harpio, R., Mikola, H., Knuuttila, P., Lindstrom, M., Mukkala, V.M., Matikainen, M.T., and Lovgren, T. (2000). Production and characterisation of monoclonal antibodies against a very small hapten, 3-methylindole. *J. Immunol. Methods* **1-2**, 111-124.

Twiner, M.J., Rehmann, N., Hess, P., and Doucette, G.J. (2008). Azaspiracid shellfish poisoning: a review on the chemistry, ecology, and toxicology with an emphasis on human health impacts. *Mar. Drugs* **2**, 39-72.

Twiner, M.J., Hess, P., Bottein Dechraoui, M., McMahon, T., Samons, M.S., Satake, M., Yasumoto, T., Ramsdell, J.S., and Doucette, G.J. (2005). Cytotoxic and cytoskeletal effects of azaspiracid-1 on mammalian cell lines. *Toxicon* **7**, 891-900.

Ubagai, T., Tansho, S., Ito, T., and Ono, Y. (2008). Influences of aflatoxin B_1 on reactive oxygen species generation and chemotaxis of human polymorphonuclear leukocytes. Toxicol. *In. Vitro*. **4**, 1115-1120.

Ueda, E.K.M., Gout, P.W., and Morganti, L. (2003). Current and prospective applications of metal ion–protein binding. *J. Chromatogr. A.* **1**, 1-23.

UK Food Standards Agency. (2003). Fumonisins in maize meal: risk assessment. Committee on Toxicity of Chemicals in Food, Consumer Products and the Environment, UK. TOX/2003/42, 1-8.

Underhill, D.M., and Ozinsky, A. (2002). Phagocytosis of microbes: complexity in action. *Annu. Rev. Immunol*. **1**, 825-852.

Vale, C., Nicolaou, K.C., Frederick, M.O., Gomez-Limia, B., Alfonso, A., Vieytes, M.R., and Botana, L.M. (2007). Effects of azaspiracid-1, a potent cytotoxic agent, on primary neuronal cultures. A structure-activity relationship study. *J. Med. Chem.* **2**, 356-363.

Van Dorst, B., Mehta, J., Bekaert, K., Rouah-Martin, E., De Coen, W., Dubruel, P., Blust, R., and Robbens, J. (2010). Recent advances in recognition elements of food and environmental biosensors: a review. *Biosens. Bioelectron*. **4**, 1178-1194.

Van Egmond, H.P. (2004). Natural toxins: risks, regulations and the analytical situation in Europe. *Anal. Bioanal Chem*. **5**, 1152-1160.

Vanhercke, T., Ampe, C., Tirry, L., and Denolf, P. (2005). Reducing mutational bias in random protein libraries. *Anal. Biochem*. **1**, 9-14.

Vasconcelos, V.M. (1995). Uptake and depuration of the heptapeptide toxin microcystin-LR in *Mytilus galloprovincialis*. *Aquatic Toxicology* **2-3**, 227-237.

Verma, R., Boleti, E., and George, A.J.T. (1998). Antibody engineering: comparison of bacterial, yeast, insect and mammalian expression systems. *J. Immunol. Methods* **1-2**, 165-181.

Vilariño, N., Nicolaou, K.C., Frederick, M.O., Vieytes, M.R., and Botana, L.M. (2007). Irreversible cytoskeletal disarrangement is independent of caspase activation during *in vitro* azaspiracid toxicity in human neuroblastoma cells. *Biochem. Pharmacol. 2*, 327-335.

Vinogradova, T., Danaher, M., Baxter, A., Moloney, M., Victory, D., and Haughey, S.A. (2011). Rapid surface plasmon resonance immunobiosensor assay for microcystin toxins in blue-green algae food supplements. *Talanta* **3**, 638-643.

Voedisch, B., and Thie, H. (2004). Size Exclusion Chromatography. In Antibody Engineering. Editors, 2nd Edition, Kontermann, R. and Dübel, S. Springer-Verlag, Berlin, Germany. 253-258.

Ward, C.J., Beattie, K.A., Lee, E.Y., and Codd, G.A. (1997). Colorimetric protein phosphatase inhibition assay of laboratory strains and natural blooms of cyanobacteria: comparisons with high-performance liquid chromatographic analysis for microcystins. *FEMS Microbiol. Lett.* **2**, 465-473.

Welker, M., Fastner, J., Erhard, M., and von Dohren, H. (2002). Applications of MALDI-TOF MS analysis in cyanotoxin research. *Environ. Toxicol*. **4**, 367-374.

Weller, M.G., Zeck, A., Eikenberg, A., Nagata, S., Ueno, Y., and Niessner, R. (2001). Development of a direct competitive microcystin immunoassay of broad specificity. *Anal. Sci*. **12**, 1445-1448.

Weng, D., Lu, Y., Wei, Y., Liu, Y., and Shen, P. (2007). The role of ROS in microcystin-LR-induced hepatocyte apoptosis and liver injury in mice. *Toxicology* **1-2**, 15-23.

Weyermann, J., Lochmann, D., and Zimmer, A. (2005). A practical note on the use of cytotoxicity assays. *Int. J. Pharm*. **2**, 369-376.

White, M. (1999). Mediators of inflammation and the inflammatory process. *J. Allergy Clin. Immunol*. **3**, S378-S381.

Whitlow, M., Bell, B.A., Feng, S.L., Filpula, D., Hardman, K.D., Hubert, S.L., Rollence, M.L., Wood, J.F., Schott, M.E., and Milenic, D.E. (1993). An improved linker for single-chain Fv with reduced aggregation and enhanced proteolytic stability. *Protein Eng*. **8**, 989-995.

Wilkinson, I.C., Hall, C.J., Veverka, V., Shi, J.Y., Muskett, F.W., Stephens, P.E., Taylor, R.J., Henry, A.J., and Carr, M.D. (2009). High resolution NMR-based model for the structure of a scFv-IL-1β complex. *J. Biol. Chem*. **46**, 31928-31935.

Williams, J.H., Phillips, T.D., Jolly, P.E., Stiles, J.K., Jolly, C.M., and Aggarwal, D. (2004). Human aflatoxicosis in developing countries: a review of toxicology, exposure, potential health consequences, and interventions. *Am. J. Clin. Nutr*. **5**, 1106-1122.

World Health Organisation (1998). Guidelines for drinking water quality, 2nd edition. Addendum to Vol.2. Health criteria and other supporting information. World Health Organisation, Geneva, 95–110.

Wörn, A., and Plückthun, A. (2001). Stability engineering of antibody single-chain Fv fragments. *J. Mol. Biol*. **5**, 989-1010.

Wright, S.D., Ramos, R.A., Tobias, P.S., Ulevitch, R.J., and Mathison, J.C. (1990). CD14, a receptor for complexes of lipopolysaccharide (LPS) and LPS binding protein. *Science* **4975**, 1431-1433.

Wu, H., and Arron, J.R. (2003). TRAF6, a molecular bridge spanning adaptive immunity, innate immunity and osteoimmunology. *Bioessays* **11**, 1096-1105.

Xi, B., Yu, N., Wang, X., Xu, X., and Abassi, Y.A. (2008). The application of cell-based label-free technology in drug discovery. *Biotechnol. J*. **4**, 484-495.

Yakes, B.J., Prezioso, S., Haughey, S.A., Campbell, K., Elliott, C.T., and DeGrasse, S.L. (2011). An improved immunoassay for detection of saxitoxin by surface plasmon resonance biosensors. *Sensors Actuators B: Chem*. **2**, 805-811.

Yang, W., Green, K., Pinz-Sweeney, S., Briones, A.T., Burton, D.R., and Barbas III, C.F. (1995). CDR walking mutagenesis for the affinity maturation of a potent human anti-HIV-1 antibody into the picomolar range. *J. Mol. Biol*. **3**, 392-403.

Yea, S.S., Kim, H.M., Oh, H.M., Paik, K.H., and Yang, K.H. (2001). Microcystin-induced down-regulation of lymphocyte functions through reduced IL-2 mRNA stability. *Toxicol. Lett*. **1**, 21-31.

Young, F.M., Metcalf, J.S., Meriluoto, J.A.O., Spoof, L., Morrison, L.F., and Codd, G.A. (2006). Production of antibodies against microcystin-RR for the assessment of purified microcystins and cyanobacterial environmental samples. *Toxicon* **3**, 295-306.

Yu, H.W., Jang, A., Kim, L.H., Kim, S.J., Kim, I.S. (2011). Bead-based competitive fluorescence immunoassay for sensitive and rapid diagnosis of cyanotoxin risk in drinking water. *Environ Sci Technol.***45**, 7804-7811.

Yu, Q., Chen, S., Taylor, A.D., Homola, J., Hock, B., and Jiang, S. (2005). Detection of low-molecular-weight domoic acid using surface plasmon resonance sensor. *Sensors Actuators B: Chem.* **1**, 193-201.

Yu, S.Z. (1995). Primary prevention of hepatocellular carcinoma. *J. Gastroenterol. Hepatol*. **6**, 674-682.

Zeck, A., Weller, M.G., Bursill, D., and Niessner, R. (2001). Generic microcystin immunoassay based on monoclonal antibodies against Adda. *Analyst* **11**, 2002-2007.

Zelikoff, J.T., and Thomas, P.T. (1998). Immunotoxicology of environmental and occupational metals, 1st Edition CRC Press, London, UK,

Zera, A.J., Sanger, T., Hanes, J., and Harshman, L. (2002). Purification and characterization of hemolymph juvenile hormone esterase from the cricket, *Gryllus assimilis*. *Arch. Insect Biochem. Physiol.* **1**, 41-55.

Zhan, L., Sakamoto, H., Sakuraba, M., Wu, D.S., Zhang, L.S., Suzuki, T., Hayashi, M., and Honma, M. (2004). Genotoxicity of microcystin-LR in human lymphoblastoid TK6 cells. *Mutat. Res.* **1**, 1-6.

Zhang, J., Lei, J., Xu, C., Ding, L., and Ju, H. (2010). Carbon nanohorn sensitized electrochemical immunosensor for rapid detection of microcystin-LR. *Anal. Chem.* **3**, 1117-1122.

Zhang, Z., Yu, S., and Chen, C. (2001). Study on the effects of DNA and natural killer cell damage induced by microcystins LR. *Zhonghua Yu Fang Yi Xue Za Zhi*, **2**, 75-78.

Zhou, H.R., Islam, Z., and Pestka, J.J. (2003). Rapid, sequential activation of mitogen-activated protein kinases and transcription factors precedes proinflammatory cytokine mRNA expression in spleens of mice exposed to the trichothecene vomitoxin. *Toxicol. Sci.* **1**, 130-142.

Zhou, H.R., Harkema, J.R., Yan, D., and Pestka, J.J. (1999). Amplified proinflammatory cytokine expression and toxicity in mice coexposed to lipopolysaccharide and the trichothecene vomitoxin (deoxynivalenol). *J. Toxicol. Environ. Health A.* **2**, 115-136.